



# UNIVERSIDAD DE MURCIA

## ESCUELA INTERNACIONAL DE DOCTORADO

Biotechnological production of antioxidant pigments  
betalains and evaluation of their functional capacity  
in the *in vivo* model *Caenorhabditis elegans*

Producción biotecnológica de los pigmentos  
antioxidantes betalaínas y evaluación de su capacidad  
funcional en el modelo *in vivo* *Caenorhabditis elegans*

**Dña. M<sup>a</sup> Alejandra Guerrero Rubio**  
**2020**



UNIVERSIDAD DE  
MURCIA

D. Fernando Gandía Herrero, Profesor Titular de Universidad del Área de Bioquímica y Biología Molecular en el Departamento de Bioquímica y Biología Molecular A, AUTORIZA:

La presentación de la Tesis Doctoral titulada "Producción biotecnológica de los pigmentos antioxidantes betalaínas y evaluación de su capacidad funcional en el modelo in vivo *Caenorhabditis elegans*. / Biotechnological production of antioxidant pigments betalains and evaluation of their functional capacity in the in vivo model *Caenorhabditis elegans*.", realizada por D<sup>a</sup>. María Alejandra Guerrero Rubio, bajo mi inmediata dirección y supervisión, y que presenta para la obtención del grado de Doctor por la Universidad de Murcia.

En Murcia, a 11 de abril de 2020

Firmante: FERNANDO GANDIA HERRERO Fecha-hora: 11/04/2020 23:12:40 Emsor del certificado: CN=AC FNMT Usuarios OU=Ceres O=FNMT-RCM C=ES



Código seguro de verificación: RUxFMmUM-J+3i7eLH-qOFKP5vi-Cm19VHUN

COPIA ELECTRÓNICA - Página 1 de 1

Esta es una copia auténtica imprimible de un documento administrativo electrónico archivado por la Universidad de Murcia, según el artículo 27.3 c) de la Ley 39/2015, de 1 de octubre. Su autenticidad puede ser contrastada a través de la siguiente dirección: <https://sede.um.es/validador/>





Los trabajos de investigación realizados en la presente Tesis Doctoral han sido financiados por los siguientes proyectos:

- “Producción biológica de los pigmentos antioxidantes betalaínas y evaluación de su capacidad funcional en modelo *in vivo*” (Proyecto AGL2014-57431-P), financiado por el Ministerio de Economía y Competitividad.
- “Protección frente a factores ambientales relacionados con el estrés oxidativo mediada por alimentos con componentes bioactivos hidrofílicos e hidrofóbicos en modelo *in vivo*” (Proyecto AGL2017-86526-P), financiado por el Ministerio de Economía, Industria y Competitividad.
- “Biotechnological design of novel health-promoting compounds: enzymatic production, molecular stabilization and testing” (Proyecto 19893/GERM/15), financiado por el programa de Ayudas a Grupos de Excelencia de la Región de Murcia, Fundación Séneca, Agencia de Ciencia y Tecnología de la Región de Murcia”

La firmante de esta Memoria ha disfrutado de una “ayuda para contrato para la formación de personal investigador (FPI)” subvencionado por el Ministerio de Economía y Competitividad mediante el Subprograma Estatal de Formación del Programa Estatal de Promoción del Talento y su Empleabilidad, en el marco del Plan Estatal de Investigación Científica y Técnica y de Innovación 2013-2016. Referencia de la ayuda: BES-2015-074284.

Murcia, 30 de mayo de 2020

Fdo. Mª Alejandra Guerrero Rubio





Los resultados obtenidos en la presente Tesis Doctoral han dado lugar a las siguientes publicaciones:

- Henarejos-Escudero, P., Guadarrama-Flores, B., **Guerrero-Rubio, M. A.**, Gómez-Pando, L. R., García-Carmona, F., & Gandía-Herrero, F. (2017). Development of betalain producing callus lines from colored quinoa varieties (*Chenopodium quinoa* Willd). Journal of Agricultural and Food Chemistry, **66**, 467-474.
- **Guerrero-Rubio, M. A.**, Hernández-García, S., García-Carmona, F., & Gandía-Herrero, F. (2019). Extension of life-span using a RNAi model and *in vivo* antioxidant effect of *Opuntia* fruit extracts and pure betalains in *Caenorhabditis elegans*. Food Chemistry, **274**, 840-847.
- Contreras-Llano, L. E., **Guerrero-Rubio, M. A.**, Lozada-Ramírez, J. D., García-Carmona, F., & Gandía-Herrero, F. (2019). First betalain-producing bacteria break the exclusive presence of the pigments in the plant kingdom. MBio, **10**, e00345-19.
- **Guerrero-Rubio, M. A.**, López-Llorca, R., Henarejos-Escudero, P., García-Carmona, F., & Gandía-Herrero, F. (2019). Scaled-up biotechnological production of individual betalains in a microbial system. Microbial Biotechnology, **12**, 993-1002.
- **Guerrero-Rubio, M. A.**, Escribano, J., García-Carmona, F., & Gandía-Herrero, F. (2020). Light Emission in Betalains: From Fluorescent Flowers to Biotechnological Applications. Trends in Plant Science, **25**, 159-175.
- **Guerrero-Rubio, M. A.**, Martínez-Zapata, J., Henarejos-Escudero, P., García-Carmona, F., & Gandía-Herrero, F. (2020). Reversible bleaching of betalains induced by metals and application to the fluorescent determination of anthrax biomarker. Dyes and Pigments, **180**, 108493.
- **Guerrero-Rubio, M. A.**, Hernández-García, S., Escribano, J., Jiménez-Atiénzar, M., Cabanes, J., García-Carmona, F., & Gandía-Herrero, F. (2020). Betalain health-promoting effects after ingestion in *Caenorhabditis elegans* are mediated by DAF-16/FOXO and SKN-1/Nrf2 transcription factors. Food Chemistry, **330**, 127228.
- **Guerrero-Rubio, M. A.**, García-Carmona, F., & Gandía-Herrero, F. (2020). First description of betalains biosynthesis in an aquatic organism: Characterization of 4,5-DOPA-extradiol dioxygenase activity in the cyanobacteria *Anabaena cylindrica*. Microbial Biotechnology, **en revisión**.

- Matencio, A., **Guerrero-Rubio, M.A.**, Gandía-Herrero, F., García-Carmona, F., & López-Nicolás, J.M. (2020). Nanoparticles of betalamic acid derivatives with cyclodextrins. A physicochemical, thermodynamic and computational study, and how to enhance production and stability. *Food Hydrocolloids*, **en revisión**.
- **Guerrero-Rubio, M. A.**, Hernández-García, S., García-Carmona, F., & Gandía-Herrero, F. (2020). Obtention of a novel polymeric chitosan betaxanthin and characterization of the first sugar-derived betalains. **En revisión**.
- **Guerrero-Rubio, M. A.**, Hernández-García, S., García-Carmona, F., & Gandía-Herrero, F. (2020). Exposition to commonly used artificial food dyes increases activity and oxidative stress in the animal model *Caenorhabditis elegans*. **En revisión**.
- **Guerrero-Rubio, M. A.**, Hernández-García, S., García-Carmona, F., & Gandía-Herrero, F. (2020). The underlying mechanisms of baicalein and related flavonoids' health-promoting effects are mediated by mTOR pathway and the transcription factors SKN-1/Nrf2 and DAF-16/FOXO in the animal model *Caenorhabditis elegans*. **En revisión**.
- Ortega-Forte, E., Ballester, F.J., Hernández-García, A., Hernández-García, S., **Guerrero-Rubio, M. A.**, Bautista, D., Santana, M. D., Gandía-Herrero, F., & Ruiz, J. (2020). Novel organo-osmium (II) proteosynthesis inhibitor active against human ovarian cancer cells reduces gonad tumor growth in *Caenorhabditis elegans* and increases lifespan in healthy animals. **En revisión**.
- Henarejos-Escuderos, P., Hernández-García, S., **Guerrero-Rubio, M. A.**, García-Carmona, F., & Gandía-Herrero, F. (2020). Antitumoral drug potential of tryptophan-betaxanthin and related plant betalains in the *Caenorhabditis elegans* tumoral model. **En revisión**.

Patentes obtenidas a partir de los trabajos realizados en la presente Tesis Doctoral:

- P201930649  
Betaxantinas derivadas de triptófano y feniletilamina para uso en el tratamiento y/o prevención del cáncer. Fecha de registro: 12/07/2019.  
Inventor/es Universidad de Murcia: Francisco García Carmona, Fernando Gandía Herrero, **María Alejandra Guerrero Rubio**, Samanta Hernández García y Paula Henarejos Escudero.
- u201931215  
Dispositivo portaobjetos para estudio de nematodos. Fecha de registro: 16/07/2019.  
Inventor/es Universidad de Murcia: Francisco García Carmona, Fernando Gandía Herrero, **María Alejandra Guerrero Rubio**, Samanta Hernández García y Paula Henarejos Escudero.

*Un viaje de mil millas  
comienza con un solo paso*

*Lao Tzu*



## Agradecimientos

---

Alguien me dijo una vez: “tu timidez te impide mostrar el gran corazón que tienes” y quizás esta sea la oportunidad perfecta para demostrar brevemente lo agradecida que estoy a la gente que me rodea ya que, sin duda, la culminación de esta tesis doctoral no es un éxito que me pertenezca en exclusividad. Sin el apoyo de esta maravillosa gente habría sido imposible. Gracias,

A **Marina**, por ser la responsable de que haya descubierto mi vocación, por dar un giro a mi vida profesional y ser un gran apoyo en la personal.

Al resto de “**los biólogos**”, por esas esporádicas reuniones que nos permiten ponernos al día, sentirnos un poco menos incomprendidos y darnos los ánimos necesarios para enfrentar las dificultades que encontramos en el camino.

A **Ana, Abel, Cristina, María del Mar y Pepe**. Por haber crecido juntos, por las vivencias compartidas y por permanecer ahí a pesar de que la rutina diaria y la vida nos haya llevado por caminos muy distintos.

A mi familia, que a pesar de no entender muy bien a qué me dedico, siempre me demuestran lo orgullosos que están de “la científica de la familia”. En especial a mis abuelos, **Catalina y Víctor**.

A mis padres, **Isabel y José Antonio**, personas imprescindibles en mi vida. Gracias por darme esa educación y esos valores que me han convertido en la persona que soy y por todo el apoyo incondicional demostrado en cada una de mis decisiones, aunque estas supongan estar separados por miles de kilómetros.

A mi hermano **Jose** por estar siempre que lo necesito y a mi cuñada **María**, por el gran corazón que tiene. Y por supuesto, gracias a los dos por traer al pequeño **Víctor** a nuestras vidas.

A **Israel**, gracias por aparecer en mi vida y hacerla más bonita y divertida. Por mostrar paciencia cuando se acaba la mía y por aportar la sangre fría que me falta cuando las circunstancias me abrumen. Seguimos cumpliendo sueños juntos.



Al departamento de **Bioquímica y Biología Molecular A** de la Universidad de Murcia, por hacerme sentir como en casa desde el primer día.

A mi director de tesis, **Fernando**, cuya calidad profesional solo puede ser superada por su gran calidad humana. Gracias por todos los consejos, profesionales y personales, por ser un mentor y un amigo, por la confianza y la paciencia depositadas en mí durante estos años y por meterme en todos esos “líos” que eran por mi bien y que me han hecho crecer personal y profesionalmente.

Al resto de profesores del Ala C, en especial a **Paco**, por guiarme en los momentos de duda aportando su extensa experiencia y sabiduría.

A los “becarios”, todos esos alumnos cuyos TFGs, TFMs y tesis doctorales han hecho que nos crucemos en el camino. En especial, a **Rubén, Antonio y Adrián**, por amenizar el (a veces) complicado día a día en el laboratorio con los debates de sobremesa y los cotilleos varios. A **Anabel y Susana**, a pesar del poco tiempo compartido. A **Mariate**, la mejor alumna de TFG que he tenido y tendré. A **Carol** y su “hoy toca marinera”, ¡lo echaré mucho de menos! A **Samanta**, por su incesable predisposición a echar una mano donde haga falta y finalmente a **Paula**, mi compi de laboratorio y de fatigas y a quien más echaré de menos.

Al “Department of Plant Sciences” de la Universidad de Cambridge (Reino Unido). A **Sam** por darme la oportunidad de colaborar y aprender con ellos, a **Hester** por su infinita paciencia y sabiduría, al resto del equipo por hacerme sentir una más durante mi corta estancia con ellos y sobre todo gracias a **Alfonso** por ser un gran apoyo y un gran amigo.

Al personal del **CAID** y el **ACTI** de la Universidad de Murcia que han contribuido con su gran profesionalidad al desarrollo de diversas técnicas empleadas en esta tesis. En especial al personal de biomasa, por hacer tan amenas las innumerables horas compartidas.

Finalmente, debo dar las gracias a las personas que me hicieron dudar de mi propia valía ya que me “obligaron” a esforzarme día a día para demostrar mi potencial y cumplir mis objetivos.

A todos y cada uno, gracias de corazón.





*A mis padres*



## Abbreviations

<b>ABTS</b>	2,2'-azino-bis (3-ethylbenzothiazoline-6-sulfonic acid)
<b>ACN</b>	Acetonitrile
<b>ADH</b>	Arogenate dehydrogenase
<b>ADHD</b>	Attention deficit hyperactivity disorder
<b>ADI</b>	Acceptable daily intake
<b>AFD</b>	Artificial food dye
<b>Amp</b>	Ampicillin
<b>AP-MALDI</b>	Atmospheric pressure-MALDI
<b>APS</b>	Ammonium persulfate
<b>BAHD</b>	Benzylalcohol O-acetyl transferase, anthocyanin O-hydroxycinnamoyl transferase, N-hydroxycinnamoyl anthranilate benzoyl transferase and deacetylvindoline 4-O-acetyltransferase
<b>BLPS</b>	Body lengths per second
<b>Cm</b>	Chloramphenicol
<b>DNA</b>	Deoxyribonucleic acid
<b>DODA</b>	DOPA-extradiol dioxygenase
<b>DPA</b>	Dipicolinic acid
<b>DTT</b>	Dithiothreitol
<b>ED</b>	Effective dose
<b>EFSA</b>	European Food Safety Authority
<b>EIC</b>	Extracted ion chromatogram
<b>ER</b>	Endoplasmic reticulum
<b>FAD</b>	Food and Drug Administration (USA)
<b>FPLC</b>	Fast protein liquid chromatography
<b>FRAP</b>	Ferric reducing antioxidant power
<b>FUdR</b>	2'-Deoxy-5-fluorouridine / Floxuridine
<b>g</b>	Gravitational constant
<b>GFP</b>	Green fluorescent protein
<b>His</b>	Histidine
<b>HPLC</b>	High performance liquid chromatography

<b>HSPs</b>	Heat shock proteins
<b>IPTG</b>	Isopropyl $\beta$ -D-1-thiogalactopyranoside
<b>kDa</b>	Kilodalton
<b>Km</b>	Kanamycin
<b>K<sub>m</sub></b>	Michaelis-Menten constant
<b>LB</b>	Luria-Bertani medium
<b>LOD</b>	Limit of detection
<b>LOQ</b>	Limit of quantification
<b>MALDI</b>	Matrix-assisted laser desorption/ionization
<b>MOPS</b>	3-morpholinopropane-1-sulfonic acid
<b>NGM</b>	Nematode growth medium
<b>O.D.</b>	Optical density
<b>ORAC</b>	Oxygen radical absorbance capacity
<b>ORO</b>	Oil Red O, 1-(2,5-dimethyl-4-(2,5-dimethylphenyl)phenyldiazenyl) azonaphthalen-2-ol
<b>PAGE</b>	Polyacrylamide gel electrophoresis
<b>PBS</b>	Phosphate-buffered saline
<b>PCR</b>	Polymerase chain reaction
<b>PDA</b>	Photometric diode array
<b>RNA</b>	Ribonucleic acid
<b>RNAi</b>	RNA interference
<b>ROS</b>	Reactive oxygen species
<b>RT</b>	Retention time
<b>SDS</b>	Sodium dodecyl sulphate
<b>ss-cDNA</b>	Single stranded complementary DNA
<b>TEAC</b>	Trolox equivalent antioxidant capacity
<b>TEMED</b>	N, N, N', N'- Tetramethylethylenediamine
<b>TFA</b>	Trifluoroacetic acid
<b>TOF</b>	Time of flight
<b>Tris</b>	Tris(hydroxymethyl)aminomethane

## **Index**



<b>Resumen</b>	<b>1</b>
<b>Abstract</b>	<b>7</b>
<b>Chapter I. Introduction</b>	<b>13</b>
1. Betalains	15
1.1. General characteristics of betalains	15
1.2. Biosynthetic pathway of betalains	16
1.2.1. Obtention of tyrosine	16
1.2.2. Tyrosine hydroxylation	17
1.2.3. Obtention of the structural unit betalamic acid	18
1.2.4. Production of betacyanins	19
1.3. Fluorescence properties	20
1.3.1. Initial discovery of fluorescence	20
1.3.2. Structure-activity relationships	22
1.3.3. Photophysics properties of betalains	24
1.3.4. Biological relevance of fluorescence	28
1.3.5. Photostability of betalains	30
1.4. Biotechnological applications of fluorescence	31
1.4.1. Improved detection of betalains in plant extracts	31
1.4.2. Fluorescent probes in microscopy	32
1.4.2.1. Visualization of natural betalains <i>in vivo</i> and <i>in vitro</i>	32
1.4.2.2. Fluorescent detection of malaria infected erythrocytes	34
1.4.3. Monitoring enzyme activities	35
1.4.3.1. Following oxidative enzymes – Tyrosinase	35
1.4.3.2. Enhancing drug production in yeast - Tyrosine hydroxylase	36
1.4.3.3. Reporter activity in transgenesis - 4,5-DOPA-extradiol-dioxygenase	38
1.4.4. Protein labeling	39
1.4.5. Output signal in biosensors	40
1.4.6. Synthesis of tailor-made probes and future prospects	40
1.5. Health-promoting effects of betalains	42
1.5.1. Antioxidant and antiradical activities	42
1.5.2. Anti-inflammatory properties	43
1.5.3. Anti-tumoral properties	44



2. <i>Caenorhabditis elegans</i>	44
2.1. Sexual forms of <i>C. elegans</i>	45
2.2. Life cycle	46
2.3. Maintenance of <i>C. elegans</i> in the laboratory	48
2.4. Applications of <i>C. elegans</i> as an animal model	49
2.4.1. Cancer	49
2.4.2. Neurodegenerative diseases	49
2.4.3. Muscle-associated diseases	50
2.4.4. Metabolic diseases	51
2.4.5. Aging	51
<b>Chapter II. Objectives</b>	<b>73</b>
<b>Chapter III. Materials and Methods</b>	<b>77</b>
1. Chemicals	79
2. Strains and plasmids	79
3. <i>Gluconacetobacter diazotrophicus</i> culture	80
4. <i>Gluconacetobacter diazotrophicus</i> DODA sequence and cloning	80
5. <i>Anabaena cylindrica</i> culture	81
6. <i>Anabaena cylindrica</i> DODA sequence and cloning	81
7. Structure modelling of novel DODA enzymes	81
8. Phylogenetic analysis of novel betalamic acid-forming DODAs	83
9. Protein characterization	83
9.1. Protein purification	83
9.2. Protein quantification	84
9.3. Gel filtration	84
9.4. MALDI-TOF MS protein analysis	84
9.5. Trypsin digestion	85
9.6. Electrophoretic techniques	85
9.7. Gel staining	86
10. Formation of betalamic acid	86
11. Betalains' extraction from plants	87
11.1. Prickly pears extracts	87
11.2. Betanin obtention	88
11.3. Betanidin obtention	88

12. Standard betalains	88
13. Production of betalains in culture media	89
14. Scaled-up production of betalains in bioreactor	90
15. Purification of betalains	90
15.1. Q-sepharose chromatography	90
15.2. Solid phase extraction	91
16. Analysis of metabolites by HPLC	91
17. Electrospray ionization mass analysis of metabolites	91
18. Quantification of betalains	92
19. Characterization of metal-betalain complexes	92
20. Colour analysis of solid polymeric betalain	93
21. Fluorescence properties of betalains	93
22. Antioxidant and free radical scavenging activities of betalains	93
22.1. FRAP method	94
22.2. ABTS method	94
22.3. ORAC assay	94
23. Calculation of LOD, LOQ and complexation constants	95
24. <i>Bacillus</i> cultures and obtaining of spores	95
25. Scanning electron microscopy	96
26. <i>Caenorhabditis elegans</i> strains and culture conditions	96
27. Synchronous worm culture	97
28. Treatment of <i>C. elegans</i> with different compounds	97
29. Survival assays	98
30. Lifespan machine temperature control	98
31. <i>C. elegans</i> sterility via gene knockdown with RNAi	98
32. Statistical analysis	99
33. Fluorescence microscopy	99
33.1. Quantification of <i>hsp-16.2::GFP</i> expression in <i>C. elegans</i> strain TJ375	99
33.2. DAF-16 transcription factor intracellular localization in <i>C. elegans</i> strain TJ356	100
33.3. SKN-1 transcription factor intracellular localization in <i>C. elegans</i> strain LD1	100
33.4. Quantification of <i>dat-1p::GFP</i> expression in <i>C. elegans</i> strain BZ555	101
33.5. Lipofuscin detection	101

34. RNA extraction	101
35. Microarray analysis	101
36. Metabolic assays	102
37. Oil Red O (ORO) lipid staining	103
38. Motility analysis	103
<b>Chapter IV. First betalain producing bacteria break the exclusive presence of the pigments in the plant kingdom</b>	<b>109</b>
1. <i>Gluconacetobacter diazotrophicus</i> cultures produce betalamic acid	111
2. <i>G. diazotrophicus</i> 4,5-DODA sequence, expression and purification	113
3. Molecular and structural characterization of <i>G. diazotrophicus</i> 4,5-DODA	115
4. Kinetic characterization	117
5. Mass spectrometry analysis of reaction products and intermediates	121
6. Chemical formation and comprehensive enzymatic-chemical mechanism	123
7. Conclusions	125
<b>Chapter V. Expanding betalains biosynthesis to the phylum cyanobacteria: Characterization of a novel enzyme with 4,5-DOPA-extradiol dioxygenase activity in <i>Anabaena cylindrica</i></b>	<b>131</b>
1. <i>Anabaena cylindrica</i> cultures produce betalamic acid	133
2. <i>A. cylindrica</i> 4,5-DODA sequence, expression and purification	135
3. Molecular characterization	137
4. Kinetic characterization	139
5. Functional characterization	140
6. Conclusions	142
<b>Chapter VI. Scaled-up biotechnological production of individual betalains in a microbial system</b>	<b>147</b>
1. Expression of 4,5-DOPA-extradiol-dioxygenase from <i>Gluconacetobacter diazotrophicus</i> in <i>Escherichia coli</i> cultures	150
2. Production of the structural unit of betalains	150
3. Production of betalamic acid in different media	153
4. Oxygen effect in the production of betalains	156
5. Addition of amines and amino acids to the medium for the production of derived betalains	157

6. Scaling-up to bioreactor level	159
7. Purification and quantification	162
8. Conclusions	163
<b>Chapter VII. Reversible bleaching of betalains induced by metals and application to the fluorescent determination of anthrax biomarker</b>	<b>167</b>
1. Selection of betalains	169
2. General effect of europium on betalains	170
3. Effect of copper and iron on betalains	174
4. Effect of $\text{Cu}^{2+}$ and $\text{Eu}^{3+}$ chelators	176
5. Determination of dipicolinic acid	179
6. Obtaining of spores from <i>Bacillus</i>	182
7. Detection of <i>Bacillus</i> spores	183
8. Conclusions	187
<b>Chapter VIII. Obtention of a novel polymeric chitosan-betaxanthin and characterization of the first sugar-derived betalains</b>	<b>191</b>
1. Obtention of a polymeric derivative of betalains	193
2. Absorbance properties of the polymeric chitosan-betaxanthin	195
3. Fluorescence of the polymeric chitosan-betaxanthin	196
4. Production of sugar-derived betalains	198
4.1. Analysis of the pigments	198
4.2. Mass spectrometry analysis	199
4.3. Spectrophotometric analysis of the novel pigments	200
5. Conclusions	202
<b>Chapter IX. Platform for the automatic control of the organism <i>C. elegans</i></b>	<b>205</b>
1. Components and system modifications	207
2. Preparation of samples	210
2.1. Worms' requirements	210
2.2. Medium's requirements	211
3. Running the lifespan machine	212
3.1. Delimitation of analysis areas	212
3.2. Data analysis and determination of lifespan	214
4. Statistical treatment of the data	215

5. Conclusions	216
<b>Chapter X. Design of a novel microscope slide for the study of nematodes</b>	<b>219</b>
1. Background	221
2. Description of the microscopy slide	222
3. Conclusions	222
<b>Chapter XI. Extension of lifespan using a RNAi model and <i>in vivo</i> antioxidant effect of <i>Opuntia</i> fruit extracts and pure betalains in <i>Caenorhabditis elegans</i></b>	<b>225</b>
1. Antioxidant capacity of betalains <i>in vivo</i> in <i>C. elegans</i> strain TJ375	228
2. Betalains effect on <i>C. elegans</i> lifespan	229
3. Novel control of progeny based on <i>pop-1</i> RNAi	231
4. Detection of betalains in worms through fluorescence	233
5. Quantification of betalains in worms	235
6. Extracts of prickly pear as a source of betalains	235
7. Conclusions	237
<b>Chapter XII. Betalain health-promoting effects after ingestion in <i>Caenorhabditis elegans</i> are mediated by DAF-16/FOXO and SKN-1/Nrf2 transcription factors</b>	<b>245</b>
1. Synthesis of betalains	247
2. Antioxidant and free radical scavenging activities of pure betalains	249
3. Antioxidant capacity of betalains <i>in vivo</i> in <i>C. elegans</i> strain TJ375	252
4. Betalains effect on <i>C. elegans</i> lifespan	256
5. Pure betalains effects on <i>C. elegans</i> gene expression	260
5.1. Indoline carboxylic acid-betacyanin	260
5.2. Phenylalanine-betaxanthin	262
5.3. Indicaxanthin	263
5.4. Dopaxanthin	263
6. Conclusions	269
<b>Chapter XIII. The underlying mechanisms of baicalein and related flavonoids' health-promoting effects are mediated by mTOR pathway and the transcription factors SKN-1/Nrf2 and DAF-16/FOXO in the animal model <i>Caenorhabditis elegans</i></b>	<b>275</b>
1. Effect of flavonoids on <i>C. elegans</i> oxidative stress resistance	278
2. Effects of flavonoids on fat accumulation in <i>C. elegans</i>	280

3. Health-promoting effect of flavonoids on <i>C. elegans</i> lifespan	281
4. Effect of flavonoids as gene modulators in longevity pathways	283
4.1. Effect of flavonoids on the IIS insulin signaling pathway	283
4.2. Effect of flavonoids on the redox active signaling pathway	285
4.3. Baicalein effect on <i>C. elegans</i> gene expression	286
5. Conclusions	291
<b>Chapter XIV. Artificial food dyes increase activity and oxidative stress in the animal model <i>Caenorhabditis elegans</i></b>	<b>301</b>
1. Effect of individual AFD on <i>C. elegans</i> lifespan	304
2. Lipofuscin accumulation in <i>C. elegans</i>	309
3. Effects of AFDs in the antioxidant system of <i>C. elegans</i>	310
4. Neurological effects of AFDs in <i>C. elegans</i>	311
5. Movement analysis of worms exposed to AFDs	313
6. Effect of tartrazine and ponceau 4R in gene expression by RNA microarray analysis	314
7. Discussion	315
8. Conclusions	322
<b>Chapter XV. Conclusions</b>	<b>331</b>
<b>Annexes</b>	<b>335</b>
Annex I	337
Annex II	339
Annex III	349
Annex IV	351



## **List of figures and tables**





**Chapter I.**

Figure 1.1. General overview of the biosynthetic pathway of betalains	17
Figure 1.2. Fluorescence of plant pigments betalains	22
Figure 1.3. Jablonski's diagram for the excitation and relaxation of absorbing molecules	25
Figure 1.4. General scheme for the transient absorption spectra UV-Vis-NIR of betalains	27
Figure 1.5. Schematic overview of the biotechnological applications developed from betalains' fluorescence	34
Figure 1.6. Schematic overview of the sexual forms of <i>C. elegans</i>	46
Figure 1.7. Life cycle of <i>Caenorhabditis elegans</i>	47
Figure 1.8. Insulin-like signaling pathway of <i>C. elegans</i>	53
Table 1.1. Quantum yield of fluorescence obtained for purified betalains	23

**Chapter III.**

Table 3.1. Amine or amino acid precursors employed for the semi-synthesis of betalains	89
Table 3.2. Strains of <i>C. elegans</i> employed in the present work	97

**Chapter IV.**

Figure 4.1. Detection of dopaxanthin in <i>Gluconacetobacter diazotrophicus</i> cultures supplemented with L-DOPA	112
Figure 4.2. Dopaxanthin accumulation in <i>G. diazotrophicus</i> cultures at different concentrations of added L-DOPA	113
Figure 4.3. Betalain production and characterization of the novel dioxygenase from <i>Gluconacetobacter diazotrophicus</i>	114
Figure 4.4. Sequence coverage of the detected fragments identified in the peptide mass fingerprint of GdDODA	117
Figure 4.5. <i>G. diazotrophicus</i> dioxygenase activity characterization	118
Figure 4.6. Effect of aeration and inert atmosphere in the formation of dopaxanthin, by GdDODA	118
Figure 4.7. Kinetic analysis of GdDODA	120
Figure 4.8. HPLC analysis of reaction products formed by <i>G. diazotrophicus</i> dioxygenase and derived compounds	121

Figure 4.9. Enzymatic-chemical mechanism in the formation of betalains	123
Figure 4.10. Biosynthetic scheme of betalains	124
Figure 4.11. Evolution of betalamic acid, muscaflavin and dopaxanthin in an enzymatic assay with GdDODA	125
Table 4.1. Expression and purification of <i>G. diazotrophicus</i> dioxygenase	115
Table 4.2. Main peptides identified to fully characterize the protein GdDODA.	116
Table 4.3. Kinetic analysis of GdDODA with different substrates	119
Table 4.4. HPLC-ESI/TOF/MS analysis of the reaction products formed by <i>G. diazotrophicus</i> dioxygenase activity in water supplemented with L-DOPA 7.6 mM	122

## Chapter V.

Figure 5.1. Detection of dopaxanthin in cultures of <i>Anabaena cylindrica</i> supplemented with L-DOPA	134
Figure 5.2. Detection of the optimal conditions for the heterologous expression of AcDODA in <i>E. coli</i> cells	136
Figure 5.3. Characterization of DODA enzyme from <i>A. cylindrica</i>	138
Figure 5.4. <i>A. cylindrica</i> dioxygenase activity characterization	140
Figure 5.5. HPLC analysis of the evolution of betalains and intermediates in <i>E. coli</i> (pRSETA-AcDODA) cultures	141
Figure 5.6. Phylogenetic analysis of characterized betalamic acid-forming DODAs and related proteobacteria sequences	142
Table 5.1. Expression and purification of <i>A. cylindrica</i> dioxygenase in <i>E. coli</i> cultures	137

## Chapter VI.

Figure 6.1. Key steps involved in the biosynthesis of betalamic acid and betalains	149
Figure 6.2. Expression of GdDODA activity in <i>E. coli</i> cells grown in agar solid medium supplemented with L-DOPA	151
Figure 6.3. Effect of adding L-DOPA to an <i>E. coli</i> culture expressing GdDODA	152
Figure 6.4. Production of dopaxanthin in microbial cultures	155
Figure 6.5. Effect of aeration in the microbial factories	156

Figure 6.6. Redirection for the production of multiple individual pigments	158
Figure 6.7. Production of indoline-betacyanin in 2L bioreactor	160
Figure 6.8. Time evolution of the scaled-up synthesis of betalains in bioreactor (volume of 2L)	161
Table 6.1. HPLC and ESI-MS/MS characteristics and identification of known and minor betalains detected after the growth of <i>E. coli</i> expressing 4,5-DODA in different media and the addition of L-DOPA	154
Table 6.2. Production of individual betalains obtained in bacterial cultures of <i>E. coli</i> expressing the DODA enzyme of <i>G. diazotrophicus</i>	159
Table 6.3. Betalain production in 2L bioreactors.	163
<b>Chapter VII.</b>	
Figure 7.1. Structures and chromatograms for the pure betalains used in this study	170
Figure 7.2. Spectrophotometric changes of betalains in presence of $\text{Eu}^{3+}$	172
Figure 7.3. Change in the absorbance values of betalains due to the presence of $\text{Eu}^{3+}$	173
Figure 7.4. Effects of dipicolinic acid on the betalain- $\text{Eu}^{3+}$ complex	177
Figure 7.5. Effect of chelating compounds on the betalain-metal complexes	178
Figure 7.6. Effects of $\text{Eu}^{3+}$ on tailor-made betalains synthesized to explore the role of sulfinyl functional group (SO), the sulphur heteroatom, and the additional carboxylic group in the complexation of $\text{Eu}^{3+}$ by miraxanthin I	181
Figure 7.7. Spores from <i>Bacillus</i>	183
Figure 7.8. Characteristics of dipicolinic acid	185
Figure 7.9. Effect of the addition of albumin, glucose, and glucosamine as models of proteins, hexoses and hexosamines in interference assays to the complex $\text{Eu}^{3+}$ -miraxanthin I	186
Table 7.1. Variations in the maximum wavelengths ( $\lambda$ ) produced by the complexation of $\text{Eu}^{3+}$ with betalains	171
Table 7.2. Values of the association constants for the complexes with $\text{Cu}^{2+}$ and $\text{Eu}^{3+}$ for the different betalains studied	174
	175

Table 7.3. Variations in the maximum wavelengths ( $\lambda$ ) produced by the complexation of copper with the betalains under study	179
Table 7.4. Detection (LOD) and quantification (LOQ) limits of dipicolinic acid obtained for the four betalains studied in absorbance and fluorescence	184
Table 7.5. Detection limits (LOD) obtained for <i>Bacillus spores</i> according to the betalain and the measurement method used	

## **Chapter VIII.**

Figure 8.1. HPLC analysis of the supernatants of <i>E. coli</i> (pET28a-GdDODA) cultures supplemented with chitin or chitosan	194
Figure 8.2. Absorbance spectrum of the new polymer derived from chitosan	195
Figure 8.3. Fluorescence of the polymeric chitosan-betaxanthin	197
Figure 8.4. Chromatograms at $\lambda = 480$ nm for the supernatants of the biofactories with <i>E. coli</i> (pET28a-GdDODA) supplemented with glucosamine and galactosamine	199
Figure 8.5. Betaxanthins obtained in this study	200
Figure 8.6. Spectrophotometric properties of the new sugar-derived betaxanthins	201
Table 8.1. Color analysis (CIELAB parameters) of chitosan particles and the novel chitosan-betaxanthin polymer	196

## **Chapter IX.**

Figure 9.1. The lifespan machine	208
Figure 9.2. Temperature evolution inside the scanners placed into the lifespan machine incubator	209
Figure 9.3. Preparation of plates for the lifespan machine	211
Figure 9.4. Mask design for the analysis of plates in the lifespan machine	213
Figure 9.5. Screenshot of a mask uploaded to worm browser to confirm the location of the analysis to be realized	214
Figure 9.6. Screenshot of the storyboard in the software worm browser	215

**Chapter X.**

Figure 10.1. Schematic representation of the slide device	223
---	-----

**Chapter XI.**

Figure 11.1. Structures of betalains used in this study	227
Figure 11.2. Antioxidant effect of betalains <i>in vivo</i>	229
Figure 11.3. Mean lifespan of <i>C. elegans</i> wild-type strain N2 sterilized by FUdR or sterilized by feed with RNAi	230
Figure 11.4. Survival plots for <i>C. elegans</i> wild-type sterilized with FUdR and pre-treated with pure betalains	231
Figure 11.5. Survival plots for <i>C. elegans</i> wild-type sterilized by feed with RNAi ( <i>E. coli</i> HT115) and pre-treated with pure betalains	232
Figure 11.6. <i>C. elegans</i> wild-type strain N2 after seven days of treatment with phenylethylamine-betaxanthin	234
Figure 11.7. Quantification of phenylethylamine-betaxanthin and indoline-betacyanin accumulated in worm's soma expressed in $\mu$ moles betalain/g protein	235
Figure 11.8. Lifespan of <i>C. elegans</i> wild type strain N2 treated with <i>Opuntia</i> extracts	236
Table 11.1. Effect of pure betalains in mean and maximum lifespan of <i>C. elegans</i> wild type strain N2 sterilized with FUdR	238
Table 11.2. Effect of pure betalains in mean and maximum lifespan of <i>C. elegans</i> wild type strain N2 sterilized by feed with RNAi ( <i>E. coli</i> HT115)	239
Table 11.3. Effect of <i>Opuntia</i> extracts in mean and maximum lifespan of <i>C. elegans</i> wild type strain N2	240
Video 11.1. <i>C. elegans</i> sterility	233

**Chapter XII.**

Figure 12.1. Chemical structures and purity analysis by HPLC for the individual betalains considered in this study	248
Figure. 12.2. Antioxidant activity of betalains measured with three different <i>in vitro</i> methods (ABTS, FRAP and ORAC)	250

Figure 12.3. Comparative analysis of antioxidant and free radical scavenging capacities of betalains by three different <i>in vitro</i> methods	251
Figure 12.4. Antioxidant effect of betalains <i>in vivo</i>	253
Figure 12.5. Calculation of the effective dose 50 (ED <sub>50</sub> ) in <i>C. elegans</i> TJ375 of the most effective betalains	254
Figure 12.6. Comparative analysis of the antioxidant capacity of betalains <i>in vivo</i> vs. <i>in vitro</i> by ABTS assay	255
Figure 12.7. Dose-dependent increased longevity effect obtained by the treatment with different concentrations of betalains	256
Figure 12.8. Effect of the different individual betalains on the lifespan of wild-type <i>C. elegans</i>	257
Figure 12.9. Comparative effect of the antioxidant capacity of betalains <i>in vivo</i> vs. longevity assays in <i>C. elegans</i>	258
Figure 12.10. Cross data of the results obtained in the antioxidant assays <i>in vitro</i> and <i>in vivo</i> and the results of the longevity experiments	259
Figure 12.11. Biological confirmation of betalains activity in the longevity pathway and in the redox active pathway using <i>C. elegans</i> mutants	265
Figure 12.12. Dopaxanthin accumulation in wild type <i>C. elegans</i>	267
Figure 12.13. Heat map showing the most differentially expressed genes in the microarrays between the groups of samples respect to the non-treatment group	268
Table 12.1. Summary of lifespan assays results for the <i>C. elegans</i> treated with betalains	270
<b>Chapter XIII.</b>	
Figure 13.1. Chemical structures of the flavonoids used in this chapter	278
Figure 13.2. Flavonoids effect on <i>C. elegans</i> strain TJ375 ( <i>hsp-16.2p::GFP</i> ) model of oxidative stress resistance	279
Figure 13.3. Effect of flavonoids on fat accumulation in <i>C. elegans</i> measured with Oil Red O (ORO)	280
Figure 13.4. Mean lifespan of wild-type <i>C. elegans</i> treated with different doses of flavonoids (0, 10, 25, 50, 100 $\mu$ M) mean lifespan	282

Figure 13.5. Biological confirmation of flavonoids activity in the insulin signaling pathway using <i>C. elegans</i> mutants	284
Figure 13.6. Effect of the different flavonoids on the redox active pathway	286
Figure 13.7. Principal component analysis (PCA) of <i>C. elegans</i> pathways altered by baicalein treatment (100 $\mu$ M) vs control worms treated with DMSO	290
Table 13.1. Survival data for the <i>C. elegans</i> treated with flavonoids	292
Table 13.2. Pathways modulated by baicalein treatment	294
 <b>Chapter XIV.</b>	
Figure 14.1. Chemical structures for the artificial food dyes (AFDs) employed in this chapter	304
Figure 14.2. Mean lifespan changes of <i>C. elegans</i> wild-type strain obtained after an acute exposure to individual AFDs	306
Figure 14.3. Lifespan curves of <i>C. elegans</i> wild-type strain obtained after an acute exposure to individual AFDs	307
Figure 14.4. Mean lifespan changes of <i>C. elegans</i> wild-type strain obtained after chronical exposure to different concentrations of individual AFDs	308
Figure 14.5. Accumulation of lipofuscin in 4-days old worms	309
Figure 14.6. Expression of HSPs measured through the fluorescence emitted in the pharynx of <i>C. elegans</i> TJ375 ( <i>hsp-16.2::GFP</i> ) strain	311
Figure 14.7. Fluorescence emitted by the dopamine receptor <i>dat-1</i> expressed in dopaminergic neurons of <i>C. elegans</i> BZ555 ( <i>dat-1p::GFP</i> ) strain	312
Figure 14.8. Changes in motility parameters of <i>C. elegans</i> wild-type after exposure to individual AFDs	313
Figure 14.9. Principal component analysis (PCA) of <i>C. elegans</i> pathways altered by ponceau 4R or tartrazine treatment (100 $\mu$ M) vs untreated control worms	319
Table 14.1. Lifespan results and statistical analysis for <i>C. elegans</i> after acute exposure to different concentration of food colorants	323
Table 14.2. Lifespan results and statistical analysis for <i>C. elegans</i> after chronical exposure to different concentration of food colorants	324





## Resumen

La biosíntesis de los pigmentos antioxidantes betaláinas siempre se ha considerado exclusiva de las plantas del orden Caryophyllales. Estas plantas presentan partes coloreadas debido a la presencia de betaláinas, pudiendo encontrar partes amarillas debido a la presencia de betaxantinas, partes violetas por la presencia de betacianinas o partes anaranjadas o rosadas debido a diferentes combinaciones de ambos pigmentos. Sin embargo, esta tesis doctoral cambia este paradigma, ya que la búsqueda de enzimas procedentes de huéspedes bacterianos promovió el descubrimiento de cultivos procariotas que producen betaláinas. Así, el espectro de posibles fuentes de los pigmentos betaláinas en la naturaleza se amplía con la descripción de la primera bacteria formadora de betaláinas, *Gluconacetobacter diazotrophicus*. El paso enzimático clave en la biosíntesis de betaláinas es la rotura del anillo aromático del aminoácido precursor L-dihidroxifenilalanina (L-DOPA) mediante la enzima 4,5-extradiol-dioxigenasa (4,5-DODA) para formar ácido betalámico, la unidad estructural que comparten todas las betaláinas (betaxantinas y betacianinas). El análisis molecular y funcional realizado en esta tesis doctoral condujo a la caracterización de una nueva dioxigenasa, un polipéptido de 17,8 kDa con una  $K_m$  de 1,36 mM, con mayor actividad y afinidad que las dioxigenasas de origen vegetal previamente caracterizadas. Su actividad superior permitió por primera vez la caracterización experimental de los primeros pasos en la biosíntesis de betaláinas al caracterizar completamente la presencia y la evolución temporal de los intermedios 2,3- y 4,5-seco-DOPA. Además, las reacciones químicas espontáneas se caracterizaron dando lugar a la descripción del “mecanismo enzimático-químico” completo que produce los pigmentos finales. En relación con la enzima DODA descrita en *G. diazotrophicus*, también se detectó por primera vez una enzima 4,5-DODA en la cianobacteria *Anabaena cylindrica*. Esta enzima es un polipéptido de 17,8 kDa con una  $K_m$  de 53 M. A pesar de que esta enzima presenta una afinidad más baja que la enzima de *Gluconacetobacter diazotrophicus*, también es capaz de producir la apertura del anillo aromático de L-DOPA, produciendo betaláinas tanto en su huésped natural como en su expresión heteróloga en cultivos de *Escherichia coli*. Estos hallazgos demuestran que la biosíntesis de betaláinas no está restringida a plantas del orden Caryophyllales, sino que puede expandirse a los procariotas.

El gran interés que se ha demostrado en las últimas décadas por las betaláinas reside en sus propiedades antioxidantes, antitumorales y antiinflamatorias. Sin embargo,

estas propiedades se han analizado principalmente a través de extractos de plantas con poca o nula purificación ya que su obtención y purificación a partir de material vegetal es un proceso muy laborioso. Esta extracción depende, además, de la estacionalidad de la disponibilidad de estructuras coloreadas como frutos o flores en las fuentes vegetales y de las variables ambientales que afectan a su producción. Estos inconvenientes han llevado a la búsqueda de nuevos enfoques para su obtención de una manera más eficiente. La clonación de la nueva y activa enzima 4,5-DOPA-extradiol dioxigenasa de *Gluconacetobacter diazotrophicus* en un vector de expresión, y su posterior expresión heteróloga en cultivos de *Escherichia coli* han permitido la puesta en marcha de un sistema de producción biotecnológico de pigmentos individuales. En la búsqueda de las condiciones óptimas para la producción de ácido betalámico y pigmentos derivados en biofactorías, se obtuvieron cuatro betaxantinas diferentes y dos betacianinas. El escalado de esta nueva técnica a biorreactores de hasta 2 litros para la obtención y purificación de betalaínas mejoró los rendimientos de las metodologías anteriores alcanzando cantidades de hasta 150 mg de compuestos puros.

Este incremento en la cantidad de betalaínas obtenidas gracias al nuevo enfoque biotecnológico ha permitido profundizar en las propiedades físico-químicas de estos pigmentos. Así, se ha podido estudiar el efecto de los metales, como el cobre y el europio, sobre las propiedades espectroscópicas de las betalaínas. Por primera vez se considera la reversibilidad de los cambios espectrales en fluorescencia y absorbancia después de la adición de sustancias quelantes. Estos resultados explican la pérdida de coloración que experimentan las betalaínas cuando son expuestas a la presencia de metales. La reversibilidad de los complejos betalaína-metal se caracterizó en presencia de esporas de *Bacillus* que provocaron la recuperación de la fluorescencia propia de las betalaínas debido a la interacción de los complejos con el ácido dipicolínico presente en las mismas. El ácido dipicolínico, componente principal y característico de las endosporas, presenta una alta afinidad por el metal europio, al que quelata, y es capaz de desplazar a la betalaína que forma parte del complejo. Así, la betalaína liberada recupera sus propiedades espectroscópicas. Este método rápido y económico permite la detección de esporas por debajo de la dosis infecciosa para el ántrax mediante el uso de un pigmento floral presente en *Mirabilis jalapa*.

La novedosa obtención biotecnológica de betalaínas desarrollada en esta tesis doctoral también ha permitido la obtención de nuevas betalaínas hasta ahora desconocidas. Estas nuevas betalaínas se han originado gracias a la condensación del

ácido betalámico, la unidad estructural de las betalainas, con grupos amina de diferentes compuestos. La obtención y caracterización de quitosano-betaxantina en este estudio ha permitido describirla como la primera betaxantina polimérica fluorescente que podría combinar las propiedades fluorescentes de las betalainas y las propiedades del quitosano, un polímero de azúcar ampliamente utilizado con fines médicos. Además, glucosamina, la unidad estructural del quitosano, y su estereoisómero galactosamina pudieron condensarse con ácido betalámico y producir nuevas moléculas con propiedades espectrofotométricas similares a las betaxantinas presentes en la naturaleza, convirtiéndose en las primeras betaxantinas derivadas de azúcares descritas.

La nueva obtención biotecnológica de betalainas ha abierto la posibilidad de analizar el efecto que tiene cada pigmento individual como compuesto bioactivo, ya que anteriormente el estudio de la bioactividad de betalainas individuales se ha visto obstaculizado por su difícil obtención y purificación. En esta tesis doctoral, estas propiedades se analizan empleando *Caenorhabditis elegans*, un pequeño nemátodo ampliamente utilizado como modelo animal debido a su rápido ciclo de vida y a su fácil mantenimiento en el laboratorio. Alrededor del 60-80% de los genes de *Caenorhabditis elegans* presentan genes ortólogos en el genoma humano, y el nematodo presenta un sistema digestivo completo, lo que beneficia su uso como modelo en alimentación. Además, su uso no presenta tantas implicaciones éticas como el trabajo con otros modelos animales, como ratones o ratas, cuyo uso en experimentación se ve reducido.

Los efectos de la administración de betalainas en *Caenorhabditis elegans* se han analizado mediante el uso de diferentes cepas mutantes y mediante el efecto que tienen las betalainas en el tiempo de vida de la cepa silvestre. El tiempo de vida de *C. elegans* es un parámetro ampliamente utilizado para describir el efecto de diferentes moléculas en el envejecimiento de este modelo animal. Con este propósito, se construyó una plataforma automática para el análisis de la vida del nematodo. Esta plataforma se basa en la máquina "Lifespan Machine" desarrollada en la Universidad de Harvard. La máquina está compuesta por escáneres que analizan el movimiento de los gusanos durante varios días, estableciendo el tiempo exacto de la muerte de cada espécimen. Esta nueva plataforma automática incorpora diferentes modificaciones respecto de la máquina original, mejorando la uniformidad de los resultados obtenidos y reduciendo el número de gusanos empleados gracias a que no existe pérdida de placas por contaminación y/o desecación como sí ha sido descrito para la máquina original. Gracias al desarrollo de esta máquina se pueden analizar alrededor de 8.000 gusanos de manera simultánea para establecer el

tiempo de vida de cada uno de ellos individualmente. Ello permite obtener resultados homogéneos que no dependen de la destreza del investigador en el conteo manual de gusanos.

La naturaleza antioxidante de cuatro betalaínas modelo se analizó en un ensayo preliminar utilizando el organismo modelo *Caenorhabditis elegans*. El estrés oxidativo causado en la cepa fluorescente TJ375 (*hsp-16.2::GFP*) se revirtió por la presencia de betalaínas tanto naturales como semisintéticas, con un valor ED<sub>50</sub> de alrededor de 25  $\mu$ M para betacianinas y hasta 10  $\mu$ M para betaxantinas, siendo indicaxantina, el pigmento principal en los frutos de *Opuntia*, la betalaína más eficaz. El efecto de estas betalaínas modelo sobre la vida útil de la cepa silvestre N2 se estudió cuidadosamente utilizando la plataforma automática desarrollada. En una búsqueda de diferentes enfoques para suprimir la progenie, se usó ARN de interferencia (ARNi) para bloquear la expresión del gen *pop-1* y así prescindir del uso de FUDR, una molécula ampliamente utilizada para evitar descendientes pero que podría afectar al tiempo de vida en algunos casos. La presencia de betalaínas en el medio, tanto como compuestos puros como en extractos de *Opuntia*, aumentó significativamente la vida útil de *C. elegans*. Además, las propiedades fluorescentes de las betaxantinas permitieron su visualización en el tracto digestivo de los gusanos, lo que confirma que las betalaínas son incorporadas mediante su ingesta.

Una vez que se caracterizaron los efectos positivos de las cuatro betalaínas modelo en el tiempo de vida de *C. elegans*, se probaron *in vivo* betalaínas puras adicionales para profundizar en su modo de acción. Entre las diecisiete betalaínas analizadas, tres betaxantinas, denominadas indicaxantina, fenilalanina-betaxantina y dopaxantina, y la betacianina indolina ácido carboxílico-betacianina mostraron una extraordinaria capacidad antioxidante *in vivo* contra el estrés oxidativo causado en la cepa fluorescente TJ375 (*hsp-16.2::GFP*). Además, estas betalaínas también mostraron ser las más eficaces contra el envejecimiento, ya que aumentaron el tiempo de vida de los gusanos hasta un 20,5%. Los efectos de las betalaínas puras en la expresión génica se han analizado por primera vez gracias a la extracción de ARN de gusanos alimentados con pigmentos individuales y al análisis mediante microarrays de la expresión. Los estudios realizados con betalaínas y la confirmación biológica con diferentes cepas mutantes mostraron que la extensión del tiempo de vida es el resultado de una reducción del estrés oxidativo combinado con la activación de diferentes factores de transcripción. Las betalaínas modulan los genes *daf-16* o *skn-1* involucrados en la longevidad y en las vías de resistencia al estrés oxidativo. Estos genes codifican factores de transcripción ortólogos

a FOXO y Nrf2 en humanos, respectivamente. En ambas especies estos genes conducen a la sobreexpresión de los genes *hsp* que codifican proteínas HSP involucradas en la resistencia al cáncer y al Alzheimer. Por tanto, los resultados obtenidos pueden abrir nuevas líneas de investigación en la búsqueda de tratamientos efectivos basados en estas moléculas de origen vegetal.

En este contexto, los flavonoides también son compuestos nutraceuticos obtenidos de plantas que han despertado un gran interés. Los flavonoides están presentes en alimentos consumidos a diario como el té, el cacao, las nueces y también están disponibles comercialmente como suplementos alimenticios. Son una de las familias más grandes de compuestos vegetales, con alrededor de 8.000 estructuras descritas, con muchas de ellas descritas como compuestos que promueven la salud y como prometedores fármacos para diferentes enfermedades como enfermedades neurológicas e inflamatorias, diabetes o cáncer. Sin embargo, se deben realizar estudios toxicológicos y mecanicistas para caracterizar los verdaderos efectos biológicos y las potenciales dianas moleculares de estas moléculas. Así, en esta Tesis Doctoral, se describe el efecto de seis flavonoides estructuralmente relacionados como son baicaleína, crisina, scutellareína, 6-hidroxi flavona, 6,7-dihidroxi flavona y 7,8-dihidroxi flavona, sobre el tiempo de vida y la resistencia al estrés de *C. elegans*. Los resultados mostraron que baicaleína, crisina y 6-hidroxi flavona tienen un fuerte efecto anti envejecimiento que actúa de manera dosis-dependiente. Estos flavonoides son capaces de aumentar la vida media de los gusanos hasta un 18,6%, 13,3% y 20,0%, respectivamente. Además, se estudió el mecanismo molecular que subyace a este efecto de extensión del tiempo de vida utilizando cepas mutantes de *C. elegans* y realizando ensayos de microarrays a partir de la extracción de ARN de gusanos de la estirpe silvestre N2. Aunque los tres flavonoides efectivos están estructuralmente relacionados, los resultados mostraron que el efecto de cada molécula sobre la longevidad depende de diferentes vías de señalización (DAF-16/FOXO o SKN-1/Nrf2) y diferentes genes diana. Los resultados sugirieron que baicaleína y 6-hidroxi flavona dependen de la vía SKN-1/Nrf2, y que además baicaleína también puede regular negativamente genes importantes relacionados con la edad, como mTOR o PARP. Mientras que el efecto de crisina depende de la vía de señalización de la insulina y su factor de transcripción DAF-16/FOXO.

Ambas familias, betalainas y flavonoides, son ampliamente empleados como nutraceuticos gracias a su efecto promotor de la salud. Además, algunos de ellos se

emplean como colorantes alimentarios, como la betanina (betalaína) o las antocianinas (flavonoides). Sin embargo, el consumo de colorantes artificiales en alimentos y bebidas consumidos por la población en general ha aumentado en las últimas décadas a pesar de la preocupación planteada por estudios que han mostrado posibles efectos nocivos. Por ello, y aprovechando el potencial de análisis desarrollado en esta Tesis Doctoral, seis colorantes artificiales, como son tartrazina, amarillo anaranjado, amarillo de quinoleína, rojo cochinilla, carmoisina y rojo allura se han empleado como compuestos puros para explorar sus efectos *in vivo* en el modelo animal *C. elegans*. La administración de estos colorantes artificiales a *C. elegans* produjo daños relacionados con el envejecimiento prematuro, como son un aumento en el estrés oxidativo y la acumulación de lipofusina. Los gusanos experimentaron un fuerte acortamiento del tiempo de vida, alteraciones en los patrones de movimiento y alteraciones en la producción de receptores de dopamina. Además, el análisis de microarrays realizado con gusanos tratados con tartrazina y rojo cochinilla mostró cómo el consumo de colorantes sintéticos puede alterar la expresión de genes involucrados en la resistencia al estrés oxidativo y la neurodegeneración.

## Abstract

The biosynthesis of antioxidant pigments betalains was believed to be restricted to plants of the Caryophyllales. These plants have colored parts due to the presence of betalains, and we find yellow parts due to the presence of betaxanthins, violet parts due to the presence of betacyanins and orange-pink parts due to the combination of both pigments in different proportions. However, this thesis changes this paradigm, and enzyme mining from bacterial hosts promoted the discovery of bacterial cultures producing betalains. The spectrum of possible sources of betalain pigments in nature is broadened by the description of the first betalain-forming bacterium, *Gluconacetobacter diazotrophicus*. The enzyme-specific step in the biosynthesis of betalains is the extradiol cleavage of the precursor amino acid L-dihydroxyphenylalanine (L-DOPA) to form betalamic acid, the structural unit of all betalains (betaxanthins and betacyanins). Molecular and functional work led to the characterization of a novel dioxygenase, a polypeptide of 17.8 kDa with a  $K_m$  of 1.36 mM, with higher activity and affinity than those found in plants. Its superior activity allowed the first experimental characterization of the early steps in the biosynthesis of betalains by fully characterizing the presence and time evolution of 2,3- and 4,5- seco-DOPA intermediates. Furthermore, spontaneous chemical reactions are characterized and incorporated into a comprehensive enzymatic-chemical mechanism that yields the final pigments. Related to the DODA enzyme described in *G. diazotrophicus*, a 4,5-DODA enzyme was also detected for the first time in the cyanobacterium *Anabaena cylindrica*. This enzyme is a polypeptide of 17.8 kDa with a  $K_m$  of 53 M. Although it presents a lower affinity than the enzyme from *Gluconacetobacter diazotrophicus*, it is also able to produce the extradiol cleavage of L-DOPA, yielding betalains both in its natural host and after its heterologous expression in *Escherichia coli* cultures. These findings demonstrate that betalain biosynthesis is not restricted to plants of the order Caryophyllales but should be considered also in the prokaryotes.

The interest in betalains resides in their well-known antioxidant, antitumoral and anti-inflammatory properties. However, these properties have been mainly analyzed through the use of plant extracts. In addition, obtaining and purifying them from whole plants depend directly on availability throughout the year and on environmental variables that affect their production. The search for new approaches to obtain them has led to the development of a new reliable and scalable process. The cloning of the novel and efficient



enzyme 4,5-DOPA-extradiol dioxygenase from *Gluconacetobacter diazotrophicus* in an expression vector, and the subsequent heterologous expression in *Escherichia coli* cultures has led to the start-up of a biotechnological production system of individual pigments. In the search for the optimal conditions for the production of betalamic acid in microbial factories and the scaled-up obtention of the derived pigments, four different betaxanthins and two betacyanins were obtained. The scaled-up obtention and purification of betalains improved the yields of the previous methodologies, reaching quantities of up to 150 mg of pure compounds.

The higher amounts of betalains obtained by the novel biotechnological approach afforded a deeper study of the physical-chemical properties of these pigments. Thus, the effect of metals, such as copper and europium, on the spectroscopic properties of betalains was studied. For the first time, the reversibility of spectral changes in fluorescence and absorbance is considered after the addition of chelating substances. These results explain the general bleaching of betalains by metals. The reversibility of the betalain-metal complexes is applied to the fluorescent detection of the presence of spores from *Bacillus* by the interaction of the complexes with the chelator dipicolinic acid, which is the main and characteristic component of endospores. This fast, economic method enables the detection of spores below the infective dose for anthrax by using a flower pigment present in *Mirabilis jalapa*.

This novel biotechnological obtention of betalains has also led to the obtention of novel, unknown betalains through the condensation of betalamic acid, their structural unit, with amine groups of different compounds. This Thesis describes the obtention and characterization of chitosan-betaxanthin, the first fluorescent polymeric betaxanthin which might combine the fluorescent properties of betalains and the properties of chitosan, a sugar polymer widely used with medical purposes. In addition, glucosamine, the structural unit of chitosan, and its stereoisomer galactosamine were able to condense with betalamic acid and to produce novel molecules with spectrophotometric properties similar to betaxanthins present in nature, and are the first sugar-derived betaxanthins ever described.

Betalain-rich extracts have been used for many years but the study of their bioactivities has always been hampered by their difficult obtention. Thanks to the novel, fast biotechnological obtention of betalains, the analysis of the properties of each betalain as bioactive compounds is now possible. In this Thesis, these properties were analyzed using *Caenorhabditis elegans*, a small nematode widely used as animal model due to its

fast, simple life cycle and its easy maintenance in the laboratory. In addition, around 60-80% genes of *Caenorhabditis elegans* present orthologous genes in the human genome and its use does not present as many ethical implications as other animal models, such as mice or rats, whose use can thus be reduced.

The effects of betalains' administration in *Caenorhabditis elegans* have been analyzed by using different mutant strains as well as the effect in the lifespan of the wild-type strain. Lifespan of *C. elegans* is a parameter widely used to describe the effect of different molecules in the aging of this animal model. With this purpose, an automatic platform for the lifespan analysis was built. This platform is based on the "Lifespan Machine" developed at the University of Harvard. The machine is composed of scanners that analyze the movement of the worms over several days and establish the exact time of death of each specimen. This new automatic platform incorporates different modifications with respect to the original one by improving the uniformity of the results obtained and reducing the number of worms used, because there was no loss of plates due to contamination and/or drying, which has been described for the original machine. Thanks to the development of this machine, around 8,000 worms can be analyzed at the same time to establish the lifespan of each one and it also offers homogeneous results which do not depend on the skills of the researcher in the manual count of worms.

Thus, the antioxidant nature of four model betalains was studied in a preliminary assay using the model organism *Caenorhabditis elegans*. The oxidative stress caused in the fluorescent strain TJ375 (*hsp-16.2::GFP*) was reversed by the presence of both natural and semi-synthetic betalains, with ED<sub>50</sub> values around 25  $\mu$ M for betacyanins and up to 10  $\mu$ M for betaxanthins, with indicaxanthin, the major pigment in prickly pear fruits, as the most effective betalain. The effect of model betalains on the lifespan of the wild type N2 strain was carefully studied using the automatic platform "Lifespan Machine". In a search for different approaches to suppress progeny, *pop-1* ARNi was used to avoid the use of FUdR, a molecule widely used to prevent descendants which could affect the life expectancy. The presence of betalains in the medium, both as pure compounds and as enriched *Opuntia* extracts, significantly increased the lifespan of *C. elegans*. In addition, the fluorescent properties of betaxanthins facilitate their visualization in the digestive tract, so confirming betalain intake by the worms.

After highlighting the positive effects of the four model betalains in the lifespan of *C. elegans*, additional pure betalains were tested *in vivo* to explore their mode of action in *C. elegans*. Among the seventeen betalains assayed, three betaxanthins - indicaxanthin,

phenylalanine-betaxanthin and dopaxanthin - and the betacyanin indoline carboxylic acid-betacyanin showed extraordinary behavior as *in vivo* antioxidants against the oxidative stress caused in the fluorescent strain TJ375 (*hsp-16.2::GFP*). In addition, they were the most promising betalains against aging, increasing the lifespan of worms up to 20.5%. The effects of the pure betalains in the gene expression have been analyzed for the first time thanks to RNA extraction from worms fed with individual betalains and microarray analysis. The first microarrays performed with betalains and the biological confirmation with different mutant strains showed that this life extension is a result of a reduction of oxidative stress combined with the activation of different transcription factors. Betalains modulate *daf-16* or *skn-1* genes involved in longevity and oxidative stress resistance pathways. They are orthologous of the human FOXO and Nrf2 gene, respectively. These genes, both in humans and worms, lead to overexpression of HSPs genes. The HSPs are involved in resistance to cancer and Alzheimer's disease, and thus, the results obtained may open novel research lines in the search for effective plant-based treatments.

Among these plant-based treatments, flavonoids are also potential nutraceutical compounds. They are present in daily-consumed foods like tea, cocoa, nuts or fruits and they are also commercially available as food supplements. They are one of the largest families of plant compounds, with around 8,000 structures described, and are considered health-promoting compounds and promising drugs for various diseases like neurological and inflammatory diseases, diabetes or cancer. However, toxicological and mechanistic studies must be performed to assess their biological effects and to identify the molecular targets of these molecules.

This Thesis describes the effects of six structurally related flavonoids - namely baicalein, chrysin, scutellarein, 6-hydroxyflavone, 6,7-dihydroxyflavone and 7,8-dihydroxyflavone - on *C. elegans* lifespan and stress resistance. The results showed that baicalein, chrysin and 6-hydroxyflavone have a strong anti-aging effect which acts in a dose-dependent manner. They are able to increase the mean lifespan of the worms up to 18.6%, 13.3% and 20.0%, respectively. In addition, the molecular mechanism underlying this lifespan extension was studied using mutant *C. elegans* strains and RNA microarray assays. Although the three effective flavonoids are structurally related, the results showed that the longevity effect of each molecule is dependent on different signaling pathways (DAF-16/FOXO or SKN-1/Nrf2) and possess different target genes. The results suggested that baicalein and 6-hydroxyflavone are dependent of the SKN-1/Nrf2

pathway, while baicalein may also downregulate important age-related genes such as mTOR or PARP. Elsewhere, chrysin effects are dependent of the insulin signaling pathway and its transcription factor DAF-16/FOXO.

Both families, betalains and flavonoids are widely used as nutraceutical compounds thanks to their health-promoting effects. In addition, some of them are employed as food colorants, such as betanin (betalain) or anthocyanins (flavonoids). However, the consumption of artificial colorants in foods and beverages has increased despite concerns in the general population raised by studies that have shown possible injurious effects. Six artificial food dyes (AFDs), tartrazine, sunset yellow, quinoline yellow, ponceau 4R, carmoisine and allura red, were employed here as pure compounds to explore their effects *in vivo* in the animal model *Caenorhabditis elegans*. The administration of these artificial dyes to *C. elegans* produced damage related to aging, such as oxidative stress and lipofuscin accumulation, as well as a strong shortening of lifespan, alterations in movement patterns and alterations in the production of dopamine receptors. Besides, microarray analysis performed with worms treated with tartrazine and ponceau 4R showed how the consumption of synthetic food colorants is able to alter the expression of genes involved in resistance to oxidative stress and neurodegeneration.



## **Chapter I. Introduction**

Part of this chapter was published in Trends in Plant Science  
Guerrero-Rubio et al. (2020) <https://doi.org/10.1016/j.tplants.2019.11.001>



## 1. Betalains

Betalains are bioactive compounds with a promising food and pharmacological potential. However, the biotechnological tools for their production are very limited and studies on their bioactivities are mainly limited to plant extracts with little or no purification.

### 1.1. General characteristics of betalains

Betalains are hydrophilic nitrogenous pigments which are characteristic of plants belonging to the order Caryophyllales. These pigments are divided into the yellow betaxanthins and the violet betacyanins (Gandía-Herrero and García-Carmona, 2013). The presence of both types of pigments is required for the orange and red colors which coexist in nature with the pure yellow and violet shades. Numerous studies were performed on the color properties of betalains since they were described as a novel family of pigments different to “nitrogenous anthocyanins” (Piattelli et al., 1964; Wyler and Dreiding, 1957). However, both families of pigments are water-soluble but mutually exclusive (Brockington et al., 2015; Timoneda et al., 2019). This phenomenon is still an evolutionary paradigm since plants from the families Molluginaceae, Kewaceae, Limeaceae, Macarthuriaceae and Simmondsiaceae, belonging to order Caryophyllales (Clement and Mabry, 1996; Thulin et al., 2016), are exceptions and they produce anthocyanins instead of betalains (Steglich and Strack, 1990). Besides, betalains have also been detected in some Basidiomycetes fungi such as *Hygrocybe conica* (Von-Ardenne et al., 1974) and *Amanita muscaria* (Musso, 1979).

Among plants of the order Caryophyllales, edible red beet roots (*Beta vulgaris*) and the fruits of cacti belonging to the genus *Opuntia* are the best-known sources of betalains, with betanin and indicaxanthin being, respectively, their main pigments (Felker et al., 2008; Hempel and Böhm, 1997). Recent research has described the betalain content of novel sources, such as the tubers from *Ullucus tuberosus* (Svenson et al., 2008) or the betalain-containing berries of *Rivina humilis* (Khan et al., 2012). The multiple shades of quinoa grains (*Chenopodium quinoa*) have also recently been reported to be based on betacyanins and betaxanthins (Escribano et al., 2017).

But the presence of betalains is not restricted to edible parts of plants, they are also present in flowers, such as in *Mirabilis* (Piattelli et al., 1965a) or *Portulaca* (Gandía-Herrero et al., 2005a), or in bracts (*Boungainvillea*) (Heuer et al., 1994).



## **1.2. Biosynthetic pathway of betalains**

Betalains are secondary metabolites derived from the amino acid L-tyrosine. Their biosynthesis is located in the cells' cytoplasm of mainly epidermal and subepidermal tissues. Then they are mobilized to the interior of vacuoles for their storage (Strack et al., 2003; Wink, 1997) as the final products betaxanthins or betacyanin, which provide yellow or violet coloration, respectively. Despite both groups share betalamic acid as structural unit, they are the result of the condensation of betalamic acid with different molecules yielding different betalains. When present in the same plant, they give rise to different shades between yellow and violet, depending on the percentage of betaxanthins and betacyanins (Kugler et al., 2004). The main steps for the synthesis of both types of betalains are described below.

### **1.2.1. Obtention of tyrosine**

The aromatic amino acid L-tyrosine is synthesized from prephenate, the final product of the shikimate pathway. In plants, prephenate is transaminated to arogenic acid which yields tyrosine due to the action of the enzyme arogenate dehydrogenase (ADH). Arogenate dehydrogenase is an oxidoreductase that is strongly regulated by the presence of tyrosine. Thus, this enzyme limits the obtention of tyrosine and, consequently, its derivatives. This is a preliminary step assumed for the beginning of the biosynthetic route of betalains and it is rarely included in the description of the pathway. However, Timoneda et al., (2018) described that plants of the order Caryophyllales present an isoform of ADH, ADH $\alpha$ , with a lower level of negative feedback by tyrosine which is involved in a 7-fold higher accumulation of betanin due to the higher obtention of tyrosine. L-tyrosine is, then, the starting molecule in the obtention of secondary metabolites as betalains (**Fig. 1.1**).

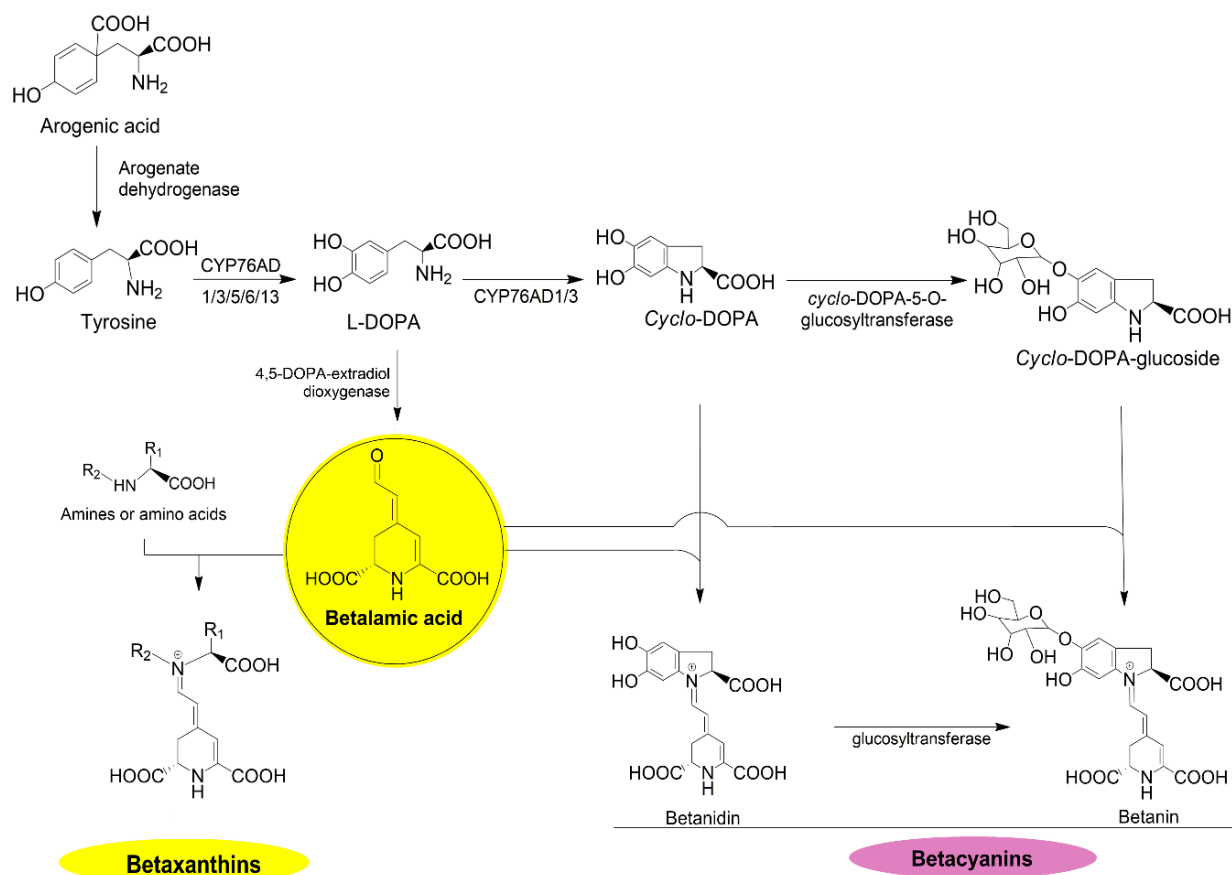


**Figure 1.1. General overview of the biosynthetic pathway of betalains.**

### 1.2.2. Tyrosine hydroxylation

The biosynthetic pathway of betalains *per se* begins with the 3-hydroxylation of L-tyrosine to produce L-3,4-dihydroxyphenylalanine (L-DOPA) thanks to the activity of cytochrome P450-type enzymes, the CYP76AD family. These enzymes have tyrosine hydroxylase activity and are responsible to the obtention of L-DOPA (**Fig. 1.1**). Recombinant expression of CYP76AD genes from *Beta vulgaris* showed that CYP76AD1 presents an additional oxidase activity which yields *cyclo*-DOPA from L-DOPA (DeLoache et al., 2015). However, recombinant expression of beet CYP76AD6 and CYP76AD5 genes are capable to produce L-DOPA from tyrosine but present a very low oxidase activity (Polturak et al., 2016; Sunnadeniya et al., 2016). A large-scale phylogenetic analysis of Caryophyllales plants suggested that CYP76AD1 and CYP76AD6/5 belong to separate clades within the CYP76AD family (Brockington et al., 2015). This analysis supports the dual activity of CYP76AD1 since it belongs to the CYP76AD1- $\alpha$  clade, while enzymes of the clade CYP76AD1- $\beta$ , as CYP76AD6 and

CYP76AD5, catalyze efficiently only L-DOPA formation. Similar results have been obtained for the recombinant expression of CYP76ADs from *Mirabilis jalapa*, where the hydroxylation of tyrosine to L-DOPA is produced by CYP76AD15 (Polturak et al., 2018) and CYP76AD3, while the oxidation of L-DOPA to *cyclo*-DOPA is only performed by CYP76AD3 (Suzuki et al., 2014). Besides, a homolog CYP76AD1 has recently been described in *Chenopodium quinoa* hypocotyls (Imamura et al., 2018). All these evidences contribute to the progress made in recent years for a better understanding of the initial steps of the biosynthetic pathway of betalains, where cytochrome P450-type enzymes have taken the role originally ascribed to tyrosinases (Gandía-Herrero et al., 2005b, 2004).

### 1.2.3. Obtention of the structural unit betalamic acid

The transformation of L-DOPA into betalamic acid is due to the activity of the enzyme DOPA-extradiol-dioxygenase (DODA) (**Fig. 1.1**). In plants, this enzyme is known as 4,5-DODA since it catalyzes the cleavage of the aromatic ring of L-DOPA between carbons in positions C<sub>4</sub>-C<sub>5</sub> (Fischer and Dreiding, 1972). This opening yields 4,5-seco-DOPA, an intermediate which by spontaneous cyclization gives rise to betalamic acid, the structural and chromophoric unit of betalains. However, in fungi, betalamic acid is produced by a DODA enzyme which presents a double activity. This enzyme is able to open the aromatic ring of L-DOPA between C<sub>4</sub>-C<sub>5</sub> positions, yielding betalamic acid, or between C<sub>2</sub>-C<sub>3</sub>, which produces 2,3-seco-DOPA. As 4,5-seco-DOPA, 2,3-seco-DOPA is an intermediate which rapidly undergoes a spontaneous intramolecular cyclization to produce muscaflavin. Muscaflavin is a final yellow pigment of this route and its biological significance is still unknown.

Preliminary cloning and expression of different DODAs showed their relationship with the formation of betalamic acid. First, the similar ability of DODA enzymes from plants and fungi to form betalamic acid was described by Mueller et al., (1997) when the enzyme described in *A. muscaria* was expressed in white petals of *Portulaca glandiflora*, producing yellow coloration due to the presence of betalains. Additionally, the characterization of a coding sequence for a DODA enzyme in *P. glandiflora* showed how its expression is limited to colored flower petals (Christinet et al., 2004). Heterologous expression in *E. coli* and purification of a DODA enzyme from *B. vulgaris* demonstrated the obtention of 4,5-seco-DOPA from L-DOPA in *E. coli* for

the first time (Gandía-Herrero and García-Carmona, 2012). The first purification of an enzyme of plant origin led to determining the DODA enzyme from *B. vulgaris* as a monomer of 32 kDa with a  $K_m = 6.9$  mM. A close homolog sequence of unknown function was detected in *E. coli*. The related-DODA protein YgiD is a monomer with a molecular mass of 32 kDa which catalyzes the transformation of L-DOPA to betalamic acid and muscaflavin (Gandía-Herrero and García-Carmona, 2014). Sequence analysis of those DODAs reveals a group of conserved amino acids close to the active site within the order Caryophyllales (Christinet et al., 2004). The presence of a related enzyme in *E. coli* could indicate that the formation of betalamic acid by 4,5-DOPA-extradiol-dioxygenase enzymes is not exclusive of Caryophyllales and fungi as *A. muscaria* and *Hygrocybe* but its obtention could be extended to prokaryotes.

There are no other enzymes involved in the biosynthesis of betaxanthins. They are imines obtained from the spontaneous reaction between betalamic acid and amino acids or amines by Schiff condensation. However, the production of betacyanins implies structural modifications by the action of additional enzymes, except for betanidin. Betanidin is the result of condensation between betalamic acid and the above-mentioned *cyclo*-DOPA which is derived from the oxidation of L-DOPA.

#### 1.2.4. Production of betacyanins

Betanidin-glucosyltransferases catalyze the incorporation of a molecule of glucose to betanidin. Two glucosyltransferases identified in *Dorotheanthus bellidiformis* showed the production of betanidin-derived betacyanins in a regiospecific manner through one of the two hydroxyl groups of the aromatic ring. Thus, the glucosylation in the 5-hydroxyl group of betanidin yields betanin (Vogt et al., 1999), whereas glucosylation in the 6-hydroxyl group gives rise to gomphrenin (Vogt, 2002).

Some species, such as *Mirabilis jalapa* (Sasaki et al., 2004), additionally present a specific *cyclo*-DOPA-5-*O*-glucosyltransferase (cDOPA5GT) which uses *cyclo*-DOPA as substrate to produce *cyclo*-DOPA-glucoside. In these plants, betanin is obtained by the condensation of betalamic acid with the *cyclo*-DOPA-glucoside. The heterologous expression of this cDOPA5GT facilitates the obtention of the stable betacyanin, betanin, and is widely employed to study the activity of the rest of enzymes involved in the betalains' route in *Saccharomyces cerevisiae* (Grewal et al., 2018) or in *Nicotiana benthamiana* (Timoneda et al., 2018).

Betacyanins can also be modified by acylation. Acyl modifications can be catalyzed by acyl-CoA-dependent acyltransferases belonging to the BAHD superfamily or by serine-carboxy-peptidase-like (SCPL) acyl-transferases (Tanaka et al., 2008). In relation to these enzymes, a recent comparative transcriptomics study identified an acyltransferase from *M. jalapa*, a hydroxycinnamate gluosyltransferase (MjHGCT) which expressed in *Nicotiana benthamiana* in conjunction with the main genes involved in the betalains' route, gives rise to the obtention of cinnamoylbetanin, coumaroyl-betanin, caffeoyl-betanin and feruloyl-betanin (Polturak et al., 2018).

### **1.3. Fluorescence properties**

#### **1.3.1. Initial discovery of fluorescence**

The discovery of fluorescence in betalains was linked to research on their biosynthetic pathway. The steps of the biosynthesis of betalains preliminarily established in the late 1960s proposed two main enzymes to build the structural units of the pigments, the enzyme 4,5-DOPA-extradiol-dyooxygenase (Fischer and Dreiding, 1972; Liebis et al., 1969) and the previous hydroxylation of tyrosine to L-DOPA by tyrosinase and further oxidation by the same enzyme to promote cyclization to *cyclo*-DOPA to form betacyanins. These preliminary experiments were performed mainly with radioactive labeled precursors and configured a simple biosynthetic pathway that was reviewed in the early 1980s in a work that established the accepted route at the time (Piattelli, 1981). The scheme derived was considered definitive until inconsistencies of the proposed reactions with the enzymatic-chemical mechanism of tyrosinase-catalyzed reactions were pointed out (Gandía-Herrero et al., 2005b, 2005a). The new biosynthetic net conversion considered betaxanthins not only as final products of a linear pathway but also as possible intermediates in the formation of other pigments. In this context, characterization of novel reactions in the biosynthetic pathway of betalains promoted the search for singular pigments in flowers of different plant species (Gandía-Herrero et al., 2005b) and the development of novel methods for their semi-synthesis and purification (Gandía-Herrero et al., 2006). As a result of those protocols, pure hydroxylated betalains were obtained to be used as substrates of the key enzymes. The resulting diluted pigment solutions needed to be concentrated and, due to the strongly hydrophilic nature of betalains, the technique used was freeze-drying. Upon freezing in liquid nitrogen, diluted aqueous solutions of betaxanthins exhibited a strong fluorescent

glow which was visible to the naked eye (**Fig. 1.2D**). Freezing a fluorescent solution causes an increase in the light emitted due to an increase in the quantum yield of fluorescence. This happens when molecules slow down their vibration, and energy loss from excited states finds a preferential relaxation through fluorescence. This serendipitous discovery provided the first evidence for the existence of fluorescence in betaxanthin solutions (Gandía-Herrero et al., 2005c, 2005a, 2005d). The previous 50 years of research on the betalain pigments (Piattelli et al., 1964; Stintzing and Carle, 2004) had not considered fluorescence.

After the initial surprise and awareness of the possible relevance of fluorescence in pigments naturally present in flowers, many efforts were made to ascertain pigment purity and to characterize multiple structures, of both betaxanthins and betacyanins, and to analyze plant extracts from different sources (Gandía-Herrero et al., 2010a, 2006, 2005a). In addition, a photographic filter system was used to visualize fluorescence and suppress the contribution of reflected light. Filters used for fluorescence photography were specially designed to enable green fluorescence detection, while suppressing UV excitation or emission (Gandía-Herrero et al., 2005a). Microscopic visualization of betaxanthins in plant tissues was technically easier because the recorded fluorescence spectra indicated a similar behavior to that obtained for the widely used green fluorescent protein (GFP) system, previously captured with standard microscopy filtercubes. *Mirabilis jalapa*, *Portulaca grandiflora*, *Lampranthus productus*, and *Carpobrotus acinaciformis* were described in the initial publications (Gandía-Herrero et al., 2005a, 2005d, 2005c) but many other single molecules (Gandía-Herrero et al., 2005e) and plant extracts were analyzed to support the novel phenomenon. This is the case for *Celosia argentea*, whose yellow inflorescences appear to glow under the blue light stimulation system developed, as shown in **Fig. 1.2A-B**. In this case, the fluorescence detected in the yellow flowers is mainly due to the presence of the pigments vulgaxanthin I and miraxanthin V. In all cases, the use of epifluorescence microscopes allows the structure of the flowers to be seen in detail (**Fig. 1.2C**).

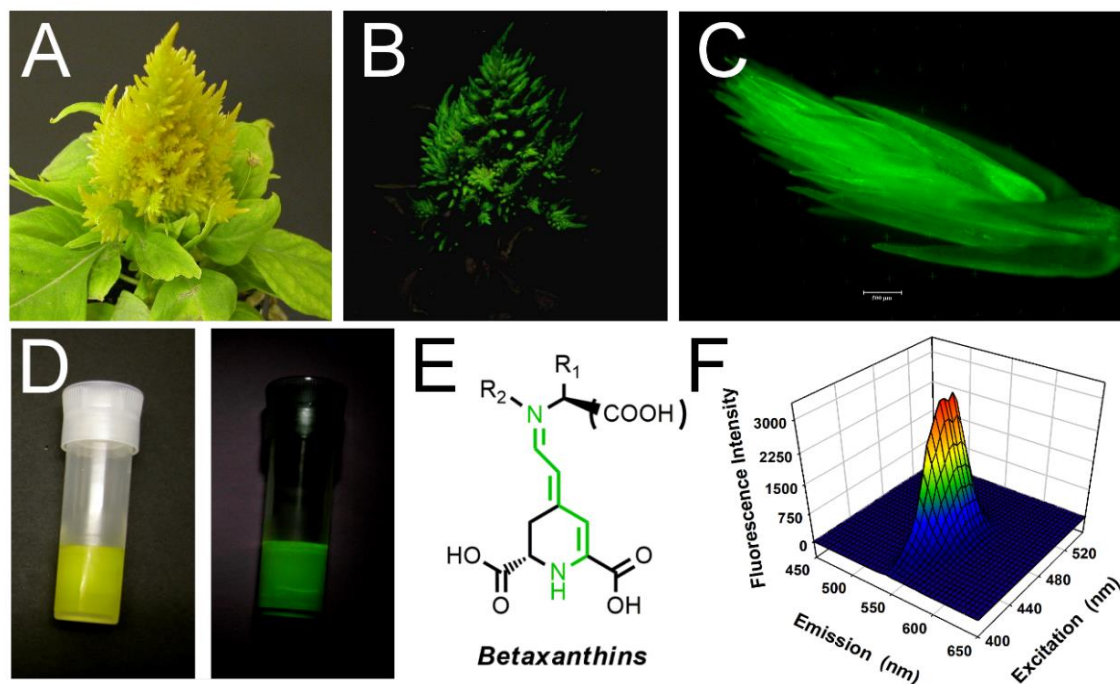


**Figure 1.2. Fluorescence of plant pigments betalains.** (A) Macroscopic image of the inflorescences of a yellow feather cockscomb, *C. argentea* var. *plumosa*, under white light. (B) The same yellow specimen visualized by fluorescence under blue light stimulation. (C) Close view of inflorescence under blue light in a microscope Leica DMRB with incident light beam using the filtercube I3 (excitation: 450-490 nm). (D) Tube containing a frozen solution of pure dopaxanthin under white light (left) and blue light stimulation (right). (E) General structures for betaxanthins indicating the electron resonance system responsible for fluorescence. (F) 3D-Fluorescence spectrum for the betaxanthin dopaxanthin in a 3  $\mu$ M solution in water at 25  $^{\circ}$ C.

Eventually, the biosynthetic pathway in plants turned out to be more complex than expected, with multiple possible branches in the scheme and with a new family of cytochrome P450 enzymes resolving the inconsistencies detected for tyrosinase as commented in section 1.2.2. (Gandía-Herrero and García-Carmona, 2013; Hatlestad et al., 2012). This was another surprise in recent betalain research, which relegated tyrosinase to a secondary role after promoting research in the biosynthetic pathway of the pigments and the discovery of fluorescence.

### 1.3.2. Structure-activity relationships

Systematic work has been performed with multiple betalains under the same conditions and has enabled the characterization of sub-structures that enhance or weaken the fluorescence described for the pigment's family. In this sense, it was initially reported that when electron density is withdrawn from the resonating system higher fluorescence can be expected. This is exemplified by the high fluorescence

exhibited in the pigment miraxanthin I, derived from methionine sulfoxide when compared with that corresponding to methionine-betaxanthin (Gandía-Herrero et al., 2005e). The betaxanthins vulgaxanthin I and vulgaxanthin II (Piattelli et al., 1965b), derived from the amino acids glutamine and glutamic acid respectively present the same situation, and the glutamic acid derived pigment presents higher fluorescence intensity due to the withdrawing effect of the carboxyl group. A similar effect was observed for semi-synthetic betalamic coumarins (Rodrigues et al., 2018). When an electron-donating methyl group was substituted from cBeet120 by an electron-withdrawing trifluoromethyl group at the C4 position of the coumarin moiety in cBeet151, the molecule became more fluorescent, with quantum yields of 0.021. The effect of electron density donating groups in betalain fluorescence is the opposite, and fluorescence intensity is reduced by the presence of hydroxyl groups (Gandía-Herrero et al., 2010a). The presence of the extra carboxylic group in dopaxanthin and tyrosine-betaxanthin (also called portulacaxanthin II) strengthens the fluorescence with respect to dopamine- and tyramine-betaxanthin (Gandía-Herrero et al., 2005e). In addition, other structural considerations should be taken into account and the effect of groups able to generate hydrogen bonds has been explored (Niziński et al., 2019). The existence of intramolecular hydrogen bonds may favor structurally constrained structures, as occurs in miraxanthin I. This reduces radiationless losses of energy and explains the high fluorescence quantum yield of this molecule (**Table 1.1**), described as the most fluorescent betaxanthin since the early description of the phenomenon (Gandía-Herrero et al., 2005e).

**Table 1.1. Quantum yield of fluorescence obtained for purified betalains.**

<b>Betalains</b>	<b><math>\Phi_F</math> in water</b>	<b><math>\Phi_F</math> in methanol</b>	<b><math>\Phi_F</math> in ethylene glycol</b>	<b>Refs.</b>
Betanin	0.0007	0.0013	0.0047	(Wendel et al., 2015a)
Indicaxanthin	0.0053	0.0081	0.033	(Wendel et al., 2015c)
Miraxanthin V	0.003	0.0047	0.015	(Nizinski et al., 2017)
Vulgaxanthin I	0.0073	0.011	0.039	(Wendel et al., 2015b)
Miraxanthin I	0.0084	---	---	(Niziński et al., 2019)



The study of structure-activity relationships in betalain fluorescence is also related to the effect of sub-structures on the absorbance of the molecules. Thus, the effect of carboxylic acid groups on the fluorescence of betalains supported existing information on the effect of this group on absorbance spectral properties. Betanin spectrum displays a maximum at 536 nm, but a hypsochromic shift occurs with the decarboxylation of the structure at C<sub>2</sub> (Kobayashi et al., 2001). A greater shift, in the same direction, occurs in the 14,15-dehydrobetanin compound (neobetainin), which is orange and not violet (Alard et al., 1985). The same effect is observed in betaxanthins absorbance, and a hypsochromic shift occurs with the decarboxylation of tyrosine-betaxanthin and dopaxanthin.

A linear relation can be found in the decrease of the Stokes shift (separation between excitation and emission spectra in fluorescence) with increasing excitation wavelengths (Gandía-Herrero et al., 2005a). In contrast to the highly fluorescent betaxanthins, their violet counterparts, betacyanins, are only weakly fluorescent. Fluorescence in this case is mainly detected in the presence of carboxylic groups and in the absence of hydroxyl ones. This enhances the fluorescence of the molecule, as occurs in the case of the indoline-derived betacyanin (Gandía-Herrero et al., 2010a). Betanidin and the glycosylated pigment betanin are only weakly fluorescent, with a very short excited state lifetime determined for betanin in 6.4 ps in water (Wendel et al., 2015a). Maximum excitation wavelengths in betacyanins occur between 521 nm and 529 nm, and emission spectra are centered around 570-575 nm.

Nowadays a wide variety of synthetic and natural betaxanthins have been obtained and their fluorescent properties have been characterized. All the pigments show similar behavior, with excitation maxima between 471 and 474 nm (blue color) and emission maxima between 548 and 551 nm (green color) (Gandía-Herrero et al., 2010a). Similarities in fluorescence characteristics point to the responsibility of betalamic acid in fluorescence (**Fig. 1.2E-F**). The nature of the amine or amino acid moiety has a limited contribution to the final spectral characteristics and there are no significant differences in relation to the chain length or its polarity.

### 1.3.3. Photophysics properties of betalains

When betalains are photoexcited, they undergo an excitation of their molecules, causing them to pass from the initial resting state S<sub>0</sub> to the excited state S<sub>1</sub>, according to

Jablonski's diagram (**Fig. 1.3**). This corresponds to the absorption measure obtained by means of UV-vis spectroscopy where a maximum absorption peak appears around  $\lambda_{\text{max}} = 475$  nm for betaxanthins and  $\lambda_{\text{max}} = 536$  nm for betacyanins (Gandía-Herrero et al., 2010a).

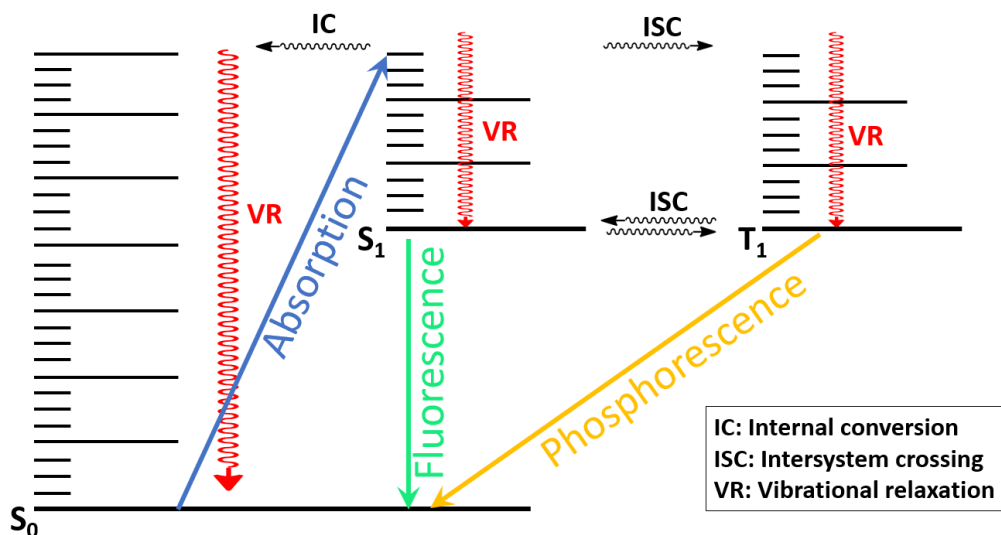


**Figure 1.3. Jablonski's diagram for the excitation and relaxation of absorbing molecules.** Betalains, after photoexcitation (absorption) experience relaxation by internal conversion (IC) or by light emission (fluorescence). Triplet  $T_1$  state (phosphorescence) has been described for betalains after the addition of potassium iodide (heavy-atom effect) and triplet sensitizers (Nizinski et al., 2017; Wendel et al., 2015c, 2015b, 2015a). IC decreases in viscous media, thus increasing the quantum yield of fluorescence.

The study of the emitted fluorescence has shown that this  $\lambda_{\text{max abs}}$  corresponds to the  $\lambda$  of excitation that produces the maximum fluorescence emission around  $\lambda = 550$  nm for betaxanthins and  $\lambda = 575$  nm for betacyanins. The subsequent relaxation of these molecules is carried out largely by internal conversion. This process releases the acquired energy in the form of heat. This energy is dissipated by convection of the excited molecules of the chromophore towards the adjacent molecules of the solvent. Only a small part of it is released as fluorescence. The quantum yield for fluorescence ( $\Phi_F$ ) gives low values if compared to compounds like rhodamine 6G, which has a value  $\Phi_F = 0.95$  (Kubin and Fletcher, 1982). In betalains it has been demonstrated that this value is proportional to the viscosity of the solvent used (**Table 1.1**). Thus, the analysis in water and methanol gives lower values than in ethylene glycol (Nizinski et al., 2017; Wendel et al., 2015c, 2015b, 2015a). This response has also been shown for betaxanthin molecules present in gelificating media, where fluorescence intensity increases with the time course of the process (Cabanés et al., 2016). These results show that an increase in

the viscosity of the medium makes the convection of the acquired energy difficult, favoring the path of the fluorescence. The presence of aromatic rings linked to the electron resonance system characteristic of betalamic acid implies a marked decrease in the fluorescence intensity. Only the fully planar aniline-derived betalain presents fluorescence intensity comparable to betaxanthins. The effect of the medium was also studied by taking indicaxanthin, vulgaxanthin I and miraxanthin V as model betaxanthins, describing how higher viscosity in the solutions increased the fluorescence quantum yields and the excited states' lifetimes (Nizinski et al., 2017; Wendel et al., 2015c, 2015b).

Transient absorption spectroscopy UV-vis-NIR has been used for the characterization of the properties of the  $S_1$  state since this excited state has a very short life (Nizinski et al., 2017; Wendel et al., 2015c, 2015b, 2015a). The excitation wavelength is adjusted to the electronic transition  $S_0 \rightarrow S_1$  and is close to the maximum of the stationary absorption. The graph resulting from this analysis (**Fig. 1.4**) shows positive and negative bands. The positive bands correspond to the transitions  $S_1 \rightarrow S_n$  ( $n > 1$ ) while the negative bands correspond to the bleaching of the  $S_0$  state and to the stimulated emission  $S_1 \rightarrow S_0$ . In this sense, it has been demonstrated the existence of conical intersections between the  $S_0$  and  $S_1$  states (He et al., 2019). This finding is related to torsional geometries of the molecules and could partially explain the quantum yields of fluorescence determined for betalains and the effect of solvents.

Over time (ps scale) it is observed that from state  $S_1$  a triplet  $T_1$  state is not produced by intersystem crossing (ISC) but that the complete recovery of the  $S_0$  state occurs, with the consequent deactivation of the excited molecules. The absence of the  $T_1$  state prevents the formation of toxic oxygen species by energy transfer, which supports the theory of the protective character of betalains in plants containing them. In extracts of vulgaxanthin,  $\text{Ru}(\text{bpy})_3^{2+}$  was used as a triplet sensitizer (Wendel et al., 2015b). Nanosecond photolysis at  $\lambda_{\text{exc}} = 355 \text{ nm}$  of the mixture  $\text{Ru}(\text{bpy})_3^{2+}$  with vulgaxanthin leads to the initial absorption band at  $\lambda_{\text{max}} = 360 \text{ nm}$ . Its decay is accompanied by the appearance of a new positive absorption band with a maximum at  $\lambda_{\text{max}} = 540 \text{ nm}$ , which can be assigned to vulgaxanthin in the  $T_1$  state. At 2,500 ns delay, besides the positive band, there is also a negative band at 460 nm, mainly reflecting vulgaxanthin ground state bleaching (Wendel et al., 2015b).

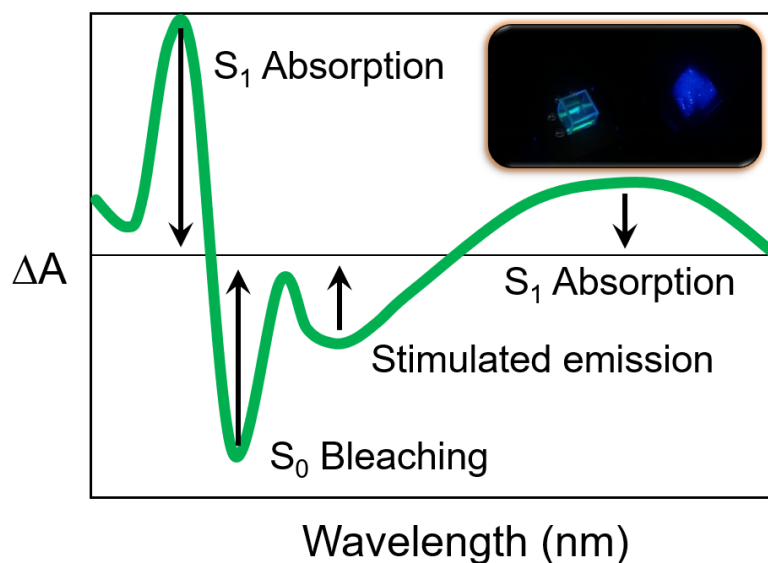


**Figure 1.4. General scheme for the transient absorption spectra UV-Vis-NIR of betalains.** Positive bands correspond to transitions from S<sub>1</sub> state and negative bands correspond to the bleaching of the S<sub>0</sub> state. Inset: Green fluorescence in a 3  $\mu$ M solution of miraxanthin I coming out from a 3 mL quartz cuvette placed in a Shimadzu RF-6000 spectrofluorometer (excitation at 470 nm).

One appropriate way of achieving an increase in the lifetime of the S<sub>1</sub> state is by increasing the viscosity of the solvent, which seems to indicate a significant change in the geometry of the molecules that precedes the S<sub>1</sub>→S<sub>0</sub> radiationless transition involved in the deactivation of S<sub>1</sub> state. In betanin, molecular rotation around the C<sub>12</sub> = C<sub>13</sub> bond may accelerate the internal conversion process (Wendel et al., 2015a). The increase in the viscosity of the medium causes the lifetime of the S<sub>1</sub> state to pass from 7.7 ps in methanol to 27 ps in ethylene glycol. This higher viscosity of the medium hinders the molecular rotation which in turn decreases the energy dissipation by convection and favors the emission of fluorescence, which is consistent with the results obtained in the quantum yield of the fluorescence.

By means of NMR it has been shown that betalains present a mixture of E/Z stereoisomers. This phenomenon has been corroborated with transient spectroscopy. Two different time constants appear corresponding to the excitation of each stereoisomer to its excited state, which subsequently relaxes, presenting in both cases, a deactivation spectrum, similar to **Fig. 1.4**. These deactivation spectra of the S<sub>1</sub> state are the fingerprint of betalains and are also observed in aqueous extracts of plants of the order *Caryophyllales*. Extracts of *O. ficus-indica*, whose major pigment is indicaxanthin, show a transient absorption spectrum at  $\lambda_{\text{exc}} = 483$  nm similar to that obtained in pure indicaxanthin aqueous solutions (Wendel et al., 2015c), whereas

extracts of *Phytolacca americana* berries show photophysical characteristics similar to extracts of pure betanin (Wendel et al., 2015a).

#### 1.3.4. Biological relevance of fluorescence

Color acts in plants as a signal for communication with other species. In general, plants take advantage of visual signals to attract animals' attention for the purpose of pollination and seed dispersal. In flowers, color represents an important characteristic known to attract pollinators (Balamurali et al., 2018; Marshall and Johnsen, 2017; Ostroverkhova et al., 2018). Insects' capacity to detect symmetry and asymmetry and the preferences described for special patterns (Plowright et al., 2017) confer relevance to color modulation in flowers, and therefore to the optical properties of the underlying pigments. The establishment of the fluorescent properties of individual pigments and flower extracts raised the question whether flowers containing betaxanthins could be considered as fluorescent items.

To observe the fluorescent phenomenon, the incident light was filtered in order to avoid contamination of the emitted fluorescence. Based on the properties of betaxanthins in aqueous solution, a photography filter system especially designed for green fluorescence visualization was used (Gandía-Herrero et al., 2005a). The resulting images showed how fluorescence is maintained in the physiological environment, as shown in **Fig. 1.2B**. Betacyanins are only weakly fluorescent (Gandía-Herrero et al., 2010a), and due to the overlapping observed between the betacyanin absorbance and the betaxanthin emission spectra, natural betacyanins are able to absorb a high degree of the light emitted by betaxanthins (Gandía-Herrero et al., 2005d). This was described as an unedited inner filter effect that was able to generate contrasting patterns in the flower fluorescence signal.

The relevance of light emission in flowers for the attraction of pollinators is a matter of current debate (García-Plazaola et al., 2015; Iriel and Lagorio, 2010; Lagorio et al., 2015; Mori et al., 2018; Rao and Ostroverkhova, 2015). The weakness of the signal in comparison with color absorption or light reflection may limit the role of fluorescence as a stand-alone communication signal. However, fluorescence may support other well-established signals and not necessarily substitute them. Some species of spiders display distinctive fluorescent signals depending on gender and life stage, with females maintaining the brightness throughout their lives (Brandt and Masta,

2017). Fluorescent external areas may serve as an additional attracting signal for preys or males. In any case, some interactions have already been described in nature to rely on emitted fluorescence, such as those involved in mating budgerigars (Arnold et al., 2002; Parker, 2002), or in attracting prey to some species of jellyfish (Haddock and Dunn, 2015). In the latter case, fluorescence is derived from a green fluorescent protein with analogous fluorescence spectra to betaxanthins which appears in yellow patches in the tentacles. Remarkably these patches are close to non-fluorescent purple ones, described by the authors to increase the contrast of the fluorescent region (Haddock and Dunn, 2015). Green fluorescence and purple contrasting patterns constitute the same tandem described for betaxanthins and betacyanins in flowers and hypothesized to be of relevance in pollination (Gandía-Herrero et al., 2005d).

It should also be considered that the different perception of light and the existence of receptors for specific wavelengths in the eyes of pollinators can make light emitted a major component of the perceived signal. This was the case hypothesized for betalains in cacti since cactus pollinating bats with specific receptors were reported as being able to see at the specific wavelengths emitted by betaxanthin fluorescence (Gandía-Herrero et al., 2005d; Winter et al., 2003). This hypothesis was confirmed by recent investigations that found how other species of bats are attracted from distances of up to 23 meters by green light with a wavelength of  $\lambda = 520$  nm (Voigt et al., 2017).

Since betaxanthins are molecules that exhibit natural fluorescence in the visible range of the electromagnetic spectrum and this phenomenon is general to all betaxanthins, potentially any solution or structure containing them should be a glowing object. In this sense, the possible influence of fluorescence in seed dispersal has a major biological relevance. To date, only quinoa grains have been demonstrated to contain significant quantities of betaxanthins in the yellow and orange varieties (Escribano et al., 2017). Color and fluorescence measurements in the grains corresponded to the colored outer layer of the grains, as visible under normal physiological conditions. Several identified betaxanthins give yellow coloration to quinoa grains and make them glow as intact viable grains. Thus, the discussion about the influence of fluorescence in pollination opens up to include a possible biological effect of this signal in seed dispersal.

### 1.3.5. Photostability of betalains

Among the properties of betalains, their stability and color permanence have received great attention by researchers due to their applications in food coloring. Therefore, factors affecting stability during processing and storage, such as pH value, temperature, oxygen and light, have been extensively studied since their early use by the food industry (Huang and von Elbe, 1987; Huang and Von Elbe, 1985; Schwartz and von Elbe, 1983; Von Elbe et al., 1974).

Exposure to light is one of the main factors affecting the stability of betalains, similar to other naturally-occurring pigments such as anthocyanins or carotenoids. In addition, the bioactive properties attributed to these compounds, such as their antioxidant activity and free radical scavenging capacity, can be altered under light exposure (Gandía-Herrero et al., 2013). Betalains obtained from several sources have been analyzed under dark and light conditions, such as the model betacyanin betanin extracted from *B. vulgaris* (Pedreño and Escribano, 2001). Pigment tolerance to light was found to be dependent on pH, and betanin in acidic solutions analogous to those found in plant cell vacuoles was stable with a limited degradation due to light exposure (Pedreño and Escribano, 2001). In the case of the betaxanthin indicaxanthin (Gandía-Herrero et al., 2010b), the presence of light increased its degradation over a wide range of pH values. Data were analyzed and adjusted to first order kinetics, with results indicating a higher stability at neutral pH, in both the presence and absence of light in short time experiments. However, when indicaxanthin was exposed to light over long periods of time, the stability of the pigment considerably diminished at all pH values. The encapsulation of pigments in polymeric matrixes greatly improves their stability in long-term experiments. In this way the color of indicaxanthin became lighter after six months in the presence of light, which was linked to the destruction of the pigment. However, the color parameters did not change noticeably after storage for the same period of time in the absence of light (Gandía-Herrero et al., 2010b). In the same manner, the betaxanthin miraxanthin V and the betacyanin betanidin, the pigments with the strongest antiradical capacity, were affected by light exposure in solution over a wide range of pH (Gandía-Herrero et al., 2013). Betanidin is known for being a very labile molecule that degrades quickly under working and storage conditions (Gandía-Herrero et al., 2007; Huang and von Elbe, 1987, 1986; Stintzing et al., 2002). Although

exposure to light reduced pigment stability, 50% of the initial pigment amount remained when encapsulated (Gandía-Herrero et al., 2013).

Stability of model betalains can be compared with that of their partner pigments' anthocyanins. When anthocyanins' stability was analyzed after encapsulation in similar conditions to those used for betalains, it was observed that storage in the absence of light also reduced the pigment content (Ersus and Yurdagel, 2007; Tonon et al., 2010). The stability of anthocyanins was lower than that shown for miraxanthin V and betanidin and the presence of light accelerated anthocyanin degradation. Comparable results were obtained for a more divergent pigment, such as lycopene encapsulated in starch matrixes (Rocha et al., 2012).

#### **1.4. Biotechnological applications of fluorescence**

Because betalain plant pigments are present in edible sources, the original discoverers of the fluorescence property suggested future applications for the food industry. Fueled by coetaneous interest in implementing fluorescence as an aesthetic color modulator (Mercuri et al., 2001), the idea arose to modify colors of food and beverages with fluorescent shades (Gandía-Herrero et al., 2005c). However, the real potential of betalain fluorescence was still to be discovered thanks to contributions from groups all around the world (**Fig. 1.5**). Precise fluorescent identification of pigments in natural sources led to methods for the visualization and staining of multiple structures and to biotechnological applications.

##### **1.4.1. Improved detection of betalains in plant extracts**

Fluorescence detection implies a high selectivity of the analysis, due to the specific excitation of the compounds. It has been extensively employed for the determination of different kinds of molecules in biosciences. Because few compounds emit a strong enough fluorescence for direct measurements, a derivatization procedure is normally necessary. This is not the case of betalains, and the native fluorescence of the molecules can be directly applied to their detection. This implies an immediate improvement of standard detection protocols.

Betalains are usually found in complex mixtures in plant extracts and thus the most suitable means for identification and quantification involve high performance liquid chromatography (HPLC) separations. The direct use of fluorescence detectors



after chromatographic separations for the accurate and sensitive quantification of betaxanthins was the first application of fluorescence. Improvement of detection involved the determination of traces of betaxanthins in white tissues of plants of the Caryophyllales (Gandía-Herrero et al., 2005c). Deeper analyses revealed an improvement in the limits of detection (LOD) and quantification (LOQ) when compared with standard protocols based on absorbance (Gandía-Herrero et al., 2005e). The average reduction of the limits is around 76% of the previous values and also implies a reduction in the amount of sample needed in the assays. The wavelengths used in the detectors were 460 nm for excitation and 510 nm for emission, which were found to be suitable for detecting the native fluorescence of all the pigments assayed, independently of the elution time and of the percentage of organic phase of the gradients.

#### **1.4.2. Fluorescent probes in microscopy**

Fluorescence of betaxanthins has been used in microscopy applications to observe betaxanthin-containing cells in both undifferentiated samples and in plant and animal tissues. Complementation of the betalains biosynthetic pathway in plants and the study of the fate of betaxanthins added to the diet of model organisms benefit from microscopy filters readily available for the GFP technology.

##### **1.4.2.1. Visualization of natural betalains *in vivo* and *in vitro***

The first descriptions of betaxanthins' strong fluorescence accompanied spectral characterization with the visualization of different pigments in the physiological environments within the plants containing them. This happened for *P. grandiflora*, *L. productus* (Gandía-Herrero et al., 2005a), and *M. jalapa*, where an inner filter effect with betacyanins was characterized under physiological conditions (Gandía-Herrero et al., 2005d). Visualization was based on microscopy filtercubes used for GFP in epifluorescence microscopes and the use of the 488 nm line of Kripto-Argon ion lasers in confocal instruments. Images of fresh samples were obtained by recording light emitted in the 500-525 nm range of wavelengths. Cells were shown with vacuoles occupying most of the cell space and with non-fluorescent black spots corresponding to nuclei. In addition, junctions between cells were visualized more clearly than with the brightfield technique (Gandía-Herrero et al., 2005a).

Further research involved visualization under the same system for the plant *Portulaca oleracea* (Gandía-Herrero et al., 2009b). In this case, fluorescence in yellow petals is mainly due to miraxanthin V. The presence of multiple shades in flowers allowed the use of violet and white controls with betacyanins and without any pigment, respectively. In this species light emission was recorded not only in yellow petals but also detected in pistils, where the same betaxanthin was also described.

A recently described source of betaxanthins is the pseudo-cereal quinoa (*C. quinoa*), where pigments can be found in their edible yellow and orange grains (Escribano et al., 2017). The presence of multiple pigments in the outer layer makes the grains of this crop fluorescent. This implies that there are glowing yellow quinoa grains while white, red or black grains do not fluoresce. Macroscopic images can be obtained with suitable macroscopes under blue light stimulation (Escribano et al., 2017). The pigments responsible in this case are mainly dopaxanthin and miraxanthin V.

Fluorescence of betaxanthins has also been applied to the determination of the pigments as a function of storage conditions in foods (Lemos et al., 2015). Time-resolved fluorescence has been applied to the study of raw beet roots that have been stored under vacuum and refrigerated for up to 41 days. The proof of concept, based on fluorescence decay, proposes the possibility of using this non-invasive technique to study the evolution of betalains in foods (Lemos et al., 2015; Rabasović et al., 2012). The addition of betaxanthins as a dye to transform dim objects into fluorescent is also possible, as has been demonstrated for wool (Guesmi et al., 2013). Indicaxanthin was used to transform white fabrics into yellow ones by adding the characteristic fluorescence of betaxanthins. In this case, maximum wavelength for emission was recorded as 576 nm. Although fluorescence was affected by light exposure, it was resistant to washing and maintained spectral properties and intensity (Guesmi et al., 2013).

The use of fluorescence as an imaging technique to identify the presence of betaxanthins in plant tissue has now been extended to betalain-producing cell cultures. This is the case of cell lines developed from *C. argentea* (Guadarrama-Flores et al., 2015). Production of the highly antioxidant diphenolic betaxanthins derived from L-DOPA and dopamine was readily followed by the presence of yellow coloration and green fluorescence with blue light stimulation under the same systems developed for tissue visualization. The existence of fluorescence and color correlated with the chromatographic identification and quantification of the pigments.

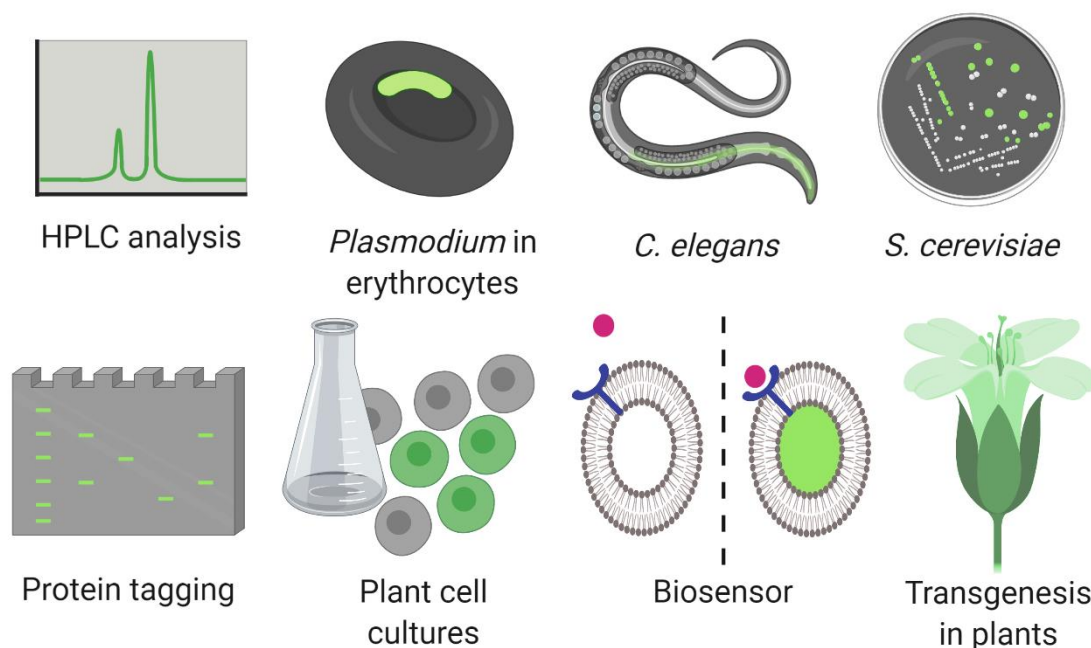


**Figure 1.5. Schematic overview of the biotechnological applications developed from betalains' fluorescence.** Fluorescence can be used for the improvement of detection procedures of the pigments separated by analytical techniques as high-performance liquid chromatography (A, (Gandía-Herrero et al., 2005e)). Specific betalains are able to stain *P. falciparum* inside erythrocytes which allows fluorescent detection of the parasite (B, (Gonçalves et al., 2013)). As it will be probed in this study, fluorescence makes betalains visible in the digestive tract of model animals as *C. elegans*, demonstrating ingestion and stability of bioactive pigments (C). Increased fluorescence due to betaxanthins can be linked to enhanced activities of enzymes of biotechnological interest, allowing high-throughput screening techniques in organisms as *S. cerevisiae* (D, (DeLoache et al., 2015)). Macromolecules condensed with one molecule of betalamic acid become fluorescent in a tagging procedure suitable for proteins in solution and in electrophoresis gels (E, (Cabanés et al., 2016)). Increased production of betalains in plant cell bioreactors can be specifically and easily followed through fluorescence (F, (Guadarrama-Flores et al., 2015)). Fluorescence of betaxanthins is a suitable output signal for virtually any biosensor provided that betalamic acid production is engineered (G, (Chen et al., 2017)). The success of transgenesis in plants can be ascertained by betaxanthin fluorescence when using genes for betalamic acid-producing dioxygenases (H, (Harris et al., 2012)). This figure was created using BioRender (<https://biorender.com/>).

#### 1.4.2.2. Fluorescent detection of malaria infected erythrocytes

The coumarinic betalain BtC is a semi-synthetic betaxanthin which behaves exactly like its natural analogues (Gonçalves et al., 2013). Like other betaxanthins, it was synthesized from betalamic acid released from betanin (Gandía-Herrero et al., 2006) after condensation with a particular amine: 7-amino-4-methylcoumarin. Condensation with this molecule provided interesting properties to the resulting betaxanthin: it was able to pass through the membrane of erythrocytes and to attach to

the parasite *Plasmodium falciparum* inside the blood cells. As a betaxanthin, it is water soluble and is a fluorescent molecule with fluorescence spectra with a maximum excitation wavelength of  $\lambda = 520$  nm, and emission with a maximum at  $\lambda = 570$  nm. This means that BtC is a fluorescent probe able to stain malaria infected erythrocytes (Gonçalves et al., 2013). BtC selectively accumulates within the infected cells at the point of the living parasite localization. The semi-synthetic betaxanthin was later characterized in depth and derivatized as its trifluoromethyl analog, cBeet151 (Rodrigues et al., 2018). The characterization of the photophysical properties of the molecule and the two-photon absorption process demonstrated that the electron density migrates from the coumarinic to the betalainic moiety upon  $S_0 \rightarrow S_1$  excitation (**Fig. 1.3**).

The novel methodology created based on betaxanthin fluorescence requires less than 5 min incubation and allows live-cell imaging with minimal cell manipulation. Malaria is a potentially deadly illness caused by the *Plasmodium* and is easily transmitted by *Anopheles* mosquitoes, mainly in wide areas of Africa, where it affects millions of people. The development of a quick and inexpensive method to detect malaria is of high medical relevance. The synthetic betaxanthin created and its quick fluorescence detection by means of microscopy may help in the important task of diagnosis by detecting the *Plasmodium* before the etiology of the illness gets severe.

### 1.4.3. Monitoring enzyme activities

Continuous spectroscopic assays are useful to follow enzyme activities with high precision. Moving from absorbance to fluorescence-based assays allows increases in sensitivity and specificity, both by following the appearance of fluorescent products or by measuring the reduction of a fluorescent substrate. In addition, the accumulation of betaxanthins as fluorescent final products has been used to indicate the activity of enzymes *in vitro* and *in vivo* with a variety of different applications.

#### 1.4.3.1. Following oxidative enzymes – Tyrosinase

By using betaxanthins as enzymes' substrates, the activity of oxidases has been followed by a continuous fluorescent method (Gandía-Herrero et al., 2009b). Dihydroxylated betaxanthins are highly antioxidant molecules due to the presence of the catecholic sub-structure (Gandía-Herrero et al., 2009a). This structure also means that the betaxanthins are substrates for oxidase enzymes like tyrosinases or peroxidases

(Gandía-Herrero et al., 2005b), while maintaining the fluorescent properties common to all betaxanthins. Oxidation generates a betaxanthin-quinone able to rearrange to leuco forms after intramolecular nucleophilic additions. The resulting compounds present highly limited fluorescence (Gandía-Herrero et al., 2009b).

The methodology used avoids the interference of non-fluorescent molecules that might be present in extracts or formulations. Spectral changes upon enzymatic extracts addition were recorded, showing the decrease of fluorescence while the substrate is converted into products. Despite the reduction in fluorescence intensity, spectral shapes and maximum wavelengths barely vary during the enzymatic activity. Selected wavelengths for the continuous recording were  $\lambda = 465$  nm for excitation and  $\lambda = 512$  nm for emission (Gandía-Herrero et al., 2009b). These wavelengths are expected to fit with the maximum signal in the spectra of most betaxanthins and are thus of use in the evaluation of the transformation or degradation of other pigments by chemical or enzymatic means.

#### **1.4.3.2. Enhancing drug production in yeast - Tyrosine hydroxylase**

Labeling of enzymatic activities through betaxanthin fluorescence is possible not only for the transformation of the pigments. Any reaction yielding betalamic acid will promote its condensation with amines or amino acids to form the corresponding betaxanthins. Thus the high fluorescence of the yellow pigments can be used as a suitable signal, being this approach applied in screening techniques (DeLoache et al., 2015; Mao et al., 2018).

The production of benzyloquinoline alkaloids in yeast relies on the use of multiple enzymes cloned from the producing plants (Hawkins and Smolke, 2008). Like betalains, alkaloids derive from L-DOPA which is transformed in multiple steps into (*S*)-reticuline, considered the starting point for a wide variety of drugs, including codeine, morphine and other opioid drugs (DeLoache et al., 2015). On the other hand, yeast *Saccharomyces cerevisiae* is able to transform simple sugars added to the growth medium and to synthesize L-tyrosine, the dehydroxylated precursor of L-DOPA, but it does not accumulate L-DOPA itself. Thus, engineered yeasts are able to produce L-tyrosine from sugars, and to produce drugs as final products from added L-DOPA (Hawkins and Smolke, 2008). There was a missing enzymatic step between these two pathways that prevented the obtention of opioids from sugars in yeast. Filling this gap

meant finding a suitable tyrosine hydroxylase activity able to convert L-tyrosine into L-DOPA without further oxidizing it to the quinone.

Because the final product of this reaction is L-DOPA, it is possible to sensor L-DOPA production by adding to the system a 4,5-DOPA-extradiol-dioxygenase enzyme (DODA). This is able to convert L-DOPA into betalamic acid, which ultimately yields betaxanthins (DeLoache et al., 2015). The dioxygenase enzyme used was the sequence from *M. jalapa* and fluorescence of betaxanthins was used then to identify L-DOPA producing enzymes using L-tyrosine as a substrate. Furthermore, massive mutagenesis studies were performed to improve the enzyme activity because the screening process detects enhanced hydroxylating activities present in single colonies by measuring increased fluorescence (DeLoache et al., 2015).

The same screening application has been extended to the discovery of strains of *S. cerevisiae* producing L-tyrosine with high yields (Mao et al., 2018). In this case, the fluorescence of betaxanthins is the signal used in the measurement of the production of L-tyrosine in yeasts from a mutant library obtained by random mutagenesis. Betaxanthins production from L-tyrosine was achieved by transformation of the wild type *S. cerevisiae* strain with the genes encoding L-tyrosine-hydroxylase and 4,5-DODA. When high yields of L-tyrosine are produced, the hydroxylase converts it into L-DOPA, which is the substrate of DODA. Then, betalamic acid is formed and condenses with amino acids and amines yielding betaxanthins which are yellow in color and highly fluorescent. This fluorescent screening technique detected yeast mutants with high production of L-tyrosine.

The combination of these two activities in yeast, high-yield L-tyrosine production (Mao et al., 2018) and L-tyrosine hydroxylation to L-DOPA (DeLoache et al., 2015), both screened thanks to betaxanthins formation, may result in an enhanced production of bioactive alkaloids. The betaxanthin fluorescence signal in microorganisms' colonies helps to assess the phenotype of interest and makes simple and inexpensive the development of high-throughput screening strategies. Thus, betalain fluorescence discovered in flowers of the Caryophyllales helps in the production of drugs in yeast cultures.

### 1.4.3.3. Reporter activity in transgenesis - 4,5-DOPA-extradiol-dioxygenase

Fluorescence is a specific signal selected to measure genetic transformation of plant models and industrial crops with the capability to produce betalains. Betalains are phytochemicals with biological activities and health-promoting potential. However, natural edible sources are mainly restricted to beets, cactus pears, and Swiss chard, with few alternative sources possible (Gandía-Herrero et al., 2016a). This has promoted interest in the generation of edible betalain-producing plants.

Transformation of the plant model *Arabidopsis thaliana* with the 4,5-DOPA-extradiol-dioxygenase from *Amanita muscaria* demonstrated the feasibility of the transgenic approach to expand the array of betalain-producing plants (Harris et al., 2012). Positively transformed plants resulted in the accumulation of betaxanthins in flowers and seedlings of the plant. The fluorescent properties of betalains allowed the visualization of cells in these structures. Equivalent results supported by fluorescence microscopy showed dioxygenase activity in transient expression experiments in petals of *Antirrhinum majus* transformed with the enzymes from *A. muscaria* and *P. grandiflora* (Harris et al., 2012). The hydroxylation of tyrosine to form L-DOPA by the specific cytochrome CYP76AD5 from *B. vulgaris* was also demonstrated by betaxanthins' fluorescence in petals of *A. thaliana* (Sunnadeniya et al., 2016). This was possible after co-expression with the 4,5-DODA from *P. grandiflora*. Furthermore, studies on different types of dioxygenases and their classification as betalamic acid forming enzymes have also been helped by the fluorescence of betaxanthins in transient expression experiments in *A. majus* petals (Chung et al., 2015). Different dioxygenases from *B. vulgaris* and *Parakeelya mirabilis* were used and positive activity was accompanied by fluorescence of petal cells under blue light stimulation. Results in this case correlated with transcript abundance in betalain accumulating tissues of the original plant (Chung et al., 2015).

By applying a similar approach, plants of agronomic and alimentary interest have finally been developed. This is the case for tobacco (*Nicotiana tabacum*), where metabolic engineering helped in the final elucidation of the biosynthetic pathway of betalains (Polturak et al., 2016). Fluorescence was the signal used to ascertain *in situ* the presence of betaxanthins, and thus the presence of active forms of the *B. vulgaris* enzymes inserted in the leaves of transgenic tobacco. Also tomatoes (*Solanum lycopersicum*), eggplants (*Solanum melongena*), potatoes (*Solanum tuberosum*) and

petunias (*Petunia × hybrida*) have been engineered to accumulate betalains and transformation was ascertained by pigments' presence (Polturak et al., 2017). Fluorescence of betaxanthins makes the tissues containing them fluorescent under blue light, as detected for tobacco flowers. Betaxanthins detected in this case were vulgaxanthin I, vulgaxanthin III, indicaxanthin, and miraxanthin III. All these plants expressed active 4,5-DODA from *B. vulgaris*, and thus were able to form betalamic acid (Gandía-Herrero and García-Carmona, 2012) which, in turn, condensed with available amines to produce the corresponding betaxanthins (Polturak et al., 2017). The presence of betalains changes the color of the vegetables developed and, in addition, enriches plants with their health-promoting activity.

In plant transformation, fluorescence demonstrates the presence of the transgene and the production of betaxanthins. The microscopy and visualization techniques used in this application are analogous to those established for plants naturally producing betalains in the Caryophyllales (Gandía-Herrero et al., 2005d). Fluorescent food has thus finally been created by the accumulation of betaxanthins in transgenic plants.

#### **1.4.4. Protein labeling**

Betalamic acid is able to react with virtually any free amine available. This leads to the wealth of pigments present in nature but also to the formation of the semi-synthetic betalains described. One notable advance in this process has been to use free amine groups present in proteins to add a molecule of betalamic acid. This results in the synthesis of the so-called yellow protein-betaxanthins (Cabanes et al., 2016). Spectral properties of the molecules are analogous to betaxanthins of low molecular weight and are fluorescent. Spectral shapes are equivalent and present maximum excitation wavelength of 476 nm and a maximum emission centered at 551 nm. The proteins studied were albumin, ovalbumin and trypsin (Cabanes et al., 2016), but the phenomenon might well be generalizable to any protein, as demonstrated by the use of standard molecular weight markers, where all proteins turned into protein-betaxanthins. This reaction results in a labeling procedure where proteins incorporating one molecule of betalamic acid turned fluorescent. Again, conventional devices already developed for the visualization of fluorescein or GFP as Typhon fluorescence scanners or ImageQuant CCD cameras can be used to reveal the presence of proteins tagged with betalamic acid.



A step forward in this procedure was to substitute purified betalamic acid as the labeling reagent with red beet root juice with minor purification (Cabanés et al., 2016). After a simple degradation procedure involving *in situ* alkalization and neutralization, proteins in electrophoresis gels can be stained and are ready for visualization. Red beet root juice is thus an unexpected but reliable staining agent yielding fluorescent proteins at low cost.

#### **1.4.5. Output signal in biosensors**

Fluorescence of betalains provides a reliable and robust signal, which is easily detected by conventional fluorescence apparatus. For this reason it is a suitable candidate signal for use in biosensors, as demonstrated in the development of whole-cell sensors for the analysis of environmental copper (Chen et al., 2017). By using the bacteria *Cupriavidus metallidurans* and *Ralstonia eutropha* it was possible to transform a copper sensing signal mediated by a kinase into protein expression and light emission mediated by betaxanthins. This was done by studying the effect of different promoters and by linking the receptor to the expression of the enzyme 4,5-DOPA from *M. jalapa*. Thus, the bacteria were able to synthesize betalamic acid, which then condensed with amines to form the corresponding fluorescent betaxanthins (Chen et al., 2017). This fluorescence was the signal measured, which turned out to be dependent on the concentration of copper. Application of this sensor is intended for environmental samples, including freshwater and tap water.

The approach developed is not restricted to metals and opens a wide field of new applications for betaxanthins. The original work is a neat demonstration that betaxanthin fluorescence can be used as the output signal of virtually any sensing device insofar as an inducible promoter can activate the expression of a 4,5-DOPA-extradioxygenase in the presence of L-DOPA. This will indefectibly lead to the production of betaxanthins and to the emission of green fluorescent light.

#### **1.4.6. Synthesis of tailor-made probes and future prospects**

Synthetic betalains can be tailor-made in order to fit specific requirements. The success of the design of a betaxanthin probe able to pass through blood cells membranes and to stain *Plasmodium falciparum* is a good example (Gonçalves et al., 2013). The amine group used in the formation of the imine pigment can be chosen or derivatized by

the researcher while maintaining the betalamic acid structure intact. It is only a matter of time that novel capabilities can be added to betaxanthins by modifying this variable substructure. Possibilities are wide as evidenced by the current works, but the success of this approach will depend on the capability of producing betalamic acid in sufficient amounts as a starting molecule.

Betalamic acid can be produced synthetically in a chemical and complex process (Büchi et al., 1977) or obtained from pigments extracted from plants after alkaline degradation (Wyler et al., 1965). In both cases yields are low. The acid can be isolated from betanin after cleavage of the Schiff base by extraction with ethyl acetate (Schliemann et al., 1999). This process also involves low yields but the amounts and purity obtained are enough to generate betaxanthins suitable as HPLC standards. After the same degradation process, betalamic acid can be purified by anion exchange chromatography if the pH of the solution is maintained high (Gandía-Herrero et al., 2012). In this case, the process can be scaled-up to yield sufficient amounts to characterize the properties and bioactivities of the isolated molecule and to produce synthetic betalains (Gandía-Herrero et al., 2006). For small-scale synthesis a betalamic acid derivatized matrix has been developed that makes affordable the one-step synthesis of individual betalains by simply adding the selected amine (Cabanès et al., 2014).

Current research on the betalamic acid-forming enzymes discovered in the biosynthetic pathway of betalains has opened a new way to produce the molecule. Enzyme assays with 4,5-DODA show that, after the cleavage of the L-DOPA aromatic ring, intramolecular rearrangement of the generated 4,5-seco-DOPA intermediate occurs and betalamic acid is formed. This had been demonstrated for the enzymes from *A. muscaria* and *P. grandiflora* *in vivo* (Christinet et al., 2004). Now enzyme-mediated formation of betalamic acid has moved from plants to *in vitro* in enzyme assays after the heterologous expression of the enzymes from *M. Jalapa* (Sasaki et al., 2009), *B. vulgaris* (Gandía-Herrero and García-Carmona, 2012), and even with bacterial enzymes.

To date, fluorescence of betaxanthins has been used to identify and characterize proteins, to stain microscopic parasites, to follow enzyme activities, and to locate pigments in the digestive tract of model organisms, in addition to ascertain the production of pigments both *in vivo* and *in vitro*, both in natural and transgenic plants (**Fig. 1.5**). Possibilities are wide, as evidenced by current works, and synthetic betalains can be tailor-made to fit specific requirements. The betaxanthins obtained may incorporate novel capabilities, depending on their substructure, but they will maintain

the same fluorescent properties described for the natural ones insofar as the betalamic acid moiety remains unaltered (**Fig. 1.2E**). It can be anticipated that the methods already developed for detection, microscopy visualization and high-throughput screening based on betaxanthin fluorescence will be straightforward to apply to novel tailor-made molecules.

## 1.5. Health-promoting effects of betalains

Betalains are not only interesting for their fluorescent properties, since they are also well-known molecules with health-promoting potential (Gandía-Herrero et al., 2016b). Betalains have pharmacological benefits thanks to their antioxidant, anti-inflammatory, and anti-tumoral properties. Studies with different human cancer cell lines have demonstrated the potential of betalains in the chemoprevention of cancer (Sreekanth et al., 2007; Wu et al., 2006). *In vivo* experiments have shown that very low concentrations of dietary pigments inhibit the formation of tumors in mice (Kapadia et al., 2003; Lechner et al., 2010) and, as will be described in this study, extend the lifespan of the model animal *Caenorhabditis elegans*. The bioactivities described are supported by the high antiradical capacity of the pigments structural unit, betalamic acid, and point to a promising potential of betalains in tumor prevention *in vivo* and a possible role for betalains in a health-promoting diet (Gandía-Herrero et al., 2016a). They have also been described in the prevention of tumors in mice and their addition to the human diet promotes protection from oxidative stress in blood cells (Tesoriere et al., 2005). Maximum plasma concentrations are reached three hours after consumption, with a decline corresponding to first-order kinetics. High bioactive potential and a strong fluorescence, both maintained under mild, physiological conditions, are fueling current research on betalains, which is enjoying a golden age (Schwinn, 2016).

### 1.5.1. Antioxidant and antiradical activities

Early studies performed with extracts from *B. vulgaris* and prickly pears (*Opuntia ficus-indica*) demonstrated the potential of betalains as antiradical scavengers (Butera et al., 2002; Escribano et al., 1998; Pedreño and Escribano, 2001). The study of this property was expanded to several natural and synthetic betalains which showed the same properties. The structure of each betalain modulates the antioxidant and antiradical “intrinsic activity” common to all betalains (Gandía-Herrero et al., 2010a, 2009a). The

presence of free hydroxyl groups confers to dopaxanthin and betanidin a high antiradical capacity, so scavenging the ABTS+• radical. However, the blockage of the hydroxyl group present in betanidin by a glycosyl group gives rise to betanin and produces a lower response as antiradical scavenger. Besides, the presence of a resonance system expanded by the connection of betalamic acid with an aromatic ring enhanced the antiradical capacity of simple betalains (Gandía-Herrero et al., 2010a). These *in vitro* redox properties have also been demonstrated *in vivo* with the administration of both prickly pears (Tesoriere et al., 2004) and beet root (Ahmadian et al., 2018) extracts to healthy humans, which contributed to a reduction of oxidative stress.

### **1.5.2. Anti-inflammatory properties**

Betalains' administration may exert an anti-inflammatory response because they are able to interact with the enzymes lipoxygenase and cyclooxygenase. Vidal et al., (2014) reported how natural and semi-synthetic betalains reduced the activity of lipoxygenase (LOX) due to the interaction of betalains with amino acids involved in substrate binding. They are also able to inactivate the cyclooxygenase (COX) active site due to binding to Tyr-385 and Ser-530 residues (Vidal et al., 2014). This anti-inflammatory potential supports the use of plants in traditional medicine for the amelioration of inflammation related diseases (Ibrahim et al., 2012). COX levels also decreased in carrageenin-induced rat pleurisy as a consequence of a pre-treatment with indicaxanthin (Allegra et al., 2014). Besides, other inflammatory markers like interleukin-1 $\beta$  (IL-1 $\beta$ ) or tumor necrosis factor- $\alpha$  (TNF- $\alpha$ ) also decreased, since indicaxanthin acts in a dose-dependent manner on the necrosis factor NF- $\kappa$ B, a key transcription factor in the inflammatory pathway. NF- $\kappa$ B has also been related to atherosclerosis, an accumulation of lipids in the wall of arteries dependent on cholesterolemia and oxidized LDL (low density lipoprotein) accumulation. Thus, indicaxanthin exerts a protective vascular effect (Attanzio et al., 2019) thanks to its bioavailability (Tesoriere et al., 2013).

### 1.5.3. Anti-tumoral properties

Betalain containing extracts have demonstrated a high chemopreventive potential against multiple cancer cells lines. Zou et al., (2005) showed that prickly pear extracts have a dose-dependent effect on the inhibition of cell growth in several cancer cell cultures and immortalized cell lines. This positive effect was mediated by a decrease in cell growth and an increase in apoptosis. In addition, indicaxanthin, the main pigment of yellow prickly pears, also increases apoptosis in the A375 human melanoma cell line and reduces the proliferation of these highly metastatic cells (Allegra et al., 2018). Similar results were obtained by the authors in the *in vivo* proliferation of tumor in mice after the oral administration of indicaxanthin.

A strong inhibition of the proliferation of melanoma cancer cells was also promoted by betanin rich extracts of *H. polyrhizus* (Wu et al., 2006). Similar results were obtained in animals exposed to betanin-containing extracts. Oral administration of beet root extracts to rats reduced the N-nitrosomethylbenzylamine (NMBA)-induced tumors in the rat esophagus by reducing cell proliferation, angiogenesis, and inflammation and stimulating apoptosis (Lechner et al., 2010).

All these findings have shown the health-promoting potential of betalains through studies that have mainly employed extracts from edible parts of plants with limited or no pigment purification (Gandía-Herrero et al., 2016a). Since extracts may have other bioactive compounds like polyphenols or flavonoids, further investigations with pure compounds are necessary to ascertain the real potential of betalains as health-promoting compounds *in vivo*.

## 2. *Caenorhabditis elegans*

*Caenorhabditis elegans* is a non-hazardous and non-pathogenic nematode belonging to the family Rhabditidae. This tiny round worm is approximately 1 mm in length and it is found worldwide as a free organism on rotting vegetables where it feeds on microbes. Despite its apparent simplicity, *C. elegans* presents a transparent body consisting of two concentric, cylindrical tubes separated by a pseudocoelomic cavity. The external layer includes a cuticle, an epidermis and digestive, muscle, nervous, and excretory systems. The internal layer is composed of the digestive and reproductive systems.

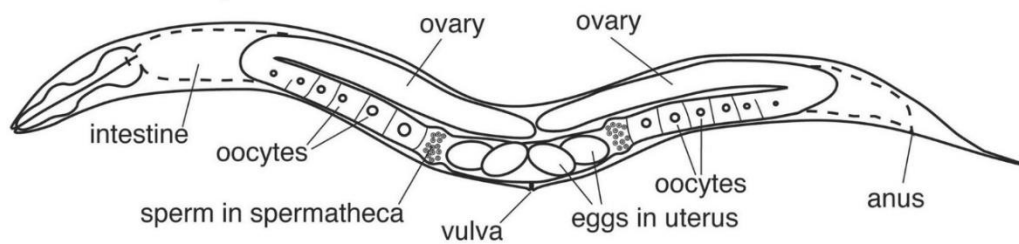
Many researchers around the world study all these tissues with different approaches giving rise to a wide community that shares results and ideas to understand the advantages of using *C. elegans* as a model organism. It is worth highlighting the pioneering works of Sidney Brenner (Brenner, 1974), who received the Noble Prize in 2002 for his works with *C. elegans* as an animal model in Biology.

## **2.1. Sexual forms of *C. elegans***

*C. elegans* has six chromosomes, five autosomal and one sexual, and presents two sexual forms which differ in the content of the sexual chromosome: hermaphrodites (XX) and males (XØ). Sex is determined by the X:autosome (X:A) ratio (Zarkower, 2006) and the incidence of males is only 0.1%-0.2% of the progeny. Hermaphrodites first produce haploid sperm, which is stored in the spermatheca in the early L4 stage, and then, near adulthood, the germ line produces haploid oocytes. The hermaphrodites are self-fertilized by the stored sperm and can yield up to 300 descendants. If a hermaphrodite mates with a male, the offspring could reach around 1,000 descendants.

In *C. elegans*, sexual dimorphism (**Fig. 1.6**) and differential gene expression have been widely studied, finding that sex-indifferent tissues are only the pharynx, the excretory system and main body muscles (Sulston et al., 1980; Sulston and Horvitz, 1977). Although morphological differences between males and hermaphrodites begin in the L2 stage, the gene lineages of the two sexual forms are different from embryonic development. Males come from the spontaneous non-disjunction of the X chromosome during meiosis in the germ line. Cells lineages are well known in both sexes and this has allowed the determination of the fate of the 959 somatic cells in hermaphrodites and the 1,033 somatic cells in males. Additionally, the proportion of sexually specialized cells is also different, with 40% in the males and 30% in the hermaphrodites. These differences play an important role in laboratory work. The genetic variability introduced by males is important to generate animals with different genotypes while their absence enhances the maintenance of well-established genotypes.

## XX hermaphrodite



## XO male

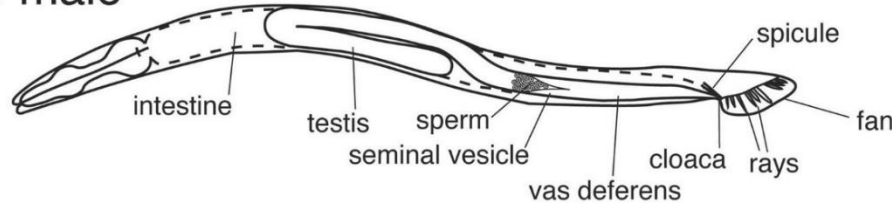


**Figure 1.6. Schematic overview of the sexual forms of *C. elegans*.** Image extracted from <http://www.wormbook.org>

## 2.2. Life cycle

*C. elegans* presents a rapid life cycle where a single hermaphrodite is able to produce a progeny of around 300 individuals. This cycle starts with an embryogenesis step which takes around 12 hours at 20 °C. Embryos are developed inside the hermaphrodite's body until they reach the 24-cell stage, when they are laid on an external surface. Their survival outside the mother's body is possible thanks to the presence of an eggshell. When free embryos hatch (**Fig. 1.7**), they become a first stage larva, L1, and they grow through four larval stages, from L1 to L4. The L1 stage lasts 16 hours and the other stages are around 12 hours long at 20 °C. Each stage ends with a short period of inactivity known as lethargus, in which a new cuticle is produced to allow the worm's growth (Raizen et al., 2008). Through the larval stages, the differentiation of both somatic and germ cells continues to establish the general organization of all tissues and especially the organization of the future gonad, which starts its organization in the spermathecae and the uterus at the L3 stage (Kimble and Hirsh, 1979).

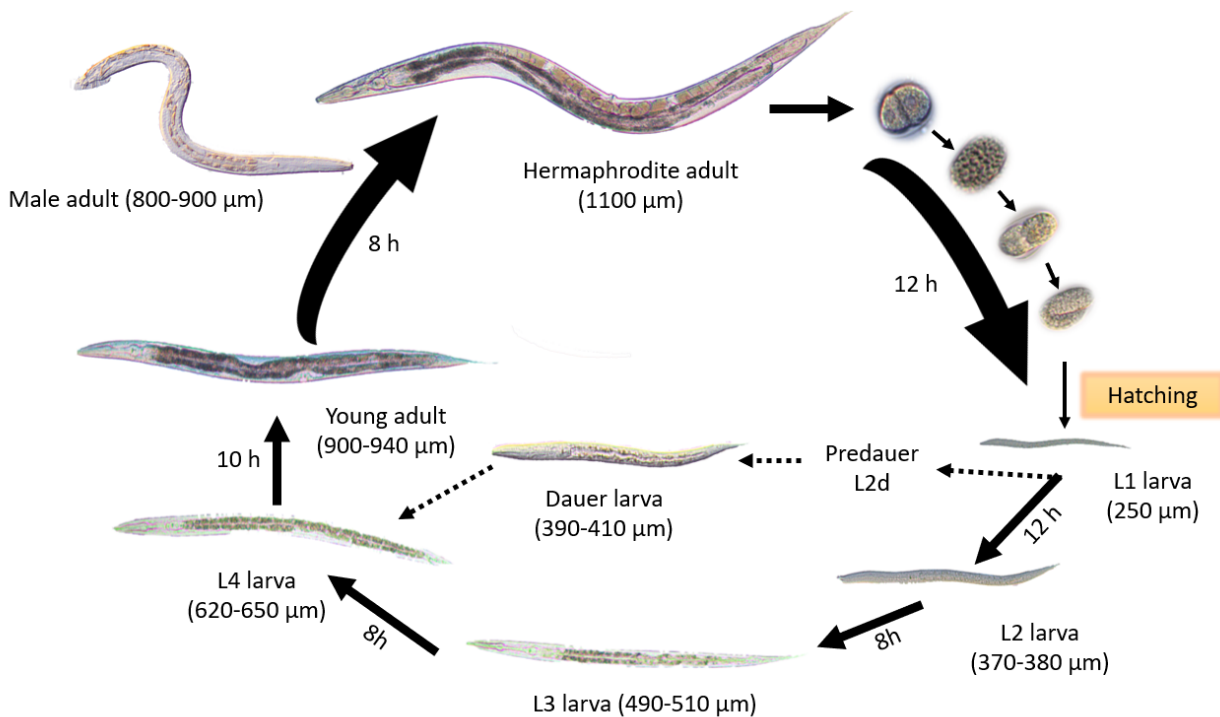


**Figure 1.7. Life cycle of *Caenorhabditis elegans*.** The periods of time correspond to the development at 20 °C. Dotted lines show the alternative route which lead to dauer larvae, which can resist up to 4 months under adverse conditions.

At the L4/adult molt, a young-adult hermaphrodite stops the production of sperm and the germline cells continue to undergo meiosis and differentiation to generate exclusively oocytes for a period of 2–3 days. When the adult form is reached, hermaphrodites undergo fertilization, employing their own sperm. Additional progeny can be generated if the hermaphrodite mates with a male. After the reproductive period, adult worms can survive an additional 10-15 days before dying.

An alternative route may be activated at the L1 stage when worms are not able to find food. This route produces a resistant form, the dauer larva (Cassada and Russell, 1975), which presents a cuticle that completely envelops the animal and plugs its mouth preventing the animal from eating and thereby arresting development. Dauer larvae are motile and can survive for several months exploring the environment until they find food (Cassada and Russell, 1975). Then, worms lose their mouth plugs, molt, and continue their development as slightly different L4 larvae. The activation of this alternative route is not only due to the lack of food since dauer recovery is inhibited by a high population density or by high temperatures (Golden and Riddle, 1984), even in the presence of adequate food sources. This provides a mean for *C. elegans* to propagate in nature under adverse conditions. In the laboratory, propagation is possible just by



transferring dauer larvae to fresh plates with bacteria as food source, which facilitates the maintenance of *C. elegans* strains for several months.

### **2.3. Maintenance of *C. elegans* in the laboratory**

Since the 1970s, when Sydney Brenner described *C. elegans* as a model organism (Brenner, 1974), more than 3,000 mutant strains and wild type have been established due to the easy maintenance of *C. elegans* in the laboratory and its resistance to freezing for a long period of time at -80 °C or indefinitely in liquid nitrogen (Stiernagle, 2006).

*C. elegans*' development is extremely sensitive to changes of temperature. The working temperature is usually established at 20 °C, where the above-described life cycle, from embryo cells to adulthood, takes 3 days. This process takes double the time at 15 °C or decreases at temperatures above 20 °C. Temperatures higher than 25 °C usually produce mutations that affect the development and viability of worms and should be avoided in standard assays.

Providing enough food is also important to complete the life cycle and to avoid the activation of the dauer stage. In the laboratory, *C. elegans* is usually fed with *E. coli* OP50, a non-pathogenic strain auxotroph for uracil which is provided on the agar surface in Petri dishes (or in the liquid culture). Since bacteria are food sources for *C. elegans*, aseptic conditions must be kept to avoid the presence of harmful strains in the worms' intestine or the colonization of the medium by fungi which could alter the experimental results. Internal contamination of worms can be eliminated by treatment with a solution of hypochlorite-sodium hydroxide. This treatment kills worms, but eggs are resistant to it thanks to the chitin shell that covers them. Placing these eggs in a new, sterile medium results not only in a non-contaminated culture but also gives rise to a synchronic population, since eggs hatch at the same time. Additionally, the obtention of a synchronic population provides a tool widely used for lifespan and aging assays.

On the other hand, the susceptibility to contamination of *C. elegans*' cultures has been used for the analysis of human, plant and animal microbial pathogens (Sifri et al., 2005). For instance, several *Pseudomonas aeruginosa* PA14 mutants employed as an additional food source have provided a step forward to set up virulence factors (genes) involved in the actuation of this human opportunistic pathogen (Mahajan-Miklos et al., 1999; Sánchez-Diener et al., 2017).

In short, precautions about temperature changes and contamination must be taken when working with *C. elegans* worms. However, once the optimal conditions are established, *C. elegans* is an excellent model for studying the biology of eukaryotes from different approaches.

## **2.4. Applications of *C. elegans* as an animal model**

*C. elegans* was the first metazoan whose genome was completely sequenced. Its genome contains over 20,000 protein-coding genes and the comparison with the human genome shows that around 60-80% of human genes have an ortholog in the *C. elegans* genome (Kaletta and Hengartner, 2006). In addition, 40% of human genes associated to different diseases have orthologs in the *C. elegans* genome (Culetto, 2000). Thus, *C. elegans* may be used for the study of human health and disease.

### **2.4.1. Cancer**

Many of the genes and pathways involved in human cancers are highly conserved in *C. elegans*. *C. elegans* as a cancer model has been employed for the development of mutant phenotypes of ortholog genes which help to understand these tangled pathologies from different perspectives. They allow the study of cell cycle process, apoptosis, growth factors signaling, metastasis or the use of new drugs to prevent or to reduce the proliferation of different human tumors (Kyriakakis et al., 2015).

### **2.4.2. Neurodegenerative diseases**

*C. elegans* has a nervous system comprising 302 neurons in the adult hermaphrodite, whose identity, position and connection with each other is well defined (White et al., 1986). This facilitates reproducibility in *in vivo* experiments. Many neurodegenerative genes of relevance in human diseases have ortholog genes in the *C. elegans*' genome and worms have also been employed for the expression of human genes. Thanks to its fast life cycle, *C. elegans* constitutes a relevant tool useful in the understanding of aspects of these multi-factorial diseases, such as Parkinson's, Alzheimer's or Huntington's diseases.

Parkinson's disease is a neurodegenerative disorder mainly characterized by locomotion deficits, the progressive loss of dopaminergic neurons and the accumulation

of protein inclusion bodies in the brain, named Lewy bodies, in which  $\alpha$ -synuclein ( $\alpha$ -syn) is the most abundant protein.  $\alpha$ -syn is a presynaptic protein encoded by the PARK1 locus whose multiplication or mutation results in the development of Parkinson's disease. PARK1 does not have an ortholog gene in *C. elegans* but the over-expression of the human gene in the worm has supposed a great advance in the characterization of the disease. This strain revealed how the progressive accumulation of misfolded  $\alpha$ -syn generates inclusion bodies when it is expressed in dopaminergic neurons (Lakso et al., 2003). Recently, the degradation of dopaminergic neurons due to the expression of deficient  $\alpha$ -syn has been related to lipid metabolism. Knockout strain for the *fat-6* and *fat-7* genes shows a lower degradation of dopaminergic neurons by the expression of  $\alpha$ -syn (Fanning et al., 2019). *fat-6* and *fat-7* encode desaturase protein and they are ortholog genes of human stearoyl-CoA-desaturase (SCD), which converts stearic acid to oleic acid. Thus, the inhibition of SCD may be a new target for the therapeutic treatment of this disease.

Alzheimer's disease is an age-associated neurological disorder characterized by progressive loss of memory, the loss of neurons in the neocortex, the accumulation of extracellular senile plaques in the brain, where  $\beta$ -amyloid peptide ( $A\beta$ ) is the primary component, and by the accumulation of intracellular neurofibrillary tangles (NFTs) which are composed of the microtubule-associated protein tau.  $A\beta$  is the result of the proteolytic breakdown of the amyloid precursor protein encoded by the *app* gene. *C. elegans* has a single APP-related gene, named *apl-1*, which is expressed in several cell types and modulates multiple metabolic pathways involved in development via DAF-16/FOXO (Ewald et al., 2012). Additionally, the transgenic expression of human  $\beta$ -amyloid ( $A\beta$ ) peptide in *C. elegans* under the muscle-specific *unc-54* promoter control, leads to the formation of amyloid deposits, which present similar characteristics to those found in human tissues (Link, 1995), making it possible to use *C. elegans* for the development and testing of new drugs against Alzheimer's disease.

*C. elegans* strains have also been developed for the study of Huntington's disease (HD). HD is a progressive neurological disorder where the expansion of huntingtin gene by several repetitions of CAG codon produces a misfolded polyglutamine (polyQ). The expression of N-terminal huntingtin fragments in ASH sensory neurons of *C. elegans* have generated a model of polyQ-mediated cellular toxicity which presents a behavior similar to the human disease (Faber et al., 1999). Studies with this strain suggest that mechanisms which involve  $\beta$ -catenin, sirtuin and

FOXO signaling protect from the early phases of mutant huntingtin toxicity (Parker et al., 2012).

#### **2.4.3. Muscle-associated diseases**

Duchenne muscular dystrophy is a human neuromuscular disease leading to a progressive necrosis of muscle cells due to the mutation in the dystrophin gene. *C. elegans* possesses a dystrophin-like gene (*dys-1*) encoding a protein showing the same structural features as human dystrophin (Bessou et al., 1998). Although there is no curative treatment for this disease, *C. elegans* is a valid model to find molecules which could palliate the degeneration of muscles. This is the case of prednisone, a steroid which reduced the number of degenerating cells in *C. elegans* assays by 40% (Gaud et al., 2004).

#### **2.4.4. Metabolic diseases**

*C. elegans* has also been employed as a model for complex metabolic disorders as obesity and type II diabetes since it possesses the evolutionary-conserved insulin-signaling pathway (Barbieri et al., 2003). There are several mutant strains of metabolism-related genes which facilitate the molecular and genetic study. In this sense, the knockout strain for *pme-1* gene, an ortholog for human PARP-1 (Poly [ADP-ribose] polymerase 1) has been related to hyperglycemia. Its pharmacological inhibition represents a new target for type II diabetes (Xia et al., 2018). As happens with *pme-1*, many genes of *C. elegans* are down or over-expressed due to the presence of high level of glucose and their study could elucidate the role of human orthologs in the type II diabetes (Zhu et al., 2016).

#### **2.4.5. Aging**

The above-mentioned insulin-like signaling pathway (IIS) has been deeply studied since it is involved in the control of several mechanisms. The most important target of these studies is the regulation of DAF-16, an ortholog of human Forkhead Box O (FOXO), a transcription factor which regulates the expression of genes involved in stress resistance, fat storage and metabolism, dauer formation and longevity (Sun et al., 2017). The IIS pathway is a signal transduction cascade (**Fig. 1.8**) where insulin-like peptides (ILPs) are ligands for the insulin/IGF-1 receptor DAF-2, an ortholog of the

mammalian insulin and insulin-like growth factor-1 (IGF-1) receptors (Kimura et al., 1997).

DAF-2 regulates the phosphorylation of a phosphoinositide 3-kinase (PI3K) by AGE-1 activation. PI3K acts on the Phosphoinositide-dependent kinase PDK-1, which activates serine/threonine kinases AKT-1, AKT-2 and SGK-1. AKTs and SGK-1 that phosphorylate and maintain DAF-16 in the cytosol, avoiding the translocation of DAF-16 to the nucleus. Therefore, knockout of upstream-DAF-16 genes or low activity rates of IIS pathway promote the translocation (Lin et al., 2001). Inside the nucleus, DAF-16 acts as a transcriptional factor, enhancing or avoiding the expression of several genes involved in aging (Sun et al., 2017).

SGK-1 can also phosphorylate SKN-1, an ortholog of the human transcription factor Nrf2 which regulates the detoxification response to oxidative stress. The phosphorylation of SKN-1 prevents its translocation to the nucleus, where it acts as transcription factor of genes involved in longevity when dephosphorylated (Blackwell et al., 2015). The translocation of dephosphorylated SKN-1 to the nucleus can also be promoted in response to oxidative stress by activating a mechanism different to the IIS longevity pathway (Tullet et al., 2017).

The activity of DAF-16 is not exclusive of the insulin-like signaling pathway. It is also regulated by cytokines or by exposure to environmental signals which produce stress by oxidation, ROS (reactive oxygen species) or heat. These signals can active the JNK-1 pathway, a signal transduction cascade involved in critical biological processes such as cancer, development, apoptosis and cell survival (Davis, 2000). Feeding also plays a role in the translocation of DAF-16 via TOR (target of rapamycin) pathway. Dietary restriction decreases the expression of TOR genes, increasing autophagy genes involved in longevity and dauer formation (Jia et al., 2004). Germline signals or AMP-activated protein kinase (AMPK) pathways have also been described as modulators of aging via DAF-16 (Sun et al., 2017) as well as SIR-2.1, a conserved deacetylase, which expands lifespan under stress conditions. SIR-2.1 binds to 14-3-3 proteins and DAF-16 to activate the transcription of DAF-16 target genes. The lifespan of *C. elegans* is increased by extra copies of SIR-2.1, showing SIR-2.1 a positive effect in the translocation of DAF-16 to the nucleus and the over-expression of longevity-involved genes (Berdichevsky et al., 2006).

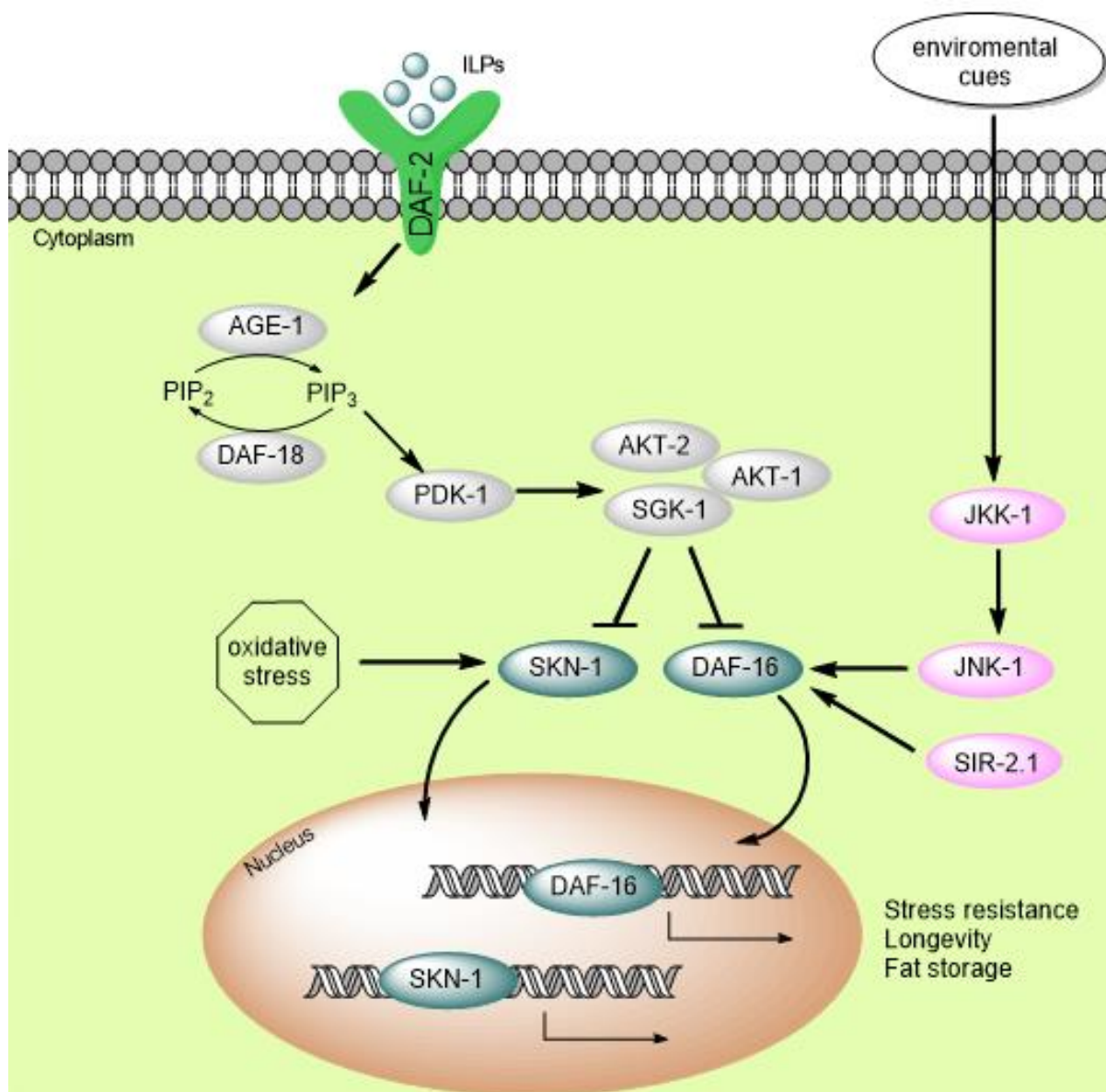


**Figure 1.8. Insulin-like signaling pathway of *C. elegans*.** The pathway presents a signaling cascade which, by dephosphorylation/phosphorylation, is involved in the translocation of DAF-16 and/or SKN-1 to the nucleus. DAF-16 and SKN-1 promote the expression of several genes related to stress resistance, longevity and fat storage. SIR-2.1 and JNK-1 are represented as examples for positive regulation of DAF-16. Oxidative stress is represented as a positive signal for SKN-1 activation.

Multiple studies have shown the effect of molecules which could potentially modulate the expression of these genes, promoting or decreasing the lifespan of *C. elegans*. Since it is a well-conserved route, lifespan of *C. elegans* is considered a useful parameter of relevance in preclinical assays to deepen into the knowledge of human aging processes and age-related illnesses. Thereby, bioactive compounds with high anti-aging potential have been studied in *C. elegans* as *in vivo* model. Some studies have reported that resveratrol increases the lifespan of *C. elegans* (Chen et al., 2013) and

similar results were obtained for other bioactive compounds such as the flavonoids myricetin, quercetin, kaempferol and naringenin (Grünz et al., 2012) or catechins from green tea extracts (Abbas and Wink, 2014). So far, no study has tested the *in vivo* effects of betalains in *C. elegans*, even though their *in vitro* effects as bioactive compounds are widely accepted.

## REFERENCES

- Abbas, S., Wink, M., 2014. Green tea extract induces the resistance of *Caenorhabditis elegans* against oxidative stress. *Antioxidants* 3, 129–143.  
<https://doi.org/10.3390/antiox3010129>
- Ahmadian, E., Khosroushahi, A.Y., Eghbal, M.A., Eftekhari, A., 2018. Betanin reduces organophosphate induced cytotoxicity in primary hepatocyte via an anti-oxidative and mitochondrial dependent pathway. *Pestic. Biochem. Physiol.* 144, 71–78.  
<https://doi.org/10.1016/j.pestbp.2017.11.009>
- Alard, D., Wray, V., Grotjahn, L., Reznik, H., Strack, D., 1985. Neobetanin: isolation and identification from *Beta vulgaris*. *Phytochemistry* 24, 2383–2385.  
[https://doi.org/10.1016/S0031-9422\(00\)83046-0](https://doi.org/10.1016/S0031-9422(00)83046-0)
- Allegra, M., De Cicco, P., Ercolano, G., Attanzio, A., Busà, R., Cirino, G., Tesoriere, L., Livrea, M.A., Ianaro, A., 2018. Indicaxanthin from *Opuntia Ficus Indica* (L. Mill) impairs melanoma cell proliferation, invasiveness, and tumor progression. *Phytomedicine* 50, 19–24. <https://doi.org/10.1016/j.phymed.2018.09.171>
- Allegra, M., Ianaro, A., Tersigni, M., Panza, E., Tesoriere, L., Livrea, M.A., 2014. Indicaxanthin from cactus pear fruit exerts anti-inflammatory effects in carrageenin-induced rat pleurisy. *J. Nutr.* 144, 185–192.  
<https://doi.org/10.3945/jn.113.183657>
- Arnold, K.E., Owens, I.P.F., Marshall, N.J., 2002. Fluorescent signaling in parrots. *Science*. 295, 92-92. <https://doi.org/10.1126/science.295.5552.92>
- Attanzio, A., Frazzitta, A., Busa, R., Tesoriere, L., Livrea, M.A., Allegra, M., 2019. Indicaxanthin from *Opuntia ficus indica* (L. Mill) inhibits oxidized LDL-mediated human endothelial cell dysfunction through inhibition of NF- $\kappa$ B activation. *Oxid. Med. Cell. Longev.* 3457846. <https://doi.org/10.1155/2019/3457846>
- Balamurali, G.S., Nicholls, E., Somanathan, H., Hempel de Ibarra, N., 2018. A comparative analysis of colour preferences in temperate and tropical social bees. *Sci. Nat.* 105, 8. <https://doi.org/10.1007/s00114-017-1531-z>
- Barbieri, M., Bonafè, M., Franceschi, C., Paolisso, G., 2003. Insulin/IGF-I-signaling pathway: An evolutionarily conserved mechanism of longevity from yeast to humans. *Am. J. Physiol. - Endocrinol. Metab.* 285, E1064-E1071.  
<https://doi.org/10.1152/ajpendo.00296.2003>
- Berdichevsky, A., Viswanathan, M., Horvitz, H.R., Guarente, L., 2006. *C. elegans* SIR-



- 2.1 interacts with 14-3-3 proteins to activate DAF-16 and extend life span. *Cell* 125, 1165–1177. <https://doi.org/10.1016/J.CELL.2006.04.036>
- Bessou, C., Giuglia, J.B., Franks, C.J., Holden-Dye, L., Ségalat, L., 1998. Mutations in the *Caenorhabditis elegans* dystrophin-like gene *dys-1* lead to hyperactivity and suggest a link with cholinergic transmission. *Neurogenetics* 2, 61–72. <https://doi.org/10.1007/s100480050053>
- Blackwell, T.K., Steinbaugh, M.J., Hourihan, J.M., Ewald, C.Y., Isik, M., 2015. SKN-1/Nrf, stress responses, and aging in *Caenorhabditis elegans*. *Free Radic. Biol. Med.* 88, 290–301. <https://doi.org/10.1016/j.freeradbiomed.2015.06.008>
- Brandt, E.E., Masta, S.E., 2017. Females are the brighter sex: Differences in external fluorescence across sexes and life stages of a crab spider. *PLoS One* 12, e0175667. <https://doi.org/10.1371/journal.pone.0175667>
- Brenner, S., 1974. The genetics of *Caenorhabditis elegans*. *Genetics* 77, 71–94.
- Brockington, S.F., Yang, Y., Gandia-Herrero, F., Covshoff, S., Hibberd, J.M., Sage, R.F., Wong, G.K.S., Moore, M.J., Smith, S.A., 2015. Lineage-specific gene radiations underlie the evolution of novel betalain pigmentation in Caryophyllales. *New Phytol.* 207, 1170–1180. <https://doi.org/10.1111/nph.13441>
- Büchi, G., Fliri, H., Shapiro, R., 1977. A Synthesis of Betalamic Acid. *J. Org. Chem.* <https://doi.org/10.1021/jo00432a048>
- Butera, D., Tesoriere, L., Di Gaudio, F., Bongiorno, A., Allegra, M., Pintaudi, A.M., Kohen, R., Livrea, M.A., 2002. Antioxidant activities of sicilian prickly pear (*Opuntia ficus indica*) fruit extracts and reducing properties of its betalains: Betanin and indicaxanthin. *J. Agric. Food Chem.* 50, 6895–6901. <https://doi.org/10.1021/jf025696p>
- Cabanes, J., Gandía-Herrero, F., Escribano, J., García-Carmona, F., Jiménez-Atiénzar, M., 2016. Fluorescent bioinspired protein labeling with betalamic acid. Derivatization and characterization of novel protein-betaxanthins. *Dye. Pigment.* 133, 458–466. <https://doi.org/10.1016/J.DYEPIG.2016.06.037>
- Cabanes, J., Gandía-Herrero, F., Escribano, J., García-Carmona, F., Jiménez-Atiénzar, M., 2014. One-step synthesis of betalains using a novel betalamic acid derivatized support. *J. Agric. Food Chem.* 62, 3776–3782. <https://doi.org/10.1021/jf500506y>
- Cassada, R.C., Russell, R.L., 1975. The dauerlarva, a post-embryonic developmental variant of the nematode *Caenorhabditis elegans*. *Dev. Biol.* 46, 326–342. [https://doi.org/10.1016/0012-1606\(75\)90109-8](https://doi.org/10.1016/0012-1606(75)90109-8)

- Chen, P.H., Lin, C., Guo, K.H., Yeh, Y.C., 2017. Development of a pigment-based whole-cell biosensor for the analysis of environmental copper. *RSC Adv.* 7, 29302–29305. <https://doi.org/10.1039/c7ra03778c>
- Chen, W., Rezaizadehnajafi, L., Wink, M., 2013. Influence of resveratrol on oxidative stress resistance and life span in *Caenorhabditis elegans*. *J. Pharm. Pharmacol.* 65, 682–688. <https://doi.org/10.1111/jphp.12023>
- Christinet, L., Burdet, F., Zaiko, M., Hinz, U., Zrýd, J.P., 2004. Characterization and functional identification of a novel plant 4,5-extradiol dioxygenase involved in betalain pigment biosynthesis in *Portulaca grandiflora*. *Plant Physiol* 134, 265–274. <https://doi.org/10.1104/pp.103.031914>
- Chung, H.-H., Schwinn, K.E., Ngo, H.M., Lewis, D.H., Massey, B., Calcott, K.E., Crowhurst, R., Joyce, D.C., Gould, K.S., Davies, K.M., Harrison, D.K., 2015. Characterisation of betalain biosynthesis in *Parakeelya* flowers identifies the key biosynthetic gene DOD as belonging to an expanded LigB gene family that is conserved in betalain-producing species. *Front. Plant Sci.* 6, 499–515. <https://doi.org/10.3389/fpls.2015.00499>
- Clement, J.S., Mabry, T.J., 1996. Pigment evolution in the caryophyllales: A systematic overview. *Bot. Acta.* 109(5), 360-367 <https://doi.org/10.1111/j.1438-8677.1996.tb00584.x>
- Culetto, E., 2000. A role for *Caenorhabditis elegans* in understanding the function and interactions of human disease genes. *Hum. Mol. Genet.* 9, 869–877. <https://doi.org/10.1093/hmg/9.6.869>
- Davis, R.J., 2000. Signal transduction by the JNK group of MAP kinases. *Inflammatory Processes.* 13-21. [https://doi.org/10.1016/S0092-8674\(00\)00116-1](https://doi.org/10.1016/S0092-8674(00)00116-1)
- DeLoache, W.C., Russ, Z.N., Narcross, L., Gonzales, A.M., Martin, V.J.J., Dueber, J.E., 2015. An enzyme-coupled biosensor enables (S)-reticuline production in yeast from glucose. *Nat. Chem. Biol.* 11, 465–471. <https://doi.org/10.1038/nchembio.1816>
- Ersus, S., Yurdagel, U., 2007. Microencapsulation of anthocyanin pigments of black carrot (*Daucus carota* L.) by spray drier. *J. Food Eng.* 80, 805–812. <https://doi.org/10.1016/J.JFOODENG.2006.07.009>
- Escribano, J., Cabanes, J., Jiménez-Atiénzar, M., Ibañez-Tremolada, M., Gómez-Pando, L.R., García-Carmona, F., Gandía-Herrero, F., 2017. Characterization of betalains, saponins and antioxidant power in differently colored quinoa (*Chenopodium*

- quinoa*) varieties. Food Chem. 234, 285–294.  
<https://doi.org/10.1016/j.foodchem.2017.04.187>
- Escribano, J., Pedreño, M.A., García-Carmona, F., Muñoz, R., 1998. Characterization of the antiradical activity of betalains from *Beta vulgaris* L. roots. Phytochem. Anal. 9, 124–127. [https://doi.org/10.1002/\(SICI\)1099-1565\(199805/06\)9:3<124::AID-PCA401>3.0.CO;2-0](https://doi.org/10.1002/(SICI)1099-1565(199805/06)9:3<124::AID-PCA401>3.0.CO;2-0)
- Ewald, C.Y., Raps, D.A., Li, C., 2012. APL-1, the Alzheimer's amyloid precursor protein in *Caenorhabditis elegans*, modulates multiple metabolic pathways throughout development. Genetics 191, 493–507.  
<https://doi.org/10.1534/genetics.112.138768>
- Faber, P.W., Alter, J.R., Macdonald, M.E., Hart, A.C., 1999. Polyglutamine-mediated dysfunction and apoptotic death of a *Caenorhabditis elegans* sensory neuron. Proc. Natl. Acad. Sci. U. S. A. 96, 179–184. <https://doi.org/10.1073/pnas.96.1.179>
- Fanning, S., Haque, A., Imberdis, T., Baru, V., Barrasa, M.I., Nuber, S., Termine, D., Ramalingam, N., Ho, G.P.H., Noble, T., Sandoe, J., Lou, Y., Landgraf, D., Freyzon, Y., Newby, G., Soldner, F., Terry-Kantor, E., Kim, T.E., Hofbauer, H.F., Becuwe, M., Jaenisch, R., Pincus, D., Clish, C.B., Walther, T.C., Farese, R. V., Srinivasan, S., Welte, M.A., Kohlwein, S.D., Dettmer, U., Lindquist, S., Selkoe, D., 2019. Lipidomic analysis of  $\alpha$ -synuclein neurotoxicity identifies stearyl CoA desaturase as a target for parkinson treatment. Mol. Cell 73, 1001-1014.e8.  
<https://doi.org/10.1016/j.molcel.2018.11.028>
- Felker, P., Stintzing, F.C., Müssig, E., Leitenberger, M., Carle, R., Vogt, T., Bunch, R., 2008. Colour inheritance in cactus pear (*Opuntia ficus-indica*) fruits. Ann. Appl. Biol. 152, 307–318. <https://doi.org/10.1111/j.1744-7348.2008.00222.x>
- Fischer, N., Dreiding, A.S., 1972. Biosynthesis of betalaines. On the cleavage of the aromatic ring during the enzymatic transformation of dopa into betalamic acid. Helv. Chim. Acta 55, 649–658. <https://doi.org/10.1002/hlca.19720550240>
- Gandía-Herrero, F., Cabanes, J., Escribano, J., García-Carmona, F., Jiménez-Atiénzar, M., 2013. Encapsulation of the most potent antioxidant betalains in edible matrixes as powders of different colors. J. Agric. Food Chem. 61, 4294–4302.  
<https://doi.org/10.1021/jf400337g>
- Gandía-Herrero, F., Escribano, J., García-Carmona, F., 2016. Biological activities of plant pigment betalains. Crit. Rev. Food Sci. Nutr. 56, 937–945.  
<https://doi.org/10.1080/10408398.2012.740103>

- Gandía-Herrero, F., Escribano, J., García-Carmona, F., 2012. Purification and antiradical properties of the structural unit of betalains. *J. Nat. Prod.* 75, 1030–1036. <https://doi.org/10.1021/np200950n>
- Gandía-Herrero, F., Escribano, J., García-Carmona, F., 2010. Structural implications on color, fluorescence, and antiradical activity in betalains. *Planta* 232, 449–460. <https://doi.org/10.1007/s00425-010-1191-0>
- Gandía-Herrero, F., Escribano, J., García-Carmona, F., 2009. The role of phenolic hydroxy groups in the free radical scavenging activity of betalains. *J. Nat. Prod.* 72, 1142–1146. <https://doi.org/10.1021/np900131r>
- Gandía-Herrero, F., Escribano, J., García-Carmona, F., 2007. Characterization of the activity of tyrosinase on betanidin. *J. Agric. Food Chem.* 55, 1546–1551. <https://doi.org/10.1021/jf062858z>
- Gandía-Herrero, F., Escribano, J., García-Carmona, F., 2005a. Betaxanthins as pigments responsible for visible fluorescence in flowers. *Planta* 222, 586–593. <https://doi.org/10.1007/s00425-005-0004-3>
- Gandía-Herrero, F., Escribano, J., García-Carmona, F., 2005b. Betaxanthins as substrates for tyrosinase. An approach to the role of tyrosinase in the biosynthetic pathway of betalains. *Plant Physiol.* 138, 421–432. <https://doi.org/10.1104/pp.104.057992>
- Gandía-Herrero, F., García-Carmona, F., 2014. *Escherichia coli* protein YgiD produces the structural unit of plant pigments betalains: Characterization of a prokaryotic enzyme with DOPA-extradiol-dioxygenase activity. *Appl. Microbiol. Biotechnol.* 98, 1165–1174. <https://doi.org/10.1007/s00253-013-4961-3>
- Gandía-Herrero, F., García-Carmona, F., 2013. Biosynthesis of betalains: yellow and violet plant pigments. *Trends Plant Sci.* 18, 334–343. <https://doi.org/10.1016/j.tplants.2013.01.003>
- Gandía-Herrero, F., García-Carmona, F., 2012. Characterization of recombinant *Beta vulgaris* 4,5-DOPA-extradiol-dioxygenase active in the biosynthesis of betalains. *Planta* 236, 91–100. <https://doi.org/10.1007/s00425-012-1593-2>
- Gandía-Herrero, F., García-Carmona, F., Escribano, J., 2006. Development of a protocol for the semi-synthesis and purification of betaxanthins. *Phytochem. Anal.* 17, 262–269. <https://doi.org/10.1002/pca.909>
- Gandía-Herrero, F., García-Carmona, F., Escribano, J., 2005c. Fluorescent pigments: New perspectives in betalain research and applications. *Food Res. Int.* 38, 879–

884. <https://doi.org/10.1016/J.FOODRES.2005.01.012>
- Gandía-Herrero, F., García-Carmona, F., Escribano, J., 2005d. Floral fluorescence effect. *Nature* 437, 334. <https://doi.org/10.1038/437334a>
- Gandía-Herrero, F., García-Carmona, F., Escribano, J., 2005e. A novel method using high-performance liquid chromatography with fluorescence detection for the determination of betaxanthins. *J. Chromatogr. A* 1078, 83–89. <https://doi.org/10.1016/j.chroma.2005.05.013>
- Gandía-Herrero, F., García-Carmona, F., Escribano, J., 2004. Purification and characterization of a latent polyphenol oxidase from beet root (*Beta vulgaris* L.). *J. Agric. Food Chem.* 52, 609–615. <https://doi.org/10.1021/jf034381m>
- Gandía-Herrero, F., Jiménez-Atiénzar, M., Cabanes, J., Escribano, J., García-Carmona, F., 2009b. Fluorescence detection of tyrosinase activity on dopamine-betaxanthin purified from *Portulaca oleracea* (common purslane) flowers. *J. Agric. Food Chem.* 57, 2523–2528. <https://doi.org/10.1021/jf803608x>
- Gandía-Herrero, F., Jiménez-Atiénzar, M., Cabanes, J., García-Carmona, F., Escribano, J., 2010b. Stabilization of the bioactive pigment of *Opuntia* fruits through maltodextrin encapsulation. *J. Agric. Food Chem.* 58, 10646–10652. <https://doi.org/DOI:10.1021/jf101695f>
- García-Plazaola, J.I., Fernández-Marín, B., Duke, S.O., Hernández, A., López-Arbeloa, F., Becerril, J.M., 2015. Autofluorescence: Biological functions and technical applications. *Plant Sci.* 236, 136–145. <https://doi.org/10.1016/J.PLANTSCI.2015.03.010>
- Gaud, A., Simon, J.M., Witzel, T., Carre-Pierrat, M., Wermuth, C.G., Ségalat, L., 2004. Prednisone reduces muscle degeneration in dystrophin-deficient *Caenorhabditis elegans*. *Neuromuscul. Disord.* 14, 365–370. <https://doi.org/10.1016/j.nmd.2004.02.011>
- Golden, J.W., Riddle, D.L., 1984. The *Caenorhabditis elegans* dauer larva: Developmental effects of pheromone, food, and temperature. *Dev. Biol.* 102, 368–378. [https://doi.org/10.1016/0012-1606\(84\)90201-X](https://doi.org/10.1016/0012-1606(84)90201-X)
- Gonçalves, L.C.P., Tonelli, R.R., Bagnaresi, P., Mortara, R.A., Ferreira, A.G., Bastos, E.L., 2013. A nature-inspired betalamic probe for live-cell imaging of Plasmodium-infected erythrocytes. *PLoS One* 8, e53874. <https://doi.org/10.1371/journal.pone.0053874>
- Grewal, P.S., Modavi, C., Russ, Z.N., Harris, N.C., Dueber, J.E., 2018. Bioproduction

- of a betalain color palette in *Saccharomyces cerevisiae*. *Metab. Eng.* 45, 180–188.  
<https://doi.org/10.1016/j.ymben.2017.12.008>
- Grünz, G., Haas, K., Soukup, S., Klingenspor, M., Kulling, S.E., Daniel, H., Spanier, B., 2012. Structural features and bioavailability of four flavonoids and their implications for lifespan-extending and antioxidant actions in *C. elegans*. *Mech. Ageing Dev.* 133, 1–10. <https://doi.org/10.1016/j.mad.2011.11.005>
- Guadarrama-Flores, B., Rodriguez-Monroy, M., Cruz-Sosa, F., García-Carmona, F., Gandía-Herrero, F., 2015. Production of dihydroxylated betalains and dopamine in cell suspension cultures of *Celosia argentea* var. *plumosa*. *J. Agric. Food Chem.* 63, 2741–2749. <https://doi.org/10.1021/acs.jafc.5b00065>
- Guerrero-Rubio, M.A., Hernández-García, S., García-Carmona, F., Gandía-Herrero, F., 2019. Extension of life-span using a RNAi model and *in vivo* antioxidant effect of *Opuntia* fruit extracts and pure betalains in *Caenorhabditis elegans*. *Food Chem.* 274, 840–847. <https://doi.org/10.1016/j.foodchem.2018.09.067>
- Guesmi, A., Hamadi, N. Ben, Ladhari, N., Saidi, F., Maaref, H., Sakli, F., 2013. Spectral characterization of wool fabric dyed with indicaxanthin natural dye: Study of the fluorescence property. *Ind. Crops Prod.* 46, 264–267.  
<https://doi.org/10.1016/j.indcrop.2013.01.029>
- Haddock, S.H.D., Dunn, C.W., 2015. Fluorescent proteins function as a prey attractant: experimental evidence from the hydromedusa *Olindias formosus* and other marine organisms. *Biol. Open* 4, 1094–1104. <https://doi.org/10.1242/bio.012138>
- Harris, N.N., Javellana, J., Davies, K.M., Lewis, D.H., Jameson, P.E., Deroles, S.C., Calcott, K.E., Gould, K.S., Schwinn, K.E., 2012. Betalain production is possible in anthocyanin-producing plant species given the presence of DOPA-dioxygenase and L-DOPA. *BMC Plant Biol.* 12, 34. <https://doi.org/10.1186/1471-2229-12-34>
- Hatlestad, G.J., Sunnadeniya, R.M., Akhavan, N.A., Gonzalez, A., Goldman, I.L., McGrath, J.M., Lloyd, A.M., 2012. The beet R locus encodes a new cytochrome P450 required for red betalain production. *Nat. Genet.* 44, 816–820.  
<https://doi.org/10.1038/ng.2297>
- Hawkins, K.M., Smolke, C.D., 2008. Production of benzyloquinoline alkaloids in *Saccharomyces cerevisiae*. *Nat. Chem. Biol.* 4, 564–573.  
<https://doi.org/10.1038/nchembio.105>
- He, J., Siddique, F., Lischka, H., Quina, F.H., Aquino, A.J.A., 2019. Conical intersections and the weak fluorescence of betalains. *Photochem. Photobiol. Sci.*

- 18, 1972–1981. <https://doi.org/10.1039/c9pp00131j>
- Hempel, J., Böhm, H., 1997. Betaxanthin pattern of hairy roots from *Beta vulgaris* var. lutea and its alteration by feeding of amino acids. *Phytochemistry* 44, 847–852. [https://doi.org/10.1016/S0031-9422\(96\)00633-4](https://doi.org/10.1016/S0031-9422(96)00633-4)
- Heuer, S., Richter, S., Metzger, J.W., Wray, V., Nimtzt, M., Strack, D., 1994. Betacyanins from bracts of *Bougainvillea glabra*. *Phytochemistry* 37, 761–767. [https://doi.org/10.1016/S0031-9422\(00\)90354-6](https://doi.org/10.1016/S0031-9422(00)90354-6)
- Huang, A.S., von Elbe, J.H., 1987. Effect of pH on the degradation and regeneration of betanine. *J. Food Sci.* 52, 1689–1693. <https://doi.org/10.1111/j.1365-2621.1987.tb05907.x>
- Huang, A.S., von Elbe, J.H., 1986. Stability comparison of two betacyanine pigments — amaranthine and betanine. *J. Food Sci.* 51, 670–674. <https://doi.org/10.1111/j.1365-2621.1986.tb13908.x>
- Huang, A.S., Von Elbe, J.H., 1985. Kinetics of the degradation and regeneration of betanine. *J. Food Sci.* 50, 1115–1120. <https://doi.org/10.1111/j.1365-2621.1985.tb13024.x>
- Ibrahim, B., Sowemimo, A., Van Rooyen, A., Van De Venter, M., 2012. Antiinflammatory, analgesic and antioxidant activities of *Cyathula prostrata* (Linn.) Blume (Amaranthaceae). *J. Ethnopharmacol.* 141, 282–289. <https://doi.org/10.1016/j.jep.2012.02.032>
- Imamura, T., Takagi, H., Miyazato, A., Ohki, S., Mizukoshi, H., Mori, M., 2018. Isolation and characterization of the betalain biosynthesis gene involved in hypocotyl pigmentation of the allotetraploid *Chenopodium quinoa*. *Biochem. Biophys. Res. Commun.* 496, 280–286. <https://doi.org/10.1016/j.bbrc.2018.01.041>
- Iriel, A., Lagorio, M.G., 2010. Is the flower fluorescence relevant in biocommunication? *Naturwissenschaften* 97, 915–924. <https://doi.org/10.1007/s00114-010-0709-4>
- Jia, K., Chen, D., Riddle, D.L., 2004. The TOR pathway interacts with the insulin signaling pathway to regulate *C. elegans* larval development, metabolism and life span. *Development* 131, 3897–3906. <https://doi.org/10.1242/dev.01255>
- Kaletta, T., Hengartner, M.O., 2006. Finding function in novel targets: *C. elegans* as a model organism. *Nat. Rev. Drug Discov.* 5(5), 387–399. <https://doi.org/10.1038/nrd2031>
- Kapadia, G.J., Azuine, M.A., Sridhar, R., Okuda, Y., Tsuruta, A., Ichiishi, E.,

- Mukainake, T., Takasaki, M., Konoshima, T., Nishino, H., Tokuda, H., 2003. Chemoprevention of DMBA-induced UV-B promoted, NOR-1-induced TPA promoted skin carcinogenesis, and DEN-induced phenobarbital promoted liver tumors in mice by extract of beetroot. *Pharmacol. Res.* 47, 141–148. [https://doi.org/10.1016/S1043-6618\(02\)00285-2](https://doi.org/10.1016/S1043-6618(02)00285-2)
- Khan, M.I., Sri Harsha, P.S.C., Giridhar, P., Ravishankar, G.A., 2012. Pigment identification, nutritional composition, bioactivity, and in vitro cancer cell cytotoxicity of *Rivina humilis* L. berries, potential source of betalains. *LWT - Food Sci. Technol.* 47, 315–323. <https://doi.org/10.1016/j.lwt.2012.01.025>
- Kimble, J., Hirsh, D., 1979. The postembryonic cell lineages of the hermaphrodite and male gonads in *Caenorhabditis elegans*. *Dev. Biol.* 70, 396–417. [https://doi.org/10.1016/0012-1606\(79\)90035-6](https://doi.org/10.1016/0012-1606(79)90035-6)
- Kimura, K.D., Tissenbaum, H.A., Liu, Y., Ruvkun, G., 1997. Daf-2, an insulin receptor-like gene that regulates longevity and diapause in *Caenorhabditis elegans*. *Science* (80-. ). 277, 942–946. <https://doi.org/10.1126/science.277.5328.942>
- Kobayashi, N., Schmidt, J., Wray, V., Schliemann, W., 2001. Formation and occurrence of dopamine-derived betacyanins. *Phytochemistry* 56, 429–436. [https://doi.org/10.1016/S0031-9422\(00\)00383-6](https://doi.org/10.1016/S0031-9422(00)00383-6)
- Kubin, R.F., Fletcher, A.N., 1982. Fluorescence quantum yields of some rhodamine dyes. *J. Lumin.* 27, 455–462. [https://doi.org/10.1016/0022-2313\(82\)90045-X](https://doi.org/10.1016/0022-2313(82)90045-X)
- Kugler, F., Stintzing, F.C., Carle, R., 2004. Identification of betalains from petioles of differently colored swiss chard (*Beta vulgaris* L. ssp. *cicla* [L.] Alef. Cv. Bright Lights) by high-performance liquid chromatography-electrospray ionization mass spectrometry. *J. Agric. Food Chem.* 52, 2975–2981. <https://doi.org/10.1021/jf035491w>
- Kyriakakis, E., Markaki, M., Tavernarakis, N., 2015. *Caenorhabditis elegans* as a model for cancer research. *Mol. Cell. Oncol.* 2(2), e975027. <https://doi.org/10.4161/23723556.2014.975027>
- Lagorio, M.G., Cordon, G.B., Iriel, A., 2015. Reviewing the relevance of fluorescence in biological systems. *Photochem. Photobiol. Sci.* 14, 1538–1559. <https://doi.org/10.1039/C5PP00122F>
- Lakso, M., Vartiainen, S., Moilanen, A.M., Sirviö, J., Thomas, J.H., Nass, R., Blakely, R.D., Wong, G., 2003. Dopaminergic neuronal loss and motor deficits in *Caenorhabditis elegans* overexpressing human  $\alpha$ -synuclein. *J. Neurochem.* 86,



- 165–172. <https://doi.org/10.1046/j.1471-4159.2003.01809.x>
- Lechner, J.F., Wang, L.-S., Rocha, C.M., Larue, B., Henry, C., McIntyre, C.M., Riedl, K.M., Schwartz, S.J., Stoner, G.D., 2010. Drinking water with red beetroot food color antagonizes esophageal carcinogenesis in N-nitrosomethylbenzylamine-treated rats. *J. Med. Food* 13, 733–739. <https://doi.org/10.1089/jmf.2008.0280>
- Lemos, M.A., Sárníková, K., Bot, F., Anese, M., Hungerford, G., 2015. Use of time-resolved fluorescence to monitor bioactive compounds in plant based foodstuffs. *Biosensors*. <https://doi.org/10.3390/bios5030367>
- Liebisch, H.W., Matschiner, B., Schutte, H.R., 1969. Beitrage zur Physiologie und Biosynthese des Betanins. *Zeitschrift fur Pflanzenphysiologie* 61, 269–278.
- Lin, K., Hsin, H., Libina, N., Kenyon, C., 2001. Regulation of the *Caenorhabditis elegans* longevity protein DAF-16 by insulin/IGF-1 and germline signaling. *Nat. Genet.* 28, 139–145. <https://doi.org/10.1038/88850>
- Link, C.D., 1995. Expression of human  $\beta$ -amyloid peptide in transgenic *Caenorhabditis elegans*. *Proc. Natl. Acad. Sci. U. S. A.* 92, 9368–9372. <https://doi.org/10.1073/pnas.92.20.9368>
- Mahajan-Miklos, S., Tan, M.W., Rahme, L.G., Ausubel, F.M., 1999. Molecular mechanisms of bacterial virulence elucidated using a *Pseudomonas aeruginosa*-*Caenorhabditis elegans* pathogenesis model. *Cell* 96, 47–56. [https://doi.org/10.1016/S0092-8674\(00\)80958-7](https://doi.org/10.1016/S0092-8674(00)80958-7)
- Mao, J., Liu, Q., Li, Y., Yang, J., Song, X., Liu, X., Xu, H., Qiao, M., 2018. A high-throughput method for screening of L-tyrosine high-yield strains by *Saccharomyces cerevisiae*. *J. Gen. Appl. Microbiol.* 64, 198–201. <https://doi.org/10.2323/jgam.2017.12.001>
- Marshall, J., Johnsen, S., 2017. Fluorescence as a means of colour signal enhancement. *Philos. Trans. R. Soc. Lond. B. Biol. Sci.* 372, 20160335. <https://doi.org/10.1098/rstb.2016.0335>
- Mercuri, A., Sacchetti, A., De Benedetti, L.D., Schiva, T., Alberti, S., 2001. Green fluorescent flowers. *Plant Sci.* 161, 961–968. [https://doi.org/10.1016/S0168-9452\(01\)00497-6](https://doi.org/10.1016/S0168-9452(01)00497-6)
- Mori, S., Fukui, H., Oishi, M., Sakuma, M., Kawakami, M., Tsukioka, J., Goto, K., Hirai, N., 2018. Biocommunication between plants and pollinating insects through fluorescence of pollen and anthers. *J. Chem. Ecol.* 44, 591–600. <https://doi.org/10.1007/s10886-018-0958-9>

- Mueller, L.A., Hinz, U., Zryd, J.-P., 1997. The formation of betalamic acid and muscaflavin by recombinant dopa-dioxygenase from *Amanita*. *Phytochemistry* 44, 567–569. [https://doi.org/10.1016/S0031-9422\(96\)00625-5](https://doi.org/10.1016/S0031-9422(96)00625-5)
- Musso, H., 1979. The pigments of fly agaric, *Amanita muscaria*. *Tetrahedron* 35, 2843–2853.
- Niziński, S., Popena, Ł., Rode, M.F., Kumorkiewicz, A., Fojud, Z., Paluch-Lubawa, E., Wybraniec, S., Burdziński, G., 2019. Structural studies on the stereoisomerism of a natural dye miraxanthin I. *New J. Chem.* 43(46), 18165–18174. <https://doi.org/10.1039/C9NJ04215F>
- Nizinski, S., Wendel, M., Rode, M.F., Prukała, D., Sikorski, M., Wybraniec, S., Burdziński, G., 2017. Photophysical properties of betaxanthins: miraxanthin V – insight into the excited-state deactivation mechanism from experiment and computations. *RSC Adv.* 7, 6411–6421. <https://doi.org/10.1039/C6RA28110A>
- Ostoverkhova, O., Galindo, G., Lande, C., Kirby, J., Scherr, M., Hoffman, G., Rao, S., 2018. Understanding innate preferences of wild bee species: responses to wavelength-dependent selective excitation of blue and green photoreceptor types. *J. Comp. Physiol. A* 204, 667–675. <https://doi.org/10.1007/s00359-018-1269-x>
- Parker, A.R., 2002. Fluorescence of yellow budgerigars. *Science*. 296, 655–655. <https://doi.org/10.1126/science.296.5568.655b>
- Parker, J.A., Vazquez-Manrique, R.P., Tourette, C., Farina, F., Offner, N., Mukhopadhyay, A., Orfila, A.M., Darbois, A., Menet, S., Tissenbaum, H.A., Neri, C., 2012. Integration of  $\beta$ -catenin, sirtuin, and FOXO signaling protects from mutant Huntingtin Toxicity. *J. Neurosci.* 32, 12630–22640. <https://doi.org/10.1523/JNEUROSCI.0277-12.2012>
- Pedreño, M.A., Escribano, J., 2001. Correlation between antiradical activity and stability of betanine from *Beta vulgaris* L roots under different pH, temperature and light conditions. *J. Sci. Food Agric.* 81, 627–631. <https://doi.org/10.1002/jsfa.851>
- Piattelli, M., 1981. The betalains: structure, biosynthesis, and chemical taxonomy. In: Conn, E.E., Ed., *The Biochemistry of Plants*, Vol. 7, Academic Press, New York, 557–575.
- Piattelli, M., Minale, L., Nicolaus, R.A., 1965a. Pigments of centrospermae-V: Betaxanthins from *Mirabilis jalapa* L. *Phytochemistry* 4, 817–823. [https://doi.org/10.1016/S0031-9422\(00\)86258-5](https://doi.org/10.1016/S0031-9422(00)86258-5)

- Piattelli, M., Minale, L., Prota, G., 1965b. Pigments of centrospermae—III. : Betaxanthins from *Beta vulgaris* L. *Phytochemistry* 4, 121–125. [https://doi.org/10.1016/S0031-9422\(00\)86153-1](https://doi.org/10.1016/S0031-9422(00)86153-1)
- Piattelli, M., Minale, L., Prota, G., 1964. Isolation, structure and absolute configuration of indicaxanthin. *Tetrahedron* 20, 2325–2329. [https://doi.org/10.1016/S0040-4020\(01\)97621-5](https://doi.org/10.1016/S0040-4020(01)97621-5)
- Plowright, C.M.S., Bridger, J.J.M., Xu, V., Herlehy, R.A., Collin, C.A., 2017. Floral guidance of learning a preference for symmetry by bumblebees. *Anim. Cogn.* 20, 1115–1127. <https://doi.org/10.1007/s10071-017-1128-0>
- Polturak, G., Breitel, D., Grossman, N., Sarrion-Perdigones, A., Weithorn, E., Pliner, M., Orzaez, D., Granell, A., Rogachev, I., Aharoni, A., 2016. Elucidation of the first committed step in betalain biosynthesis enables the heterologous engineering of betalain pigments in plants. *New Phytol.* 210, 269–283. <https://doi.org/10.1111/nph.13796>
- Polturak, G., Grossman, N., Vela-Corcía, D., Dong, Y., Nudel, A., Pliner, M., Levy, M., Rogachev, I., Aharoni, A., 2017. Engineered gray mold resistance, antioxidant capacity, and pigmentation in betalain-producing crops and ornamentals. *Proc. Natl. Acad. Sci.* 114, 201707176. <https://doi.org/10.1073/pnas.1707176114>
- Polturak, G., Heinig, U., Grossman, N., Battat, M., Leshkowitz, D., Malitsky, S., Rogachev, I., Aharoni, A., 2018. Transcriptome and metabolic profiling provides insights into betalain biosynthesis and evolution in *Mirabilis jalapa*. *Mol. Plant* 11, 189–204. <https://doi.org/10.1016/j.molp.2017.12.002>
- Rabasović, M.S., Šević, D., Terzić, M., Marinković, B.P., 2012. Comparison of beetroot extracts originating from several sites using time-resolved laser-induced fluorescence spectroscopy. *Phys. Scr.* T149, 014076. <https://doi.org/10.1088/0031-8949/2012/T149/014076>
- Raizen, D.M., Zimmerman, J.E., Maycock, M.H., Ta, U.D., You, Y.J., Sundaram, M. V., Pack, A.I., 2008. Lethargus is a *Caenorhabditis elegans* sleep-like state. *Nature* 451, 569–572. <https://doi.org/10.1038/nature06535>
- Rao, S., Ostroverkhova, O., 2015. Visual outdoor response of multiple wild bee species: highly selective stimulation of a single photoreceptor type by sunlight-induced fluorescence. *J. Comp. Physiol. A* 201, 705–716. <https://doi.org/10.1007/s00359-015-0983-x>
- Rocha, G.A., Fávaro-Trindade, C.S., Grosso, C.R.F., 2012. Microencapsulation of

- lycopene by spray drying: Characterization, stability and application of microcapsules. *Food Bioprod. Process.* 90, 37–42.  
<https://doi.org/10.1016/j.fbp.2011.01.001>
- Rodrigues, A.C.B., Mariz, I. de F.A., Maçoas, E.M.S., Tonelli, R.R., Martinho, J.M.G., Quina, F.H., Bastos, E.L., 2018. Bioinspired water-soluble two-photon fluorophores. *Dye. Pigment.* 150, 105–111.  
<https://doi.org/10.1016/j.dyepig.2017.11.020>
- Sánchez-Diener, I., Zamorano, L., López-Causapé, C., Cabot, G., Mulet, X., Peña, C., Del Campo, R., Cantón, R., Doménech-Sánchez, A., Martínez-Martínez, L., Arcos, S.C., Navas, A., Oliver, A., 2017. Interplay among resistance profiles, high-risk clones, and virulence in the *Caenorhabditis elegans Pseudomonas aeruginosa* infection model. *Antimicrob. Agents Chemother.* 61(12), e01586-17.  
<https://doi.org/10.1128/AAC.01586-17>
- Sasaki, N., Abe, Y., Goda, Y., Adachi, T., Kasahara, K., Ozeki, Y., 2009. Detection of DOPA 4,5-dioxygenase (DOD) activity using recombinant protein prepared from *Escherichia coli* cells harboring cDNA encoding DOD from *Mirabilis jalapa*. *Plant Cell Physiol.* 50, 1012–1016. <https://doi.org/10.1093/pcp/pcp053>
- Sasaki, N., Adachi, T., Koda, T., Ozeki, Y., 2004. Detection of UDP-glucose:cyclo-DOPA 5-O-glucosyltransferase activity in four o'clocks (*Mirabilis jalapa* L.). *FEBS Lett.* 568, 159–162. <https://doi.org/10.1016/j.febslet.2004.04.097>
- Schliemann, W., Kobayashi, N., Strack, D., 1999. The decisive step in betaxanthin biosynthesis is a spontaneous reaction. *Plant Physiol.* 119, 1217–1232.  
<https://doi.org/10.1104/pp.119.4.1217>
- Schwartz, S.J., von Elbe, J.H., 1983. Identification of betanin degradation products. *Z. Lebensm. Unters. Forsch.* 176, 448–453. <https://doi.org/10.1007/BF01042560>
- Schwinn, K.E., 2016. The dope on L-DOPA formation for betalain pigments. *New Phytol.* 210, 6–9. <https://doi.org/10.1111/nph.13901>
- Sifri, C.D., Begun, J., Ausubel, F.M., 2005. The worm has turned - microbial virulence modeled in *Caenorhabditis elegans*. *Trends Microbiol.* 13(3), 119–127.  
<https://doi.org/10.1016/j.tim.2005.01.003>
- Sreekanth, D., Arunasree, M.K., Roy, K.R., Chandramohan Reddy, T., Reddy, G. V., Reddanna, P., 2007. Betanin a betacyanin pigment purified from fruits of *Opuntia ficus-indica* induces apoptosis in human chronic myeloid leukemia cell line-K562. *Phytomedicine* 14, 739–746. <https://doi.org/10.1016/j.phymed.2007.03.017>

- Steglich, W., Strack, D., 1990. Betalains. *Alkaloids Chem. Pharmacol.* 39, 1–62.  
[https://doi.org/10.1016/S0099-9598\(08\)60163-7](https://doi.org/10.1016/S0099-9598(08)60163-7)
- Stiernagle, T., 2006. Maintenance of *C. elegans*. In *WormBook*. Ed. The *C. elegans* research community, *WormBook*, doi/10.1895/wormbook.1.101.1,  
<http://www.wormbook.org>.
- Stintzing, F.C., Carle, R., 2004. Functional properties of anthocyanins and betalains in plants, food, and in human nutrition. *Trends Food Sci. Technol.* 15, 19–38.  
<https://doi.org/10.1016/J.TIFS.2003.07.004>
- Stintzing, F.C., Schieber, A., Carle, R., 2002. Betacyanins in fruits from red-purple pitaya, *Hylocereus polyrhizus* (Weber) Britton & Rose. *Food Chem.* 77, 101–106.  
[https://doi.org/10.1016/S0308-8146\(01\)00374-0](https://doi.org/10.1016/S0308-8146(01)00374-0)
- Strack, D., Vogt, T., Schliemann, W., 2003. Recent advances in betalain research. *Phytochemistry*. 62(3), 247–269. [https://doi.org/10.1016/S0031-9422\(02\)00564-2](https://doi.org/10.1016/S0031-9422(02)00564-2)
- Sulston, J.E., Albertson, D.G., Thomson, J.N., 1980. The *Caenorhabditis elegans* male: Postembryonic development of nongonadal structures. *Dev. Biol.* 78, 542–576.  
[https://doi.org/10.1016/0012-1606\(80\)90352-8](https://doi.org/10.1016/0012-1606(80)90352-8)
- Sulston, J.E., Horvitz, H.R., 1977. Post-embryonic cell lineages of the nematode, *Caenorhabditis elegans*. *Dev. Biol.* 56, 110–156. [https://doi.org/10.1016/0012-1606\(77\)90158-0](https://doi.org/10.1016/0012-1606(77)90158-0)
- Sun, X., Chen, W.-D., Wang, Y.-D., 2017. DAF-16/FOXO transcription factor in aging and longevity. *Front. Pharmacol.* 8, 548. <https://doi.org/10.3389/fphar.2017.00548>
- Sunnadeniya, R., Bean, A., Brown, M., Akhavan, N., Hatlestad, G., Gonzalez, A., Symonds, V.V., Lloyd, A., 2016. Tyrosine hydroxylation in betalain pigment biosynthesis is performed by cytochrome P450 enzymes in beets (*Beta vulgaris*). *PLoS One* 11, 1–16. <https://doi.org/10.1371/journal.pone.0149417>
- Suzuki, M., Miyahara, T., Tokumoto, H., Hakamatsuka, T., Goda, Y., Ozeki, Y., Sasaki, N., 2014. Transposon-mediated mutation of CYP76AD3 affects betalain synthesis and produces variegated flowers in four o'clock (*Mirabilis jalapa*). *J. Plant Physiol.* 171, 1586–1590. <https://doi.org/10.1016/j.jplph.2014.07.010>
- Svenson, J., Smallfield, B.M., Joyce, N.I., Sansom, C.E., Perry, N.B., 2008. Betalains in red and yellow varieties of the andean tuber crop ulluco (*Ullucus tuberosus*). *J. Agric. Food Chem.* 56, 7730–7737. <https://doi.org/10.1021/jf8012053>
- Tanaka, Y., Sasaki, N., Ohmiya, A., 2008. Biosynthesis of plant pigments: anthocyanins, betalains and carotenoids. *Plant J.* 54, 733–749.

- <https://doi.org/10.1111/j.1365-313X.2008.03447.x>
- Tesoriere, L., Butera, D., Allegra, M., Fazzari, M., Livrea, M.A., 2005. Distribution of betalain pigments in red blood cells after consumption of cactus pear fruits and increased resistance of the cells to ex vivo induced oxidative hemolysis in humans. *J. Agric. Food Chem.* 53, 1266–1270. <https://doi.org/10.1021/jf048134+>
- Tesoriere, L., Butera, D., Pintauro, A.M., Allegra, M., Livrea, M.A., 2004. Supplementation with cactus pear (*Opuntia ficus-indica*) fruit decreases oxidative stress in healthy humans: A comparative study with vitamin C. *Am. J. Clin. Nutr.* 80, 391–395. <https://doi.org/10.1093/ajcn/80.2.391>
- Tesoriere, L., Gentile, C., Angileri, F., Attanzio, A., Tutone, M., Allegra, M., Livrea, M.A., 2013. Trans-epithelial transport of the betalain pigments indicaxanthin and betanin across Caco-2 cell monolayers and influence of food matrix. *Eur. J. Nutr.* 52, 1077–1087. <https://doi.org/10.1007/s00394-012-0414-5>
- Thulin, M., Moore, A.J., El-Seedi, H., Larsson, A., Christin, P.A., Edwards, E.J., 2016. Phylogeny and generic delimitation in molluginaceae, new pigment data in caryophyllales, and the new family corbichoniaceae. *Taxon* 65, 775–793. <https://doi.org/10.12705/654.6>
- Timoneda, A., Feng, T., Sheehan, H., Walker-Hale, N., Pucker, B., Lopez-Nieves, S., Guo, R., Brockington, S.F., 2019. The evolution of betalain biosynthesis in Caryophyllales. *New Phytol.* 224, 71–85. <https://doi.org/10.1111/nph.15980>
- Timoneda, A., Sheehan, H., Feng, T., Lopez-Nieves, S., Maeda, H.A., Brockington, S., 2018. Redirecting Primary Metabolism to Boost Production of Tyrosine-Derived Specialised Metabolites in Planta. *Sci. Rep.* 8, 17256 <https://doi.org/10.1038/s41598-018-33742-y>
- Tonon, R. V., Brabet, C., Hubinger, M.D., 2010. Anthocyanin stability and antioxidant activity of spray-dried açai (*Euterpe oleracea* Mart.) juice produced with different carrier agents. *Food Res. Int.* 43, 907–914. <https://doi.org/10.1016/J.FOODRES.2009.12.013>
- Tullet, J.M.A., Green, J.W., Au, C., Benedetto, A., Thompson, M.A., Clark, E., Gilliat, A.F., Young, A., Schmeisser, K., Gems, D., 2017. The SKN-1/Nrf2 transcription factor can protect against oxidative stress and increase lifespan in *C. elegans* by distinct mechanisms. *Aging Cell* 16, 1191–1194. <https://doi.org/10.1111/accel.12627>
- Vidal, P.J., López-Nicolás, J.M., Gandía-Herrero, F., García-Carmona, F., 2014.

- Inactivation of lipoxygenase and cyclooxygenase by natural betalains and semi-synthetic analogues. *Food Chem.* 154, 246–254.  
<https://doi.org/10.1016/j.foodchem.2014.01.014>
- Vogt, T., 2002. Substrate specificity and sequence analysis define a polyphyletic origin of betanidin 5- and 6-O-glucosyltransferase from *Dorotheanthus bellidiformis*. *Planta* 214, 492–495. <https://doi.org/10.1007/s00425-001-0685-1>
- Vogt, T., Grimm, R., Strack, D., 1999. Cloning and expression of a cDNA encoding betanidin 5-O-glucosyltransferase, a betanidin- and flavonoid-specific enzyme with high homology to inducible glucosyltransferases from the Solanaceae. *Plant J.* 19, 509–519. <https://doi.org/10.1046/j.1365-3113X.1999.00540.x>
- Voigt, C.C., Roeleke, M., Marggraf, L., Pētersons, G., Voigt-Heucke, S.L., 2017. Migratory bats respond to artificial green light with positive phototaxis. *PLoS One* 12, e0177748. <https://doi.org/10.1371/journal.pone.0177748>
- Von-Ardenne, R., Döpp, H., Musso, H., Steglich, W., 1974. Isolation of muscaflavin from *Hygrocybe* species (Agaricales) and its dihydroazepine structure. *Z. Naturforsch* 29, 637–639.
- Von Elbe, J.H., Maing, I. -Y., Amundson, C.H., 1974. Color stability of betanine. *J. Food Sci.* 39, 334–337. <https://doi.org/10.1111/j.1365-2621.1974.tb02888.x>
- Wendel, M., Nizinski, S., Tuwalska, D., Starzak, K., Szot, D., Prukala, D., Sikorski, M., Wybraniec, S., Burdzinski, G., 2015a. Time-resolved spectroscopy of the singlet excited state of betanin in aqueous and alcoholic solutions. *Phys. Chem. Chem. Phys.* 17, 18152–18158. <https://doi.org/10.1039/c5cp00684h>
- Wendel, M., Szot, D., Starzak, K., Tuwalska, D., Gapinski, J., Naskrecki, R., Prukala, D., Sikorski, M., Wybraniec, S., Burdzinski, G., 2015b. Photophysical properties of betaxanthins: Vulgaxanthin I in aqueous and alcoholic solutions. *J. Lumin.* 167, 289–295. <https://doi.org/10.1016/j.jlumin.2015.06.030>
- Wendel, M., Szot, D., Starzak, K., Tuwalska, D., Prukala, D., Pedzinski, T., Sikorski, M., Wybraniec, S., Burdzinski, G., 2015c. Photophysical properties of indicaxanthin in aqueous and alcoholic solutions. *Dye. Pigment.* 113, 634–639. <https://doi.org/10.1016/j.dyepig.2014.09.036>
- White, J.G., Southgate, E., Thomson, J.N., Brenner, S., 1986. The structure of the nervous system of the nematode *Caenorhabditis elegans*. *Philos. Trans. R. Soc. B Biol. Sci.* 314, 1–340. <https://doi.org/10.1098/rstb.1986.0056>
- Wink, M., 1997. Compartmentation of Secondary Metabolites and Xenobiotics in Plant

- Vacuoles. *Adv. Bot. Res.* 25, 141–169. [https://doi.org/10.1016/S0065-2296\(08\)60151-2](https://doi.org/10.1016/S0065-2296(08)60151-2)
- Winter, Y., López, J., Von Helversen, O., 2003. Ultraviolet vision in a bat. *Nature* 425, 612–614. <https://doi.org/10.1038/nature01971>
- Wu, L., Hsu, H.-W., Chen, Y.-C., Chiu, C.-C., Lin, Y.-I., Ho, J.A., 2006. Antioxidant and antiproliferative activities of red pitaya. *Food Chem.* 95, 319–327. <https://doi.org/10.1016/J.FOODCHEM.2005.01.002>
- Wyler, H., Dreiding, A.S., 1957. Kristallisiertes Betanin. Vorläufige Mitteilung. *Helv. Chim. Acta* 40, 191–192. <https://doi.org/10.1002/hlca.19570400122>
- Wyler, H., Wilcox, M.E., Dreiding, A.S., 1965. Umwandlung eines Betacyans in ein Betaxanthin. Synthese von Indicaxanthin aus Betanin. *Helv. Chim. Acta* 48, 361–366. <https://doi.org/10.1002/hlca.19650480214>
- Xia, Q., Lu, S., Ostrovsky, J., McCormack, S.E., Falk, M.J., Grant, S.F.A., 2018. PARP-1 inhibition rescues short lifespan in hyperglycemic *C. elegans* and improves GLP-1 secretion in human cells. *Aging Dis.* 9, 17–30. <https://doi.org/10.14336/AD.2017.0230>
- Zarkower, D., 2006. Somatic sex determination. In *WormBook*. Ed. The *C. elegans* research community, WormBook. <https://doi.org/10.1895/wormbook.1.84.1>
- Zhu, G., Yin, F., Wang, L., Wei, W., Jiang, L., Qin, J., 2016. Modeling type 2 diabetes-like hyperglycemia in *C. elegans* on a microdevice. *Integr. Biol.* 8, 30–38. <https://doi.org/10.1039/c5ib00243e>
- Zou, D.M., Brewer, M., Garcia, F., Feugang, J.M., Wang, J., Zang, R., Liu, H., Zou, C., 2005. Cactus pear: A natural product in cancer chemoprevention. *Nutr. J.* 4, 25. <https://doi.org/10.1186/1475-2891-4-25>





## **Chapter II. Objectives**



The properties of betalains as bioactive compounds have been outlined in the introduction section. They have antioxidant, anti-tumoral and anti-inflammatory effects which have been mainly studied by employing extracts of plants of the order Caryophyllales.

Betalains production and purification from edible parts of the plants have been limiting factors in the analysis of individual compounds. In addition, the lack of studies with pure, individual betalains has hindered the unequivocal confirmation of betalains as health-promoting compounds and the characterization of the most active structures.

Thus, the **main objective** of this Thesis was:

The production of individual betalains by biotechnological means and the characterization of their health-promoting properties *in vivo* in the animal model *Caenorhabditis elegans*.

In order to develop the main objective, the following **specific objectives** were defined:

1. Searching for alternative sources of betalamic acid-forming dioxygenases through enzyme-mining in non-native hosts.
2. Biotechnological production of individual betalains by heterologous expression of efficient DODA enzymes in bacterial cultures.
3. Construction and optimization of a machine for the automatic control of worms' lifespan and its application to the characterization of betalains.
4. Analysis of transcriptional changes in worms treated with betalains and subsequent biological confirmation by using mutant strains of *C. elegans*.

Parallel to the main topic, the device for the automatic analysis of *C. elegans* lifespan facilitates the study of other individual compounds, both natural and synthetic, *in vivo* in the animal model for the first time.



## **Chapter III. Materials and Methods**



## 1. Chemicals

All compounds and reagents employed in this Thesis were purchased from Sigma-Aldrich (St. Louis, MO, USA), except the flavonoids, which were obtained from Extrasynthese (Genay, France), HPLC-grade acetonitrile, purchased from Fisher Scientific UK (Leicestershire, UK) and TRIzol reagent, obtained from Invitrogen (Carlsbad, California, USA). Distilled water was purified using a Milli-Q system (Millipore, Bedford, MA, USA).

## 2. Strains and plasmids

*Gluconacetobacter diazotrophicus*, *Bacillus subtilis* and *Bacillus halodurans* were acquired from DSMZ (Deutsche Sammlung von Mikroorganismen und Zellkulturen, German collection of microorganisms and cell cultures). *Anabaena cylindrica* was acquired from the Spanish Bank of Algae (BEA - Banco Español de Algas, Gran Canaria, Spain). All strains of *Caenorhabditis elegans* and *Escherichia coli* strains OP50 and HT115 were acquired from the Caenorhabditis Genetic Center (CGC, St Paul, MN, USA). Strains of *E. coli* DH5 $\alpha$  and Rosetta 2 (DE3) were obtained from Novagen (Merck KGaA, Darmstadt, Germany). *E. coli* BL21 (DE3) was purchased from Invitrogen (Waltham, Massachusetts, USA). *E. coli* DH5 $\alpha$  was employed for expression of recombinant proteins and Rosetta 2 and BL21 strains were employed with protein purification's purposes. Recipes of culture media for each strain are detailed in Annex I.

Different plasmids were employed for the expression of recombinant proteins in *E. coli* strains. For expression of 4,5-DODA from *Gluconacetobacter diazotrophicus*, pET28a was employed. The plasmid pRSET-A was employed for the expression of the dioxygenase from *Anabaena cylindrica*. They both are plasmids widely used for the heterologous expression of proteins in *E. coli* since they present a high-level expression controlled by the bacteriophage T7 promoter and T7 terminator which limits a region containing a multi-cloning site as well as a 6xHis tag in the N-terminal region which facilitates the purification of proteins.



### 3. *Gluconacetobacter diazotrophicus* culture

*Gluconacetobacter diazotrophicus* was inoculated in 20 mL cultures of a specific media detailed in Annex I. The cultures were maintained overnight at 25 °C with agitation. Afterwards half of the cultures were centrifuged for 10 min at 5,000 g and resuspended in 20 mL distilled water. The other half were kept in the culture medium. Both water and medium cultures were supplemented with varying concentrations of L-DOPA (from 0 to 7.6 mM) and sodium ascorbate 15 mM and further incubated at 25 °C. Appropriate control media without L-DOPA were also incubated at 25 °C for each condition. After two days, the media were collected and analysed by HPLC-ESI/TOF/MS in the search for compounds derived from the synthesis of betalamic acid.

Additionally, liquid cultures of *G. diazotrophicus* were laying over semi-solid culture plates supplemented with IPTG 1 mM, L-DOPA 7.6 mM and sodium ascorbate 15 mM to promote the formation of betalamic acid. Plates without these compounds were employed as negative controls.

### 4. *Gluconacetobacter diazotrophicus* DODA sequence and cloning

The sequence of the protein WP\_012222467 from *Gluconacetobacter diazotrophicus* deposited at the National Center for Biotechnology Information (NCBI, Bethesda, MD, USA) was used as a template to synthetically obtain the 4,5-DODA sequence (Geneart, Regensburg, Germany). PCR amplification was performed using *Pfu* DNA polymerase and the following primers, which include the restriction sequences recognized by the enzymes *NdeI* and *XhoI*: GdDODA-F (5'TATATATACATATGACACCGGTGCCGGAA) and GdDODA-R (5'ATATATATCTCGAGTTAAATCGGGGTTGC). This amplification yielded a 457 bp product. The PCR product was digested with *NdeI* and *XhoI*, purified by QIAquick PCR purification kit, and inserted into the expression vector pET28a downstream of the T7 RNA polymerase promoter, the expression vector was previously digested with the same restriction enzymes. This produced the recombinant plasmid pET28a-GdDODA, which encodes for an additional 22 amino acid N-terminal sequence containing a 6 His-tag. The plasmid was transformed into *E. coli* DH5 $\alpha$  (Novagen) electrocompetent cells and plated onto LB agar plates containing kanamycin (Km) 100  $\mu$ g/mL. The resulting colonies were then analysed by PCR. The plasmid pET28a-GdDODA was obtained

from positive colonies using the QIAprep spin plasmid miniprep kit. The sequence was confirmed by DNA sequencing of the plasmid and subsequently transformed into *E. coli* Rosetta 2 for further experiments.

## 5. *Anabaena cylindrica* culture

*Anabaena cylindrica* was cultivated in 20 mL cultures of liquid BG-11 medium (Annex I). The cultures were maintained at 20 °C with agitation under a daily light/dark cycles of 14:8 h. After 7 days, cultures media were supplemented with varying concentrations of L-DOPA (from 0 to 7.6 mM) and sodium ascorbate 15 mM and further incubated at 20 °C. After 24 h, the media were collected and analysed by HPLC-ESI/TOF/MS in the search for compounds derived from the synthesis of betalamic acid.

## 6. *Anabaena cylindrica* DODA sequence and cloning

The sequence of the protein WP\_015213489 from *Anabaena cylindrica* deposited at the National Center for Biotechnology Information (NCBI, Bethesda, MD, USA) was used as a template to synthetically obtain the 4,5-DODA sequence from *A. cylindrica*, enhanced for *E. coli* expression (Geneart, Regensburg, Germany). The synthetic DODA gene yielded a 357 bp product that was expressed into the expression vector pRSETa, which encodes for an additional N-terminal sequence containing a 6 His-tag. The new plasmid pRSETa-AcDODA was transformed into *E. coli* BL21 (Invitrogen) thermocompetent cells and plated onto LB agar plates containing ampicillin (Amp) 50 µg/mL. The resulting colonies were then analysed by PCR.

PCR amplification was performed using Taq DNA polymerase and the primers AcDODA-F (5' TGGGGACATATGAAAAGCAAAAC) and AcDODA-R (5' GCTGCAGATCTCGAGTTACAGAC). This amplification yielded a 384 bp product, which coincides with the entire DODA synthetic gene plus the additional 6 His-tag sequence. The plasmid pRSETa-AcDODA was subsequently used in further experiments.

## 7. Structure modelling of novel DODA enzymes

Structure homology of DODA enzymes from *G. diazotrophicus* and *A. cylindrica* were computed by the SWISS-MODEL (Swiss Institute of Bioinformatics, Biozentrum, University of Basel, Switzerland) homology server (Bienert et al., 2017;

Waterhouse et al., 2018) which relies on ProMod3, an inhouse comparative modelling engine based on OpenStructure (Biasini et al., 2013). The SWISS-MODEL template library (SMTL version 2018-02-28, PDB release 2018-02-23 for modelling of *G. diazotrophicus* protein and SMTL version 2020-03-04, PDB release 2020-02-28 for modelling of *A. cylindrica* enzyme) was searched with BLAST (Camacho et al., 2009) and HHBlits (Remmert et al., 2012) for evolutionary related structures matching the target sequence.

ProMod3 extracts initial structural information from the selected template structure. Insertions and deletions, as defined by the sequence alignment, are resolved by first searching for viable candidates in a structural database. Final candidates are then selected using statistical potentials of mean force scoring methods. If no candidates can be found, a conformational space search is performed using Monte Carlo techniques. Non-conserved side chains are modelled using the 2010 backbone-dependent rotamer library from the Dunbrack group (Shapovalov and Dunbrack, 2011). The optimal configuration of rotamers is estimated using the graph-based TreePack algorithm (McPake et al., 2009) by minimising the SCWRL4 energy function (Krivov et al., 2009). As a final step, small structural distortions, unfavourable interactions or clashes introduced during the modelling process are resolved by energy minimisation. ProMod3 uses the OpenMM library (Eastman et al., 2017) to perform the computations and the CHARMM27 force field (Mackerell et al., 2004) for parameterisation.

In SWISS-MODEL, the quaternary structure annotation of the template is used to model the target sequence in its oligomeric form. The method used is based on a supervised machine learning algorithm, Support Vector Machines (SVM), which combines interface conservation, structural clustering, and other template features to provide a quaternary structure quality estimate (QSQE) (Bertoni et al., 2017). The QSQE score is only computed if it is possible to build an oligomer and only for the top ranked templates. In this model, the *in silico* results were corroborated by molecular characterization of the expressed and purified proteins, experimentally determined to be homodimers, as will be exposed in chapter IV and V.

The GMQE and QMEAN parameters were determined to ascertain enough model quality. GMQE provides a quality estimation which combines properties from the target-template alignment and the template search method. The resulting GMQE score is expressed as a number between 0 and 1, reflecting the expected accuracy of a model built with that alignment and template and the coverage of the target. Higher

numbers indicate higher reliability. The QMEAN parameter is a composite estimator based on different geometrical properties and provides both global (entire structure) and local (per residue) absolute quality estimates on the basis of the single model used (Benkert et al., 2011). The QMEAN score provides an estimate of the "degree of nativeness" of the structural features observed in the model on a global scale. It indicates whether the model is comparable to what one would expect from experimental structures of similar size. If QMEAN scores between zero and -4.0 indicate good agreement between the model structure and experimental structures of similar size (higher quality around 0.0). Scores of -4.0 or below are indicative of models of low quality.

## 8. Phylogenetic analysis of novel betalamic acid-forming DODAs

The novel enzyme from *G. diazotrophicus* was searched against similar enzymes and the 100 most similar sequences were used to construct a Neighbour-Joining phylogenetic tree (Altschul et al., 2005; Li et al., 2015). Additionally, an expanded analysis was performed and the DODA enzyme from *A. cylindrica* was found. The relationship of the novel enzymes with betalamic acid-forming dioxygenases previously reported was performed from the conserved block of *G. diazotrophicus* which includes the His 101. In all cases, multiple sequence alignment was performed using Clustal Omega from the EMBL-EBI (European Molecular Biology Laboratory - European Bioinformatics Institute) (Madeira et al., 2019) and the phylogenetic tree was inferred by using the phylogeny tool from the ClustalW2 package of the same platform and plotted using ITOL (Interactive Tree of Life) (Letunic and Bork, 2019).

## 9. Protein characterization

### 9.1. Protein purification

Recombinant proteins were expressed in *E. coli* cultures grown at 37 °C in LB supplemented with antibiotics up to an O.D.<sub>600</sub> = 0.8–1.0. Induction was then performed with IPTG and after 20 h at 20 °C, cells were harvested by centrifugation for 10 min at 6,000 g and resuspended in sodium phosphate buffer 50 mM, pH 8.0, supplemented with 0.3 M sodium chloride. Cell lysis was performed by sonication in a Cole-Palmer 4710 series ultrasonic homogenizer (Chicago, IL, USA). The extracts were centrifuged for 10 min at 13,000 g and proteins in the supernatants were collected by using His-

select nickel affinity gel (Sigma-Aldrich) following the manufacturer's instructions. The bound DODA proteins were released from the gel matrix with elution buffer containing imidazole (250 mM) and the proteins were then desalted on PD10 columns (General Electric Healthcare, Milwaukee, USA) using 20 mM sodium phosphate buffer, pH 8.5.

## **9.2. Protein quantification**

Protein concentration was determined according to the Bradford protein assay using bovine serum albumin as standard (Bradford, 1976).

## **9.3. Gel filtration**

Samples of pure recombinant protein were applied to a Superdex 200 10/300 GL column equilibrated with sodium phosphate buffer 50 mM, pH 7.5, supplemented with 150 mM sodium chloride. The protein was eluted by isocratic chromatography at a constant flow rate of 0.5 mL min<sup>-1</sup>. Elutions were performed in an Äkta purifier apparatus (General Electric Healthcare) and monitored at 280 nm. Column calibration was performed with the following protein markers (Sigma-Aldrich): cytochrome C (12.4 kDa), carbonic anhydrase (29 kDa), albumin (66 kDa), alcohol dehydrogenase (150 kDa), and  $\beta$ -amylase (200 kDa).

## **9.4. MALDI-TOF MS protein analysis**

Matrix solution for peptide analyses was  $\alpha$ -cyano-4-hydroxycinnamic acid (20 mg/mL) in ACN/water/TFA (70:30:0.1). The peptide samples were dissolved in 0.1% TFA and mixed with the matrix solution. One microliter of this mixture was applied to the atmospheric pressure matrix-assisted laser desorption ionization (AP-MALDI) target plate and allowed to dry. Experiments were carried out with an Agilent Time of Flight (TOF) Mass Spectrometer (Agilent Technologies, Santa Clara, CA, USA), equipped with an AP-MALDI Ion Source with an N<sub>2</sub> laser (337 nm). Samples were measured in reflectron mode to identify molecular formulas based on precise mass measurements in positive mode. External calibration of the spectrometer was performed with standard peptides from the ProteoMass<sup>TM</sup> Peptide MALDI-MS Calibration Kit (Sigma-Aldrich). Data were recorded and processed with Agilent MassHunter Workstation Software. Peptide Mass Fingerprint determination was carried out using Agilent Spectrum Mill Software. Determination of protein absolute molecular mass was

carried out using an HPLC-ESI-MS TOF system. This system comprises an HPLC Agilent VL 1100 apparatus equipped with an autosampler  $\mu$ -wellplate and a capillary pump, connected to an Agilent 6100 Mass Spectrometer Time of Flight (MS TOF), and an electrospray ionization interface (ESI) was used. The column employed was a Zorbax Poroshell 300SB-C18, 1 x 75 mm with 5  $\mu$ m (Agilent Technologies). The column was operated at 60 °C, and the samples were injected with a flux of 0.2 mL min<sup>-1</sup>. The protein was eluted with a linear gradient using water/ACN/formic acid (95:4.9:0.1) as solvent A, and water/ACN/formic acid (10:89.9:0.1) as solvent B. A linear gradient was performed for 30 min from 0% to 90% of B. Protein separation was monitored at 210 and 280 nm using a multiple wavelength detector. The mass spectrometer was operated in positive mode in the range of 100-2200  $m/z$ , using a capillary voltage of 3.5 kV. Nebulizer gas pressure was 30 psi, and drying gas flux was 8 L/min at a temperature of 350 °C. External spectrometer calibration was carried out using the ProteoMass<sup>TM</sup> Peptide MALDI-MS Calibration Kit (Sigma-Aldrich, St. Louis, MO, USA). Two different peptides were used as controls (Cytochrome C, and carbonic anhydrase, Sigma-Aldrich). All data were recorded and processed through the software Agilent MassHunter Workstation Qualitative Analysis Software (Agilent Technologies), and the intact molecular weight of the protein was obtained using the deconvolution algorithm from this software.

### 9.5. Trypsin digestion

The protein samples were prepared in 100  $\mu$ L of ammonium bicarbonate buffer 50 mM, pH 8.0, with 0.02% ProteaseMAX<sup>TM</sup> Surfactant (Promega, Madison, WI, USA). After that, the samples were reduced with DTT 10 mM at 56°C for 20 min and alkylated with iodoacetamide 50 mM at room temperature in the dark for 20 min. One microgram of proteomics grade trypsin (Promega) was added and the samples were incubated at 37 °C for 4 h. Finally, the sample were centrifuged at 15,000 g for 1 min to collect the condensate and 0.5% TFA was added to stop the digestion. Peptides were cleaned up with C18 ZipTips (Millipore) and evaporated using an Eppendorf vacuum concentrator model 5301.

### 9.6. Electrophoretic techniques

For SDS-PAGE technique, samples were prepared by 1:2 dilution in denaturing sample buffer (2x) composed, per 10 mL, of 0.25 mL of water, 1.25 mL of Tris-HCl 1

M pH 6.8, 0.5 g of SDS, 0.4 mL of bromophenol blue 0.1%, 2 mL of glycerol and 1 mL of  $\beta$ -mercaptoethanol. After 5 min at 95 °C, samples were applied to the polyacrylamide gel comprising a stacking gel (4% acrylamide) and a resolving gel (15% acrylamide) (Laemmli, 1970). Gels were run in a miniProtean II (BioRad Laboratories, Hercules, CA, USA), containing 400 mL of running buffer, for 80 min at a constant voltage of 200 V. EZ-Run™ Prestained Rec Protein Ladder (Fisher Bioreagents, Pittsburgh, PA, USA) was used to estimate the size of proteins.

### 9.7. Gel staining

After electrophoresis by SDS-PAGE, gels were stained using a standard Coomassie Blue solution, which contains 100 mL of water, 100 mL of ethanol, 25 mL of glacial acetic acid and 25 mL of Coomassie Brilliant Blue R-250 (0.1% w/v) (Sigma-Aldrich). Gels were submerged in this solution shaking at room temperature for 90 min. A destaining solution was employed overnight to remove the excess of staining. The destaining solution contains 30% ethanol, 10% acetic acid and 60% water.

## 10. Formation of betalamic acid

Enzyme activities were determined using a continuous spectrophotometric method by measuring the absorbance due to betalamic acid and muscaflavin appearance at  $\lambda = 414$  nm (Gandía-Herrero and García-Carmona, 2012; Girod and Zryd, 1991). Unless otherwise stated, the reaction medium contained 50 mM sodium phosphate buffer, pH 6.5, 2.5 mM L-DOPA, and 10 mM sodium ascorbate. Measurements were performed at 25 °C in 96-well plates in a Synergy HT plate reader (Bio-Tek Instruments, Winooski, USA). The final sample volume was 300  $\mu$ L.

The plate reader detector signal was calibrated with betalamic acid solutions of known concentration. Kinetic data analysis was carried out by using non-linear regression fitting with the SigmaPlot Scientific Graphing for Windows version 10.0 (Systat Software, San Jose, CA, USA).

Chemical condensation of betalamic acid with L-DOPA was kinetically characterized by determining the kinetic constant of the reaction. The kinetic scheme for a second order reaction where two reactants yield a single product following a stoichiometry 1:1 was considered. The mass balance of the system was according to the following scheme:

$$v = k \cdot [\text{bet}] \cdot [\text{DOPA}]$$

$$[\text{bet}]_0 = [\text{bet}] + [\text{dopax}]$$

By maintaining constant the concentration of L-DOPA, a pseudo first order kinetics can be obtained:

$$v = k_{app} \cdot [\text{bet}]$$

$$k_{app} = k \cdot [\text{DOPA}]$$

and the substrate concentration equation  $[\text{bet}] = [\text{bet}]_0 \cdot e^{-k_{app} \cdot t}$  can be transformed into product accumulation  $[\text{dopax}] = [\text{bet}]_0 \cdot (1 - e^{-k_{app} \cdot t})$ , where  $[\text{bet}]$  represents the concentration of betalamic acid,  $[\text{bet}]_0$ , the initial acid concentration before the reaction is triggered, and  $[\text{dopax}]$  is the concentration of dopaxanthin formed by the chemical reaction. By representing the accumulation of dopaxanthin,  $[\text{dopax}]$ , versus the initial concentration of betalamic acid,  $[\text{bet}]_0$ , the apparent constant can be determined from the slope of the linear representation obtained in the graph as  $k_{app} = (\text{Ln slope} - \text{Ln } 1) / t$ , and then the kinetic constant of the second order reaction can be determined.

## 11. Betalains' extraction from plants

### 11.1. Prickly pears extracts

Red and yellow prickly pears from *Opuntia ficus-indica* were purchased from a local distributor. The fruits were peeled, chopped into small pieces and stored at -20 °C in tightly closed containers. 10 grams of red fruit and another 10 grams of yellow fruit were weighed in 50 mL centrifuge tubes and crushed using a spatula to form a soft pulp, which was then passed through a cheese cloth to remove the seeds and tissue debris. The extracts were then diluted with 10 mL of sterile M9 buffer, centrifuged at 5,000 g, filtered through a nylon cloth and finally filtered through a 22 µm sterile filter. The red and yellow extracts prepared were maintained at -20 °C until use.



### 11.2. Betanin obtention

Betanin from commercial red beet was extracted in 10 mM phosphate buffer, pH 6.0, in a 230 Omnimixer (Sorvall, Norwalk, CT, USA) at maximum speed for 10 s. The homogenate was filtered through cheesecloth and centrifuged at 120,000 g for 40 min. the supernatant was then filtered using a YM-10 membrane (Millipore) to remove proteins. All steps were carried out at 4 °C.

### 11.3. Betanidin obtention

Betanidin was obtained from violet flowers of *Lampranthus productus*. The process was performed in 10 mM sodium acetate buffer, pH 5.0 in a polytron homogenizer (5 s, 2 pulses at medium speed; Kinematica AG, Littau, Switzerland). The homogenate was filtered through nylon cloth and centrifuged at 120,000 g for 40 min. the supernatant was then filtered through Centriplus YM-10 membranes (Millipore) to remove proteins. All steps were carried out at 4 °C.

## 12. Standard betalains

Betalamic acid and all betalains described in this Thesis, except for betanidin and betanin, were obtained by a semi-synthesis method for use as real standards for identification purposes. First, 10 mL of purified betanin from red beet yielded betalamic acid by basic hydrolysis (pH 11.4). Then, 0.2 M of the corresponding amine or amino acid was added and the pH was lowered with acetic acid to pH 5.0, allowing the condensation of betalamic acid with the corresponding amine (Wyler et al., 1965) (**Table 3.1**). All solutions were degassed and the whole process was carried out under N<sub>2</sub> atmosphere. Once semi-synthesis was achieved, purification steps were carried out for the obtention of pure compounds.

**Table 3.1. Amine or amino acid precursors employed for the semi-synthesis of betalains.**

<b>Amine or amino acid</b>	<b>Betalain</b>
Aniline	Aniline-betalain
L-Asparagine	Vulgaxanthin III
L-Glutamic acid	Vulgaxanthin II
L-Glutamine	Vulgaxanthin I
Indoline	Indoline-betacyanin
L-Indoline carboxylic acid	Indoline carboxylic acid-betacyanin
L-DOPA	Dopaxanthin
L-Leucine	Vulgaxanthin IV
L-Methionine sulfoxide	Miraxanthin I
L-Phenylalanine	Phenylalanine-betaxanthin
2-Phenylethylamine	Phenylethylamine-betaxanthin
L-Proline	Indicaxanthin
Pyrrolidine	Pyrrolidine-betaxanthin
L-Tryptophan	Tryptophan-betaxanthin
L-Valine	Valine-betaxanthin

### 13. Production of betalains in culture media

The enzyme 4,5-DOPA-extradiol dioxygenase (DODA) was chosen for biotransformation assays in *E. coli* because it is the key enzyme in the betalains biosynthesis pathway. *E. coli*, harbouring the above-mentioned pET28a-GdDODA, was cultured in Luria Bertani (LB) or NZCYM media (Sambrook et al., 2001). Both media were supplemented with chloramphenicol (Cm) 35 µg/mL and kanamycin (Km) 100 µg/mL at 37 °C until a O.D.<sub>600nm</sub> 0.8-1.0. Then, IPTG 1mM was added and the culture was maintained for 15 hours at 20 °C. After that, the culture was centrifuged 10 min at 5,000 g. The pellet obtained was resuspended in Milli-Q water and kept at 20 °C and shaking at 120 rpm. Optimal conditions for the production of each betalain were established considering different concentrations of L-DOPA and amines, varying from 0.76 to 22.32 mM and from 0.38 to 38 mM respectively. In optimal conditions L-DOPA 7.6 mM and sodium ascorbate 15 mM were added. In the case of the addition of amines, these were added at a final optimized concentration of 38 mM, except for indoline, which was added at 0.38 mM, and indoline-2-carboxylic acid added, at 3.8 mM. The

culture media were centrifuged 1 min at 14,000 g and the supernatants were analysed. The resulting pellets were disrupted by sonication with a Branson Digital sonifier (Branson Ultrasonic Corporation, Connecticut, USA) with 5 pulses of 10 seconds (medium intensity). The cells content was further analysed under the same conditions that the supernatants.

## 14. Scaled-up production of betalains in bioreactor

The EZ - Control system from Applikon Biotechnology (Delft, The Netherlands) was used to control the production of betalains in bioreactors. *E. coli* harbouring pET28a-GdDODA was cultivated in 20 mL LB supplemented with Cm (35 µg/mL) and Km (100 µg/mL) at 37 °C as starter culture. After 15 hours, the culture was diluted in a reactor with 2 L LB supplemented with the same antibiotics and grown up at 37 °C until an O.D.<sub>600nm</sub> 0.8-1.0 was reached. Temperature was then dropped to 20 °C and IPTG 1 mM was added. 15 hours later, the culture was centrifuged 10 min at 5,000 g and the medium was replaced in the reactor by 1 L of sterile MilliQ water. Furthermore, 500 mL of sterile water was employed to resuspend the cell pellet and another 500 mL was employed to add L-DOPA, sodium ascorbate and the corresponding amines, giving place to a reactor with a final volume of 2 L. The culture was kept in the dark and shaken at 50 rpm and 20 °C during 96 hours with 50-65% dO<sub>2</sub>.

## 15. Purification of betalains

Immediately after the obtention of betalains by the semi-synthesis method, by biotransformation in cell cultures or from plant extracts, the following steps for their purification were carried out.

### 15.1. Q-sepharose chromatography

Anionic exchange chromatography of betalains was performed in an Äkta purifier apparatus (General Electric Healthcare). The equipment was operated via a PC using Unicorn software version 3.00. Elutions were monitored at 280, 480 and 536 nm. The solvents used were 20 mM sodium phosphate buffer, pH 6.0 (solvent A), and 20 mM sodium phosphate buffer, pH 6.0, with 2 M NaCl (solvent B). A 25 x 16 mm, 20-mL Q-Sepharose Fast Flow column (cross-linked agarose with quaternary ammonium as exchanger group, 90 µm of particle size) purchased from General Electric Healthcare

was used. After sample injection, the elution process was as follows: 0% B from 0.0 to 10.0 mL, then a linear gradient from 0% to 26% B was performed over 120 mL, collecting 3 mL fractions. Cleaning was done with 50% B for 30 mL and re-equilibration with 0% B for 30 mL. Injection volume was 25 mL and the flow rate was 2.5 mL/min.

### **15.2. Solid phase extraction**

After anionic exchange chromatography, pigment-containing fractions were pooled and salts removed by solid phase extraction in C-18 cartridges (35 cc, Waters, MA, USA) (Gandía-Herrero et al., 2006). Columns were conditioned with 70 mL ethanol followed by 70 mL purified water. Betalains were injected and bound to the column, washed with water or acidified water (0.1% HCl) and eluted later with ethanol. Finally, samples were dried under vacuum to remove ethanol and pigments were re-dissolved with distilled water.

## **16. Analysis of metabolites by HPLC**

A Shimadzu LC-10A apparatus (Kyoto, Japan) equipped with a SPD-M10A PDA detector was used for analytical HPLC separations. Reversed phase chromatography was performed with a 250 x 4.6 mm Kinetex 5 $\mu$  C-18 column (Phenomenex, Torrance, CA, USA). Gradients were formed with the following solvents: solvent A was water with 0.05% TFA, and solvent B was composed of acetonitrile with 0.05% TFA. A linear gradient was performed for 25 min from 0% B to 35% B and the column operation temperature was 30 °C. The flow rate was 1 mL/min, operated at 25°C. In all cases, injection volume was 50  $\mu$ L.

## **17. Electrospray ionization mass analysis of metabolites**

An Agilent VL 1100 apparatus with LC/MSD Trap (Agilent Technologies) was used for HPLC–ESI–MS analyses of metabolites and pigments. Elution conditions were the same as described above (HPLC analysis section) using a Kinetex 5 $\mu$  C-18 column with a flow rate of 0.8 mL/min. Vaporizer temperature was 350°C, and voltage was maintained at 3.5 kV. The sheath gas was nitrogen, operated at a pressure of 45 psi. Samples were ionized in positive mode. Ion monitoring mode was full scan in the range  $m/z$  50–600. The electron multiplier voltage for detection was 1,350 V.

## 18. Quantification of betalains

Pigment concentration was evaluated through absorbance. A Jasco V-630 spectrophotometer (Jasco Corporation, Tokyo, Japan) was used to measure the absorbance spectra of betalains. The measures were carried out with a wavelength scan from 250 to 700 nm at 25 °C. For known betaxanthins, molar extinction coefficient ( $\epsilon$ ) described in the bibliography were employed (Schliemann et al., 1999; Trezzini and Zrýb, 1991). For betanin and betanidin,  $\epsilon = 65,000 \text{ M}^{-1} \text{ cm}^{-1}$  and  $\epsilon = 54,000 \text{ M}^{-1} \text{ cm}^{-1}$  were employed, respectively (Schwartz and von Elbe, 1980). For new betaxanthins, molar extinction coefficients were determined by following an end-point method for measuring the degradation of the betalain, yielding free betalamic acid. The spectra of new betaxanthins were obtained in solution and then subjected to hydrolysis using ammonia diluted 1:50 in water. The degradation processes were monitored for 30 min, performing spectra every 2 minutes. The resulting betalamic acid solutions provided the concentration of each sample, and from this the  $\epsilon$  of the new betalains were calculated at maximum wavelengths. All measures were performed at 25 °C.

## 19. Characterization of metal-betalain complexes

The complexation studies between individual betalains and europium or copper were performed in betalain solutions with MOPS buffer (10 mM, pH 7.5) at a constant concentration of 13  $\mu\text{M}$  of the pigment and variable concentrations (6-260  $\mu\text{M}$ ) of  $\text{Eu}^{3+}$  or  $\text{Cu}^{2+}$ . End-time measurements of the spectra of each molecule were made at different concentrations of metals. The same spectrophotometer described above was used for dipicolinic acid (DPA) detection studies, a betalain solution was used in MOPS buffer (10 mM, pH 7.5) at a constant concentration of 13  $\mu\text{M}$  of the pigments and at fixed europium concentrations determined for each betalain. A variable DPA concentration (1.3-130  $\mu\text{M}$ ) was used. The end-point spectra for each DPA concentration were measured. For measurements with spores of *Bacillus*, solutions of the betalains were used in MOPS buffer at a constant concentration of 13  $\mu\text{M}$  and europium at the respective optimum concentration. Serial dilutions of the spore suspensions were used to perform the measurements. In all cases, the experiments were carried out at 25 °C in quartz cuvettes with a final volume of 1 mL.

## 20. Colour analysis of solid polymeric betalain

The absorbance spectrum of a novel solid betalain was measured by an integrating sphere (Jasco Corporation) in the same spectrophotometer described above. The colour properties of the solid betalain were quantitated by the analysis of the CIELAB colour space (Cabanés et al., 2014; Noor et al., 2012) for colour ( $a^*$ ,  $b^*$ ,  $h^\circ$ ), intensity ( $C^*$ ), and lightness ( $L^*$ ).

## 21. Fluorescence properties of betalains

A Shimadzu RF-6000 spectrofluorometer (Kyoto, Japan) was used for fluorescence spectroscopy measurements. Excitation spectra of betalains at a concentration 3  $\mu\text{M}$  were obtained following the emission at the maximum emission wavelength detected in a previous measurement and emission spectra were obtained after excitation at the maximum wavelength. For the complexating experiments with metals, a solution of the betalains in MOPS buffer with a fixed concentration of 3  $\mu\text{M}$  and variable  $\text{Eu}^{3+}$  and  $\text{Cu}^{2+}$  concentrations (3-90  $\mu\text{M}$ ) was used. The end-point spectra were obtained for each of the different concentrations of metals, also obtaining the maximum fluorescence values. For the DPA detection assays, a solution of each betalain at the same concentration was used as in the previous test with a fixed concentration of  $\text{Eu}^{3+}$ . The concentration of DPA was varied in the range of 0.3-45  $\mu\text{M}$ . The end-point spectra were obtained for each of the different concentrations of DPA together with the maximum fluorescence intensity values. In all cases the measurements were carried out at 25  $^\circ\text{C}$  in quartz cuvettes with a final volume of 3 mL.

## 22. Antioxidant and free radical scavenging activities of betalains

Three different methods (ABTS, FRAP and ORAC) were used to estimate the potential of the produced betalains as antioxidants and radical scavengers *in vitro*. The compounds analyses were prepared by diluting a 20  $\mu\text{M}$  stock solutions of each betalain. In all cases Trolox (6-hydroxy-2,5,7,8-tetramethylchroman-2-carboxylic acid) was used as a reference antioxidant for calibration curves and the results were referred to Trolox equivalent antioxidant capacity (TEAC). Reactions were prepared in 96 well plates and the measurements were performed in a Synergy HT plate reader (Bio-Tek Instruments, Winooski, USA). All experiments were performed in triplicate and mean

values and standard deviations were plotted. Data analysis was carried out using linear regression fitting under Sigma Plot Scientific Graphing software (Systat software).

### **22.1. FRAP method**

The antioxidant activity of betalains was characterized by following the ferric reducing antioxidant power (FRAP) (Benzie and Strain, 1996).  $\text{FeCl}_3$  solutions in sodium acetate buffer, pH 3.6 were used and the reduction of Fe (III) to Fe (II) was measured by adding the chromogenic reagent 2,4,6-tri(2-pyridyl)-s-triazine (TPTZ) as previously described (Gandía-Herrero et al., 2013). Reaction was monitored at  $\lambda = 593$  nm. Betalains stock solution (20  $\mu\text{M}$ ) was diluted to different concentrations in 250  $\mu\text{L}$  FRAP reactive and distilled water was added up to final volume of 300  $\mu\text{L}$ .

### **22.2. ABTS method**

Betalains were assayed for antiradical capacity by following their effect on the stable free radical  $\text{ABTS}^{\bullet+}$  [2,2'-azino-bis(3-ethylbenzothiazoline-6-sulfonic acid)]. Decolorizing activity of the different betalains in various concentrations on  $\text{ABTS}^{\bullet+}$  solutions was monitored at  $\lambda = 414$  nm (Gandía-Herrero et al., 2010) in sodium phosphate buffer, pH 7.0 in a final volume of 300  $\mu\text{L}$  as previously described (Gandía-Herrero et al., 2013).

### **22.3. ORAC assay**

The hydrogen atom transfer assay ORAC (oxygen radical absorbance capacity) was performed with fluorescein as fluorescent probe and 2,2'-azobis(2-amidinopropane) dihydrochloride (AAPH) as the free radical generator as previously described [25]. The latter produces the peroxy radicals which damage the fluorescent probe, thus resulting in the loss of fluorescence. The reaction medium (200  $\mu\text{L}$ ) contained 50  $\mu\text{L}$  of fluorescein (0.15  $\mu\text{M}$ ), 50  $\mu\text{L}$  of AAPH (76 mM), and betalains diluted in sodium phosphate, pH 7.4 at different concentrations.

## 23. Calculation of LOD, LOQ and complexation constants

Limits of detection (LOD) and limits of quantification (LOQ) of dipicolinic acid for betalains were determined from the value of three times the standard deviation ( $3\sigma$ ) or ten times the standard deviation ( $10\sigma$ ), respectively, around the regression line obtained from the calibration curve using the Sigma Plot Scientific Graphing software. To obtain the complexation constants of betalains with metals, the same Sigma Plot program was used in a non-linear regression process to adjust a sigmoid curve to the absorbance/fluorescence values vs. concentration plots. The constants were determined by adjustments to the points obtained experimentally.

By using a Bio-Tek Synergy HT device (Winooski, VT, USA) and 96-well plates with 0.3 mL final volume, the number absorbance and fluorescence assays performed with the pieces of equipment above described, was increased. Assays were performed in MOPS buffer (10 mM, pH 7.5) with a fixed concentration of betalain (26  $\mu$ M for absorbance assays and 13  $\mu$ M for fluorescence assays).  $\text{Eu}^{3+}$  was used with the optimal concentration according to the employed betalain and the type of the test. Dipicolinic acid concentrations were varied between 1.3 and 260  $\mu$ M. End-time measurements of the absorbance and fluorescence values were made using the wavelength filters available in the equipment:  $485 \pm 20$  nm for the excitation process and  $528 \pm 20$  nm for emission.

## 24. *Bacillus* cultures and obtaining of spores

*Bacillus subtilis* and *Bacillus halodurans* were cultured in Nutrient Broth (NB) medium supplemented with 0.003%  $\text{MnSO}_4$  to promote the sporulation process (Parry and Gilbert, 1980). To facilitate the growth of *B. halodurans*,  $\text{NaHCO}_3$  and  $\text{Na}_2\text{CO}_3$  were added to the medium at 4.2% and 5.3% respectively. The cultures were carried out in semi-solid and in liquid media, maintaining constant orbital shaking at 130 rpm for the liquid cultures. The cultures were carried out for 10 days at 30 °C. Cells were separated from the culture plate by adding distilled water and scraping the surface of the agar with a spatula. These cells were washed five times with distilled water by centrifuging for 2 min at 1,500 g. The suspensions obtained were again washed three times by centrifuging 2 min at 10,000 g, resuspended in 40% v/v ethanol and heated at 65 °C for 25 min to remove the living *Bacillus* cells and thus a spore suspension was obtained. Once the spores were obtained, they were quantified using the most probable



number (MPN) method (Woomer, 1994). The spores were used directly or subjected to a heat treatment (autoclave, 121 °C, 20 min) to facilitate the release of dipicolinic acid. In the latter case, the samples were centrifuged at 10,000 g for 2 min and the supernatant was transferred to a new microtube. The treatment of liquid cultures was as described above after the collection of the spores in order to compare the yields obtained with the two culturing techniques.

## **25. Scanning electron microscopy**

A Jeol JSM-6100 (Tokyo, Japan) equipment was used to visualize the spores of *Bacillus subtilis* and *Bacillus halodurans* by scanning electron microscopy. Cells were fixed in Trump's fixative (McDowell and Trump, 1976) for 24 hours, then washed and treated with 1% osmium tetroxide (OsO<sub>4</sub>). Subsequently, the cells passed through increasing concentrations of acetone until they reached pure acetone and were dried by the critical point technique before being coated in gold.

## **26. *Caenorhabditis elegans* strains and culture conditions**

All strains of *C. elegans* employed in this Thesis are detailed in **Table 3.2**. The strains were obtained from the Caenorhabditis Genetic Center (CGC, St Paul, MN, USA), which is funded by NIH Office of Research Infrastructure Programs (P40 OD010440). The strains were maintained at 20 °C in solid nematode growth medium (NGM) and the experiments were performed in liquid S medium (Stiernagle, 2006) with age-synchronized worms as described below. The strain OP50 of *E. coli* was used as a food source. *E. coli* was grown overnight in LB medium at 37 °C and was concentrated 10X in sterile M9 buffer.

**Table 3.2. Strains of *C. elegans* employed in the present work.**

Strain	Genotype	Description
N2	Wild type	Wild type
TJ375	<i>hsp-16.2</i> /GFP	Inducible GFP expression in pharynx cells
CF1038	<i>daf-16(mu86)</i>	Deficient DAF-16 strain
TJ356	<i>zIs356</i> [ <i>daf-16p::daf-16a/b::GFP</i> + <i>rol-6(su1006)</i> ]	Bright GFP in DAF-16 transcription factor
QV225	<i>skn-1(zj15)</i>	Deficient SKN-1 strain
LD01	<i>IdIs7</i> [ <i>skn-1b/c::GFP</i> + <i>rol-6(su1006)</i> ]	Bright GFP in SKN-1 transcription factor
BZ555	<i>dat-1p::GFP</i>	Bright GFP in dopaminergic neurons

## 27. Synchronous worm culture

All the worms used in the experiments were age-synchronized. Synchronic cohorts of *C. elegans* were prepared using the bleaching method. Briefly, stock plates with many gravid adults were collected with 3.5 mL of sterile M9 buffer in a 15 mL centrifuge tube, and then 1.5 mL of freshly prepared household bleach/5N NaOH solution (2:1) was added. The mix was incubated at room temperature for ten minutes mixing by vortex every two minutes. The bleached eggs were then centrifuged at 7,500 g and washed twice with 5 mL of M9 buffer. The eggs were left to hatch overnight in 10 mL of the same buffer under orbital shaking at 20 °C.

## 28. Treatment of *C. elegans* with different compounds

The strains above described were employed to characterized the effects of three different families of compounds: betalains, flavonoids and artificial food dyes (AFDs). In all cases, arrested larvae, L1, were collected and transferred to 25 mL sterile flasks containing 250 µL of an *E. coli* OP50 culture 10X concentrated in M9 buffer. The concentrations employed for each compound were 10, 25, 50 and 100 µM for betalains and flavonoids assays and 100 µM for AFDs assays. For a final volume of 5 mL, sterile S medium was added and the flasks were kept under orbital shaking at 20 °C. Prickly pear extracts were used in the same way, but the final concentration of the extracts in the assays was 0.1, 0.5, and 1% w/v.

## 29. Survival assays

Lifespan machine, the platform for the automatic control of the organism *C. elegans* mobility, was used in the survival assays. After 48 hours in liquid culture in S medium supplemented with the tested compounds, synchronic worms were centrifuged at 2,000 g and washed with M9 buffer three times. Then, 40-50 worms were transferred to 35 mm analysis plates, containing 8 mL of NGM agar, 30 µg/mL of nystatin, 100 µM of ampicillin and 10 µg/mL of FUdR (2'-Deoxy-5-fluorouridine) to avoid progeny (Alvarez-Illera et al., 2017; García-Casas et al., 2019). Plates were seeded with 100 µL of heat inactivated *E. coli* OP50 (an overnight culture in LB at 37 °C was concentrated 10X in sterile M9 buffer and then the concentrated *E. coli* was incubated for 30 minutes at 65 °C for its inactivation). All the experiment plates were done in triplicate. Plates were closed and incubated 20 minutes at 20 °C. Plates that presented condensation were opened under sterile conditions and the lids dried with disposable sterile wipers. Closed lid plates were loaded into the lifespan machine's scanners. The experiments were performed in the lifespan machine at 25 °C for 25 days.

## 30. Lifespan machine temperature control

*C. elegans* life cycle is very sensitive to temperature, so in order to avoid differences in lifespan due to temperature, the incubator temperature was adjusted to maintain a temperature of 25 °C inside the scanners, using external temperature probes (USB Reference Thermometers purchased from Thermoworks, Utah, USA). The external probes allowed to record the temperature inside the scanner for the duration of the experiments.

## 31. *C. elegans* sterility via gene knockdown with RNAi

Gene knockdown by RNAi feeding was used to cause sterility in the N2 strain to avoid the use of FUdR to avoid progeny. The *E. coli* strain HT115 (DE3) with the homologous DNA sequence for the *pop-1* (W10C8.2) gene inside the vector pL4440 DEST was obtained from Source BioScience (Nottingham, UK) from the library *C. elegans* ORF-RNAi (Rual et al., 2004). The RNAi feeding was done following the standard protocol (Ahringer, 2006). Briefly, the HT115 strain was cultured in LB supplemented with 100 µg/mL of ampicillin overnight at 37 °C, after which the cells were induced with 1 mM of IPTG at 37 °C for one hour. Cultures were then centrifuged

to remove LB and cells were concentrated to 10X with M9 buffer. The effectivity of the gene knockdown vs. the use of FUdR to avoid progeny was done by comparing the obtained results for survival assays for worms pre-treated with four model betalains (Chapter XI). For gene knockdown assay, the survival assay was performed by changing the OP50 for HT115 and adding to the reaction medium 100 µg/mL of ampicillin and IPTG to a final concentration of 1 mM.

### 32. Statistical analysis

Mathematical analysis of the data obtained in the lifespan machine was performed using the on-line application for survival analysis OASIS 2 (Han et al., 2016), with the Kaplan-Meier estimator, Boschloo's Test, Kolmogorov-Smirnov Test and Survival Time F-Test.

In the rest of experiments, one-way ANOVA Calculator for independent measures was performed for numeric data while Chi-square Calculator Contingency Table was used for nominal data. Both analyses were performed using the online Social Sciences Calculator <https://www.socscistatistics.com>. The significance level for all the data was 0.05.

### 33. Fluorescence microscopy

Images of fluorescence from worms were taken at constant exposure times using a Leica DM 2500 LED microscope fitted with a Leica DFC550 camera (Leica Microsystems, Wetzlar, Germany) with incident light beam. All worms' cultures contained *E. coli* OP50 as food, and FUdR to avoid progeny. To quantify fluorescence, images of 12-13 worms per condition were taken and analysed using ImageJ software (NIH) (Abràmoff et al., 2004). For each raw image, worms were outlined black-to-white inverted and the mean pixel density was measured.

#### 33.1. Quantification of *hsp-16.2::GFP* expression in *C. elegans* strain TJ375

TJ375 (*hsp-16.2::GFP*) worms were cultured in liquid S medium at 20 °C and the expression of *hsp-16.2* was measured by observing the fluorescence of the green fluorescent protein (GFP). TJ375 age-synchronized worms were treated for 48 h with different concentrations of betalains, flavonoids or AFDs beginning on the day after hatching. The worms were then transferred to a fresh medium, and oxidative stress was

exerted by adding a solution of juglone 20  $\mu$ M to the liquid medium. After 24 h of induction, the worms were washed with M9 buffer and mounted on glass slides containing 10 mM sodium azide to reduce their mobility. The images taken using filtercube I3 (Leica, excitation range: 450-490 nm) included the anterior part of the worms from the back of the pharynx.

### **33.2. DAF-16 transcription factor intracellular localization in *C. elegans* strain TJ356**

*C. elegans* strain TJ356 (*daf-16::GFP*) expresses the green fluorescent protein fused to the transcription factor DAF-16. TJ356 worms were synchronized and treated with different concentrations of betalains, flavonoids or AFDs. After 72 hours at 20 °C, worms were washed with M9 buffer twice and mounted onto glass slides containing 10 mM sodium azide to reduce their mobility. Worms were catalogued as “nuclear” when GFP fluorescence was visible in the nuclei, “cytoplasmic” when GFP fluorescence was diffused in the whole soma and “intermediate” if fluorescence was present in both nuclei and soma locations. Positive control (DAF-16 nuclear localization) was prepared by “heat shocking” non-treated TJ356 worms at 37 °C for one hour and water was used as negative control (cytosolic localization). Images were taken using filtercube I3 (Leica, excitation range: 450-490 nm).

### **33.3. SKN-1 transcription factor intracellular localization in *C. elegans* strain LD1**

The LD1 worms express *skn-1b/c::GFP* in the gut and in the ASI neurons. SKN-1 regulates a key Phase II detoxification gene through constitutive and stress-inducible mechanisms in the ASI chemosensory neurons and intestine, respectively. SKN-1 is present in ASI nuclei under normal conditions, and accumulates in intestinal nuclei in response to oxidative stress. LD1 worms were age-synchronized and treated with the tested compounds in S medium at 20 °C. After 72 hours, the worms were washed with M9 buffer twice and mounted on glass slides containing 10 mM sodium azide. Water was used as negative control. Images were taken using filtercube I3 (Leica, excitation range: 450-490 nm). Gut fluorescence was measured with ImageJ software (NIH).

### 33.4. Quantification of *dat-1p::GFP* expression in *C. elegans* strain BZ555

BZ555 (*dat-1p::GFP*) strain expresses the green fluorescent protein fused to the promoter of the *dat-1* gene in dopaminergic neurons. Age-synchronized worms were kept in 5 mL of liquid S medium supplemented with 100  $\mu$ M of individual AFDs tartrazine, sunset yellow, quinoline yellow, carmoisine, ponceau 4R and allura red. After 6 days at 20 °C, worms were washed with M9 buffer and mounted onto glass slides containing 10 mM sodium azide. Images were taken using filtercube I3 (Leica, excitation range: 450-490 nm).

### 33.5. Lipofuscin detection

The accumulation of lipofuscin in worms pre-treated with AFDs was measured as an aging marker. Age-synchronized N2 worms were kept in 5 mL of liquid S medium supplemented with 100  $\mu$ M of tartrazine, sunset yellow, quinoline yellow, carmoisine, ponceau 4R or allura red. After 4 days at 20 °C, worms were washed with M9 buffer and mounted onto glass slides containing 10 mM sodium azide. Images were taken using filtercube A (Leica, excitation range: 340-380 nm).

## 34. RNA extraction

The day after hatching, synchronized-worms were treated with 25  $\mu$ M of the pure betalains, 100  $\mu$ M of the baicalein and 100  $\mu$ M of the selected AFDs in S medium and kept at 20 °C with orbital shaking at 120 rpm. After 48 h, worms were washed with M9 buffer ten times for the complete elimination of *E. coli* bacteria present in the medium. Then, the clean worms were resuspended in 250  $\mu$ L of M9 buffer and 750  $\mu$ L of reactive TRIzol® was employed for the RNA extraction. RNA extraction and its purification were realized following the protocol of PureLink™ RNA Mini Kit from Invitrogen (Carlsbad, California, USA). The amount and quality of the RNA were checked by Bioanalyzer (Agilent Technologies) and it was then used for microarray analysis.

## 35. Microarray analysis

Ss-cDNA was synthesized from 3.5 ng of each sample using the GeneChip WT Pico Reagent kit (Affymetrix, P/N 703262) purchased from Thermo Fisher Scientific (Thermo Fisher Scientific Inc., USA), according to the protocol supplied by the

manufacturer. The amount and quality of ss-cDNA were checked by Nanodrop and Bioanalyzer (Agilent Technologies). ss-cDNA targets were cleaned up, and after fragmentation and terminal labelling, 3.75 µg of fragmented and biotinylated ss-cDNA were included in the hybridization mix, using the GenAtlas Hybridization, Wash and Stain kit for WT Array Strips (Affymetrix, P/N 901667) according to the recommendations of the manufacturer. The resulting preparations were hybridized to GeneChip® *C. elegans* Gene 1.1 ST Array Strip (Affymetrix, 902157) with 26 unique sequences of each transcript. After applying hybridization and labeling tests it was observed that the all chips had fulfilled the quality criteria.

After scanning, microarrays data were processed using Affymetrix Expression Command Console (Affymetrix, Thermofisher) and all samples were within bounds for hybridization and labeling tests.

Three independent RNA samples were employed. Samples from worms treated with betalains, baicalein, or AFDs were grouped as “treatment” and worms without compounds exposition were grouped as “control”. Data analysis was then performed with RMA (Robust Multiarray Average) allowing raw intensity values to be background corrected, log2 transformed and then quantile normalized in order to obtain an individual intensity value for each probe set. Partek Genomics Suite and Partek Pathways software (Partek Incorporated, St. Louis, USA) were used for the statistical analysis and an ANOVA test was applied with a restrictive threshold at  $p\text{-value} \leq 0.05$ . The molecular interaction, reaction and relation networks that showed differentially expressed genes (DEGs) were then analysed using KEGG Pathways (Kyoto Encyclopaedia of Genes and Genomes).

### 36. Metabolic assays

On the seventh day of the compounds treatment assays, worms were collected, centrifuged and washed three times with sterile M9 buffer. Once cleaned, the worms were resuspended in 20 mM phosphate buffer pH 7.0 supplemented with 10 mM of sodium ascorbate. Then the worms were disrupted by sonication with 3 pulses of 20 seconds in a Branson Digital sonifier (Branson Ultrasonic Corporation). The debris was precipitated by centrifugation and the supernatant transferred to a clean tube. The samples obtained were stored at -20 °C until analysis.

### 37. Oil Red O (ORO) lipid staining

Quantification of lipids in *C. elegans* was performed using the Oil Red O protocol (O'Rourke et al., 2009) with some modifications. Briefly, one day-adult worms treated with 100  $\mu$ M of individual flavones were fixed in a formaldehyde PBS solution (4%) for 24 hours at 4 °C. Then, the worms were washed and permeabilized using a 5%  $\beta$ -mercaptoethanol, 1% Triton-100 solution in tris/HCl buffer pH 7.4 for 24 hours at 37 °C. Then the fixed and permeabilized worms were washed twice with PBS. Meanwhile, an ORO working solution (60%) was prepared diluting a stock solution of ORO (0.5 g ORO in 100 mL of isopropanol) in distilled water and filtered through a 0.22  $\mu$ m syringe filter. Fixed worms were treated with the ORO working solution for five minutes at room temperature, then washed three times with PBS-Triton (0.01%) buffer. ORO stained animals were mounted onto glass slides and brightfield images were taken with the 40x lens of a Leica DM 2500 LED microscope fitted with a Leica DFC550 camera (Leica Microsystems). ORO quantification of the images was performed with the free software Fiji (NIH), an improved ImageJ (Schindelin et al., 2012). Firstly, the images were split with the colour deconvolution tool using the H AEC vector, followed by applying the thresholding tool only in the red channel and measuring the intensity in the threshold area.

### 38. Motility analysis

The effects of the six AFDs in the motility of *C. elegans* were measured by evaluating the average speed, maximum speed and number of bendings of the animals. Synchronized worms in the first larva stage L1 were treated with 100  $\mu$ M of each colorant in S basal medium supplemented with *E. coli* as food source. After 48 hours, plates were acclimated to the room temperature 30 minutes and then, videos of worms' movements were recorded using an Optika SZO series stereomicroscope (OPTIKA S.r.l., Italy) fitted with an Optika H series camera (OPTIKA). Image analysis was performed by using the worMTracker -wrMTrck- plugin of imageJ software (NIH) following the Pederson's protocol (Pederson, 2008).



## REFERENCES

- Abràmoff, M.D., Magalhães, P.J., Ram, S.J., 2004. Image processing with ImageJ. *Biophotonics Int.* 11, 36–42.
- Ahringer, J., 2006. Reverse genetics. In *WormBook*, ed. The *C. elegans* research community, *WormBook*, doi/10.1895/wormbook.1.47.1, <http://www.wormbook.org>.
- Altschul, S.F., Wootton, J.C., Gertz, E.M., Agarwala, R., Morgulis, A., Schaffer, A.A., Yu, Y.-K., 2005. Protein database searches using compositionally adjusted substitution matrices. *FEBS J.* 272, 5101–5109. <https://doi.org/10.1111/j.1742-4658.2005.04945.x>
- Alvarez-Illera, P., García-Casas, P., Arias-del-Val, J., Fonteriz, R.I., Alvarez, J., Montero, M., 2017. Pharynx mitochondrial  $[Ca^{2+}]$  dynamics in live *C. elegans* worms during aging. *Oncotarget* 8, 55889–55900. <https://doi.org/10.18632/oncotarget.18600>
- Benkert, P., Biasini, M., Schwede, T., 2011. Toward the estimation of the absolute quality of individual protein structure models. *Bioinformatics* 27, 343–350. <https://doi.org/10.1093/bioinformatics/btq662>
- Benzie, I.F.F., Strain, J.J., 1996. The ferric reducing ability of plasma (FRAP) as a measure of “antioxidant power”: The FRAP assay. *Anal. Biochem.* 239, 70–76. <https://doi.org/10.1006/abio.1996.0292>
- Bertoni, M., Kiefer, F., Biasini, M., Bordoli, L., Schwede, T., 2017. Modeling protein quaternary structure of homo- and hetero-oligomers beyond binary interactions by homology. *Sci. Rep.* 7. <https://doi.org/10.1038/s41598-017-09654-8>
- Biasini, M., Schmidt, T., Bienert, S., Mariani, V., Studer, G., Haas, J., Johner, N., Schenk, A.D., Philippsen, A., Schwede, T., 2013. OpenStructure: An integrated software framework for computational structural biology. *Acta Crystallogr. Sect. D Biol. Crystallogr.* 69, 701–709. <https://doi.org/10.1107/S0907444913007051>
- Bienert, S., Waterhouse, A., De Beer, T.A.P., Tauriello, G., Studer, G., Bordoli, L., Schwede, T., 2017. The SWISS-MODEL Repository-new features and functionality. *Nucleic Acids Res.* 45, D313–D319. <https://doi.org/10.1093/nar/gkw1132>
- Bradford, M.M., 1976. A rapid and sensitive method for the quantitation of microgram quantities of protein utilizing the principle of protein-dye binding. *Anal. Biochem.* 72, 248–254. [https://doi.org/10.1016/0003-2697\(76\)90527-3](https://doi.org/10.1016/0003-2697(76)90527-3)

- Cabanes, J., Gandía-Herrero, F., Escribano, J., García-Carmona, F., Jiménez-Atiénzar, M., 2014. One-step synthesis of betalains using a novel betalamic acid derivatized support. *J. Agric. Food Chem.* 62, 3776–3782. <https://doi.org/10.1021/jf500506y>
- Camacho, C., Coulouris, G., Avagyan, V., Ma, N., Papadopoulos, J., Bealer, K., Madden, T.L., 2009. BLAST+: Architecture and applications. *BMC Bioinformatics* 10, 421. <https://doi.org/10.1186/1471-2105-10-421>
- Eastman, P., Swails, J., Chodera, J.D., McGibbon, R.T., Zhao, Y., Beauchamp, K.A., Wang, L.P., Simmonett, A.C., Harrigan, M.P., Stern, C.D., Wiewiora, R.P., Brooks, B.R., Pande, V.S., 2017. OpenMM 7: Rapid development of high performance algorithms for molecular dynamics. *PLoS Comput. Biol.* 13, e1005659. <https://doi.org/10.1371/journal.pcbi.1005659>
- Gandía-Herrero, F., Cabanes, J., Escribano, J., García-Carmona, F., Jiménez-Atiénzar, M., 2013. Encapsulation of the most potent antioxidant betalains in edible matrixes as powders of different colors. *J. Agric. Food Chem.* 61, 4294–4302. <https://doi.org/10.1021/jf400337g>
- Gandía-Herrero, F., Escribano, J., García-Carmona, F., 2010. Structural implications on color, fluorescence, and antiradical activity in betalains. *Planta* 232, 449–460. <https://doi.org/10.1007/s00425-010-1191-0>
- Gandía-Herrero, F., García-Carmona, F., 2012. Characterization of recombinant *Beta vulgaris* 4,5-DOPA-extradiol-dioxygenase active in the biosynthesis of betalains. *Planta* 236, 91–100. <https://doi.org/10.1007/s00425-012-1593-2>
- Gandía-Herrero, F., García-Carmona, F., Escribano, J., 2006. Development of a protocol for the semi-synthesis and purification of betaxanthins. *Phytochem. Anal.* 17, 262–269. <https://doi.org/10.1002/pca.909>
- García-Casas, P., Arias-Del-Val, J., Alvarez-Illera, P., Wojnicz, A., De Los Ríos, C., Fonteriz, R.I., Montero, M., Alvarez, J., 2019. The neuroprotector benzothiazepine CGP37157 extends lifespan in *C. elegans* worms. *Front. Aging Neurosci.* 11, 440. <https://doi.org/10.3389/fnagi.2018.00440>
- Girod, P.-A., Zryd, J.-P., 1991. Biogenesis of betalains: Purification and partial characterization of dopa 4,5-dioxygenase from *Amanita muscaria*. *Phytochemistry* 30, 169–174. [https://doi.org/10.1016/0031-9422\(91\)84119-D](https://doi.org/10.1016/0031-9422(91)84119-D)
- Han, S.K., Lee, D., Lee, H., Kim, D., Son, H.G., Yang, J.-S., Lee, S.-J. V, Kim, S., 2016. OASIS 2: online application for survival analysis 2 with features for the analysis of maximal lifespan and healthspan in aging research. *Oncotarget* 7,

- 56147–56152. <https://doi.org/10.18632/oncotarget.11269>
- Krivov, G.G., Shapovalov, M. V., Dunbrack, R.L., 2009. Improved prediction of protein side-chain conformations with SCWRL4. *Proteins Struct. Funct. Bioinforma.* 77, 778–795. <https://doi.org/10.1002/prot.22488>
- Laemmli, U.K., 1970. Cleavage of structural proteins during the assembly of the head of bacteriophage T4. *Nature* 227, 680–685. <https://doi.org/10.1038/227680a0>
- Letunic, I., Bork, P., 2019. Interactive Tree Of Life (iTOL) v4: recent updates and new developments. *Nucleic Acids Res.* 47, W256–W259. <https://doi.org/10.1093/nar/gkz239>
- Li, W., Cowley, A., Uludag, M., Gur, T., McWilliam, H., Squizzato, S., Park, Y.M., Buso, N., Lopez, R., 2015. The EMBL-EBI bioinformatics web and programmatic tools framework. *Nucleic Acids Res.* 43, W580–W584. <https://doi.org/10.1093/nar/gkv279>
- Mackerell, A.D., Feig, M., Brooks, C.L., 2004. Extending the treatment of backbone energetics in protein force fields: Limitations of gas-phase quantum mechanics in reproducing protein conformational distributions in molecular dynamics simulation. *J. Comput. Chem.* 25, 1400–1415. <https://doi.org/10.1002/jcc.20065>
- Madeira, F., Park, Y.M., Lee, J., Buso, N., Gur, T., Madhusoodanan, N., Basutkar, P., Tivey, A.R.N., Potter, S.C., Finn, R.D., Lopez, R., 2019. The EMBL-EBI search and sequence analysis tools APIs in 2019. *Nucleic Acids Res.* 47, W636–W641. <https://doi.org/10.1093/nar/gkz268>
- McDowell, E.M., Trump, B.F., 1976. Histologic fixatives suitable for diagnostic light and electron microscopy. *Arch. Pathol. Lab. Med.* 100, 405–414.
- McPake, C.B., Murray, C.B., Sandford, G., 2009. Epoxidation of alkenes using HOF·MeCN by a continuous flow process. *Tetrahedron Lett.* 50, 1674–1676. <https://doi.org/10.1016/j.tetlet.2008.12.073>
- Noor, A.I., Mokhtar, M.H., Rafiqul, Z.K., Pramod, K.M., 2012. Understanding color models : A review. *ARPN J. Sci. Technol.* 2, 265–275.
- O’Rourke, E.J., Soukas, A.A., Carr, C.E., Ruvkun, G., 2009. *C. elegans* major fats are stored in vesicles distinct from lysosome-related organelles. *Cell Metab.* 10, 430–435. <https://doi.org/10.1016/j.cmet.2009.10.002>
- Parry, J.M., Gilbert, R.J., 1980. Studies on the heat resistance of *Bacillus cereus* spores and growth of the organism in boiled rice. *J. Hyg. (Lond).* 84, 77–82. <https://doi.org/10.1017/S0022172400026541>

- Pederson, J.S., 2008. *C. elegans* motility analysis in ImageJ - A practical approach. <https://docplayer.net/14385273-C-elegans-motility-analysis-in-imagej-a-practical-approach.html>
- Remmert, M., Biegert, A., Hauser, A., Söding, J., 2012. HHblits: Lightning-fast iterative protein sequence searching by HMM-HMM alignment. *Nat. Methods* 9, 173–175. <https://doi.org/10.1038/nmeth.1818>
- Rual, J.F., Ceron, J., Koreth, J., Hao, T., Nicot, A.S., Hirozane-Kishikawa, T., Vandenhaute, J., Orkin, S.H., Hill, D.E., van den Heuvel, S., Vidal, M., 2004. Toward improving *Caenorhabditis elegans* phenome mapping with an ORFeome-based RNAi library. *Genome Res.* 14, 2162–2168.
- Schindelin, J., Arganda-Carreras, I., Frise, E., Kaynig, V., Longair, M., Pietzsch, T., Preibisch, S., Rueden, C., Saalfeld, S., Schmid, B., Tinevez, J.Y., White, D.J., Hartenstein, V., Eliceiri, K., Tomancak, P., Cardona, A., 2012. Fiji: An open-source platform for biological-image analysis. *Nat. Methods.* 9(7), 676–682. <https://doi.org/10.1038/nmeth.2019>
- Schliemann, W., Kobayashi, N., Strack, D., 1999. The decisive step in betaxanthin biosynthesis is a spontaneous reaction. *Plant Physiol.* 119, 1217–1232. <https://doi.org/10.1104/pp.119.4.1217>
- Schwartz, S.J., von Elbe, J.H., 1980. Quantitative determination of individual betacyanin pigments by High-Performance Liquid Chromatography. *J. Agric. Food Chem.* 28, 540–543. <https://doi.org/10.1021/jf60229a032>
- Shapovalov, M. V., Dunbrack, R.L., 2011. A smoothed backbone-dependent rotamer library for proteins derived from adaptive kernel density estimates and regressions. *Structure* 19, 844–858. <https://doi.org/10.1016/j.str.2011.03.019>
- Stiernagle, T., 2006. Maintenance of *C. elegans*. In *WormBook*. Ed. The *C. elegans* research community, *WormBook*, doi/10.1895/wormbook.1.101.1, <http://www.wormbook.org>.
- Trezzini, G.F., Zrýb, J.-P., 1991. Characterization of some natural and semi-synthetic betaxanthins. *Phytochemistry* 30, 1901–1903. [https://doi.org/10.1016/0031-9422\(91\)85036-Y](https://doi.org/10.1016/0031-9422(91)85036-Y)
- Waterhouse, A., Bertoni, M., Bienert, S., Studer, G., Tauriello, G., Gumienny, R., Heer, F.T., De Beer, T.A.P., Rempfer, C., Bordoli, L., Lepore, R., Schwede, T., 2018. SWISS-MODEL: Homology modelling of protein structures and complexes. *Nucleic Acids Res.* 46, W296–W303. <https://doi.org/10.1093/nar/gky427>

- Woomer, P.L., 1994. Most probable number counts. In *Methods of soil analysis. Part 2.* Eds. R W Weaver, S Angle, P Bottomley, D Bezdicek, S Smith, A Tabatabai and A Wollum. Microbiological and biochemical properties, Soil Science Society of America, Wisconsin. 59-79. Print ISBN: 9780891188100
- Wyler, H., Wilcox, M.E., Dreiding, A.S., 1965. Umwandlung eines Betacyans in ein Betaxanthin. Synthese von Indicaxanthin aus Betanin. *Helv. Chim. Acta* 48, 361–366. <https://doi.org/10.1002/hlca.19650480214>

**Chapter IV.** First betalain producing bacteria break  
the exclusive presence of the pigments in the plant kingdom

Part of this chapter was published in mBio  
Contreras-Llano et al. (2019) <https://doi.org/10.1128/mBio.00345-19>



### **Contextualization**

As it is described in the introduction section, the biosynthesis of betalains has always been believed to be restricted to Caryophyllales plants and some species of fungi which produce betalain-related pigments. However, no evidence exists in the bibliography that bacteria may synthesize betalains. The search for novel biological systems and enzyme mining from non-native hosts led to establishing bacterial cultures of microorganisms and supplementing them with L-DOPA as precursor able to yield betalamic acid thanks to activity of 4,5-DOPA-extradiol-dioxygenase enzyme. The spectrum of possible sources of betalain pigments in nature is here broadened by describing the first betalain forming bacteria, *Gluconacetobacter diazotrophicus*.

### **1. *Gluconacetobacter diazotrophicus* cultures produce betalamic acid**

*Gluconacetobacter diazotrophicus* is a proteobacteria first described in roots and stems of sugarcane (Gilliss et al., 1989) with no evident relationship with plants of the order Caryophyllales, but their cultures supplemented with L-DOPA 7.6 mM showed yellow coloration. HPLC analysis of yellow *G. diazotrophicus* cultures showed the presence of a peak with a retention time (RT) of 13.67 min and with an exact mass detected by HPLC-ESI/TOF/MS of 391.1144 *m/z*. This mass corresponded to the pigment dopaxanthin, the DOPA-derived betaxanthin first described in *Glottiphyllum longum* flowers (Impellizzeri et al., 1973) and its identity was corroborated using a real dopaxanthin standard (**Fig. 4.1**).

This positive result was further investigated by harvesting *G. diazotrophicus* cells and resuspending them in water supplemented with increasing concentrations of L-DOPA until its solubility limit was reached at 7.6 mM. After 24 hours, this medium showed yellow coloration and the presence of dopaxanthin was confirmed by HPLC-ESI/TOF/MS. The exact mass of 391.1144 *m/z*, corresponding to dopaxanthin, was detected in all the samples and its accumulation was higher as concentration of L-DOPA increased (**Fig. 4.2**).



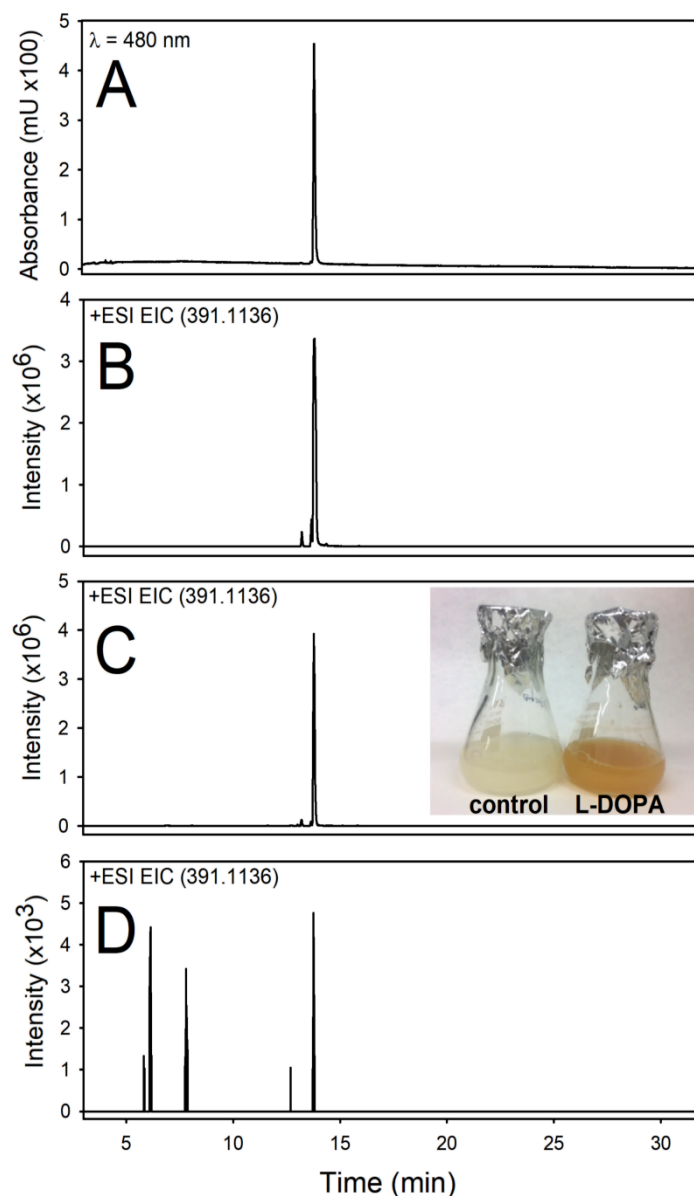


**Figure 4.1. Detection of dopaxanthin in *Gluconacetobacter diazotrophicus* cultures supplemented with L-DOPA.** Standard dopaxanthin was followed by HPLC-DAD at  $\lambda=480$  nm (A) and by HPLC-ESI-TOF-MS at EIC 391.1136  $m/z$  (B). The same peak was detected in EIC of *G. diazotrophicus* transformations in water (C) and culture medium (D), both supplemented with L-DOPA 7.6 mM.

The presence of L-DOPA stimulated the production of dopaxanthin but low amounts of dopaxanthin were also detected in the absence of added L-DOPA. Therefore, *Gluconacetobacter diazotrophicus* is able to produce the betalain dopaxanthin under physiological conditions in the absence of exogenous L-DOPA. Thus *G. diazotrophicus* expresses a dioxygenase enzyme able to cleave the aromatic ring of L-DOPA in the same manner as the 4,5-extradiol-DOPA-dioxygenases of plant origin. HPLC-DAD was used to follow the reaction and to determine the

spectral maximum wavelength of a main peak found a retention time (RT) of 13,67 min at  $\lambda = 470$  nm. This peak was identified as dopaxanthin. A minor peak with maximum wavelength of  $\lambda = 405$  nm and a RT of 14.46 min was also detected, compatible with the presence of betalamic acid. HPLC-ESI/TOF/MS and a real standard of betalamic acid were used to confirm its presence, with an exact mass of 212.0554  $m/z$ .

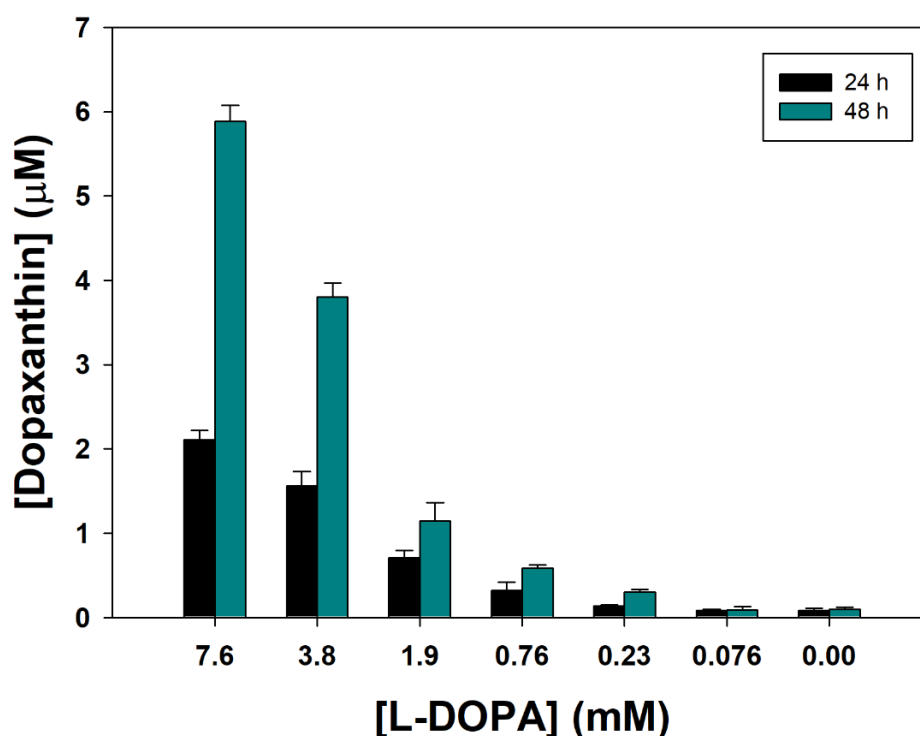


**Figure 4.2.** Dopaxanthin accumulation in *G. diazotrophicus* cultures at different concentrations of added L-DOPA. Samples were analyzed at 24 and 48 h and showed accumulation of dopaxanthin even in the absence of exogenous L-DOPA.

## 2. *G. diazotrophicus* 4,5-DODA sequence, expression and purification

A sequence with suitable characteristics to provide the dopaxanthin-forming activity described in the cultures of *G. diazotrophicus* was found in its genome, the WP\_012222467 protein (gi:501179334) from which an optimized synthetic sequence was expressed in *Escherichia coli* Rosetta 2 (DE3) cells. The DODA enzyme from *G. diazotrophicus* (GdDODA) was expressed accounting for 46% of the total soluble protein in the cell extract. Recombinant protein was purified by  $\text{Ni}^{2+}$ -chelating affinity chromatography, run on an SDS-PAGE and purified to homogeneity (**Fig. 4.3A**) with a purification fold of 1.8 (**Table 4.1**), in accordance to the electrophoretic estimation of DODA expression.

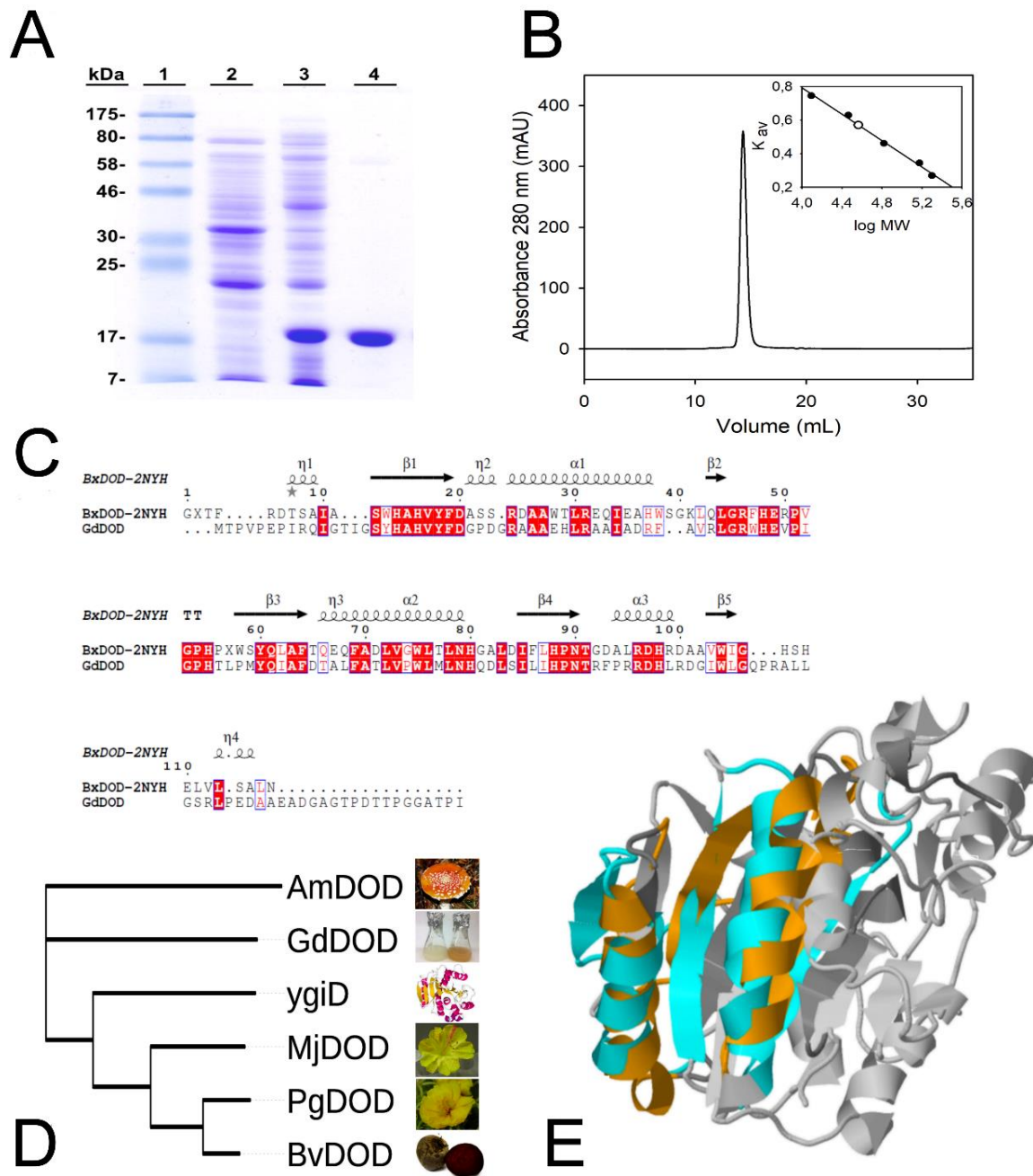


**Figure 4.3. Betalain production and characterization of the novel dioxygenase from *Gluconacetobacter diazotrophicus*.** **A:** Electrophoretic analysis for the expression and purification of recombinant GdDODA from *E. coli* culture. Lane 1: molecular weight markers; lane 2: soluble protein content of cells harvested prior to IPTG induction; lane 3: soluble protein content of cells harvested 20 h after IPTG induction (0.5 mM); lane 4: eluted protein after affinity chromatography purification. **B:** Analysis of GdDODA by gel filtration chromatography. The profile shows a single peak corresponding to a homodimeric form. Inset: Calibration curve and molecular mass determination. **C:** Sequence comparison of GdDODA with the structurally characterized protein PDB ID: 2NYH from *Burkholderia xenovorans*. Multiple sequence alignment using structural information was performed with Expresso (Armougom et al., 2006). Conserved blocks of amino acids are squared and strictly conserved residues are shown in red. Information was displayed with ESPrpt program (Robert and Gouet, 2014) (Continues on the next page).

**D:** Phylogenetic analysis of all characterized 4,5-DOPA-dioxygenases known to produce betalamic acid. Multiple sequence alignment was performed using ClustalW2. The unrooted tree was obtained with the Phylogeny inference package from EMBL (Neighbor-Joining algorithm) (Letunic and Bork, 2016; Li et al., 2015) using the conserved block among residues His91 and Asp122. This block contains one of the three strictly conserved histidines in the plant enzymes which also appears in the novel dioxygenase from *G. diazotrophicus* as His101. **E:** Structural model for the DODA from *G. diazotrophicus* (orange and dark grey) superimposed to the YgiD protein from *E. coli* (blue and pale grey). Orange (GdDODA) and blue (YgiD-EcDOD) portions of the protein indicate structural similarity according to the Combinatorial Extension (CE) algorithm.

**Table 4.1. Expression and purification of *G. diazotrophicus* dioxygenase.**

	Volume (mL)	Protein (mg/mL)	Total Prot. (mg)	<sup>a</sup> Activity ( $\mu\text{M} \cdot \text{min}^{-1}$ )	Specific Activity ( $\mu\text{mol} \cdot \text{min}^{-1} \cdot \text{mg}^{-1}$ )	Purif. fold	Yield (%)
<sup>b</sup> Crude extract	6.0	15.9	95.4	1.578	0.595	1.0	100
Ni <sup>2+</sup> chrom.	7.0	4.5	31.8	0.823	1.087	1.8	61

<sup>a</sup>Activity was determined using 50  $\mu\text{L}$  of protein solution under the assay conditions.

<sup>b</sup>Crude extract was obtained from a cellular paste harvested from a 0.5 L culture.

### 3. Molecular and structural characterization of *G. diazotrophicus* 4,5-DODA

HPLC-ESI/TOF/MS mass spectra showed a single peak with a molecular mass of 17.822 kDa, consistent with the molecular weight calculated using the protein sequence (17.8 kDa). Peptide Mass Fingerprint analysis further support the identity of protein (Table 4.2, Fig. 4.4). In addition, *G. diazotrophicus* 4,5-DODA was determined to be a dimer under native conditions after gel filtration because different samples from 2.5  $\mu\text{g}$  up to 0.39 mg eluted as a single peak with a molecular mass estimated at 36.5 kDa (Fig. 4.3B). These results further support the sequence homology found for GdDODA. A 46% identity (56.6% similarity, local alignment) was determined (Fig. 4.3C) with a structurally characterized enzyme from *Burkholderia xenovorans* Lb400 (Li et al., 2015; Smith and Waterman, 1981), a dioxygenase (PDB entry 2NYH) that also demonstrated to be a dimer, which is the closest homolog structurally characterized. By structurally assisted sequence

comparison, GdDODA residues were assigned to specific secondary motifs (Armougom et al., 2006; Robert and Gouet, 2014). A three dimensional model of the novel enzyme from *G. diazotrophicus* was performed by the comparative modelling engine ProMod3 (Biasini et al., 2014; Bienert et al., 2017) and then used for comparison with the only crystallized protein known to form betalamic acid from L-DOPA in enzyme assays - the protein YgiD (PDB entry 2PW6) from *E. coli*, a homologue of the plant enzymes (Gandía-Herrero and García-Carmona, 2014) (**Fig. 4.3D**). Structural comparison (Prlić et al., 2010) shows how both enzymes share common local structural features. Despite of the protein size differences the small monomer of GdDODA superimposes well with one portion of the YgiD protein, and the structures composed of the amino acids Gly28-Asp41, Val45-Pro57, His58-Thr59, Leu60-Ala66, Phe67-His83, and Gln84-Pro97 in the *G. diazotrophicus* sequence are also present in the plant homologue protein.

**Table 4.2. Main peptides identified to fully characterize the protein GdDODA.** Its peptide mass fingerprint was determined by MALDI-TOF analysis after trypsin digestion. Amino acids in brackets correspond to the theoretical residue after trypsin digestion. (-) corresponds to the beginning of the sequence.

Peptide identified	<i>m/z</i>
[(-)MTPVPEPIRQIGTIGSYHAHVYFDGPDGR(A)]	3210.58
[(R)QIGTIGSYHAHVYFDGPDGR(A)]	2190.04
[(R)DGIWLGQPRALLGSR(L)]	1638.91
[(R)DGIWLGQPR(A)]	1041.55
[(-)MTPVPEPIR(Q)]	1039.56
[(R)AAIADR(F)]	616.34
[(R)DHLLR(D)]	540.29

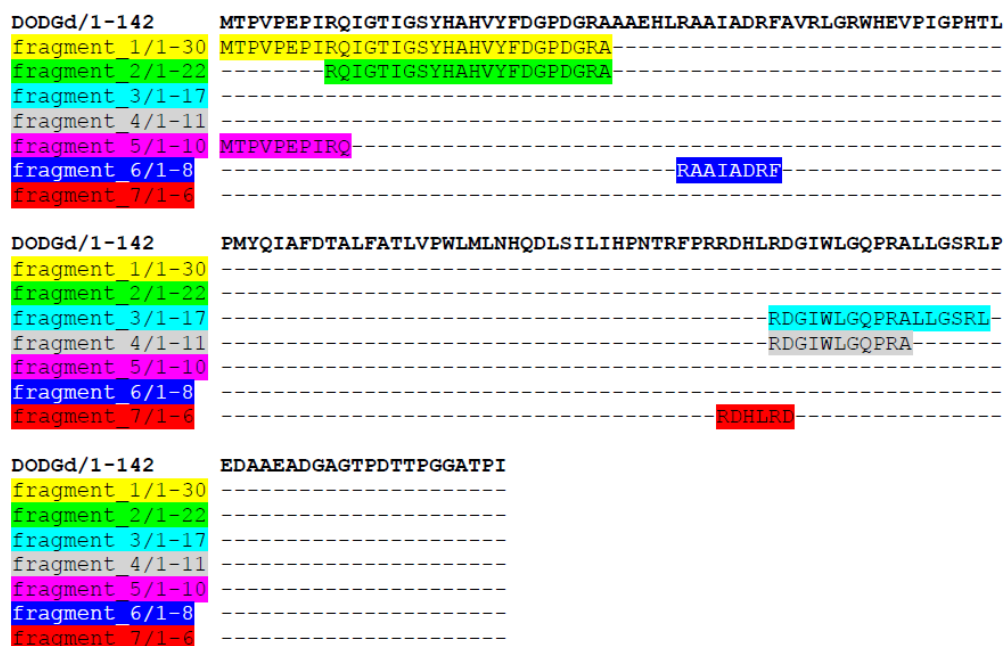
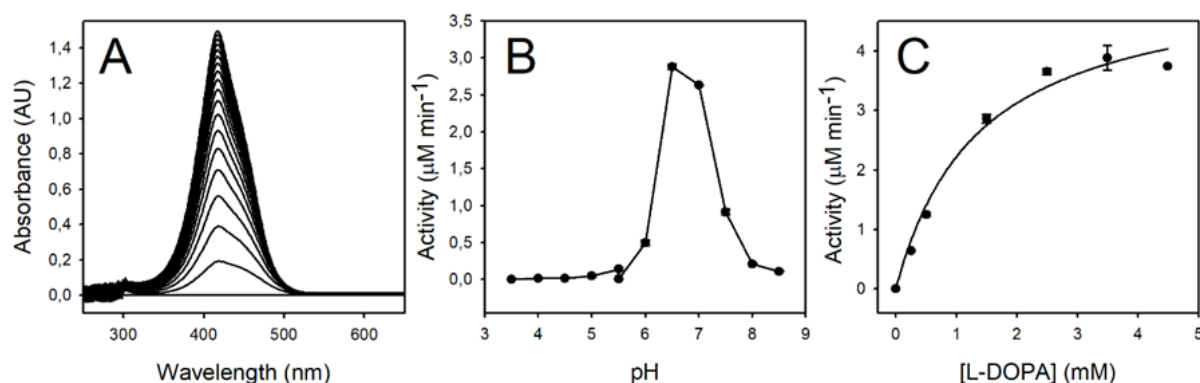


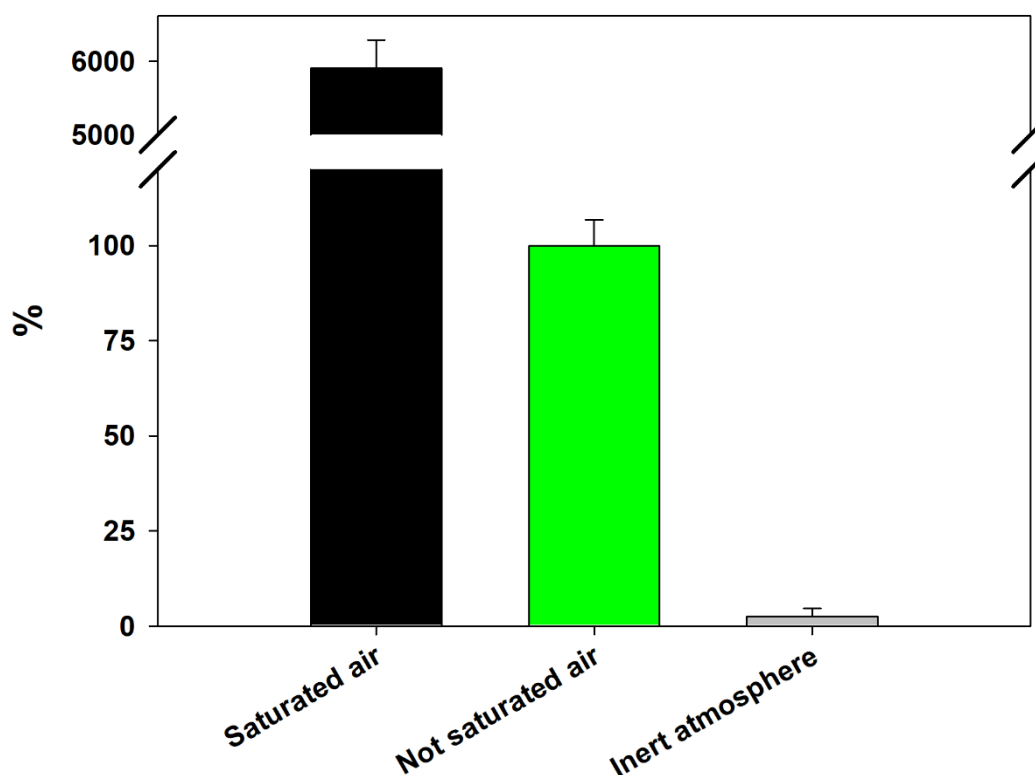
Figure 4.4. Sequence coverage of the detected fragments identified in the peptide mass fingerprint of GdDODA.

#### 4. Kinetic characterization

The addition of the novel *G. diazotrophicus* enzyme to a reaction media containing L-DOPA produced a yellow coloration with a  $\lambda_{\max}$  of 414 nm (Fig. 4.5A). The optimum pH for the DOPA-dioxygenase activity was determined as pH 6.5 (Fig. 4.5B), and this pH was used to characterize the kinetic parameters (Fig. 4.5C), determined as  $K_m = 1.36 \pm 0.31$  mM and  $V_{\max} = 5.26 \pm 0.43$   $\mu$ M/min. This  $K_m$  value is lower than those obtained for *B. vulgaris* 4.5-DODA (6.9 mM) (Gandía-Herrero and García-Carmona, 2012), *E. coli* YgiD (7.9 mM) (Gandía-Herrero and García-Carmona, 2014) and for *A. muscaria* dioxygenase (3.9 mM) (Girod and Zryd, 1991), making GdDODA the enzyme with the highest affinity for L-DOPA in the formation of the structural unit of betalains and the fastest one. The value for the turnover number was calculated as  $k_{\text{cat}} = 0.50 \pm 0.019$   $\text{min}^{-1}$ , and the value for the specificity constant as  $k_{\text{cat}}/K_m = 0.36 \pm 0.01$   $\text{min}^{-1} \cdot \text{mM}^{-1}$ .



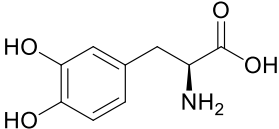
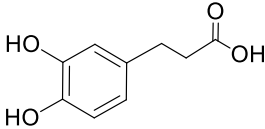
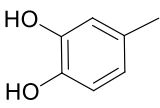
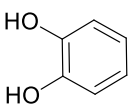
**Figure 4.5. *G. diazotrophicus* dioxygenase activity characterization.** A: Spectral evolution of the transformation of DOPA (2.5 mM) by the addition of pure 4,5-DODA enzyme to the reaction medium. Spectra were recorded at 10-min interval, for 180 minutes, using a scanning speed of 2,000 nm·min<sup>-1</sup>. B: Effect of pH on the dioxygenase activity. Reactions were performed with 2.5 mM L-DOPA in 50 mM sodium acetate buffer for pH values ranging from 3.5 to 5.5 and 50 mM sodium phosphate for 5.5 to 8.5. C: Enzyme activity dependence on L-DOPA concentration measured in 50 mM sodium phosphate buffer pH 6.5.



**Figure 4.6. Effect of aeration and inert atmosphere in the formation of dopaxanthin, by GdDODA.** Enzyme assays without stirring were considered as standard conditions (Not saturated air). Inert atmosphere was obtained with nitrogen gas.

Oxygen exchange was determinant in the production of betalains (**Fig. 4.6**). The production of dopaxanthin under inert atmosphere was negligible while saturation with air provoked a production of dopaxanthin 50 times higher compared to the formation of the pigments when the exchange of oxygen is limited by diffusion. Structurally related substrates to L-DOPA, such as catechol, 4-methyl-catechol, and dihydrocaffeic acid, were also tested. These substrates showed kinetic parameters of  $K_m$  three orders of magnitude higher than the  $K_m$  for L-DOPA (**Table 4.3**).

**Table 4.3. Kinetic analysis of GdDODA with different substrates.** Strong inhibition by excess of substrate was shown for dihydrocaffeic acid, 4-methyl-catechol and catechol.

Compound	Structure	$V_{max}$ ( $\mu\text{M}\cdot\text{min}^{-1}$ )	$K_m$ (mM)	Inhibition constant
L-DOPA		5.26	1.36	No inhibition
Dihydrocaffeic acid		$63.60\cdot 10^3$	$108.17\cdot 10^3$	0.0004
4-Methyl-catechol		$70.99\cdot 10^3$	$111.24\cdot 10^3$	0.0003
Catechol		$32.60\cdot 10^3$	$21.66\cdot 10^3$	0.0011

In addition, these alternative substrates showed a strong inhibition of the DOPA-dioxygenase of *G. diazotrophicus* by excess of substrate, also called substrate inhibition (Segel, 1975). Inhibition curves and the kinetic mechanism are shown in **Fig. 4.7**. This makes L-DOPA the substrate most likely to be of physiological relevance. This is also supported by the presence of dopaxanthin, the final product of L-DOPA transformation in the culture medium.



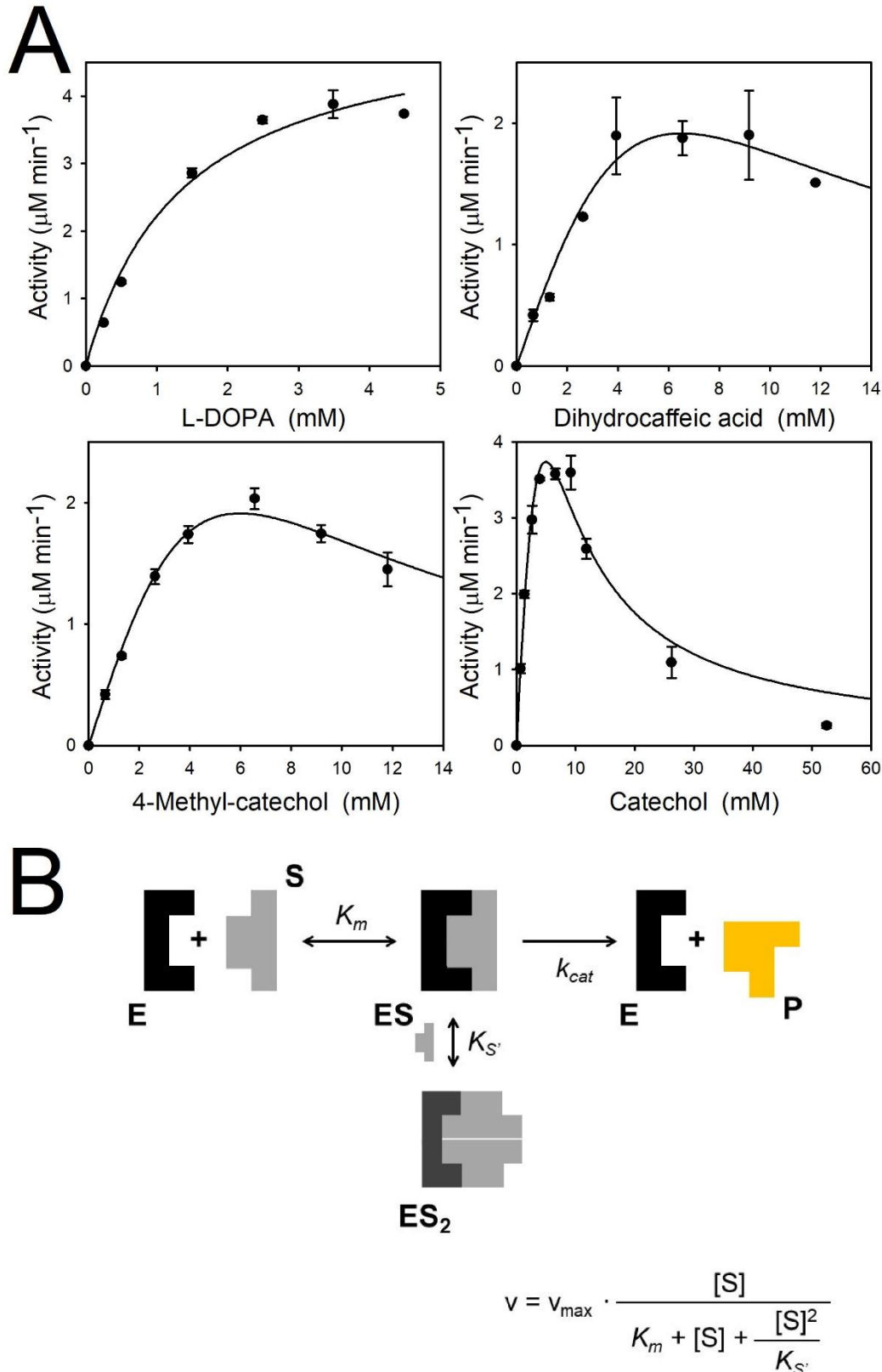


**Figure 4.7. Kinetic analysis of GdDODA.** **A:** Activity measured for the enzyme under growing concentrations of the substrates L-DOPA, dihydrocaffeic acid, 4-methyl-catechol and catechol. L-DOPA behave as a Michaelis-Menten substrate while dihydrocaffeic acid, 4-methyl-catechol and catechol present substrate inhibition kinetics. **B:** Kinetic mechanism and rate equation for inhibition by excess of substrate.

## 5. Mass spectrometry analysis of reaction products and intermediates

The nature of the products derived from the enzymatic activity was analyzed by HPLC. The presence of betalamic acid and dopaxanthin described above for *G. diazotrophicus* cultures were confirmed (**Fig. 4.8**, peaks 3 and 5). Additionally, a peak with RT 16.32 min and  $\lambda_{\max} = 403$  nm (**Fig. 4.8**, peak 4) was found in the reaction media, consistent with the product of 2,3-DOPA-extradiol-dioxygenase activity, muscaflavin. Two additional earlier peaks with  $\lambda_{\max} = 361$  nm were obtained with RT of 8.04 and 8.54 min (**Fig. 4.8**, peaks 1 and 2) and identified as the 4,5-seco-DOPA and 2,3-seco-DOPA precursors. All products were characterized by ESI-MS and TOF-MS confirming the proposed nature above (**Table 4.4**).

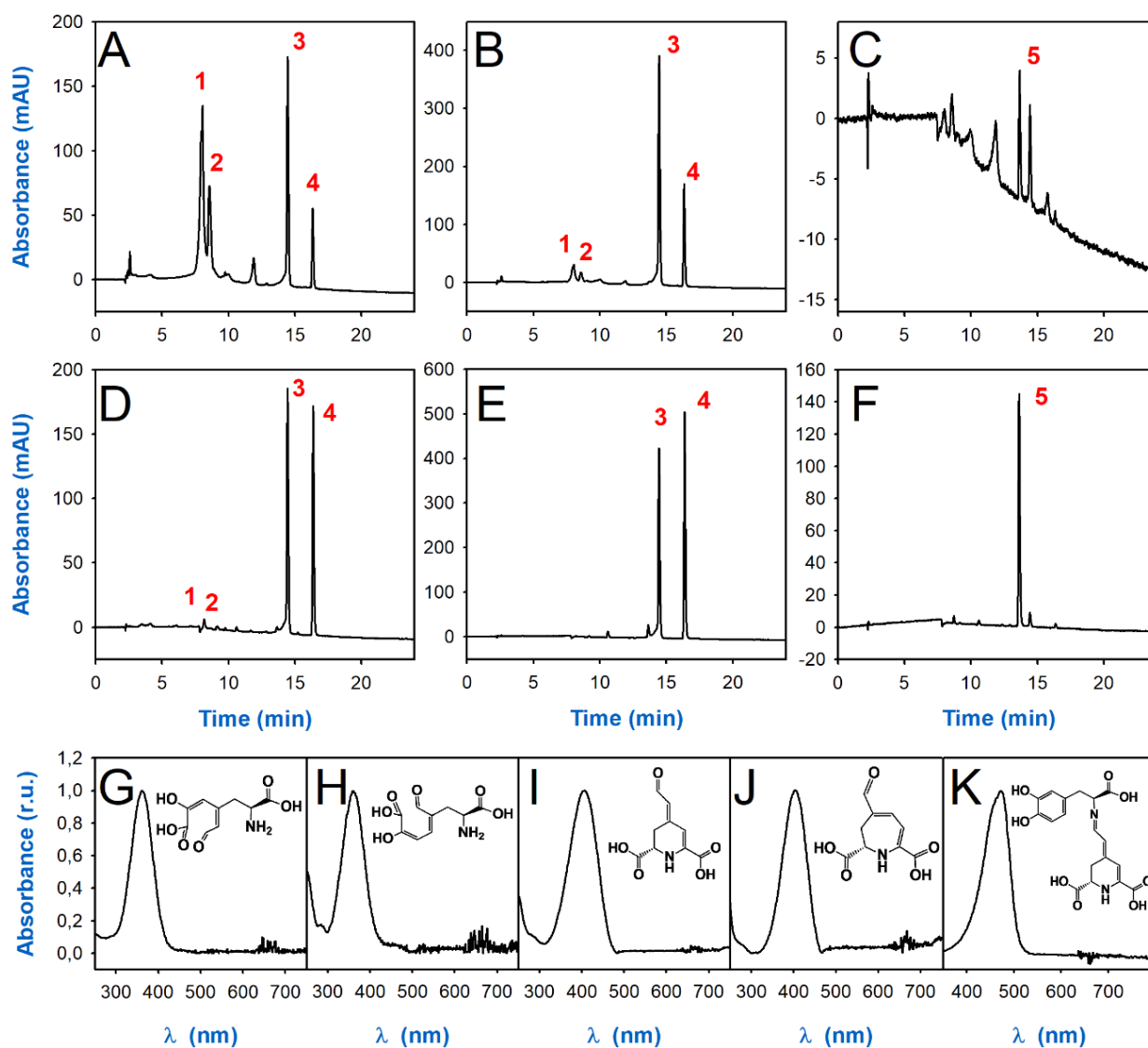


**Figure 4.8.** HPLC analysis of reaction products formed by *G. diazotrophicus* dioxygenase and derived compounds. (Continues on the next page)

**A, B, C:** Chromatograms obtained at  $\lambda=360$  nm (**A**),  $\lambda=405$ nm (**B**), and  $\lambda=480$  nm (**C**) for a reaction medium containing 2.5 mM L-DOPA and 10 mM AA in phosphate buffer 50 mM, pH 6.5 at 25 °C, 3.3 hours after the addition of the purified enzyme. **D, E, F:** The same reaction monitored at  $\lambda=360$  nm (**D**),  $\lambda=405$ nm (**E**), and  $\lambda=480$  nm. (**F**) 31.5 hours after the reaction was triggered. **G-K:** Normalized spectra shown correspond to peak 1 (4,5-seco-DOPA) (**G**), peak 2 (2,3-seco-DOPA) (**H**), peak 3 (betalamic acid) (**I**), peak 4 (muscaflavin) (**J**), and peak 5 (dopaxanthin) (**K**).

Fragmentation spectra for all the reported compounds with annotations are provided in the **Annex II**. The ESI accurate mass spectra showed the detection of molecular protonated ions  $[M+H]^+$  with exact mass values of 230.0665  $m/z$ , 212.0562  $m/z$  y 391.1141  $m/z$  (experimental masses). These results are consistent with the calculated masses for the molecules 4,5 and 2,3-seco-DOPAs (230.0659  $m/z$ ) with a difference of 2.52 ppm, betalamic acid and muscaflavin (212.0553  $m/z$ ) with a difference of 2.07 ppm, and dopaxanthin (391.1136  $m/z$ ) with a difference of 1.25 ppm. All the different values in this analysis are below the accepted accuracy threshold for elemental composition analysis, established at 5 ppm (Ferrer et al., 2005). For the first time, these masses are experimentally determined for readily obtained seco-DOPAs intermediates and hence a complete and unambiguous picture of intermediates and final products of the evolution of L-DOPA in the presence of DOPA-dioxygenase is obtained.

**Table 4.4. HPLC-ESI/TOF/MS analysis of the reaction products formed by *G. diazotrophicus* dioxygenase activity in water supplemented with L-DOPA 7.6 mM.**

Compound	Chemical formula	$[M+H]^+$ (m/z)	Main daughter ion (m/z)	Secondary daughter ions (m/z)	TOF Exact mass (m/z) (experimental)	Calculated mass (m/z) (theoretical)	$\Delta$ ppm
4,5-seco-DOPA	C <sub>9</sub> H <sub>11</sub> NO <sub>6</sub>	230.2	140.0	187.1, 94.1	230.0665	230.0659	2.52
2,3-seco-DOPA	C <sub>9</sub> H <sub>11</sub> NO <sub>6</sub>	230.2	140.0	94.1	230.0665	230.0659	2.52
Betalamic acid	C <sub>9</sub> H <sub>9</sub> NO <sub>5</sub>	212.0	166.1	138.0	212.0562	212.0553	2.07
Muscaflavin	C <sub>9</sub> H <sub>9</sub> NO <sub>5</sub>	212.0	166.0	149.0	212.0562	212.0553	2.07
Dopaxanthin	C <sub>18</sub> H <sub>18</sub> N <sub>2</sub> O <sub>8</sub>	391.3	347.1	301.1, 255.1	391.1141	391.1136	1.25

## 6. Chemical formation and comprehensive enzymatic-chemical mechanism

The presence of the intermediates 4,5 and 2,3-seco-DOPAs reaches a maximum 5 h after the reaction started and then decreases until they disappear (**Fig. 4.9A**). Betalamic acid reaches its maximum value at 20 h and experiences a further decrease, while muscaflavin accumulates during the time in which the reaction was monitored. The formation of both, betalamic acid and muscaflavin is preceded by a lag period, justified by the need for the formation of the corresponding seco-intermediates before these molecules can be obtained. The lag period was 33 min for betalamic acid and after its maximum, the concentration decreases due to its condensation with intact L-DOPA molecules, resulting in the formation of dopaxanthin (**Fig. 4.10**), after a lag period of 3.35 hours (**Fig. 4.9A**).

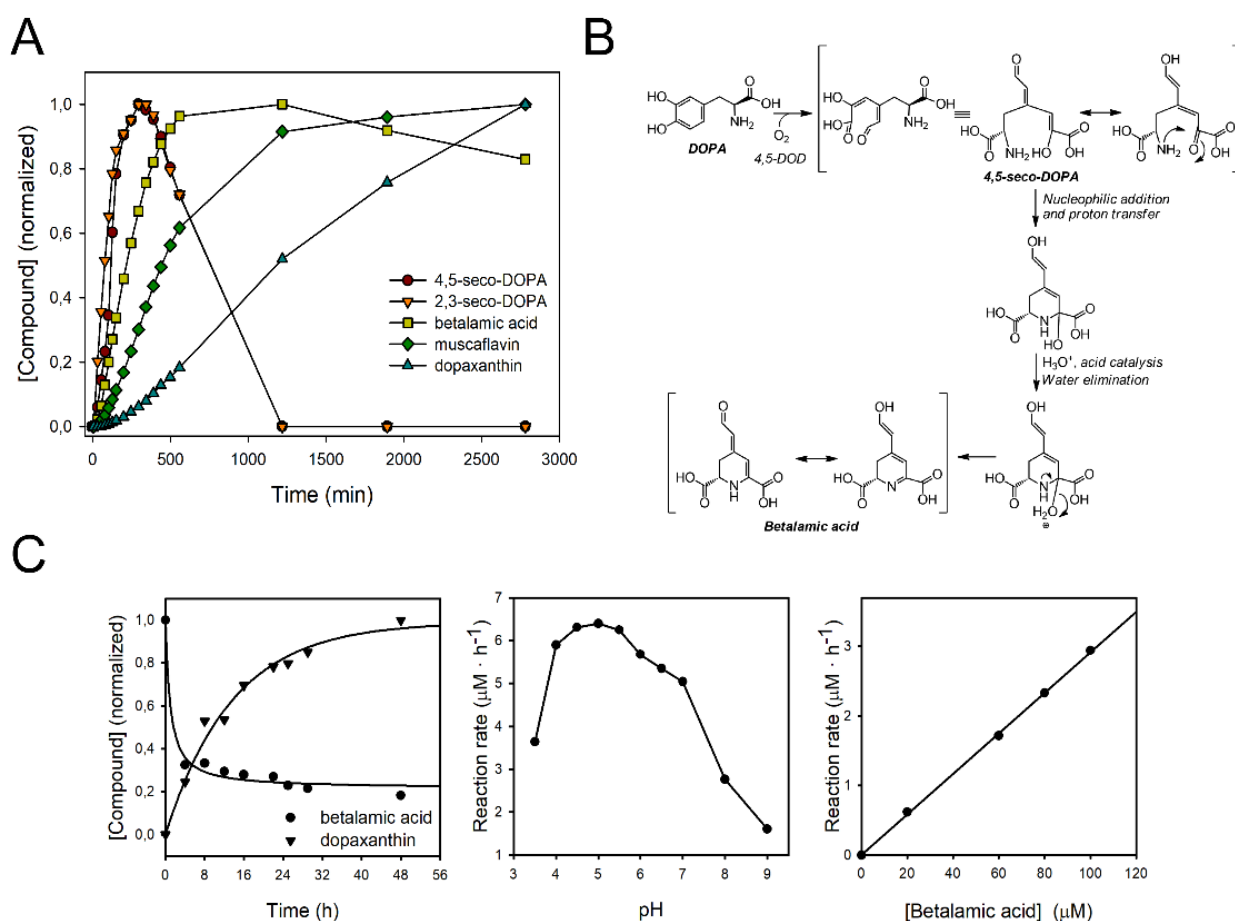


**Figure 4.9.** Enzymatic-chemical mechanism in the formation of betalains. (Continues on the next page)

**A:** Time evolution of the reaction's products formed by *G. diazotrophicus* dioxygenase activity and their derived compounds. Normalized data are based on pigment content determination by HPLC at the wavelengths  $\lambda=360$  nm (seco-DOPAs),  $\lambda=405$  nm (betalamic acid and muscaflavin), and  $\lambda=480$  nm (dopaxanthin). **B:** Proposed chemical reactions underlying the spontaneous cyclization of the enzyme-generated 4,5-seco-DOPA intermediate into betalamic acid. **C:** Formation of betalamic acid. Left: Time course for the formation of dopaxanthin from betalamic acid (100  $\mu$ M) and L-DOPA (3.5 mM) at pH 5.0. Center: pH effect on the rate of dopaxanthin synthesis. Right: Effect of betalamic acid concentration on the formation of dopaxanthin at a fixed concentration of L-DOPA 3.5 mM. Rates were calculated based on dopaxanthin concentration in the reaction medium after 12 h.

Absolute concentrations of dopaxanthin, betalamic acid and muscaflavin in the medium are provided in **Fig. 4.11**. The analysis of this chemical reaction yields a kinetic constant of  $k = 189 \text{ h}^{-1} \cdot \text{M}^{-1}$ . The timescale obtained (**Fig. 4.9C**) is in accordance to the results shown in **Fig. 4.9A**, and justifies the time needed to obtain color in developing flowers even when the initial enzyme-catalyzed reaction is finished. This chemical reaction implies a not-previously considered additional time in the formation of the final pigments in the betalains biosynthesis. It is a chemical spontaneous - but not immediate - reaction which depends on pH (**Fig. 4.9C**).

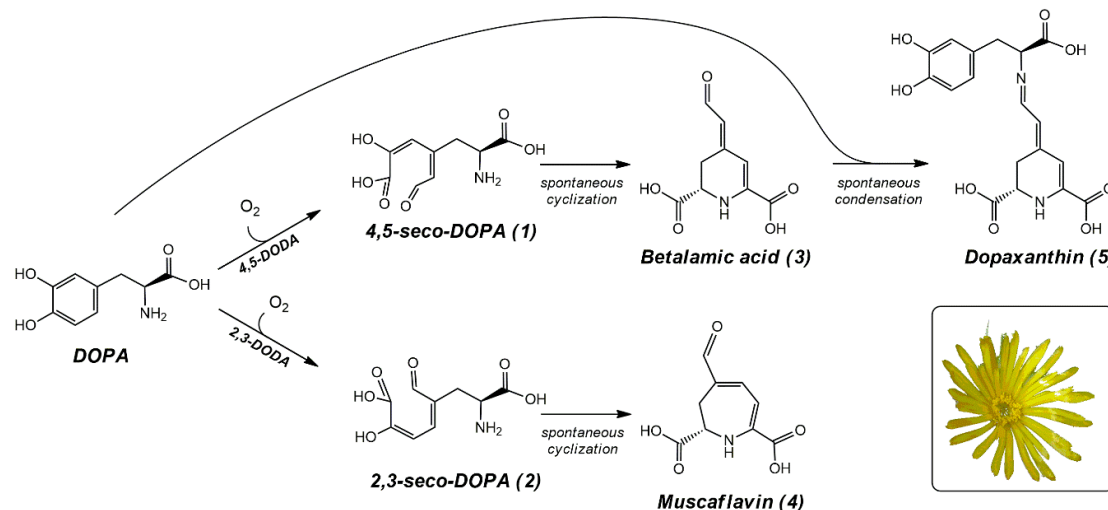


**Figure 4.10. Biosynthetic scheme of betalains.** The enzyme catalyzed reactions and the chemical spontaneous cyclization and condensation ultimately yielding the flower pigment dopaxanthin are shown. Flower shown corresponds to *Glottiphyllum oligocarpum* which produces dopaxanthin as the only pigment responsible for its coloration. Numbers in brackets correspond to the intermediates and final products described in Fig. 4.8.

Taking into account the evolution described and the nature of the intermediates characterized, the scheme shown in **Fig. 4.9B** is proposed for the “spontaneous cyclization” of the first compound in the biosynthesis of betalains. It shows how a nucleophilic addition with a concomitant proton transfer is possible and favored by the presence of the carboxylic group generated in the enzymatic cleavage of the ring. Water elimination by acid catalysis gives the structural unit of betalains. The same scheme can be proposed for muscaflavin, considering the different isomer forms derived from the 2,3-extradiol cleavage.

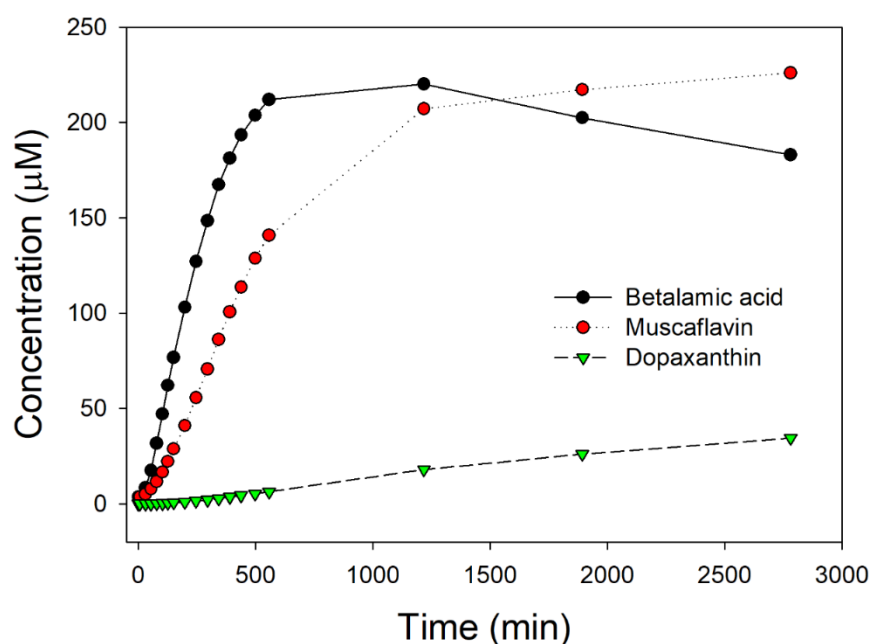


**Figure 4.11. Evolution of betalamic acid, muscaflavin and dopaxanthin in an enzymatic assay with GdDODA.** Absolute concentrations are expressed in micromolar and conditions are as those commented in Fig. 4.9.

## 7. Conclusions

The identification of the final product and intermediates makes GdDODA the smallest dioxygenase able to produce betalamic acid described in the bibliography (Christinet et al., 2004; Gandía-Herrero and García-Carmona, 2014, 2012; Mueller et al., 1997; Sasaki et al., 2009). All betalamic acid forming dioxygenases described up to now can be analyzed in terms of sequence homology and phylogeny (**Fig. 4.3E**). There is a compact clade formed by plant sequences (Gandía-Herrero and García-Carmona, 2013) and the YgiD protein separated from *A. muscaria* dioxygenase. The dioxygenase from *G. diazotrophicus* stands apart from these two branches. Extended

phylogenetic analysis attached in the **Annex II** reveals homology of *G. diazotrophicus* DODA with sequences from *Bradyrhizobium*, *Komagataeibacter*, *Mesorhizobium*, and *Inquilius*. All these sequences stand apart from previously characterized enzymes. Thus, sequence analysis reveals that GdDODA corresponds to a hitherto unknown group of enzymes involved in this biosynthetic pathway. The reactions, intermediates, products, constants and lag periods described constitute the clearest experimental evidences of the first reactions involved in the route of betalains biosynthesis, expanded now to prokaryotes.

## REFERENCES

- Armougom, F., Moretti, S., Poirot, O., Audic, S., Dumas, P., Schaeli, B., Keduas, V., Notredame, C., 2006. Espresso: Automatic incorporation of structural information in multiple sequence alignments using 3D-Coffee. *Nucleic Acids Res.* 34, W604–W608. <https://doi.org/10.1093/nar/gkl092>
- Biasini, M., Bienert, S., Waterhouse, A., Arnold, K., Studer, G., Schmidt, T., Kiefer, F., Cassarino, T.G., Bertoni, M., Bordoli, L., Schwede, T., 2014. SWISS-MODEL: Modelling protein tertiary and quaternary structure using evolutionary information. *Nucleic Acids Res.* 42, W252–W258. <https://doi.org/10.1093/nar/gku340>
- Bienert, S., Waterhouse, A., De Beer, T.A.P., Tauriello, G., Studer, G., Bordoli, L., Schwede, T., 2017. The SWISS-MODEL Repository-new features and functionality. *Nucleic Acids Res.* 45, D313–D319. <https://doi.org/10.1093/nar/gkw1132>
- Christinet, L., Burdet, F., Zaiko, M., Hinz, U., Zrýd, J.P., 2004. Characterization and functional identification of a novel plant 4,5-extradiol dioxygenase involved in betalain pigment biosynthesis in *Portulaca grandiflora*. *Plant Physiol* 134, 265–274. <https://doi.org/10.1104/pp.103.031914>
- Escribano-Cebrián, J., Pedreño, M.A., García-Carmona, F., Muñoz, R., 1998. Characterization of the antiradical activity of betalains from *Beta vulgaris* L. roots. *Phytochem. Anal.* 9, 124–127. [https://doi.org/10.1002/\(SICI\)1099-1565\(199805/06\)9:3<124::AID-PCA401>3.0.CO;2-0](https://doi.org/10.1002/(SICI)1099-1565(199805/06)9:3<124::AID-PCA401>3.0.CO;2-0)
- Ferrer, I., García-Reyes, J.F., Fernandez-Alba, A., 2005. Identification and quantitation of pesticides in vegetables by liquid chromatography time-of-flight mass spectrometry. *Trends Anal. Chem.* 24, 671–682. <https://doi.org/10.1016/j.trac.2005.04.004>
- Gandía-Herrero, F., García-Carmona, F., 2014. *Escherichia coli* protein YgiD produces the structural unit of plant pigments betalains: Characterization of a prokaryotic enzyme with DOPA-extradiol-dioxygenase activity. *Appl. Microbiol. Biotechnol.* 98, 1165–1174. <https://doi.org/10.1007/s00253-013-4961-3>
- Gandía-Herrero, F., García-Carmona, F., 2013. Biosynthesis of betalains: yellow and violet plant pigments. *Trends Plant Sci.* 18, 334–343. <https://doi.org/10.1016/j.tplants.2013.01.003>



- Gandía-Herrero, F., García-Carmona, F., 2012. Characterization of recombinant *Beta vulgaris* 4,5-DOPA-extradiol-dioxygenase active in the biosynthesis of betalains. *Planta* 236, 91–100. <https://doi.org/10.1007/s00425-012-1593-2>
- Gilliss, M., Kersters, K., Hoste, B., Janssens, D., Kroppenstedt, R.M., Stephan, M.P., Teixeira, K.R.S., Dobereiner, J., De Ley, J., 1989. *Acetobacter diazotrophicus* sp. nov., a nitrogen-fixing acetic acid bacterium associated with sugarcane. *Int. J. Syst. Bacteriol.* 39, 361–364. <https://doi.org/10.1099/00207713-39-3-361>
- Girod, P.-A., Zryd, J.-P., 1991. Biogenesis of betalains: Purification and partial characterization of dopa 4,5-dioxygenase from *Amanita muscaria*. *Phytochemistry* 30, 169–174. [https://doi.org/10.1016/0031-9422\(91\)84119-D](https://doi.org/10.1016/0031-9422(91)84119-D)
- Impellizzeri, G., Piattelli, M., Sciuto, S., 1973. A new betaxanthin from *Glottiphyllum longum*. *Phytochemistry* 12, 2293–2294. [https://doi.org/10.1016/0031-9422\(73\)85137-4](https://doi.org/10.1016/0031-9422(73)85137-4)
- Letunic, I., Bork, P., 2016. Interactive tree of life (iTOL) v3: an online tool for the display and annotation of phylogenetic and other trees. *Nucleic Acids Res.* 44, W242–W245. <https://doi.org/10.1093/nar/gkw290>
- Li, W., Cowley, A., Uludag, M., Gur, T., McWilliam, H., Squizzato, S., Park, Y.M., Buso, N., Lopez, R., 2015. The EMBL-EBI bioinformatics web and programmatic tools framework. *Nucleic Acids Res.* 43, W580–W584. <https://doi.org/10.1093/nar/gkv279>
- Mueller, L.A., Hinz, U., Zryd, J.-P., 1997. The formation of betalamic acid and muscaflavin by recombinant dopa-dioxygenase from *Amanita*. *Phytochemistry* 44, 567–569. [https://doi.org/10.1016/S0031-9422\(96\)00625-5](https://doi.org/10.1016/S0031-9422(96)00625-5)
- Prlić, A., Bliven, S., Rose, P.W., Bluhm, W.F., Bizon, C., Godzik, A., Bourne, P.E., 2010. Pre-calculated protein structure alignments at the RCSB PDB website. *Bioinformatics* 26, 2983–2985. <https://doi.org/10.1093/bioinformatics/btq572>
- Robert, X., Gouet, P., 2014. Deciphering key features in protein structures with the new ENDscript server. *Nucleic Acids Res.* 42, W320–W324. <https://doi.org/10.1093/nar/gku316>
- Sasaki, N., Abe, Y., Goda, Y., Adachi, T., Kasahara, K., Ozeki, Y., 2009. Detection of DOPA 4,5-dioxygenase (DOD) activity using recombinant protein prepared from *Escherichia coli* cells harboring cDNA encoding DOD from *Mirabilis jalapa*. *Plant Cell Physiol.* 50, 1012–1016. <https://doi.org/10.1093/pcp/pcp053>
- Segel, I.H., 1975. Enzyme kinetics : behavior and analysis of rapid equilibrium and

steady state enzyme systems. New York-Wiley.

- Smith, T.F., Waterman, M.S., 1981. Identification of common molecular subsequences. J. Mol. Biol. 147, 195–197. [https://doi.org/10.1016/0022-2836\(81\)90087-5](https://doi.org/10.1016/0022-2836(81)90087-5)
- Stintzing, F., Schliemann, W., 2007. Pigments of fly agaric (*Amanita muscaria*). Zeitschrift fur Naturforsch. - Sect. C J. Biosci. 62, 779–785.
- Von-Ardenne, R., Döpp, H., Musso, H., Steglich, W., 1974. Isolation of muscaflavin from *Hygrocybe* species (Agaricales) and its dihydroazepine structure. Z. Naturforsch 29, 637–639.



**Chapter V.** Expanding betalains biosynthesis to the phylum  
cyanobacteria: Characterization of a novel enzyme with  
4,5-DOPA-extradiol dioxygenase activity in *Anabaena cylindrica*



## Contextualization

Chapter IV reported the presence of betalain-forming bacteria by describing a DODA enzyme with a high affinity towards L-DOPA. The discovery of *Gluconacetobacter diazotrophicus* as the first betalain-forming bacterium has opened a new field in the search for novel biological systems able to produce betalains. The phylogenetic analysis in **Annex II** shows the sequence homology for the novel dioxygenase enzyme from *G. diazotrophicus* in several proteobacteria, such as *Bradyrhizobium*, *Komagataeibacter*, *Mesorhizobium*, and *Inquilius*. An extended phylogenetic analysis, provided in **Annex III**, shows the presence of homologous proteins not only in proteobacteria but also in the phylum cyanobacteria. Within the sequences found in the extended analysis, *Anabaena cylindrica*, an autotrophic filamentous bacterium with nitrogen-fixing capabilities, was identified and chosen as a representative species of the phylum cyanobacteria to study the possible betalamic acid-producing abilities in this group of water organisms.

### 1. *Anabaena cylindrica* cultures produce betalamic acid

*A. cylindrica* cultures enriched with increasing concentrations of L-DOPA up to its solubility limit at 7.6 mM were employed. Preliminary assays of *A. cylindrica* cultures supplemented with L-DOPA as a precursor in the formation of betalamic acid did not produce any yellow pigmentation, but they produced the darkening of the medium. It was hypothesized that this was due to the production of DOPA-chrome, a product derived from L-DOPA in the production of melanins by oxidase enzymes. Previous studies have reported that ascorbic acid or an analogous reducing agent is necessary in the biosynthesis pathway to recover the pool of L-DOPA, thus avoiding the accumulation of DOPA-chrome (Gandía-Herrero and García-Carmona, 2013). The addition of sodium ascorbate 15 mM to the media did not produce the expected results and the conversion of L-DOPA to DOPA-chrome was again evident from the darkening of culture media.

Then it was considered that this may be due to the presence of an ascorbate peroxidase particularly active in *A. cylindrica*, demonstrated to be involved in the scavenging of hydrogen peroxide (Miyake et al., 1991). This enzyme is able to capture sodium ascorbate molecules, by reducing them and limiting their bioavailability to revert the conversion of L-DOPA to DOPA-chrome. Taking these

considerations into account, EDTA 100 mM was also added to the reaction media in order to avoid the reduction of sodium ascorbate. 7-day cultures of *A. cylindrica* were supplemented with L-DOPA at concentrations 0.23, 0.76, 1.90, 3.80, and 7.60 mM, 15 mM sodium ascorbate and 100 mM EDTA. Non-supplemented cultures were employed as controls. After two days, supernatants were analysed by HPLC-ESI/TOF/MS and pure pigment dopaxanthin was employed as a standard to check out the activity of a hypothetical DODA enzyme. This betaxanthin is the result of the condensation of betalamic acid with L-DOPA and its presence reveals the formation of betalamic acid from L-DOPA through the presence of a 4,5-DOPA-extradiol-dioxygenase enzyme. Control pigment analysis yielded a retention time of 12.1 min with an exact mass value of 391.1136  $m/z$  (**Fig. 5.1**). The same peak was obtained in cultures of *A. cylindrica* supplemented with 3.8 and 7.6 mM of L-DOPA but it was not found at lower concentrations of the added substrate neither in its absence.

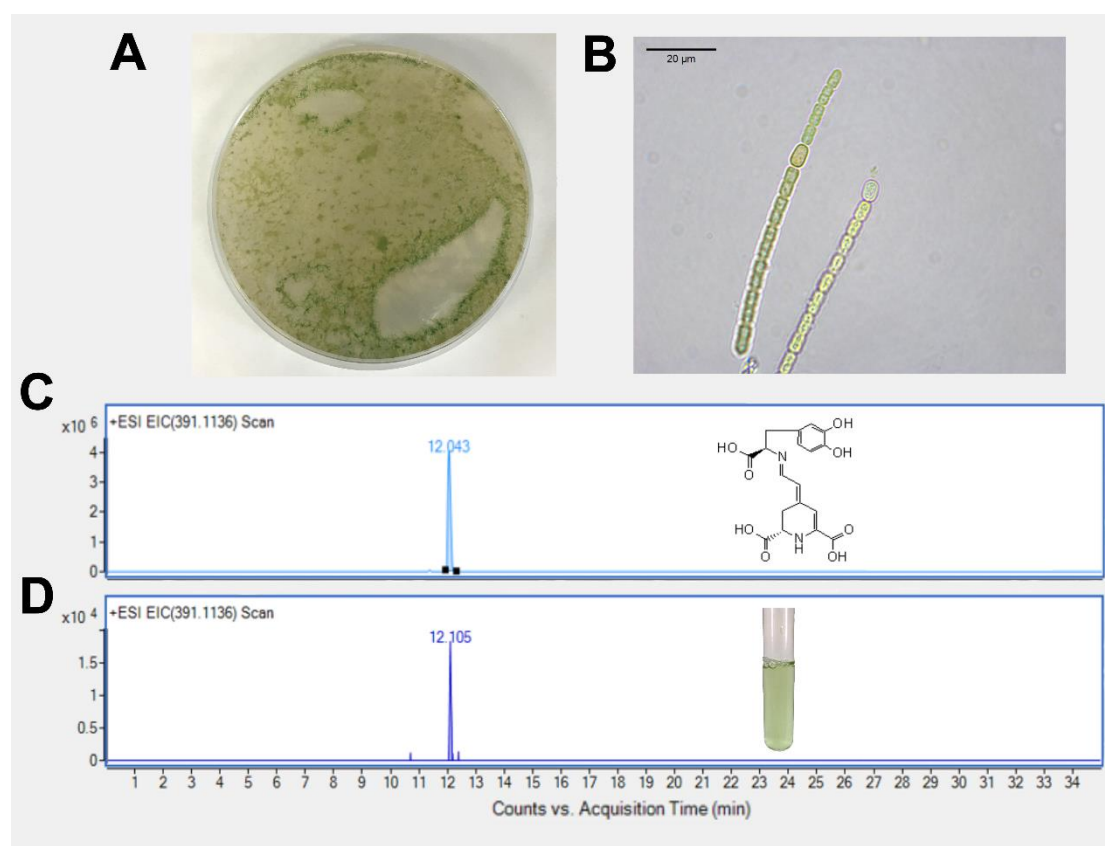


**Figure 5.1. Detection of dopaxanthin in cultures of *Anabaena cylindrica* supplemented with L-DOPA.** **A.** 3-day plate of BG-11 medium containing *A. cylindrica*. **B.** Microscopy image of the filamentous distribution of *A. cylindrica* cells. Scale bar: 20 μm. **C** and **D.** Chromatograms from HPLC-ESI-TOF-MS analysis. Standard dopaxanthin was followed at EIC 391.1136  $m/z$  (**C**) and the same peak was detected in culture media of *A. cylindrica* supplemented with L-DOPA 7.6 mM, 15 mM sodium ascorbate and 100 mM EDTA (**D**).

Therefore, the existence of a betalamic acid-forming DODA activity has been demonstrated. This metabolism does not seem active or relevant in the development of *A. cylindrica* but it is able to produce betalamic acid when the precursor amino acid is present in the medium. The betalamic acid produced condenses with L-DOPA to yield its derived betaxanthin, dopaxanthin.

## **2. *A. cylindrica* 4,5-DODA sequence, expression and purification**

The search for non-plant L-DOPA dioxygenases able to produce betalamic acid and thus to start the biosynthetic pathway of betalains in prokaryotes has led to search for sequences related to that described for *G. diazotrophicus*. Phylogenetic analysis shows a sequence susceptible to produce betalains in the genome of *Anabaena cylindrica*. This autotrophic cyanobacterium presents the sequence for the protein WP\_015213489.1 deposited at the NCBI database. The sequence obtained from the database was used as a template to obtain a synthetic sequence optimized for expression in *E. coli*. This optimization introduced mutations which did not change the amino acid sequence coded. The modified sequence was inserted into the multiple cloning site of the expression vector pRSETA, obtaining the recombinant plasmid pRSETA-AcDODA.

This plasmid was used to transform thermocompetent *E. coli* BL21 (DE3) cells. For an increased expression of activity in transformed *E. coli* cultures, optimization conditions of IPTG concentration and temperature of induction was performed using IPTG at final concentrations of 0.1, 0.5, and 1 mM and temperatures of 20 and 25 °C. In all cases, 20 h after induction L-DOPA 7.6 mM and ascorbate 15 mM were added to the cultures and dopaxanthin formation was evaluated by HPLC. This measure allowed to establish the optimal conditions for the activity, and thus protein expression. The highest dopaxanthin content was achieved after induction with 0.1 mM IPTG at 20 °C, as shown in **Fig. 5.2**.



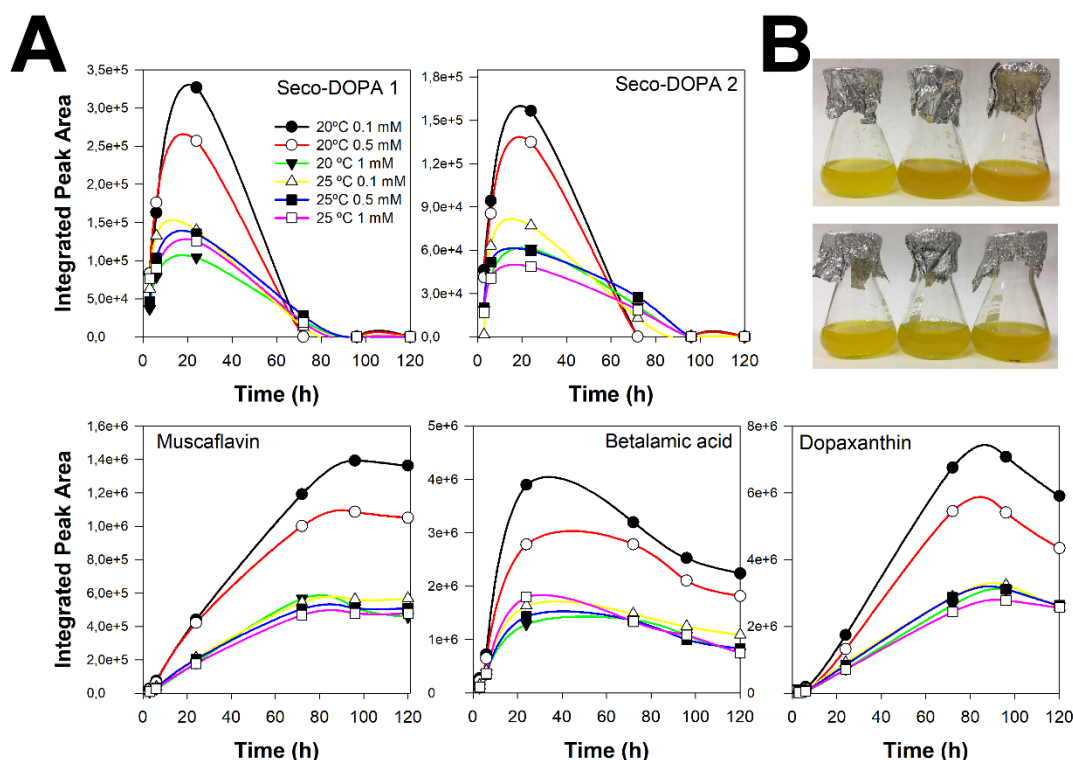


**Figure 5.2. Determination of the optimal conditions for the heterologous expression of AcDODA in *E. coli* cells.** A: Comparison of the obtention of the products from the activity of AcDODA and derived compounds in *E. coli* cultures supplemented with different concentrations of IPTG and maintained under different temperatures. The reactions were followed by HPLC in order to evaluate the presence of the enzyme. B: Macroscopic images of *E. coli* (pRSETA-AcDODA) cultures, after 24 hours of reaction, supplemented with 1.0 (left), 0.5 (centre) or 0.1 (right) mM IPTG and maintained at 20 °C (top) or 25 °C (bottom).

Protein production for the following steps was performed in 0.5 L cultures of LB medium under the optimized conditions. Recombinant *A. cylindrica* DODA was purified from *E. coli* cells by Ni<sup>2+</sup>-chelating affinity chromatography. After non-tagged proteins were washed, the His-tagged protein was eluted with a buffer supplemented with 250 mM imidazole. Immediately after the elution, the protein solution buffer was changed to phosphate buffer 20 mM, pH 7.5. Preliminary assays were performed with a phosphate buffer pH 8.5 but the activity recorded was negatively affected, as **Fig. 5.3A** shows. The purified enzyme was run on an SDS-PAGE electrophoresis gel, revealing that the recombinant *A. cylindrica* DODA was purified to homogeneity after the affinity separation (**Fig. 5.3A**). The results of the purification process are shown in **Table 5.1**, where it can be seen that a purification yield of 75% and a purification fold of 1.6 were obtained, in accordance with the electrophoretic estimation of DODA expression.

**Table 5.1.** Expression and purification of *A. cylindrica* dioxygenase in *E. coli* cultures.

	Volume (mL)	Protein (mg/mL)	Total Prot. (mg)	<sup>a</sup> Activity ( $\mu\text{M}\cdot\text{min}^{-1}$ )	Specific Activity ( $\mu\text{mol}\cdot\text{min}^{-1}\cdot\text{mg}^{-1}$ )	Purif. fold	Yield (%)
<sup>b</sup> Crude extract	7.0	6.18	43.29	0.743	0.773	1.0	100
Ni <sup>2+</sup> chr om.	7.0	2.82	19.7	0.594	1.264	1.6	75

<sup>a</sup>Activity was determined using 100  $\mu\text{L}$  of protein solution under the assay conditions.

<sup>b</sup>Crude extract was obtained from a cellular paste harvested from a 0.5 L culture.

### 3. Molecular characterization

The band corresponding to the recombinant protein obtained by SDS-PAGE yields an estimated molecular mass of 17 kDa (**Fig. 5.3A**), consistent with the molecular weight calculated according to the protein sequence (17.8 kDa). The purified protein was analysed by HPLC-ESI-MS TOF in order to determine its accurate molecular mass. Mass spectra showed a single peak with a molecular mass of 17.806 kDa, which agrees with the above-mentioned values obtained by SDS-PAGE and for the theoretical molecular weight. To fully characterize the protein, its peptide mass fingerprint was determined by MALDI-TOF analysis after trypsin digestion. The main peptides identified corresponded to the masses 437,89  $m/z$  [(R)WHEQPVGPHPK(S)], 1052,51  $m/z$  [(R)EGLDILVHPETGDDVKDHTDHSLWLGEK(L)], 621,86  $m/z$  [(K)LPLNIEFLQR(L)], 479,89  $m/z$  [(K)DHTDHSLWLGEK(L)], 868,94  $m/z$  [(R)EGLDILVHPETGDDVK(D)].

The purified protein was subjected to gel filtration chromatography on a Superdex 200 column under native conditions in order to determine whether this DODA enzyme is a monomer or if it forms oligomers. In this sense, different concentrations of purified protein were employed to investigate the possibility of an equilibrium among the monomer and the possible oligomers. A single peak eluting at the same volume was obtained in all cases, with a molecular mass estimated of 32.9 kDa (**Fig. 5.3B**). This value doubles the expected mass according to the SDS-PAGE and TOF analyses. Therefore, the results obtained by gel filtration shows that the DODA protein of *A. cylindrica* is a dimer under native conditions.

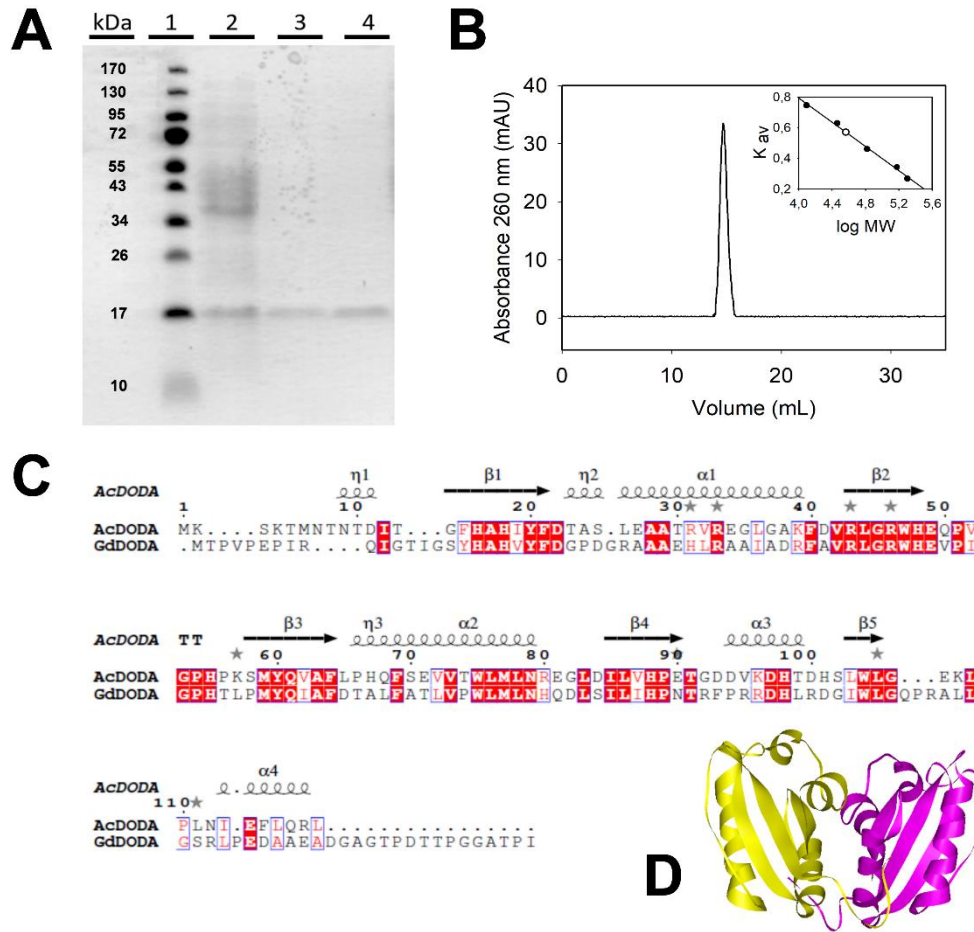


**Figure 5.3. Characterization of DODA enzyme from *A. cylindrica*.** **A.** SDS-PAGE electrophoretic analysis of the expression and purification of AcDODA from *E. coli* BL21 cells. Lane 1, molecular weight markers; lane 2, soluble protein content of cells harvested 20 h after IPTG induction (0.1 mM); lane 3, eluted protein after affinity chromatography purification; lane 4, final purified protein obtained after desalting on PD-10 columns. **B.** Analysis of the AcDODA enzyme by gel filtration chromatography. Elution was followed at a wavelength of  $\lambda=260$  nm. Inset: Calibration curve and molecular mass determination of the detected dimer. **C.** Comparison of DODA sequences from *A. cylindrica* and *G. diazotrophicus*. Sequence alignment with structural considerations was performed with Expresso (Armougom et al., 2006). Conserved blocks of amino acids are squared. Strictly conserved residues are shown in red. **D.** Structural model for the dimer of DODA enzyme from *A. cylindrica* by using the template PDB-ID 2PEB from *Nostoc punctiforme*. The two monomeric units are shown in yellow and purple.

These results strongly support the sequence homology found by a search performed on the databases for sequences with known structures. The *A. cylindrica* DODA has 71.3% identity (83.0% similarity) with a dioxygenase enzyme characterized from *Nostoc punctiforme* PCC 73102 (Camacho et al., 2009; Li et al., 2015). The protein (PDB entry 2PEB) has been demonstrated to be a dimer by X-ray crystallography at 1.46 Å resolution. The similarity between these two enzymes agrees with the molecular characterization performed for AcDODA in the present

study. In addition, *A. cylindrica* DODA residues can be assigned to specific secondary motifs also found in the enzyme from the only prokaryote known to produce betalains, *G. diazotrophicus*, by structurally assisted sequence comparison (Armougom et al., 2006; Robert and Gouet, 2014). **Figure 5.3C** shows the structural similitude between both enzymes with respect to the residues involved in the formation of  $\beta$ -strands and  $\alpha$ -helices. Taking into account the molecular similarities between the *A. cylindrica* DODA and *G. diazotrophicus* enzymes and with the protein crystalized from *N. punctiforme*, a three-dimensional model of the novel DODA from *A. cylindrica* was performed (Biasini et al., 2014; Bienert et al., 2017). The resulting structure can be found in **Fig. 5.3D** where a dimer modelled by the bioinformatic techniques is shown. The predicted dimeric protein finds experimental support in **Fig. 5.3B** where the multimeric nature of the novel enzyme is unambiguously determined.

#### 4. Kinetic characterization

The activity of the DODA enzyme from *A. cylindrica* was characterized spectrophotometrically by its addition to a reaction medium with the amino acid L-DOPA as substrate. The addition of the enzyme yielded a yellow coloration with a  $\lambda_{\text{max}}$  of 414 nm. Spectral changes were not observed in the absence of the enzyme and, therefore, they were considered proof of the activity of AcDODA. As happened with the DODA enzyme from *G. diazotrophicus* described in the previous chapter IV, the product of AcDODA activity agrees with the properties reported for betalamic acid and muscaflavin extracted from plants and fungi (Gandía-Herrero et al., 2012; Mueller et al., 1997; Trezzini and Zrýb, 1991) and for those formed *in vitro* by the enzyme from the fungus *A. muscaria* (Girod and Zryd, 1991), and from the plants *B. vulgaris* (Gandía-Herrero and García-Carmona, 2012) and *M. jalapa* (Sasaki et al., 2009).

The highest activity for the novel DODA enzyme was determined at pH 7.0 (**Fig. 5.4C**). Dependence of the activity rate on substrate concentration was analysed at the optimum pH determined. In these assays AcDODA enzyme showed a reduction of its activity at high L-DOPA concentrations, and thus a strong inhibition by excess of L-DOPA as clearly shown in **Fig. 5.4A**. This phenomenon is known as inhibition by excess of substrate. In this kinetic model, the plot of the double-reciprocal (inverse activity rate as a function of the inverse of L-DOPA concentration) provides a curve

like that shown in (**Fig. 5.4B**) (Segel, 1975). The equation for the obtained curve showed the kinetic parameters estimated as  $K_m = 53 \text{ M}$  and  $V_{max} = 105.8 \text{ mM/min}$ , and a substrate inhibition constant of  $31.9 \text{ }\mu\text{M}$ . The kinetic mechanism and its corresponding equation are shown in the previous chapter IV, where the same model was found for alternative substrates. The values determined are far from those obtained for previously characterized DODA enzymes, which did not show substrate inhibition for L-DOPA. Previous works reported that values determined for  $K_m$  were  $6.9 \text{ mM}$  for *B. vulgaris* 4,5-DODA (Gandía-Herrero and García-Carmona, 2012),  $7.9 \text{ mM}$  for *E. coli* YgiD (Gandía-Herrero and García-Carmona, 2014),  $3.9 \text{ mM}$  for *A. Muscaria* dioxygenase (Girod and Zryd, 1991) and  $1.4 \text{ mM}$  for *G. diazotrophicus* dioxygenase (Chapter IV). Thus, the novel enzyme here described presents a singular behaviour with respect to the activity in the presence of L-DOPA as substrate.

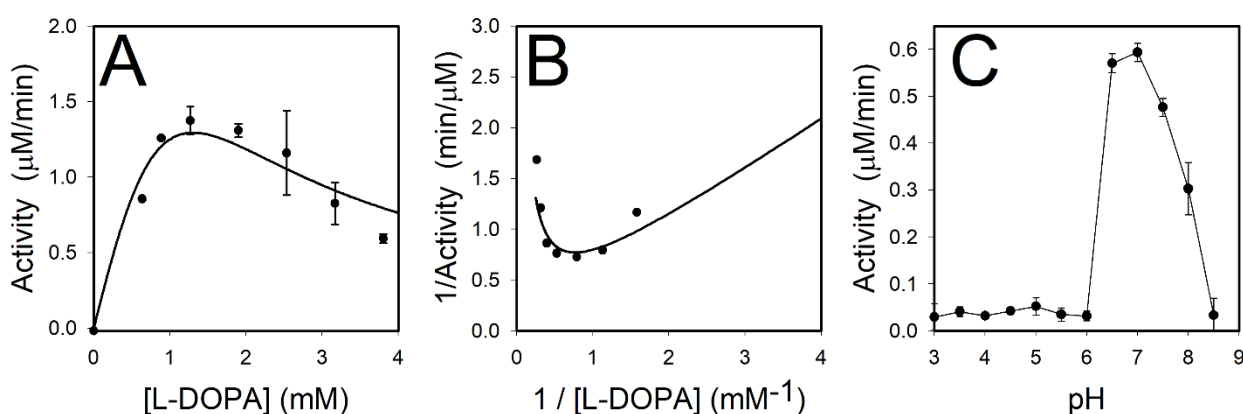


**Figure 5.4. *A. cylindrica* dioxygenase activity characterization.** **A:** Enzyme activity at different concentrations of L-DOPA, measured in 50 mM sodium phosphate buffer pH 7.0. **B:** Double-reciprocal plot showing the inverse activity rate as a function of the inverse of substrate concentration. **C:** Effect of pH on the activity of the novel dioxygenase enzyme. Reactions were performed with 2.5 mM L-DOPA in 50 mM sodium acetate buffer for pH values ranging from 3.5 to 5.0 and in 50 mM sodium phosphate buffer for pH values ranging from 5.5 to 8.5.

## 5. Functional characterization

*E. coli* (pRSETA-AcDODA) expressing the novel DODA from *A. cylindrica* was used to study the evolution of the intermediates of the biosynthetic pathway of betalains and for the biotechnological obtention of their products. The induced expression of the enzyme was performed in LB media under optimal conditions of temperature and IPTG concentration as mentioned above. Then, the reaction was

followed for 100 hours by the analysis of culture supernatants by HPLC. As **Fig. 5.5** shows, the formation of intermediates 2,3- and 4,5-seco-DOPA occurs in the first hours of reaction and these reached the maximum concentrations after 7 h. They were detected at  $\lambda = 360$  nm with retention times of 6.7 and 7.1 min, respectively. Betalamic acid was detected at  $\lambda = 405$  nm with a retention time of 13.8 min and a minor peak was detected with a  $\lambda_{\text{max}}$  of 403 nm and a retention time of 15.5 min. This peak corresponds to muscaflavin. HPLC analysis also showed a peak with a  $\lambda_{\text{max}}$  of 470 nm and a retention time of 13.2 min, corresponding to dopaxanthin, which is accumulated due to the condensation of betalamic acid and L-DOPA.

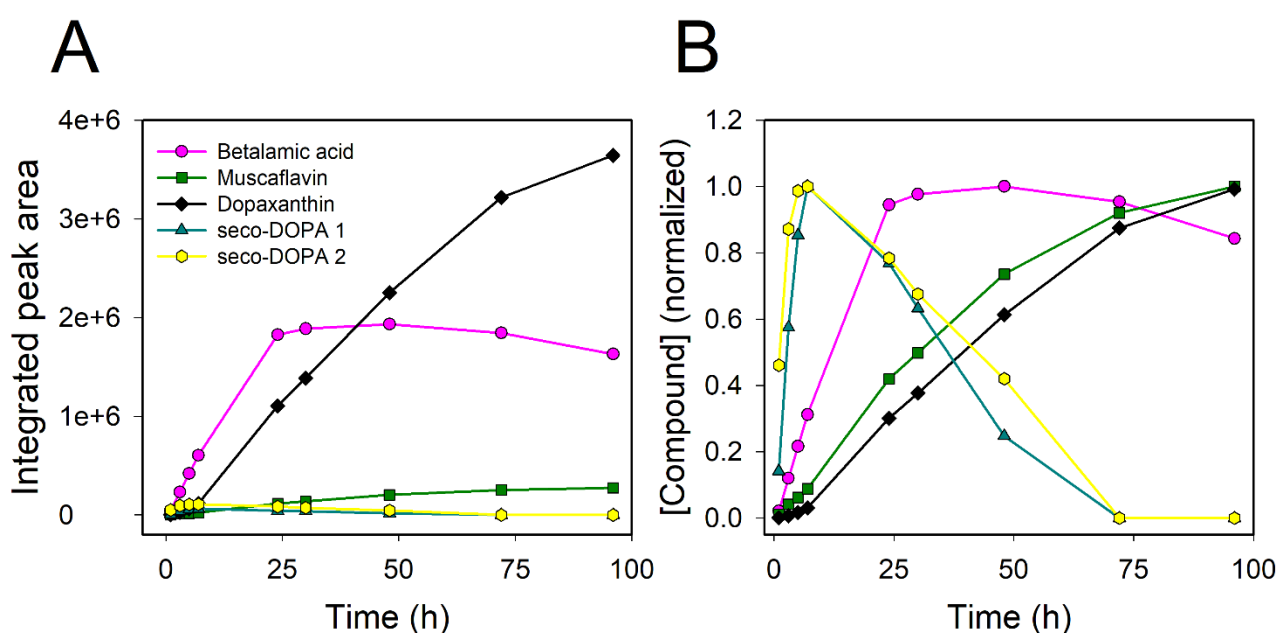


**Figure 5.5. HPLC analysis of the evolution of betalains and intermediates in *E. coli* (pRSETA-AcDODA) cultures.** Time evolution of intermediates and final compounds in the supernatant of the culture medium follow for 100 hours under optimal conditions. Seco-DOPAs were detected at  $\lambda_{\text{max}} = 60$  nm, betalamic acid and muscaflavin were detected at  $\lambda_{\text{max}} = 405$  nm, and dopaxanthin was detected at  $\lambda_{\text{max}} = 480$  nm.

Thus, the DODA enzyme from *A. cylindrica* presents dual 2,3- and 4,5-DOPA-extradiol-dioxygenase activities similar to those described for the dioxygenase enzymes characterized from *G. diazotrophicus* (chapter IV), *E. coli* (Gandía-Herrero and García-Carmona, 2014) and *A. muscaria* (Mueller et al., 1997).

DODA enzyme from *A. cylindrica* was compared, in terms of sequence homology and phylogeny, with the dioxygenase enzymes previously characterized to produce betalains and to the sequence of potential dioxygenase enzymes related to the *G. diazotrophicus* sequence. The conserved block of *G. diazotrophicus* among



residues His91 and Asp122 was used for sequence evaluation of the *A. cylindrica* enzyme (Chang et al., 2015; Li et al., 2015). This block includes one of the three strictly conserved histidines present in the plant enzymes, which is present in GdDODA and in the novel AcDODA as His 101. It also presents acid (Asp100) and hydrophobic (Leu102) residues flanking out the His101, as occurs in the enzymes described from plants (Gandía-Herrero and García-Carmona, 2014). Phylogenetic analysis (**Fig. 5.6**) of the region conserved showed that there is a compact clade formed by plant sequences and the homologue YgiD protein separated from *A. muscaria* dioxygenase and another compact clade formed by proteobacteria enzymes. However, *A. cylindrica* appears as an individual clade apart, showing that although its enzyme produces betalamic acid and muscaflavin, AcDODA is not closely related to these two branches.

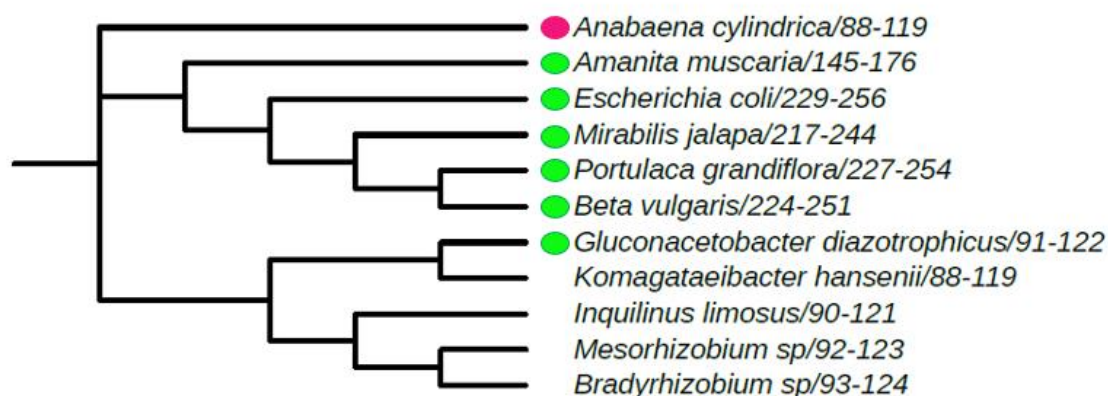


**Figure 5.6. Phylogenetic analysis of characterized betalamic acid-forming DODAs and related proteobacteria sequences.** The analysis was performed with the conserved block of *G. diazotrophicus* which includes the His 101. This residue is conserved in all characterized 4,5-DOPA-dioxygenases known to produce betalamic acid (green dot) and several proteobacteria. The conserved residues were also detected in the novel *A. cylindrica* enzyme here described to produce dopaxanthin (pink dot) and it conforms an independent clade. Multiple sequence alignment was performed using Clustal Omega and the phylogenetic tree was inferred by using the phylogeny tool from the ClustalW2 package and plotted using ITOL.

## 6. Conclusions

DOPA-extradiol-dioxygenase, the key enzyme involved in the betalains' biosynthetic pathway of Caryophyllales plants, is also present in the cyanobacterium *Anabaena cylindrica*. The protein sequence has been optimized for its recombinant expression in *E. coli*, purified to homogeneity and characterized for the first time as a protein of 17.8 kDa which forms dimers under native conditions. Reactions performed in one-pot experiments show how this enzyme is able to produce betalamic acid and

muscaflavin from the amino acid L-DOPA due to a dual activity 2,3- and 4,5-DOPA-extradiol-dioxygenase. This work provides evidence of the presence of DODA enzymes in the phylum cyanobacteria and expands the presence of betalain-forming capabilities in prokaryotes along with the previously described enzymes from *E. coli* (Gandía-Herrero and García-Carmona, 2014) and *G. diazotrophicus* (chapter IV). The sequence analysis of the known enzymes has shown little phylogenetic relationship of the *A. cylindrica* DODA with those previously described. This seems to indicate that dioxygenase enzymes able to cleave the ring of L-DOPA to produce betalamic acid may be more diverse and frequent than expected. This opens the possibility of finding novel betalamic acid-forming dioxygenases in organisms of different nature with no apparent relationship among them.



## REFERENCES

- Armougom, F., Moretti, S., Poirot, O., Audic, S., Dumas, P., Schaeli, B., Keduas, V., Notredame, C., 2006. Espresso: Automatic incorporation of structural information in multiple sequence alignments using 3D-Coffee. *Nucleic Acids Res.* 34, W604–W608. <https://doi.org/10.1093/nar/gkl092>
- Biasini, M., Bienert, S., Waterhouse, A., Arnold, K., Studer, G., Schmidt, T., Kiefer, F., Cassarino, T.G., Bertoni, M., Bordoli, L., Schwede, T., 2014. SWISS-MODEL: Modelling protein tertiary and quaternary structure using evolutionary information. *Nucleic Acids Res.* 42, W252–W258. <https://doi.org/10.1093/nar/gku340>
- Bienert, S., Waterhouse, A., De Beer, T.A.P., Tauriello, G., Studer, G., Bordoli, L., Schwede, T., 2017. The SWISS-MODEL Repository-new features and functionality. *Nucleic Acids Res.* 45, D313–D319. <https://doi.org/10.1093/nar/gkw1132>
- Camacho, C., Coulouris, G., Avagyan, V., Ma, N., Papadopoulos, J., Bealer, K., Madden, T.L., 2009. BLAST+: Architecture and applications. *BMC Bioinformatics* 10, 421. <https://doi.org/10.1186/1471-2105-10-421>
- Chang, J.M., Di Tommaso, P., Lefort, V., Gascuel, O., Notredame, C., 2015. TCS: A web server for multiple sequence alignment evaluation and phylogenetic reconstruction. *Nucleic Acids Res.* 43, W3–W6. <https://doi.org/10.1093/nar/gkv310>
- Gandía-Herrero, F., Escribano, J., García-Carmona, F., 2012. Purification and antiradical properties of the structural unit of betalains. *J. Nat. Prod.* 75, 1030–1036. <https://doi.org/10.1021/np200950n>
- Gandía-Herrero, F., García-Carmona, F., 2014. *Escherichia coli* protein YgiD produces the structural unit of plant pigments betalains: Characterization of a prokaryotic enzyme with DOPA-extradiol-dioxygenase activity. *Appl. Microbiol. Biotechnol.* 98, 1165–1174. <https://doi.org/10.1007/s00253-013-4961-3>
- Gandía-Herrero, F., García-Carmona, F., 2013. Biosynthesis of betalains: yellow and violet plant pigments. *Trends Plant Sci.* 18, 334–343. <https://doi.org/10.1016/j.tplants.2013.01.003>
- Gandía-Herrero, F., García-Carmona, F., 2012. Characterization of recombinant *Beta vulgaris* 4,5-DOPA-extradiol-dioxygenase active in the biosynthesis of betalains.

- Planta 236, 91–100. <https://doi.org/10.1007/s00425-012-1593-2>
- Girod, P.-A., Zryd, J.-P., 1991. Biogenesis of betalains: Purification and partial characterization of dopa 4,5-dioxygenase from *Amanita muscaria*. *Phytochemistry* 30, 169–174. [https://doi.org/10.1016/0031-9422\(91\)84119-D](https://doi.org/10.1016/0031-9422(91)84119-D)
- Li, W., Cowley, A., Uludag, M., Gur, T., McWilliam, H., Squizzato, S., Park, Y.M., Buso, N., Lopez, R., 2015. The EMBL-EBI bioinformatics web and programmatic tools framework. *Nucleic Acids Res.* 43, W580–W584. <https://doi.org/10.1093/nar/gkv279>
- Miyake, C., Michihata, F., Asada, K., 1991. Scavenging of hydrogen peroxide in prokaryotic and eukaryotic algae: acquisition of ascorbate peroxidase during the evolution of cyanobacteria. *Plant Cell Physiol.* 32, 33–43. <https://doi.org/10.1093/oxfordjournals.pcp.a078050>
- Mueller, L.A., Hinz, U., Zryd, J.-P., 1997. The formation of betalamic acid and muscaflavin by recombinant dopa-dioxygenase from *Amanita*. *Phytochemistry* 44, 567–569. [https://doi.org/10.1016/S0031-9422\(96\)00625-5](https://doi.org/10.1016/S0031-9422(96)00625-5)
- Robert, X., Gouet, P., 2014. Deciphering key features in protein structures with the new ENDscript server. *Nucleic Acids Res.* 42, W320–W324. <https://doi.org/10.1093/nar/gku316>
- Sasaki, N., Abe, Y., Goda, Y., Adachi, T., Kasahara, K., Ozeki, Y., 2009. Detection of DOPA 4,5-dioxygenase (DOD) activity using recombinant protein prepared from *Escherichia coli* cells harboring cDNA encoding DOD from *Mirabilis jalapa*. *Plant Cell Physiol.* 50, 1012–1016. <https://doi.org/10.1093/pcp/pcp053>
- Segel, I.H., 1975. Enzyme kinetics : behavior and analysis of rapid equilibrium and steady state enzyme systems. New York-Wiley.
- Trezzini, G.F., Zryb, J.-P., 1991. Characterization of some natural and semi-synthetic betaxanthins. *Phytochemistry* 30, 1901–1903. [https://doi.org/10.1016/0031-9422\(91\)85036-Y](https://doi.org/10.1016/0031-9422(91)85036-Y)



## **Chapter VI.** Scaled-up biotechnological production of individual betalains in a microbial system

Part of this chapter was published in Microbial Biotechnology  
Guerrero-Rubio et al. (2019) <https://doi.org/10.1111/1751-7915.13452>



### Contextualization

The renewed interest in betalains contrasts with the limited number of biotechnological tools to produce them. Obtaining individual pigments is necessary to characterize and apply the potent health-promoting activities described for betalains (Gandía-Herrero et al., 2016). To date, obtaining betalains and purifying them from whole plants has depended on their availability throughout the year and on environmental variables that may affect their production (Khan et al., 2012). Other methods used are the production of betalains by a semi-synthesis method, which requires obtaining betalamic acid from the degradation of betanin (Gandía-Herrero et al., 2006) or the production of betalains in plant cell cultures (Guadarrama-Flores et al., 2015; Henarejos-Escudero et al., 2018; Milech et al., 2017), but the main problem these techniques present is the low efficiency in the production of pure betalains. The aim of this chapter is to describe a novel technique for the obtention of betalains through the development of microbial factories as a controllable system. The cloning of the novel and efficient enzyme 4,5-DOPA-extradiol dioxygenase from *Gluconacetobacter diazotrophicus* in an expression vector and the subsequent heterologous expression in *Escherichia coli* cultures has enabled the start-up of a biotechnological production system of individual pigments.

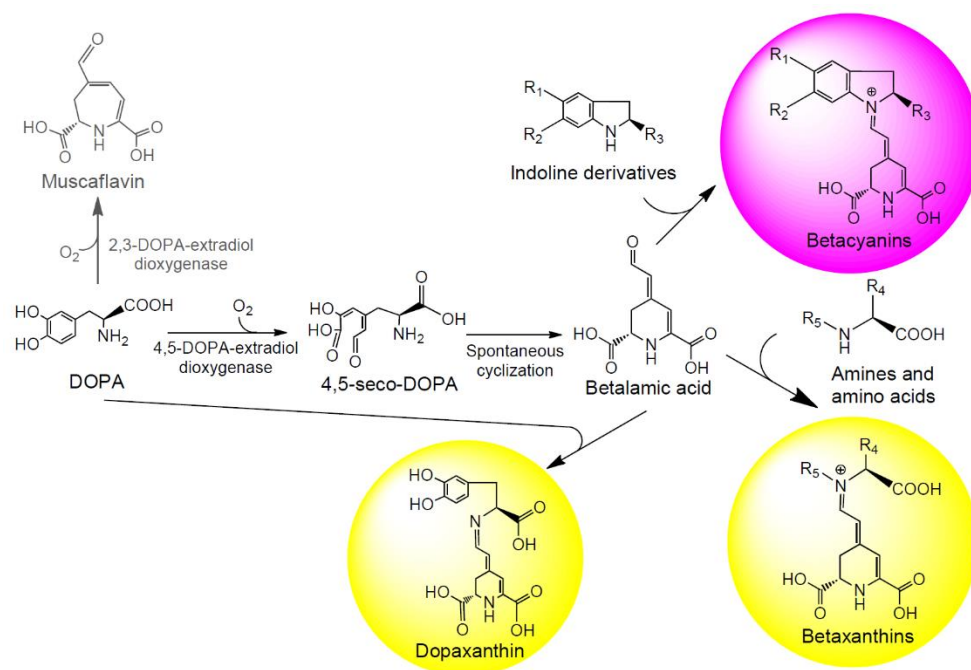


**Figure 6.1. Key steps involved in the biosynthesis of betalamic acid and betalains.** R<sub>1</sub> and R<sub>2</sub> can be hydroxyl groups with or without sugar derivatives. R<sub>3</sub> can be a carboxylic acid group. R<sub>4</sub> can be side chains of amino acids.

## 1. Expression of 4,5-DOPA-extradiol-dioxygenase from

### *Gluconacetobacter diazotrophicus* in *Escherichia coli* cultures

The 4,5-DODA enzyme from *Gluconacetobacter diazotrophicus* described in the chapter IV was used due to its higher activity, affinity towards L-DOPA substrate and stability compared with others dioxygenases previously described, as *Beta vulgaris* DODA or *E. coli* YgiD. The gene sequence of *G. diazotrophicus* (sequence WP\_012222467.1, GI:501179334) was used as a template to obtain the DODA sequence for protein expression in *E. coli* and inserted into the expression vector pET28a as it is described in Chapter IV. *E. coli* Rossetta 2 (DE3) was transformed with the vector pET28a-GdDODA and selected in LB supplemented with chloramphenicol (Cm) and kanamycin (Km) and then was cultured as little drops of 10  $\mu$ L in LB plates supplemented with IPTG, L-DOPA and sodium ascorbate to check the ability of *E. coli* expressing DODA to form betalamic acid (**Fig. 6.1**). After incubation for 24 hours at 20°C these plates showed a yellow coloration around the drops. Plates without IPTG were used as a control and these plates did not show any change of color (**Fig. 6.2**). The yellow halos around the drops confirmed the expression and activity of heterologous DODA protein induced by IPTG. The use of L-DOPA as a precursor in the synthesis of betaxanthins and the excretion of pigments thus resulted in yellow coloration. The positive results in the plate assays promoted the transfer of the production to *E. coli* liquid cultures.

## 2. Production of the structural unit of betalains

Thanks to the expression of the enzyme in *E. coli* Rossetta 2 (DE3) transformed with pET28a-GdDODA, the production of betalamic acid was obtained in cells grown and selected in medium LB supplemented with Cm and Km. IPTG was used for the induction of GdDODA's expression, and 15 hours later L-DOPA was added as the substrate of the reaction and as the precursor of betalains' obtention. The optimal concentration of L-DOPA was obtained by varying its concentration in the medium between 0.76 to 22.32 mM. The higher production was reached at 7.6 mM (**Fig. 6.3A**), the solubility limit of the substrate. Sodium ascorbate was added to prevent spontaneous oxidation. After the addition of any L-DOPA concentration assayed, the culture began to show a yellow coloration.

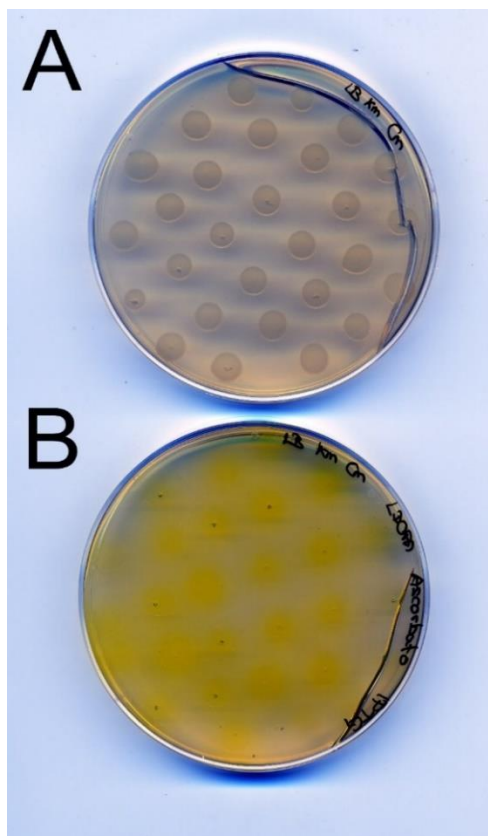


**Figure 6.2. Expression of GdDODA activity in *E. coli* cells grown in agar solid medium supplemented with L-DOPA. A:** Control plate without IPTG. **B:** Yellow halos formed around the bacterial colonies in the presence of L-DOPA 7.6 mM indicate the formation and excretion of betalain related compounds. The image was taken at the same time (same shot) for both 60 mm petri plates.

HPLC analyses of the supernatant medium showed that the yellow coloration was due to the presence of betalamic acid and due to other compound with lower retention time and spectrum compatible with betaxanthins. Betalamic acid was detected at  $\lambda_m = 405$  nm with a retention time of 14.9 minutes. To confirm its nature, betalamic acid obtained from the degradation of betanin was used as standard (**Fig. 6.3C**) (Gandía-Herrero et al., 2009). Muscaflavin was also detected with a maximum at 403 nm and a retention time of 16.6 min. By using real standards (Gandía-Herrero et al., 2005a), the peak compatible with betaxanthins was identified as dopaxanthin (**Fig. 6.3D**), the same betaxanthin obtained in cultures of *G. diazotrophicus* enriched with L-DOPA (Chapter IV), which was detected with a maximum wavelength at  $\lambda_m = 471$  nm and a retention time of 13.91 min. The presence of dopaxanthin is the result of the condensation of betalamic acid with L-DOPA used as a substrate. Therefore, this betaxanthin is obtained in cell cultures of *E. coli* due to the expression of the enzyme 4,5-DODA in one-pot experiments.



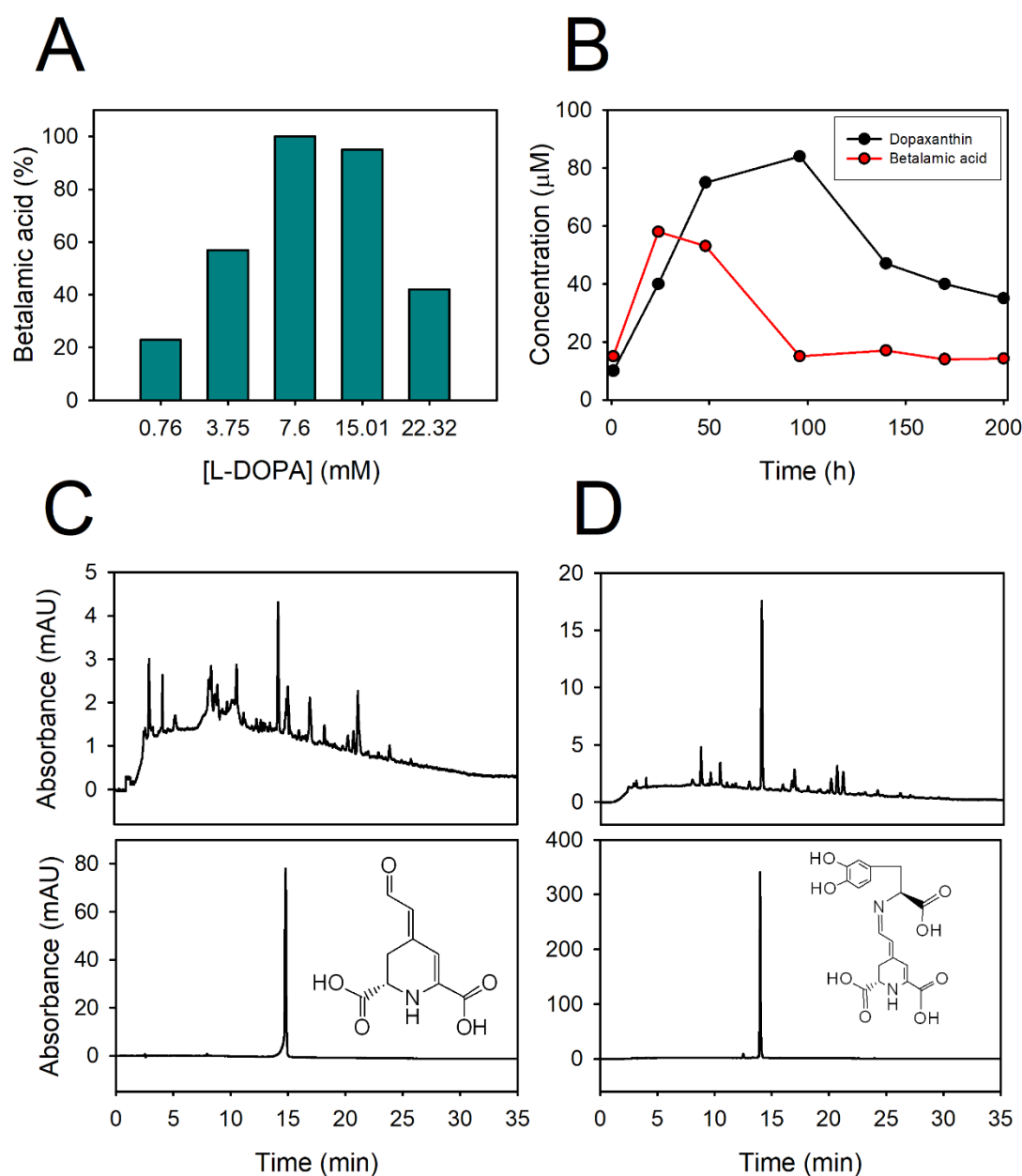


**Figure 6.3. Effect of adding L-DOPA to an *E. coli* culture expressing GdDODA. A.** Production of betalamic acid at different concentrations of L-DOPA (mM). Production is expressed in % considering the highest value as 100% production. **B.** Time course of the betalamic acid and dopaxanthin production. **C.** Chromatogram at  $\lambda=405$  nm of LB medium after the addition of L-DOPA. The employment of betalamic acid standard (below) confirmed its presence. **D.** Chromatogram at  $\lambda=480$  nm of LB medium after the addition of L-DOPA. The use of dopaxanthin standard (below) confirmed its presence as a major peak with a retention time of 13.9 min.

The evolution of the concentration of both betalamic acid and dopaxanthin was followed over time by HPLC analysis. Both products were monitored for a period of 200 hours after adding L-DOPA as substrate of the reaction (**Fig. 6.3B**). In the first

hours, a peak with retention time of 8.54 min was obtained at  $\lambda_m = 361$  nm. This peak corresponded to 4,5-seco-DOPA, the intermediate product of 4,5-DODA activity that yields betalamic acid by spontaneous cyclization. The maximum concentration of betalamic acid was obtained at 24-30 hours, after which it drastically decreased. However, dopaxanthin concentration increases progressively until a maximum production at 96 hours. This lag period is due to the condensation of betalamic acid with the L-DOPA used as a substrate for the production of betalamic acid. On the other hand, the cell pellet was centrifuged and analyzed by HPLC after washing and sonication but it did not show accumulation of betalamic acid or dopaxanthin, indicating that products obtained by the L-DOPA transformation are excreted to the culture medium, as 4,5-seco-DOPA intermediate or as betalamic acid.

### 3. Production of betalamic acid in different media

HPLC analyses showed the presence of betalamic acid, dopaxanthin and muscaflavin in the above-mentioned LB culture but also showed the formation of minor peaks detected at 480 nm (**Fig. 6.4A**) which had different retention times (**Table 6.1**) and evolved independently with the reaction time. The spectral analysis of the compounds was compatible with the presence of unknown betaxanthins whose formation could be promoted by the presence of free amines in LB medium. To study this phenomenon, different media were used to determine the formation of the new betaxanthins depending on the medium composition. The media used were NZCYM, fresh LB and the same LB medium where the bacteria were grown. The optimum conditions for substrate concentration and temperature were used in all cases. After addition of the substrate L-DOPA, there was no difference between fresh LB and LB used in the growth of bacteria.

Various betaxanthins with different retention times in the LB and NZCYM media were observed by HPLC analysis (**Fig. 6.4A-B**). Betaxanthins with retention times of 13.9, 14.9, 21.7, 22.8, 26.1 and 26.9 minutes were detected in both media. Furthermore, betaxanthins with retention times of 9.2, 16.7 and 20.5 minutes were exclusively detected in samples from LB medium. The mass values determined by electrospray ionization mass spectrometry (ESI-MS) are shown in **Table 6.1**.

**Table 6.1. HPLC and ESI-MS/MS characteristics and identification of known and minor betalains detected after the growth of *E. coli* expressing 4,5-DODA in different media and the addition of L-DOPA.**

Rt (min)	Name	Media	PDA- $\lambda_m$ (nm)	[M+H] ( $m/z$ )	Main daughter ion ( $m/z$ )
9.2	---	LB	471	235	162
13.9	Dopaxanthin	LB/NZCYM	471	391	347
14.9	Betalamic acid	LB/NZCYM	405	212	166
16.7	Muscaflavin	LB	405	212	166
20.5	---	LB	471	385	215
21.7	---	LB/NZCYM	471	326	244
22.8	---	LB/NZCYM	471	374	365
26.1	---	LB/NZCYM	471	288	461
26.9	---	LB/NZCYM	471	411	385

The mass of 391.1  $m/z$  obtained at 13.91 min and the mass exact of 212.0  $m/z$  obtained at 14.9 min were compatible with the presence of dopaxanthin and betalamic acid, respectively, in LB and NZCYM media. In addition, the mass of 212.0  $m/z$  obtained at 16.7 min in LB medium was compatible with muscaflavin. The rest of mass values were not compatible with known betaxanthins.

It is concluded that LB and NZCYM media have a series of elements with amino groups in their composition which condense with the betalamic acid formed by the bacterial culture, giving rise to different betaxanthins. No differences were found between fresh LB and the LB medium used in the bacterial growth. This indicates that elements with amine groups are still available for the condensation with the betalamic acid formed by the engineered bacteria. In order to simplify the final pigments obtained by the transformation of the precursor molecule L-DOPA, water was added, instead of the amine-containing media, after harvesting and washing of the induced cells. In this case, the production of betalamic acid and dopaxanthin experienced an increase, doubling the results obtained with the other media. Neither was the presence of any other derived betaxanthin observed (**Fig. 6.4C**), thus yielding dopaxanthin in a purer form.

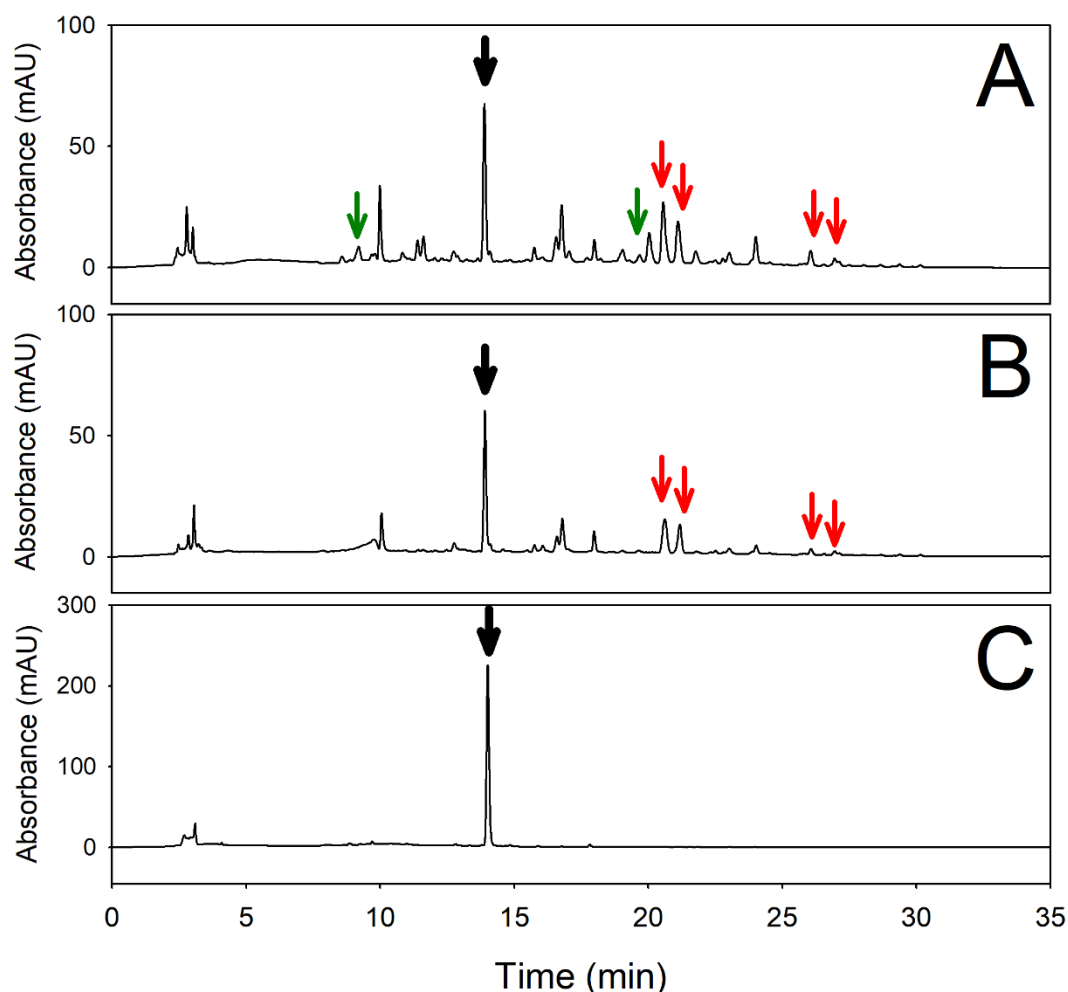
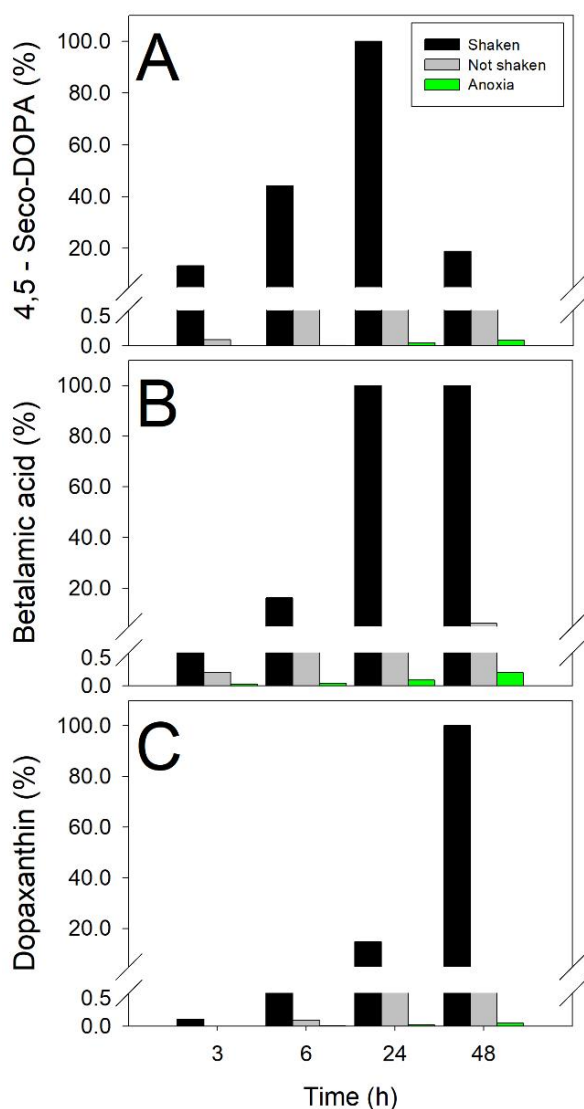


**Figure 6.4. Production of dopaxanthin in microbial cultures.** Chromatograms at  $\lambda=480$  nm for the production betaxanthins in the media LB (A), NZCYM (B) and water (C). Dopaxanthin was detected at 13.9 min with a signal intensity higher in water than in LB and NZCYM (black arrows). The exclusive betaxanthins present in LB medium are indicated with green arrows. Red arrows indicate betaxanthins present in both LB and NZCYM media.

In the transformation in water, only the formation of betalamic acid and dopaxanthin was achieved. This raises the possibility of using water in the transformation phase as a way to reduce production costs and simplify future purification processes, since the culture medium is only necessary for the initial growth of the cells.

#### 4. Oxygen effect in the production of betalains

Previous studies on the enzymatic activity of GdDODA showed the importance of oxygen exchange in the formation of betalains, as it is described in the chapter IV. Thus, once water was established as the optimum medium for the biotransformation of L-DOPA, *E. coli* (pET28a-GdDODA) was grown in LB medium, centrifuged and cell pellet was transferred to water for the production of 4,5-



seco-DOPA, betalamic acid and dopaxanthin. The reaction was followed under different atmospheric conditions, in order to evaluate the effect of oxygen. As **Fig. 6.5** shows, a shaken medium, which favors the oxygen exchange, increases the production of pigments respect to the values obtained in a non-shaken medium where the oxygen exchange is limited by diffusion. Furthermore, deaeration and the use of nitrogen atmosphere in the culture produced a pronounced decrease in the yield of the final product dopaxanthin (**Fig. 6.5**).

**Figure 6.5. Effect of aeration in the microbial factories.** Production was followed for 4,5-seco-DOPA (A), betalamic acid (B) and dopaxanthin (C). **D.** Products accumulation was due to *E. coli* (pET28a-GdDODA) biotransformation in water solution supplemented with L-DOPA in a shaken, not shaken and anoxic media. Anoxia conditions were obtained with deaeration and nitrogen atmosphere.

## 5. Addition of amines and amino acids to the medium for the production of derived betalains

The addition of amines and amino acids to a medium which produces betalamic acid may lead to the obtention of betalains. This phenomenon is due to Schiff condensation, where the spontaneous reaction between the  $\text{-NH}_2$  group of an amine and the aldehyde group of betalamic acid form the corresponding imine. Successful approaches for betalain production have been carried out in semi-synthesis processes previously described to obtain betalains standards (Materials and Methods section). Betalamic acid obtained by basic hydrolysis from betanin extracted from red beet, is able to condense with the amines added to the medium (Gandía-Herrero et al., 2006). However, betalamic acid is obtained more efficiently by the novel biotechnological technique described in this chapter and its capability to react with free amines is maintained. In this context, the biosynthesis of betaxanthins and betacyanins could be achieved by adding selected amino acids and amines. The addition of the compounds 2-phenylethylamine, L-phenylalanine, indoline, indoline-2-carboxylic acid and proline gave rise to the betalains phenylethylamine-betaxanthin, phenylalanine-betaxanthin, indoline-betacyanin, indoline carboxylic acid-betacyanin and indicaxanthin, respectively.

The obtention of each amine-derived betalain was performed in flasks containing 100 mL of water, and they were shaken at 120 rpm to favor the oxygen exchange previously described. The addition of these compounds was carried out at a concentration of 38 mM, five times higher than the concentration used for L-DOPA. This favors the condensation of betalamic acid with these molecules instead of the condensation with L-DOPA, which acts as a substrate for DODA enzyme and as precursor in the synthesis of dopaxanthin (**Fig. 6.1**). Condensation with 2-phenylethylamine, L-phenylalanine and L-proline led to the production of the betaxanthins phenylethylamine-betaxanthin, phenylalanine-betaxanthin and indicaxanthin, respectively. On the other hand, the condensation with indoline and indoline-2-carboxylic acid led to the production of indoline-betacyanin and indoline-carboxylic acid-betacyanin, respectively (**Fig. 6.6A**). Indoline and its carboxylated derivative added at 38 mM negatively affected the activity of the dioxygenase enzyme produced. Indoline and indoline-carboxylic acid formed water-insoluble droplets in the biotransformation medium that may negatively affect the integrity of

the bacterial membrane or the stability of the protein. To avoid the formation of these drops, their concentrations were lowered by several orders of magnitude, reaching a maximum betacyanin production at 3.8 mM for indoline-2-carboxylic acid and at 0.38 mM for indoline.



**Figure 6.6. Redirection for the production of multiple individual pigments.** **A:** Structures of the betalains produced in this study. From left to right: indicaxanthin, dopaxanthin, phenylalanine-betaxanthin, phenylethylamine-betaxanthin, indoline carboxylic acid-betacyanin and indoline-betacyanin. **B:** 100-mL cultures of *E. coli* expressing 4,5-DODA in the production of the individual molecules shown above. **C-D:** Scaled-up synthesis of phenylethylamine-betaxanthin (**C**) and indoline-betacyanin (**D**) in bioreactors with a volume of 2L.

In all cases, the compounds obtained were analyzed by mass spectrometry and HPLC to confirm the structures proposed (**Table 6.2**). The values for absorption maximum wavelengths and retention times shown in **Table 6.2** were in accordance to the values reported previously for standards obtained using a semi-synthetic method (Gandía-Herrero et al., 2005b, 2010a). Under the optimal conditions determined for each compound in volumes of 100 mL, it was possible to obtain up to 3.1 mg in total of indoline-betacyanin, 1.9 mg of indoline-2-carboxylic acid-betacyanin, 2.6 mg of L-phenylalanine-betaxanthin, 1.1 mg of phenylethylamine-betaxanthin, 2.2 mg of indicaxanthin and 4.3 mg of dopaxanthin. Once the technique was optimized and its efficiency in the synthesis of individual betalains was confirmed, the possibility of using these microbial cultures in bioreactors for a higher production of betalains was studied.

**Table 6.2. Production of individual betalains obtained in bacterial cultures of *E. coli* expressing the DODA enzyme of *G. diazotrophicus* (flasks, 100mL).**

Betalain	Rt (min)	PDA- $\lambda_m$ (nm)	[M+H] <sup>+</sup> (m/z)	Yield (mg/100mL)	Main daughter ion (m/z)
Indicaxanthin	12.65	471	308	2.2	264
Dopaxanthin	13.91	471	391	4.3	347
Phenylethylamine-betaxanthin	20.08	471	315	2.6	271
Phenylalanine-betaxanthin	22.11	471	359	1.1	315
Indoline-2-carboxylic acid- betacyanin	19.17	524	357	1.9	313
Indoline-betacyanin	22.10	524	313	3.1	269

## 6. Scaling-up to bioreactor level

Indicaxanthin, dopaxanthin, phenylethylamine-betaxanthin and indoline-betacyanin were chosen for the scaled-up production. Indicaxanthin and dopaxanthin were chosen for their relevance in preliminary bioactivity assays (Wendel et al., 2015) and strong antioxidant activity (Escribano et al., 2017). Furthermore, indicaxanthin is the main bioactive pigment of cactus pears (Gandía-Herrero et al., 2010b) and dopaxanthin is the only pigment in *Glottiphyllum* flowers (Impellizzeri et al., 1973). Phenylethylamine-betaxanthin and indoline-betacyanin (**Fig. 6.6C-D**) were chosen for their close structural similarity as pigment models of betaxanthins and betacyanins. In addition, phenylethylamine-betaxanthin is a minor pigment present in cactus pears (Castellanos-Santiago and Yahia, 2008).

The biotechnological synthesis of betalains in bioreactor was intended to allow a greater production. In addition, it made possible to control all the variables that may affect the synthesis, such as pH, temperature and oxygen demand. Temperature control made on a small scale was also performed in the bioreactor thanks to the use of a heating jacket that allows large temperature changes in a few hours.

In preliminary assays, the synthesis of indoline-betacyanin was carried out controlling the pH at a value of 7.0, as it is done for bacterial growth. After 96 hours, the culture did not show the pink coloration characteristic of betacyanins (**Fig. 6.7A**). It was observed that, after the addition of the reagents, the culture did not consume



acid, but it continued to consume alkali at a high rate in order to maintain pH 7 (**Fig. 6.7C**).

Samples were taken over time to follow the evolution of the reaction and they were analyzed by HPLC. The analysis showed the accumulation of betalamic acid, but that it did not condense with indoline as expected. In an alternative experiment, the pH of the culture was allowed to evolve freely. In this way, after 48 hours, a deep purple indoline-betacyanin culture with pH = 5.8 was obtained (**Fig. 6.7B**). HPLC analysis showed that betalamic acid reacted rapidly with indoline in the synthesis of indoline-betacyanin and it accumulated over time up to a maximum value at 72 hours after the addition of the compounds. Thus, betalamic acid requires a slightly acidic medium in order to be able to condense with available amines or amino acids.

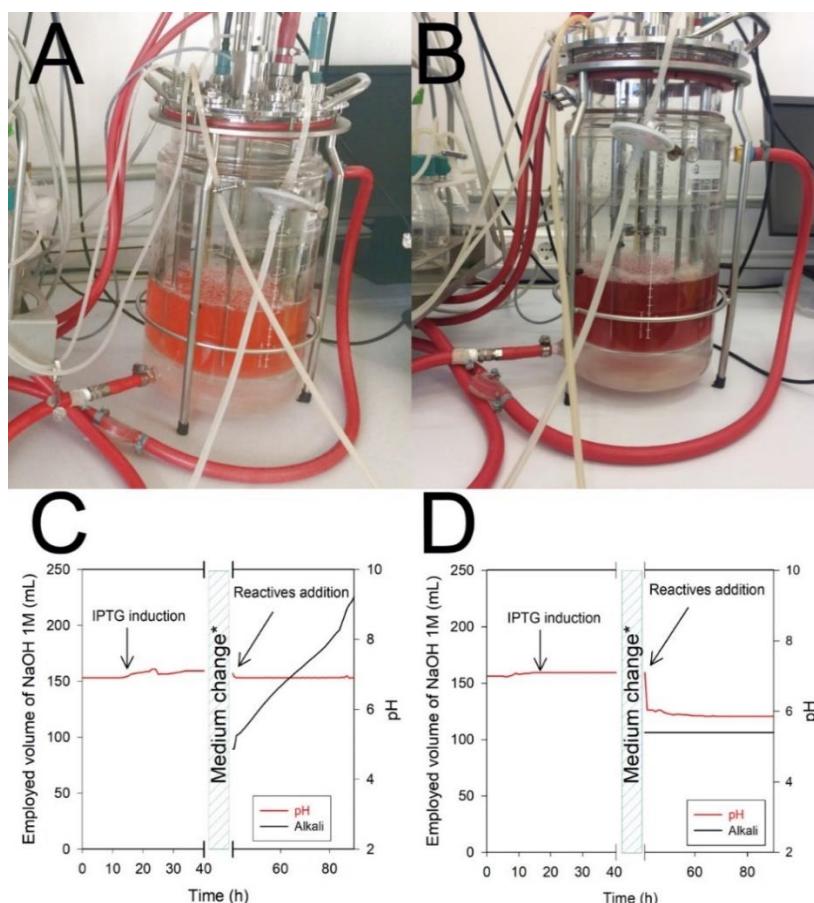


**Figure 6.7. Production of indoline-betacyanin in 2L bioreactor.** Different trends in the synthesis of indoline-betacyanin can be observed when pH is controlled to 7.0 (**A**) and when pH drops freely to 5.8 (**B**). Pictures are shown after 96 hours incubation. When carrying out the reaction at pH 7.0 (**C**), the consumption of alkali increases progressively due to the tendency of acidification in the synthesis of betalamic acid. **D**: Effect of stopping the consumption of alkali after the addition of reactives on pH when it evolves freely in the reactor. \*Medium change: cells in LB medium were centrifuged and the pellet was resuspended in water.

After observing the pronounced pH effect in the synthesis of betalains, and its favorable evolution towards acidic values in order to yield betalains, the following assays were performed without the addition of base. In this sense, the sole addition of L-DOPA and sodium ascorbate to the bioreactor led to the synthesis of dopaxanthin. The addition, besides, of 2-phenylethylamine or proline, gave rise to the synthesis of phenylethylamine-betaxanthin and indicaxanthin, respectively. The reaction medium for the biotransformations leading to the obtention of betaxanthins showed a final pH value of 5.7. The needed time to reach maximum production of each betalain was established after the addition of reagents. Thus, time for optimal production was 48 hours for phenylethylamine-betaxanthin and indicaxanthin, 72 hours for indoline-derived betacyanin and 96 hours for dopaxanthin (**Fig. 6.8**).

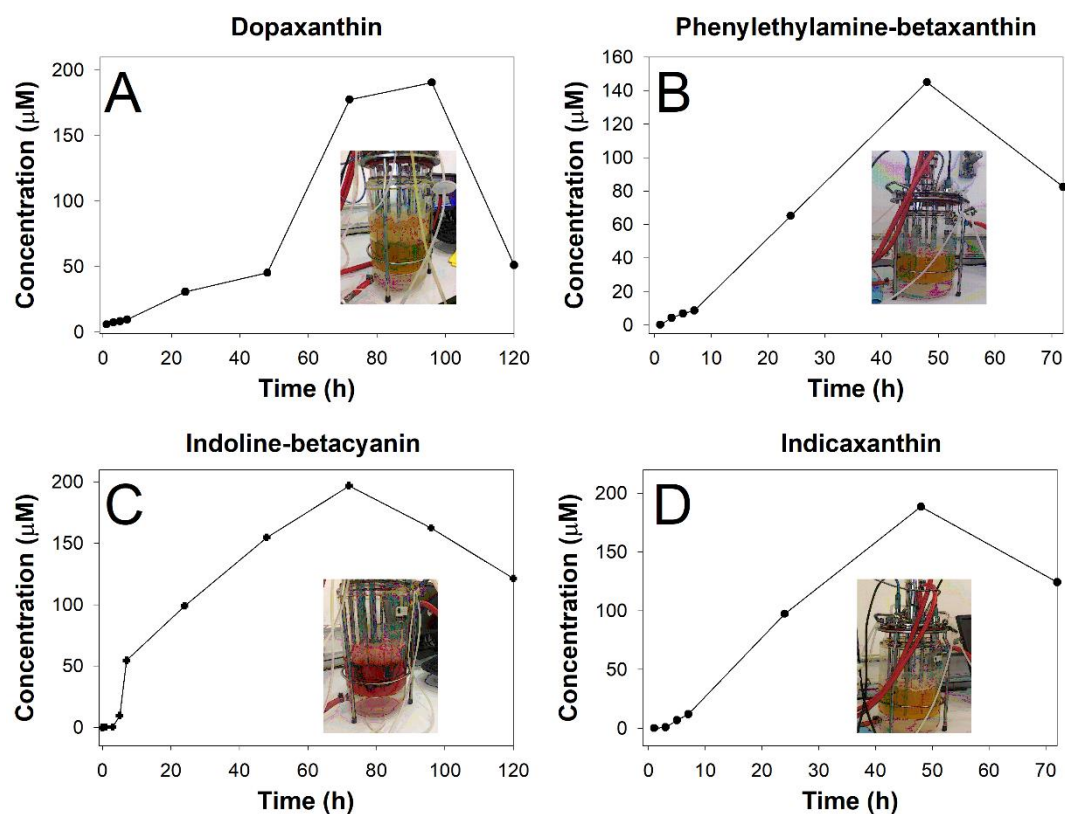


**Figure 6.8.** Time evolution of the scaled-up synthesis of betalains in bioreactor (volume of 2L) (A) Dopaxanthin. (B) Phenylethylamine-betaxanthin. (C) Indoline-betacyanin. (D) Indicaxanthin.

## 7. Purification and quantification

Once the optimal production conditions for each compound were established, the media were collected and the pigments were then purified. Dopaxanthin was collected 96 hours after the addition of the reagents, while the betaxanthins phenylethylamine-betaxanthin and indicaxanthin were recovered 48 hours after amines addition. The indoline-derived betalain was collected 72 hours after the addition of the reagents. The cultures were then centrifuged twice for 10 minutes at 5,000 g to remove the cell pellet and the supernatants were analyzed by HPLC and submitted to purification. Although the concentration of amines was 5 times higher than L-DOPA concentration (except for indoline), all the analyzed samples showed a residual presence of dopaxanthin, at a much lower concentration than the betalain corresponding to the added amine. The proportion of dopaxanthin obtained respect to the major betalain was 4.3% in the production of indoline-betacyanin, 2.1% in phenylethylamine-betaxanthin and 13.8% in indicaxanthin. L-DOPA, as a precursor of betalamic acid synthesis was present in all biotransformation media and the amount of residual dopaxanthin obtained was inversely proportional to the affinity that betalamic acid shows for the major amine.

In order to remove the substrates added and dopaxanthin, the media were purified by automatic anionic exchange chromatography (FPLC) and subsequent extraction in solid phase C-18 columns (Gandía-Herrero et al., 2006). The compounds were purified with a recovery of 92.7% for dopaxanthin, 91.2% for indoline-betacyanin, 96.0% for phenylethylamine-betaxanthin and 42.0% for indicaxanthin (**Table 6.3**). Pure compounds obtained in the scaled-up bioreactors were quantified, with 148.25 mg of dopaxanthin, 112.22 mg of indoline-betacyanin, 91.11 mg of phenylethylamine-betaxanthin and 48.75 mg of indicaxanthin. These values are 4 orders of magnitude higher than those obtained by semi-synthesis, where the limitations of the technique gave between 40 and 90 µg of pure betalains (Gandía-Herrero et al., 2006).

**Table 6.3. Betalain production in 2L bioreactors.**

<b>Betalain</b>	<b>Amino acid or amine</b>	<b><math>\lambda_{\text{abs}}</math> (nm)</b>	<b>Pure final pigment (mg)</b>	<b>Purification yield (%)</b>
Indicaxanthin	L-Proline	483	48.75	42.03
Dopaxanthin	L-DOPA	478	148.25	92.7
Phenylethylamine-betaxanthin	2-phenylethylamine	473	91.11	96.04
Indoline-betacyanin	Indoline	524	112.22	91.24

## 8. Conclusions

A novel scalable bioprocess is here described to produce the plant pigments betalains in a fast and simple system. The process is performed in bioreactors controlled by the heterologous expression of GdDODA, the most efficient DODA enzyme described so far. The biotransformations performed in water minimize the costs of large-scale biological production and allow the easy purification of the compounds. Furthermore, the number of possible betaxanthin is reduced from eight in enriched media (LB, NZCYM) to only one main pigment in costless water. The scaling-up of this technique to large bioreactors would enable large amounts of betalains to be obtained and would increase the applicability of their health-promoting potential in the food, pharmaceutical, and cosmetic industries.

## REFERENCES

- Castellanos-Santiago, E., Yahia, E.M., 2008. Identification and quantification of betalains from the fruits of 10 Mexican prickly pear cultivars by high-performance liquid chromatography and electrospray ionization mass spectrometry. *J. Agric. Food Chem.* 56, 5758–5764.  
<https://doi.org/10.1021/jf800362t>
- Escribano, J., Cabanes, J., Jiménez-Atiénzar, M., Ibañez-Tremolada, M., Gómez-Pando, L.R., García-Carmona, F., Gandía-Herrero, F., 2017. Characterization of betalains, saponins and antioxidant power in differently colored quinoa (*Chenopodium quinoa*) varieties. *Food Chem.* 234, 285–294.  
<https://doi.org/10.1016/j.foodchem.2017.04.187>
- Gandía-Herrero, F., Escribano, J., García-Carmona, F., 2016. Biological activities of plant pigments betalains. *Crit. Rev. Food Sci. Nutr.* 56, 937–945.
- Gandía-Herrero, F., Escribano, J., García-Carmona, F., 2010a. Structural implications on color, fluorescence, and antiradical activity in betalains. *Planta* 232, 449–460.  
<https://doi.org/10.1007/s00425-010-1191-0>
- Gandía-Herrero, F., Escribano, J., García-Carmona, F., 2005a. Betaxanthins as substrates for tyrosinase. An approach to the role of tyrosinase in the biosynthetic pathway of betalains. *Plant Physiol.* 138, 421–432.  
<https://doi.org/10.1104/pp.104.057992>
- Gandía-Herrero, F., Escribano, J., García-Carmona, F., 2005b. Betaxanthins as pigments responsible for visible fluorescence in flowers. *Planta* 222, 586–593.  
<https://doi.org/10.1007/s00425-005-0004-3>
- Gandía-Herrero, F., García-Carmona, F., Escribano, J., 2006. Development of a protocol for the semi-synthesis and purification of betaxanthins. *Phytochem. Anal.* 17, 262–269. <https://doi.org/10.1002/pca.909>
- Gandía-Herrero, F., Jiménez-Atiénzar, M., Cabanes, J., Escribano, J., García-Carmona, F., 2009. Fluorescence detection of tyrosinase activity on dopamine-betaxanthin purified from *Portulaca oleracea* (common purslane) flowers. *J. Agric. Food Chem.* 57, 2523–2528. <https://doi.org/10.1021/jf803608x>
- Gandía-Herrero, F., Jiménez-Atiénzar, M., Cabanes, J., García-Carmona, F., Escribano, J., 2010b. Stabilization of the bioactive pigment of *Opuntia* fruits through maltodextrin encapsulation. *J. Agric. Food Chem.* 58, 10646–10652.  
<https://doi.org/DOI:10.1021/jf101695f>

- Guadarrama-Flores, B., Rodriguez-Monroy, M., Cruz-Sosa, F., García-Carmona, F., Gandía-Herrero, F., 2015. Production of dihydroxylated betalains and dopamine in cell suspension cultures of *Celosia argentea* var. *plumosa*. J. Agric. Food Chem. 63, 2741–2749. <https://doi.org/10.1021/acs.jafc.5b00065>
- Henarejos-Escudero, P., Guadarrama-Flores, B., Guerrero-Rubio, M.A., Gómez-Pando, L.R., García-Carmona, F., Gandía-Herrero, F., 2018. Development of betalain producing callus lines from colored quinoa varieties (*Chenopodium quinoa* Willd). J. Agric. Food Chem. 66, 467–474. <https://doi.org/10.1021/acs.jafc.7b04642>
- Impellizzeri, G., Piattelli, M., Sciuto, S., 1973. A new betaxanthin from *Glottiphyllum longum*. Phytochemistry 12, 2293–2294. [https://doi.org/10.1016/0031-9422\(73\)85137-4](https://doi.org/10.1016/0031-9422(73)85137-4)
- Khan, M.I., Sri Harsha, P.S.C., Giridhar, P., Ravishankar, G.A., 2012. Pigment identification, nutritional composition, bioactivity, and in vitro cancer cell cytotoxicity of *Rivina humilis* L. berries, potential source of betalains. LWT - Food Sci. Technol. 47, 315–323. <https://doi.org/10.1016/j.lwt.2012.01.025>
- Milech, C., Lucho, S.R., Kleinowski, A.M., Dutra, D.B., Soares, M.M., Jacira, E., Braga, B., 2017. Production of pigments in *Alternanthera sessilis* calli mediated by plant growth regulators and light. Acta Sci. Biol. Sci. Mar. 39, 381–388. <https://doi.org/10.4025/actascibiolsci.v39i3.36312>
- Wendel, M., Szot, D., Starzak, K., Tuwalska, D., Prukala, D., Pedzinski, T., Sikorski, M., Wybraniec, S., Burdzinski, G., 2015. Photophysical properties of indicaxanthin in aqueous and alcoholic solutions. Dye. Pigment. 113, 634–639. <https://doi.org/10.1016/j.dyepig.2014.09.036>



**Chapter VII.** Reversible bleaching of betalains induced by metals and application to the fluorescent determination of anthrax biomarker

Part of this chapter was published in Dyes and Pigments  
Guerrero-Rubio et al. (2020) <https://doi.org/10.1016/j.dyepig.2020.108493>





### **Contextualization**

For many decades, the degradation of betalains has been related to the presence of metals. However, the ability of betanin to interact with europium was recently described. Europium is a metal of the lanthanide series in the group of the so-called rare earths, and it forms a complex that produces a change in the absorbance spectrum (Gonçalves et al., 2013). This characteristic has not been investigated in other betalains and the existence of possible effects of complexation on other properties is unknown. The association with europium is sensitive to the presence in the medium of dipicolinic acid (DPA), a compound present in the core of bacterial spores of the genus *Bacillus*. Bacteria that are part of this genus pass to a dormant spore state to survive adverse environmental conditions (Setlow, 2000). Among the bacteria that constitute the genus *Bacillus*, there are some species with positive applications for human activities, such as *B. thuringensis* (Schnepf et al., 1998), and other species, such as *B. anthracis*, which represent a great threat to public health due to their use as bioterrorist agents. Therefore, the development of a fast, simple and sensitive method for the detection of *Bacillus* spores is of great interest.

This chapter is an overall study on the existence of complexes of betalains with metals. Different metals and types of molecules, both betaxanthins and betacyanins, are used for the first time and the effect of the complexes is evaluated not only on color, but also on the fluorescent properties of the pigments.

## **1. Selection of betalains**

To characterize the possible general effect of metal addition on the spectrophotometric properties of plant pigments betalains, four model molecules were chosen: two violet betacyanins and two yellow betaxanthins (**Fig. 7.1**). Among the betacyanins, betanin was chosen for its physiological relevance and for being a model molecule widely used in betalains studies (Gliszczyńska-Świgło et al., 2006). Indoline-betacyanin was selected for being the simplest betacyanin and structural and chromophoric unit of these pigments. Two betaxanthins were selected, one for its structural similarity with the simplest betacyanin (phenylethylamine-betaxanthin), and the other one for being the most fluorescent betaxanthin (miraxanthin I) (Gandía-Herrero et al., 2005a). Both betaxanthins are natural compounds identified in *Opuntia* fruits (Castellanos-Santiago and Yahia, 2008) and flowers of *Mirabilis jalapa* (Piattelli

et al., 1965). The indoline-betacyanin and betaxanthins used in this work were obtained by the biotechnological method described in the chapter VI, while betanin was obtained from extracts of red beet (*Beta vulgaris*). All of them were purified to homogeneity by ion exchange chromatography and solid phase extraction, obtaining the total yields for the process reported in **Table 7.1** together with the retention times of the four pigments in the analysis by high performance liquid chromatography (HPLC).

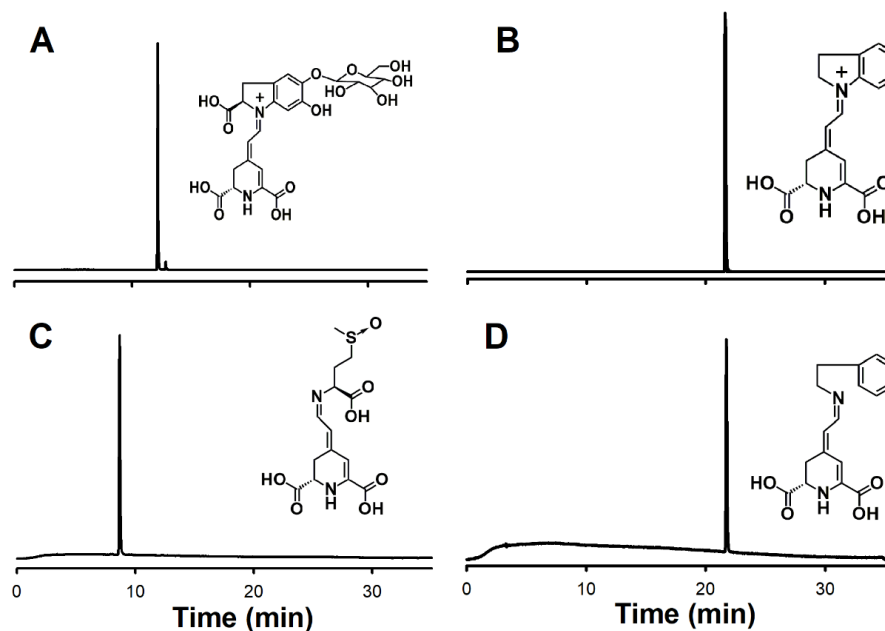


**Figure 7.1. Structures and chromatograms for the pure betalains used in this study:** Betanin (**A**), indoline-betacyanin (**B**), miraxanthin I (**C**) and phenylethylamine-betaxanthin (**D**). Elutions were followed at maximum wavelengths: 536 nm for **A** and **B**, and at 480 nm for **C** and **D**.

## 2. General effect of europium on betalains

The effect of  $\text{Eu}^{3+}$ , a rare earth of the lanthanide group, was evaluated on the color of the pigment betanin in a previous work (Gonçalves et al., 2013). Here, we expand the number of evaluated molecules in an attempt to generalize the phenomenon and to explore a possible effect on the fluorescence of the pigments. Both betacyanins and betaxanthins with related structures were used for the first time. Europium altered the spectrophotometric properties of betalains immediately after its addition. In **Table 7.1**, the variation of the wavelengths is shown after the complexation process for both the absorbance and the fluorescence phenomena.

**Table 7.1. Variations in the maximum wavelengths ( $\lambda$ ) produced by the complexation of  $\text{Eu}^{3+}$  with betalains.** The data correspond to measurements of 13  $\mu\text{M}$  betalains for absorbance and 3  $\mu\text{M}$  for fluorescence with concentrations of europium 39  $\mu\text{M}$  for betanin, 130  $\mu\text{M}$  for indoline-betacyanin and 260  $\mu\text{M}$  for phenylethylamine-betaxanthin and miraxanthin I. The retention times of the same in HPLC and the performance of the purification process are also shown.

	Absorbance		Fluorescence				Analysis and purification	
	$\lambda_{\text{max}}$ (control) (nm)	$\lambda_{\text{max}}$ ( $\text{Eu}^{3+}$ ) (nm)	$\lambda_{\text{max}}^{\text{emi}}$ (control) (nm)	$\lambda_{\text{max}}^{\text{emi}}$ ( $\text{Eu}^{3+}$ ) (nm)	$\lambda_{\text{max}}^{\text{exc}}$ (control) (nm)	$\lambda_{\text{max}}^{\text{exc}}$ ( $\text{Eu}^{3+}$ ) (nm)	Retention Time (min)	Yield purification (%)
Betanin	537	477	--	--	--	--	12.1	70.0%
Indoline- Betacyanin	524	466	575	575	526	525	21.7	91.2%
Miraxanthin I	474	433	511	515	478	476	8.6	41.6%
Phenylethylamine- betaxanthin	474	449	510	509	477	475	21.7	96.0%

At the absorbance level, the four molecules studied experience a hipsochromic displacement of the wavelength (**Table 7.1**) as well as a decrease in the absorbance value (**Fig. 7.2A-D**). The recorded effect for betanin is identical to that previously described (Gonçalves et al., 2013). The structural unit indoline-betacyanin behaves analogously and thus indicates a general tendency. For betaxanthins, a metal induced change of color is recorded for the first time towards shorter wavelengths and a notable reduction of absorbance was observed. On the other hand, the effect of europium on the fluorescence of the three fluorescent betalains (indoline-betacyanin, miraxanthin I and phenylethylamine-betaxanthin) was evaluated for the first time and consisted of the almost total reduction in the intensity of fluorescence obtained (**Fig. 7.2E-G**). However, there is no significant variation in the maximum wavelengths for all excitation and emission processes (**Table 7.1**).

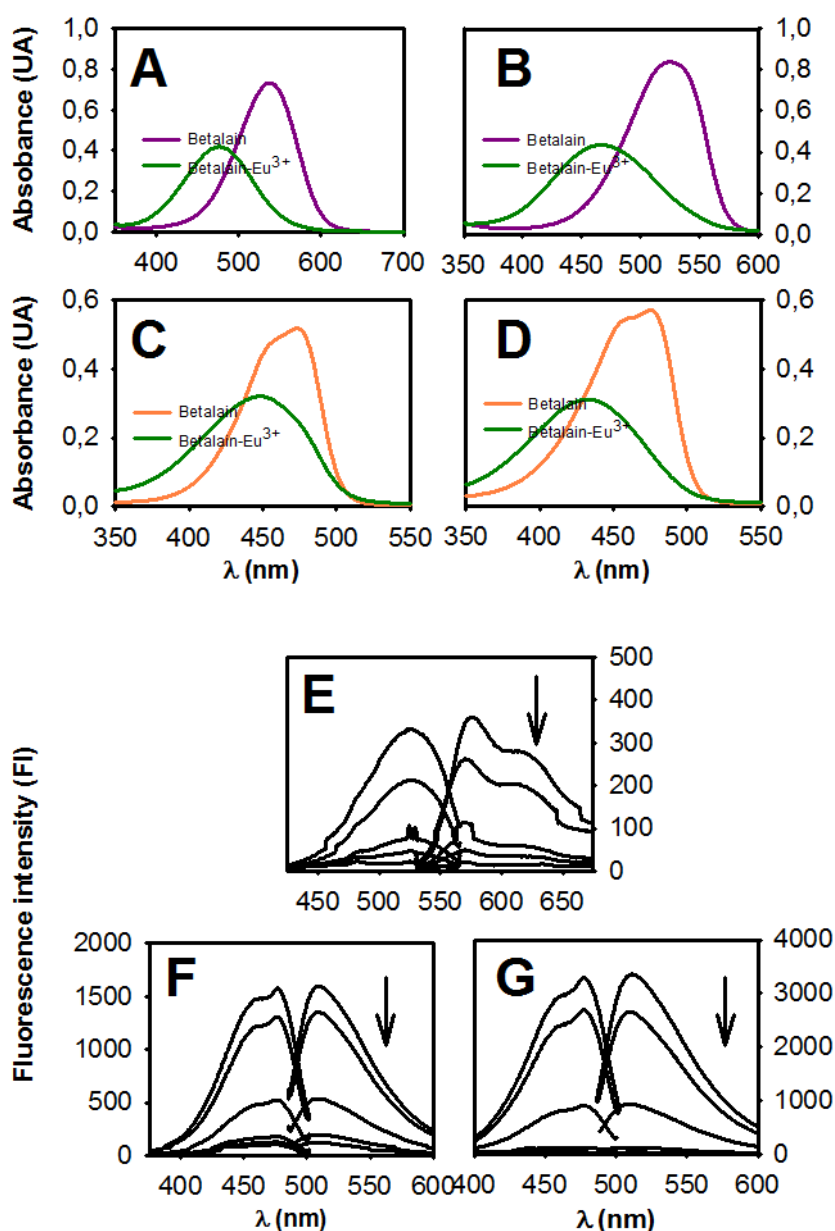


**Figure 7.2. Spectrophotometric changes of betalains in presence of  $\text{Eu}^{3+}$ .** Absorbance and fluorescence spectra of betanin (A), indoline-betacyanin (B and E), phenylethylamine-betaxanthin (C and F) and miraxanthin I (D and G), where the native absorbance of the molecule (purple line for betacyanins and orange for betaxanthins) is shown together with the absorbance spectrum of the complexes with  $\text{Eu}^{3+}$  (green line in all cases). Spectra were obtained at concentrations of 13  $\mu\text{M}$  of pigment in all cases and 39  $\mu\text{M}$  (A), 130  $\mu\text{M}$  (B), and 260  $\mu\text{M}$  (C and D) of europium. In the fluorescence figures, the highest spectrum represents the native fluorescence of the compound (without europium) while the following lines represent the spectra at increasing concentrations of europium (6, 12, 18, 18, 30  $\mu\text{M}$  (E); 12, 30, 60, 90  $\mu\text{M}$  (F); 18, 30, 45, 90  $\mu\text{M}$  (G)). Arrows indicate the order of increasing concentrations of europium and show how fluorescence intensity is lowered as the concentration of europium increases.

This indicates that complexed forms are not fluorescent at all and that the fluorescence values registered in the presence of europium were due solely to the presence of the remaining free betalain molecules. These effects were observed in concentration ranges varying from 0 to 130  $\mu\text{M}$   $\text{Eu}^{3+}$  in betacyanins and from 0 to 260  $\mu\text{M}$  in betaxanthins, for absorbance measurements, and 0-90  $\mu\text{M}$  in betaxanthins and 0-30  $\mu\text{M}$  in indoline-betacyanin for the analysis of fluorescence. In all cases, the lowest metal concentration necessary to produce the maximum spectral difference was obtained. That maximum spectral difference was used in a following step to optimize the sensitivity of an  $\text{Eu}^{3+}$  capture system. The absorbance variations obtained at the maximum wavelength of the betalain used as a function of  $\text{Eu}^{3+}$  concentration is shown in **Fig. 7.3**. Sigmoid-type curves were obtained, indicating that the relationship between europium and betalains is a process of complexation between metal and pigment, which acts as a binder. Through a non-linear regression to the experimental data shown it was possible to extract the corresponding formation constants of the complexes as shown in **Table 7.2**.

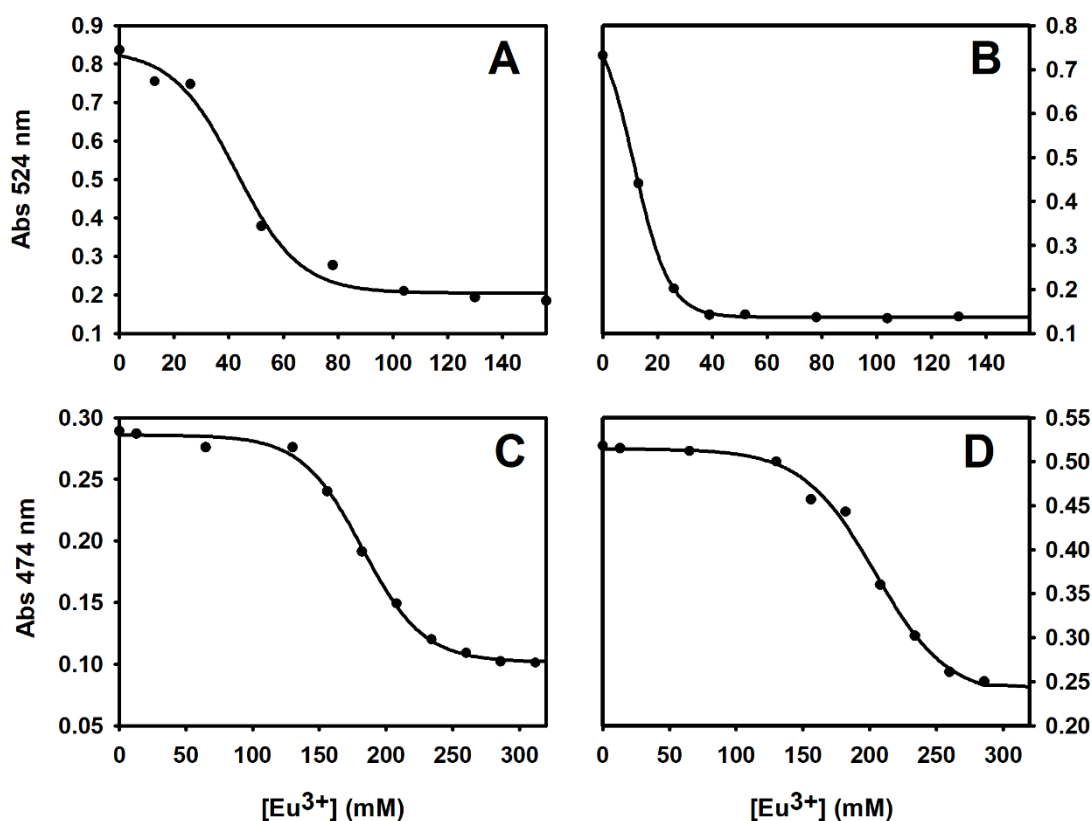


**Figure 7.3.** Change in the absorbance values of betalains due to the presence of  $\text{Eu}^{3+}$ . Changes observed in solution of indoline-betacyanin (A), betanin (B), miraxanthin I (C) and phenylethylamine-betaxanthin (D) at the maximum signal wavelength of the native betalain by adding increasing concentrations of europium to the medium.

**Table 7.2. Values of the association constants for the complexes with  $\text{Cu}^{2+}$  and  $\text{Eu}^{3+}$  for the different betalains studied.**

	Stability constant for $\text{Eu}^{3+}$ -complex ( $\text{L}\cdot\text{mol}^{-1}$ )	Stability constant for $\text{Cu}^{2+}$ -complex ( $\text{L}\cdot\text{mol}^{-1}$ )
Betanin	$1.2 \pm 0.3 \times 10^5$	$4.4 \pm 1.0 \times 10^6$
Indoline-betacyanin	$4.3 \pm 0.4 \times 10^5$	$7.5 \pm 0.8 \times 10^6$
Miraxanthin I	$1.8 \pm 0.2 \times 10^4$	$5.3 \pm 1.5 \times 10^6$
Phenylethylamine-betaxanthin	$2.0 \pm 0.4 \times 10^4$	$6.5 \pm 0.7 \times 10^6$

### 3. Effect of copper and iron on betalains

The presence of metal ions in the medium such as copper ( $\text{Cu}^{2+}$ ) or iron ( $\text{Fe}^{2+}$ ) has been described in the literature as one of the factors that favor the degradation of betalains (Herbach et al., 2006). The presence of these ions produces bleaching and changes in the spectrophotometric characteristics of solutions containing betalains, resulting in decreases in absorbance values. This reduction has, until now, been considered irreversible and a result of the pigment degradation process (Khan and Giridhar, 2014).

The addition of  $\text{Cu}^{2+}$  to the four related betalains in this study causes the alteration of the absorbance and fluorescence spectra. Copper was added in the range of 1.3  $\mu\text{M}$  to 52  $\mu\text{M}$  to solutions 13  $\mu\text{M}$  of betalains. We propose that the changes are due to complexation processes between the betalains and copper instead of to pigment degradation induced by the metals. In the case of the addition of iron, no immediate effect on the spectrophotometric properties was observed and the absorbance and fluorescence remained unchanged when  $\text{Fe}^{2+}$  was added to the medium in the range of 13  $\mu\text{M}$  to 130  $\mu\text{M}$ . As shown in **Table 7.3**, the maximum wavelengths varied, producing a hypsochromic displacement in absorbance after the addition of  $\text{Cu}^{2+}$ , except for phenylethylamine-betaxanthin which did not vary significantly. In all cases, bleaching was observed and the maximum absorbance value obtained was reduced when adding  $\text{Cu}^{2+}$ . As regards fluorescence, a pronounced decrease in the intensity of the measured fluorescence was observed. However, there was no displacement of the maximum emission or excitation wavelengths.

**Table 7.3. Variations in the maximum wavelengths ( $\lambda$ ) produced by the complexation of copper with the betalains under study.** The concentrations of betalains used were 13  $\mu$ M and 3  $\mu$ M for absorbance and fluorescence respectively and the  $\text{Cu}^{2+}$  concentrations used were 52  $\mu$ M for betanin, 39  $\mu$ M for indoline-betalain, 26  $\mu$ M for miraxanthin I and 39  $\mu$ M for phenylethylamine-betaxanthin.

	Absorbance		Fluorescence			
	$\lambda_{\text{max}}$ (control) (nm)	$\lambda_{\text{max}}$ ( $\text{Cu}^{2+}$ ) (nm)	$\lambda_{\text{max}}^{\text{emi}}$ (control) (nm)	$\lambda_{\text{max}}^{\text{emi}}$ ( $\text{Cu}^{2+}$ ) (nm)	$\lambda_{\text{max}}^{\text{exc}}$ (control) (nm)	$\lambda_{\text{max}}^{\text{exc}}$ ( $\text{Cu}^{2+}$ ) (nm)
Betanin	537	508	-	-	-	-
Indoline- Betacyanin	524	504	575	574	526	527
Miraxanthin I	474	450	511	511	478	477
Phenylethylamine- betaxanthin	474	473	510	511	477	477

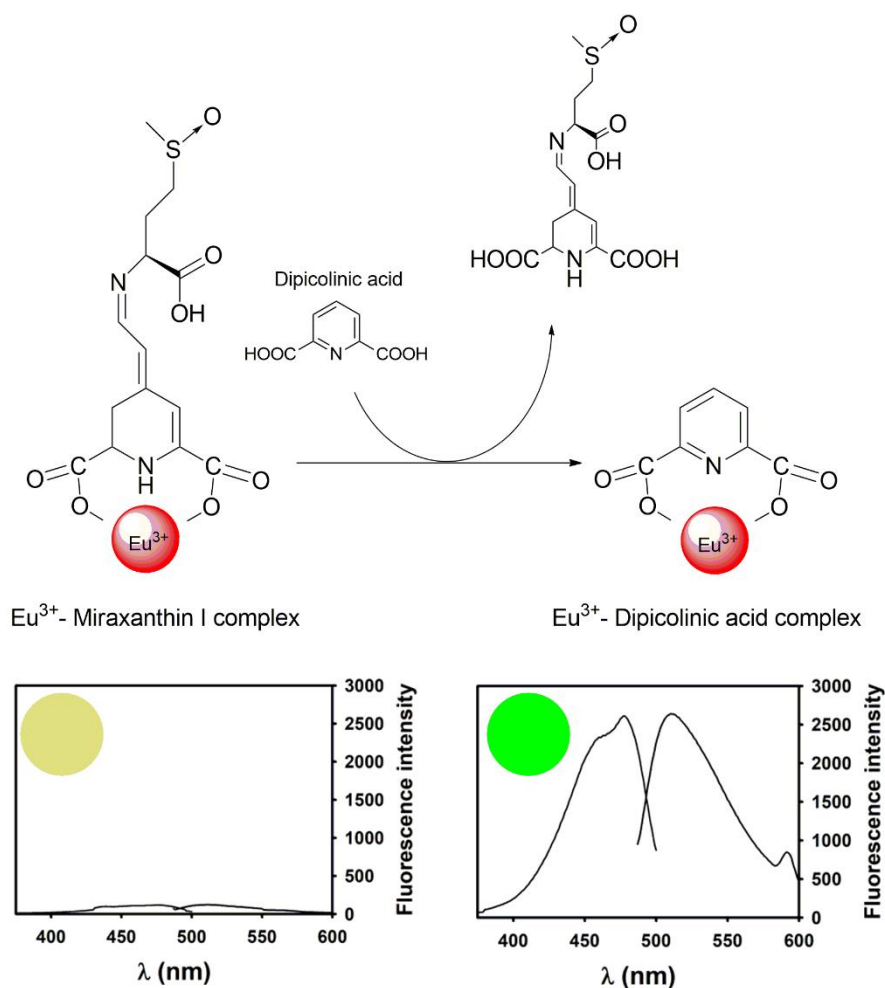
Stability constants were obtained by applying increasing concentrations of metal ion with respect to a fixed amount of betalain of 13  $\mu$ M. These constants are shown in **Table 7.2**. Thus, complexation of metals by betalains has been detected not only for betanin and  $\text{Eu}^{3+}$  but for model betacyanins and betaxanthins and different metals. The data obtained suggest that this is a general process in betalains which may involve the betalamic acid substructure where two carboxylic groups are available to chelate metals. Betalains are plant pigments present in flowers and thus a major biological function in plant signaling and pollinators attraction has been reported (Gandía-Herrero et al., 2005b; Iriel and Lagorio, 2010). However, their presence in roots is not understood. A possible role in sequestration and mobilization of metals in these structures can be proposed in relation to metal complexation. This would help in the intake of metals, as also happens for other known chelators of plant origin, such as some flavonoids (Korkina and Afanas'ev, 1996).



#### 4. Effect of $\text{Cu}^{2+}$ and $\text{Eu}^{3+}$ chelators

The immediacy of the spectral changes described and the constants determined suggested a possible competition of betalains with chelating substances of the metals involved. Among the compounds capable of chelating copper, tropolone was chosen because of its stability constant of  $1.2 \times 10^8 \text{ (L} \cdot \text{mol}^{-1})$  (Bryant et al., 1972), which is higher than that obtained for the complexes with betalains. The addition of tropolone to the medium was able to reverse the effect that the formation of the betalain-copper complex had on the spectral properties, with the initial conditions being recovered. This indicates a higher affinity of copper for tropolone than for the betalains and thus confirms the range of the constants determined in this work for the plant pigments. In the case of europium, dipicolinic acid (DPA) is a chelator able to compete with betalains for  $\text{Eu}^{3+}$  ions due to the high structural similarity between DPA and betalains (**Fig. 7.4**). The complex formed presents the following formula  $[\text{Eu}(\text{DPA})_n]^{3-2n}$ , with the stability constants  $k_1 = 6.92 \times 10^8 \text{ (L} \cdot \text{mol}^{-1})$  ( $n = 1$ ),  $k_2 = 1.38 \times 10^5 \text{ (L} \cdot \text{mol}^{-1})$  ( $n = 2$ ),  $k_3 = 3.23 \times 10^5 \text{ (L} \cdot \text{mol}^{-1})$  ( $n = 3$ ) (Grenthe, 1961) being higher than those determined for the complexes between  $\text{Eu}^{3+}$  and the four model betalains studied. It was observed how the addition of DPA displaces the complexes of betalains, releasing the pigment in its free state to the medium and thus recovering its color characteristics (results not shown) and original fluorescence (**Fig. 7.5**).

**A**



**B**

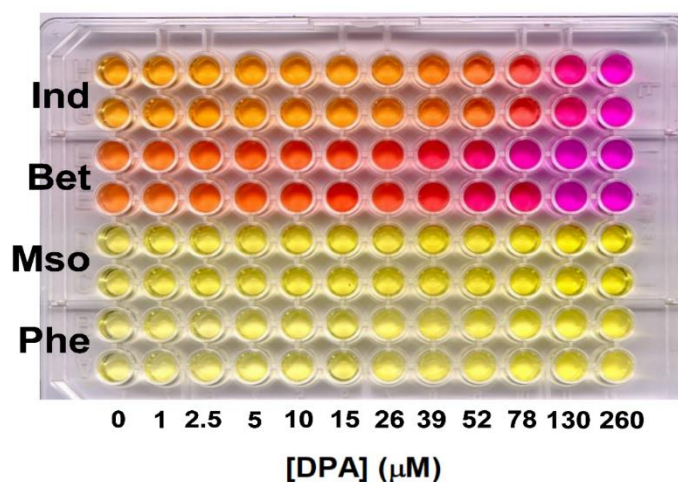


**Figure 7.4. Effects of dipicolinic acid on the betalain- $\text{Eu}^{3+}$  complex.** **A.** The scheme shows the structural similarity between betalains and dipicolinic acid. The dissociation of the  $\text{Eu}^{3+}$ -betalain complex allows the release of the betalain miraxanthin I, which results in the recovery of its fluorescent properties. **B.** A 96-well plate in which a dipicolinic acid concentration scan was performed for the  $\text{Eu}^{3+}$  complexes of the four betalains, in duplicate, from 0  $\mu\text{M}$  DPA to 260  $\mu\text{M}$ , from left to right.

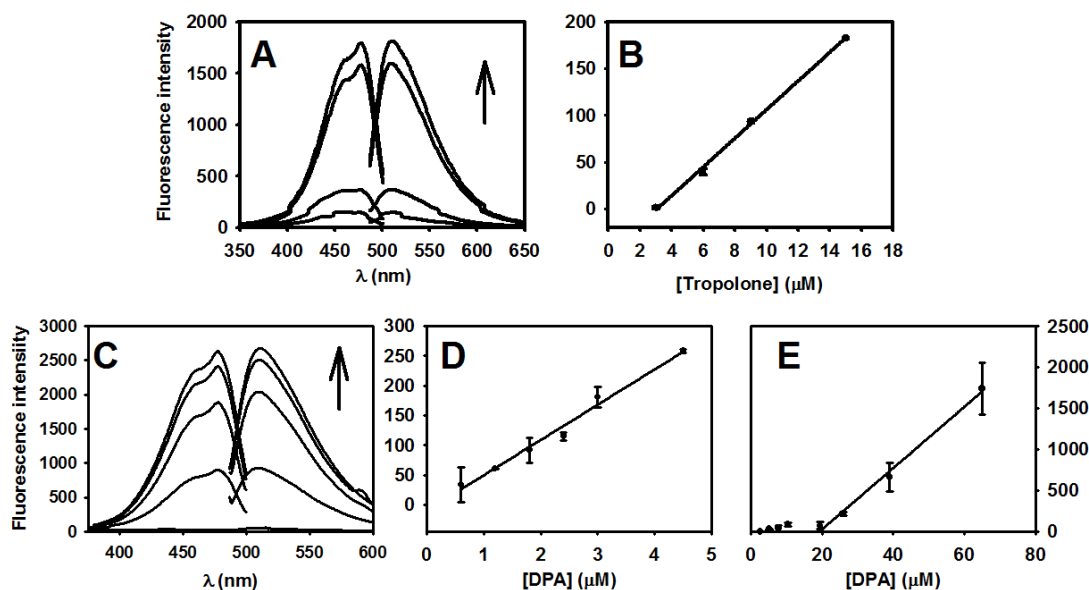


**Figure 7.5. Effect of chelating compounds on the betalain-metal complexes.** **A:** Effect of tropolone addition on the fluorescence of the  $\text{Cu}^{2+}$ -miraxanthin I 3  $\mu\text{M}$  complex, showing the partial recovery of the fluorescence thereof when adding increasing concentrations of tropolone between 0  $\mu\text{M}$  and 60  $\mu\text{M}$  (0, 6, 12, 30, 45, 60  $\mu\text{M}$ ), **B:** Calibration line of fluorescence recovery by adding increasing concentrations of tropolone to fixed concentrations of miraxanthin I (3  $\mu\text{M}$ ) and  $\text{Cu}^{2+}$  (9  $\mu\text{M}$ ). **C:** Effect of DPA addition on the fluorescence of the  $\text{Eu}^{3+}$ -miraxanthin I complex showing the fluorescence recovery of miraxanthin I by adding of increasing concentrations of dipicolinic acid to reach the initial value corresponding to free betaxanthin. The concentration of the betalain was 3  $\mu\text{M}$ , the europium concentration was 60  $\mu\text{M}$  and the DPA ranges from 0 to 90  $\mu\text{M}$  (0, 6, 18, 45, 90  $\mu\text{M}$ ). **D:** Calibration for the recovery of fluorescence with fixed concentrations of 3  $\mu\text{M}$  of miraxanthin I and 75  $\mu\text{M}$  of europium and variable concentration of DPA between 0.3 and 4.5  $\mu\text{M}$ . **E:** Calibration line obtained by measuring in the plate reader using fixed concentrations of 13  $\mu\text{M}$  of betaxanthin and 325  $\mu\text{M}$  of europium and variable concentration of DPA.

The recovery of absorbance and fluorescence was carried out in all cases taking a fixed europium concentration, which corresponded to the minimum concentration necessary to achieve the maximum reduction of the absorbance and fluorescence values. These concentrations in absorbance are 39  $\mu\text{M}$  for betanin, 130  $\mu\text{M}$  for indoline-betacyanin, and 260  $\mu\text{M}$  for both betaxanthins. In fluorescence the maximum effect was obtained starting at concentrations 75  $\mu\text{M}$  for the betaxanthins and 30  $\mu\text{M}$  for indoline-betacyanin. The DPA concentration was varied in the range from 0  $\mu\text{M}$  to 130  $\mu\text{M}$ .

## 5. Determination of dipicolinic acid

From the variations in the absorbance and fluorescence values of the betalain- $\text{Eu}^{3+}$  complexes in the presence of dipicolinic acid it was possible to obtain calibration curves where the increase in absorbance or fluorescence was related to the concentration of DPA (**Fig. 7.5**). From these calibration lines, the limits of detection (LOD) and quantification (LOQ) for dipicolinic acid were obtained using the variations on color and fluorescence of the complexes of the four pigments (**Table 7.4**). In absorbance, betanin presented the lowest LOD and LOQ in the measurement systems used with values of 1.6  $\mu\text{M}$  and 9.1  $\mu\text{M}$ , respectively. As regards fluorescence, miraxanthin I, the most fluorescent betalain (Gandía-Herrero et al., 2005a), presented the lowest LOD and LOQ with 1.0  $\mu\text{M}$  and 2.9  $\mu\text{M}$ , respectively. These data improve on the limits of detection and quantification of dipicolinic acid previously described in the literature (Gonçalves et al., 2013; Lin and Zhigang, 2018; Shi et al., 2018) and are a consequence of the extraordinary fluorescence exhibited by this betalain.

**Table 7.4. Detection (LOD) and quantification (LOQ) limits of dipicolinic acid obtained for the four betalains studied in absorbance and fluorescence.** The values obtained in parallel plate reader tests are also shown.

	Absorbance		Absorbance reader		Fluorescence		Fluorescence reader	
	LOD ( $\mu\text{M}$ )	LOQ ( $\mu\text{M}$ )	LOD ( $\mu\text{M}$ )	LOQ ( $\mu\text{M}$ )	LOD ( $\mu\text{M}$ )	LOQ ( $\mu\text{M}$ )	LOD ( $\mu\text{M}$ )	LOQ ( $\mu\text{M}$ )
Betanin	1.6	9.1	16.0	23.3	-	-	-	-
Indoline-betacyanin	6.3	20.7	34.6	49.8	2.9	9.6	33.2	52.7
Miraxanthin I	4.1	16.1	65.3	94.3	1.0	2.9	32.4	62.5
Phenylethylamine-betaxanthin	2.5	10.4	45.3	64.6	1.3	4.3	16.5	55.1

The proposed interaction mode of miraxanthin I with  $\text{Eu}^{3+}$  shown in **Fig. 7.4A** was confirmed by the synthesis and analysis of tailor-made structurally related betalains, synthetic analogs of miraxanthin I.  $\text{Eu}^{3+}$  may have the potential to interact with the methionine sulphoxide specific groups of the betalain. Thus, the characteristic sub-structures present in the most fluorescent betaxanthin used to detect dipicolinic acid were removed in novel compounds designed to explore the role of the sulfinyl

functional group (SO), the Sulphur heteroatom, and the additional carboxylic group in the complexation of  $\text{Eu}^{3+}$ . If any of these functional groups takes part in the complexation of Europium by miraxanthin I, and not the dipicolinic acid-like substructure (**Fig. 7.4A**), a reduction of the complexation capacity should be observed in the novel molecules. In order to study this, the tailor-made betalains synthesized were exposed to  $260\ \mu\text{M}\ \text{Eu}^{3+}$ , the minimum concentration needed to obtain a full spectral change by metal complexation in miraxanthin I as seen in **Fig. 7.3**.

All the betalains showed identical spectral properties in the absence of Europium and spectral changes were identical in its presence, regardless the presence or absence of the selected functional groups (**Fig. 7.6**). This reveals that the formation of the complex was analogous in miraxanthin I and in the structurally related compounds and strongly suggests that the complexation process is independent on the presence of the carboxyl and the sulfinyl groups and on the presence of the Sulphur heteroatom (**Fig. 7.6M**). This was observed not only for absorbance, but also for fluorescence, where analogous reductions of fluorescence were observed upon  $\text{Eu}^{3+}$ -complexes formation (**Fig. 7.6**), exactly as seen for miraxanthin I. The identity of the novel molecules synthesized was corroborated by Q-TOF mass spectrometry and exact mass determination as shown in **Fig. 7.6**.

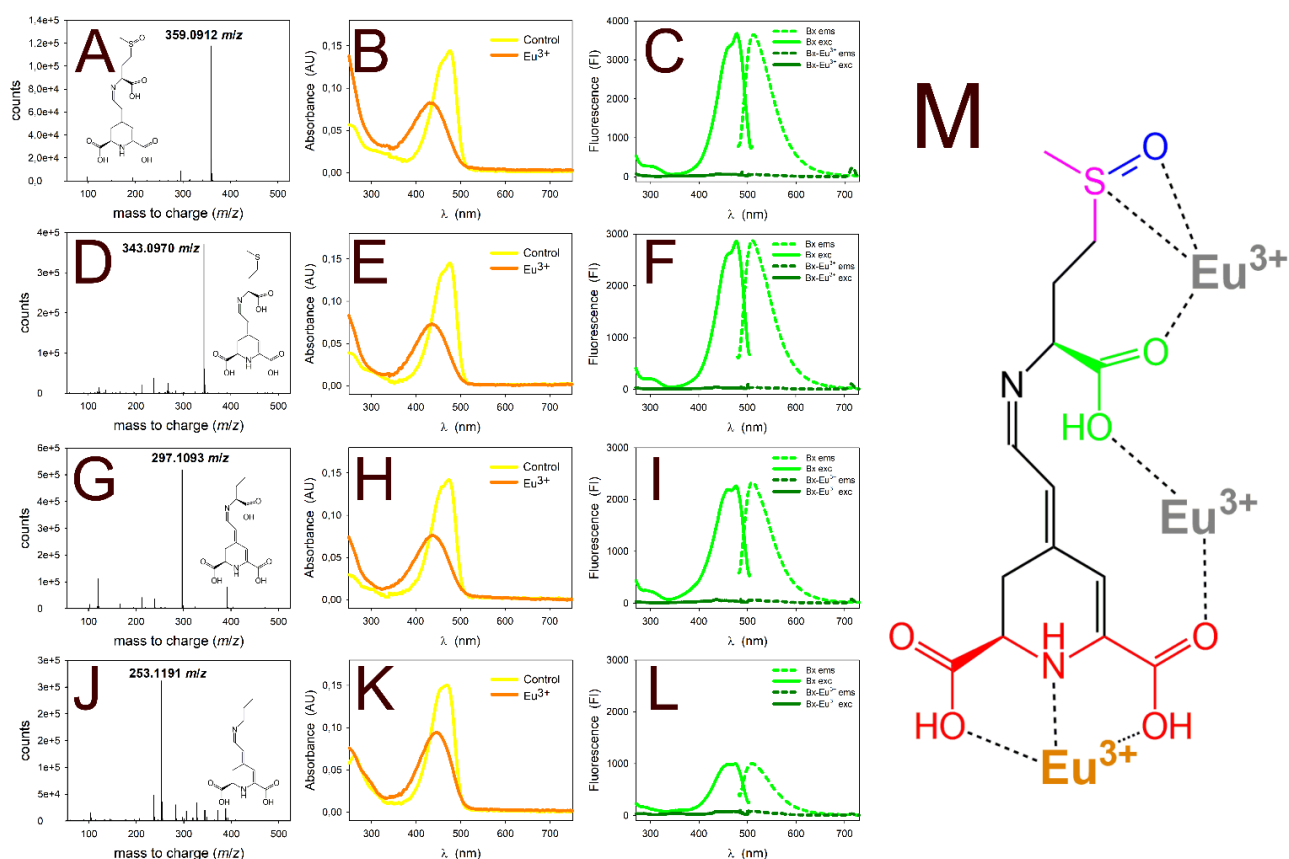


**Figure 7.6.** Effects of  $\text{Eu}^{3+}$  on tailor-made betalains synthesized to explore the role of sulfinyl functional group (SO), the sulphur heteroatom, and the additional carboxylic group in the complexation of  $\text{Eu}^{3+}$  by miraxanthin I. Left: Q-TOF mass analysis and exact mass is shown in A, D, G and J for the chemical structures shown inset. Center: Effect of the presence of  $\text{Eu}^{3+}$  (260  $\mu\text{M}$ ) in the absorbance spectra of the molecules miraxanthin I (B), miraxanthin I derived betalain without sulfinyl group (E), miraxanthin I derived betalain without sulfinyl and Sulphur (H), and miraxanthin I derived betalain without sulfinyl, Sulphur and carboxylic acid (K). Right: Effect of  $\text{Eu}^{3+}$  (260  $\mu\text{M}$ ) in the fluorescence spectra of the same molecules miraxanthin I (C), miraxanthin I derived betalain without sulfinyl group (F), miraxanthin I derived betalain without sulfinyl and Sulphur (I), and miraxanthin I derived betalain without sulfinyl, Sulphur and carboxylic acid (L). M: Structural scheme for the interactions analyzed, showing in blue the possible contribution of the sulfinyl group, in magenta the possible role of Sulphur, and in green the possible effect of the carboxylic group of the methionine part of the molecule miraxanthin I. According to the spectral changes observed in fluorescence and absorbance for the molecules designed none of these groups contribute to the complexation of  $\text{Eu}^{3+}$  (shown in grey). Only the common part to all betalains, shown in red and structural analog to dipicolinic acid, is able to interact with  $\text{Eu}^{3+}$  (shown in orange), being responsible of spectral changes and complexation in all the betalains.

In an approach to the realization of automated and massive measurements (high throughput), the conditions used to detect dipicolinic acid were transferred to a plate reader in both absorbance and fluorescence. Intensity changes and limits of detection and quantification were recalculated. The limits obtained in the plate reader were an order of magnitude higher (Table 7.4) than those obtained in the conventional

spectrophotometer and fluorimeter. This is due to the specific detection equipment and the filter system, which avoids the selection of wavelengths for optimum detection of each betalain, thus, reducing sensitivity. Although the limits obtained in the plate reader were higher than those obtained in conventional spectrophotometer and fluorimeter, the use of a high throughput screening equipment would allow the application of the technique to a greater number of samples. In any case, the detection limits obtained both for conventional and high throughput techniques are very relevant compared with the infective dose of the spores of the most pathogenic *Bacillus* species described, used in bioterrorist attacks, *Bacillus anthracis* (Spencer, 2003), which is described in 60  $\mu\text{M}$  of DPA (Oh et al., 2011).

## 6. Obtaining of spores from *Bacillus*

Dipicolinic acid is the most representative chemical compound inside endospores of some gram-positive bacteria such as *Bacillus* or *Clostridium*. The development of calibration curves for the concentration of DPA results in a system for the quantification of spores because DPA is not present in vegetative cells. In this work, the species *B. subtilis* (**Fig. 7.7E**) and *B. halodurans* (**Fig. 7.7F**) were used to produce spores. These species were chosen for feasibility of their manipulation but they can be considered as models of other *Bacillus* species capable of producing toxic endospores, such as *B. anthracis* (Spencer, 2003), which is used as the infectious agent anthrax in bioterrorist attacks. After the development of the cultures and the concentration of the spores, the quantification of the same isolates was performed with the MPN technique, resulting in a concentration of  $2.4 \times 10^7$  spores $\cdot\text{mL}^{-1}$  for *B. subtilis*, and  $1.6 \times 10^6$  spores $\cdot\text{mL}^{-1}$  for *B. halodurans*.

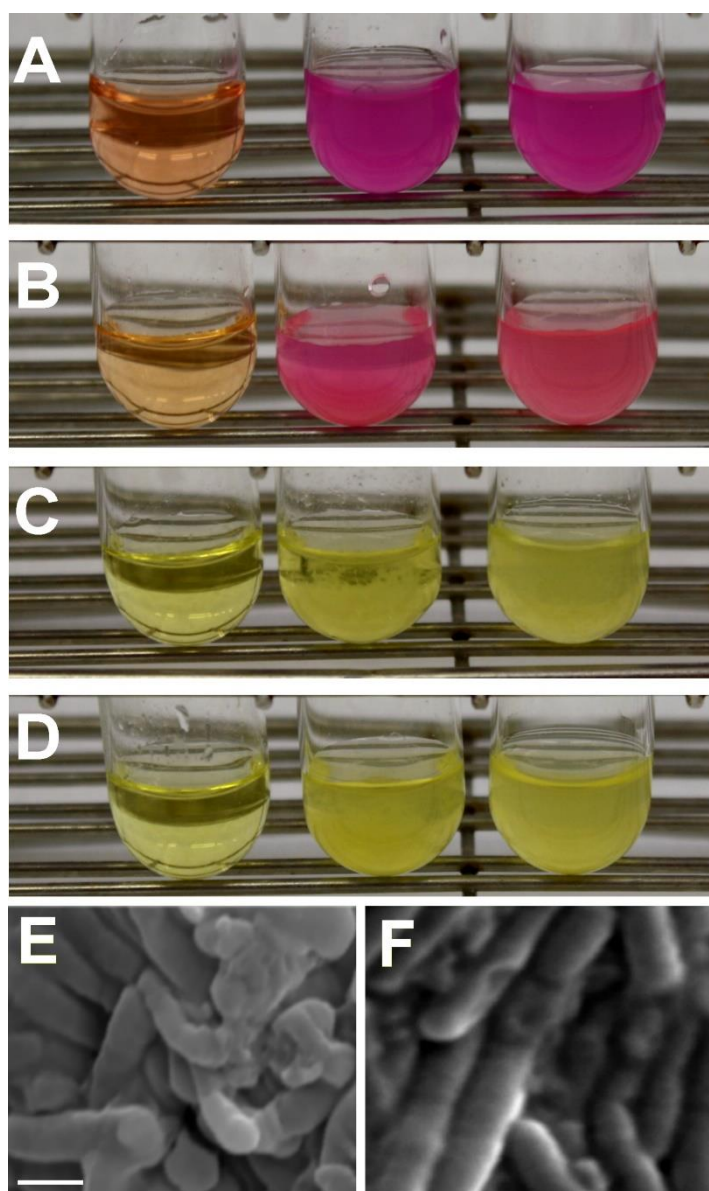


**Figure 7.7. Spores from *Bacillus*.** A-D: Qualitative measurements of the effect of the spores of *B. halodurans* (center) and *B. subtilis* (right) with respect to the betalain-europium complex (left) for betanin (A), indoline-betalain (B), phenylethylamine-betaxanthin (C) and miraxanthin I (D). E: *Bacillus subtilis* spores visualized by scanning electron microscopy. F: *Bacillus halodurans* spores visualized by scanning electron microscopy. Scale bar: 1µm.

## 7. Detection of *Bacillus* spores

The detection of dipicolinic acid was carried out with raw spores as obtained above and with spores that had been subjected to heat treatment. This process is described in the literature as being of use for the release of DPA from the spores. Both untreated and treated spores produced a strong signal detected in the presence of all the complexes of the betalains with europium. As shown in **Table 7.5**, betalains with better



LOD for the detection of *Bacillus* spores were the betaxanthins phenylethylamine-betaxanthin and miraxanthin I, which allow a more sensitive detection. In our assays the thermal treatment of the spores did not represent an improvement in the sensitivity of the detection, possibly due to the degradation of dipicolinic acid, after its release from the spores (Gonçalves et al., 2013). Dipicolinic acid detected was 95.7  $\mu\text{M}$  and 6.4  $\mu\text{M}$  for *B. subtilis* and *B. halodurans* spores' samples respectively.

**Table 7.5. Detection limits (LOD) obtained for *Bacillus* spores according to the betalain and the measurement method used.**

	LOD <sub>Abs</sub> (spores/mL)	LOD <sub>Abs</sub> (autoclaved) (spores/mL)	LOD <sub>Fluor</sub> (spores/mL)	LOD <sub>Fluor</sub> (autoclaved) (spores/mL)
Betanin	146,000	250,000	-	-
Indoline-betacyanin	137,000	273,000	149,000	183,000
Miraxanthin I	20,000	31,000	41,000	50,000
Phenylethylamine- betaxanthin	11,000	84,000	44,000	90,000

The presence of dipicolinic acid was validated with an alternative method based on the chromatographic separation of the acid (Fichtel et al., 2008). It was detected by UV absorbance at  $\lambda = 198$  nm, where absorbance is maximum, and its nature confirmed under analogous conditions with Q-TOF mass spectrometry (Supplementary Materials and Methods). Same retention time at 5.4 min was obtained for samples and standard. Accurate mass detection of dipicolinic acid yielded the value 168.0285  $m/z$ . This value implies a variation of 3.7 ppm respect to the calculated exact mass (168.0291  $m/z$ ), and it is well below the accepted accuracy threshold for elemental composition analysis, established at 5 ppm (Ferrer and Thurman, 2003), thus confirming the presence and nature of the acid detected in all samples. **Fig. 7.8** shows a UV-vis spectrum of dipicolinic acid together with a representative chromatogram.

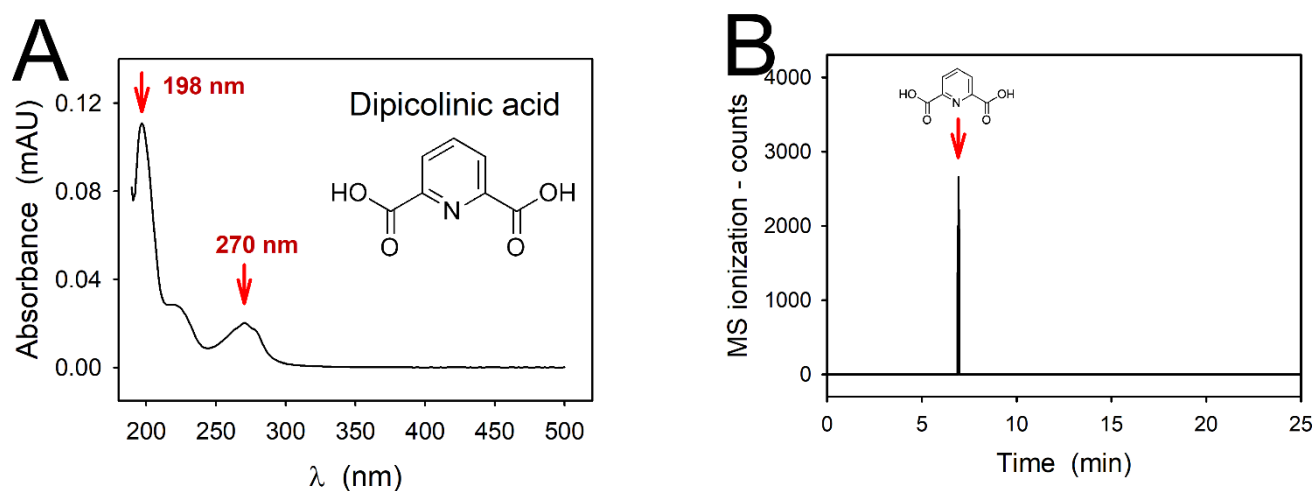


**Figure 7.8. Characteristics of dipicolinic acid.** **A:** UV-vis spectrum for dipicolinic acid. Inset: Structure of the molecule. **B:** Representative chromatogram for ESI-EIC for the detection of dipicolinic acid at 168.0291  $m/z$ .

**Fig. 7.7** shows the qualitative effect of the addition of *Bacillus* spores to the betalain- $\text{Eu}^{3+}$  complexes, proposed to be used in the rapid detection of the possible presence of *Bacillus* spores. The addition of spores provoked the dissociation of the complex with the pigment, due to the association of  $\text{Eu}^{3+}$  and dipicolinic acid, the consequent release of the betalains, and the recovery of their characteristic colors.

Exactly the same spectral changes in fluorescence and absorbance of betalains were observed after the addition of spores than for the presence of pure dipicolinic acid. This strongly suggests that the described complexes between  $\text{Eu}^{3+}$  and dipicolinic acid naturally present in the spores are competing with the complex between the metal and the betalains, and thus are the responsible of the recovery of color and fluorescence. Both signals are specific and dose-dependent. In order to further confirm that the recovered color and fluorescence was caused by the sole interaction with dipicolinic acid, rather than with interferences in the spores, the other major components of spores were studied in interference assays. In addition to dipicolinic acid, spores contain a protein fraction and small molecules as hexose and hexosamine (Warth et al., 1963). This way, albumin, glucose, and glucosamine were used as model protein, hexose and hexosamine in interference assays performed in order to test the robustness of the assay. The complex  $\text{Eu}^{3+}$ -miraxanthin I proved to be resistant to the presence of added glucose and glucosamine at concentrations three orders of magnitude higher than that used for the betaxanthin (3mM). In both cases, absorbance and fluorescence were not recovered

by the addition of the hexose and the hexosamine (**Fig. 7.9**), thus indicating that the miraxanthin I pigment was not released. This demonstrates the permanence of the complex, with its characteristic absorbance spectrum and negligible fluorescence (**Fig. 7.9**). The addition of protein neither promoted the release of miraxanthin I, and the only remarkable change observed was a limited turbidity in the cell, as seen in **Fig. 7.9A**, but the original absorbance and fluorescence spectra of miraxanthin I were not recovered (**Fig. 7.9**). Thus, the presence of protein and the hexose and hexosamine tested in great excess did not interfere. They are unable to compete with the betaxanthin for  $\text{Eu}^{3+}$  and thus they were not able to recover the fluorescence, as done by dipicolinic acid.

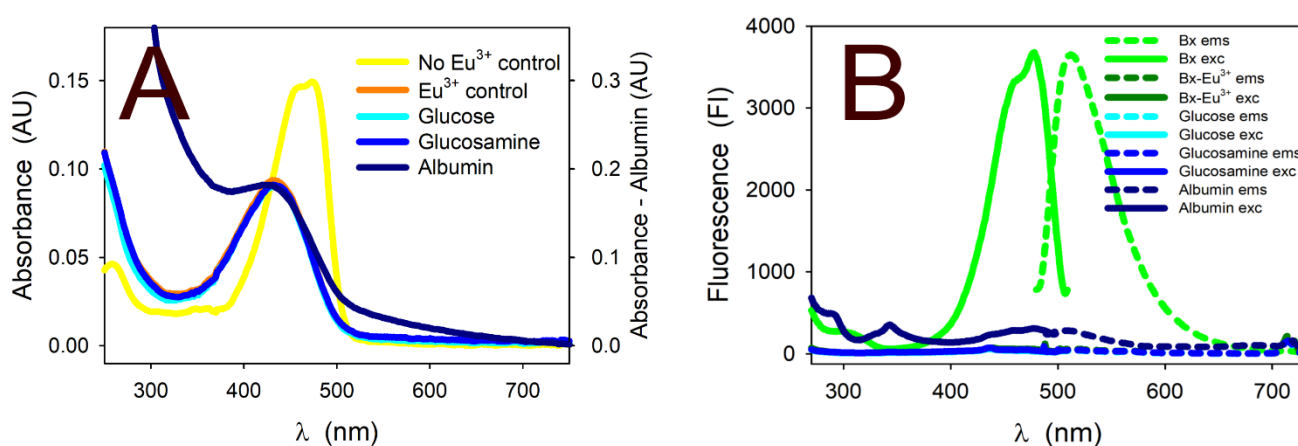


**Figure 7.9. Effect of the addition of albumin, glucose, and glucosamine as models of proteins, hexoses and hexosamines in interference assays to the complex  $\text{Eu}^{3+}$ -miraxanthin I.** The assays were performed in order to follow spectral changes in absorbance (**A**) and fluorescence (**B**) recordings. Glucose and glucosamine were added at concentrations three orders of magnitude higher than that used for the betaxanthin (3mM) and albumin at a final concentration 1.2 mg/mL. None of the molecules added interfered in the interaction between  $\text{Eu}^{3+}$  and miraxanthin I, maintaining the spectral properties of the formed complex  $\text{Eu}^{3+}$ -miraxanthin I.

The described assay can be used for a rapid test in the detection of bioterrorist attacks with spores of *B. anthracis* (anthrax). In this case, if another compound which can form complex with miraxanthin I more stable than  $\text{Eu}^{3+}$  is maliciously added into a real sample containing no anthrax, in fake attacks, the pigment will probably lose the fluorescence but this will never be recovered, avoiding a false alarm. This can be considered a double check analysis, since fluorescence of the flower pigment is lost by specific complexation and then recovered by specific competence. Furthermore, if

another metal ion which can form complex with miraxanthin I is maliciously added into a real sample containing anthrax, the recovery of fluorescence will depend on the relative strength of the complex between the metal and the flower pigment and that formed by the metal and dipicolinic acid. Due to close similarities in the substructures responsible for metal complexation in the betaxanthin and in dipicolinic acid, it is likely that the competence phenomenon will exist for any active metal with total or partial recovery of fluorescence upon addition of spores' samples. Although it is likely that the present work will promote research in this field, currently there is no other metal reported in the bibliography able to give the effects here described.

## 8. Conclusions

The interaction between betalains and metals such as  $\text{Cu}^{2+}$  and  $\text{Eu}^{3+}$  is general and due to complexation processes that involve significant changes in absorbance and fluorescence both for betacyanins and betaxanthin. These changes are reversible. Beyond the possible physiological implications of the phenomenon in metal sequestration and mobilization inside the plant, the nature of the interactions described allows the modulation of the color and fluorescence of the complexes. These properties depend on the presence of the metal and on the presence of agents that may combine with the metals, such as dipicolinic acid. The competition of dipicolinic acid with the betalains to form  $\text{Eu}^{3+}$ -betalain complexes means it can be used as a sensitive, rapid and simple method to detect the presence of dipicolinic acid and, therefore, of endospores from harmless or health-threatening species, such as *B. anthracis*. The developed method allows the detection of endospores below infective levels, and therefore it is a tool to detect false alarms and fake attacks quickly.

## REFERENCES

- Bryant, B.E., Fernelius, W.C., Douglas, B.E., 1972. Formation constants of metal complexes of tropolone and its derivatives. I. Tropolone. *Acta Chem. Scand.* <https://doi.org/10.3891/acta.chem.scand.02-0297>
- Castellanos-Santiago, E., Yahia, E.M., 2008. Identification and quantification of betalains from the fruits of 10 Mexican prickly pear cultivars by high-performance liquid chromatography and electrospray ionization mass spectrometry. *J. Agric. Food Chem.* 56, 5758–5764. <https://doi.org/10.1021/jf800362t>
- Ferrer, I., Thurman, E.M., 2003. Liquid chromatography/time-of-flight/mass spectrometry (LC/TOF/MS) for the analysis of emerging contaminants. *TrAC - Trends Anal. Chem.* 22, 750–756. [https://doi.org/10.1016/S0165-9936\(03\)01013-6](https://doi.org/10.1016/S0165-9936(03)01013-6)
- Fichtel, J., Sass, H., Rullkötter, J., 2008. Assessment of spore contamination in pepper by determination of dipicolinic acid with a highly sensitive HPLC approach. *Food Control* 19, 1006–1010. <https://doi.org/10.1016/J.FOODCONT.2007.09.006>
- Gandía-Herrero, F., García-Carmona, F., Escribano, J., 2005a. A novel method using high-performance liquid chromatography with fluorescence detection for the determination of betaxanthins. *J. Chromatogr. A* 1078, 83–89. <https://doi.org/10.1016/j.chroma.2005.05.013>
- Gandía-Herrero, F., García-Carmona, F., Escribano, J., 2005b. Floral fluorescence effect. *Nature* 437, 334. <https://doi.org/10.1038/437334a>
- Gliszczyńska-Świgło, A., Szymusiak, H., Malinowska, P., 2006. Betanin, the main pigment of red beet: Molecular origin of its exceptionally high free radical-scavenging activity. *Food Addit. Contam.* 23, 1079–1087. <https://doi.org/10.1080/02652030600986032>
- Gonçalves, L.C.P., Da Silva, S.M., DeRose, P.C., Ando, R.A., Bastos, E.L., 2013. Beetroot-pigment-derived colorimetric sensor for detection of calcium dipicolinate in bacterial spores. *PLoS One* 8, 1–6. <https://doi.org/10.1371/journal.pone.0073701>
- Grenthe, I., 1961. Stability relationships among the rare earth dipicolinates. *J. Am. Chem. Soc.* 83, 360–364. <https://doi.org/10.1021/ja01463a024>
- Herbach, K.M., Stintzing, F.C., Carle, R., 2006. Betalain stability and degradation -

- structural and chromatic aspects. J. Food Sci. <https://doi.org/10.1111/j.1750-3841.2006.00022.x>
- Iriel, A., Lagorio, M.G., 2010. Is the flower fluorescence relevant in biocommunication? *Naturwissenschaften* 97, 915–924. <https://doi.org/10.1007/s00114-010-0709-4>
- Khan, M.I., Giridhar, P., 2014. Enhanced chemical stability, chromatic properties and regeneration of betalains in *Rivina humilis* L. berry juice. *LWT - Food Sci. Technol.* 58, 649–657. <https://doi.org/10.1016/j.lwt.2014.03.027>
- Lin, C., Zhigang, F., 2018. Modifying luminescent metal-organic frameworks with rhodamine dye: aiming at the optical sensing of anthrax biomarker dipicolinic acid. *Inorganica Chim. Acta* 477, 51–58. <https://doi.org/10.1016/j.ica.2018.02.032>
- Korkina, Ludmila G. and Afanas'ev, Igor B., 1996. Antioxidant and chelating properties of flavonoids. *Advances Pharmacol.* 38, 151–163. [https://doi.org/10.1016/S1054-3589\(08\)60983-7](https://doi.org/10.1016/S1054-3589(08)60983-7)
- Oh, W.K., Jeong, Y.S., Song, J., Jang, J., 2011. Fluorescent europium-modified polymer nanoparticles for rapid and sensitive anthrax sensors. *Biosens. Bioelectron.* 29, 172–177. <https://doi.org/10.1016/j.bios.2011.08.013>
- Piattelli, M., Minale, L., Nicolaus, R.A., 1965. Pigments of centrospermae-V: Betaxanthins from *Mirabilis jalapa* L. *Phytochemistry* 4, 817–823.
- Schnepf, E., Crickmore, N., Van Rie, J., Lereclus, D., Baum, J., Feitelson, J., Zeigler, D.R., Dean, D.H., 1998. *Bacillus thuringiensis* and its pesticidal crystal proteins. *Microbiol. Mol. Biol. Rev.* 62, 775–806. <https://doi.org/10.1092-2172>
- Setlow, P., 2000. Resistance of bacterial spores. *Bact. Stress responses* 217–230. <https://doi.org/10.1128/9781555816841.ch18>
- Shi, K., Yang, Z., Dong, L., Yu, B., 2018. Dual channel detection for anthrax biomarker dipicolinic acid: The combination of an emission turn on probe and luminescent metal-organic frameworks. *Sensors Actuators, B Chem.* 266, 263–269. <https://doi.org/10.1016/j.snb.2018.03.128>
- Spencer, R.C., 2003. *Bacillus anthracis*. *J. Clin. Pathol.* <https://doi.org/10.1136/jcp.56.3.182>
- Warth, A.D., Ohye, D.F., Murrell, W.G., 1963. The composition and structure of bacterial spores. *J. Cell Biol.* 16, 579–592. <https://doi.org/10.1083/jcb.16.3.579>



**Chapter VIII.** Obtention of a novel polymeric chitosan-betaxanthin  
and characterization of the first sugar-derived betalains





### **Contextualization**

The new biotechnological obtention of betalains described in chapter VI opens up the possibility to produce not only higher amounts of known betaxanthins but also new betaxanthins in a simple and reliable way thanks to the ability of betalamic acid to condense with amine groups. One of the most important sugar polymers, chitosan, presents -NH<sub>2</sub> groups susceptible to produce this reaction.

Chitosan is a cationic compound obtained by the deacetylation of chitin, a polysaccharide biopolymer produced by organisms such as crabs and shrimps. Thanks to its biocompatible and biodegradable nature, chitosan is widely used with medical purposes in encapsulating materials (Cheng et al., 2017; Hao et al., 2017), to create artificial skin (Dhandayuthapani et al., 2010) or dental implants (Bumgardner et al., 2003), or in antibacterial biofilms (Sano et al., 2001).

In this chapter a new polymer that may combine the properties of chitosan and betalains is proposed for the first time.

## **1. Obtention of a polymeric derivative of betalains**

Chitosan is the result of the deacetylation of chitin in the C<sub>2</sub> position of the side chain. Chitin is the second most important polymer in nature, after cellulose. Chitin is a polymer composed by *n* repetitions of N-acetylglucosamine which can experiment deacetylation in different grades. Thus, it is possible to obtain mixtures of N-acetylglucosamine and its deacetylated derivate, glucosamine, or a complete deacetylated polymer. In order to explore the different reactivity of both compounds, chitin and pure chitosan, defined as a completely deacetylated chitin, were employed for the first biotechnological obtention of carbohydrate derived betalains. 38 mM of chitin or chitosan were added to microbial bioreactors of *E. coli* harboring the vector (pET28a-GdDODA) culture in order to produce betalamic acid in the presence of the polymers to yield Schiff condensation reactions between the acid and the available amine groups.

Bioreactors with chitin or chitosan yield a yellow coloration in the medium with aggregated particles from these polymers. Cultures were then centrifuged and supernatants were analyzed by HPLC. Analysis showed how the yellow coloration of the liquid medium was due to a single peak detected at  $\lambda = 480$  nm with a retention time (RT) of 13.91 min. Co-elution with pure standards showed that this peak belonged to

the pigment dopaxanthin. As it is indicated in the chapter VI, dopaxanthin was present in the reaction media as a result of the condensation of betalamic acid with L-DOPA which, at the same time, is the precursor of betalamic acid production. However, the presence of dopaxanthin in chitin was an order of magnitude higher than that obtained in the medium with chitosan (**Fig. 8.1**). This indicates that the betalamic acid produced in the medium supplemented with chitosan did not condense with L-DOPA to yield dopaxanthin but it condensed with the free amine groups present in the side chain of chitosan. This yielded in a new polymeric derivative of betalains, tentatively named chitosan-betaxanthin.

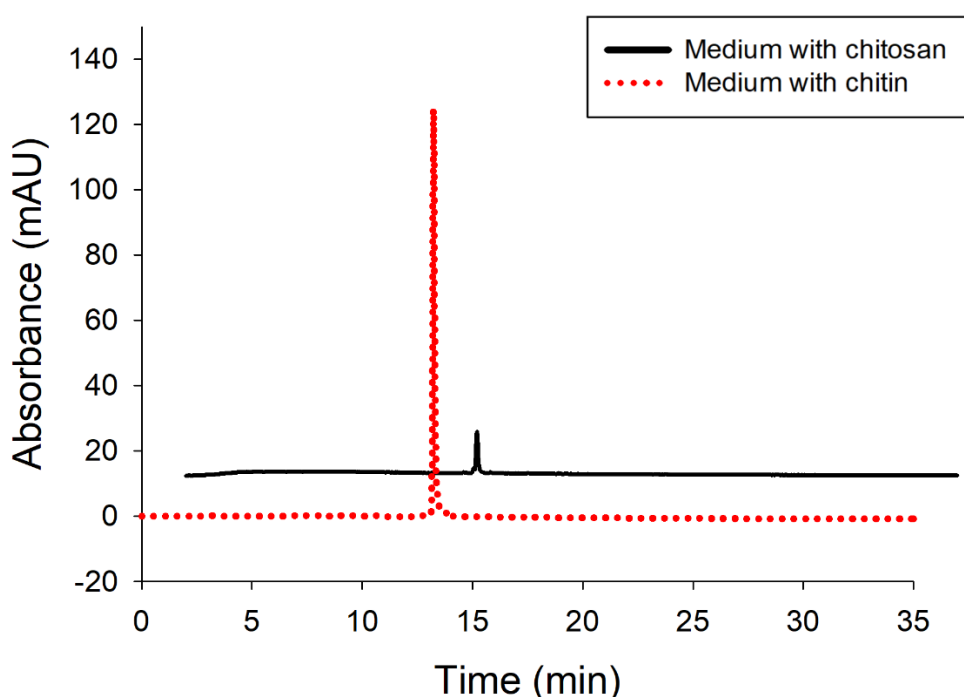


**Figure 8.1. HPLC analysis of the supernatants of *E. coli* (pET28a-GdDODA) cultures supplemented with chitin or chitosan.** Chromatograms at  $\lambda=480$  nm showed the higher detection of dopaxanthin in the medium supplemented with chitin (dotted red line) respect to the dopaxanthin present in the medium supplemented with chitosan (continuous line).

The precipitate of the reaction medium contained the novel polymer that showed an insoluble nature and a deep yellow color. In the case of chitin, N-acetylglucosamine was not viable to produce the condensation, and the polymer obtained did not differ of the starting material.

## 2. Absorbance properties of the polymeric chitosan-betaxanthin

The yellow particles obtained in the *E. coli* (pET28a-GdDODA) culture supplemented with L-DOPA and chitosan were washed 5 times with water to discard the presence of dopaxanthin. Absorbance properties of the new polymer were characterized thanks to an integrating sphere, which allows to measure the absorbance spectrum of solid substances. In addition, the absorbance spectrum of chitosan's particles was measured and used as control. The values obtained for chitosan (**Fig. 8.2A**) were subtracted to those obtained for the new polymer (**Fig. 8.2B**) and a spectrum with a maximum absorbance at  $\lambda = 471$  nm was obtained as the result of the condensation of chitosan with betalamic acid (**Fig. 8.2C**).

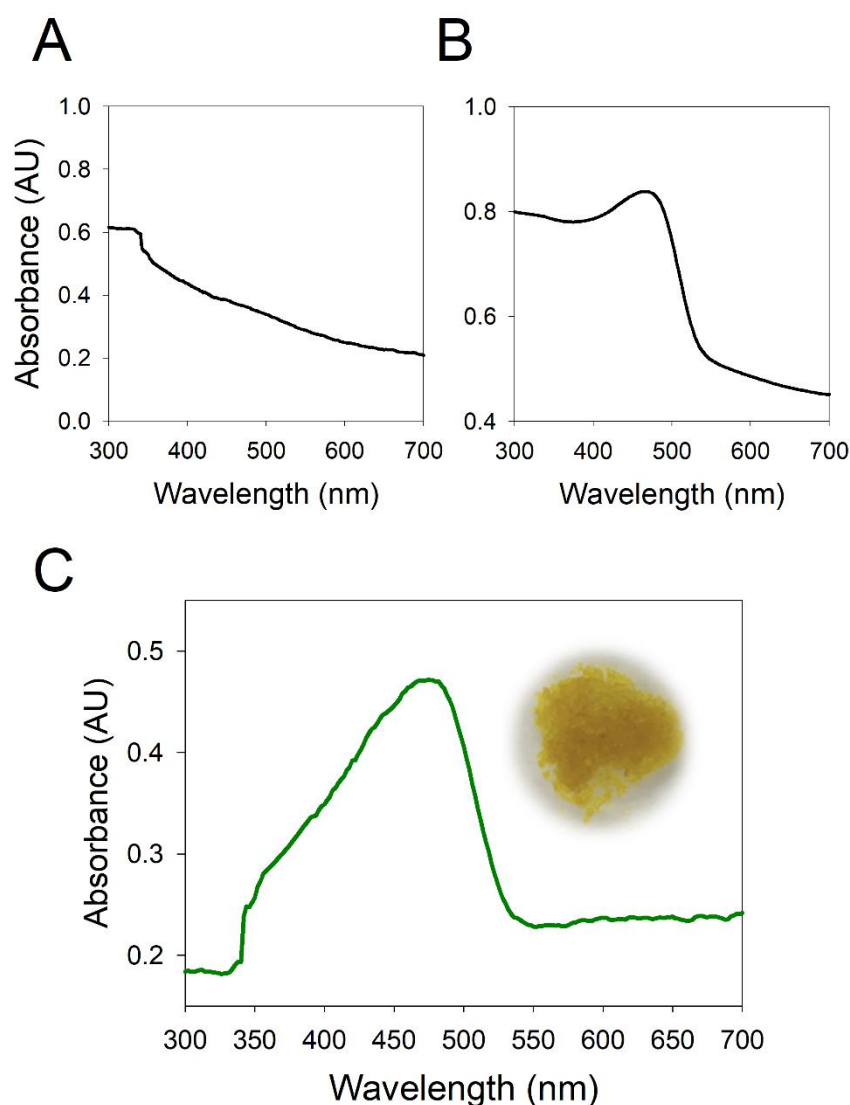


**Figure 8.2. Absorbance spectrum of the new polymer derived from chitosan.** **A:** Absorbance spectrum of chitosan. **B:** Absorbance spectrum of the new chitosan-betaxanthin polymer. **C:** Absorbance spectrum of chitosan-betaxanthin after subtraction of the spectrum of chitosan. Inset: macroscopic image of the chitosan-betaxanthin polymer.

The colorimetric changes of the new polymer respect to chitosan were quantitated through the analysis of the CIELAB color space (Cabanés et al., 2014; Noor et al., 2012) of the spectra obtained by the integrating sphere. The parameters for color ( $b^*$ ,  $h^\circ$ ), intensity ( $C^*$ ), and lightness ( $L^*$ ) were higher in the new polymer (**Table 8.1**). The  $a^*$  value slightly decreased with respect to the raw chitosan, corresponding to a decrease in the red tonality. These results agree with the bright yellow appearance of the new polymer observed to the naked eye (**Fig. 8.2C**) and related to the proposed betaxanthin nature of the novel polymeric compound.

**Table 8.1. Color analysis (CIELAB parameters) of chitosan particles and the novel chitosan-betaxanthin polymer.**

	Chitosan	Chitosan-betaxanthin
$L^*$	77.21	79.05
$a^*$	1.70	-2.95
$b^*$	11.08	20.95
$C^*$	11.21	21.16
$h^\circ$	81.29	98.00

### 3. Fluorescence of the polymeric chitosan-betaxanthin

Betalains are fluorescent plant pigments in the visible range of the electromagnetic spectrum, as it is showed in the chapter I of this thesis. All betalains are fluorescent given the nature of the betalamic acid, with a limited contribution of the condensed amine. This opens the possibility of the presence of fluorescence in the novel material here obtained. The yellow particles were washed 5 times with water to discard dopaxanthin in the supernatant and were observed by fluorescence microscopy under blue light employing a I3 filtercube (Leica) which present an excitation range of 450-490 nm. The polymer showed a strong green fluorescence (**Fig. 8.3A**) similar to those obtained for betalains previously described (Gandía-Herrero et al., 2010).

As it is described in the previous chapter VII, metals such as europium ( $\text{Eu}^{3+}$ ) or copper ( $\text{Cu}^{2+}$ ) are capable to produce a complexation with molecules of the betalains' family. This produces a decrease in the fluorescence of betalains which may be recovered by a solution of a quelating substance with a higher affinity to these metals, releasing the molecules of betalains. In this sense, the spectrophotometric changes of

the novel polymer derived to the condensation of betalamic acid with chitosan was measured in presence to  $\text{Eu}^{3+}$ . The addition of a solution 5  $\mu\text{M}$  of  $\text{Eu}^{3+}$  to the polymeric chitosan-betaxanthin produced a decrease in the fluorescence emitted by the polymer due to the complexation of  $\text{Eu}^{3+}$  with the molecule of betalain (**Fig. 8.3B**) and it was partially recovered by adding a solution of dipicolinic acid 40  $\mu\text{M}$  (**Fig. 8.3C**).

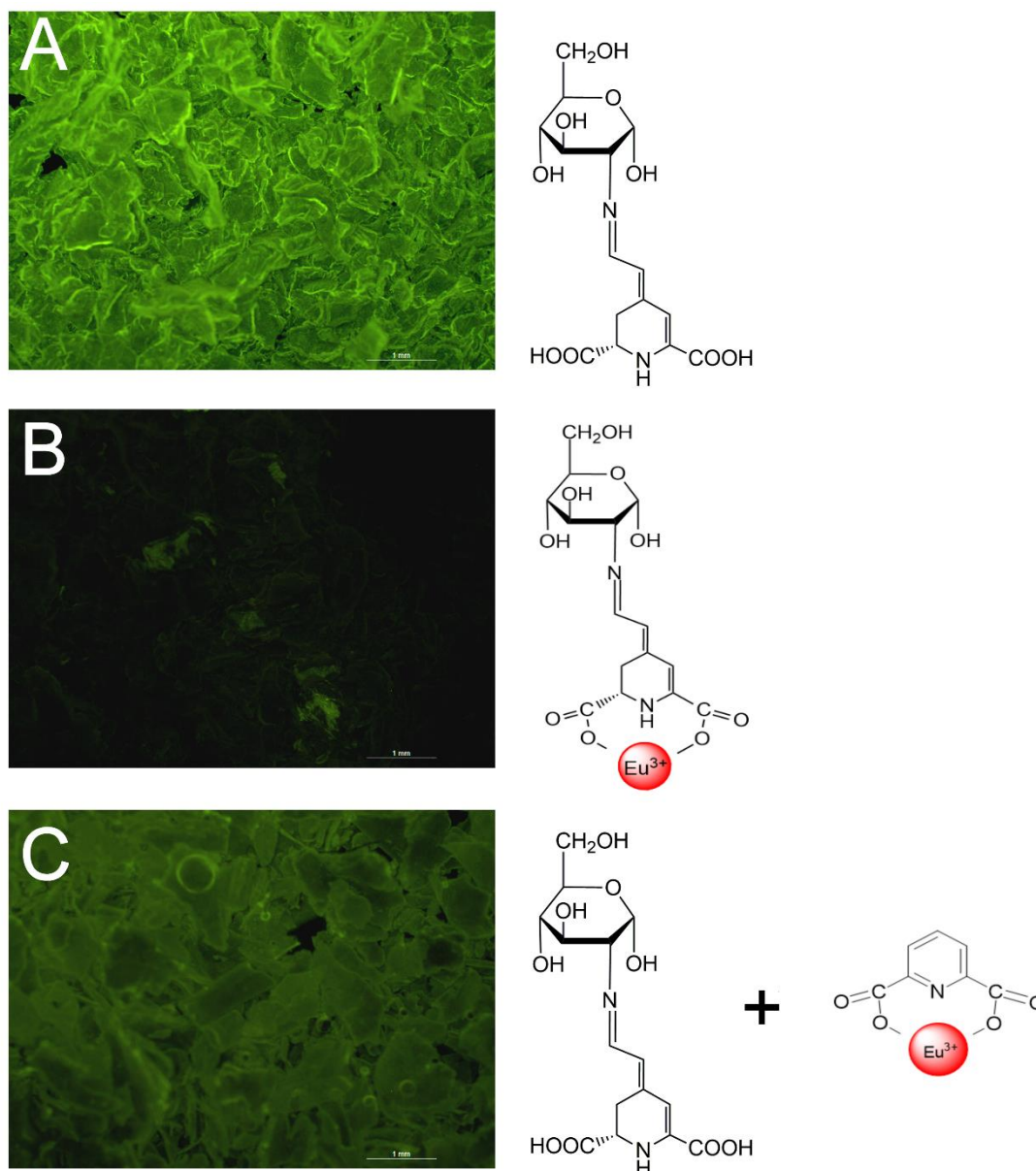


**Figure 8.3. Fluorescence of the polymeric chitosan-betaxanthin.** The initial fluorescence of the polymer (**A**) is lost in the presence of a solution of 5  $\mu\text{M}$   $\text{Eu}^{3+}$  (**B**). **C:** The addition of a solution of dipicolinic acid 40  $\mu\text{M}$  to the complex  $\text{Eu}^{3+}$ -betaxanthin produces the partial recovery of the fluorescence of the polymer. Scale bar: 1 mm.

Thus, the fluorescence properties of this novel polymer adds to the described characteristics of chitosan as a polymer employed with medical and pharmaceutical purposes (Dodane and Vilivalam, 1998). Chitosan is widely employed as a carrier to enhance the bioavailability of drugs and this new polymer might allow its detection due to the fluorescent properties that the betalain moiety provides. In addition, chitosan is a polymer biocompatible and biodegradable, now labelled with the fluorescent properties of betaxanthins.

#### **4. Production of sugar-derived betalains**

Chitosan is composed of units of glucosamine which present amine group able to condense with betalamic acid and, as a result, the monomer could form a new type of betaxanthin derived from sugars. This structural unit of the described polymer was used to produce a new betalain as well as N-acetyl-D-glucosamine, the structural unit of chitin. Both were employed to elucidate whether simple sugars are able to condense with betalamic acid. With this purpose, *E. coli* pET28a (GdDODA) was employed in biofactories for the possible obtention of sugar-derived betaxanthins due to the condensation of betalamic acid with N-acetyl-D-glucosamine or glucosamine. Additionally, their stereoisomers N-acetylgalactosamine and galactosamine, respectively, were also employed to obtain the corresponding betalains.

##### **4.1. Analysis of the pigments**

The addition of these sugars to the cultures of *E. coli* yielded yellow coloration in all cases. HPLC analysis showed that the yellow coloration in cultures containing N-acetyl-D-glucosamine or N-acetyl-D-galactosamine was due to the presence of dopaxanthin (a single peak detected at  $\lambda = 480$  nm and RT = 13.91 min). Thus, no new betaxanthins could be obtained due to the condensation of betalamic acid with N-acetyl-D-glucosamine or N-acetyl-D-galactosamine and this was used to confirm the results obtained with chitin, where the presence of an acetyl group joined to the amine blocks the condensation with the nitrogen atom.

On the other hand, the analysis of samples from cultures containing galactosamine or glucosamine showed the minor presence of dopaxanthin. However, a major unknown peak was detected in each case. In the presence of glucosamine or galactosamine, peaks at  $\lambda = 480$  m with retention times of 8.1 min and 4.1 min were

detected respectively (**Fig. 8.4**). These peaks corresponded to the condensation of betalamic acid with the  $-NH_2$  group present in the C<sub>2</sub> position of these molecules, giving rise to the formation of two new betaxanthins (**Fig. 8.5A**). These results indicate that the  $-NH_2$  residues present in molecules of glucosamine are responsible of the formation of the chitosan-betaxanthin polymer and thus the structure of this new polymer is proposed in **Fig. 8.5B**.

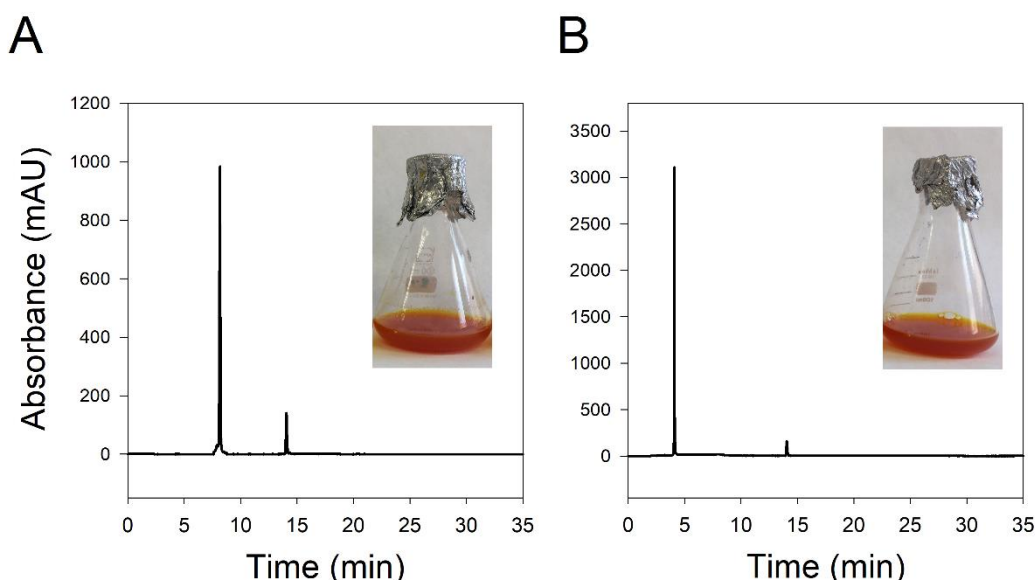


**Figure 8.4.** Chromatograms at  $\lambda=480$  nm for the supernatants of the biofactories with *E. coli* (pET28a-GdDODA) supplemented with glucosamine (A) and galactosamine (B). In both cases, the minor peak obtained at 13.9 min corresponds to dopaxanthin.

#### 4.2. Mass spectrometry analysis

The new betaxanthins were purified by ion exchange and C18 reversed phase chromatography and then characterized by ESI-MS, to confirm the structures proposed. The analysis of pure glucosamine-betaxanthin showed the detection of molecular protonated ion,  $[M+H]^+$ , with a mass value of 373,12  $m/z$ . Analogously, the analysis of pure galactosamine-betaxanthin showed a peak with a mass value of 373,12  $m/z$ . Thus, the retention times obtained were similar to those obtained by HPLC analysis. Both compounds are isomers only different by the position of  $-OH$  group at the C<sub>2</sub> position as illustrated in **Fig. 8.5**. The molecules differ in the retention times under the HPLC system, 8.1 min for glucosamine-betaxanthin and 4.1 min for galactosamine-betaxanthin.

The mass values obtained corresponded to the theoretical mass values calculated for the condensation of betalamic acid with a molecule of galactosamine or



glucosamine. These results unambiguously demonstrate the obtention of two novel betaxanthins, being the first sugar-derived betaxanthins ever described.

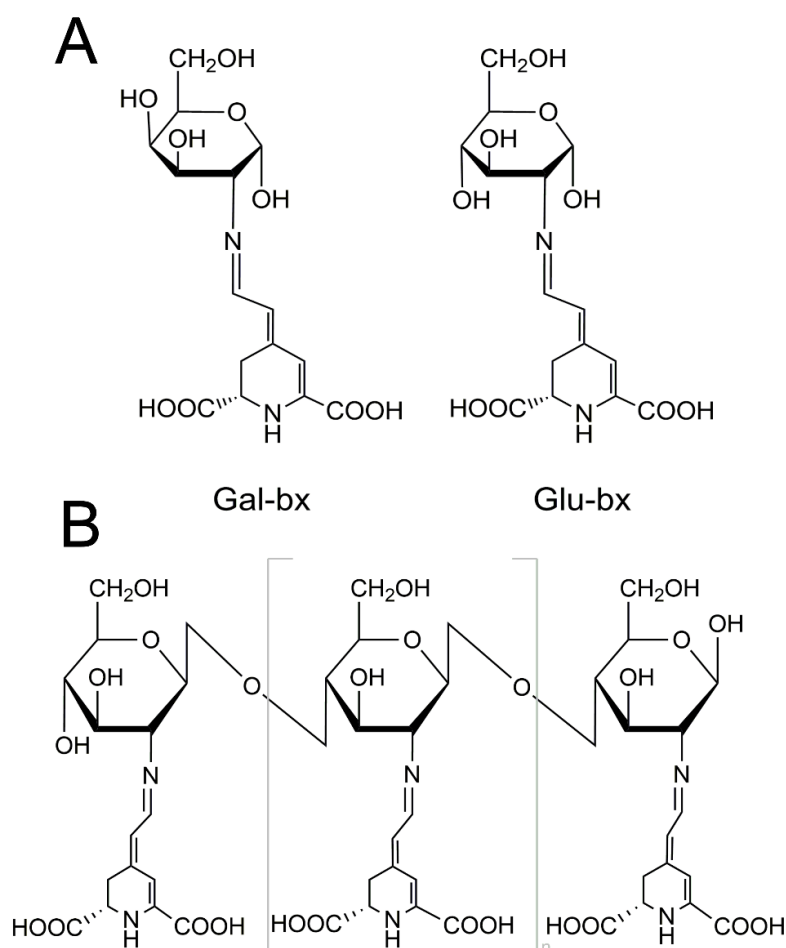


**Figure 8.5. Betaxanthins obtained in this study.** **A:** sugar-derived betaxanthins obtained by the condensation of betalamic acid with galactosamine or glucosamine. **B:** Proposed structure of the polymeric chitosan-betaxanthin.

#### 4.3. Spectrophotometric analysis of the novel pigments

Absorbance and fluorescence properties of the novel betaxanthins were studied by spectrophotometry. The absorbance spectrum recorded showed a maximum absorbance of glucosamine-betaxanthin at  $\lambda = 475$  nm and exactly the same result was obtained for the betaxanthin derived from galactosamine (**Fig. 8.6**). In addition, the molar absorption coefficient ( $\epsilon$ ) for both molecules were obtained by basic hydrolysis. This analysis was followed until the complete degradation of the molecules to betalamic acid and it led to determine an  $\epsilon = 51,100 \text{ M}^{-1} \text{ cm}^{-1}$  for both glucosamine-betaxanthin and galactosamine-betaxanthin. Thus, both isomers share spectral properties, as shown **Fig. 8.6**.

Regarding fluorescence analysis, excitation spectra were obtained following the emission at the maximum emission wavelength detected in a previous measurement and emission spectra were obtained after excitation at maximum wavelength. Glucosamine-betaxanthin showed an emission maximum at  $\lambda = 513$  nm and an excitation maximum at  $\lambda = 478$  nm. For galactosamine-betaxanthin, an emission maximum was detected at  $\lambda = 510$  nm and the excitation maximum was obtained at  $\lambda = 477$  nm. These results (**Fig. 8.6**) agree with spectrophotometric properties previously described for betaxanthins derived from amines and amino acids instead of from sugars (Gandía-Herrero et al., 2010). In nature, the action of *O*-glycosyltransferase enzymes yields betanin and amaranthin, which are classified as betacyanin due to their spectrophotometric properties. However, the new betaxanthins here described for the first time are obtained without additional enzymes and present the same electron resonance system responsible of the yellow pigmentation and fluorescence properties of betaxanthins (Gandía-Herrero et al., 2005).

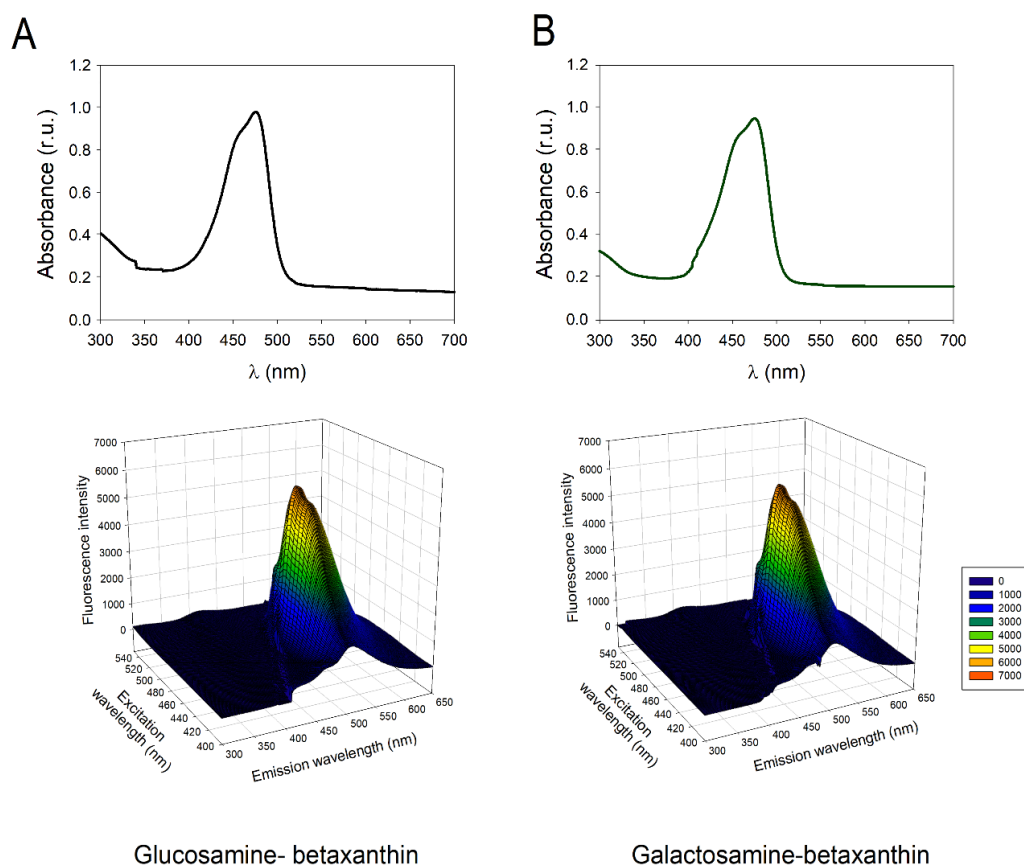


**Figure 8.6. Spectrophotometric properties of the new sugar-derived betaxanthins. A.** Absorbance spectrum (top) and 3D fluorescence plot (bottom) for glucosamine-betaxanthin. **B.** Absorbance spectrum (top) and 3D fluorescence plot (bottom) for galactosamine-betaxanthin.

The spectroscopic properties of the novel sugar-derived betalains are analogous to those reported for betalains derived from amino acids, thus indicating a common pattern derived from the common structural feature, the betalamic acid. Thus, all betalains may provide the same colour and fluorescent properties insofar betalamic acid is condensed to an amino group regardless the nature of the molecule. This, induces amino acids, sugars and polymers.

## 5. Conclusions

The polysaccharide chitosan has been employed to produce a new polymeric betaxanthin. Glucosamine, the structural unit of chitosan, and its stereoisomer galactosamine are able to condense with betalamic acid to produce two new betaxanthins. The new polymer and the new individual betaxanthins present spectrophotometric properties similar to those obtained for betaxanthins previously described. Thus, glucosamine-betaxanthin, galactosamine-betaxanthin and polymeric chitosan-betaxanthin are the first betaxanthins obtained from sugars. The obtention of a fluorescent, non-toxic polymer that combines the properties of chitosan and betaxanthins may be of use for medical and pharmaceutical applications.

## REFERENCES

- Bumgardner, J.D., Wiser, R., Gerard, P.D., Bergin, P., Chestnutt, B., Marini, M., Ramsey, V., Elder, S.H., Gilbert, J.A., 2003. Chitosan: Potential use as a bioactive coating for orthopaedic and craniofacial/dental implants. *J. Biomater. Sci. Polym. Ed.* 14, 423–438. <https://doi.org/10.1163/156856203766652048>
- Cabanes, J., Gandía-Herrero, F., Escribano, J., García-Carmona, F., Jiménez-Atiénzar, M., 2014. One-step synthesis of betalains using a novel betalamic acid derivatized support. *J. Agric. Food Chem.* 62, 3776–3782. <https://doi.org/10.1021/jf500506y>
- Cheng, N.C., Lin, W.J., Ling, T.Y., Young, T.H., 2017. Sustained release of adipose-derived stem cells by thermosensitive chitosan/gelatin hydrogel for therapeutic angiogenesis. *Acta Biomater.* 51, 258–267. <https://doi.org/10.1016/j.actbio.2017.01.060>
- Dhandayuthapani, B., Krishnan, U.M., Sethuraman, S., 2010. Fabrication and characterization of chitosan-gelatin blend nanofibers for skin tissue engineering. *J. Biomed. Mater. Res. Part B Appl. Biomater.* 94(1), 264–272. <https://doi.org/10.1002/jbm.b.31651>
- Dodane, V., Vilivalam, V.D., 1998. Pharmaceutical applications of chitosan. *Pharm. Sci. Technol. Today.* 1(6), 246–253. [https://doi.org/10.1016/S1461-5347\(98\)00059-5](https://doi.org/10.1016/S1461-5347(98)00059-5)
- Gandía-Herrero, F., Escribano, J., García-Carmona, F., 2010. Structural implications on color, fluorescence, and antiradical activity in betalains. *Planta* 232, 449–460. <https://doi.org/10.1007/s00425-010-1191-0>
- Gandía-Herrero, F., Escribano, J., García-Carmona, F., 2005. Betaxanthins as pigments responsible for visible fluorescence in flowers. *Planta* 222, 586–593. <https://doi.org/10.1007/s00425-005-0004-3>
- Hao, J., Guo, B., Yu, S., Zhang, W., Zhang, D., Wang, J., Wang, Y., 2017. Encapsulation of the flavonoid quercetin with chitosan-coated nano-liposomes. *LWT - Food Sci. Technol.* 85, 37–44. <https://doi.org/10.1016/j.lwt.2017.06.048>
- Noor, A.I., Mokhtar, M.H., Rafiqul, Z.K., Pramod, K.M., 2012. Understanding color models : A review. *ARPN J. Sci. Technol.* 2, 265–275.
- Sano, H., Shibasaki, K., Matsukubo, T., Takaesu, Y., 2001. Comparison of the activity of four chitosan derivatives in reducing initial adherence of oral bacteria

onto tooth surfaces. Bull. Tokyo Dent. Coll. 42, 243–249.

<https://doi.org/10.2209/tdcpublish.42.243>

**Chapter IX.** Platform for the automatic control  
of the organism *C. elegans*

Part of this chapter was published in Food Chemistry  
Guerrero-Rubio et al. (2019) <https://doi.org/10.1016/j.foodchem.2018.09.067>



### **Contextualization**

Once the biotechnological obtention of betalains led to a higher amount of pure pigments, the study of their individual health-promoting properties, as bioactive compounds, was possible. In this thesis, those properties are evaluated for the first time in the *in vivo* model animal *Caenorhabditis elegans*. For this purpose, a platform for the automatic control of the organism *C. elegans* was developed.

This machine is able to follow the movements of up to 8,000 worms at the same time and to accurately and objectively determine their lifespan. Lifespan is a biologically relevant parameter used to estimate the health-promoting potential of biomolecules when working with the model animal *C. elegans* based on the original one developed at the University of Harvard (Cambridge, MA, USA) and it was built following the indications published by their constructors (Stroustrup et al., 2013). However, minor modifications described in this chapter were applied to improve some disadvantages of the original device.

## **1. Components and system modifications**

The machine is composed of an incubator that houses 10 high-quality photographic scanners (**Fig. 9.1A**) connected to a high-power Linux computer which processes and analyzes the images obtained by each scanner. This close system avoids the fluctuations of the temperature produced by the human manipulation of plates when manual counting of worms (alive and dead) must be performed every day. The scanners used were Epson PerfectionV800 Photo instead of the V700 used in the original design, being this one of the modifications made with respect to the original machine. The V800 model has a LED lamp unlike the V700 which has a cold cathode lamp. This change improves temperature control and stability, since LED lamps generate less heat than cold cathode lamps. Even so, the maintenance of plates in a close system as the incubator is, could generate local heat inside the scanners that could affect the lifespan of worms due to the continuous activation of scanners' lamps.

To dissipate the heat generated by the lamps and keep the temperature stable, the photographic scanners were modified incorporating 8 fans per scanner (7 of 8 cm of diameter and 1 of 12 cm) (**Fig. 9.1B-C**) connected to an external power supply.



These fans generate an air current that reduces the temperature of the scanner when it is running and homogenize the local temperature with the temperature of the chamber.

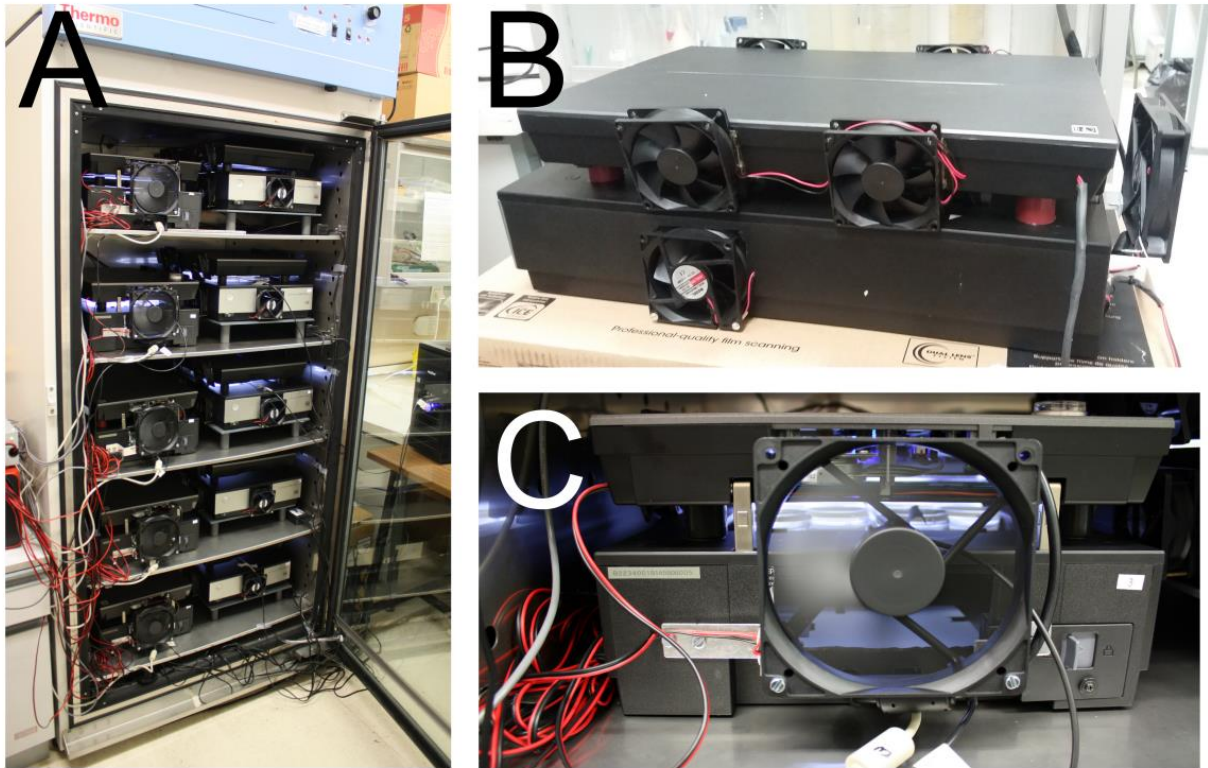


**Figure 9.1. The lifespan machine.** A. Overall image of the incubator of the lifespan machine showing the ten modified scanners. B. Side view of an modified Epson V800 scanner modified. C. LED light coming out from an Epson V800 scanner placed inside the incubator.

In order to improve the control of temperature, five temperature probes were installed inside the machine and continuously recorded the temperature of scanners. The maximum temperature on the scanners' surface was produced every 15 minutes when the scanner lamp passes through the temperature probe while digitalizing the plates. As **Fig. 9.2** shows, this instant increase in temperature has an amplitude of 0.1 °C and heat dissipation is fast thanks to the eight fans mounted in the scanners. The temperature of the incubator is adjusted to ensure that the temperature inside the scanners, where the plates are located, is 25 °C.

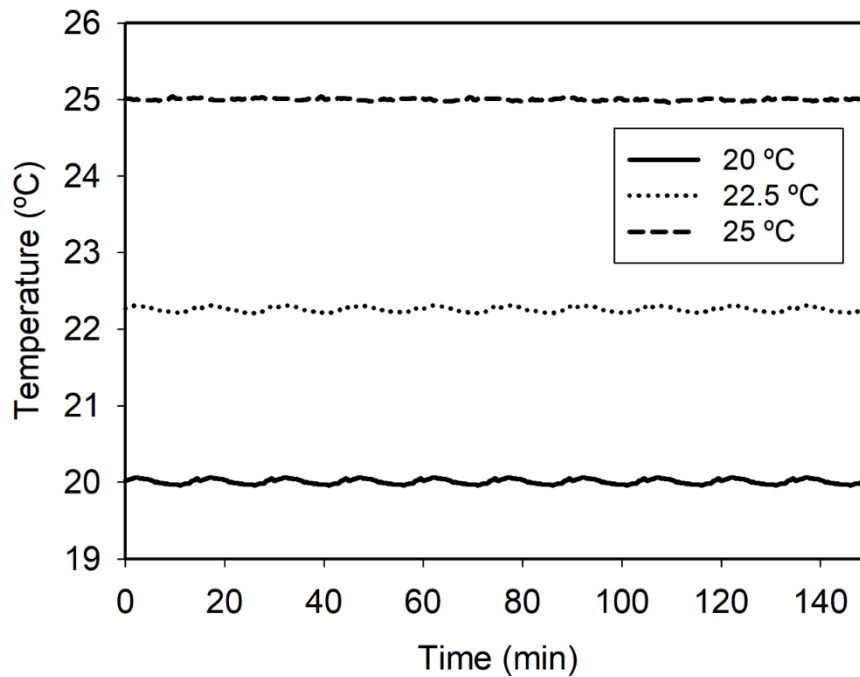


**Figure 9.2. Temperature evolution inside the scanners placed into the lifespan machine incubator.** Temperature stability is shown at three different temperatures. The local oscillations every 15 minutes are due to the scanner bar while images are acquired. Amplitude of the oscillation is reduced by the use of multiple fans attached to the scanner.

A second important improvement introduced in the system was the design of plastic trays which have been incorporated in order to raise the scanners of the right side of the incubator. This modification avoids the air flows of the fans from facing each other, thus homogenizing the temperature more efficiently and preventing hot air flows causing condensation on the test plates.

The employment of closed Petri dishes instead of the system used in the original design also avoided the loss of plates affected by desiccation of agar or cross contamination. In the original machine, the authors placed sixteen Petri dishes (35 mm) without a lid on a glass tray, and then sealed them using rubber sheets placed on the scanner tray. However, the machine here described proposed to directly place sixteen Petri dishes, closed with their own cover, on the scanner tray. This modification had implications at the focus point of the scanners, which were adjusted accordingly. For this re-focusing of the scanners, lens had to be accessed, completely dismantling them. The resin that keeps lens fixed to the carousel was removed and then the lens was moved until finding a position in which the nematodes of the plate looked sharp. This adjustment, guided by a trial-error process, significantly improved the visualization and the correct detection of *C. elegans* on the surface of plates.

It should be noted that ten percent of the experiment plates are censored (removed from the analysis) in the original machine due to contamination, condensation or drying (Stroustrup et al., 2013). The modifications here described alleviated these problems and the number of censored plates, not useful, is reduced to nil. Once all modifications were performed and tested, the machine was ready to start the analysis of worms.

## **2. Preparation of samples**

### **2.1. Worms' requirements**

The aim of this machine is to allow the visualization and detection of *C. elegans* worms throughout their life cycle. Therefore, all worms belonging to the same experiment must be synchronous, starting their life cycle at the same time. This is a mandatory requirement to obtain a successful experiment and significant results since the machine is able to measure mean and maximum lifespan of a population, thanks to the ability of the following each individual worm. Monitoring each individual worm allows to established the mean lifespan as the survival time of 50% of the population and the maximum lifespan as the survival time of the last worm alive.

The other important requisite to measure the lifespan of worms with this machine is to avoid progeny. As it is described in the introduction section, a hermaphrodite worm is able to produce around 300 individuals in a short time of 3-5 days and it may be increased by the presence of a male in the medium culture. Therefore, this rapid expansion of population must be avoided to have significant lifespan data from the original worms laying on the plate. The most frequent method to determine lifespan is the daily hand-counting assay and the transfer of adult worms to fresh plates leaving the progeny in the original ones. This manual manipulation may damage the worms and alter environmental conditions (temperature, light, humidity...) and is only suitable for a small number of assays. Therefore, the use of the machine needs the addition of a chemical reagent able to sterilize worms and to avoid the manual manipulation of plates due to the high number of worms and conditions that it is able to analyzed. Floxuridine (FUdR) is the chemical agent most widely used to prevent the proliferation of progeny. FUdR is an antineoplastic

antimetabolite used as a chemotherapeutic agent (Allen-Mersh et al., 1994) in gastrointestinal tract cancer that spreads to the liver.

## 2.2. Medium's requirements

Because to the scanners' lenses were manipulated to obtain sharp images of the agar surface, all plates must contain exactly the same volume of NGM medium. To avoid human mistakes in the measurement of volume in the preparation of a large number of the plates, an automatic dispenser is employed to prepare plates (**Fig. 9.3**). This machine supplies 8 mL of NGM medium every 5 seconds, with enough time to move from one plate to another to refill them efficiently. This ensures a homogeneous volume in all plates and thus proper visualization of worms. Besides, this NGM medium is supplemented with FUDR, to avoid progeny as stated above, nystatin, to avoid contamination by fungi, and ampicillin, to avoid contamination by bacteria. *E. coli* OP50 is also provided over the agar surface as food source. Additionally, the medium may contain compounds to analyze their effects in the survival rate of *C. elegans*. These compounds must be water-soluble, non-volatile and dissolved in a non-volatile solvent. Insoluble compounds cannot be analyzed by the machine since they produce aggregates that hinder the resolution and the analysis of the images.

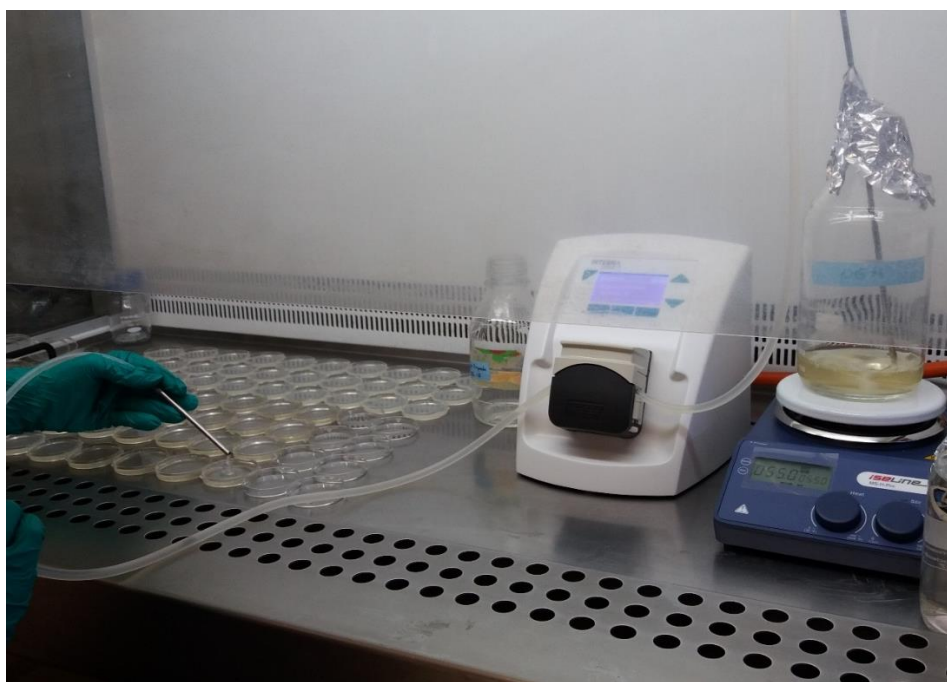


**Figure 9.3. Preparation of plates for the lifespan machine.** An automatic dispenser allows the distribution of 8 mL of NGM to several plates (35 mm). Although NGM medium is supplemented with nystatin and ampicillin to avoid contamination, plates must be filled under aseptic conditions.

### 3. Running the lifespan machine

The control software and the analysis software are specific and have been developed for this machine by the authors of the original work. It works under Scientific Linux environment and it is able to control the operation of scanners, to acquire images, to fragment them and to associate them with each specific experiment in the programmed time. This analysis is able to identify each nematode individually on its plate from the beginning of the experiment and to follow its movement or lack thereof until its death, thanks to different algorithms which analyze the posture of each worm at each moment. The program identifies a series of possible events, but always requires confirmation from a human operator to validate its interpretation. Only then, the software executes the analysis of the events and transfer processed data of files on survival in each of the analyzed conditions. That part of the process is controlled by two computers working in Windows environment which communicate, through a network established for this purpose, with the main Linux computer ultimately which controls the machine.

As Stroustrup et al., (2013) detailed, given the complexity of the system it is not necessary to understand all informatic components and how they are connected to each other but it is extremely recommended the installation of the system by a professional, especially for the possible appearance of connection issues when installing the system for the first time. The researcher only needs to manipulate the scanners, to load plates with worms, to run the “worm browser”, to schedule and set up experimental conditions, and to run the “web browser” and schedule the data analysis.

#### 3.1. Delimitation of analysis areas

Worm browser is the software especially designed by the authors of the original machine to set up the conditions of analysis. First, a preliminary scan of the entire scanner surface allows to determine the position of each plate. This information is sent to worm browser in order to mark the area to scan and to avoid the accumulation of irrelevant information, that is, the part of the scanner that does not contain any plates. Although each scan works with intervals of 15 minutes, a single plate will be only analyzed with 1 hour-intervals. Thus, the scanner surface is first divided into four columns (**Fig. 9.4A**), each one containing four plates.

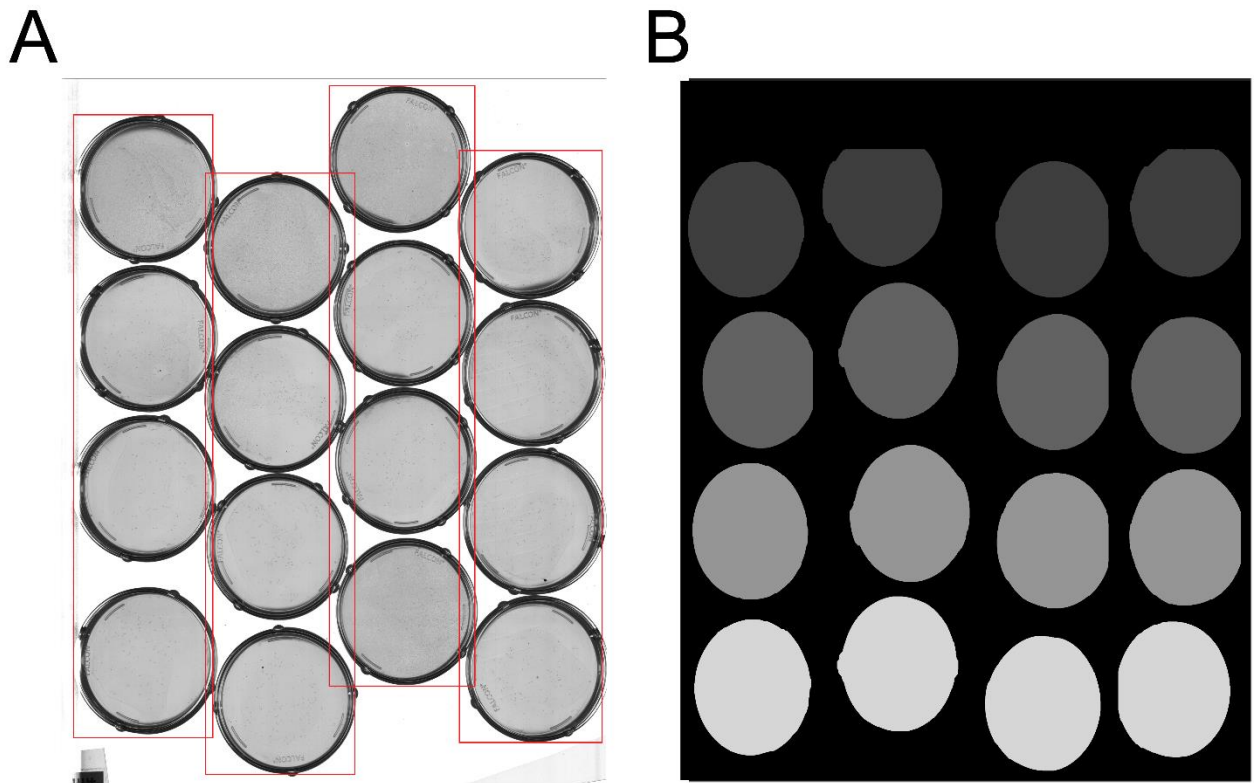


**Figure 9.4. Mask design for the analysis of plates in the lifespan machine. (A)** Delimitation of columns from the preliminary scan of the entire surface. **(B)** Image obtained after modifications realized with Adobe Photoshop where plates, in each column, are recognized by a grey subtone.

Additionally, each plate must be identified to collect images separately. This part needs Adobe Photoshop or a similar software in order to convert the image obtained by scan in a plane, black background picture (without layers) where each plate, per column, will be identified with a tone of the grey scale (**Fig. 9.4B**). Since each column corresponds to an individual read of the scanner, the pattern of four grey subtones can be repeated in the following columns. All these modifications give rise to the mask, which will be uploaded to “worm browser” in order to confirm the location of each plate as well as the recognition of the delimited area to analyze per plate (**Fig. 9.5**). Then, the mask is sent to the analysis server (“web browser”) in order to run the analysis and to collect the pictures of each plate separately.



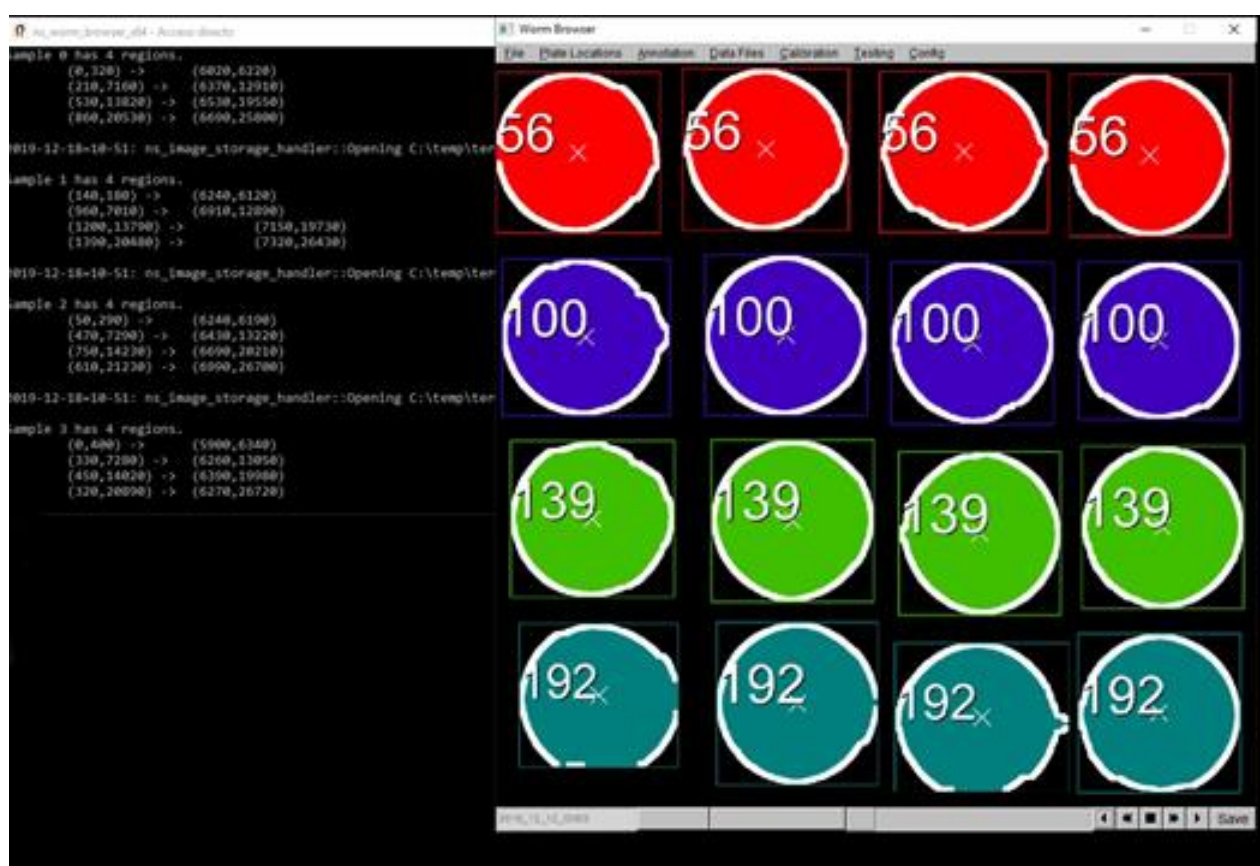


**Figure 9.5. Screenshot of a mask uploaded to worm browser to confirm the location of the analysis to be realized.** The system visually confirms that there is no error in the mask and that it is ready to be sent to the analysis server.

### 3.2. Data analysis and determination of lifespan

Once the mask is performed and validated by worm browser, it is sent to the web browser to start the assay and the collection of images. The web browser is the online interface that allows to determine the parameters that will be analyzed to estimate the lifespan of the worms. The image analysis performed by the “web browser” through this thesis was based on the model “mixed genotype”. This model allows detecting each worm of each image and indicating its movement based on its position and its posture.

Thanks to all the images collected, the analysis server is able to re-create the movement pattern of each worm, from the beginning of the experiment to its death, generating a compact file called storyboard (**Fig. 9.6**). This storyboard is then available for its visualization in the worm browser, where the researcher must confirm or modify the “death event” pointed out by the automatic analysis.

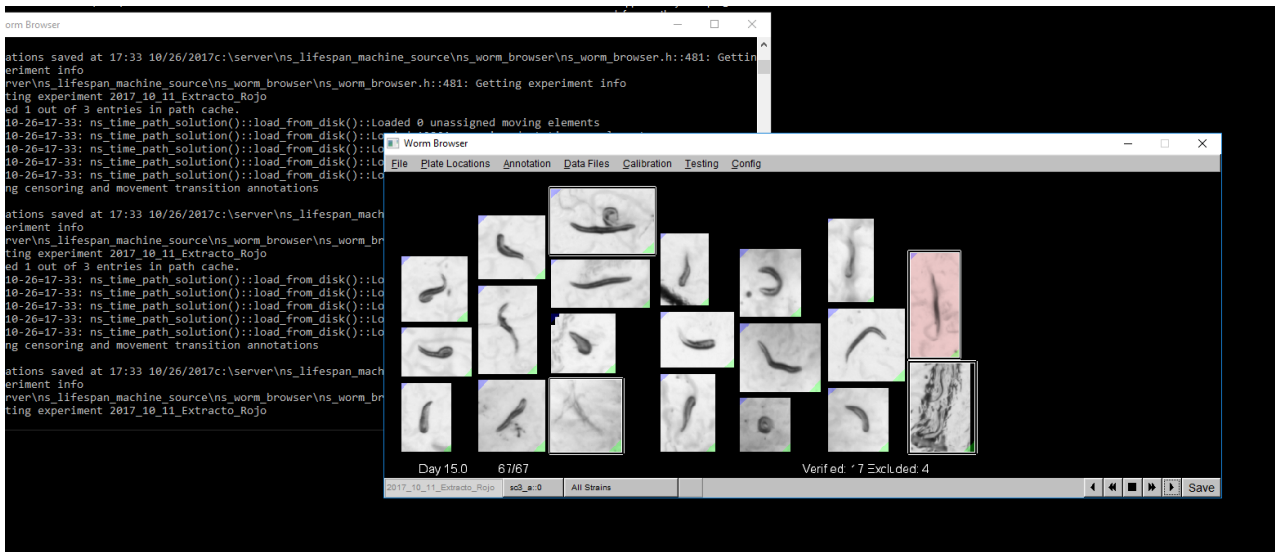


**Figure 9.6. Screenshot of the storyboard in the software worm browser.** Here, each worm on the screen contains the photograms' collection of its lifespan from the beginning to its death. The researcher must check them one by one to validate or modify the death event set up by the automatic analysis as well as to discard any possible error.

The death event is determined by the position and the posture of the worm since it suffers an expansion and a later contraction of the body as well as the loss of its "elegant" morphology. After the confirmation or modification of these death events, the "web browser" generates a comma separated value (CSV) file which contains the death time of each worm which is used to generate a survival curve of the population.

#### 4. Statistical treatment of the data

The statistical treatment of the data obtained with the lifespan machine is carried out by means of the OASIS2 (Han et al., 2016), an online application which allows to adjust the data to the Kaplan-Meier function. This function shows the probability of survival at a certain time interval. In addition, the different conditions of an entire assay are compared each other by means of the F-test in order, to establish whether the data obtained from the lifespan are significant. This allows to obtain significant results avoiding unnecessary repetitions and sacrificing the least number of specimens. It has been established that all tests must be carried out at least in triplicate, in order to obtain significant data and reduce the possibility of errors.



## 5. Conclusions

In the current state of optimized operation of the lifespan machine, around 8,000 individuals of *C. elegans* are being followed independently and simultaneously, determining their lifespan with an accuracy of minutes in experiments that last 25 days. Each error detected in the management and culture of the *C. elegans* organism, each failure in the use of the machine, each improvement solution, and each condition tested has involved these 25 days of experimentation and analysis. The effort and time devoted to this platform has been great and it is being rewarded with the relevance of the biological data obtained for the molecules tested.

## REFERENCES

- Allen-Merish, T.G., Earlam, S., Fordy, C., Abrams, K., Houghton, J., 1994. Quality of life and survival with continuous hepatic-artery floxuridine infusion for colorectal liver metastases. *Lancet* 344, 1255–1260. [https://doi.org/10.1016/S0140-6736\(94\)90750-1](https://doi.org/10.1016/S0140-6736(94)90750-1)
- Han, S.K., Lee, D., Lee, H., Kim, D., Son, H.G., Yang, J.-S., Lee, S.-J. V, Kim, S., 2016. OASIS 2: online application for survival analysis 2 with features for the analysis of maximal lifespan and healthspan in aging research. *Oncotarget* 7, 56147–56152. <https://doi.org/10.18632/oncotarget.11269>
- Stroustrup, N., Ulmschneider, B.E., Nash, Z.M., López-Moyado, I.F., Apfeld, J., Fontana, W., 2013. The *Caenorhabditis elegans* lifespan machine. *Nat. Methods* 10, 665–670. <https://doi.org/10.1038/nmeth.2475>



**Chapter X.** Design of a novel microscope  
slide for the study of nematodes

This chapter has been registered as the utility model ES1235378Y  
“Dispositivo portaobjetos para estudio de nemátodos”.



### **Contextualization**

The observation of *C. elegans* is strongly conditioned by its tiny size. The “elegant” movement of adults might be visible to naked eye but a deeper observation involving techniques such as staining or dissection needs of tools for a closer view. Besides, sometimes the microscopic visualization used in the *C. elegans*’ studies requires that worms stay close to their optimal physiological state. Sodium azide is widely used as anaesthetic but Massie et al., (2003) reported the possibility of sodium azide could imply physiological consequences for the animal.

## **1. Background**

Nowadays some devices that facilitate the study of nematodes are known, such as the patent US20120129726A1 (Rohde and Yanik, 2012) which details a subcellular multi-well plate imaging system, or patents US10052631B2 (Ben-Yakar et al., 2018) and US8961877B2 (Yanik et al., 2015), which describe high performance screening systems. These devices are complex and hardly applicable to the current available imaging and analysis systems.

On the other hand, JP2015230377A (Tadao, 2014) patent refers to a microscopic slide made of optically transparent glass or resin for microscopic observation of biological specimens such as microorganisms or plankton. The slide has a plurality of microcavities of a size between 0.01 and 0.5 mm and with a depth between 0.001 and 0.2 mm, in which the specimens to be observed can be housed without being damaged. The microcavities can be sealed by applying a conventional glass coverslip to form chambers in which the specimen is confined. However, the morphology of these cavities does not prevent the mobility of the specimen, and allows the accommodation of more than one specimen, thus making observation difficult.

Therefore, there is a need to create a microscopic slide that allows isolation and immobilization of nematodes individually to facilitate their observation and manipulation in a simple and economical mean. The novel device should be able to adapt the majority of currently existing laboratory display devices and microscopes.

## 2. Description of the microscopy slide

The aim of this chapter consists on the description of a novel microscopic slide designed for the study of nematodes, specially configured and sized for *C. elegans*. The device comprises a support plate and a coverslip sheet, linkable to the plate. Both elements, plate and coverslip, are made with optically transparent materials to allow the observation of the nematodes as well as to avoid the dispersion of light and the autofluorescence of the supports.

The plate contains a plurality of micro grooves on one of its faces, each of them being configured and sized to house a single worm. Thus, they present an essentially elongated geometry with dimensions in the range between 0.5 mm and 2.0 mm for the length, between 0.02 mm and 0.2 mm for the width, and between 0.02 mm and 0.2 mm deep. In a preferent embodiment of the device, in which the nematode to be studied belongs to the species *C. elegans*, each microgroove has dimensions of 1.5 mm long, 0.05 mm wide, and 0.05 mm deep. Once the nematodes have been introduced inside, the microgrooves are over-coated by means of the coverslip, generating closed chambers that prevent the scape of the nematodes as well as avoid the need for additional immobilization techniques, such as sedation.

The technical effect that derives from the elongated morphology of the microgrooves consists in facilitating the manipulation, visualization and dissection of the nematode. It stays physically trapped and with a limited or impeded movement capacity. In order to help a better understanding of the characteristics of this invention which has been accepted with the patent ES1235378Y (Gandía-Herrero et al., 2019) for its practical implementation for the study of *C. elegans*, a set of drawings is attached in **Fig. 10.1** where, for illustrative and non-limiting purposes, it has been represented.

## 3. Conclusions

The novel device here described for the study of nematodes provides a number of advantages over existing devices. First, it constitutes a simple device that can be applied to the image and analysis systems currently available in the market. The device is attachable to existing mechanical stages in the visualization systems commonly used today (microscopes, macroscopes, magnifiers, X-ray systems, or ultrasound scanners) which may be present or not retention systems or clips.. On the

other hand, it facilitates the process of manipulation, visualization and dissection of the nematode, since the worm is physically trapped and its movement is limited. In addition, the immobilization achieved by the additional use of a coverslip facilitates observation without the need to completely or partially numb of the specimen.

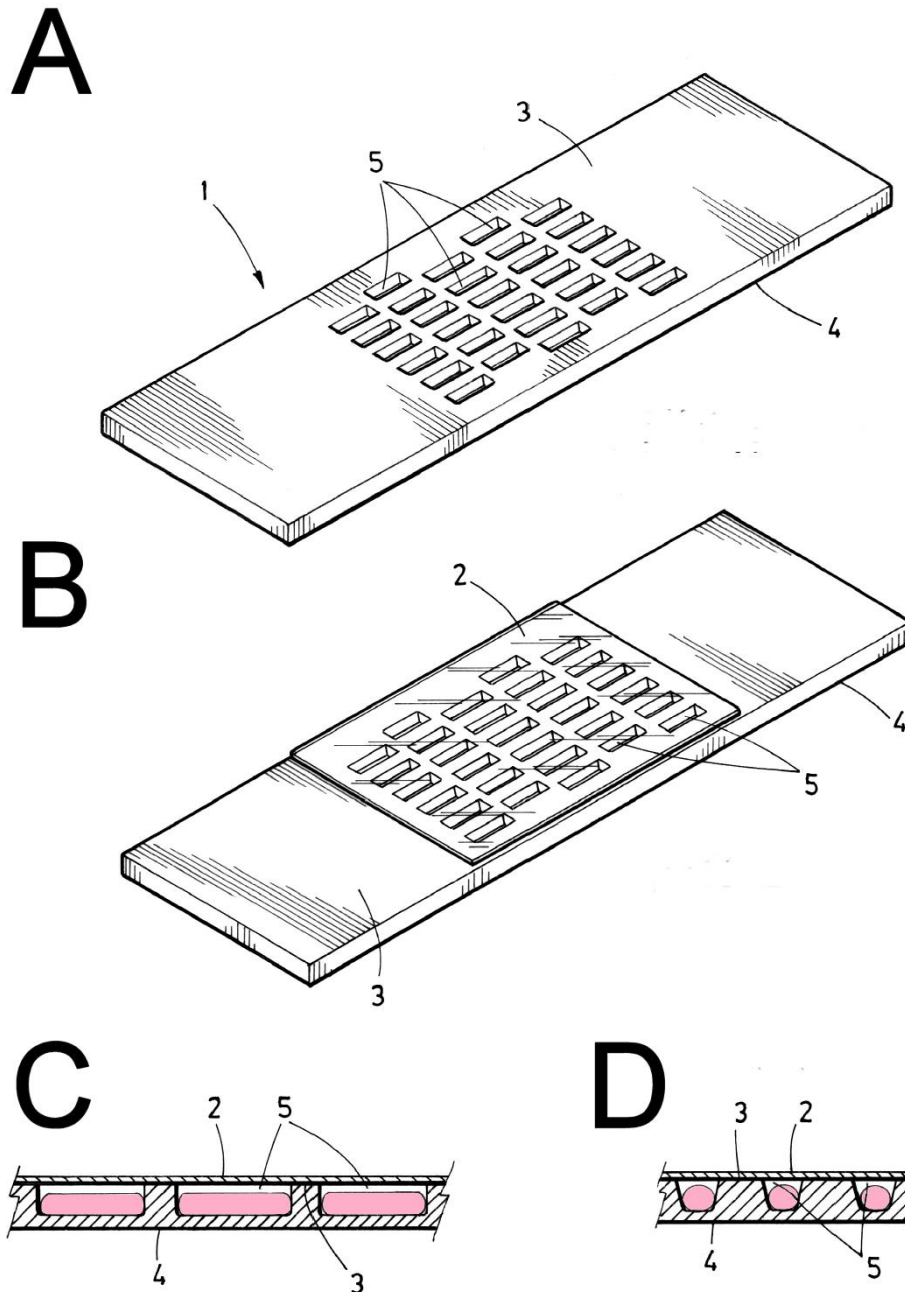


**Figure 10.1. Schematic representation of the slide device.** **(A)** A top view of the slide device for the study of nematodes, in which its main constituent elements are observed. **(B)** A slide device covered by a sheet coverslip. **(C)** Detail of a longitudinal section of the device, in which a side view of some housings can be seen, each of them having a nematode specimen inside (pink). **(D)** A detail of a cross-section of the device, in which a front view of some housings can be seen. Numbers in images correspond to the slide (1), the sheet (2) coverslip, the anterior face (3) and the posterior face (4) of the slide and the micro grooves (5).



## REFERENCES

- Ben-Yakar, A., Ghorashian, N., Gökçe, S.K., Guo, S.X., Everett, W.N., Bourgeois, F., 2018. Microfluidic devices for the rapid and automated processing of sample populations. US10052631B2.
- Gandía-Herrero, F., García-Carmona, F., Guerrero-Rubio, M.A., Henarejos-Escudero, P., Hernández-García, S., 2019. Dispositivo portaobjetos para estudio de nematodos. ES1235378Y
- Massie, M.R., Lapoczka, E.M., Boggs, K.D., Stine, K.E., White, G.E., 2003. Exposure to the metabolic inhibitor sodium azide induces stress protein expression and thermotolerance in the nematode *Caenorhabditis elegans*. Cell Stress Chaperones 8, 1–7. [https://doi.org/10.1379/1466-1268\(2003\)8<1:ettmis>2.0.co;2](https://doi.org/10.1379/1466-1268(2003)8<1:ettmis>2.0.co;2)
- Rohde, C.B., Yanik, M.F., 2012. Subcellular in vivo time-lapse imaging and surgery of *C. elegans* in standard multiwell plates. US20120129726A1.
- Tadao, I., 2014. Microcavity preparation. JP2015230377A.
- Yanik, M.F., Rohde, C., Angel, M.M., Gilleland, C.L., 2015. High-throughput, whole-animal screening system. US8961877B2.

**Chapter XI.** Extension of lifespan using a RNAi model  
and *in vivo* antioxidant effect of *Opuntia* fruit extracts  
and pure betalains in *Caenorhabditis elegans*

Part of this chapter was published in Food Chemistry  
Guerrero-Rubio et al. (2019) <https://doi.org/10.1016/j.foodchem.2018.09.067>



### Contextualization

Once the lifespan machine was ready for its use, a preliminary assay was carried out with four different model betalains (**Fig. 11.1**): betanin, indicaxanthin, phenylethylamine-betaxanthin and indoline-betacyanin. Betanin (betacyanin), the well-known pigment of beetroots, and indicaxanthin (betaxanthin), the main pigment of *Opuntia* fruits were chosen because they are the most abundant betalains in nature. Phenylethylamine-betaxanthin, naturally present in prickly pear (Castellanos-Santiago and Yahia, 2008), and indoline-betacyanin were chosen for their simple structure and close similarity as pigment models of betaxanthins and betacyanins, respectively, in addition to having a high antioxidant capacity (Gandía-Herrero et al., 2010a). In this chapter, the antioxidant and health-promoting effect of these betalains *in vivo* are detailed for the first time thanks to their administration as pure compounds to the model *C. elegans* as well as prickly pears extracts' administration as a natural source of betalains. Besides, the measurement of betalains' effect in the lifespan machine led the develop of a new method to avoid the progeny without the necessity of using of FUDR.

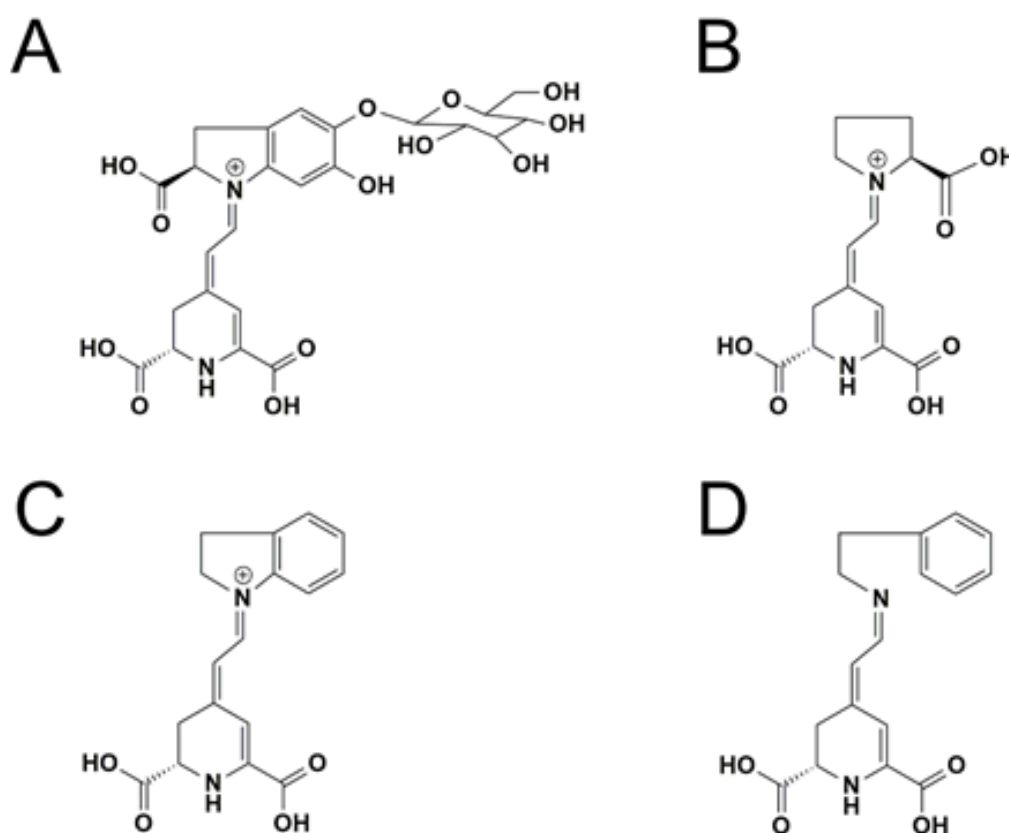


**Figure 11.1. Structures of betalains used in this study. A. Betanin. B. Indicaxanthin. C. Indoline-betacyanin. D. Phenylethylamine-betaxanthin.**

## 1. Antioxidant capacity of betalains *in vivo* in *C. elegans* strain TJ375

The fluorescence emitted by *C. elegans* strain TJ375 was employed to measure the antioxidant capacity of betalains. This strain contains a reporter transgene that expresses green fluorescence protein (GFP) upregulated by a promoter of a small heat shock protein (HSPs). HSPs are proteins widely present in the animal kingdom (Tower, 2009) and they are expressed in a stress situation (Feder and Hofmann, 1999). In *C. elegans*, HSPs are a group of 16 kDa proteins and their expression are induced in response to heavy metals (Stringham and Candido, 1994) or quinones (Link et al., 1999). Under oxidative stress, the fluorescence of the strain TJ375 is located in the pharynx because these worms contain the *hsp-16.2::GFP* (Link et al., 1999) construction which helps to determine the redox state of the worms. In this assay, the oxidative stress was induced to worms previously treated with betalains by the presence of juglone (naphthoquinone) 20  $\mu$ M.

For the four betalains studied, it was observed that as the concentration of the betalain in the medium increases, the expression of *hsp-16.2::GFP* decreases, evidenced by a decrease of the fluorescence intensity (**Fig. 11.2A-F**). At the lowest concentration assayed of 10  $\mu$ M, the betalains already produce a protection of the worms against the induced oxidative stress. At that concentration betacyanins' administration was less effective with a decrease in fluorescence of 11% for betanin and 27% for indoline-betacyanin in comparison to the untreated control group. The maximum effect in the decrease of fluorescence due to exposure to betanin or indoline-betacyanin were obtained at 100  $\mu$ M, reaching values of 76% and 85%, respectively. The values obtained for the betaxanthins indicaxanthin and phenylethylamine-betaxanthin were higher than those obtained for the betacyanins. Phenylethylamine-betaxanthin reached a fluorescence decrease of 93% at 100  $\mu$ M while indicaxanthin reached 94% at the same concentration.

The effective dose 50 (ED<sub>50</sub>) was established as the amount of betalain that produced a reduction of 50% of the initial fluorescence. The values obtained for each betalain were 24.4  $\mu$ M for betanin, 24.5  $\mu$ M for indoline-betacyanin, 9.4  $\mu$ M for indicaxanthin and 13.2  $\mu$ M for phenylethylamine-betaxanthin. Indicaxanthin was the most protective betalain *in vivo* against the oxidative stress (**Fig. 11.2G**) induced by juglone in *C. elegans*. The protective effect of some antioxidants had already been studied in the *C. elegans* TJ375 model with positive results, like resveratrol (Chen et

al., 2013b) or green tea extracts (Abbas and Wink, 2014), rich in catechins, which decreased the fluorescence emission by 40.7% and 68.4%, respectively. However, no antioxidant studied to date has given a 94% decrease, as indicaxanthin did.

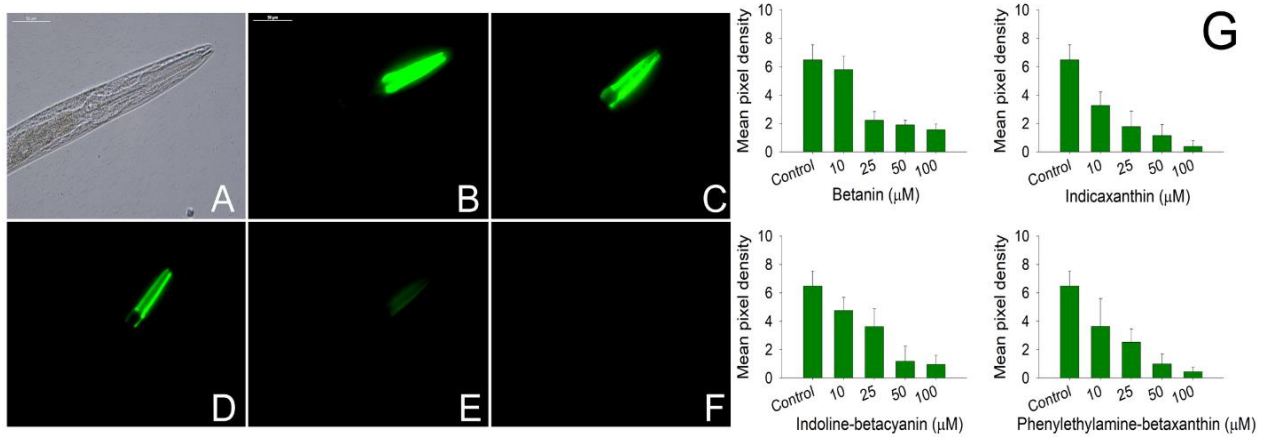


**Figure 11.2. Antioxidant effect of betalains *in vivo*.** A: Control worm of *C. elegans* strain TJ375 visualized under the bright field technique. B: The same specimen under fluorescence microscopy using the I3 filtercube. Fluorescence is located in the pharynx after juglone exposure. The decrease of fluorescence was observed in worms pre-treated with 10 (C), 25 (D), 50 (E) and 100 (F) μM of indicaxanthin. G: Quantification of the effect of pre-treatment with pure betalains measured through fluorescence integration.

## 2. Betalains effect on *C. elegans* lifespan

The wild-type N2 strain was used to study the health-protective effect of betalains by increasing the lifespan of *C. elegans*. Wild-type worms were exposed during 48 hours to concentrations of 10, 25, 50 and 100 μM of betalains. The worms were then transferred to fresh NGM plates supplemented with *E. coli* as a food source and incubated at 25 °C in the lifespan machine, where mean and maximum lifespan were measured. Mean lifespan was measured as the survival time of 50% of the population. Maximum lifespan refers to the survival time of the last worm alive. As shown in the **Table 11.1**, betanin did not produce a significant effect on the lifespan of the worms. However, indoline-betacyanin increased the mean lifespan by 10% at 25 and 50 μM and its effect reached a maximum value of 21.67% when the highest tested concentration (100 μM) was used (**Fig. 11.3**). In addition, exposure to indoline-betacyanin increased the maximum lifespan by 0.5 days. These values were even higher in worms exposed to the yellow betalains phenylethylamine-betaxanthin and indicaxanthin (**Fig. 11.3A**). Phenylethylamine-betaxanthin achieved an increase in mean survival of 14.29% and an increase of 2.4 days in the maximum lifespan when the worms were exposed to a 50 μM dose. The exposure to 50 μM of indicaxanthin

was the most efficient treatment, increasing the maximum lifespan by 3.96 days (Table 11.1, Fig. 11.4) and the mean survival by 32.42% (Table 11.1, Fig. 11.3A). At 25  $\mu$ M, mean survival increased by 34.34% and a maximum lifespan increase was recorded of 3.9 days. Although the maximum duration of life increased significantly ( $p < 0.05$ ) with these betaxanthins around 2-3 days, the use of the highest dose (100  $\mu$ M) resulted in a decrease in the mean and maximum life expectancy, respect to lower doses.

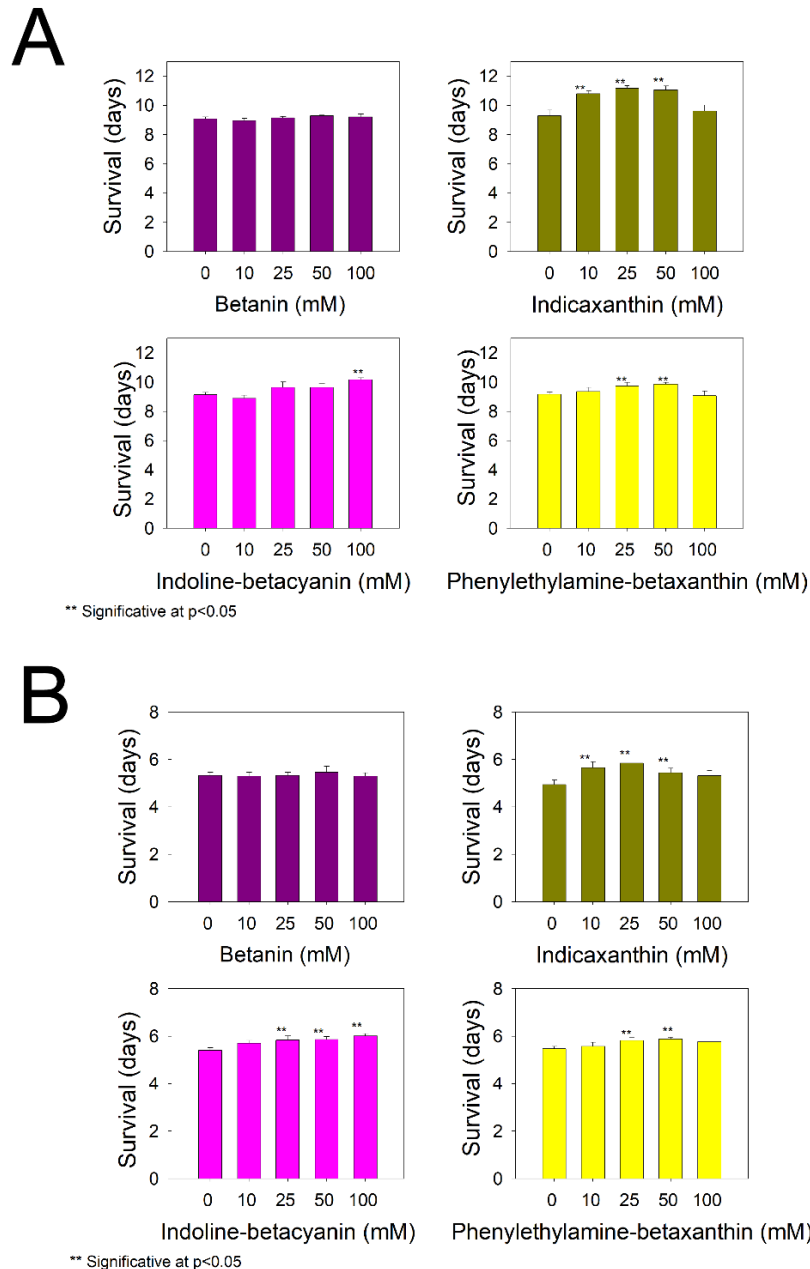


**Figure 11.3. Mean lifespan of *C. elegans* wild-type strain N2 sterilized by FUDR (A) or sterilized by feed with RNAi (B). Both groups of experiments were pre-treated with betanin, indicaxanthin, indoline-betacyanin and phenylethylamine-betaxanthin.**

Therefore, the optimal dose for indicaxanthin was 25  $\mu$ M, whereas for phenylethylamine-betaxanthin it was 50  $\mu$ M. Effective concentrations of betalains are much lower than those used for other antioxidant molecules like catechin, which enabled an increase of 13% in the maximum lifespan of *C. elegans* at 200  $\mu$ M concentration (Saul et al., 2009) or the flavonoids myricetin, quercetin and kaempferol, which at 100  $\mu$ M provoked an increase in the maximum lifespan (Grünz et al., 2012) of 21,7%, 18.4% and 6.7%, respectively. Thus, betalains are the most active antioxidants assayed in the life extension of *C. elegans*.

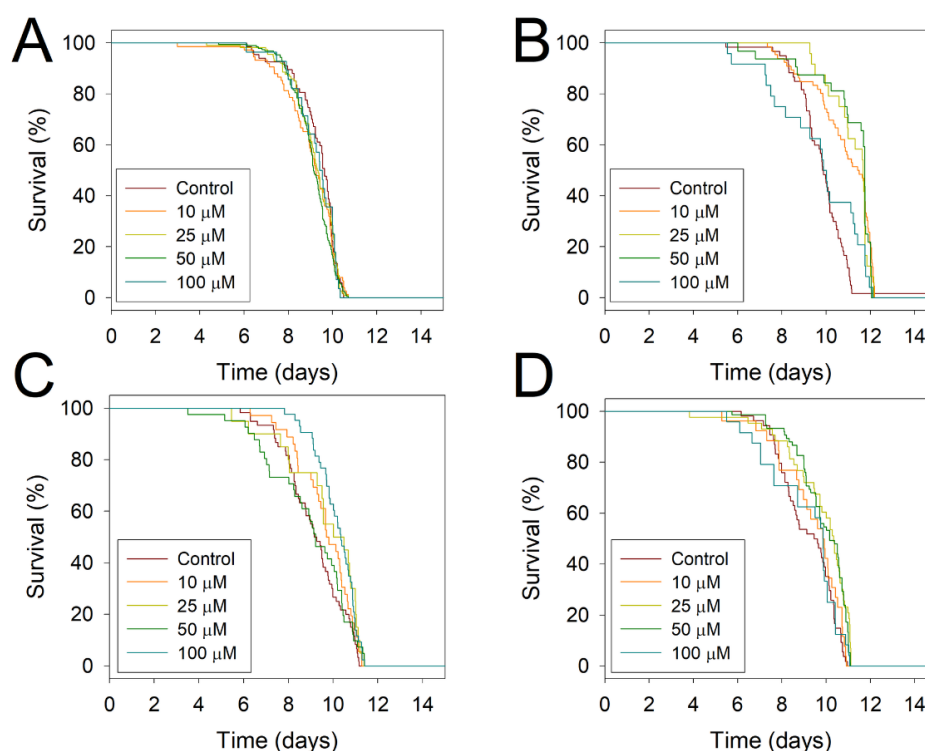


**Figure 11.4. Survival plots for *C. elegans* wild-type sterilized with FUDR and pre-treated with pure betalains. (A) Betanin, (B) indicaxanthin, (C) indoline-betacyanin and phenylethylamine-betaxanthin (D).**

### 3. Novel control of progeny based on *pop-1* RNAi

The lifespan assay was also performed employing RNAi instead of FUDR to produce sterility. FUDR is an antineoplastic antimetabolite that may expand the *C. elegans* lifespan via thymidylate synthase inhibition, and that may have impacts on FoxO transcription factors, sirtuins, and DNA repair pathways. It also increases the resistance of *C. elegans* to acute hypertonic stress, thermal stress, and anoxia (Anderson et al., 2016).



The chosen gene to knockdown was *pop-1*, which is involved in the development of the vulva and cell fate ([www.wormbase.org](http://www.wormbase.org)). The silencing of this gene causes sterility in L1 worms and embryonic death in L4 worms (Lin et al., 1995).

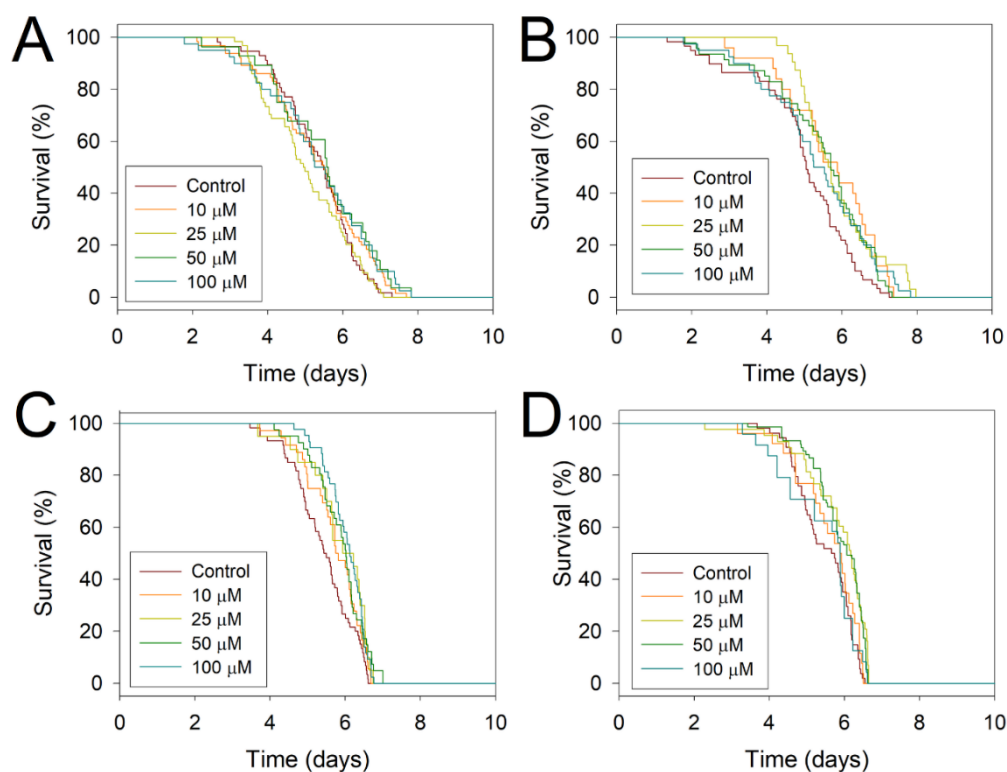
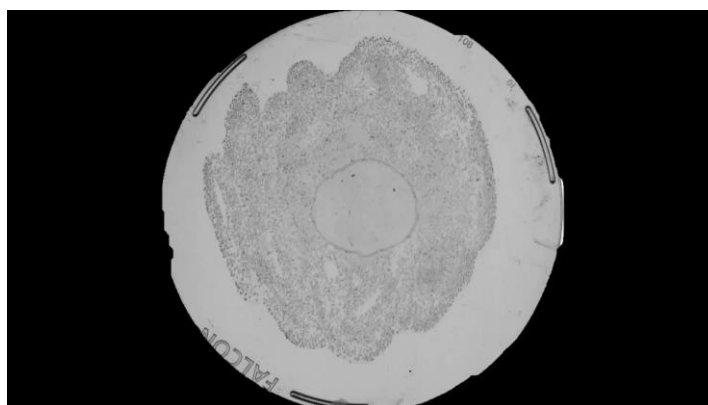


**Figure 11.5.** Survival plots for *C. elegans* wild-type sterilized by feed with RNAi (*E. coli* HT115) and pre-treated with pure betalains. (A) Betanin, (B) indicaxanthin, (C) indoline-betacyanin and phenylethylamine-betaxanthin (D).

Under the RNAi *C. elegans* assay, the tested betalains showed the same trend respect to the mean (**Fig. 11.3B**) and maximum lifespan (**Fig. 11.5**) effects than under the FUDR system. The exposure to betanin did not show any significant effect in the lifespan of worms while the betacyanin derived from indoline at 100  $\mu$ M increased the mean survival by 11.09% (**Table 11.2**). As shown in **Fig. 11.3B**, the lower effective concentration of betalains was obtained with the yellow ones. Phenylethylamine-betaxanthin used at 50  $\mu$ M increased 7.5% the lifespan and indicaxanthin expanded the mean lifespan up to 18.0% when used at 25  $\mu$ M. Therefore, the health-protective effect of indicaxanthin was confirmed with this alternative method and, as **Video 11.1** shows, the use of both FUDR or RNAi are efficient to avoid the presence of progeny.



**Video 11.1. *C. elegans* sterility.** The images obtained from the lifespan machine have been compacted into a video, with the three experiments: **A:** *C. elegans* strain N2 on NGM-agar plates treated with 40  $\mu$ M of FUDR to avoid progeny. **B:** *C. elegans* strain N2 feed with RNAi (*E. coli* HT115) to achieve sterility. **C:** Control *C. elegans* strain N2 without using a sterility method.

Video available:

<https://www.sciencedirect.com/science/article/pii/S0308814618316406?via%3Dihub#s0165>

The worms sterilized with FUDR and fed with heat shocked *E. coli* lived longer than the RNAi ones where the *E. coli* is active. Overall the effect of FUDR combined with heat shocked bacteria results in around a 40% expansion of lifespan in control worms. These results agree with Anderson *et al.*, (2016) research which stated that FUDR treated worms live longer than untreated ones and Stroustrup *et al.*, (2016), who obtained a longer lifespan when UV inactivated bacteria were used.

#### 4. Detection of betalains in worms through fluorescence

The natural fluorescence of betaxanthins could be quantified inside the worm's body and their position was also observed thanks to the thin epidermis of *C. elegans*. After seven days of incubation with betalains, worms treated with betacyanins did not present any color or fluorescence signal in microscopy assays. Previous studies demonstrated that betaxanthins maintain their fluorescent properties under physiological conditions and are responsible for visible fluorescence in flowers (Gandía-Herrero *et al.*, 2005b). Phenylethylamine-betaxanthin fluorescence was observed in *C. elegans* and reached a maximum value when worms were exposed to a 50  $\mu$ M dose (**Fig. 11.6D**). This result agrees with the maximum values obtained for this betalain in the lifespan assay and might to be indicative of its prevalence in the worm.

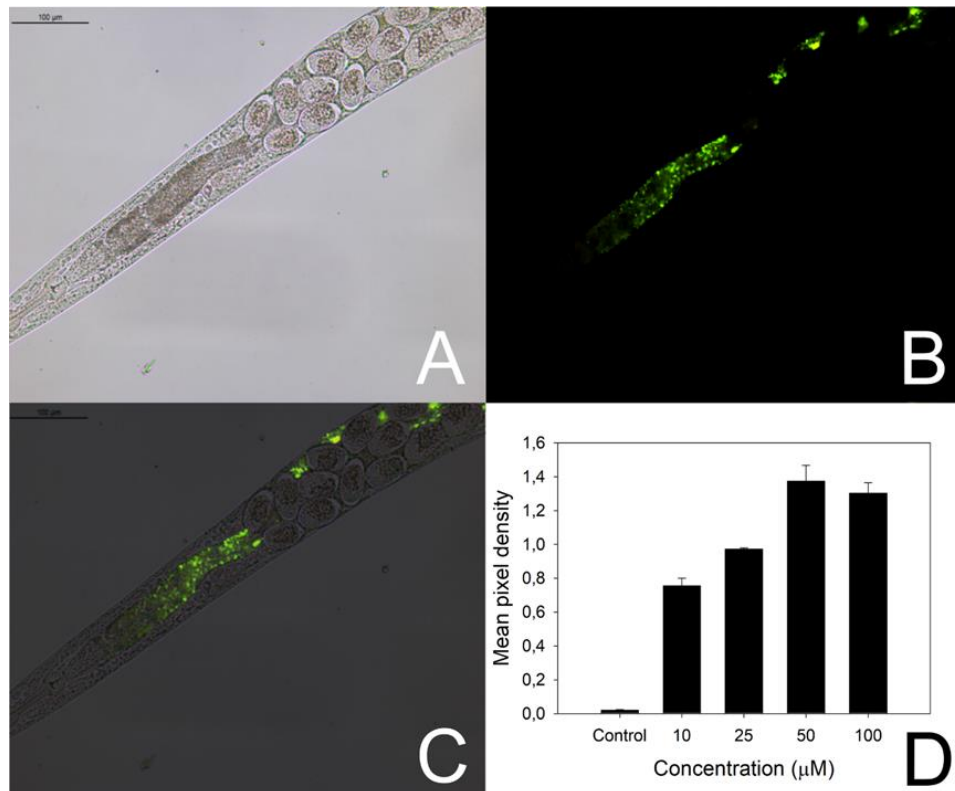


**Figure 11.6.** *C. elegans* wild-type strain N2 after seven days of treatment with phenylethylamine-betaxanthin. **A.** Brightfield image. **B.** Fluorescence emitted followed with Leica I3 filtercube. **C.** Merged image showing the location of the fluorescence in the digestive tube of *C. elegans*. **D.** Fluorescence emitted by *C. elegans* after treatments with different concentrations of phenylethylamine-betaxanthin.

Regarding localization of phenylethylamine-betaxanthin's fluorescence, **Fig. 11.6A-C** shows that this was detected in the digestive tube, indicating that betalains were incorporated into the organism through feeding. No fluorescence was detected for indicaxanthin fed *C. elegans*, which may be due to a higher metabolization. Phenylethylamine-betaxanthin is more hydrophobic and might be incorporated more efficiently into the worm tissues in the digestive system.

As it is exposed in the introduction section, fluorescence of betaxanthins has previously been employed to visualize petal cells (Gandía-Herrero et al., 2005a), to detect the presence of *Plasmodium falciparum* (malaria) in erythrocytes (Gonçalves et al., 2013), and to follow the accumulation of betaxanthins in *Celosia argentea* and *Chenopodium quinoa* cell cultures (Guadarrama-Flores et al., 2015; Henarejos-Escudero et al., 2018). This is the first time betaxanthins fluorescence is used to visualize animal tissues, confirming the potential of these pigments in microscopy applications.

## 5. Quantification of betalains in worms

HPLC was used to follow the presence of betalains and their derived product, betalamic acid, in worms extracts after seven days of exposure to betalains. Detection of supplemented betalains confirmed the accumulation of phenylethylamine-betaxanthin observed by microscopy. The accumulation of indoline-betacyanin was also detected at lower quantities. Indicaxanthin and betanin were not detected in the worm extracts, an indication -as commented above- that the most hydrophobic betalains tended to accumulate, whereas the most hydrophilic ones were rapidly metabolized. Between indoline-betacyanin and phenylethylamine-betaxanthin, the second was accumulated in higher proportions and both responses were dose-dependent (**Fig. 11.7**). Worms treated with a dose of 50  $\mu\text{M}$  of phenylethylamine-betaxanthin accumulated 26.35 moles per gram of protein. Worms treated with the same dose of indoline-betacyanin only accumulated 4.4 mols per gram of protein. Betalamic acid, analyzed as a possible metabolization product was not detected.

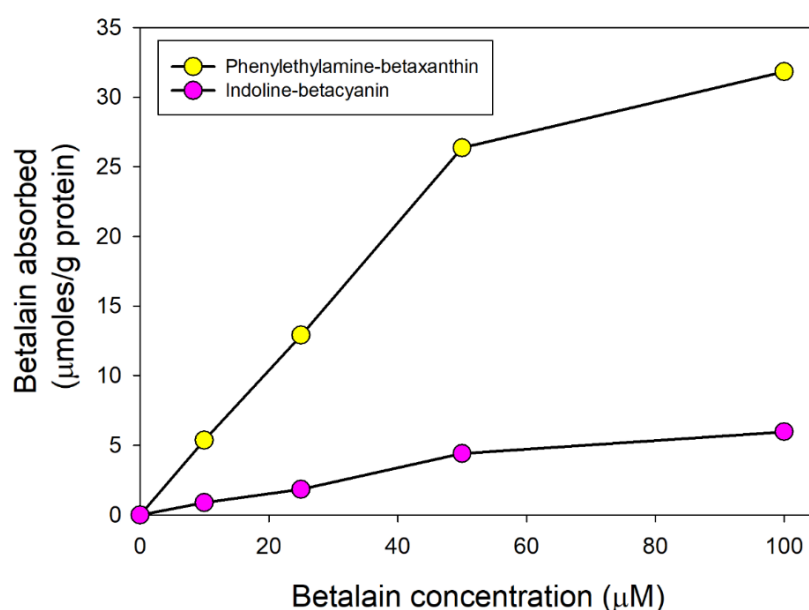


**Figure 11.7.** Quantification of phenylethylamine-betaxanthin and indoline-betacyanin accumulated in worm's soma expressed in  $\mu\text{moles betalain/g protein}$ .

## 6. Extracts of prickly pear as a source of betalains

Indicaxanthin was the most effective betalain in increasing the lifespan of *C. elegans*. This betalain is the main pigment found in yellow fruits of *Opuntia ficus-indica* (Gandía-Herrero et al., 2010b), although it is also present in red pears, where betanin is the main betalain (Forni et al., 1992). Extracts of red and yellow prickly

pears were employed to study their effect on the lifespan of *C. elegans* (**Fig. 11.8**). Different weight/volume (w/v) concentrations from extracts were used in the assay and were analyzed by HPLC. Pure indicaxanthin and betanin were used as standards to ascertain the concentration, expressed in  $\mu\text{M}$ , in prickly pear extracts. **Table 11.3** shows the relationship between w/v concentration from extracts and the concentration of the major pigment, expressed in  $\mu\text{M}$ . The analysis in the lifespan machine shows a significant increase in the average lifespan of *C. elegans* in the presence of 0.5% w/v from yellow extract, where the maximum lifespan was increased from 12.8 to 14.2 days and the mean survival increased by 21.06%. The red extract also increased the maximum lifespan from 12.8 to 13.7 days. This supposes an increase of 0.85 days in total lifespan but in this case, the mean survival did not increase significantly at any concentration of red extract, even having a negative effect on lifespan when the highest concentration was used.

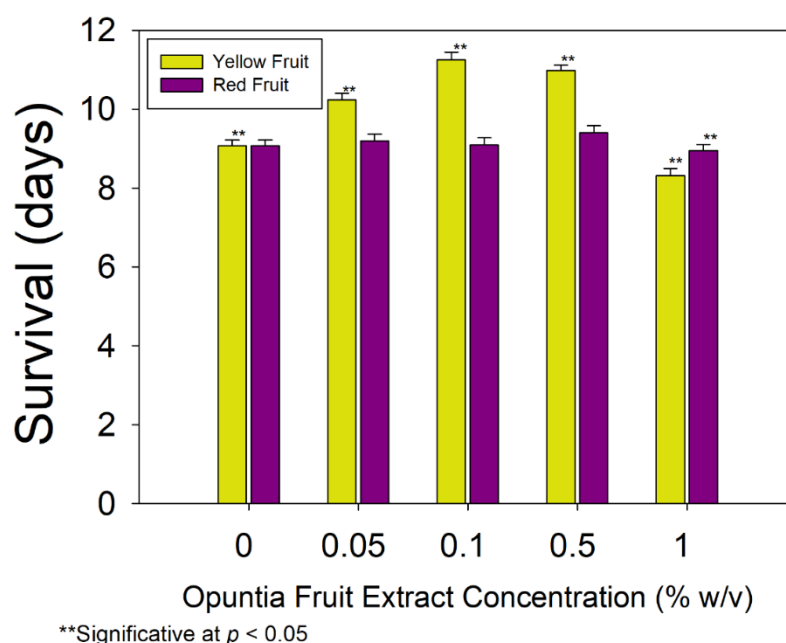


**Figure 11.8.** Lifespan of *C. elegans* wild type strain N2 treated with *Opuntia* extracts.

The antioxidant capacity of prickly pear had been demonstrated in *in vitro* assays (Butera et al., 2002) and the present results from tests in an *in vivo* system agree with the described effect against aging. In addition, our results are comparable with extracts rich in other antioxidant pigments, like purple wheat (Chen et al., 2013a) or Acai (*Euterpe precatoria*) (Peixoto et al., 2016) extracts, both rich in anthocyanins or Tsai Tai (*Brassica chinensis*) extract (Chen et al., 2016), rich in flavonoids and

hydroxycinnamic acid derivatives. The strong effect demonstrated for pure indicaxanthin justified the effect shown for the yellow extract of *Opuntia* fruits in the increase of the lifespan of *C. elegans*.

## 7. Conclusions

Pure individual betalains, both natural and semi-synthetic, have proven to exert health-promoting benefits *in vivo* in the *C. elegans* animal model. For the first time, antioxidant activity *in vivo* is demonstrated for betalains and justifies an increase in lifespan of more than 30% for treated *C. elegans*. The activity is also demonstrated for a natural edible source of the pigments, prickly pears, whose consumption had been previously demonstrated to present health-promoting benefits linked to the presence of indicaxanthin. The results of the present work open up new perspectives in the research and application of betalains as phytochemicals of interest for the food, cosmetic and pharmaceutical industries.

**Table 11.1. Effect of pure betalains in mean and maximum lifespan of *C. elegans* wild type strain N2 sterilized with FUDR.**

<b>Betalain</b>	<b>Concentration (<math>\mu</math>M)</b>	<b>Number of subjects</b>	<b>Survival (days)</b>	<b>Mean survival increase (%)</b>	<b>Maximum Lifespan (days)</b>
Betanin	0	167	9.09	0.00	10.5
	10	75	8.96	-1.43	10.7
	25	114	9.16	0.77	10.7
	50	195	9.29	2.20	10.7
	100	98	9.22	1.43	10.35
Indicaxanthin	0	75	9.9	0.00	10.9
	10	66	12.66	27.88	13.5
	25	64	13.3	34.34	14.8
	50	72	13.11	32.42	14.86
	100	64	10.54	6.46	14.4
Indoline- betacyanin	0	90	9.09	0.00	12.97
	10	76	8.73	-3.96	13.21
	25	80	10.05	10.56	13.4
	50	91	10.08	10.89	13.46
	100	73	11.06	21.67	13.45
Phenylethylamine- betaxanthin	0	94	9.45	0.00	10.9
	10	66	9.83	4.02	12.87
	25	83	10.65	12.70	13.3
	50	75	10.8	14.29	13.26
	100	74	9.28	-1.80	13.19

**Table 11.2. Effect of pure betalains in mean and maximum lifespan of *C. elegans* wild type strain N2 sterilized by feed with RNAi (*E. coli* HT115).**

Betalain	Concentration (uM)	Number of subjects	Survival (days)	Mean survival increase (%)	Maximum Lifespan (days)
Betanin	0	57	5.32	0.00	7.31
	10	65	5.3	-0.38	7.7
	25	64	5.32	0.00	7.08
	50	78	5.46	2.63	7.82
	100	54	5.31	-0.19	7.7
Indicaxanthin	0	59	4.95	0.00	7.26
	10	75	5.65	14.14	7.37
	25	82	5.84	17.98	7.97
	50	47	5.43	9.70	7.33
	100	40	5.31	7.27	7.82
Indoline- betacyanin	0	60	5.41	0.00	6.61
	10	66	5.71	5.55	6.68
	25	80	5.84	7.95	6.74
	50	71	5.87	8.50	7.5
	100	63	6.01	11.09	6.76
Phenylethylamine- betaxanthin	0	54	5.47	0.00	6.54
	10	76	5.58	2.01	6.61
	25	43	5.82	6.40	6.64
	50	75	5.88	7.50	6.62
	100	54	5.77	5.48	6.6



**Table 11.3. Effect of *Opuntia* extracts in mean and maximum lifespan of *C. elegans* wild type strain N2.**

Extract	Quantity of Extract (%)	Main pigment concentration ( $\mu$ M)	Survival (days)	Mean survival increase (%)	Maximum Lifespan (days)
Yellow	0	0	9.07	0	12.83
<i>Opuntia</i> fruit	0.05	0.029	10.24	12.89	12.71
	0.1	0.058	11.25	24.04	13.64
	0.5	0.29	10.98	21.06	14.21
	1	0.58	8.32	-8.27	12.68
Red <i>Opuntia</i>	0	0	9.07	0	12.83
fruit	0.05	0.033	9.2	1.43	12.52
	0.1	0.066	9.09	0.22	13.68
	0.5	0.33	9.4	3.64	12.56
	1	0.66	8.95	-1.32	11.9

## REFERENCES

- Abbas, S., Wink, M., 2014. Green tea extract induces the resistance of *Caenorhabditis elegans* against oxidative stress. *Antioxidants* 3, 129–143.  
<https://doi.org/10.3390/antiox3010129>
- Anderson, E.N., Corkins, M.E., Li, J.C., Singh, K., Parsons, S., Tucey, T.M., Sorkaç, A., Huang, H., Dimitriadi, M., Sinclair, D.A., Hart, A.C., 2016. *C. elegans* lifespan extension by osmotic stress requires FUDR, base excision repair, FOXO, and sirtuins. *Mech. Ageing Dev.* 154, 30–42.  
<https://doi.org/10.1016/j.mad.2016.01.004>
- Butera, D., Tesoriere, L., Di Gaudio, F., Bongiorno, A., Allegra, M., Pintaudi, A.M., Kohen, R., Livrea, M.A., 2002. Antioxidant activities of sicilian prickly pear (*Opuntia ficus indica*) fruit extracts and reducing properties of its betalains: Betanin and indicaxanthin. *J. Agric. Food Chem.* 50, 6895–6901.  
<https://doi.org/10.1021/jf025696p>
- Castellanos-Santiago, E., Yahia, E.M., 2008. Identification and quantification of betalains from the fruits of 10 Mexican prickly pear cultivars by high-performance liquid chromatography and electrospray ionization mass spectrometry. *J. Agric. Food Chem.* 56, 5758–5764.  
<https://doi.org/10.1021/jf800362t>
- Chen, J., Zhang, J., Xiang, Y., Xiang, L., Liu, Y., He, X., Zhou, X., Liu, X., Huang, Z., 2016. Extracts of Tsai Tai (*Brassica chinensis*): enhanced antioxidant activity and anti-aging effects both in vitro and in *Caenorhabditis elegans*. *Food Funct.* 7, 943–952. <https://doi.org/10.1039/C5FO01241D>
- Chen, W., Müller, D., Richling, E., Wink, M., 2013a. Anthocyanin-rich purple wheat prolongs the life span of *Caenorhabditis elegans* probably by activating the DAF-16/FOXO transcription factor. *J. Agric. Food Chem.* 61, 3047–3053.  
<https://doi.org/10.1021/jf3054643>
- Chen, W., Rezaizadehnajafi, L., Wink, M., 2013b. Influence of resveratrol on oxidative stress resistance and life span in *Caenorhabditis elegans*. *J. Pharm. Pharmacol.* 65, 682–688. <https://doi.org/10.1111/jphp.12023>
- Feder, M.E., Hofmann, G.E., 1999. Heat-shock proteins, molecular chaperones, and the stress response: evolutionary and ecological physiology. *Annu. Rev. Physiol.* 61, 243–282. <https://doi.org/10.1146/annurev.physiol.61.1.243>

- Forni, E., Polesello, A., Montefiori, D., Maestrelli, A., 1992. High-performance liquid chromatographic analysis of the pigments of blood-red prickly pear (*Opuntia ficus indica*). J. Chromatogr. 593, 177–183. [https://doi.org/10.1016/0021-9673\(92\)80284-2](https://doi.org/10.1016/0021-9673(92)80284-2)
- Gandía-Herrero, F., Escribano, J., García-Carmona, F., 2010a. Structural implications on color, fluorescence, and antiradical activity in betalains. Planta 232, 449–460. <https://doi.org/10.1007/s00425-010-1191-0>
- Gandía-Herrero, F., Escribano, J., García-Carmona, F., 2005a. Betaxanthins as pigments responsible for visible fluorescence in flowers. Planta 222, 586–593. <https://doi.org/10.1007/s00425-005-0004-3>
- Gandía-Herrero, F., García-Carmona, F., Escribano, J., 2005b. Floral fluorescence effect. Nature 437, 334. <https://doi.org/10.1038/437334a>
- Gandía-Herrero, F., Jiménez-Atiénzar, M., Cabanes, J., García-Carmona, F., Escribano, J., 2010b. Stabilization of the bioactive pigment of *Opuntia* fruits through maltodextrin encapsulation. J. Agric. Food Chem. 58, 10646–10652. <https://doi.org/DOI:10.1021/jf101695f>
- Gonçalves, L.C.P., Tonelli, R.R., Bagnaresi, P., Mortara, R.A., Ferreira, A.G., Bastos, E.L., 2013. A nature-inspired betalamic probe for live-cell imaging of Plasmodium-infected erythrocytes. PLoS One 8, e53874. <https://doi.org/10.1371/journal.pone.0053874>
- Grünz, G., Haas, K., Soukup, S., Klingenspor, M., Kulling, S.E., Daniel, H., Spanier, B., 2012. Structural features and bioavailability of four flavonoids and their implications for lifespan-extending and antioxidant actions in *C. elegans*. Mech. Ageing Dev. 133, 1–10. <https://doi.org/10.1016/j.mad.2011.11.005>
- Guadarrama-Flores, B., Rodríguez-Monroy, M., Cruz-Sosa, F., García-Carmona, F., Gandía-Herrero, F., 2015. Production of dihydroxylated betalains and dopamine in cell suspension cultures of *Celosia argentea* var. plumosa. J. Agric. Food Chem. 63, 2741–2749. <https://doi.org/10.1021/acs.jafc.5b00065>
- Henarejos-Escudero, P., Guadarrama-Flores, B., Guerrero-Rubio, M.A., Gómez-Pando, L.R., García-Carmona, F., Gandía-Herrero, F., 2018. Development of betalain producing callus lines from colored quinoa varieties (*Chenopodium quinoa* Willd). J. Agric. Food Chem. 66, 467–474. <https://doi.org/10.1021/acs.jafc.7b04642>

- Lin, R., Thompson, S., Priess, J.R., 1995. pop-1 encodes an HMG box protein required for the specification of a mesoderm precursor in early *C. elegans* embryos. *Cell* 83, 599–609. [https://doi.org/10.1016/0092-8674\(95\)90100-0](https://doi.org/10.1016/0092-8674(95)90100-0)
- Link, C.D., Cypser, J.R., Johnson, C.J., Johnson, T.E., 1999. Direct observation of stress response in *Caenorhabditis elegans* using a reporter transgene. *Cell Stress Chaperones* 4, 235. DOI: 10.1379/1466-1268(1999)004<0235:doosri>2.3.co;2
- Peixoto, H., Roxo, M., Krstin, S., Röhrig, T., Richling, E., Wink, M., 2016. An anthocyanin-rich extract of acai (*Euterpe precatoria* Mart.) Increases stress resistance and retards aging-related markers in *Caenorhabditis elegans*. *J. Agric. Food Chem.* 64, 1283–1290. <https://doi.org/10.1021/acs.jafc.5b05812>
- Saul, N., Pietsch, K., Menzel, R., Stürzenbaum, S.R., Steinberg, C.E.W., 2009. Catechin induced longevity in *C. elegans*: From key regulator genes to disposable soma. *Mech. Ageing Dev.* 130, 477–486. <https://doi.org/10.1016/j.mad.2009.05.005>
- Stringham, E.G., Candido, E.P.M., 1994. Transgenic hsp 16-Lacz strains of the soil nematode *Caenorhabditis elegans* as biological monitors of environmental stress. *Environ. Toxicol. Chem.* 13, 1211–1220. <https://doi.org/10.1002/etc.5620130802>
- Stroustrup, N., Anthony, W.E., Nash, Z.M., Gowda, V., Gomez, A., López-Moyado, I.F., Apfeld, J., Fontana, W., 2016. The temporal scaling of *Caenorhabditis elegans* ageing. *Nature* 530, 103–107. <https://doi.org/10.1038/nature16550>
- Tower, J., 2009. Hsps and aging. *Trends Endocrinol. Metab.* 20, 216–222. <https://doi.org/10.1016/j.tem.2008.12.005>



**Chapter XII.** Betalain health-promoting effects after ingestion in  
*Caenorhabditis elegans* are mediated by  
DAF-16/FOXO and SKN-1/Nrf2 transcription factors

Part of this chapter was published in Food Chemistry  
Guerrero-Rubio et al. (2020) <https://doi.org/10.1016/j.foodchem.2020.127228>



### **Contextualization**

The preliminary assays described in chapter XI demonstrated *in vivo* the health-promoting effects of pure betalains as well as the positive effect of cactus pears. In the present chapter the study of pure compounds is expanded to seventeen pure betalains which allows to deepen on the knowledge of the individual behavior of betalains tested *in vivo* and allows for the first time to study the mechanisms and pathways involved in their bioactivities using the model animal *C. elegans*.

## **1. Synthesis of betalains**

Using the novel approach previously described in the chapter VI, 15 different betalains were obtained in the biofactories. Some of these betalains are naturally present in plants, such as dopaxanthin, present in the yellow flowers of *L. productus* (Gandía-Herrero et al., 2005a), or miraxanthin I, present in *Mirabilis jalapa* flowers (Piattelli et al., 1965). However, their presence in plants is in small quantities and usually in complex mixtures and the production in bioreactors offers higher amounts and purity than extraction procedures from plants.

After ion exchange and C18 reversed phase chromatography applied to each betalain obtained by biotransformation, HPLC analyses were performed to confirm their purity (**Fig. 12.1**). Twelve different yellow betaxanthins with maximum absorbance values around 475 nm were obtained: miraxanthin I, vulgaxanthin I, vulgaxanthin II, vulgaxanthin III, vulgaxanthin IV, indicaxanthin, dopaxanthin, and the betaxanthins derived from phenylalanine, phenylethylamine, pyrrolidine, valine, and tryptophan. The retention times (RT) of these betaxanthins were 6.17 min for vulgaxanthin III, 8.21 for vulgaxanthin I, 8.67 min for miraxanthin I, 9.82 min for vulgaxanthin II, 12.65 min for indicaxanthin, 13.91 min for dopaxanthin, 13.99 min for pyrrolidine-betaxanthin, 15.45 min for valine-betaxanthin, 18.82 min for vulgaxanthin IV, 20.08 min for phenylalanine-betaxanthin, 20.28 min for tryptophan-betaxanthin, and 22.10 min for phenylethylamine-betaxanthin. Aniline precursor produced a soft pink colored betalain considered an intermediate pigment between a yellow betaxanthin, and a red-violet betacyanin with a  $\lambda_{\text{max}} = 507$  nm and with a retention time of 19.29 min., as it is described in the bibliography (Gandía-Herrero et al., 2010).



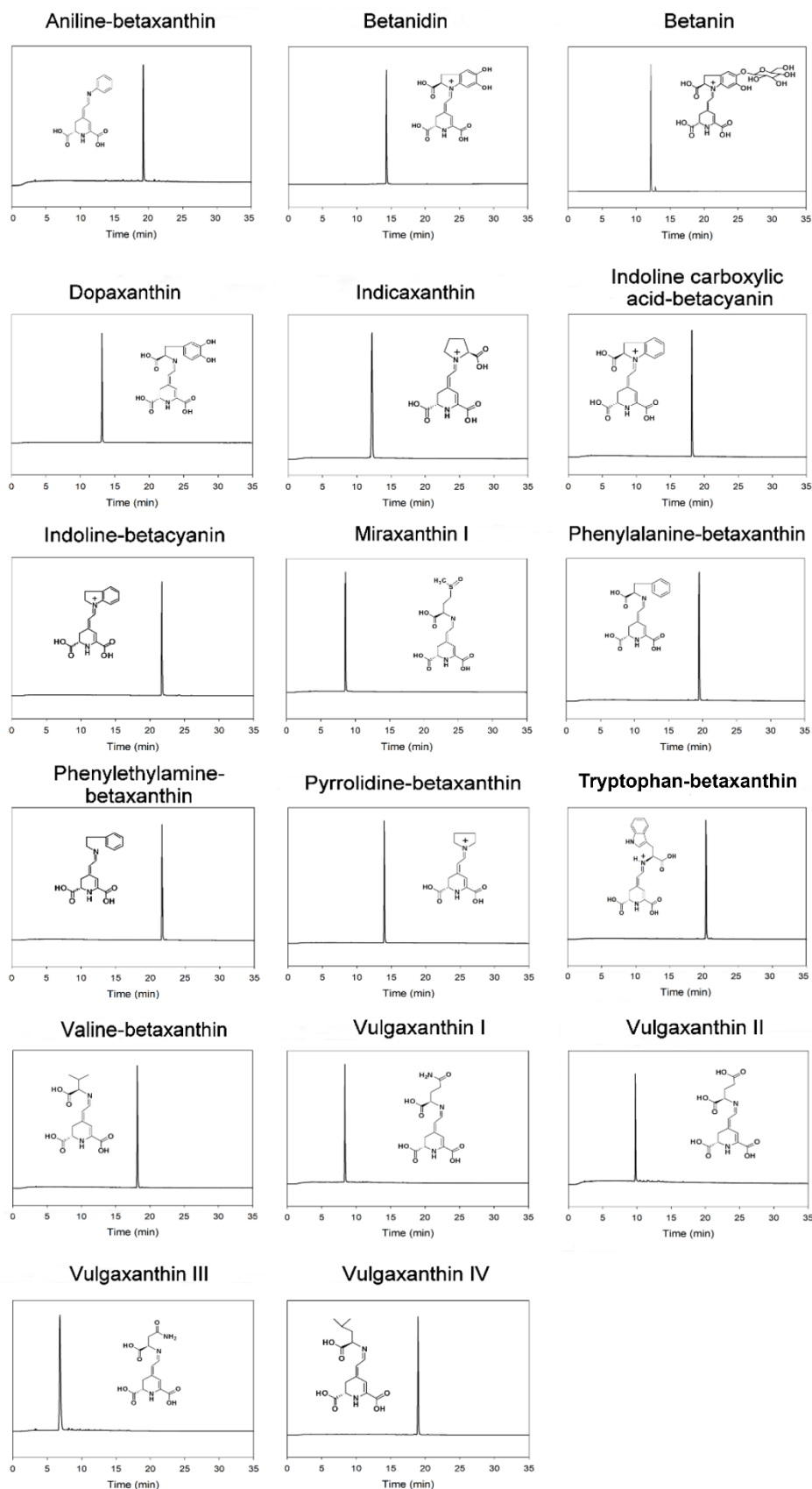


**Figure 12.1. Chemical structures and purity analysis by HPLC for the individual betalains considered in this study.** (Continues on the next page)

Chromatograms are shown at a wavelength of 480 nm for betaxanthins, at 508 nm for aniline-betaxanthin and at 536 nm for the betacyanins betanin, betanidin, indoline-betacyanin and indoline carboxylic acid-betacyanin, in all cases demonstrating the presence of pure individual betalains.

The betacyanins derived from indoline carboxylic acid and indoline were also obtained and showed a red-violet color characteristic of betacyanins and the HPLC analysis confirmed a maximum absorbance at  $\lambda_{\text{max}} = 524$  nm with retention times of 19.17 min and 22.10 min, respectively. Betanidin (RT = 14.31 min,  $\lambda_{\text{max}} = 542$  nm) and betanin (RT = 12.14 min,  $\lambda_{\text{max}} = 536$  nm) were obtained and purified from plant extracts, providing a total of seventeen pure betalains obtained for the present study.

## 2. Antioxidant and free radical scavenging activities of pure betalains

The pure betalains obtained were assayed for *in vitro* antioxidant and antiradical scavenging activities using three different methods: ABTS, FRAP and ORAC. ABTS assay is based on the capacity of the molecules to reduce ABTS  $\cdot^+$  radical to ABTS; FRAP assay is based on the capacity to reduce Fe (III) to Fe (II); and ORAC is based on the capacity of the molecules to protect the fluorescent probe fluorescein from peroxy radicals. The seventeen pure molecules' activity was measured and compared with Trolox (6-hydroxy-2,5,7,8-tetramethylchroman-2-carboxylic acid) activity, and the results were given as Trolox equivalent antioxidant capacity (TEAC).

The results were consistent among the three assays with slight differences as shown in **Fig. 12.2** and **Fig. 12.3**. Betanidin and dopaxanthin were the most antioxidant betalains tested with ABTS values of 6.9 and 6.8 TEAC, respectively. Both pigments present an *ortho*-diphenol structural motif that might be responsible for their enhanced radical scavenging activity (Gandía-Herrero et al., 2009; Gliszczyńska-Świgło et al., 2006). When one of the hydroxyl groups of the *o*-diphenol was blocked, as occurs in betanin, the antioxidant activity decreased to 4.3 TEAC in the ABTS assay. The absence of hydroxyl groups affects the antioxidant activity deeply, as occurs with phenylalanine-betaxanthin, which presents a value of 2.6 TEAC in the ABTS assay, 4.2 units lower than dopaxanthin, which presents the same structure but holds two hydroxyl groups in the aromatic ring. Tryptophan-betaxanthin has a value of 5.28 TEAC in the ABTS assay. Its structure does not have any hydroxyl groups; therefore, the antioxidant activity may be due to the nitrogen atom of the indole ring. Nayak *et al.* (Nayak and Buttar, 2016) obtained similar results for the free amino acid tryptophan

(7.9 TEAC units) using the ORAC assay and argued that the measured antioxidant activity could be due to the indole ring or also due to the conversion from tryptophan to 3-hydroxykynurenine or 3-hydroxy anthranilic acid, which are potent antioxidants.

Betacyanins derived from indoline and indoline 2-carboxylic acid also have an indole-like ring. However, the nitrogen atom of the indoline forms part of the core structure of the betalains and has no hydrogen atoms. The blockage of the nitrogen group results in a decrease in the antioxidant activity to 4.10 units for indoline-betacyanin and to 3.8 for indoline carboxylic acid-betacyanin. Herraiz and Galisteo (2004), measured the antioxidant activity of free indoline and indoline 2-carboxylic acid and reported activities of 1.39 and 1.04 respectively for ABTS assay, indicating that the fusion of the indole group with betalamic acid increases the antioxidant activity.

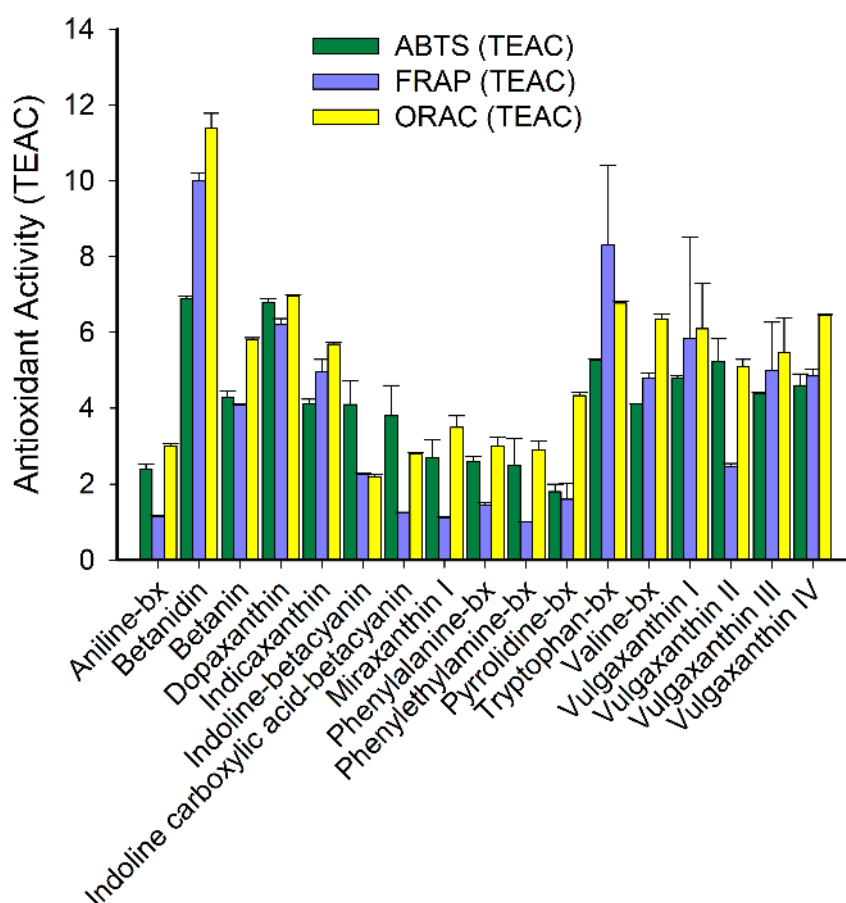


**Figure. 12.2. Antioxidant activity of betalains measured with three different *in vitro* methods (ABTS, FRAP and ORAC).** Three independent trials were assayed in each case, being represented the average value. Error bars represent standard deviation.

Vulgaxanthins (I to IV) and valine-betaxanthin showed intermediate antioxidant activities in the range of 5.23 to 4.11 units for ABTS assay. These structures have lineal

side chains, positively or negatively charged with primary amines and carboxylic acids. While these groups have not been reported to have high antioxidant activities, their reaction with betalamic acid seems to enhance the antioxidant activity of betalamic acid between 2.53 and 1.41 units. Interestingly, the results for the different molecules were quite similar for ABTS, FRAP and ORAC. However, vulgaxanthin II had lower activity in the FRAP assay than in ABTS and ORAC assays, probably due to the low pH used for the FRAP method.

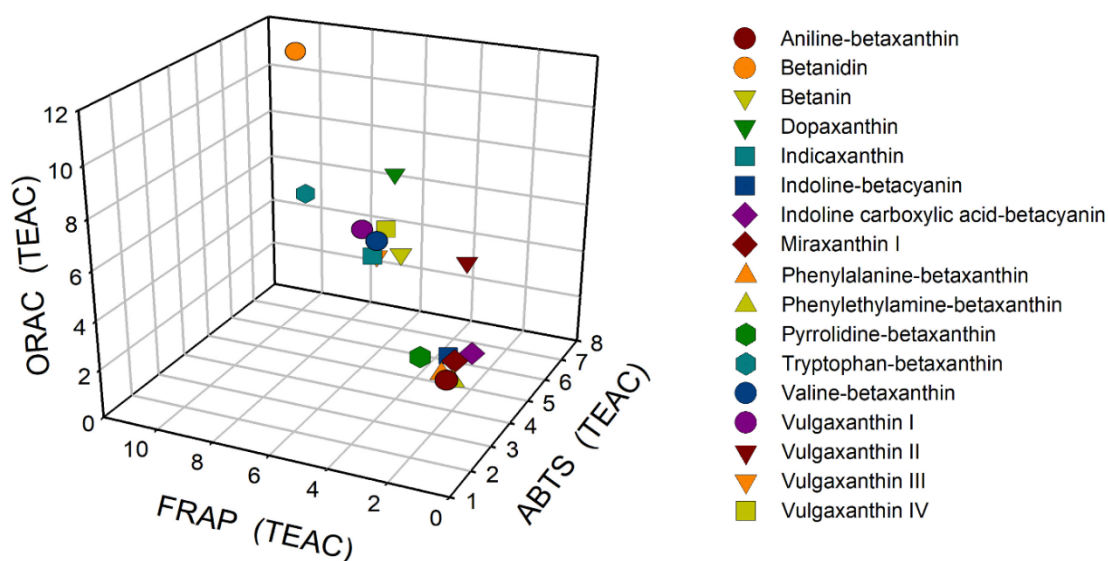


**Figure 12.3. Comparative analysis of antioxidant and free radical scavenging capacities of betalains by three different *in vitro* methods.**

Indicaxanthin and pyrrolidine-betaxanthin have a pyrrolidine ring motif. Additionally, indicaxanthin has a carboxylic acid group attached to the ring, which might be responsible for its enhanced antioxidant activity. Miraxanthin I, phenylethylamine-betaxanthin and aniline-betaxanthin had antioxidant values ranging from 2.7 to 2.4. Miraxanthin I has an aliphatic chain and a sulfoxide group, but the similar antioxidant activity with betalamic acid suggests that the methionine sulfoxide group was not involved in the antioxidant activity of the molecule. Aniline-betaxanthin and phenylethylamine-betaxanthin structures differ in an ethylene group ( $-\text{CH}_2\text{-CH}_2-$ ) that connects the amine and the aromatic ring and, like pyrrolidine-betaxanthin, they lack free hydroxyl groups. The influence of these structural motifs on the antioxidant capacity of betalains is limited and pyrrolidine, aniline and phenylethylamine-derived betalains show similar antioxidant activity than betalamic acid (Gandía-Herrero et al., 2012).

### 3. Antioxidant capacity of betalains *in vivo* in *C. elegans* strain TJ375

The antioxidant capacity of betalains was also studied *in vivo* by measuring the fluorescence intensity emitted by *C. elegans* TJ375. This strain contains a reporter transgene that expresses a green fluorescence protein (GFP) upregulated by a promoter of small heat shock proteins (HSPs) (Feder and Hofmann, 1999). Their expression is induced in response to heavy metals (Stringham and Candido, 1994) or quinones (Link et al., 1999). The *hsp-16.2::GFP* construction is responsible for the fluorescence emitted in the pharynx cells of *C. elegans* TJ375 under oxidative stress. The previously purified betalains were used in this assay at 25  $\mu$ M. The antioxidant *in vivo* effect of betanin, indoline-betacyanin, indicaxanthin and phenylethylamine-betaxanthin was reported in the previous chapter with indicaxanthin being the most antioxidant. As for the previous molecules studied, their presence in the culture medium produced a decrease in the expression of *hsp-16.2::GFP*, showing a decrease in the fluorescence intensity of 7.96% for miraxanthin I, 17.21% for pyrrolidine-betaxanthin, 23.03% for tryptophan-betaxanthin, 29.88% for vulgaxanthin III, 38.95% for aniline-betaxanthin, 42.28% for vulgaxanthin IV, 58.75% for vulgaxanthin I, 65.31% for betanidin, 68.83% for phenylalanine-betaxanthin, 77.06% for indoline carboxylic acid-betacyanin, and 84% for dopaxanthin (**Fig. 12.4**). Only two molecules (valine-betaxanthin and vulgaxanthin II) failed to significantly decrease the oxidative stress in the animals - an indication that not all the molecules characterized as antioxidants *in vitro* are effective *in vivo*. Dopaxanthin was the most protective betalain *in vivo* against the oxidative stress induced in *C. elegans*. The decreases of fluorescence obtained at 25  $\mu$ M for dopaxanthin, indoline carboxylic acid-betacyanin, and phenylalanine-betaxanthin were higher than the value obtained for the betalains previously studied in the chapter XI, where the fluorescence decreased up to 66.59% in the presence of indicaxanthin. To set up the effective dose 50 (ED<sub>50</sub>) for these three betalains, concentrations of 5, 10, 25 and 50  $\mu$ M were employed. ED<sub>50</sub> was established as the amount of betalain that produced a reduction of 50% of the initial fluorescence.

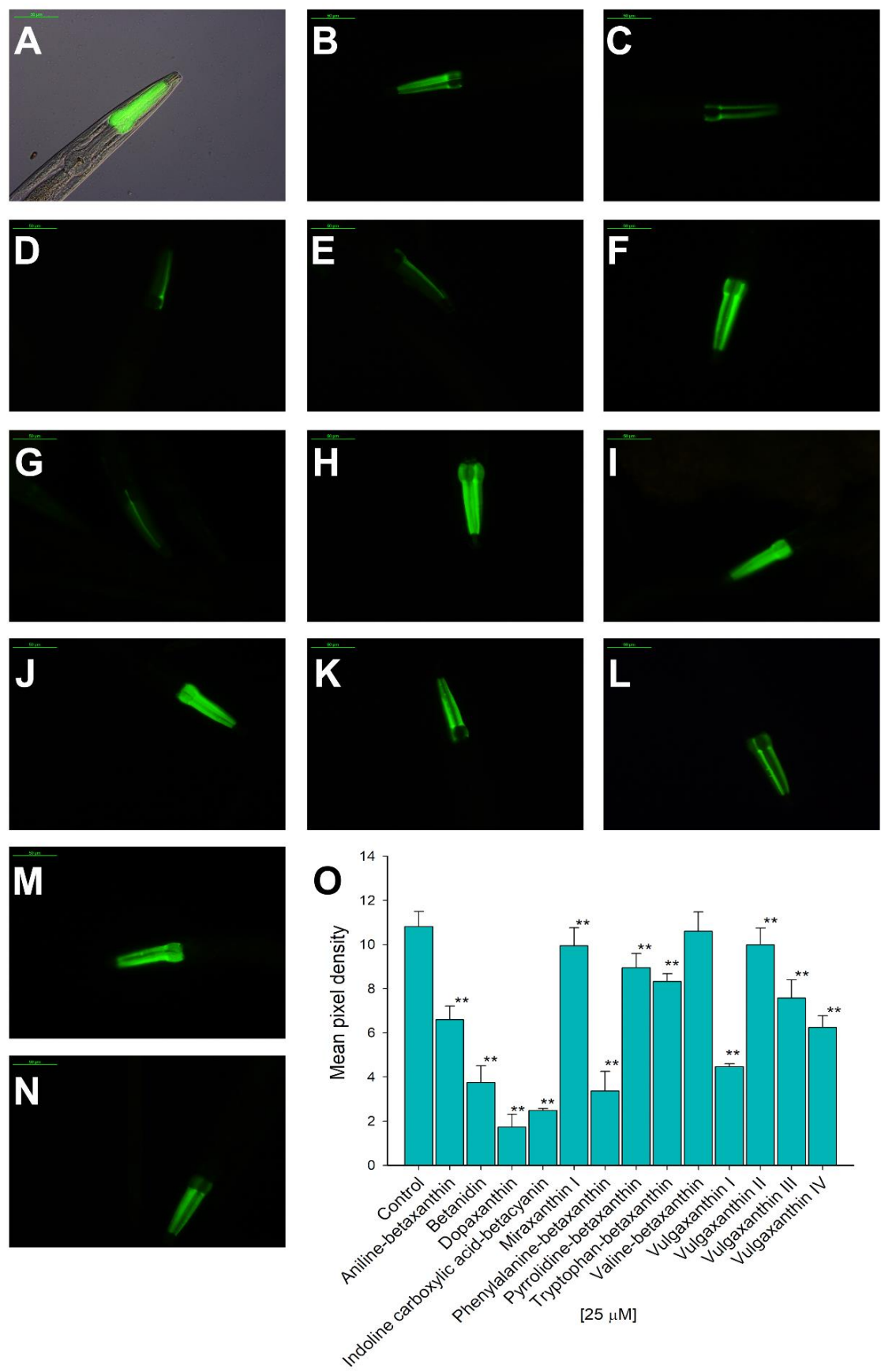
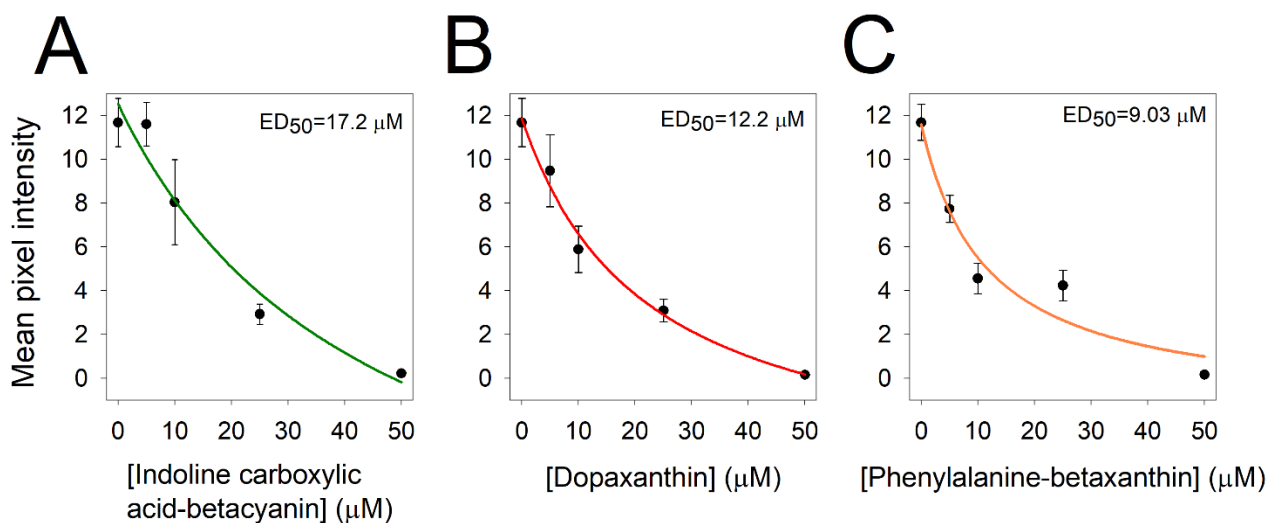


Figure 12.4. Antioxidant effect of betalains *in vivo*. (Continues on the next page)

**A** Merged image from a control worm of TJ375 *C. elegans* visualized under bright field technique and fluorescence microscopy using the I3 filtercube. Fluorescence is located in the pharynx of the worms after juglone exposure. **B-N** The diminution of fluorescence was observed in worms pre-treated with 25  $\mu\text{M}$  of: aniline-betaxanthin **B**, betanidin **C**, dopaxanthin **D**, indoline carboxylic acid-betacyanin **E**, miraxanthin **F**, phenylalanine-betaxanthin **G**, pyrrolidine-betaxanthin **H**, tryptophan-betaxanthin **I**, valine-betaxanthin **J**, vulgaxanthin I **K**, vulgaxanthin II **L**, vulgaxanthin III **M** and vulgaxanthin IV **N**. **O**. Quantification of the effect of pre-treatment with pure betalains measured through fluorescence integration. Two independent trials were made using  $n \geq 10$  in each trial. Scale bars: 50  $\mu\text{m}$ , data is presented as mean  $\pm$  S.D, statistical results are summarized in the Annex III.

The  $\text{ED}_{50}$  values obtained for each betalain were 17.2  $\mu\text{M}$  for indoline carboxylic acid-betacyanin, 12.2  $\mu\text{M}$  for dopaxanthin and 9.03  $\mu\text{M}$  for phenylalanine-betaxanthin (**Fig. 12.5**). So far, indicaxanthin was the most antioxidant pigment described, with an  $\text{ED}_{50} = 9.4$   $\mu\text{M}$  for *in vivo* *C. elegans* assays (chapter XI). However, the  $\text{ED}_{50}$  value obtained for the three best betalains of this work revealed phenylalanine-betaxanthin has a lower value than indicaxanthin, making it the most antioxidant pigment described *in vivo* in the *C. elegans* animal model.



**Figure 12.5. Calculation of the effective dose 50 ( $\text{ED}_{50}$ ) in *C. elegans* TJ375 of the most effective betalains. A. Indoline carboxylic acid-betacyanin. B. Dopaxanthin. C. Phenylalanine-betaxanthin. Data information:  $\text{ED}_{50}$  is established as the amount of betalain that produced a reduction of 50% of the initial fluorescence in the pharynx of the worms.**

The discrepancies between *in vitro* and *in vivo* results (**Fig. 12.6**) may be caused by the bioavailability and reactivity of the compounds. A rapidly oxidizable or difficult to absorb compound may be active in *in vitro* assays but could show low activity *in vivo*. The data indicated that molecules with positive charge are less efficient in reducing reactive oxygen species (ROS) *in vivo*, although they showed some potential *in vitro*. The use of the described library of compounds has allowed this level of discussion in the family of betalains for the first time.

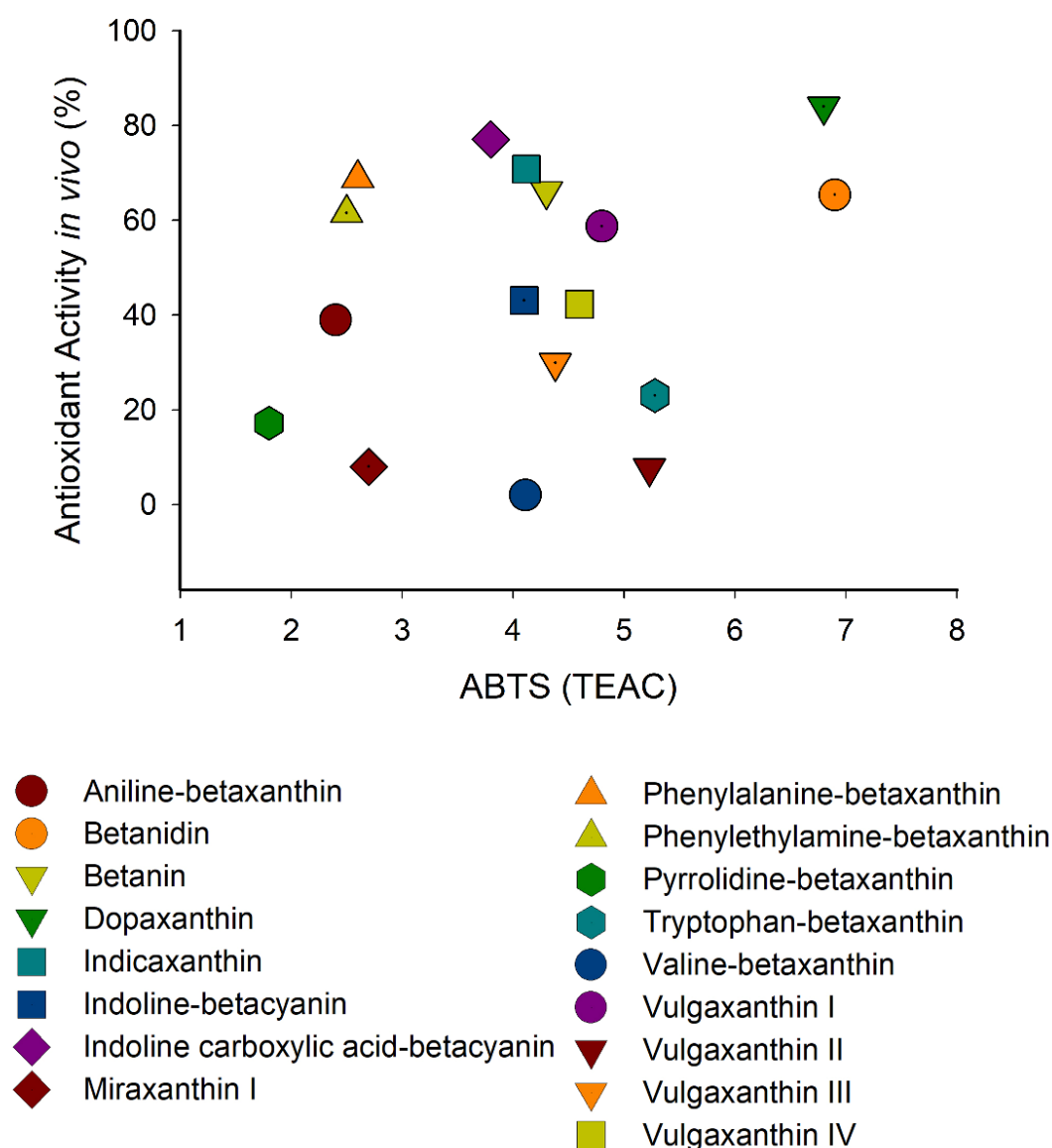


**Figure 12.6.** Comparative analysis of the antioxidant capacity of betalains *in vivo* vs. *in vitro* by ABTS assay.



#### 4. Betalains effect on *C. elegans* lifespan

The health-promoting effect of betalains was asserted by measuring the capacity of the molecules to extend *C. elegans* lifespan. Although, betanin and indicaxanthin effects on lifespan have already been reported in the previous chapter, they were included in this experiment as they are the two most representative molecules of the betacyanins and betaxanthins families, respectively. As shown in **Table 12.1** and **Fig. 12.8**, betalains treatment increased the mean lifespan of the wild type strain by the following values: 3.45% for vulgaxanthin IV, 3.52% for vulgaxanthin II, 3.56% for aniline-betaxanthin, 4.40% for vulgaxanthin, 4.44% for tryptophan-betaxanthin, 5.72% for pyrrolidine-betaxanthin, 6.15% for miraxanthin I, 12.93% for dopaxanthin, 16.53% for phenylalanine-betaxanthin and 16.65% for indoline-carboxylic acid-betacyanin. Vulgaxanthin II, valine-betaxanthin, betanidin or betanin did not present any positive effect on the *C. elegans* lifespan. However, as the results showed, they were non-toxic.

The optimal dose for the three best betalains was also obtained. Mean lifespan was measured for worms treated with 10, 25, 50 and 100  $\mu\text{M}$  of dopaxanthin, phenylalanine-betaxanthin and indoline carboxylic acid-betacyanin. The optimal dose for phenylalanine-betaxanthin was 25  $\mu\text{M}$ , 10  $\mu\text{M}$  for indoline carboxylic acid-betacyanin and 100  $\mu\text{M}$  for dopaxanthin, with remarkable increases in the lifespan of 16.55%, 12.92% and 20.52%, respectively (**Fig. 12.7**).

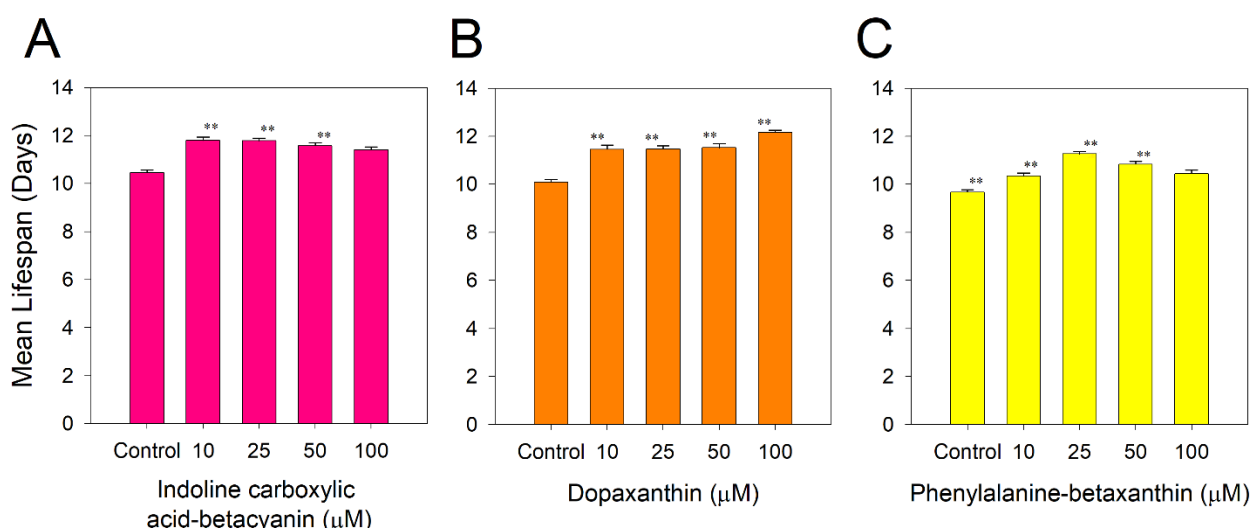


**Figure 12.7. Dose-dependent increased longevity effect obtained by the treatment with different concentrations of betalains. A.** Indoline carboxylic acid-betacyanin. **B.** Dopaxanthin. **C.** Phenylalanine-betaxanthin. Data information: \*\*Significative at  $p \leq 0.05$ ,  $p$  values, standard errors, and  $n$  are given in Table 12.1.

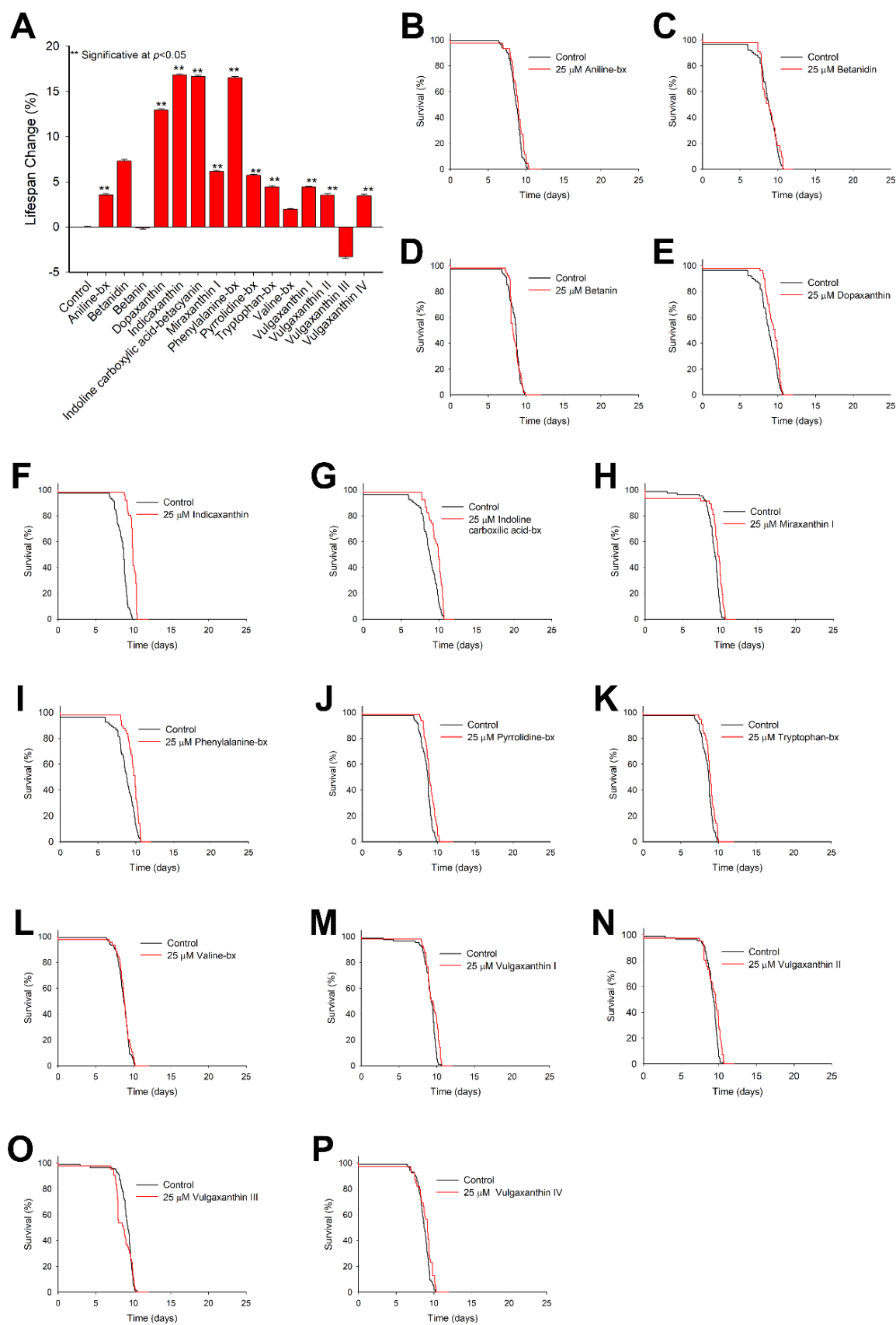


**Figure 12.8.** Effect of the different individual betalains on the lifespan of wild-type *C. elegans*. (Continues on the next page)

**A** Mean lifespan histogram, where the data were obtained from the survival curves. Error bars depicted the standard error and the double asterisk indicated statistical significance with a  $p$  value  $\leq 0.05$ . The survival data  $p$  values, standard errors, confidence intervals and  $n$  are summarized in the Annex III. **B-P** Lifespan curves were adjusted to Kaplan-meier estimator for the *C. elegans* strain N2 treated with 25  $\mu$ M of **B** Aniline-betaxanthin, **C** Betanidin, **D** Betanin, **E** Dopaxanthin, **F** Indicaxanthin, **G** Indoline carboxylic acid-betacyanin, **H** Miraxanthin I, **I** Phenylalanine-betaxanthin, **J** Pyrrolidine-betaxanthin, **K** Tryptophan-betaxanthin, **L** Valine-betaxanthin, **M** Vulgaxanthin I, **N** Vulgaxanthin II, **O** Vulgaxanthin III, and **P** Vulgaxanthin IV.

The synthesized betalains with the highest antioxidant effect *in vivo* were also the most effective in expanding the wild type worm's life: indoline carboxylic acid-betacyanin, phenylalanine-betaxanthin, indicaxanthin and dopaxanthin. These results showed that betalains with a cyclized amino-acid and that were negatively charged, like indoline carboxylic acid-betacyanin, phenylalanine-betaxanthin, indicaxanthin and dopaxanthin were the most effective betalains against oxidative stress *in vivo* and also the most effective in the longevity assays (**Fig. 12.9**).

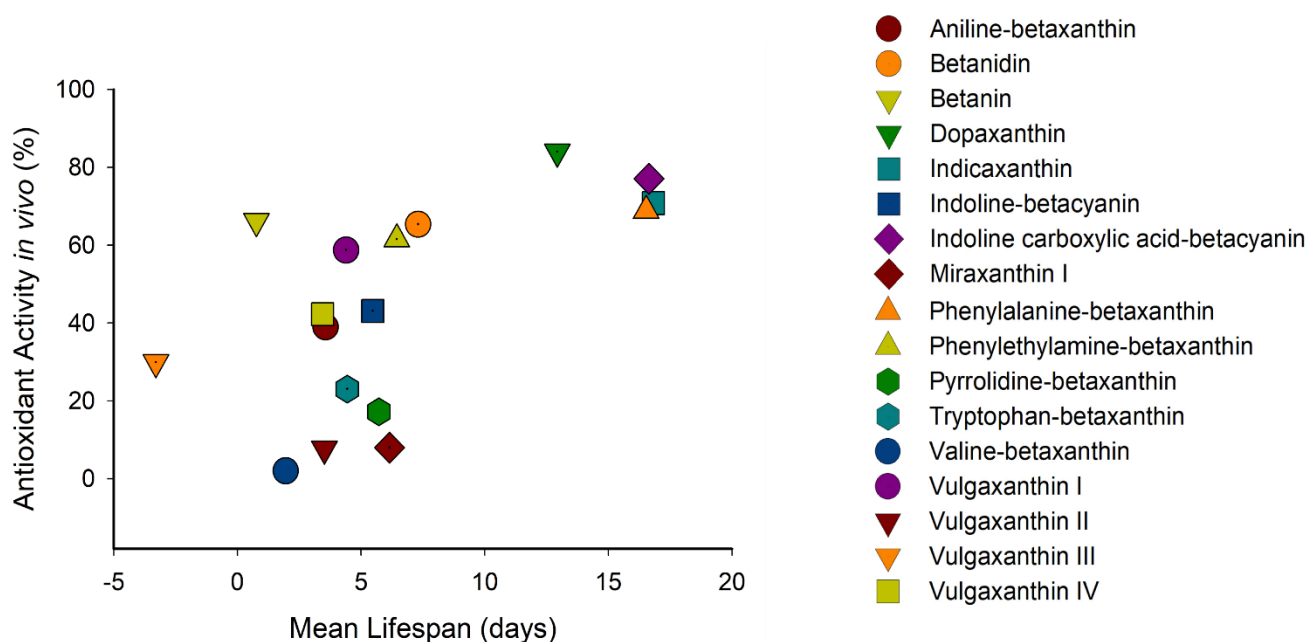


**Figure 12.9.** Comparative effect of the antioxidant capacity of betalains *in vivo* vs. longevity assays in *C. elegans*.

A triple comparative analysis of the assays performed (**Fig. 12.10**) showed how betanidin had a high activity as antioxidant both *in vitro* and *in vivo* assays. However, the results showed low efficiency in the lifespan assay. Indoline carboxylic acid-betacyanin, phenylalanine-betaxanthin, indicaxanthin and dopaxanthin showed

noteworthy activities in the three assays. Indoline carboxylic acid-betacyanin showed a 77.0% reduction in oxidative stress and a 16.6% increase in lifespan, phenylalanine-betaxanthin and indicaxanthin behaved similarly. Dopaxanthin was the best antioxidant *in vivo* (84.0%), but only increased the lifespan by 13%, an indication that the molecules not only increased the lifespan by reducing oxidative stress but may modulate signaling pathways.

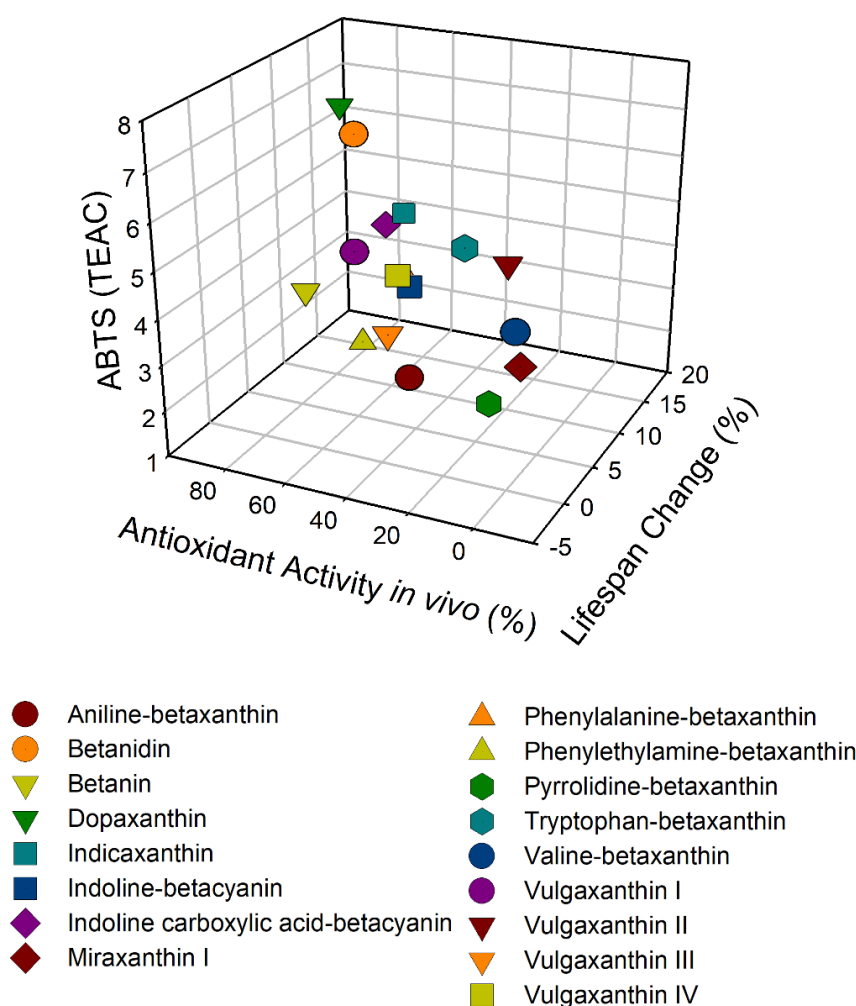


**Figure 12.10.** Cross data of the results obtained in the antioxidant assays *in vitro* and *in vivo* and the results of the longevity experiments.

The increase on the worms' lifespan producing by betalains was higher than those reported for other natural compounds previously assayed as resveratrol, which did not produce a health-promoting effect (Chen et al., 2013), or the flavonoids myricetin, quercetin and kaempferol, which increased the mean lifespan of worms up to 18%, 5.8% and 5.6%, respectively (Grünz et al., 2012). However, this healthy effect was reached when worms were exposed to a flavonoid's concentration of 200  $\mu$ M, higher than the necessary for betalains' effects.

## 5. Pure betalains effects on *C. elegans* gene expression

Once the positive effect on *C. elegans* lifespan by some of the pure betalains tested in this work had been established, the next step was to determine whether the effect was merely a result of the strong antioxidant activity of these compounds or if they could actually alter the worm's gene expression. More accurately the question is if they could modulate the longevity pathways, either the insulin signaling pathway or the redox-active Nrf2/ARE signaling pathway (**Fig. 12.11Q**).

RNA microarray assays were performed for worms treated with the betalains that extended most the lifespan of the wild type animals, namely indoline carboxylic acid-betacyanin, phenylalanine-betaxanthin and indicaxanthin. Besides, the microarray data from these analyses have been deposited to the GEO database (NCBI) [<https://www.ncbi.nlm.nih.gov/geo/>] and assigned the identifier GSE134614.

The biological verification of the microarray results was made using the *C. elegans* strains CF1038 (*daf-16(mu86)*) and TJ356 (*zIs356 [daf-16p::daf-16a/b::GFP + rol-6(su1006)]*) to assert the effect of betalains in the insulin like signaling pathway and QV225 (*skn-1(zj15)*) and LD1 *ldIs7 [skn-1b/c::GFP + rol-6(su1006)]*) was used for the redox-active Nrf2/ARE signaling pathway.

### 5.1. Indoline carboxylic acid-betacyanin

RNA microarray for indoline carboxylic acid-betacyanin showed an overexpression of *skn-1* gene (1.64-fold vs control,  $p \leq 0.05$ ), the *C. elegans* ortholog of human Nrf2, a transcription factor that regulates the phase 2 detoxification response to oxidative stress (Blackwell et al., 2015). In *C. elegans*, SKN-1 activates enzymes that work as radical scavengers and transfer glutathione. It is located in the ASI neurons (putative hypothalamus), in response to dietary restrictions, or in the gut nuclei, in response to oxidative stress. Its accumulation in gut nuclei activates the phase 2 gene expression in response to stress and is regulated by *sgk-1* (Tullet et al., 2008). *Sgk-1* is a serine/threonine kinase that can phosphorylate the SKN-1 transcription factor and modulate its nuclear localization (A. T.-Y. Chen et al., 2013). Therefore, RNAi knockdown of *sgk-1* increases the presence of SKN-1::GFP in the gut nuclei (Tullet et al., 2008). The microarray showed a downregulation of *sgk-1* (-1.45-fold vs control,  $p \leq 0.05$ ) in worms treated with indoline carboxylic acid-betacyanin, and also a modulation of some *skn-1* dependent genes related to resistance to oxidative stress

(Park et al., 2009) *cup-4* (2.08-fold vs control,  $p \leq 0.05$ ), *nlp-7* (2.1-fold vs control,  $p \leq 0.05$ ), *ent-1* (-2.2-fold vs control,  $p \leq 0.05$ ) and *nhx-2* (-1.68-fold vs control,  $p \leq 0.05$ ). *Cup-4* encodes a non-alpha ligand-gated ion channel with similarity to the nicotinic acetylcholine receptors. It is located in the cytoplasmic vesicles of the coelomocytes, and it is suggested that *cup-4* may regulate endocytosis *via* regulation of phospholipase C activity (wormbase.com). *Nlp-7* a neuropeptide like protein is expressed in several tissues including the nervous and reproductive systems. It is related to response to caloric restriction and adult lifespan. As Tullet et al., (2008) reported, the knockdown of these two genes reduces the oxidative stress resistance and lifespan (12-14%) of the wild type animals, suggesting an important role of these genes in longevity. *ent-1* is an ortholog of human SLC29A1, a transmembrane glycoprotein that localizes to the plasma and mitochondrial membranes and mediates the cellular uptake of nucleosides from the surrounding medium (Huang et al., 2017), in *C. elegans*. It is located in the plasma membrane and it is predicted to have nucleoside transmembrane activity (Appleford et al., 2004). Finally, *nhx-2* is an ortholog of human SLC9A3. It encodes a sodium/proton exchanger that is expressed in the intestine and is involved in larvae development, lifespan and fat storage (Wang et al., 2014). Inactivation of *nhx-2* gene by RNAi increases the *C. elegans* lifespan by 40% (Tullet et al., 2008; Wang et al., 2014).

Therefore, the lifespan extension shown in worms treated with indoline carboxylic acid-betacyanin could be a result of the repression of *sgk-1*, the activation of *skn-1* and the regulation of its downstream genes *cup-4*, *nlp-7* and *nhx-2*.

As commented above, biological verification of these results was done using *C. elegans* strains CF1038 (*daf-16(mu86)*) and TJ356 (*zIs356 [daf-16p::daf-16a/b::GFP + rol-6(su1006)]*) to assert the effect of indoline carboxylic acid-betacyanin in the insulin like signaling pathway and QV225 (*skn-1(zj15)*) and LD1 *ldIs7 [skn-1b/c::GFP + rol-6(su1006)]* for the redox-active Nrf2/ARE signaling pathway.

There was an increase in lifespan produced by indoline carboxylic acid-betacyanin in the *daf-16* mutant CF1038 (**Fig. 12.11N**) of a 6.72% ( $p \leq 0.05$ ), an indication that the compound effect is not dependent on *daf-16*. However, the fluorescent strain TJ356 showed a partial translocation of DAF-16 (**Fig. 12.11E**) into the cell nuclei (44.5%), most probably due to an effect on the upregulation of *jkn-1* (2.94-fold vs control,  $p \leq 0.05$ ), coding for a c-Jun N-terminal kinase that regulates the

longevity pathway interacting with DAF-16 (Oh et al., 2005). *jkn-1* phosphorylates DAF-16, allowing it to translocate to the cell nucleus. RNA microarray showed that the heat shock proteins downstream of DAF-16 were upregulated by the betalain, as seen for *hsp-16.1* (4.0-fold vs control,  $p \leq 0.05$ ) or *hsp-70* (2.0-fold vs control,  $p \leq 0.05$ ). The loss of elongation of lifespan in the mutant strain QV225 (**Fig. 12.11P**) suggests the life extension was due to the activation of the redox-active Nrf2/ARE signaling pathway. Indeed, when the fluorescent strain LD1 was exposed to the betalain, the accumulation of *skn-1::GFP* in the gut nuclei was increased 2.3-fold (**Fig. 12.11L** and **12.11O**). *skn-1* accumulation in the gut is an essential step for the activation of phase 2 detoxification and stress resistance.

Therefore, indoline carboxylic acid-betacyanin confers stress resistance to the wild type worms, downregulating *sgk-1*, upregulating *skn-1* and modulating *skn-1* downstream genes *cup-4*, *nlp-7*, *ent-1* and *nhx-2*, resulting in an extension of lifespan.

## 5.2. Phenylalanine-betaxanthin

In contrast, phenylalanine-betaxanthin treatment did not shown an overexpression of genes involved in the SKN-1 pathway. Microarray data showed an increase in the expression of *daf-2* (insulin/IGF pathway) (1.34-fold vs control,  $p \leq 0.05$ ), which should produce a repression in the translocation of DAF-16 into the nuclei. However, phenylalanine-betaxanthin treatment induced a 30% nuclear translocation of DAF-16 in the fluorescent strain TJ356 (**Fig. 12.11F** and **12.11I**). The transcription factor DAF-16 is not only regulated via insulin/IGF pathway but is also regulated by the expression of SIR-2.1, a NAD-dependent protein deacetylase ortholog of human sirtuin SIRT1. SIR-2.1 is able to bind and translocate the transcription factor DAF-16 by acting in parallel to the insulin-like pathway (Berdichevsky et al., 2006).

The significant increased lifespan (16.55%) shown in the wild type worms treated with phenylalanine-betaxanthin was lost in the mutant animals *daf-16 (mu86)* (**Fig. 12.11N**). These results show that the overexpression of *sir2.1* obtained from worms treated with phenylalanine-betaxanthin (1.96-fold vs control,  $p \leq 0.05$ ) had a direct effect in the lifespan via DAF-16. The nuclear translocation of DAF-16 is an essential requisite for the transcriptional activation of target genes (Murphy et al., 2003).

Phenylalanine-betaxanthin treatment also increased the expression of some heat shock protein genes like *hsp-16.2* (2.7- fold vs control,  $p \leq 0.05$ ), *hsp-16.1* (1.8- fold vs control,  $p \leq 0.05$ ) and *hsp-16.48* (1.6- fold vs control,  $p \leq 0.05$ ).

In conclusion, phenylalanine-betaxanthin, a minor betalain present in the *Opuntia ficus-indica* fruits, expands *C. elegans* lifespan by promoting an increase in the expression of *sir 2.1*, which enhances the translocation of DAF-16 to the nuclei, and DAF-16 induces the *sHSPs* gene overexpression.

### 5.3. Indicaxanthin

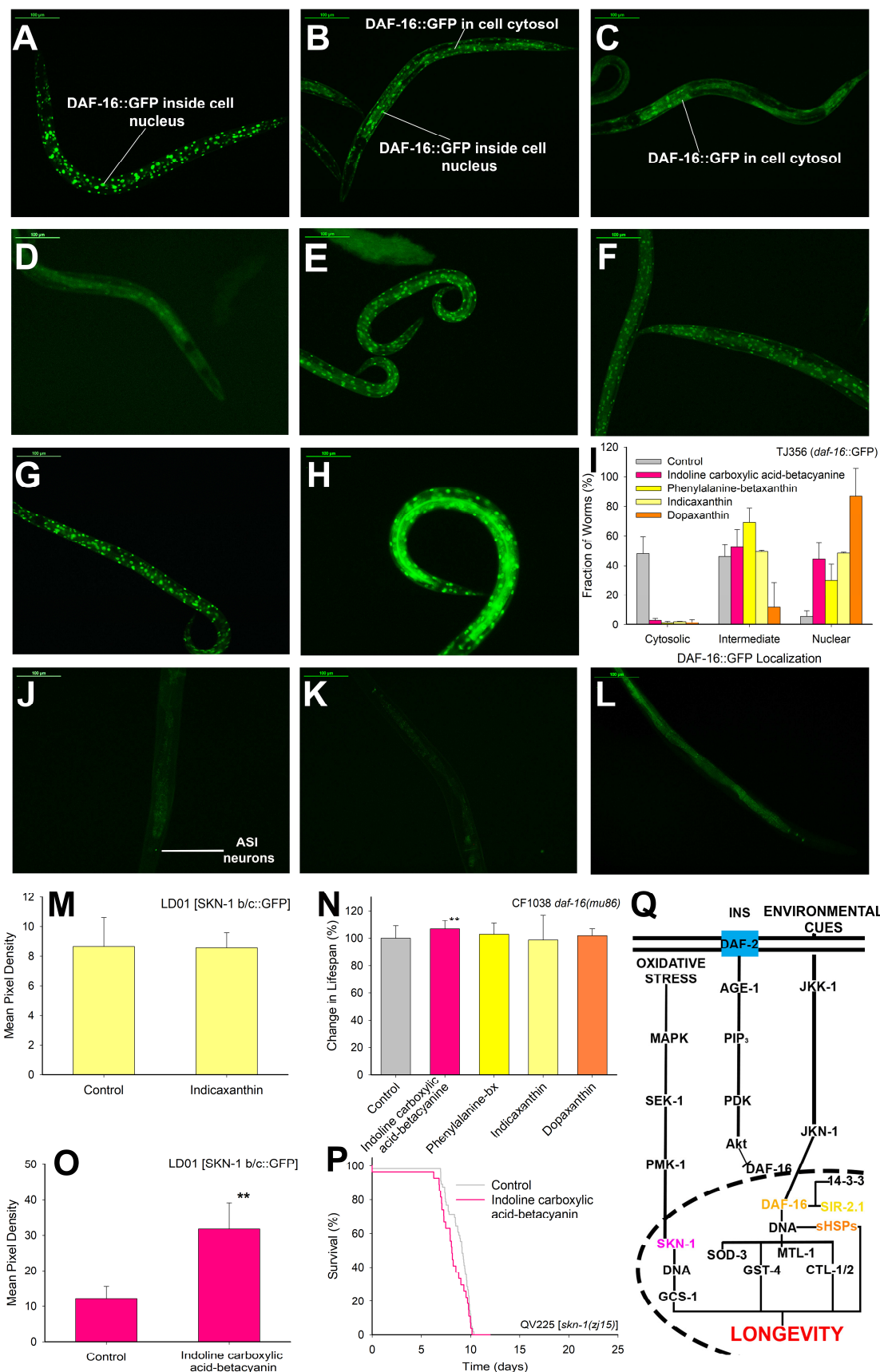
Indicaxanthin is the main and characteristic bioactive pigment of the cactus pears, and worms treated with this pure molecule showed that two DAF-16 target genes were upregulated: *hsp-12.1* (1.12- fold vs control,  $p \leq 0.05$ ) and *lips-17* (1.67- fold vs control,  $p \leq 0.05$ ). *Lips-17* is predicted to encode a lipase involved in fat metabolism (Sun et al., 2017) that has been linked to a lifespan extension of germ-less animals (Hansen et al., 2013; McCormick et al., 2012). The lifespan extension effect produced by indicaxanthin in wild type animals was lost in the mutant strain *daf-16 (mu86)* (**Fig. 12.11N**), indicating that the effect is mediated by DAF-16. Indicaxanthin treatment was also able to induce the nuclear translocation of DAF-16 (48.4%) in the mutant strain TJ356 (**Fig. 12.11G** and **12.11I**) and, at the same time, it did not have any effect on mutants of the SKN-1 route (**Fig. 12.11K** and **12.11M**). This indicates that indicaxanthin expands *C. elegans* lifespan via DAF-16 translocation and subsequent upregulation of the target genes *hsp-12.1* and *lips-17*, involved respectively in protein unfolding and fat metabolism.

### 5.4. Dopaxanthin

In addition to a lifespan extension, wild type worms treated with dopaxanthin showed fluorescence in the digestive tube. The green light emission was due to the natural autofluorescence of these molecules commented in the introduction chapter (Gandía-Herrero et al., 2005b), and shows how dopaxanthin was ingested by the worms and then accumulated. The fluorescence of worms treated with 10  $\mu$ M of the compound was 2-fold higher than the control and 6.94-fold higher in animals treated with 100  $\mu$ M (**Fig. 12.12**).



Overall, dopaxanthin was the compound with the greatest effect on the nuclear translocation of *daf-16* of the four tested betalains (**Fig. 12.11H** and **12.11I**). When fluorescent TJ356 worms were treated with dopaxanthin, 86.76% of the animals presented nuclear translocation of *daf-16*. These results, together with the loss of effect on the lifespan in the strain *daf-16(mu86)* (**Fig. 12.11N**), are a neat indication that DAF-16 is responsible for the increased longevity in worms treated with dopaxanthin.



**A-H.** Representative images are shown for **A.** TJ356 strain (*daf-16::GFP*) nuclear translocation, **B.** TJ356 (*daf-16::GFP*) intermediate localization, **C.** TJ356 (*daf-16::GFP*) cytosolic localization, **D.** TJ356 (*daf-16::GFP*) solvent control, **E.** TJ356 (*daf-16::GFP*) localization with indoline carboxylic acid-betacyanin treatment, **F.** TJ356 (*daf-16::GFP*) localization with phenylalanine-betaxanthin treatment, **G** (*daf-16::GFP*) localization with indicaxanthin treatment, **H.** TJ356 (*daf-16::GFP*) localization with dopaxanthin treatment. Scale bars: 100  $\mu$ m. **I.** Histogram summarizing the fraction of TJ356 worms with either cytosolic, intermediate or nuclear localization of DAF-16 (*daf-16::GFP*) after betalains treatment (100  $\mu$ M). Three independent trials were made using  $n \geq 25$  in each trial. Statistical results are summarized in the Annex III. **J-L.** Representative images of **J.** Control LD1 strain (*skn-1 b/c::GFP*), **K.** LD1 strain treated with 25  $\mu$ M of indicaxanthin, **L.** LD1 strain treated with 25  $\mu$ M of indoline carboxylic acid- betacyanin. **M.** Results of the integrated fluorescence of the gut in LD1 worms treated with 25  $\mu$ M indicaxanthin versus control worms. Two independent trials were made using  $n \geq 10$  in each trial. Statistical results are summarized in the Annex III. **N.** Mean lifespan results for mutant worms CF1038 (*daf-16 (mu86)*) treated with 25  $\mu$ M of indicaxanthin, dopaxanthin, phenylalanine-betaxanthin and indoline carboxylic acid-betacyanin. *p* values, standard errors, confidence intervals and *n* are given in the Annex III. **O.** Results of the integrated fluorescence of the gut in LD1 worms treated with 25  $\mu$ M indoline carboxylic acid-betacyanin versus control worms. Two independent trials were made using  $n \geq 10$  in each trial, statistical results are summarized in the Annex III. **P.** Survival curves for QV225 strain treated with 25  $\mu$ M of indoline carboxylic acid-betacyanin vs control QV225 worms, *p* values, standard errors, confidence intervals and *n* are given in the Annex III. **Q.** Scheme of the pathways modulated by the tested betalains involved in longevity and oxidative stress resistance.

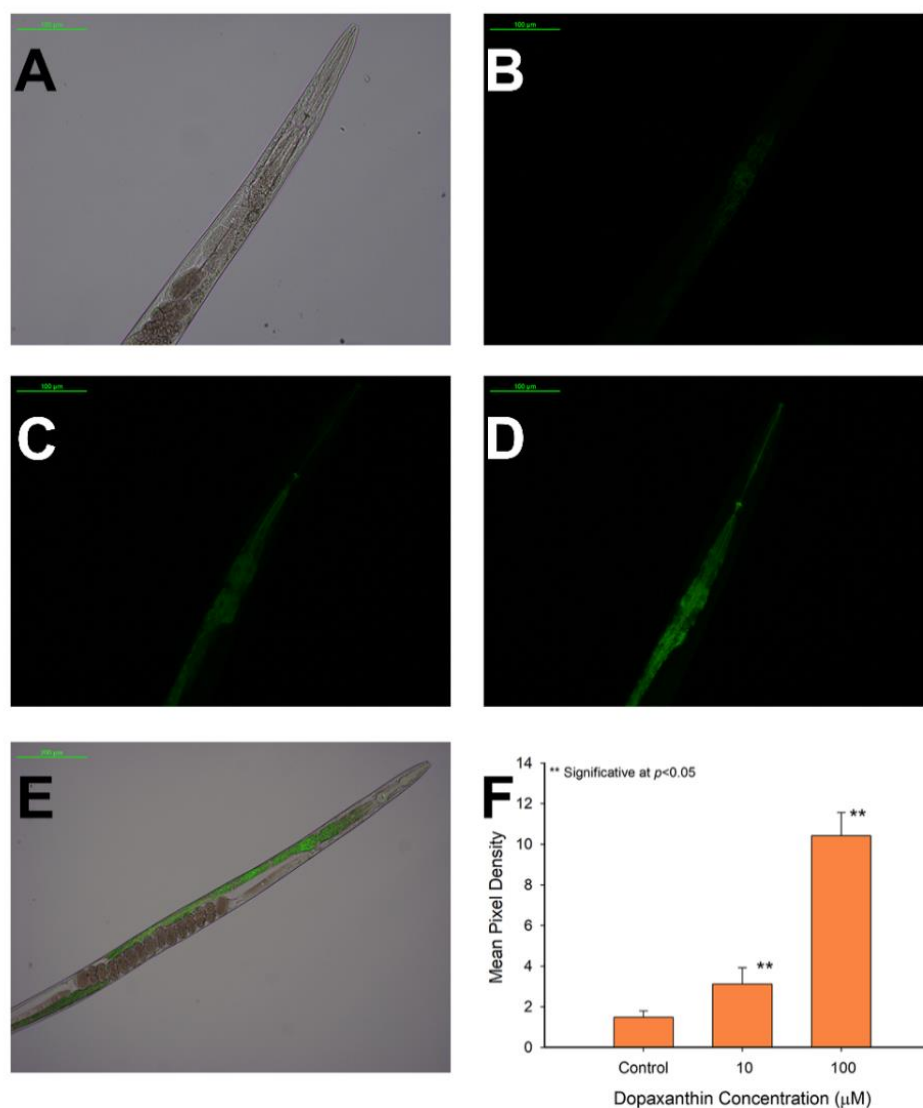
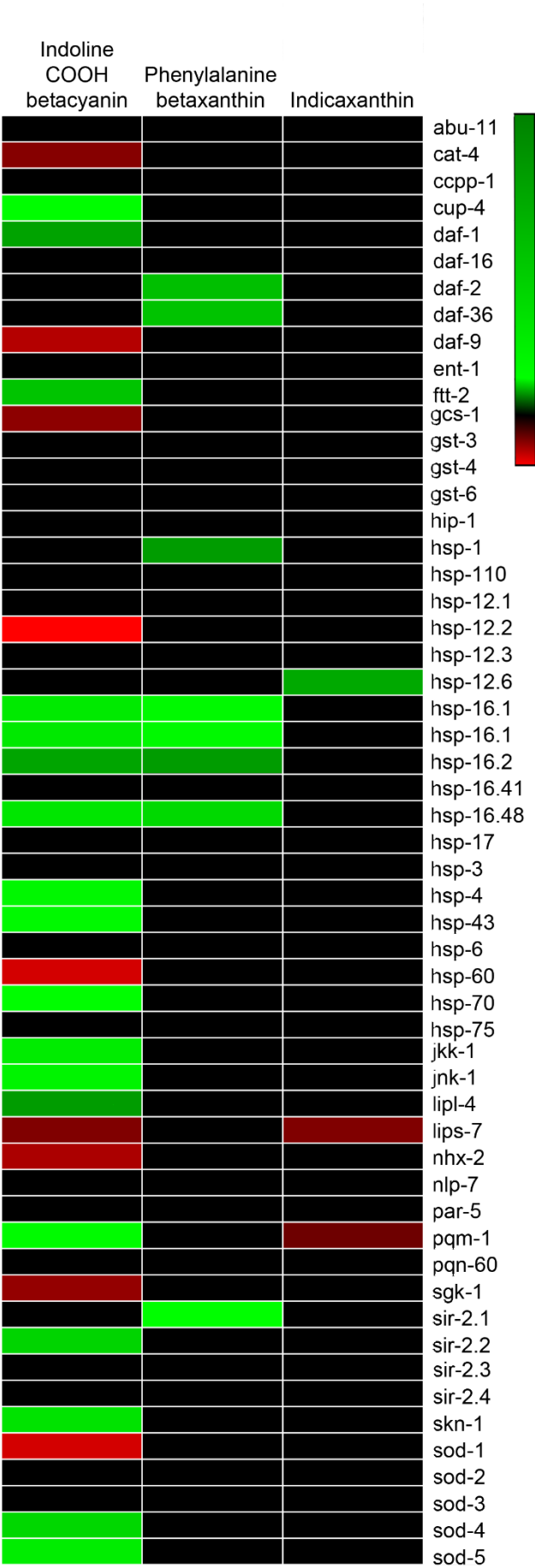


**Figure 12.12. Dopaxanthin accumulation in wild type *C. elegans*.** A-E. Representative images of wild-type worms visualized with different techniques: **A.** Bright Field image of a control worm, **B.** Same control worm visualized in fluorescence (I3 filtercube, Leica), **C.** Fluorescence image of a worm treated with 10  $\mu\text{M}$  of dopaxanthin, **D.** Fluorescence image of a worm treated with 100  $\mu\text{M}$  of dopaxanthin, **E.** Merged image of brightfield and fluorescence for a worm treated with 100  $\mu\text{M}$  of dopaxanthin. Scale bars **A-D:** 100  $\mu\text{m}$ , Scale bar **E:** 200  $\mu\text{m}$ . **F.** Integrated fluorescence results of the captured images. Two independent assays were made with  $n \geq 10$ , statistical analysis of the data is summarized in Annex III.

The results obtained by the microarray analysis indicated that the preferred target proteins of betalains are the heat shock proteins (Fig. 12.13), the small peptides that exhibit a chaperone-like activity, maintaining proteome stability by preventing of misfolded proteins and protein aggregation, and by reducing the production of reactive oxygen species (ROS). The sHSPs expression is altered in diseases like Alzheimer's, Parkinson's or cancer (Bakthisaran et al., 2015). The modulation of the sHSPs by molecules of the diet is not only useful in longevity but may also be of interest in these diseases.

**Figure 12.13.** Heat map showing the most differentially expressed genes in the microarrays between the groups of samples respect to the non-treatment group. The positive values (green) correspond to overexpression of genes and negative values (red) correspond to repressed expression due to effect of betalains in *C. elegans*.



## 6. Conclusions

Although all betalains belong to the same family of compounds, the seventeen pigments assayed in this chapter presented different behavior in the *in vivo* assays due to their bioavailability. The presence of a cyclized amino-acid and a negative charge in the chemical structure seems to enhance the effectivity of the pigment by expanding the *C. elegans* lifespan. Thus, indoline carboxylic acid-betacyanin, phenylalanine-betaxanthin, indicaxanthin and dopaxanthin were the most effective betalains not only by reducing reactive oxygen species but also by modulating the longevity pathways (**Fig. 12.11Q**). The first microarrays performed with betalains showed that as their chemical structures are different, so are the transcriptional changes. Although worms treated with indoline carboxylic acid-betacyanin, phenylalanine-betaxanthin and indicaxanthin showed different target proteins, the extension of lifespan performed by these pigments lead to the modulation of HSPs genes which mainly work in the proteome stability of the organism. The in-depth work here performed demonstrates the health-promoting effect of individual betalains *in vivo*, supporting the biological activities attributed to betalains since many decades.

**Table 12.1. Summary of lifespan assays results for the *C. elegans* treated with betalains.**

<i>C. elegans</i> strain	Betalain	Concentration ( $\mu$ M)	n	Mean Lifespan (days)	S. E ( $\pm$ day)	Lifespan Change (%)	<i>p</i> -value vs Control
Wild-Type (N2)	Control	0	80	8.56	0.08	0.00	
	Tryptophan-betaxanthin	25	56	8.94	0.09	4.44	0.0038
	Betanin	25	54	8.55	0.09	-0.12	0.9559
	Pyrrolidine-betaxanthin	25	62	9.05	0.09	5.72	0.0001
	Indicaxanthin	25	51	10.00	0.07	16.82	0
	Control	0	87	9.10	0.12	0.00	
	Vulgaxanthin I	25	56	9.50	0.11	4.40	0.0004
	Miraxanthin I	25	47	9.66	0.12	6.15	0.00002
	Vulgaxanthin II	25	41	9.42	0.15	3.52	0.0017
	Vulgaxanthin III	25	43	8.80	0.15	-3.30	0.6703
	Control	0	117	8.70	0.08	0.00	
	Aniline-betaxanthin	25	44	9.01	0.12	3.56	0.0279
	Valine-betaxanthin	25	45	8.87	0.12	1.95	0.2477
	Vulgaxanthin IV	25	69	9.00	0.15	3.45	0.0122
	Control	0	145	8.35	0.2	0.00	
	Betanidin	25	56	8.96	0.15	7.31	0.3178
	Indoline carboxilic acid-betacyanin	25	52	9.74	0.12	16.65	9e-7
	Dopaxanthin	25	52	9.43	0.12	12.93	0.0051
	Phenylalanine-betaxanthin	25	49	9.73	0.11	16.53	0.000027
	Control	0	95	9.67	0.1	0.00	
	Phenylalanine-betaxanthin	10	58	10.35	0.12	7.03	0.0001
	Phenylalanine-betaxanthin	25	80	11.27	0.09	16.55	0
	Phenylalanine-betaxanthin	50	73	10.83	0.13	12.00	0
	Phenylalanine-betaxanthin	100	80	10.45	0.15	8.07	0.0000015
	Control	0	70	10.45	0.11	0.00	
	Indoline carboxilic acid- betacyanin	10	118	11.80	0.14	12.92	0

	Indoline carboxilic acid- betacyanin	25	154	11.78	0.11	12.73	0
	Indoline carboxilic acid- betacyanin	50	155	11.58	0.12	10.81	0
	Indoline carboxilic acid- betacyanin	100	125	11.40	0.13	9.09	
	Control	0	100	10.09	0.11	0.00	
	Dopaxanthin	10	46	11.45	0.19	13.48	0
	Dopaxanthin	25	109	11.47	0.13	13.68	0
	Dopaxanthin	50	92	11.53	0.16	14.27	0
	Dopaxanthin	100	188	12.16	0.1	20.52	0
<b><i>daf-16 (mu86)</i> CF1038</b>	Control	0	205	9.41	0.13	0.00	
	Indicaxanthin	25	145	9.30	0.18	-1.17	0.0521
	Control	0	43	3.87	0.09	0.00	
	Indoline carboxilic acid- betacyanin	25	75	4.13	0.06	6.72	0.0564
	Phenylalanine-betaxanthin	25	65	3.98	0.08	2.84	0.2544
	Dopaxanthin	25	75	3.94	0.05	1.81	0.98
<b><i>skn-1(zj15)</i> LD1</b>	Control	0	44	9.71	0.16	0.00	
	Indicaxanthin	25	56	10.84	0.12	11.64	5e-7
	Control	0	56	8.91	0.14	0.00	
	Indoline carboxylic acid- betacyanin	25	67	8.42	0.24	-5.50	0.3701



## REFERENCES

- Appleford, P.J., Griffiths, M., Yao, S.Y.M., Ng, A.M.L., Chomey, E.G., Elwyn Isaac, R., Coates, D., Hope, I.A., Cass, C.E., Young, J.D., Baldwin, S.A., 2004. Functional redundancy of two nucleoside transporters of the ENT family (CeENT1, CeENT2) required for development of *Caenorhabditis elegans*. *Mol. Membr. Biol.* 21, 247–259. <https://doi.org/10.1080/09687680410001712550>
- Bakthisaran, R., Tangirala, R., Rao, C.M., 2015. Small heat shock proteins: Role in cellular functions and pathology. *Biochim. Biophys. Acta - Proteins Proteomics* 1854, 291–319. <https://doi.org/10.1016/J.BBAPAP.2014.12.019>
- Berdichevsky, A., Viswanathan, M., Horvitz, H.R., Guarente, L., 2006. *C. elegans* SIR-2.1 interacts with 14-3-3 proteins to activate DAF-16 and extend life span. *Cell* 125, 1165–1177. <https://doi.org/10.1016/J.CELL.2006.04.036>
- Blackwell, T.K., Steinbaugh, M.J., Hourihan, J.M., Ewald, C.Y., Isik, M., 2015. SKN-1/Nrf, stress responses, and aging in *Caenorhabditis elegans*. *Free Radic. Biol. Med.* 88, 290–301. <https://doi.org/10.1016/j.freeradbiomed.2015.06.008>
- Chen, A.T.-Y., Guo, C., Dumas, K.J., Ashrafi, K., Hu, P.J., 2013. Effects of *Caenorhabditis elegans* *sgk-1* mutations on lifespan, stress resistance, and DAF-16/FoxO regulation. *Aging Cell* 12, 932–940. <https://doi.org/10.1111/accel.12120>
- Chen, W., Rezaizadehnajafi, L., Wink, M., 2013. Influence of resveratrol on oxidative stress resistance and life span in *Caenorhabditis elegans*. *J. Pharm. Pharmacol.* 65, 682–688. <https://doi.org/10.1111/jphp.12023>
- Feder, M.E., Hofmann, G.E., 1999. Heat-shock proteins, molecular chaperones, and the stress response: evolutionary and ecological physiology. *Annu. Rev. Physiol.* 61, 243–282. <https://doi.org/10.1146/annurev.physiol.61.1.243>
- Gandía-Herrero, F., Escribano, J., García-Carmona, F., 2012. Purification and antiradical properties of the structural unit of betalains. *J. Nat. Prod.* 75, 1030–1036. <https://doi.org/10.1021/np200950n>
- Gandía-Herrero, F., Escribano, J., García-Carmona, F., 2010. Structural implications on color, fluorescence, and antiradical activity in betalains. *Planta* 232, 449–460. <https://doi.org/10.1007/s00425-010-1191-0>
- Gandía-Herrero, F., Escribano, J., García-Carmona, F., 2009. The role of phenolic hydroxy groups in the free radical scavenging activity of betalains. *J. Nat. Prod.* 72, 1142–1146. <https://doi.org/10.1021/np900131r>

- Gandía-Herrero, F., Escribano, J., García-Carmona, F., 2005a. Betaxanthins as substrates for tyrosinase. An approach to the role of tyrosinase in the biosynthetic pathway of betalains. *Plant Physiol.* 138, 421–432.  
<https://doi.org/10.1104/pp.104.057992>
- Gandía-Herrero, F., García-Carmona, F., Escribano, J., 2005b. Floral fluorescence effect. *Nature* 437, 334. <https://doi.org/10.1038/437334a>
- Gliszczynska-Świgło, A., Szymusiak, H., Malinowska, P., 2006. Betanin, the main pigment of red beet: molecular origin of its exceptionally high free radical-scavenging activity. *Food Addit. Contam.* 23, 1079–1087.  
<https://doi.org/10.1080/02652030600986032>
- Grünz, G., Haas, K., Soukup, S., Klingenspor, M., Kulling, S.E., Daniel, H., Spanier, B., 2012. Structural features and bioavailability of four flavonoids and their implications for lifespan-extending and antioxidant actions in *C. elegans*. *Mech. Ageing Dev.* 133, 1–10. <https://doi.org/10.1016/j.mad.2011.11.005>
- Hansen, M., Flatt, T., Aguilaniu, H., 2013. Reproduction, fat metabolism, and life span: What is the connection? *Cell Metab.* 17, 10–19.  
<https://doi.org/10.1016/J.CMET.2012.12.003>
- Herraiz, T., Galisteo, J., 2004. Endogenous and dietary indoles: A class of antioxidants and radical scavengers in the ABTS assay. *Free Radic. Res.* 38, 323–331. <https://doi.org/10.1080/10611860310001648167>
- Huang, W., Zeng, X., Shi, Y., Liu, M., 2017. Functional characterization of human equilibrative nucleoside transporter 1. *Protein Cell* 8, 284–295.  
<https://doi.org/10.1007/s13238-016-0350-x>
- Link, C.D., Cypser, J.R., Johnson, C.J., Johnson, T.E., 1999. Direct observation of stress response in *Caenorhabditis elegans* using a reporter transgene. *Cell Stress Chaperones* 4, 235. [https://doi.org/10.1379/1466-1268\(1999\)004<0235:doosri>2.3.co;2](https://doi.org/10.1379/1466-1268(1999)004<0235:doosri>2.3.co;2)
- McCormick, M., Chen, K., Ramaswamy, P., Kenyon, C., 2012. New genes that extend *Caenorhabditis elegans*’ lifespan in response to reproductive signals. *Aging Cell* 11, 192–202. <https://doi.org/10.1111/j.1474-9726.2011.00768.x>
- Murphy, C.T., McCarroll, S.A., Bargmann, C.I., Fraser, A., Kamath, R.S., Ahringer, J., Li, H., Kenyon, C., 2003. Genes that act downstream of DAF-16 to influence the lifespan of *Caenorhabditis elegans*. *Nature* 424, 277–283.

<https://doi.org/10.1038/nature01789>

- Nayak, B.N., Buttar, H.S., 2016. Evaluation of the antioxidant properties of tryptophan and its metabolites in in vitro assay. *J. Complement. Integr. Med.* 13, 129–136. <https://doi.org/10.1515/jcim-2015-0051>
- Oh, S.W., Davis, R.J., Tissenbaum, H.A., Mukhopadhyay, A., Jiang, F., Svazikapa, N., 2005. JNK regulates lifespan in *Caenorhabditis elegans* by modulating nuclear translocation of forkhead transcription factor/DAF-16. *Proc. Natl. Acad. Sci.* 102, 4494–4499. <https://doi.org/10.1073/pnas.0500749102>
- Park, S.-K., Tedesco, P.M., Johnson, T.E., 2009. Oxidative stress and longevity in *Caenorhabditis elegans* as mediated by SKN-1. *Aging Cell* 8, 258–269. <https://doi.org/10.1111/j.1474-9726.2009.00473.x>
- Piattelli, M., Minale, L., Nicolaus, R.A., 1965. Pigments of centrospermae-V: Betaxanthins from *Mirabilis jalapa* L. *Phytochemistry* 4, 817–823. [https://doi.org/10.1016/S0031-9422\(00\)86258-5](https://doi.org/10.1016/S0031-9422(00)86258-5)
- Stringham, E.G., Candido, E.P.M., 1994. Transgenic hsp 16-Lacz strains of the soil nematode *Caenorhabditis elegans* as biological monitors of environmental stress. *Environ. Toxicol. Chem.* 13, 1211–1220. <https://doi.org/10.1002/etc.5620130802>
- Sun, X., Chen, W.-D., Wang, Y.-D., 2017. DAF-16/FOXO transcription factor in aging and longevity. *Front. Pharmacol.* 8, 548. <https://doi.org/10.3389/fphar.2017.00548>
- Tullet, J.M.A., Hertweck, M., An, J.H., Baker, J., Hwang, J.Y., Liu, S., Oliveira, R.P., Baumeister, R., Blackwell, T.K., 2008. Direct inhibition of the longevity-promoting factor SKN-1 by insulin-like signaling in *C. elegans*. *Cell* 132, 1025–1038. <https://doi.org/10.1016/J.CELL.2008.01.030>
- Wang, M.C., Oakley, H.D., Carr, C.E., Sowa, J.N., Ruvkun, G., 2014. Gene pathways that delay *Caenorhabditis elegans* reproductive senescence. *PLoS Genet.* 10, e1004752. <https://doi.org/10.1371/journal.pgen.1004752>

**Chapter XIII.** The underlying mechanisms of baicalein and related flavonoids' health-promoting effects are mediated by mTOR pathway and the transcription factors SKN-1/Nrf2 and DAF-16/FOXO in the animal model *Caenorhabditis elegans*



### **Contextualization**

In the two previous chapters, the nature of betalains as bioactive compounds has been studied with the animal model *C. elegans*. The administration of pure betalains is able to modulate different genes and transcription factors which are involved in different pathways that converge in an extension of the lifespan, activating genes-promoted longevity. As betalains, flavonoids are secondary metabolites of plants that are commonly consumed in several foods as cocoa, tea, fruits or wine (Panche et al., 2016). They have been considered health-promoting and disease-preventing compounds, since they are associated with several effects related to their antioxidant, anti-inflammatory (González-Gallego et al., 2013), anti-mutagenic and anti-carcinogenic activities (Birt et al., 2001; Le Marchand, 2002). In addition, they are possible candidates in neurodegenerative disease treatments like Alzheimer's or Parkinson's (Baptista et al., 2014; Williams and Spencer, 2012).

In this chapter, the health-promoting effects and the molecular mechanisms of action of six structurally related flavonoids were investigated in *C. elegans*: Baicalein (5,6,7-trihydroxyflavone), which is mainly present in the roots of *Scutellaria baicalensis* and *Scutellaria lateriflora* (Li-Weber, 2009), chrysin (5,7-dihydroxyflavone) present in honey, propolis and *Passiflora incarnata* leaves (Baltrušaitytė et al., 2007; Zanolini et al., 2000), scutellarein (5,6,7,4'-tetrahydroxyflavone) from *Scutellaria lateriflora* (Islam et al., 2011), 6-hydroxyflavone, the naturally occurring monoflavone present in the leaves of *Barleria prionitis* (Ren et al., 2010), 6,7-dihydroxyflavone, a synthetic analogue chosen for its structural similarity to the natural molecules and 7,8-dihydroxyflavone which appears in the leaves of *Primula* species (Colombo et al., 2014). **Fig. 13.1** shows the structures of the flavonoids selected for this study.

Several reports have studied the effects of these molecules as antioxidants and radical scavengers or their effects in cell lines (Ren et al., 2010; Shieh et al., 2000; Zanolini et al., 2000). However, there are few studies in *C. elegans*, and they are mainly focused on baicalein (Havermann et al., 2016). Other flavonoids as myricetin, quercetin or kaempferol present positive effects in *C. elegans* lifespan and ROS-levels as it has previously been reported (Grünz et al., 2012), but the performed studies did not elucidate the molecular mechanisms underlying the effects described.

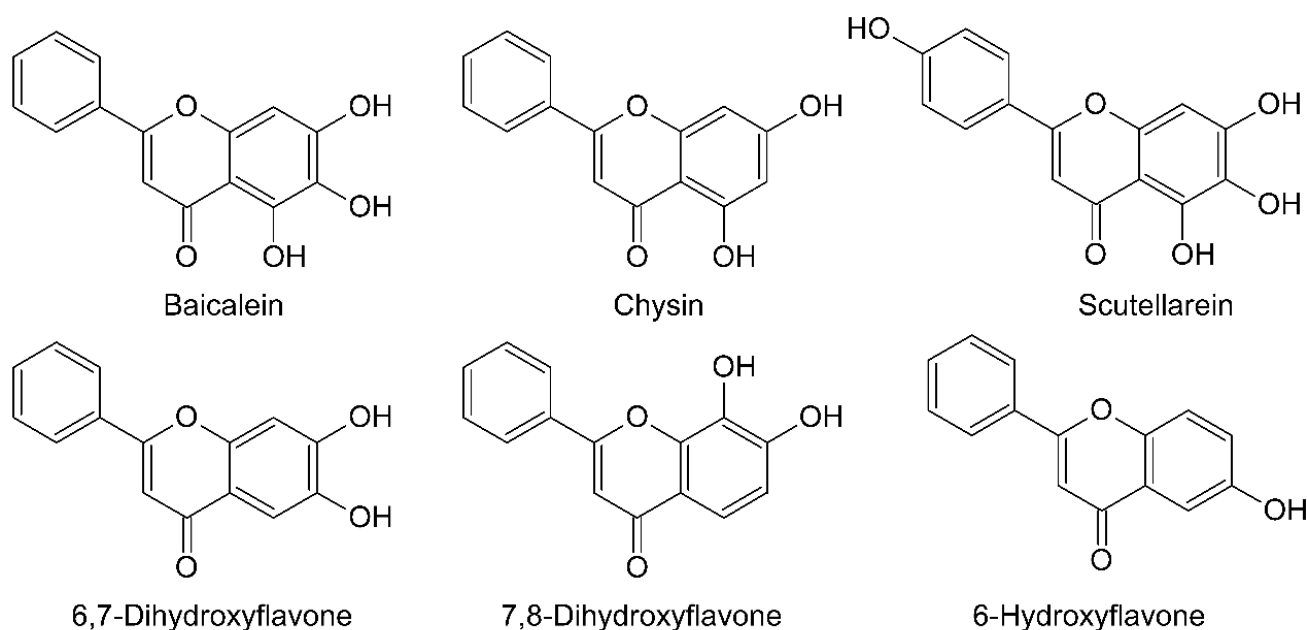


Figure 13.1. Chemical structures of the flavonoids used in this chapter.

## 1. Effect of flavonoids on *C. elegans* oxidative stress resistance

In response to oxidative stress, all the organisms generate heat shock proteins (HSPs) as a mean of protection from the oxidative damage. This response could be enhanced by the addition of bioactive compounds which confer resistance to oxidative stress to cells and organisms, as it has been demonstrated for the betalains described in the previous chapters XI and XII.

To estimate the ability of the six flavonoids to enhance the defense against oxidative stress, the TJ375 strain of *C. elegans* was fed with them individually and then *C. elegans* was exposed to oxidative stress chemically induced with juglone (**Fig. 13.2A**). This strain presents the HSP16.2 fused with the green fluorescent protein GFP. HSP16.2-GFP is located in the pharynx and, in response to oxidative stress, *hsp-16.2p::GFP* accumulate bright green fluorescence (**Fig. 13.2A**). When TJ375 worms were treated with 100  $\mu$ M of flavonoids, only 6,7-dihydroxyflavone and chrysin (**Fig. 13.2D**) had a protective effect against the induced stress. 6,7-dihydroxyflavone presented the highest potential as *in vivo* antioxidant with a decrease of fluorescence of 88.9%.

Other polyphenols previously studied such as aspalathin or epigallocatechin gallate increased the oxidative stress resistance of the treated *C. elegans* by 27.0% and 26.74% respectively (Abbas and Wink, 2014, 2009), suggesting that 6,7-dihydroxyflavone was stronger as stress-response gene modulator than the previously tested polyphenols. The rest of the flavonoids showed little activity towards oxidative stress in the worms (**Fig. 13.2B and 13.2D**), suggesting that even being structurally similar, their effects, stability or bioavailability may be different.

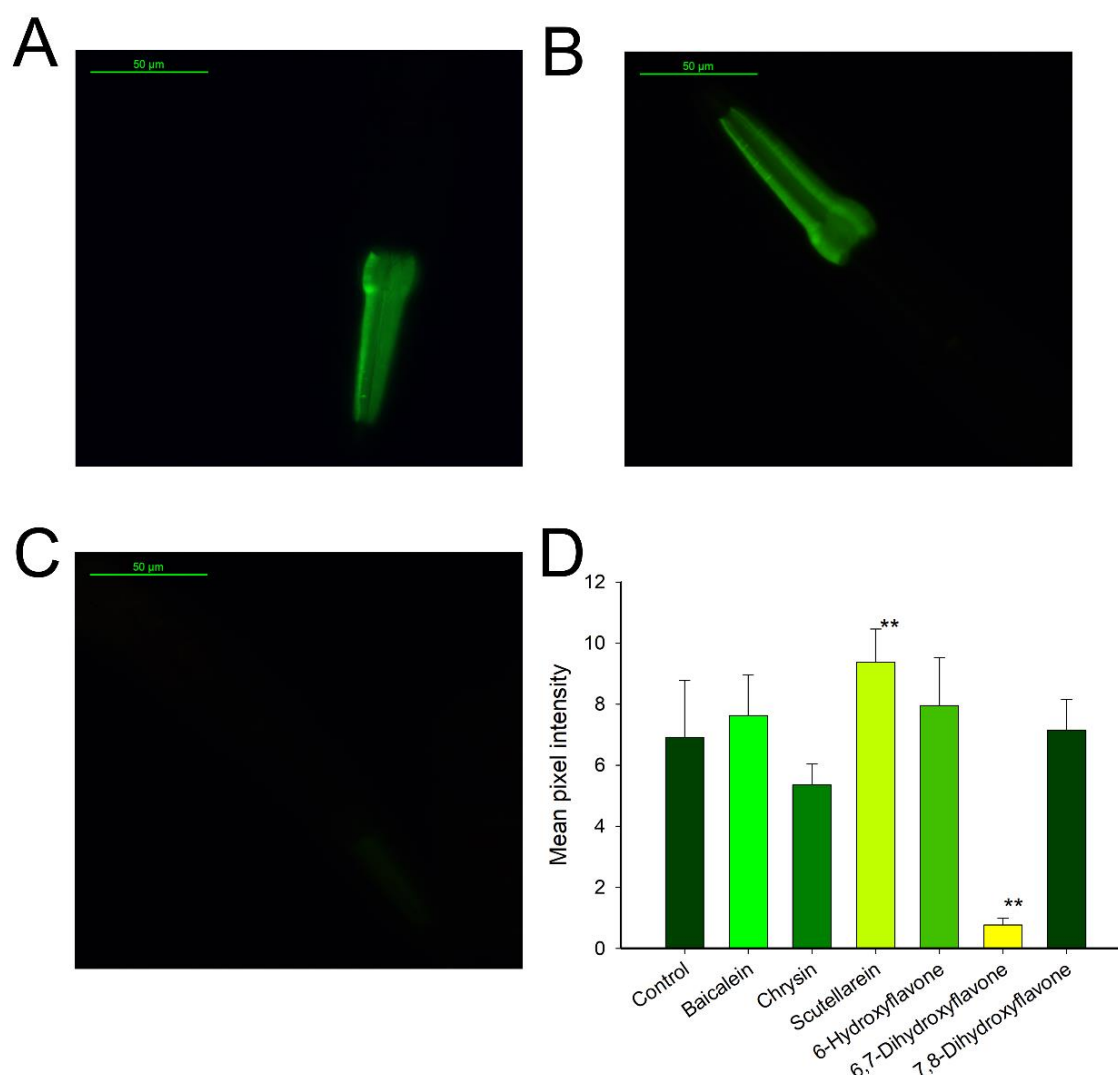


**Figure 13.2. Flavonoids effect on *C. elegans* strain TJ375 (*hsp-16.2p::GFP*) model of oxidative stress resistance.** A. Representative image of a TJ375 control worm, B. Representative image of a TJ375 worm treated with 100 µM of baicalein, C. Representative image of a TJ375 worm treated with 100 µM of 6,7-dihydroxyflavone and D. Quantification of the effect of pre-treatment with flavones in oxidative stress resistance measured through fluorescence integration. Scale bar: 50 µm.



## 2. Effects of flavonoids on fat accumulation in *C. elegans*

The bioactive properties of flavonoids seem to promote fat metabolism and a consequent reduction of fat storage and obesity (Assini et al., 2013; Barth et al., 2012), a situation that increases the risk of suffering several pathologies that nowadays affect 11-15% of the worldwide population (Jaacks et al., 2019), including cardiovascular diseases, type 2 diabetes and cancer. To evaluate the *in vivo* effect of flavonoids as fat mobilizers, the stored fat of *C. elegans* was measured in worms treated with 100  $\mu$ M of flavonoids and in control worms using the Oil Red O (ORO) staining protocol (**Fig. 13.3**). The results showed that all the tested molecules were able to reduce the fat storage in the animals (**Fig. 13.3D**). The most effective flavonoids in reducing the animal's fat were chrysin and scutellarein with a 38.9% (**Fig. 13.3C and 13.3D**) and a 36.6% (**Fig. 13.3B and 13.3D**) less fat than control worms, respectively. The effect of other flavonoids like naringenin or kaempferol on fat reduction has been previously reported (Bhattacharya et al., 2013) with a 60-80% of fat reduction, an indication of the ability of these compounds to improve the health by reducing fat accumulation.

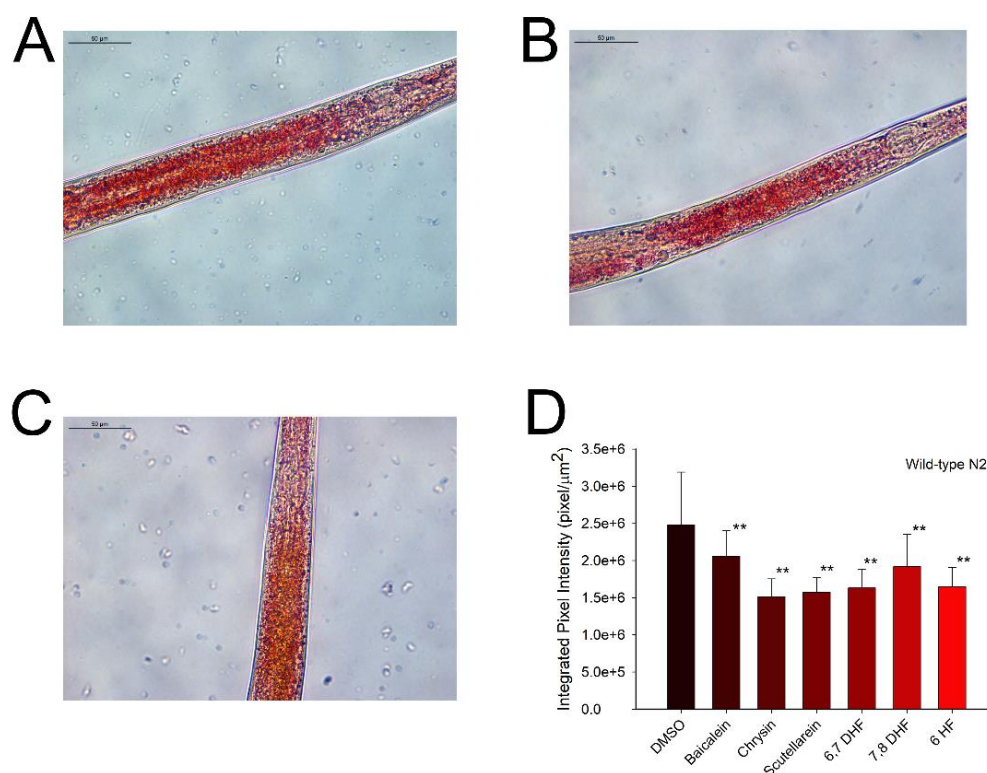


**Figure 13.3. Effect of flavonoids on fat accumulation in *C. elegans* measured with Oil Red O (ORO).** A. DMSO control worms. B. Worm treated with 100  $\mu$ M of scutellarein. C. Worm treated with 100  $\mu$ M of chrysin. D. Lipid content measurement with ORO staining in *C. elegans* treated with 100  $\mu$ M of each flavonoid. Scale bar: 50  $\mu$ m.

### 3. Health-promoting effect of flavonoids on *C. elegans* lifespan

The health-promoting effects of flavonoids in the diet were also measured as their ability to expand the lifespan of the wild-type *C. elegans*. The lifespan machine was employed to measure the mean lifespan of the flavonoid-fed worms. The obtained survival curves and mean lifespans indicated that the flavonoids tested expanded the *C. elegans* mean lifespan in a dose-dependent manner over the concentration range used (**Fig. 13.4, Table 13.1**). The results showed that a dose of 10  $\mu\text{M}$  of baicalein was able to improve the animal's lifespan up to 16.5% (**Fig. 13.4A**). At the same concentration, chrysin, 7,8-dihydroxyflavone and 6-hydroxyflavone treated worms had an increase in the mean lifespan of 8.46% (**Fig. 13.4C**), 4.9% (**Fig. 13.4F**) and 2.36% (**Fig. 13.4D**), respectively. The best result was obtained at 100  $\mu\text{M}$  for 6-hydroxyflavone with an increase of 11.8% in the animal longevity (**Fig. 13.4D**). On the other hand, scutellarein (**Fig. 13.4B**) and 6,7-dihydroxyflavone (**Fig. 13.4E**) had a little negative effect on the lifespan of treated worms as well as the highest concentration of 7,8-dihydroxyflavone also decrease the lifespan of *C. elegans* (**Fig. 13.4F**).

Prior studies have shown similar results with other flavonoids, like myricetin or quercetin that prolonged the *C. elegans* lifespan a 18.0% and a 5.8%, respectively when worms were treated with 100  $\mu\text{M}$  of each compound (Grünz et al., 2012). The researchers associated this lifespan extension effect to the number of hydroxyl groups in the B-ring and to the structure of the C-ring, being the most active molecule myricetin, which presents three hydroxyl groups in the B-ring. According to this hypothesis, 6-hydroxyflavone should be the molecule with the lowest antioxidant activity, and therefore less active since it presents only one hydroxyl group. However, with only one hydroxyl group it was probably the most stable and the less prone to form oxidation species that may reduce the bioactive potential of the molecules when exposed to the medium for 48 hours. Scutellarein, having four hydroxyl groups, and 6,7-dihydroxyflavone and 7,8-dihydroxyflavone, with two hydroxyl groups in *ortho* positions, are more susceptible to oxidation than 6-hydroxyflavone, with one hydroxyl group, chrysin, with two hydroxyls in *meta* positions, and baicalein, with three hydroxyl groups in *ortho* positions. Nevertheless, the assay revealed the potential of all the tested flavonoids as health-promoting compounds, mainly baicalein, chrysin and 6-hydroxyflavone.

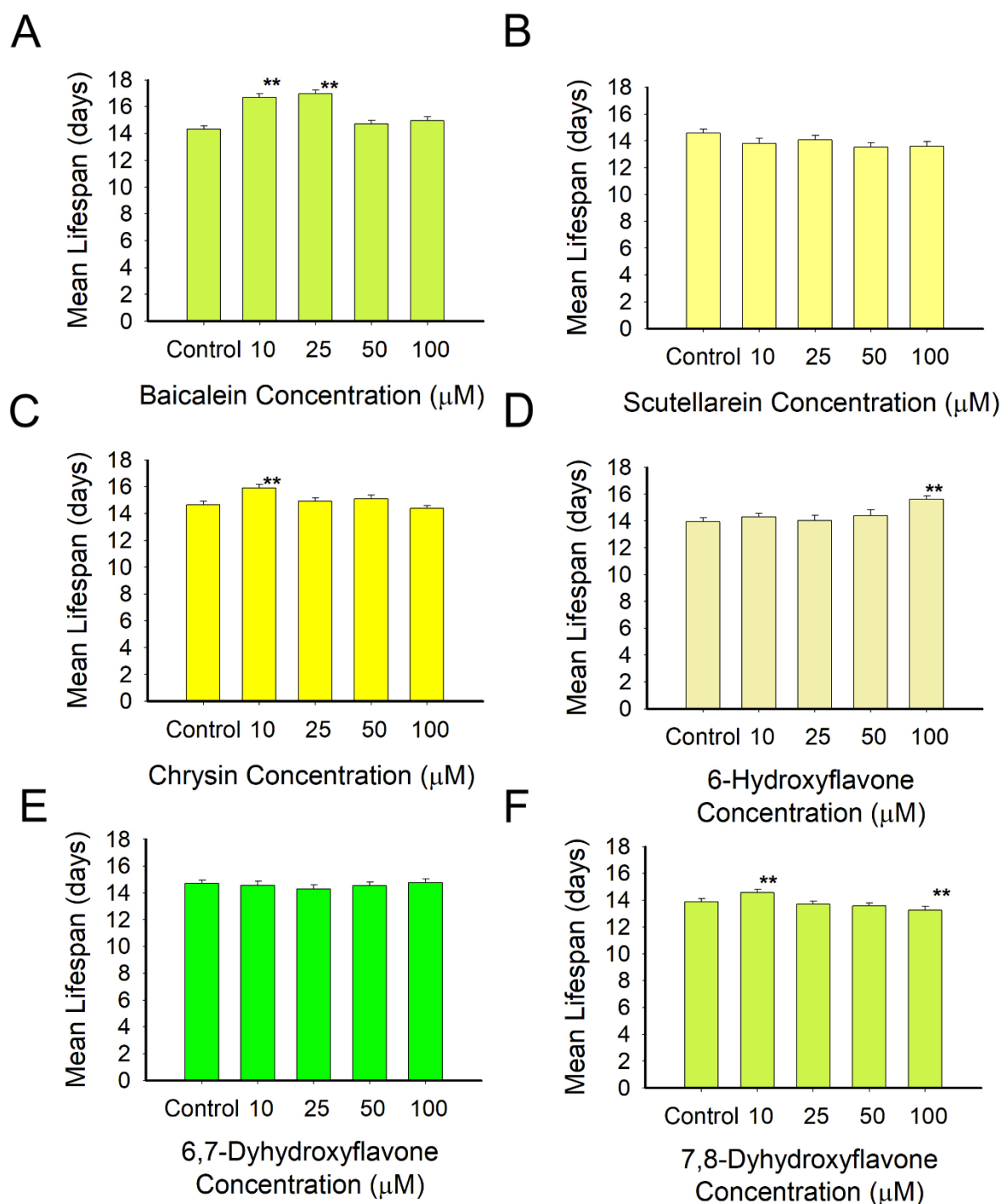


**Figure 13.4. Mean lifespan of wild-type *C. elegans* treated with different doses of flavonoids (0, 10, 25, 50, 100 μM) mean lifespan. A. Baicalein, B. Scutellarein, C. Chrysin, D. 6-Hydroxyflavone, E. 6,7-Dyhydroxyflavone and F. 7,8-Dyhydroxyflavone.**

#### 4. Effect of flavonoids as gene modulators in longevity pathways

Baicalein, chrysin and 6-hydroxyflavone showed the highest extension of the lifespan and at the same time were able to produce a significant decrease in fat storage in *C. elegans*. These two events are related since they might be responses to the modulation of genes' expression which depend of the IIS insulin signaling pathway *via* DAF-16 or depend of the redox active signaling pathway *via* SKN-1. In order to elucidate which pathway is involved in the effect of these three flavonoids related mutant strains were employed at the optimal concentration obtained in the lifespan's assay. Thus, 25  $\mu$ M of baicalein, 10  $\mu$ M of chrysin or 100  $\mu$ M of 6-hydroxyflavone were employed to further investigated the pathways involved in their health-promoting effects in *C. elegans*.

##### 4.1. Effect of flavonoids on the IIS insulin signaling pathway

The effect of the flavonoids on the insulin signaling pathway was estimated *in vivo* with the *daf-16* deficient strain CF1038 (*daf-16(mu86)*) and the fluorescent strain of *C. elegans* TJ356 (**Fig. 13.5**).

Chrysin effect on lifespan was lost in the mutant strain CF1038, where *daf-16* is not present, but baicalein and 6-hydroxyflavone increased the lifespan of the *daf-16* deficient mutants, indicating that chrysin effects are strictly DAF-16 dependent, while baicalein and 6-hydroxyflavone are not dependent on DAF-16 (**Fig. 13.5F**). These results were further supported by the fluorescent strain TJ356, which presents GFP fused with the transcription factor DAF-16 (**Fig. 13.5A-D**). The transcription factor is active when it is translocated into the cell nuclei, and it is inactive when it shows low diffuse fluorescence in the cytoplasm. The results (**Fig. 13.5E**) show that chrysin activated the translocation of DAF-16 to the cell nuclei with a 58.6% of worms showing nuclear fluorescence (**Fig. 13.5D and 13.5E**). Baicalein and 6-hydroxyflavone showed less effect on DAF-16 translocation than the dissolvent (16.1%) (**Fig. 13.5C and 13.5E**). Therefore, it can be concluded that chrysin prolongs *C. elegans* lifespan in a DAF-16 dependent manner. The basal effect of DMSO is well-known as reported before, it is able to modulate lifespan of the worms *via* DAF-16 (Wang et al., 2010).

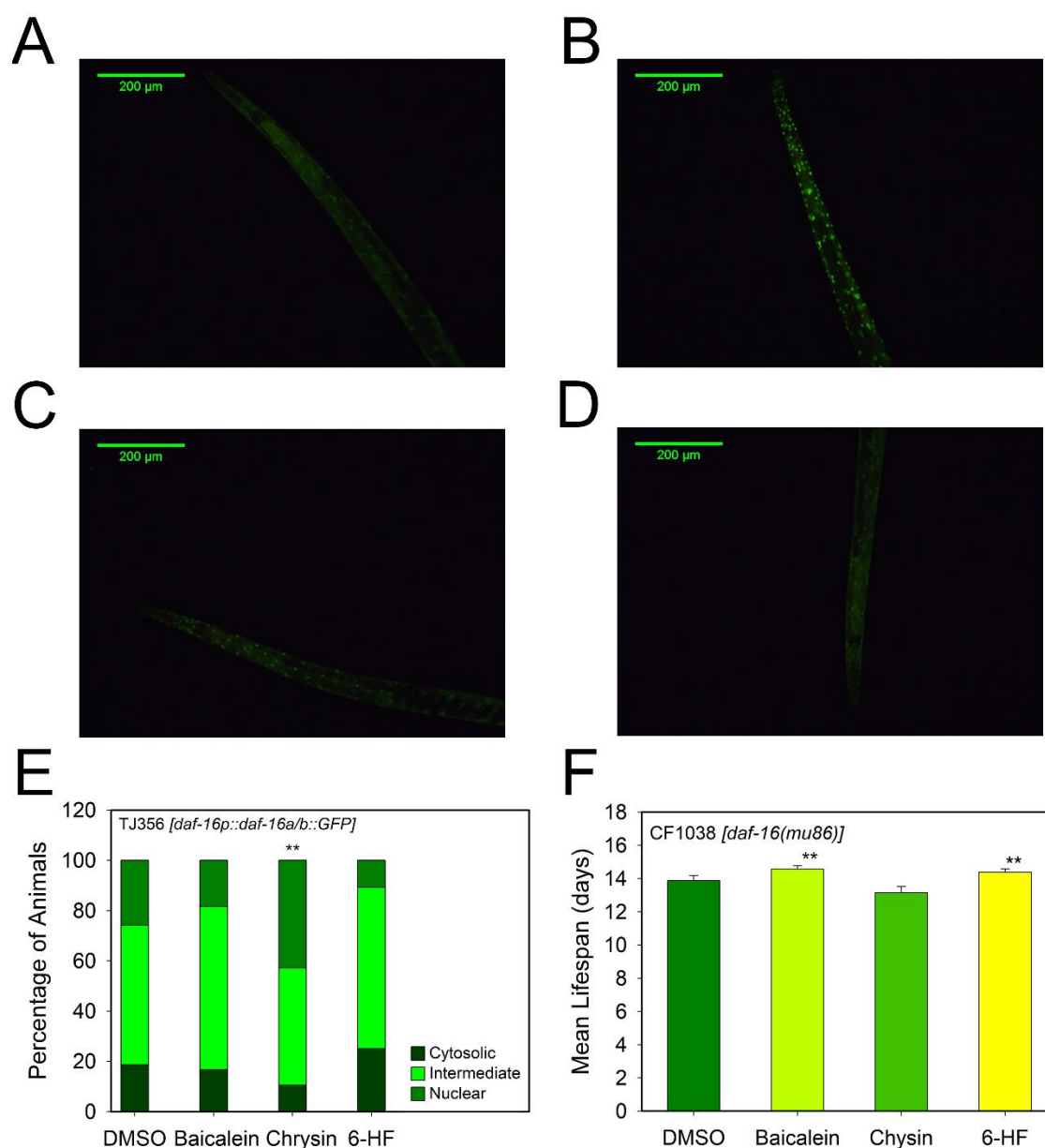


**Figure 13.5. Biological confirmation of flavonoids activity in the insulin signaling pathway using *C. elegans* mutants.** Representative images are shown for TJ356 (*daf-16::GFP*) negative control (A), TJ356 (*daf-16::GFP*) localization with DMSO treatment (B), TJ356 (*daf-16::GFP*) localization after baicalein treatment (C) and (*daf-16::GFP*) localization after chrysin treatment (D). E. Histogram summarizing the fraction of TJ356 worms with either cytosolic, intermediate or nuclear localization of DAF-16 (*daf-16::GFP*) after flavonoid treatment. F. Mean lifespan results for mutant worms CF1038 (*daf-16(mu86)*) treated with 25  $\mu$ M of baicalein, 10  $\mu$ M of chrysin or 100  $\mu$ M of 6-hydroxyflavone. Scale bar: 50  $\mu$ m.

#### 4.2. Effect of flavonoids on the redox active signaling pathway

The possible effects of baicalein and 6-hydroxyflavone *in vivo* due to the redox active pathway were measured with the SKN-1 deficient strain QV225 (*skn-1(zj15)*) of *C. elegans* and the fluorescent strain LD1 [*skn-1 b/c::GFP*] (**Fig. 13.6**). SKN-1 is the *C. elegans* ortholog to the human Nrf2, a transcription factor that regulates de phase II detoxification response to oxidative stress (Blackwell et al., 2015). SKN-1 activates enzymes that work as radical scavengers and transfer glutathione. SKN-1 is located in the ASI neurons (putative hypothalamus) in response to dietary restrictions, and in the gut nuclei in response to oxidative stress.

The lifespan machine showed that the extension effects produced on the lifespan of the wild-type worms treated with baicalein and 6-hydroxyflavone were lost in the *skn-1* deficient strain (**Fig. 13.6D**). This suggests that the longevity effect of these flavones is dependent on the redox active pathway which involves SKN-1. To further investigate this hypothesis, the LD1 strain of *C. elegans* was used. LD1 has the transcription factor SKN-1 fused to the protein GFP, showing green fluorescence in the gut cell nuclei and ASI neurons when the transcription factor is active (**Fig. 13.6A and 13.6B**).

The flavonoid 6-hydroxyflavone produced the translocation of the SKN-1 transcription factor to the nuclei, while baicalein did not produce a significant translocation of the transcription factor to the gut cell nuclei (**Fig. 13.6C**). These results clearly indicate for the first time that the longevity effects of 6-hydroxyflavone in *C. elegans* is mediated by SKN-1 transcription factor and the redox active pathway. However, lifespan expansion effects of baicalein are not totally dependent of SKN-1 or totally dependent of the IIS insulin signaling pathway and further investigation at transcriptomic level is necessary to dilucidate the mechanisms involved in its lifespan extension.

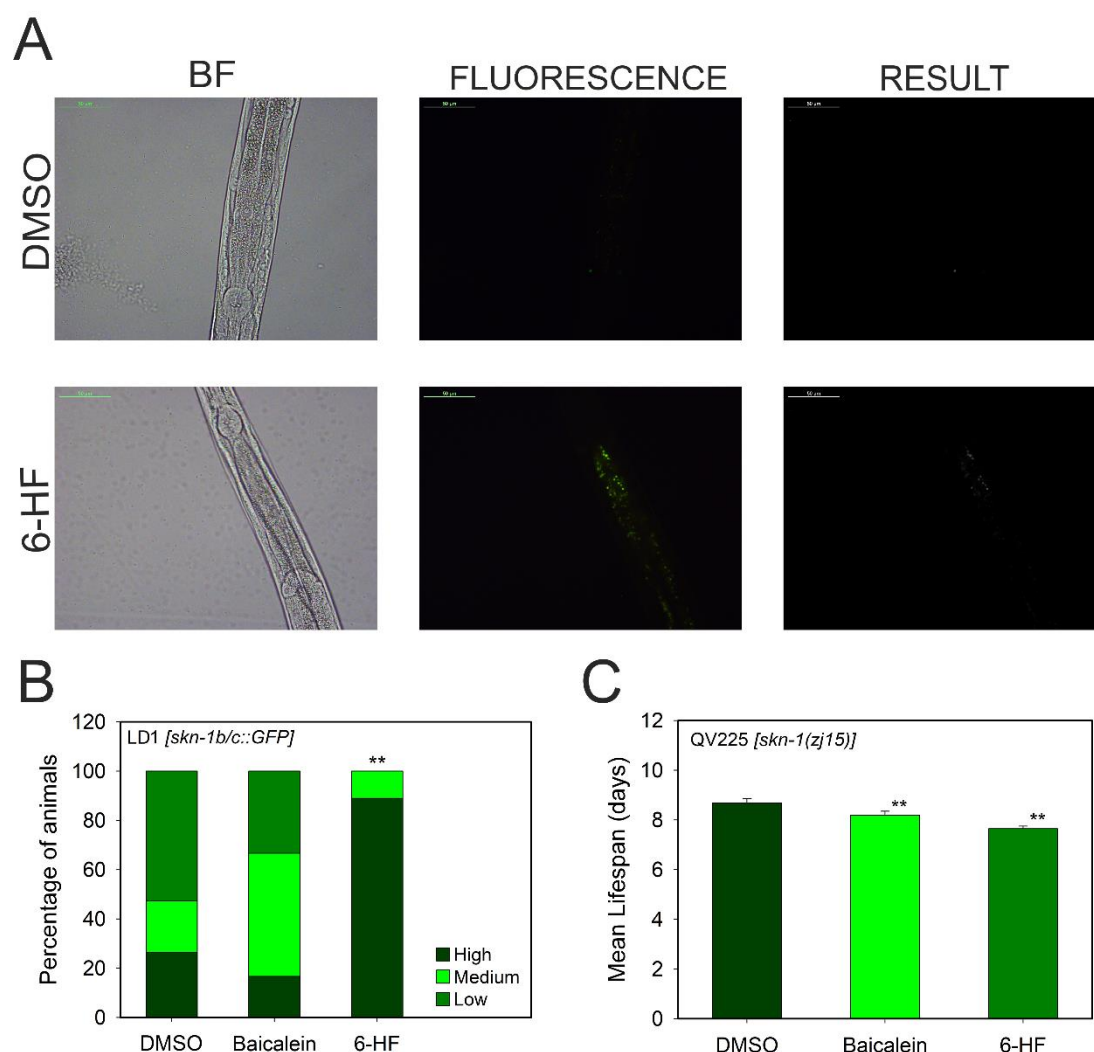


**Figure 13.6. Effect of the different flavonoids on the redox active pathway.** **A.** LD1 strain (*skn-1 b/c::GFP*) treated with DMSO as control, **B.** LD1 strain treated with 100  $\mu$ M of 6-hydroxyflavone. **C.** Results of the integrated fluorescence of the gut in LD1 worms treated with 100  $\mu$ M of each flavone. **D.** Changes in mean lifespan results for mutant worms QV255 (*skn-1(zj15)*) treated with 100  $\mu$ M of each flavone. Scale bar: 50  $\mu$ m.

### 4.3. Baicalein effect on *C. elegans* gene expression

RNA microarray assays from worms treated with baicalein were performed to investigate the possibility that the molecule could modulate *C. elegans* gene expression. The microarray data obtained from this analysis have been deposited to the GEO database (NCBI) [<https://www.ncbi.nlm.nih.gov/geo/>] and assigned the identifier GSE134775. DMSO treated worms were used as a control and their results were compared with water treated ones, to further characterize the solvent effects and compare them with those obtained from baicalein treated worms. DMSO microarray showed the upregulation of microbial defense and innate immune response genes as

*lys-7* (3.35-fold vs control,  $p \leq 0.05$ ) that encoded an antimicrobial lysozyme or the SPP family (Saposin like protein family) with *spp-1* (1.59-fold vs control,  $p \leq 0.05$ ), *spp-2* (3.15-fold vs control,  $p \leq 0.05$ ) or *spp-8* (3.78-fold vs control,  $p \leq 0.05$ ), that are antibacterial peptides present in the *C. elegans* lumen (Roeder et al., 2010). Overexpression of *lys-7* by DMSO has been previously reported in the bibliography using quantitative real-time-PCR (Wang et al., 2010), supporting the results obtained in this microarray.

Additionally, the microarray results for baicalein-treated worms indicated that several pathways were modulated as illustrated in **Fig. 13.7** and in **Table 13.2**. The microarrays showed that baicalein treatment downregulated the insulin signaling pathway including *daf-16* (-1.33-fold vs control,  $p \leq 0.05$ ), *sir 2.1* (-1.5-fold vs control,  $p \leq 0.05$ ), *akt-1* (-1.58-fold vs control,  $p \leq 0.05$ ), *age-1* (-2.1-fold vs control,  $p \leq 0.05$ ) and heat shock proteins.

These results are consistent with the results obtained with the DAF-16 deficient mutant strain and the above-mentioned TJ375 strain which was used to evaluate the antioxidant effect *in vivo* of the compounds. Although baicalein is not DAF-16 dependent, the molecule is able to upregulated the gene expression of some enzymes downstream of DAF-2/DAF-16 involved in stress resistance such as catalase (*ctl-2* 2.5-fold vs control,  $p \leq 0.05$ ) and metallothioneins (*mtl-1* 6.7-fold vs control,  $p \leq 0.05$  and *mtl-2* 8.8-fold vs control,  $p \leq 0.05$ ), and elevated levels of these proteins may contribute to ROS degradation and therefore to a lifespan extension (Barsyte et al., 2001). Gene expression of mitochondrial proteins such as PARPs (poly(ADP-ribose) polymerase) was also downregulated by baicalein treatment: *parp-1* (formerly known as *pme-1*, -4.14-fold vs control,  $p \leq 0.05$ ) and *parp-2* (-3.8-fold vs control,  $p \leq 0.05$ ). It has been reported that RNAi silencing of *parp-1* or treatment with PARP inhibitors in wild-type worms increased their lifespan in the range 15-29% by rising the NAD<sup>+</sup> levels (Mouchiroud et al., 2013). Several studies had concluded that the repression of *parp-1* could be an interesting approach to develop synthetic lethality in cancer cells (Tempka et al., 2018) and in the regulation of the anti-inflammatory response (Aguilar-Quesada et al., 2007).

Baicalein also produced an inhibition of the mTOR (mammalian target of rapamycin) pathway by downregulating *let-363* (-1.26-fold vs control,  $p \leq 0.05$ ), the *C. elegans* ortholog to human mTOR, *daf-15* (-1.7-fold vs control,  $p \leq 0.05$ ), the



ortholog to human RPTOR, *ife-3* (-2.8-fold vs control,  $p \leq 0.05$ ), *riect-1* (-2.00-fold vs control,  $p \leq 0.05$ ) and a overexpression of *pha-4* (1.03-fold vs control,  $p \leq 0.05$ ). Many studies have reported a relationship between mTOR and human diseases such as cancer, cardiovascular diseases, diabetes, obesity and neurological disorders, being involved in age-related diseases and in lifespan regulation (Tsang et al., 2007). mTOR is the main component of two different multiprotein complexes mTORC1 and mTORC2, which are involved in the regulation of the synthesis of proteins needed for cell growth and proliferation (Zarogoulidis et al., 2014). It has been reported that an inhibition of mTORC1 (mTOR complex 1) or mTORC2 (mTOR complex 2) in *C. elegans* produced a lifespan extension dependent of SKN-1, however that inhibition of mTOR did not increase the presence of SKN-1 in cell nuclei (Blackwell et al., 2015; Robida-Stubbs et al., 2012; J. Wang et al., 2010) as happened to the worms treated with baicalein in this study. In addition, PHA-4 transcription factor is described as necessary for the longevity effects associated to mTOR inhibition (Bishop and Guarente, 2007; Panowski et al., 2007), and indeed *pha-4* was upregulated in the worms treated with baicalein as showed in the microarrays performed.

Altogether, the effects of the flavonoid baicalein on *C. elegans* may be partially a result of the molecule downregulation of the expression of mTOR which produced a lifespan extension dependent on SKN-1, being the same effect reported in worms treated with rapamycin (Robida-Stubbs et al., 2012). These results agree with the mechanism of action proposed for baicalein in human cancer cell lines (Aryal et al., 2014; Guo et al., 2015; Wang et al., 2017), that showed growth inhibition of cancer cells via mTOR inhibition. Thus, lifespan extension of *C. elegans* and human cancer cells inhibition by baicalein share the same molecule mechanism.

Baicalein seems also to be a repressor of DAF-18 gene expression (*daf-18* - 5.55-fold vs control,  $p \leq 0.05$ ). DAF-18 is the ortholog of human PTEN tumor suppressor, which is involved in several diseases such as Bannayan-Riley-Ruvalcaba syndrome, carcinoma (multiple), and reproductive organ cancer (multiple). It is proposed that a reduction of PTEN may increase insulin and/or insulin-like growth factor signaling. However an increase of PTEN activity may cause insulin resistance, as happens in late onset diabetes disease (Ogg and Ruvkun, 1998). In *C. elegans* *age-1* mutants, the suppression of *daf-18* caused a decrease in fat storage (Ogg and

Ruvkun, 1998), and adipogenesis reduction has also been reported as a response of mTOR and RPTOR inhibition (Laplane and Sabatini, 2009; Polak et al., 2008).

Thus, the fat storage reduction reported in this work by the worms treated with baicalein (**Fig. 13.3**) agrees with the inhibition of mTOR and RPTOR and the additional activation of the redox active pathway and SKN-1 transcription factor. Besides, the downregulation of PARP expression may increase the NAD<sup>+</sup> levels and therefore contribute to the lifespan extension.

The underlying mechanisms of baicalein and related flavonoids' health promoting effects are mediated by mTOR pathway and the transcription factors SKN-1/Nrf2 and DAF-16/FOXO in the animal model *C. elegans*

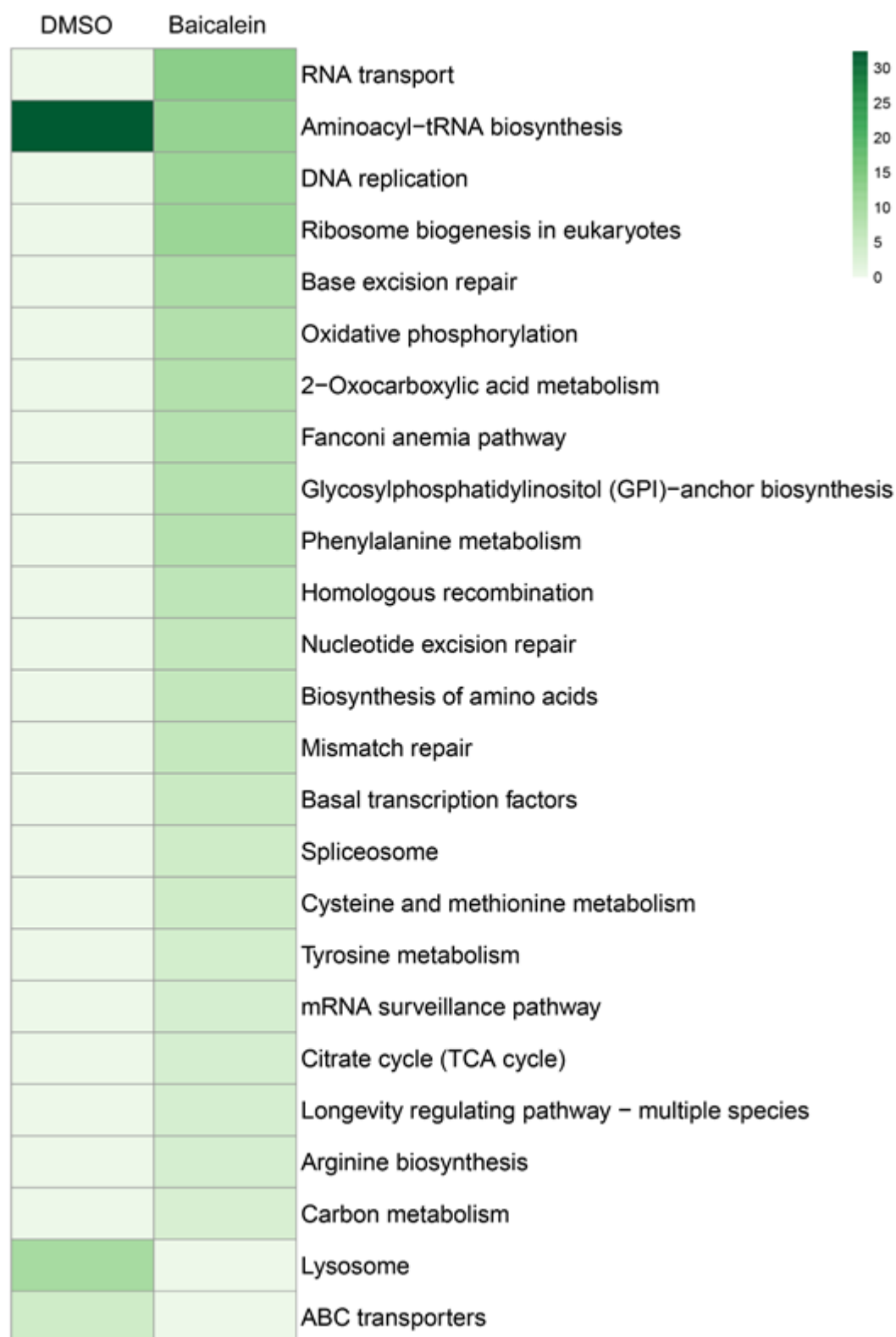


**Figure 13.7. Principal component analysis (PCA) of *C. elegans* pathways altered by baicalein treatment (100  $\mu$ M) vs control worms treated with DMSO.**

## 5. Conclusions

The results showed that all flavonoids tested increase the mean lifespan of the model animal *C. elegans* in a dose-dependent manner, being the most active molecules baicalein, chrysin and 6-hydroxyflavone. Stress resistance assay showed that only 6,7-dihydroxyflavone is able to enhance the oxidative stress resistance of *C. elegans* by reducing an 88.9% the pharynx fluorescence of the strain TJ375 (*hsp-16.2p::GFP*). The other flavonoids had little effect, suggesting that their positive effects on lifespan are not directly related to oxidative stress resistance and radical scavenging properties. The results from the mutant strains for DAF-16 and SKN-1 transcription factors treated with the best enhancers of lifespan showed how different pathways are involved in the flavonoids lifespan extension of *C. elegans*.

Chrysin expanded the lifespan of the worms in a DAF-16 dependent manner, whereas baicalein and 6-hydroxyflavone prolonged the *C. elegans* lifespan via SKN-1 pathway. RNA microarray for baicalein-treated worms showed the downregulation of the mTOR pathway which leads to a reduction in lipids and to an activation of the redox active pathway and SKN-1 transcription factor, being responsible for the lifespan extension in *C. elegans*. Also, the repression of some mitochondrial protein's genes such as *parp-1* and *parp-2* may contribute to the longevity effects showed. Altogether, the results are an indication that baicalein may be a potential drug for the treatment of diseases in which mTOR or PARPs are involved. Also, the tested flavonoids should be further investigated for a possible effect in the prevention and treatment of obesity as they reduced fat accumulation in the model animal. In this sense, the most effective molecule was chrysin, that was able to reduce a 38.9% the fat storage compared to control animals.

**Table 13.1. Survival data for the *C. elegans* treated with flavonoids**

<i>C. elegans</i> Strain	Flavonoid	Concentration ( $\mu$ M)	n	Mean Lifespan (days)	S. E ( $\pm$ day)	Lifespan Change (%)	<i>p</i> -value vs Control
N2 Wild-type	Baicalein	0	166	14.33	0.24		
		10	98	16.7	0.25	16.54	0**
		25	95	16.98	0.27	18.49	0**
		50	80	14.72	0.28	2.72	0.0576
		100	72	14.96	0.29	4.40	0.0077**
	Chrysin	0	90	14.66	0.28		
		10	104	15.9	0.28	8.46	0.000006**
		25	110	14.92	0.25	1.77	0.1914
		50	76	15.1	0.29	3.00	0.226
		100	124	14.38	0.23	-1.91	0.4426
	Scutellarein	0	163	14.58	0.29		
		10	109	13.79	0.4	-5.42	0.3076
		25	105	14.08	0.31	-3.43	0.3288
		50	136	13.54	0.32	-7.13	0.0457**
		100	123	13.59	0.36	-6.79	0.3814
	7,8- Dihydroxyflavone	0	175	13.89	0.21		
		10	105	14.58	0.23	4.97	0.0263**
		25	160	13.71	0.22	-1.30	0.4389
		50	156	13.59	0.2	-2.16	0.1045
		100	83	13.24	0.31	-4.68	0.0177
	6,7- Dihydroxyflavone	0	88	14.71	0.24		
		10	70	14.55	0.3	-1.09	0.4585
		25	86	14.29	0.29	-2.86	0.5925
		50	86	14.52	0.28	-1.29	0.8729
		100	88	14.77	0.27	0.41	0.2216
	6-Hydroxyflavone	0	111	13.96	0.29		
		10	140	14.29	0.3	2.36	0.3262
		25	88	14.04	0.4	0.57	0.5242
		50	74	14.41	0.45	3.22	0.1312
		100	159	15.61	0.25	11.82	0.0001**

The underlying mechanisms of baicalein and related flavonoids' health promoting effects are mediated by mTOR pathway and the transcription factors SKN-1/Nrf2 and DAF-16/FOXO in the animal model *C. elegans*

		0	82	13.87	0.31		
QV255	Baicalein	25	86	14.56	0.21	4.97	0.0168**
( <i>skn-1(zj15)</i> )	Chrysin	10	89	13.15	0.37	-5.19	0.4943
	6-Hydroxyflavone	100	108	14.38	0.21	3.68	0.0079**
		0	85	8.68	0.17		
CF1038 ( <i>daf-16(mu86)</i> )	Baicalein	25	61	8.19	0.16	-5.65	0.0172**
	6-Hydroxyflavone	100	70	7.65	0.1	-11.87	7.8e-8**

**Table 13.2. Pathways modulated by baicalein treatment.** Data obtained from the RNA microarray results vs DMSO control worms.

Pathway Name	DMSO			Baicalein		
	Enrichment	Enrichment	%	Enrichment	Enrichment	%
	Score	<i>p</i> -value	genes	Score	<i>p</i> -value	genes
RNA transport	0.00	0.00	0.00	13.31	1.66E-06	60.00
Aminoacyl-tRNA biosynthesis	32.42	8.30E-15	52.94	12.05	5.84E-06	70.59
DNA replication	0.00	0.00	0.00	11.64	8.78E-06	78.26
Ribosome biogenesis in eukaryotes	0.00	0.00	0.00	11.49	1.03E-05	76.00
Base excision repair	0.00	0.00	0.00	9.16	1.05E-04	90.91
Oxidative phosphorylation	0.00	0.00	0.00	8.31	2.45E-04	56.60
2-Oxocarboxylic acid metabolism	0.00	0.00	0.00	8.12	2.96E-04	90.00
Fanconi anemia pathway	0.00	0.00	0.00	8.10	3.03E-04	71.43
Glycosylphosphatidylinositol (GPI)-anchor biosynthesis	0.00	0.00	0.00	7.84	3.93E-04	140.00
Phenylalanine metabolism	0.00	0.00	0.00	7.83	3.97E-04	100.00
Homologous recombination	0.00	0.00	0.00	6.52	1.48E-03	73.33
Nucleotide excision repair	0.00	0.00	0.00	6.09	2.28E-03	61.54
Biosynthesis of amino acids	0.00	0.00	0.00	5.92	2.69E-03	53.19
Mismatch repair	0.00	0.00	0.00	5.69	3.39E-03	71.43
Basal transcription factors	0.00	0.00	0.00	5.09	6.13E-03	63.16
Spliceosome	0.00	0.00	0.00	4.52	1.09E-02	45.95
Cysteine and methionine metabolism	0.00	0.00	0.00	4.45	1.16E-02	55.56
Tyrosine metabolism	0.00	0.00	0.00	3.74	2.37E-02	58.82
mRNA surveillance pathway	0.00	0.00	0.00	3.56	2.86E-02	46.15
Citrate cycle (TCA cycle)	0.00	0.00	0.00	3.47	3.11E-02	50.00
Longevity regulating pathway - multiple species	0.00	0.00	0.00	3.31	3.64E-02	48.57
Arginine biosynthesis	0.00	0.00	0.00	3.25	3.87E-02	66.67
Carbon metabolism	0.00	0.00	0.00	3.01	4.91E-02	42.47
Lysosome	10.01	4.49E-05	18.67	0.00	0.00	0.00
ABC transporters	4.48	0.01	20.00	0.00	0.00	0.00

## REFERENCES

- Abbas, S., Wink, M., 2014. Green tea extract induces the resistance of *Caenorhabditis elegans* against oxidative stress. *Antioxidants* 3, 129–143.  
<https://doi.org/10.3390/antiox3010129>
- Abbas, S., Wink, M., 2009. Epigallocatechin gallate from green tea (*Camellia sinensis*) increases lifespan and stress resistance in *Caenorhabditis elegans*. *Planta Med.* 75, 216–221. <https://doi.org/10.1055/s-0028-1088378>
- Aguilar-Quesada, R., Munoz-Gamez, J.A., Martin-Oliva, D., Peralta-Leal, A., Quiles-Perez, R., Rodriguez-Vargas, J.M., Ruiz de Almodovar, M., Conde, C., Ruiz-Extremera, A., Oliver, F.J., 2007. Modulation of transcription by PARP-1: consequences in carcinogenesis and inflammation. *Curr. Med. Chem.* 14, 1179–1187. <https://doi.org/10.2174/092986707780597998>
- Aryal, P., Kim, K., Park, P., Ham, S., Cho, J., Song, K., 2014. Baicalein induces autophagic cell death through AMPK/ULK1 activation and downregulation of mTORC1 complex components in human cancer cells. *FEBS J.* 281, 4644–4658.  
<https://doi.org/10.1111/febs.12969>
- Assini, J.M., Mulvihill, E.E., Huff, M.W., 2013. Citrus flavonoids and lipid metabolism. *Curr. Opin. Lipidol.* 24(1), 34–40. doi: 10.1097/MOL.0b013e32835c07fd
- Baltrušaitytė, V., Venskutonis, P.R., Čeksterytė, V., 2007. Radical scavenging activity of different floral origin honey and beebread phenolic extracts. *Food Chem.* 101, 502–514. <https://doi.org/10.1016/j.foodchem.2006.02.007>
- Baptista, F.I., Henriques, A.G., Silva, A.M.S., Wiltfang, J., da Cruz e Silva, O.A.B., 2014. Flavonoids as therapeutic compounds targeting key proteins involved in Alzheimer's disease. *ACS Chem. Neurosci.* 5, 83–92.  
<https://doi.org/10.1021/cn400213r>
- Barsyte, D., Lovejoy, D.A., Lithgow, G.J., 2001. Longevity and heavy metal resistance in *daf-2* and *age-1* long-lived mutants of *Caenorhabditis elegans*. *FASEB J.* 15, 627–634. <https://doi.org/10.1096/fj.99-0966com>
- Barth, S.W., Koch, T.C.L., Watzl, B., Dietrich, H., Will, F., Bub, A., 2012. Moderate effects of apple juice consumption on obesity-related markers in obese men: Impact of diet-gene interaction on body fat content. *Eur. J. Nutr.* 51, 841–850.  
<https://doi.org/10.1007/s00394-011-0264-6>



- Bhattacharya, S., Christensen, K.B., Olsen, L.C.B., Christensen, L.P., Grevsen, K., Færgeman, N.J., Kristiansen, K., Young, J.F., Oksbjerg, N., 2013. Bioactive components from flowers of *Sambucus nigra* L. increase glucose uptake in primary porcine myotube cultures and reduce fat accumulation in *Caenorhabditis elegans*. *J. Agric. Food Chem.* 61, 11033–11040.  
<https://doi.org/10.1021/jf402838a>
- Birt, D.F., Hendrich, S., Wang, W., 2001. Dietary agents in cancer prevention: flavonoids and isoflavonoids. *Pharmacol. Ther.* 90, 157–177.  
[https://doi.org/10.1016/S0163-7258\(01\)00137-1](https://doi.org/10.1016/S0163-7258(01)00137-1)
- Bishop, N.A., Guarente, L., 2007. Two neurons mediate diet-restriction-induced longevity in *C. elegans*. *Nature* 447, 545–549.  
<https://doi.org/10.1038/nature05904>
- Blackwell, T.K., Steinbaugh, M.J., Hourihan, J.M., Ewald, C.Y., Isik, M., 2015. SKN-1/Nrf, stress responses, and aging in *Caenorhabditis elegans*. *Free Radic. Biol. Med.* 88, 290–301. <https://doi.org/10.1016/j.freeradbiomed.2015.06.008>
- Colombo, P.S., Flamini, G., Christodoulou, M.S., Rodondi, G., Vitalini, S., Passarella, D., Fico, G., 2014. Farinose alpine *Primula* species: Phytochemical and morphological investigations. *Phytochemistry* 98, 151–159.  
<https://doi.org/10.1016/j.phytochem.2013.11.018>
- González-Gallego, J., García-Mediavilla, M.V., Sánchez-Campos, S., Tuñón, M.J., 2013. Anti-inflammatory and immunomodulatory properties of dietary flavonoids. *Polyphenols Hum. Heal. Dis.* 1, 435–452.  
<https://doi.org/10.1016/B978-0-12-398456-2.00032-3>
- Grünz, G., Haas, K., Soukup, S., Klingenspor, M., Kulling, S.E., Daniel, H., Spanier, B., 2012. Structural features and bioavailability of four flavonoids and their implications for lifespan-extending and antioxidant actions in *C. elegans*. *Mech. Ageing Dev.* 133, 1–10. <https://doi.org/10.1016/B978-0-12-398456-2.00032-3>
- Guo, Z., Hu, X., Xing, Z., Xing, R., Lv, R., Cheng, X., Su, J., Zhou, Z., Xu, Z., Nilsson, S., 2015. Baicalein inhibits prostate cancer cell growth and metastasis via the caveolin-1/AKT/mTOR pathway. *Mol. Cell. Biochem.* 406, 111–119.  
<https://doi.org/10.1007/s11010-015-2429-8>
- Havermann, S., Humpf, H.U., Wätjen, W., 2016. Baicalein modulates stress-resistance and life span in *C. elegans* via SKN-1 but not DAF-16. *Fitoterapia*

- 113, 123–127. <https://doi.org/10.1016/j.fitote.2016.06.018>
- Islam, M.N., Downey, F., Ng, C.K.Y., 2011. Comparative analysis of bioactive phytochemicals from *Scutellaria baicalensis*, *Scutellaria lateriflora*, *Scutellaria racemosa*, *Scutellaria tomentosa* and *Scutellaria wrightii* by LC-DAD-MS. *Metabolomics* 7, 446–453. <https://doi.org/10.1007/s11306-010-0269-9>
- Jaacks, L.M., Vandevijvere, S., Pan, A., McGowan, C.J., Wallace, C., Imamura, F., Mozaffarian, D., Swinburn, B., Ezzati, M., 2019. The obesity transition: stages of the global epidemic. *Lancet Diabetes Endocrinol.* 7, 231–240. [https://doi.org/10.1016/S2213-8587\(19\)30026-9](https://doi.org/10.1016/S2213-8587(19)30026-9)
- Laplante, M., Sabatini, D.M., 2009. An emerging role of mTOR in lipid biosynthesis. *Curr. Biol.* 19, R1046–R1052. <https://doi.org/10.1016/j.cub.2009.09.058>
- Le Marchand, L., 2002. Cancer preventive effects of flavonoids—a review. *Biomed. Pharmacother.* 56, 296–301. [https://doi.org/10.1016/S0753-3322\(02\)00186-5](https://doi.org/10.1016/S0753-3322(02)00186-5)
- Li-Weber, M., 2009. New therapeutic aspects of flavones: the anticancer properties of *Scutellaria* and its main active constituents Wogonin, Baicalein and Baicalin. *Cancer Treat. Rev.* 35, 57–68. <https://doi.org/10.1016/j.ctrv.2008.09.005>
- Mouchiroud, L., Houtkooper, R.H., Moullan, N., Katsyuba, E., Ryu, D., Cantó, C., Mottis, A., Jo, Y.-S., Viswanathan, M., Schoonjans, K., 2013. The NAD<sup>+</sup>/sirtuin pathway modulates longevity through activation of mitochondrial UPR and FOXO signaling. *Cell* 154, 430–441. <https://doi.org/10.1016/j.cell.2013.06.016>
- Murphy, C.T., Hu, P.J., 2005. Insulin/insulin-like growth factor signaling in *C. elegans*. *WormBook*, ed. The *C. elegans* research community. doi/10.1895/wormbook.1.164.1, <http://www.wormbook.org>
- Ogg, S., Ruvkun, G., 1998. The *C. elegans* PTEN homolog, DAF-18, acts in the insulin receptor-like metabolic signaling pathway. *Mol. Cell* 2, 887–893. [https://doi.org/10.1016/S1097-2765\(00\)80303-2](https://doi.org/10.1016/S1097-2765(00)80303-2)
- Panche, A.N., Diwan, A.D., Chandra, S.R., 2016. Flavonoids: an overview. *J. Nutr. Sci.* 5, E47. doi:10.1017/jns.2016.41
- Panowski, S.H., Wolff, S., Aguilaniu, H., Durieux, J., Dillin, A., 2007. PHA-4/Foxa mediates diet-restriction-induced longevity of *C. elegans*. *Nature* 447, 550–555. <https://doi.org/10.1038/nature05837>
- Polak, P., Cybulski, N., Feige, J.N., Auwerx, J., Rüegg, M.A., Hall, M.N., 2008. Adipose-specific knockout of raptor results in lean mice with enhanced

- mitochondrial respiration. *Cell Metab.* 8, 399–410.  
<https://doi.org/10.1016/j.cmet.2008.09.003>
- Ren, L., Wang, F., Xu, Z., Chan, W.M., Zhao, C., Xue, H., 2010. GABAA receptor subtype selectivity underlying anxiolytic effect of 6-hydroxyflavone. *Biochem. Pharmacol.* 79, 1337–1344. <https://doi.org/10.1016/j.bcp.2009.12.024>
- Robida-Stubbs, S., Glover-Cutter, K., Lamming, D.W., Mizunuma, M., Narasimhan, S.D., Neumann-Haefelin, E., Sabatini, D.M., Blackwell, T.K., 2012. TOR signaling and rapamycin influence longevity by regulating SKN-1/Nrf and DAF-16/FoxO. *Cell Metab.* 15, 713–724. <https://doi.org/10.1016/j.cmet.2012.04.007>
- Roeder, T., Stanisak, M., Gelhaus, C., Bruchhaus, I., Grötzinger, J., Leippe, M., 2010. Caenopores are antimicrobial peptides in the nematode *Caenorhabditis elegans* instrumental in nutrition and immunity. *Dev. Comp. Immunol.* 34, 203–209.  
<https://doi.org/10.1016/j.dci.2009.09.010>
- Shieh, D., Liu, L.-T., Lin, C.-C., 2000. Antioxidant and free radical scavenging effects of baicalein, baicalin and wogonin. *Anticancer Res.* 20, 2861–2865.
- Tempka, D., Tokarz, P., Chmielewska, K., Kluska, M., Pietrzak, J., Rygielska, Ż., Virág, L., Robaszkiewicz, A., 2018. Downregulation of PARP1 transcription by CDK4/6 inhibitors sensitizes human lung cancer cells to anticancer drug-induced death by impairing OGG1-dependent base excision repair. *Redox Biol.* 15, 316–326. <https://doi.org/10.1016/j.redox.2017.12.017>
- Tsang, C.K., Qi, H., Liu, L.F., Zheng, X.F.S., 2007. Targeting mammalian target of rapamycin (mTOR) for health and diseases. *Drug Discov. Today* 12, 112–124.  
<https://doi.org/10.1016/j.drudis.2006.12.008>
- Wang, J., Robida-Stubbs, S., Tullet, J.M.A., Rual, J.-F., Vidal, M., Blackwell, T.K., 2010. RNAi screening implicates a SKN-1–dependent transcriptional response in stress resistance and longevity deriving from translation inhibition. *PLoS Genet.* 6, e1001048. <https://doi.org/10.1371/journal.pgen.1001048>
- Wang, X., Wang, Xiaoyan, Li, L., Wang, D., 2010. Lifespan extension in *Caenorhabditis elegans* by DMSO is dependent on *sir-2.1* and *daf-16*. *Biochem. Biophys. Res. Commun.* 400, 613–618.  
<https://doi.org/10.1016/j.bbrc.2010.08.113>
- Wang, Y.-F., Xu, Y.-L., Tang, Z.-H., Li, T., Zhang, L.-L., Chen, X., Lu, J.-H., Leung, C.-H., Ma, D.-L., Qiang, W.-A., 2017. Baicalein induces beclin 1-and

extracellular signal-regulated kinase-dependent autophagy in ovarian cancer cells. *Am. J. Chin. Med.* 45, 123–136.

<https://doi.org/10.1142/S0192415X17500094>

Williams, R.J., Spencer, J.P.E., 2012. Flavonoids, cognition, and dementia: actions, mechanisms, and potential therapeutic utility for Alzheimer disease. *Free Radic. Biol. Med.* 52, 35–45. <https://doi.org/10.1016/j.freeradbiomed.2011.09.010>

Zanoli, P., Avallone, R., Baraldi, M., 2000. Behavioral characterisation of the flavonoids apigenin and chrysin. *Fitoterapia* 71, S117–S123.

[https://doi.org/10.1016/S0367-326X\(00\)00186-6](https://doi.org/10.1016/S0367-326X(00)00186-6)

Zarogoulidis, P., Lampaki, S., Turner, J.F., Huang, H., Kakolyris, S., Syrigos, K., Zarogoulidis, K., 2014. mTOR pathway: A current, up-to-date mini-review. *Oncol. Lett.* 8, 2367–2370. <https://doi.org/10.3892/ol.2014.2608>



**Chapter XIV.** Artificial food dyes increase activity and oxidative stress  
in the animal model *Caenorhabditis elegans*



### **Contextualization**

In the current world of stimuli, appearance has become an important topic in all aspects, including food. It is essential that foods present colors that make them appetizing and visually attractive, and the use of dyes has spread in response. There are different natural pigments that are used by the food industry like  $\beta$ -carotene, betanin, or curcumin (Wrolstad and Culver, 2012). However, the requirements of the food industry are so high that obtaining these natural pigments is not economically feasible. In addition, they have low durability in the food and cannot cover the whole range of necessary colors. Therefore, in recent decades the consumption of artificial food dyes (AFD) has increased significantly (Stevens et al., 2015). These compounds are found in foods and beverages consumed by the entire world population, and they especially influence children, due to their presence in candies and desserts. Some studies have shown that children consume AFD in higher amounts than recommended by official agencies such as EFSA (European Food Safety Authority) or FAD (United States Food and Drug Administration) (Husain et al., 2006; Stevens et al., 2015). The lack of awareness by the consumer may be responsible for this high intake, since several studies have shown that an excessive consumption can be harmful to health (Khayyat et al., 2017; Macioszek and Kononowicz, 2004; Mohamed et al., 2015; Sasaki et al., 2002). One of the most relevant studies in this field is known as "Southampton studies" (McCann et al., 2007) where mixtures of six of the most used AFDs were related to an increase in the hyperactivity of children diagnosed with attention deficit hyperactivity disorder (ADHD). After these studies, EFSA reevaluated and decreased the ADI (Acceptable Daily Intake) of three dyes: quinoline yellow, sunset yellow and ponceau 4R ("Scientific Opinion on the re-evaluation of Ponceau 4R (E 124) as a food additive," 2009, "Scientific Opinion on the re-evaluation of Quinoline Yellow (E 104) as a food additive," 2009, "Scientific Opinion on the re-evaluation of Sunset Yellow FCF (E 110) as a food additive," 2009). However, this measure could be considered preventive because the study did not show a direct relationship between hyperactivity and consumption of these dyes. In addition, the "Southampton studies" lack individual assays that may highlight the effect of each dye used in their mixtures. Based on these studies and in view of the increased consumption of artificial food colorants, the aim of this chapter is to provide information about the *in vivo* effect of six AFDs (**Fig. 14.1**) in *Caenorhabditis elegans*.



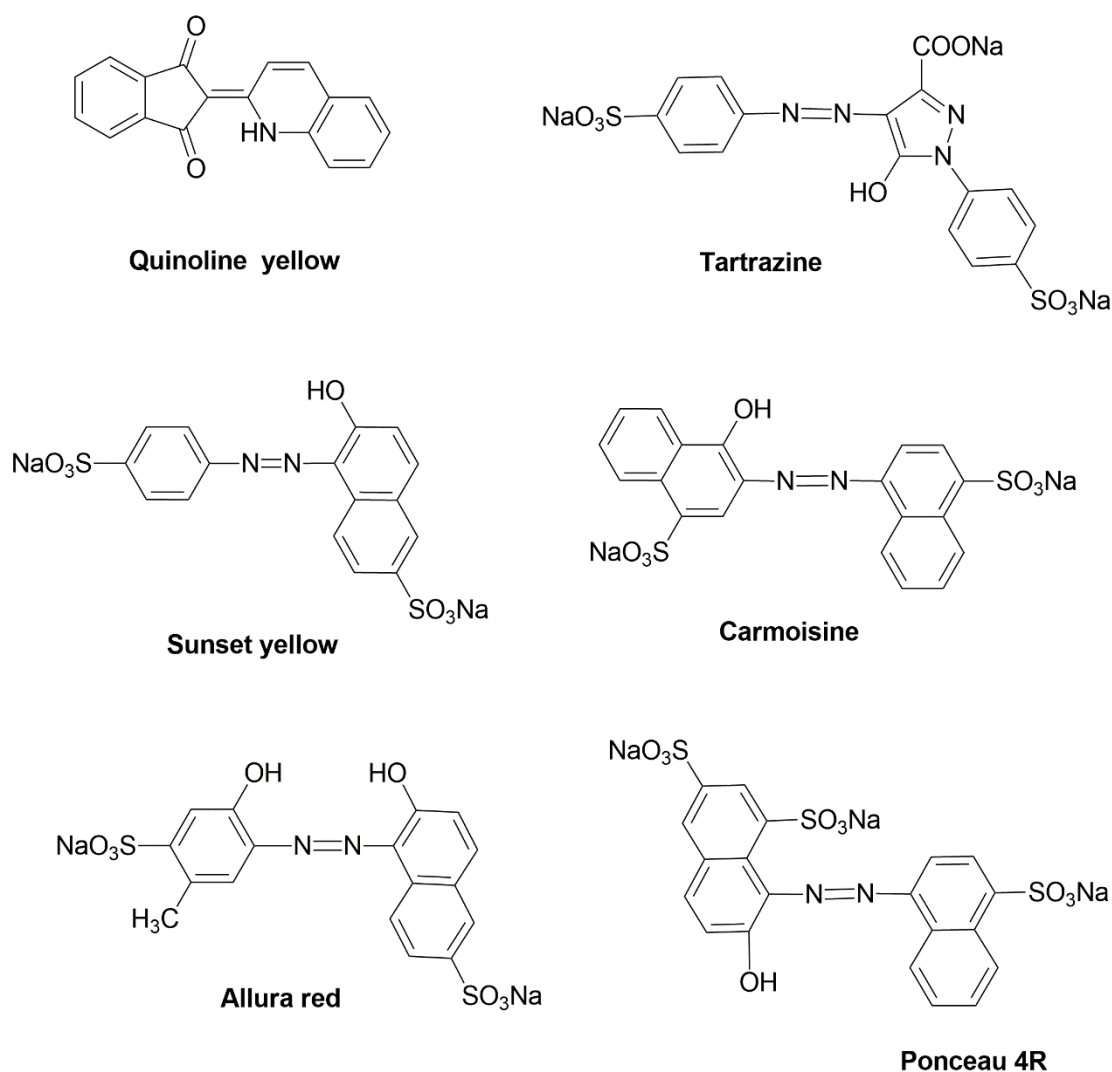


**Figure 14.1.** Chemical structures for the artificial food dyes (AFDs) employed in this chapter.

## 1. Effect of individual AFD on *C. elegans* lifespan

The wild-type N2 strain was used to study the effect of each individual dye in the lifespan of *C. elegans*. Wild-type worms were exposed for 48 hours to concentrations of 10, 25, 50 and 100  $\mu$ M of colorants in acute exposure assay (**Table 14.1**). The worms were then transferred to fresh NGM supplemented with *E. coli* as food source and incubated at 25 °C in the lifespan machine. Acute exposure to colorants negatively affected the mean lifespan of worms (**Fig. 14.2**). **Fig. 14.2** shows relative decrease of lifespan in the presence of AFDs and the survival curves are included in the **Fig. 14.3**.

The negative effect shown was dose-dependent and directly proportional to colorant concentration. At the highest concentration, mean lifespan decreased 10.6% for allura red exposure, 25.0% for ponceau, 31.2% for carmoisine, 10.0% for tartrazine, 20.2% for sunset yellow and 20.2% for quinoline yellow with respect to non-treated worms. This reduction in the lifespan was higher when chronic exposure of colorants was assayed (**Fig. 14.4** and **Table 14.2**). Concentrations of 10, 50 and 100  $\mu\text{M}$  were used directly on the plates in order to evaluate the effects of a chronic exposure to individual colorants, producing a decrease of up to 28.6% with respect to the control worms with the exposure at 100  $\mu\text{M}$  of allura red and ponceau (**Fig. 14.4**). This corresponds to 2.4 days less of mean lifespan in the model animal. For carmoisine exposure a decrease in lifespan of 26.8% was experienced by *C. elegans*. The yellow colorants provoked a decrease of 25.6% for tartrazine, 23.0% for sunset yellow and 24.4% for quinoline yellow.

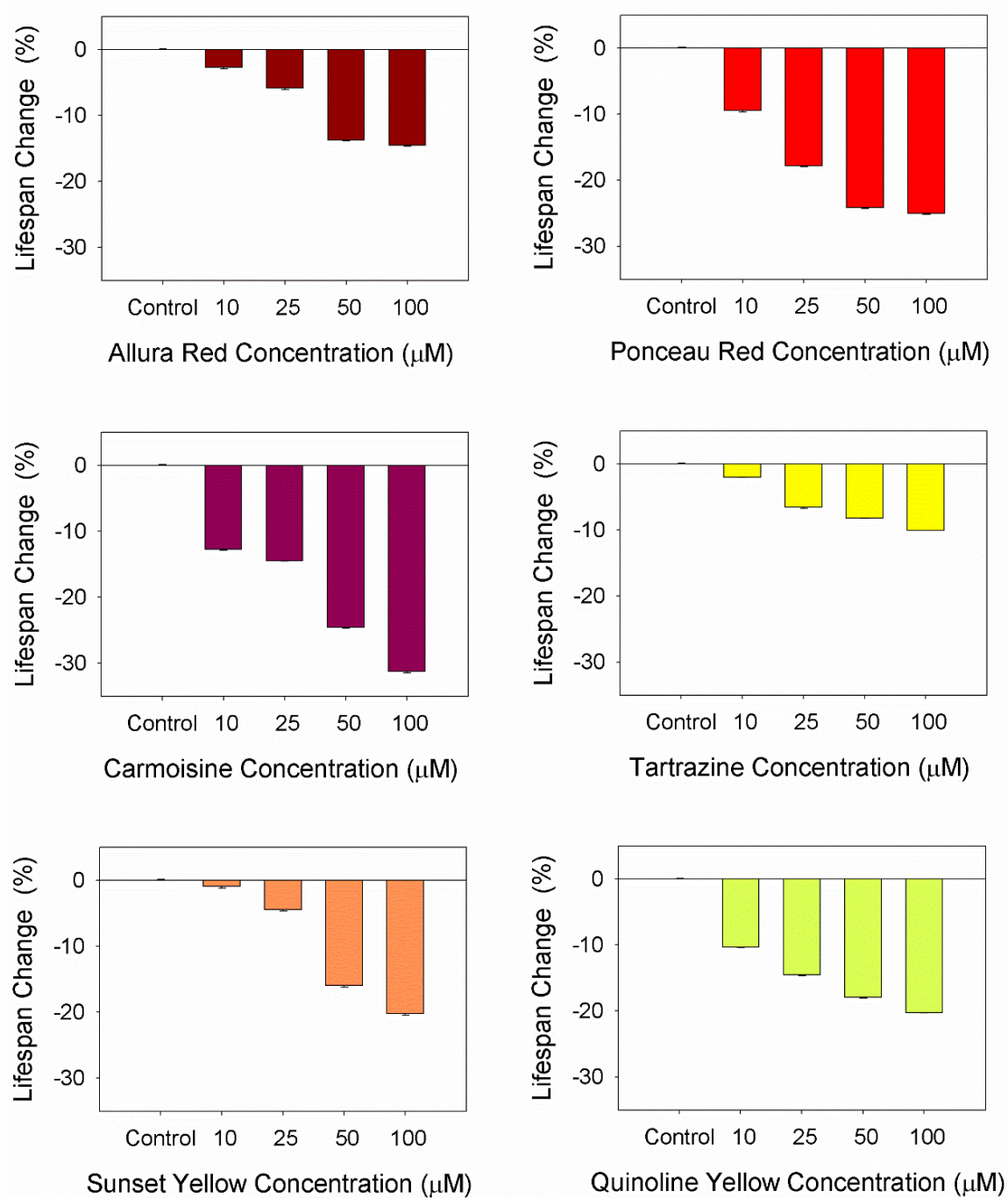


**Figure 14.2.** Mean lifespan changes of *C. elegans* wild-type strain obtained after an acute exposure to individual AFDs. Histograms show the negative effect produced by an exposition of 48 hours to individual artificial food dyes at 10, 25, 50 and 100 μM concentrations.

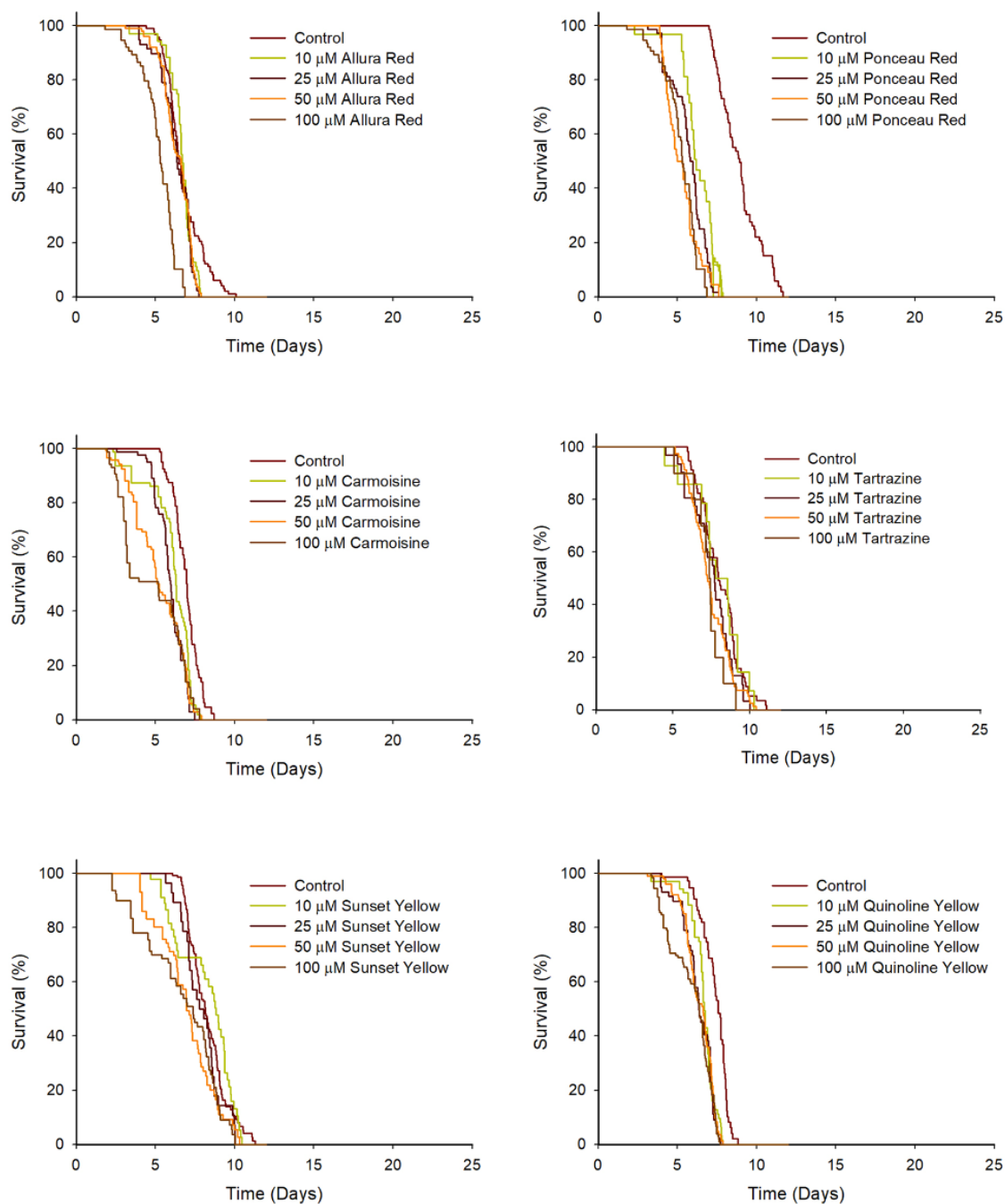


**Figure 14.3. Lifespan curves of *C. elegans* wild-type strain obtained after an acute exposure to individual AFDs.** Curves show the evolution of worms' survival after an exposition of 48 hours to individual artificial food dyes at 10, 25, 50 and 100  $\mu$ M concentrations.

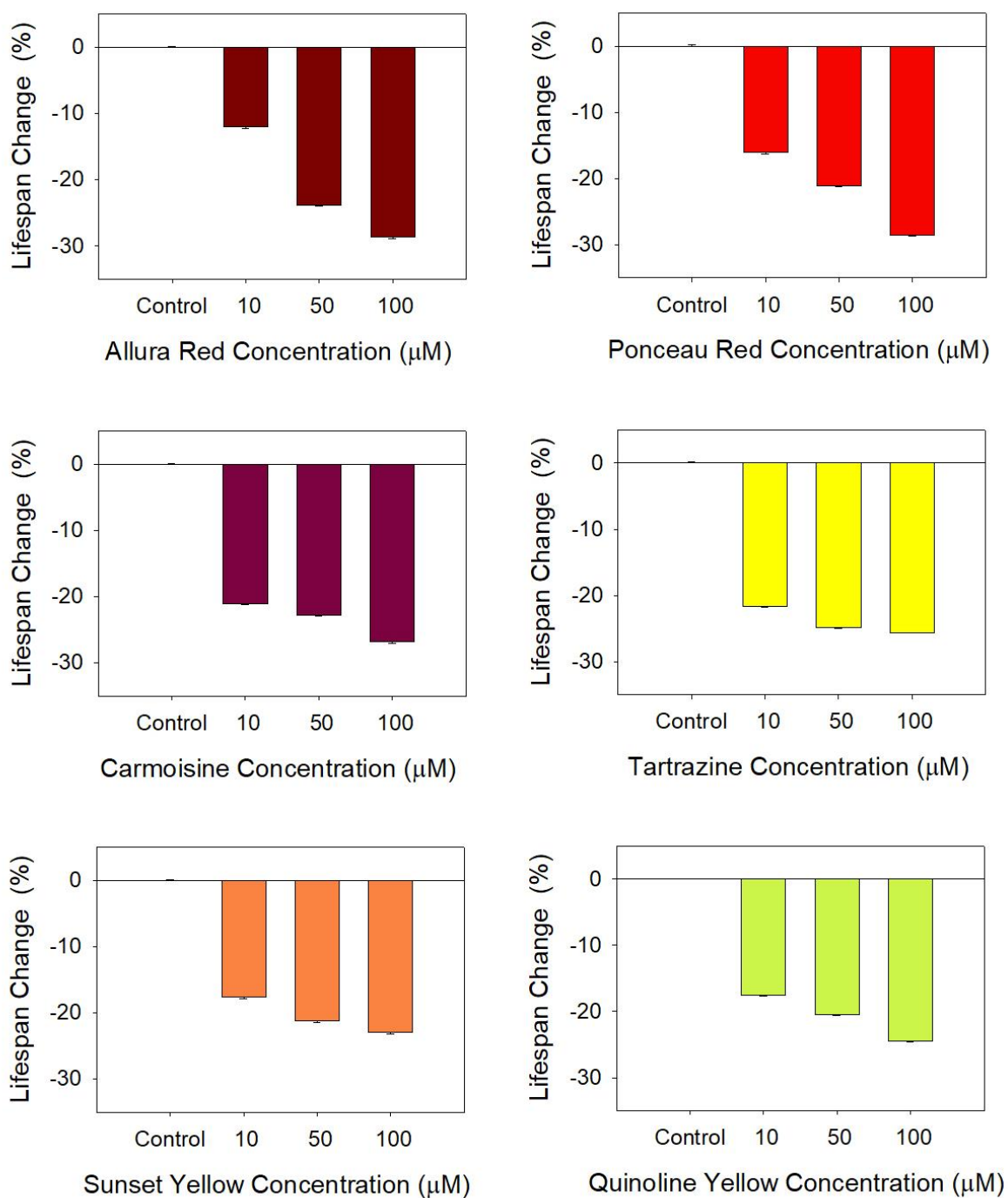


**Figure 14.4. Mean lifespan changes of *C. elegans* wild-type strain obtained after chronic exposure to different concentrations of individual AFDs.** Histograms show the negative effect produced by continuous exposition to individual artificial food dyes at 10, 50 and 100  $\mu$ M concentrations.

## 2. Lipofuscin accumulation in *C. elegans*

Worms treated with AFDs presented a higher accumulation of lipofuscin than untreated worms. For comparative purposes, the blue fluorescence emitted by the intestinal region of untreated worms was taken as 100% of fluorescence and then compared with the emission from treated worms (**Fig. 14.5**). The amount of lipofuscin increased in worms exposed to quinoline yellow (154%), ponceau 4R (182%) and carmoisine (169%) with respect to untreated worms while sunset yellow did not produce a higher accumulation of lipofuscin (88%). Allura red and tartrazine exposition produced the highest values (277% and 344%, respectively) in the accumulation of lipofuscin.

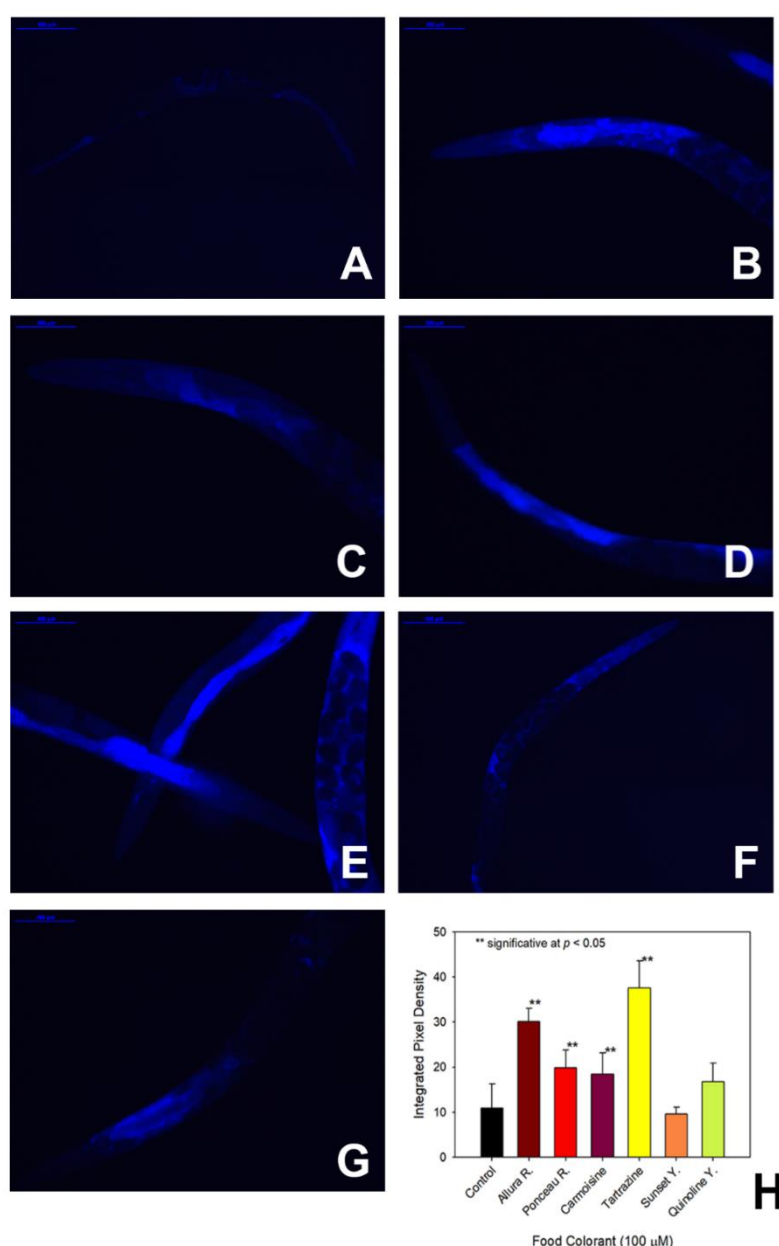


**Figure 14.5. Accumulation of lipofuscin in 4-days old worms.** (Continues on the next page).

**A-G** show representative images of untreated worms (**A**) and worms treated with 100  $\mu$ M of allura red (**B**), ponceau 4R (**C**), carmoisine (**D**), tartrazine (**E**), sunset yellow (**F**) and quinoline yellow (**G**). **H**: Quantification of fluorescence emitted by lipofuscin accumulation.

### 3. Effects of AFDs in the antioxidant system of *C. elegans*

The effects of the exposition to colorants in the antioxidant system of *C. elegans* were studied measuring the fluorescence intensity emitted by *C. elegans* strain TJ375. This strain contains a reporter transgene that expresses green fluorescence protein (GFP) linked to a promoter of small heat shock protein (HSPs), expressed in a stress situation (Feder and Hofmann, 1999). In *C. elegans*, HSPs are a group of 16 kDa proteins and their expression are induced in response to heavy metals (Stringham and Candido, 1994) or quinones (Link et al., 1999). The strain TJ375 contains the *hsp-16.2::GFP* construction, responsible for the fluorescence emitted in the pharynx cells under oxidative stress (Link et al., 1999). In this assay, exposition to juglone (naphthoquinone) 20  $\mu$ M was employed as a positive control of oxidative stress. The addition of the six colorants produced worms with green fluorescence in the pharynx, an indication of oxidative stress. Tartrazine, carmoisine and quinoline yellow were less harmful dyes, producing a fluorescence of 19.5%, 19.6% and 18.7%, respectively, with respect to the juglone effect (100%). The fluorescence values due to ponceau 4R, sunset yellow, and allura red exposure were 31.9%, 36.7%, and 44.8%, respectively, while in the absence of juglone or dyes there was no response (**Fig. 14.6A**). The added oxidative effect produced by the presence of juglone in combination with each AFD was also assayed. In this case, the fluorescence of TJ375 worms increased as a result of a higher oxidative stress. The combination of juglone and colorants yielded the following values: 184.5% (respect to juglone only control) for tartrazine, 316.2% for sunset yellow, 282.5% for quinoline yellow, 232.9% for ponceau 4R, 190.5% for carmoisine and 321.6% for allura red (**Fig. 14.6B**).

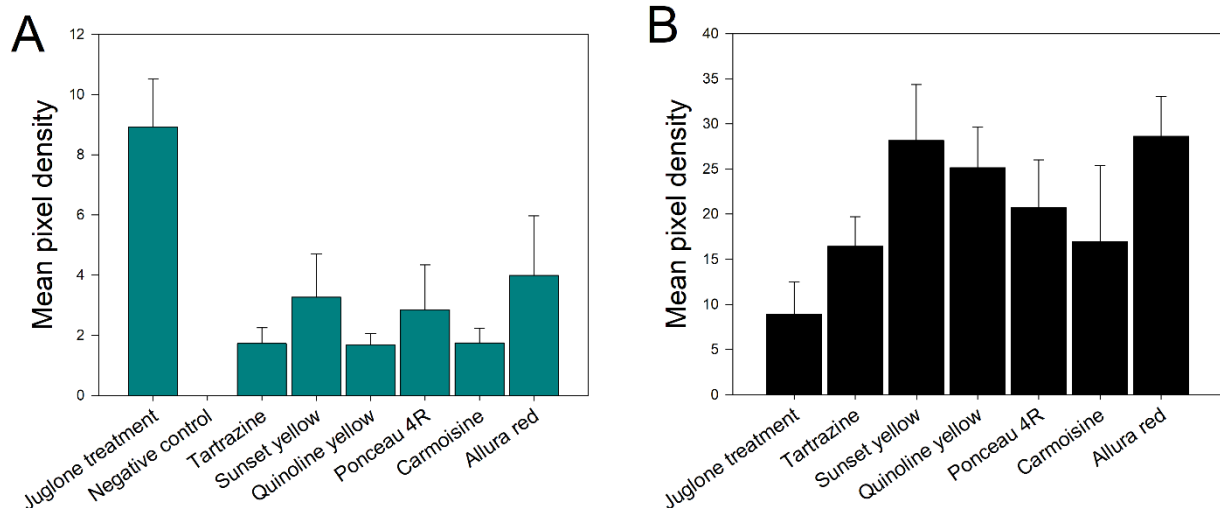


**Figure 14.6. Expression of HSPs measured through the fluorescence emitted in the pharynx of *C. elegans* TJ375 (*hsp-16.2::GFP*) strain.** **A.** Effect of individual AFDs in the fluorescence located in the pharynx. **B.** Effect of exposure to individual AFDs in worms treated with juglone. In all cases, AFDs were administered at 100  $\mu$ M concentration.

#### 4. Neurological effects of AFDs in *C. elegans*

AFDs have been related to attention deficit hyperactivity disorder (ADHD), one of the most common behavioural disorder in children (Schab and Trinh, 2004). Some reports also associate ADHD with alterations in the expression of genes involved in dopaminergic, serotonergic and noradrenergic neurotransmission systems (Banaschewski et al., 2010). In order to explore the relationship between AFDs and neuronal alterations in the animal model, BZ555 (*dat-1p::GFP*) strain of *C. elegans* was employed. This strain expresses GFP under *dat-1* promoter, which encodes a plasma membrane dopamine transporter. The administration of tartrazine or quinoline yellow produced an increase in the expression of *dat-1* promoter and, consequently, a higher accumulation of dopamine into the dopaminergic neurons (**Fig. 14.7E and G**). On the other hand, allura red, ponceau red, carmoisine and sunset yellow produced a slight decrease in the fluorescence of dopaminergic neurons.



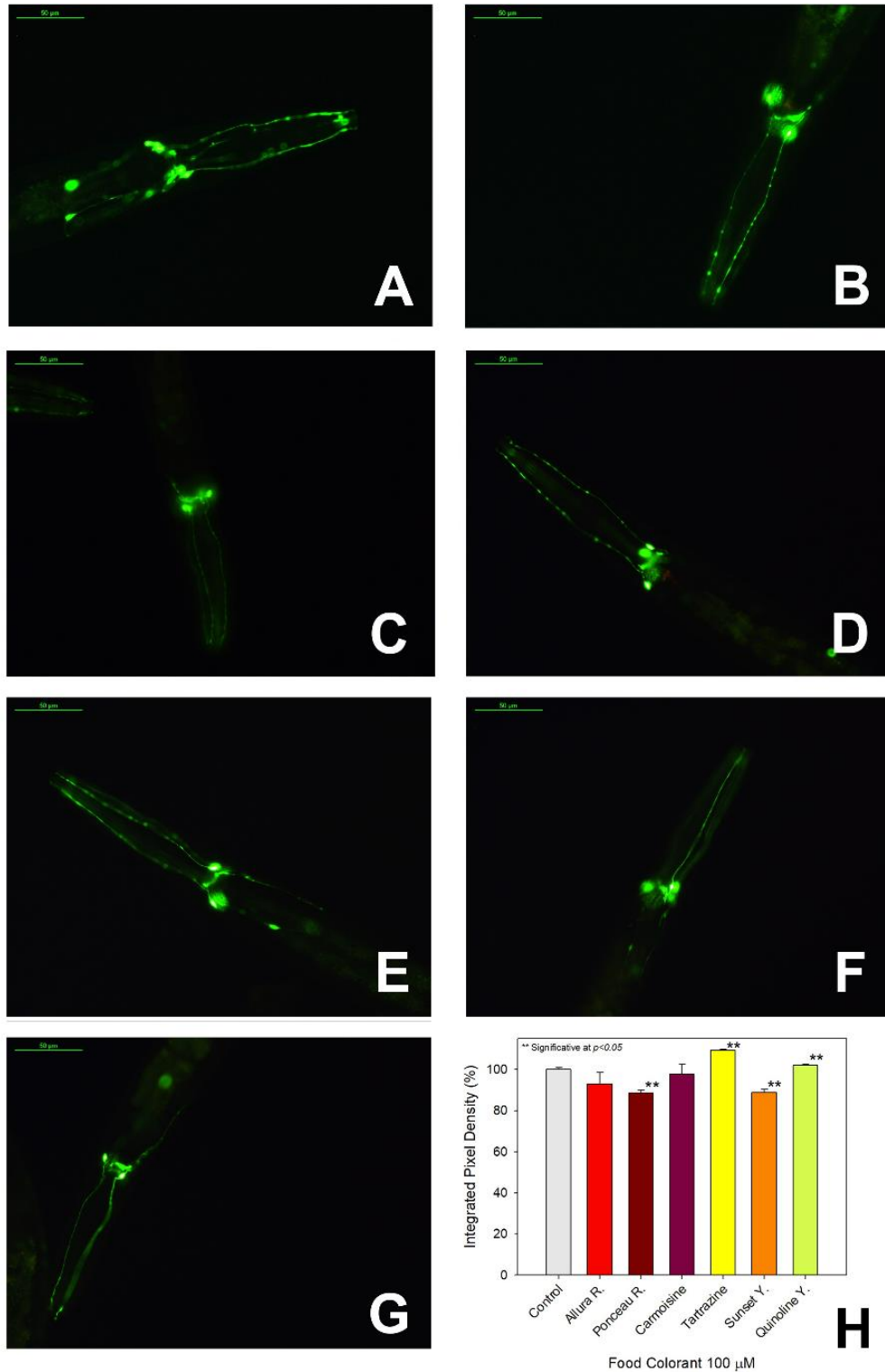


**Figure 14.7. Fluorescence emitted by the dopamine receptor *dat-1* expressed in dopaminergic neurons of *C. elegans* BZ555 (*dat-1p::GFP*) strain.** A-G show representative images of dopaminergic neurons visualized through the fluorescence (I3 filtercube, Leica microscope) of *dat-1* receptor expressed in untreated worms (A) and worms treated with 100 µM of allura red (B), ponceau 4R (C), carmoisine (D), tartrazine (E), sunset yellow (F) and quinoline yellow (G). H: Quantification of fluorescence emitted by expression of *dat-1p::GFP*.

## 5. Movement analysis of worms exposed to AFDs

The motility of untreated worms showed an average speed of 0.21 mm/s but this value was higher in *C. elegans* treated with some of the AFDs. Worms exposed to 100  $\mu$ M of tartrazine or sunset yellow had an increase of 25% ( $p$  value of 0.025) and 66% ( $p$  value  $\leq 0.00001$ ) in average speed, respectively (Fig. 14.8A). Additionally, the treatment of worms with tartrazine or sunset yellow produced an increase in their maximum speed and their number of body lengths per second (BLPS), as Fig. 14.8B-C shows. The rest of colorants had no significant effect in the motility of the animals.

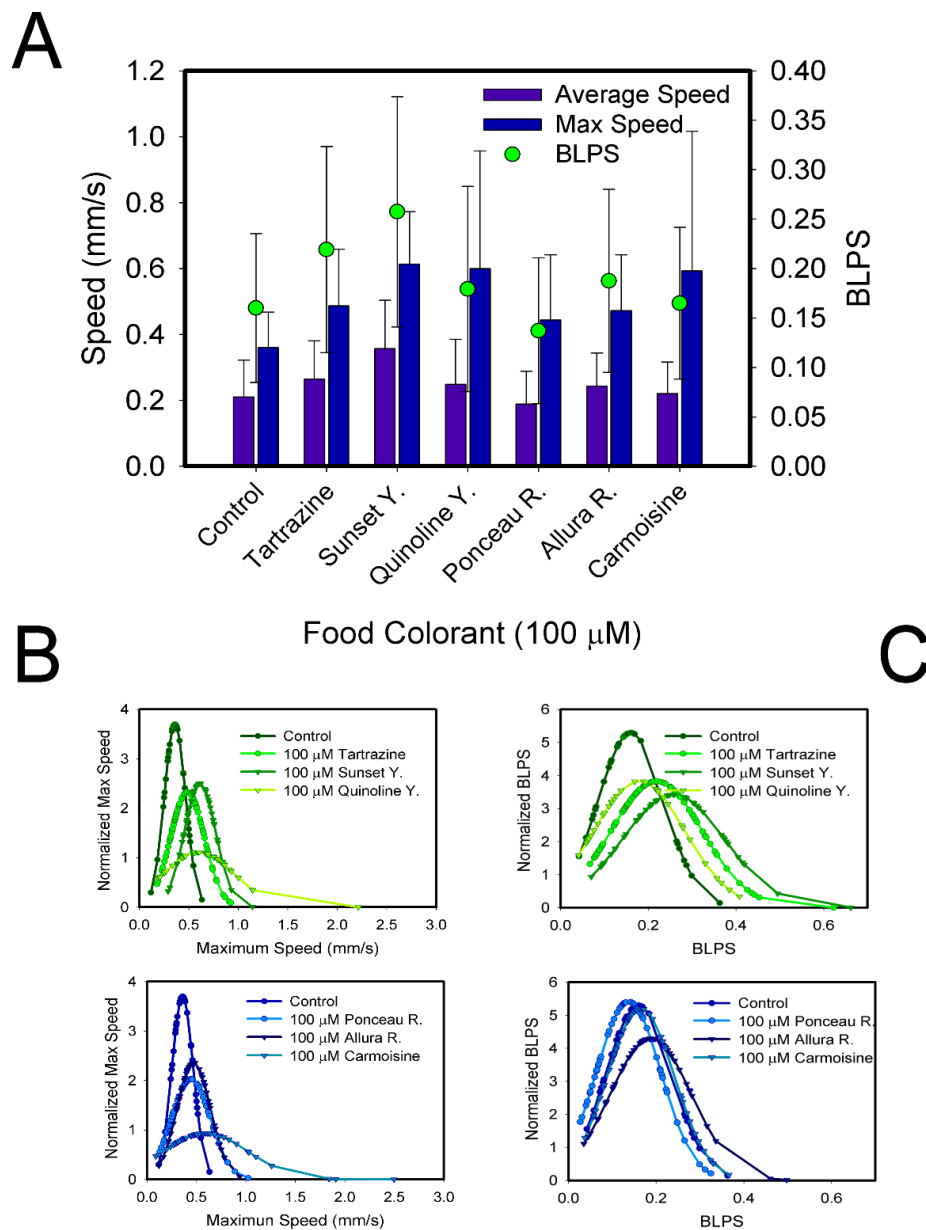


**Figure 14.8. Changes in motility parameters of *C. elegans* wild-type after exposure to individual AFDs.** (Continues on the next page)

A. Effect of AFDs 100  $\mu$ M in mean speed, maximum speed and blps (body length per second) of worms. Normal distributions are shown for the maximum speed (**B**) and blps (**C**) of the control and treated worms (100  $\mu$ M AFDs). Values are clustered around the mean average speed obtained in each case.

## 6. Effect of tartrazine and ponceau 4R in gene expression by RNA microarray analysis

The six colorants used in this chapter showed potential toxic effects in the *C. elegans* lifespan assays. Thus, RNA microarrays were used to estimate whether these toxic effects could involve changes in gene expression of worms treated with the colorants. Tartrazine and ponceau 4R were chosen for being well-known colorants used worldwide in a wide variety of alimentary products and in cosmetic formulations and have presented high toxicity in chronic assays performed with *C. elegans*. In addition, tartrazine was selected because some reports suggest that tartrazine consumption is linked to ADHD (attention deficit/hyperactivity disorder) in children (Stevens et al., 2011). The microarray data from these analysis have been deposited to the GEO database (NCBI) [<https://www.ncbi.nlm.nih.gov/geo/>] and assigned the identifier GSE143611.

RNA microarray of *C. elegans* treated with tartrazine showed genes of the insulin signaling pathway up or down regulated like *ins-7* (9.5-fold,  $p$  vs control  $\leq 0.05$ ), *ins-10* (3.6-fold,  $p$  vs control  $\leq 0.05$ ), *ins-19* (1.3-fold,  $p$  vs control  $\leq 0.05$ ) and *ins-11* (-2.5-fold,  $p$  vs control  $\leq 0.05$ ). Tartrazine treatment also downregulated other immune related genes such as *sek-1* (-1.9-fold,  $p$  vs control  $\leq 0.05$ ), *pmk-1* (-2.1-fold,  $p$  vs control  $\leq 0.05$ ) and their target gene *gcs-1* (-1.25-fold,  $p$  vs control  $\leq 0.05$ ). Heat shock factor (HSF) was also modulated by tartrazine, upregulating the upstream genes *hsb-1* (2.7-fold,  $p$  vs control  $\leq 0.05$ ) and *ddl-1* (2.4-fold,  $p$  vs control  $\leq 0.05$ ). Worms treated with ponceau 4R showed an alteration in the metabolic pathway (5.2-fold,  $p$  vs control  $\leq 0.05$ ). The microarrays showed that the main genes affected were *lips-17* (-1.79-fold,  $p$  vs control  $\leq 0.05$ ), the steroid dehydrogenase gen *stdh-3* (-1.4-fold,  $p$  vs control  $\leq 0.05$ ), infection response genes like *lys-7* (3.1-fold,  $p$  vs control  $\leq 0.05$ ) and *spp-1* (1.4-fold,  $p$  vs control  $\leq 0.05$ ) as well as the heat shock protein *hsp-16.2* (4.55-fold,  $p$  vs control  $\leq 0.05$ ).

## 7. Discussion

The experiments performed in this chapter provide a new insight into the effects of AFDs *in vivo* by using the animal model *C. elegans*. The safety of such colorants widely used by the food industry has been questioned by studies that have reported negative health effects after their consumption ((Amin et al., 2010; Gao et al., 2011; Macioszek and Kononowicz, 2004; Sasaki et al., 2002; Stevens et al., 2011). *C. elegans* is well-accepted animal model for use in experiments related to the bioactivity of low molecular weight molecules that are incorporated into their standard diet constituted by bacteria (Abbas and Wink, 2009; Chen et al., 2013; García-Casas et al., 2018; Guerrero-Rubio et al., 2019). For the first time AFDs have been introduced in the nematode with this purpose. The effects of artificial food colorants after their consumption by *C. elegans* show that acute or chronic exposure to individual AFDs produced a decrease in the lifespan of worms. Lifespan of *C. elegans* is considered a standard parameter in the evaluation of the biological activity of molecules in preclinical studies. In the case of AFDs, an acute exposure produced a shortening in the worms' lifespan in a dose-dependent trend (**Fig. 14.2** and **Fig. 14.3**). This toxicity of AFDs in the worms' lifespan was higher under chronic exposure, where it produced a shorter lifespan even at low concentrations. The highest difference between acute and chronic exposure was obtained with tartrazine. In the acute assay, tartrazine was one of the least harmful dye at 100  $\mu$ M (**Table 14.1**) but its effect in the chronic experiments was close to that of the other colorants (**Table 14.2**). The maximum damage in the lifespan of *C. elegans* occurred with chronic exposure to 100  $\mu$ M for all dyes tested, except carmoisine, which produced greater damage when administered in an acute manner. Mean lifespan of *C. elegans* indicates an accelerated cellular aging, where many factors intervene. Thus, it is possible that different dyes may follow different modes of action in the negative bioactivity shown in the animal model.

In this sense, the intestinal accumulation of lipofuscin is also evidence of cellular damage during aging (Gerstbrein et al., 2005). Lipofuscin is a degradation metabolite derived from the peroxidation of polyunsaturated lipids that is progressively accumulated during ageing. By following the autofluorescence of this compound in worms exposed to artificial dyes a higher accumulation is seen in the treated animals with respect to the control. This strongly suggests an accelerated ageing, which agrees with the results of lifespan. As **Fig. 14.5** shows, after 4 days of adulthood, worms

exposed to dyes were ‘physiologically older’ than untreated worms since the accumulation of lipofuscin is gradual until early adulthood and rapid in midlife (Gerstbrein et al., 2005).

The metabolic transformation of AFDs after ingestion could also be related to their harmful effect. Tartrazine and sunset yellow are metabolized by the intestinal microflora to sulfanilic acid, which generates reactive oxygen species (ROS) (Ameur et al., 2018). Therefore, the decrease measured in the lifespan may be due to the accumulation of sulfanilic acid and the production of ROS, causing a consequent decrease in the antioxidant capacity of cells (Himri et al., 2011). In *C. elegans*, the presence of ROS directly affects to the expression of the heat shock protein hsp-16.2. In order to evaluate the potential effect of AFDs consumed by *C. elegans* in the expression of hsp-16.2, the transgenic strain TJ375 was used. The co-expression of hsp-16.2 fused to GFP into the pharynx cells of these animals is an indication of oxidative stress *in vivo*. The *C. elegans* TJ375 strain showed harmful effect promoted by the exposure to sunset yellow and tartrazine. These two artificial colorants increased the fluorescence induced by juglone exposure and produced the signal by themselves. Thus, it can be concluded that the colorants were able to induce oxidative stress by themselves and to exacerbate the damage provoked by the juglone. Previously there have been no reports of oxidative stress induced by tartrazine due to a low expression of catalase and superoxide dismutase (SOD) (Gao et al., 2011). In *C. elegans* both routes, catalase/superoxide dismutase and hsp, are regulated via DAF-2 insulin/IGF-1 signaling pathway and DAF-16 (Murphy et al., 2003). Therefore, the results obtained suggest that tartrazine may affect the expression of the hsp-16.2 gene, as will later be demonstrated by microarray experiments. The oxidative stress produced by sunset yellow exposure could be due to its metabolization to 1-amino-2-naphtol-6-sulphonic acid (ANSA) (“Scientific Opinion on the re-evaluation of Sunset Yellow FCF (E 110) as a food additive,” 2009) but there is not enough evidence to relate ANSA and ROS.

Despite the lack of evidence of its metabolization or its relationship with ROS accumulation, quinoline yellow administration also produced an increase in the fluorescence of *C. elegans* TJ375. This is an indication of increased oxidative damage after feeding, to be added to its genotoxic effects (Macioszek and Kononowicz, 2004), which may explain the shortening of lifespan in *C. elegans*. Carmoisine and ponceau 4R present the same main metabolite, naphthionic acid, but there is no evidence of a possible negative effect of naphthionic acid (“Scientific Opinion on the re-evaluation

of Azorubine/Carmoisine (E 122) as a food additive,” 2009, “Scientific Opinion on the re-evaluation of Ponceau 4R (E 124) as a food additive,” 2009). However, the consumption of carmoisine *per se* is related to renal and hepatic damage in young male rats and also produced a decrease in SOD and catalase (Amin et al., 2010). Carmoisine and ponceau 4R are present in several foods consumed by children and some studies have demonstrated that their consumption is above their ADI (Husain et al., 2006), so a deeper study on carmoisine and ponceau 4R effects and their derivatives is necessary. Regarding allura red consumption, there is not enough evidence in the bibliography about whether its metabolization could imply a harmful oxidative effect. In this sense, our results with the *C. elegans* model of oxidative stress show that allura red is the dye with the highest oxidative effect.

The accumulation of ROS is closely related to different neurogenerative diseases (Mancuso et al., 2006) like Parkinson's or Alzheimer's, also characterized by alterations in dopamine levels. The results with the mutant strain BZ555 (*dat-1p::GFP*) of *C. elegans* show how AFDs are able to contribute to this alteration by producing a disarrangement in the dopamine receptors *dat-1*. These dopamine receptors have been related to neurodegenerative disorders and they are targets of current pharmacological treatments (Joyce and Millan, 2007). The alterations of dopamine receptors are also related to behavioral alterations such as ADHD. There is evidence suggesting that infants susceptible to ADHD show a notable increase of dopamine receptor D2 (Lou et al., 2004). Besides, it is known that ADHD symptoms improve with dietary restrictions, such as a low consumption of AFDs (Stevens et al., 2011). The results show the relationship between the intake of artificial colorants and the disarrangement of dopamine receptors, with tartrazine administration contributing to the increase of dopamine receptors. Additionally, the analysis of the motility of worms shows how tartrazine, the main colorant related to ADHD (Stevens et al., 2011), increased the average speed of the animals. In addition, the treatment with sunset yellow, which has also been related to ADHD, produced a pronounced effect in the worms' behaviour, by increasing the worms' speed (**Fig. 14.8**). The normal distribution on **Fig. 14.8** describes how the values of a variable are distributed. Values around the centre of the curve are more likely to occur than further values. In statistics, the normal distribution is one of the most important probability distributions since it fits many natural phenomena. The normal distribution of these curves showed how the speed of the worms is clustered

around the mean of the average speeds obtained and the differences in locomotion between the animals treated with tartrazine and sunset yellow and the non-treated (control) animals is easily observed. These facts in the model animal agree with the wide bibliography which describes a correlation between hyperactivity and AFDs' intake (Arnold et al., 2012; McCann et al., 2007; Schab and Trinh, 2004; Stevens et al., 2015, 2011).

The results indicate that colorants may have different ways of altering processes involved in the lifespan of *C. elegans*, as ROS accumulation and antioxidant capacity, motility, or neurological changes. In order to get a deeper understanding of the effects of AFDs in the animal model *C. elegans*, gene expression was analyzed after the treatment with the colorants tartrazine and ponceau 4R. The RNA microarray of *C. elegans* treated with tartrazine showed several genes of the insulin signaling pathway with altered expression (**Fig. 14.9**). INS is a family of forty insulin/IGF-1 (insulin growth factor) like peptides, which serve as hormones, neurotransmitters and growth factors during post-embryonic stages in invertebrates but also in higher animals (Antonova et al., 2012). Tartrazine treatment up-regulated the expression of *ins-7*, which seems to function as antagonist of DAF-2 insulin/IGF-1 receptor. *ins-7* is expressed in amphid sensory neurons, labial neurons, nerve ring, ventral cord and tail neurons. RNAi silencing of *ins-7* increased the lifespan of wild type worms but this effect was lost in the long-lived *daf-2* mutants suggesting that *ins-7* lifespan modulation is dependent of *daf-2*. Kawli and Tan, (2008) concluded that INS-7 neuropeptide secretion from the dense core vesicles (DCVs) suppresses the immune function by activating DAF-2 signaling, suppressing DAF-16 nuclear translocation, and consequently reducing the expression of the immunity related gene.

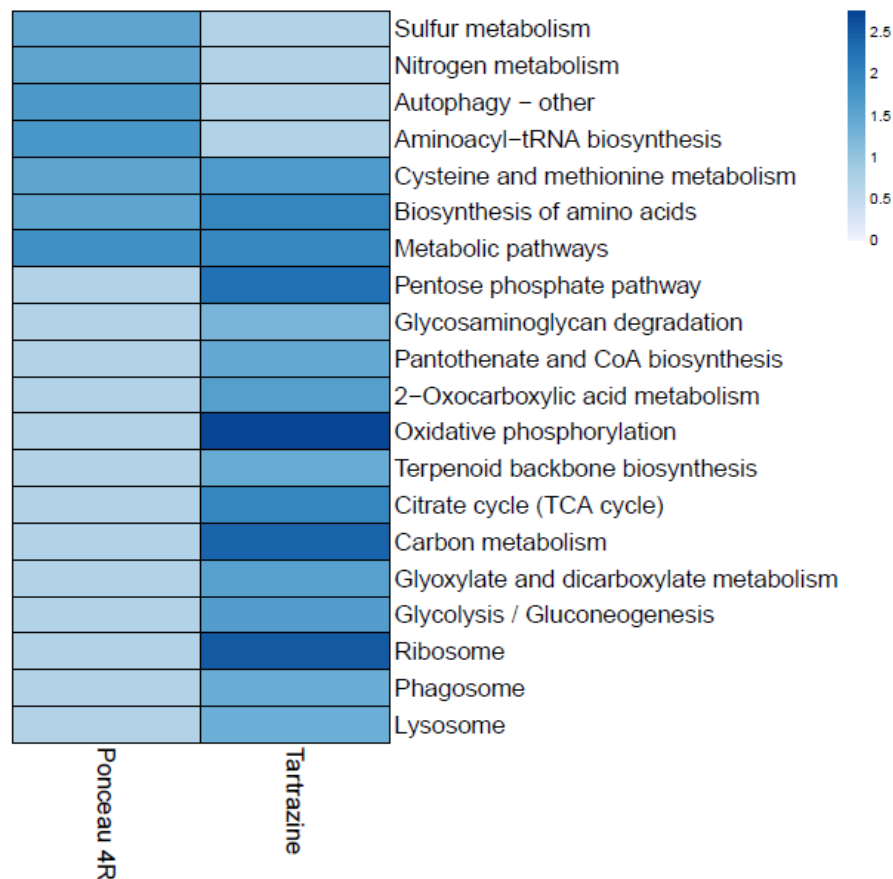


**Figure 14.9. Principal component analysis (PCA) of *C. elegans* pathways altered by ponceau 4R or tartrazine treatment (100  $\mu$ M) vs untreated control worms.**

Tartrazine treatment directly down-regulated other immune related genes such as *sek-1* (-1.9-fold,  $p$  vs control  $\leq 0.05$ ), *pmk-1* (-2.1-fold,  $p$  vs control  $\leq 0.05$ ) and their target gene *gcs-1* (-1.25-fold,  $p$  vs control  $\leq 0.05$ ). These genes appear in the longevity pathway, specifically in the phase 2 detoxification response to oxidative stress pathway that confers oxidative stress resistance in *C. elegans*. *sek-1* is an ortholog of human MAP2K3 (mitogen activated protein kinase kinase 3) expressed in several tissues of the worm including the gonads and the nervous system. This gene is related to the activation of MAPK (mitogen activated protein kinase) signaling pathway, defense response against other organisms, determination of asymmetry in nervous system (Cochella et al., 2014) and it has been shown to promote synaptic transmission in GABA (gamma-Aminobutyric acid) neurons (Vashlishan et al., 2008). *pmk-1* encodes a mitogen activated kinase, which is a downstream gene of *sek-1* and also related to p38 MAPK activation. It has transcription factor binding and kinase activities and it is involved in several processes, such as defense response to other organisms or positive regulation of response to biotic stimuli. Like *sek-1*, *pmk-1* is expressed in head neurons



and the intestine. *sek-1* and *pmk-1* target gene *gcs-1* was also down-regulated when worms were exposed to tartrazine. *gcs-1* encodes a gamma glutamine cysteine synthetase and it is involved in the phase 2 detoxification in the oxidative stress response pathway (Papp et al., 2012). RNAi silencing of *gcs-1* produced worms with intestinal abnormalities, an indication that *gcs-1* is also involved in post-embryonic development. Fluorescent mutants for this protein labeled with green fluorescent protein, GCS-1::GFP, showed that GCS-1 is accumulated in the intestine and ASI chemosensory neurons in response to harmful stimuli (An and Blackwell, 2003). Tartrazine also modulated heat shock factor (HSF) by up-regulating the upstream genes *hsb-1* (2.7-fold,  $p$  vs control  $\leq 0.05$ ) and *ddl-1* (2.4-fold,  $p$  vs control  $\leq 0.05$ ). Heat-shock proteins appear at high levels in inflammatory diseases as a consequence of the temperature increase. These proteins have many purposes in *C. elegans* including thermotolerance, apoptosis or enhancement of the innate immune system. HSF acts downstream DAF-2/DAF-16 and contributes to the worm immunity against bacterial pathogens, by the activation of HSPs (Singh and Aballay, 2006). *hsb-1* encodes a heat shock factor binding protein, ortholog to the human HSBP1. This gene is involved in the negative regulation of the heat-shock response and may have a role in the suppression of the activation of the stress response in aging (Satyal et al., 1998). In *C. elegans*, over-expression of this gene generates animals that are more sensitive to heat stress, and the survival rates of these mutants were reported to be a 48% for the wild type worms (Satyal et al., 1998). Furthermore, *ddl-1* encodes a protein homolog to human CCDC53 (human coiled-coil domain-containing protein 53). CCDC53 modulates HSF-1 activity by forming a complex with it, but it has also been reported to form complex with the HSF-1 negative regulator of CCDC53 (Rual et al., 2005). Inhibition on *ddl-1* produced worms with longer lifespan and enhanced thermotolerance dependent on *hsf-1* and the IIS (insulin/IGF-1-like signaling) pathway (Chiang et al., 2012). Therefore, exposure to tartrazine increases its expression and decreases the lifespan and the thermotolerance in *C. elegans*. The transcription factor PHA-4, which is involved in the TOR (target of Rapamycin) pathway, was also down-regulated in worms fed with tartrazine (*pha-4* -4.47-fold,  $p$  vs control  $\leq 0.05$ ). PHA-4 is an ortholog of human FOXA3 (forkhead box A3), a transcription factor located in hepatocytes that regulates the expression of several genes such as AFP, albumin, tyrosine aminotransferase, or PEPCK, and it plays an essential role in early stages of development and later in the regulation of glucagon production and glucose

homeostasis (Kaestner, 2000). In *C. elegans*, the suppression of *pha-4* in the first larval stage L1 was reported to produce larval lethality and pharyngeal defects (Mango et al., 1994) while its suppression in adult worms shortened the lifespan (Panowski et al., 2007). Like other genes altered by tartrazine, *pha-4* is expressed in some of the head neurons as previously reported (Panowski et al., 2007). Overall, the microarray results for tartrazine indicate that the reduction in lifespan may be explained as a result of an alteration in key genes expression. The pathways most affected by tartrazine are those associated with resistance to oxidative stress, the innate immune system and thermotolerance, all linked by DAF-2 and INS. Interestingly, some of the altered genes are expressed in neurons involved in neuronal formation and activity, suggesting that neurons could be target cells for tartrazine.

On the other hand, worms treated with ponceau 4R showed an alteration in the metabolic pathways (5.2-fold,  $p$  vs control  $\leq 0.05$ ) (**Fig. 14.9**). The microarray showed that the gene *lips-17* is down-regulated (-1.79-fold,  $p$  vs control  $\leq 0.05$ ) along with the steroid dehydrogenase gene *stdh-3* (-1.4-fold,  $p$  vs control  $\leq 0.05$ ). The first gene is predicted to encode a triacylglycerol lipase involved in lipolysis and longevity (McCormick et al., 2012). Instead, *stdh-3* encodes a hydroxysteroid 17-beta dehydrogenase enzyme, predicted to have oxidoreductase activity (Maglioni and Ventura, 2016). The human ortholog HSD17B12 encodes a mitochondrial multifunctional enzyme (HSD10) which plays an important role in the metabolism of neuroactive steroids and the degradation of isoleucine (Yang et al., 2007), the loss of this protein is known as HSD10 disease, a mitochondrial metabolic disorder. HSD10 deficiency that may cause acidosis, neurodegeneration, loss of motor skills, epilepsy or blindness (Zschocke, 2012). Indeed, some reports have shown that in *Drosophila melanogaster* (Torroja et al., 1998) and mice (Rauschenberger et al., 2010) the gene knock-down causes embryonic lethality and it is likely that the same may occur in humans, where RNAi silencing of HSD17B12 gene expression caused mitochondrial tRNA precursors accumulation (Holzmann et al., 2008). This is in agreement with our microarray results that showed an up-regulation of 4.7-fold ( $p$  vs control  $\leq 0.05$ ) in the aminoacyl-tRNA biosynthesis pathway in worms treated with ponceau 4R. Although other genes are altered by ponceau 4R exposition, such as infection response genes *lys-7* (3.1-fold,  $p$  vs control  $\leq 0.05$ ) and *spp-1* (1.4-fold,  $p$  vs control  $\leq 0.05$ ) or the heat shock protein *hsp-16.2* (4.55-fold,  $p$  vs control  $\leq 0.05$ ), overall these alterations may

not have a direct impact in the *C. elegans* lifespan. The down-regulation of *stdh-3* and the accumulation of tRNA could be the main cause of premature death in worms treated with ponceau 4R.

Microarray assays have shown that the reduced lifespan of the worms treated with these AFDs could be partially explained by an effect in gene regulation. Genes and pathways affected are different and there is not a common trend (**Fig. 14.9**). Although all are artificial colorants, the chemical structures and properties are different. Ponceau was the most lethal of both in the lifespan experiments, and its effect on gene regulation may explain this result. Nevertheless, tartrazine shortened the lifespan and down-regulated longevity genes.

## 8. Conclusions

Altogether, these results indicate the need for new and exhaustive studies on the effects of AFDs on health, development, and genetic regulation. The data suggest that caution should be taken to avoid excessive consumption of artificial food dyes, and the search for alternatives should be promoted (Wrolstad and Culver, 2012). There is enough evidence for the use of natural dyes that are not only innocuous but which show health-promoting effects. For instance, one alternative to red colorants is betanin, the betacyanin employed as food colorant E-162 in the European Union and 73.40 in the 21 CFR section of the FDA in the USA. As it is described in the chapter XI, betanin has a health-promoting effect *in vivo* with an extraordinary antioxidant effect in *C. elegans*. Other natural yellow pigments such as curcumin or carotenoids are also used in the food and cosmetic industries as E-100 and E-160a respectively. These compounds also have antioxidant and anti-inflammatory properties (Ammon et al., 1993; Stahl and Sies, 2003) and they are potential alternatives to the employment of artificial colorants.

**Table 14.1. Lifespan result and statistical analysis for *C. elegans* after acute exposure to different concentration of food colorants. \*\*significant at  $p \leq 0.05$** 

Food Colorant	Concentration ( $\mu$ M)	n° subjects	Mean Lifespan (days)	S. E ( $\pm$ days)	Life shortening (%)	<i>p</i> vs Control
Allura Red	0	128	7.63	0.08	0.00	
	10	67	7.42	0.18	-2.75	0.1447
	25	82	7.18	0.17	-5.90	0.0152**
	50	70	6.58	0.14	-13.76	0**
	100	70	6.52	0.15	-14.55	0.00000074**
Ponceau Red	0	78	6.95	0.15	0.00	
	10	92	6.29	0.19	-9.50	0**
	25	71	5.71	0.13	-17.84	0**
	50	94	5.27	0.16	-24.17	0**
	100	76	5.21	0.13	-25.04	0**
Carmoisine	0	80	6.92	0.09	0.00	
	10	81	6.04	0.15	-12.72	0.00003**
	25	83	5.92	0.1	-14.45	0**
	50	123	5.22	0.15	-24.57	0**
	100	88	4.76	0.22	-31.21	0**
Tartrazine	0	57	8.08	0.17	0.00	
	10	74	7.92	0.43	-1.98	0.9538
	25	51	7.55	0.25	-6.56	0.1085
	50	80	7.42	0.14	-8.17	0.0094**
	100	90	7.27	0.33	-10.02	0.0532*
Sunset Yellow	0	139	8.27	0.11	0.00	
	10	86	8.19	0.27	-0.97	0.5699
	25	98	7.9	0.23	-4.47	1.43E-01
	50	72	6.95	0.22	-15.96	0.0001**
	100	80	6.6	0.28	-20.19	0.000026**
Quinoline Yellow	0	74	7.37	0.1	0.00	
	10	70	6.61	0.1	-10.31	0**
	25	59	6.3	0.13	-14.52	0**
	50	103	6.05	0.1	-17.91	0**
	100	127	5.88	0.12	-20.22	0**

**Table 14.2. Lifespan result and statistical analysis for *C. elegans* after chronical exposure to different concentration of food colorants. \*\*significant at  $p \leq 0.05$** 

<b>Food Colorant</b>	<b>Concentration (μM)</b>	<b>n° subjects</b>	<b>Mean Lifespan (days)</b>	<b>S. E (± days)</b>	<b>Life shortening (%)</b>	<b>p vs Control</b>
<b>Control</b>	0	132	8.39	0.16	0.00	
<b>Allura Red</b>	10	194	7.38	0.12	-12.04	0.8152
	50	165	6.39	0.09	-23.84	0**
	100	197	5.99	0.13	-28.61	0**
<b>Ponceau Red</b>	10	105	7.04	0.11	-16.09	0.0028**
	50	116	6.62	0.1	-21.10	0.00000028**
	100	159	5.99	0.25	-28.61	0.0012**
<b>Carmoisine</b>	10	124	6.62	0.15	-21.10	0.0001**
	50	137	6.48	0.16	-22.77	0.000000045**
	100	134	6.14	0.11	-26.82	0.0000009**
<b>Tartrazine</b>	10	76	6.57	0.19	-21.69	0.0000072**
	50	233	6.30	0.1	-24.91	0.00000031**
	100	72	6.24	0.09	-25.63	0**
<b>Sunset Yellow</b>	10	60	6.91	0.08	-17.64	0.0589
	50	197	6.61	0.13	-21.22	0.0008**
	100	268	6.46	0.11	-23.00	0.0000000033**
<b>Quinoline Yellow</b>	10	138	6.92	0.11	-17.52	0.0116**
	50	137	6.67	0.12	-20.50	0.0000077**
	100	66	6.34	0.16	-24.43	0.000000017**

## REFERENCES

- Abbas, S., Wink, M., 2009. Epigallocatechin gallate from green tea (*Camellia sinensis*) increases lifespan and stress resistance in *Caenorhabditis elegans*. *Planta Med.* 75, 216–221. <https://doi.org/10.1055/s-0028-1088378>
- Ameur, F.Z., Mehedi, N., Kheroua, O., Saïdi, D., Salido, G.M., Gonzalez, A., 2018. Sulfanilic acid increases intracellular free-calcium concentration, induces reactive oxygen species production and impairs trypsin secretion in pancreatic AR42J cells. *Food Chem. Toxicol.* 120, 71–80. <https://doi.org/10.1016/j.fct.2018.07.001>
- Amin, K.A., Abdel Hameid, H., Abd Elsttar, A.H., 2010. Effect of food azo dyes tartrazine and carmoisine on biochemical parameters related to renal, hepatic function and oxidative stress biomarkers in young male rats. *Food Chem. Toxicol.* 48, 2994–2999. <https://doi.org/10.1016/j.fct.2010.07.039>
- Ammon, H.P.T., Safayhi, H., Mack, T., Sabieraj, J., 1993. Mechanism of antiinflammatory actions of curcumine and boswellic acids. *J. Ethnopharmacol.* 38, 105–112. [https://doi.org/10.1016/0378-8741\(93\)90005-P](https://doi.org/10.1016/0378-8741(93)90005-P)
- An, J.H., Blackwell, T.K., 2003. SKN-1 links *C. elegans* mesendodermal specification to a conserved oxidative stress response. *Genes Dev.* 17, 1882–1893. <https://doi.org/10.1101/gad.1107803>
- Antonova, Y., Arik, A.J., Moore, W., Riehle, M.A., Brown, M.R., 2012. Insulin-like peptides: structure, signaling, and function. In *Insect endocrinology*. Academic Press. 63–92. <https://doi.org/10.1016/B978-0-12-384749-2.10002-0>
- Arnold, L.E., Lofthouse, N., Hurt, E., 2012. Artificial food colors and attention-deficit/hyperactivity symptoms: conclusions to dye for. *Neurotherapeutics.* 9(3), 599–609. <https://doi.org/10.1007/s13311-012-0133-x>
- Banaschewski, T., Becker, K., Scherag, S., Franke, B., Coghill, D., 2010. Molecular genetics of attention-deficit/hyperactivity disorder: an overview. *Eur. Child Adolesc. Psychiatry* 19, 237–257. <https://doi.org/10.1007/s00787-010-0090-z>
- Chen, W., Müller, D., Richling, E., Wink, M., 2013. Anthocyanin-rich purple wheat prolongs the life span of *Caenorhabditis elegans* probably by activating the DAF-16/FOXO transcription factor. *J. Agric. Food Chem.* 61, 3047–3053. <https://doi.org/10.1021/jf3054643>
- Chiang, W.C., Ching, T.T., Lee, H.C., Mousigian, C., Hsu, A.L., 2012. HSF-1 regulators DDL-1/2 link insulin-like signaling to heat-shock responses and modulation of longevity. *Cell* 148, 322–334.

<https://doi.org/10.1016/j.cell.2011.12.019>

- Cochella, L., Tursun, B., Hsieh, Y.-W., Galindo, S., Johnston, R.J., Chuang, C.-F., Hobert, O., 2014. Two distinct types of neuronal asymmetries are controlled by the *Caenorhabditis elegans* zinc finger transcription factor *die-1*. *Genes Dev.* 28, 34–43. <https://doi.org/10.1101/gad.233643.113>
- Feder, M.E., Hofmann, G.E., 1999. Heat-shock proteins, molecular chaperones, and the stress response: evolutionary and ecological physiology. *Annu. Rev. Physiol.* 61, 243–282. <https://doi.org/10.1146/annurev.physiol.61.1.243>
- Gao, Y., Li, C., Shen, J., Yin, H., An, X., Jin, H., 2011. Effect of food azo dye tartrazine on learning and memory functions in mice and rats, and the possible mechanisms involved. *J. Food Sci.* 76(6), T125-T129. <https://doi.org/10.1111/j.1750-3841.2011.02267.x>
- García-Casas, P., Arias-del-Val, J., Alvarez-Illera, P., Wojnicz, A., de los Ríos, C., Fonteriz, R.I., Montero, M., Alvarez, J., 2018. The neuroprotector benzothiazepine CGP37157 extends lifespan in *C. elegans* worms. *Front. Aging Neurosci.* 10, 440. <https://doi.org/10.3389/fnagi.2018.00440>
- Gerstbrein, B., Stamatatos, G., Kollias, N., Driscoll, M., 2005. In vivo spectrofluorimetry reveals endogenous biomarkers that report healthspan and dietary restriction in *Caenorhabditis elegans*. *Aging Cell* 4, 127–137. <https://doi.org/10.1111/j.1474-9726.2005.00153.x>
- Guerrero-Rubio, M.A., Hernández-García, S., García-Carmona, F., Gandía-Herrero, F., 2019. Extension of life-span using a RNAi model and in vivo antioxidant effect of Opuntia fruit extracts and pure betalains in *Caenorhabditis elegans*. *Food Chem.* 274, 840–847. <https://doi.org/10.1016/j.foodchem.2018.09.067>
- Himri, I., Bellahcen, S., Souna, F., Belmekki, F., Aziz, M., Bnouham, M., Zoheir, J., Berkia, Z., Mekhfi, H., Saalaoui, E., 2011. A 90 day oral toxicity study of tartrazine, a synthetic food dye, in wistar rats. *Int. J. Pharm. Pharm. Sci.*, 3 (3), 159-169.
- Holzmann, J., Frank, P., Löffler, E., Bennett, K.L., Gerner, C., Rossmanith, W., 2008. RNase P without RNA: identification and functional reconstitution of the human mitochondrial tRNA processing enzyme. *Cell* 135, 462–474. <https://doi.org/10.1016/j.cell.2008.09.013>
- Husain, A., Sawaya, W., Al-Omair, A., Al-Zenki, S., Al-Amiri, H., Ahmed, N., Al-Sinan, M., 2006. Estimates of dietary exposure of children to artificial food colours

- in Kuwait. Food Addit. Contam. 23, 245–251.  
<https://doi.org/10.1080/02652030500429125>
- Joyce, J.N., Millan, M.J., 2007. Dopamine D3 receptor agonists for protection and repair in Parkinson's disease. Curr. Opin. Pharmacol. 7(1), 100–105.  
<https://doi.org/10.1016/j.coph.2006.11.004>
- Kaestner, K.H., 2000. The hepatocyte nuclear factor 3 (HNF3 or FOXA) family in metabolism. Trends Endocrinol. Metab. 11(7), 281–285.  
[https://doi.org/10.1016/S1043-2760\(00\)00271-X](https://doi.org/10.1016/S1043-2760(00)00271-X)
- Kawli, T., Tan, M.W., 2008. Neuroendocrine signals modulate the innate immunity of *Caenorhabditis elegans* through insulin signaling. Nat. Immunol. 9, 1415–1424.  
<https://doi.org/10.1038/ni.1672>
- Khayyat, L., Essawy, A., Sorour, J., Soffar, A., 2017. Tartrazine induces structural and functional aberrations and genotoxic effects in vivo. PeerJ 5, e3041.  
<https://doi.org/10.7717/peerj.3041>
- Link, C.D., Cypser, J.R., Johnson, C.J., Johnson, T.E., 1999. Direct observation of stress response in *Caenorhabditis elegans* using a reporter transgene. Cell Stress Chaperones 4, 235. doi: 10.1379/1466-1268(1999)004<0235:doosri>2.3.co;2
- Lou, H.C., Rosa, P., Pryds, O., Karrebæk, H., Lunding, J., Cumming, P., Gjedde, A., 2004. ADHD: increased dopamine receptor availability linked to attention deficit and low neonatal cerebral blood flow. Dev. Med. Child Neurol. 46, 179–183.  
<https://doi.org/10.1017/S0012162204000313>
- Macioszek, V.K., Kononowicz, A.K., 2004. The evaluation of the genotoxicity of two commonly used food colors: Quinoline Yellow (E 104) and Brilliant Black BN (E 151). Cell. Mol. Biol. Lett. 9, 107–122.
- Maglioni, S., Ventura, N., 2016. *C. elegans* as a model organism for human mitochondrial associated disorders. Mitochondrion. 30, 117–125.  
<https://doi.org/10.1016/j.mito.2016.02.003>
- Mancuso, M., Coppede, F., Migliore, L., Siciliano, G., Murri, L., 2006. Mitochondrial dysfunction, oxidative stress and neurodegeneration. J. Alzheimer's Dis. 10, 59–73. <https://doi.org/10.3233/JAD-2006-10110>
- Mango, S.E., Lambie, E.J., Kimble, J., 1994. The *pha-4* gene is required to generate the pharyngeal primordium of *Caenorhabditis elegans*. Development 120, 3019–3031.
- McCann, D., Barrett, A., Cooper, A., Crumpler, D., Dalen, L., Grimshaw, K., Kitchin,



- E., Lok, K., Porteous, L., Prince, E., Sonuga-Barke, E., Warner, J.O., Stevenson, J., 2007. Food additives and hyperactive behaviour in 3-year-old and 8/9-year-old children in the community: a randomised, double-blinded, placebo-controlled trial. *Lancet* 370, 1560–1567. [https://doi.org/10.1016/S0140-6736\(07\)61306-3](https://doi.org/10.1016/S0140-6736(07)61306-3)
- McCormick, M., Chen, K., Ramaswamy, P., Kenyon, C., 2012. New genes that extend *Caenorhabditis elegans*’ lifespan in response to reproductive signals. *Aging Cell* 11, 192–202. <https://doi.org/10.1111/j.1474-9726.2011.00768.x>
- Mohamed, A.A.R., Galal, A.A.A., Elewa, Y.H.A., 2015. Comparative protective effects of royal jelly and cod liver oil against neurotoxic impact of tartrazine on male rat pups brain. *Acta Histochem.* 117, 649–658. <https://doi.org/10.1016/j.acthis.2015.07.002>
- Murphy, C.T., McCarroll, S.A., Bargmann, C.I., Fraser, A., Kamath, R.S., Ahringer, J., Li, H., Kenyon, C., 2003. Genes that act downstream of DAF-16 to influence the lifespan of *Caenorhabditis elegans*. *Nature* 424, 277–283. <https://doi.org/10.1038/nature01789>
- Panowski, S.H., Wolff, S., Aguilaniu, H., Durieux, J., Dillin, A., 2007. PHA-4/Foxa mediates diet-restriction-induced longevity of *C. elegans*. *Nature* 447, 550–555. <https://doi.org/10.1038/nature05837>
- Papp, D., Csermely, P., Soti, C., 2012. A role for SKN-1/Nrf in pathogen resistance and immunosenescence in *Caenorhabditis elegans*. *PLoS Pathog.* 8, e1002673. <https://doi.org/10.1371/journal.ppat.1002673>
- Rauschenberger, K., Schöler, K., Sass, J.O., Sauer, S., Djuric, Z., Rumig, C., Wolf, N.I., Okun, J.G., Kölker, S., Schwarz, H., Fischer, C., Grziwa, B., Runz, H., Astrid, N., Shafqat, N., Kavanagh, K.L., Hämmering, G., Wanders, R.J.A., Shield, J.P.H., Wendel, U., Stern, D., Nawroth, P., Hoffmann, G.F., Bartram, C.R., Arnold, B., Bierhaus, A., Oppermann, U., Steinbeisser, H., Zschocke, J., 2010. A non-enzymatic function of 17 $\beta$ -hydroxysteroid dehydrogenase type 10 is required for mitochondrial integrity and cell survival. *EMBO Mol. Med.* 2, 51–62. <https://doi.org/10.1002/emmm.200900055>
- Rual, J.F., Venkatesan, K., Hao, T., Hirozane-Kishikawa, T., Dricot, A., Li, N., Berriz, G.F., Gibbons, F.D., Dreze, M., Ayivi-Guedehoussou, N., Klitgord, N., Simon, C., Boxem, M., Milstein, S., Rosenberg, J., Goldberg, D.S., Zhang, L. V, Wong, S.L., Franklin, G., Li, S., Albala, J.S., Lim, J., Fraughton, C., Llamasas, E., Cevik, S., Bex, C., Lamesch, P., Sikorski, R.S., Vandenhaute, J., Zoghbi, H.Y., Smolyar, A.,

- Bosak, S., Sequerra, R., Doucette-Stamm, L., Cusick, M.E., Hill, D.E., Roth, F.P., Vidal, M., 2005. Towards a proteome-scale map of the human protein-protein interaction network. *Nature* 437, 1173–1178. <https://doi.org/10.1038/nature04209>
- Sasaki, Y.F., Kawaguchi, S., Kamaya, A., Ohshita, M., Kabasawa, K., Iwama, K., Taniguchi, K., Tsuda, S., 2002. The comet assay with 8 mouse organs: Results with 39 currently used food additives. *Mutat. Res. - Genet. Toxicol. Environ. Mutagen.* 519, 103–119. [https://doi.org/10.1016/S1383-5718\(02\)00128-6](https://doi.org/10.1016/S1383-5718(02)00128-6)
- Satyal, S.H., Chen, D., Fox, S.G., Kramer, J.M., Morimoto, R.I., 1998. Negative regulation of the heat shock transcriptional response by HSBP1. *Genes Dev.* 12, 1962–1974. <https://doi.org/10.1101/gad.12.13.1962>
- Schab, D.W., Trinh, N.H.T., 2004. Do artificial food colors promote hyperactivity in children with hyperactive syndromes? A meta-analysis of double-blind placebo-controlled trials. *J. Dev. Behav. Pediatr.* 25, 423–434. <https://doi.org/10.1097/00004703-200412000-00007>
- Scientific Opinion on the re-evaluation of Azorubine/Carmoisine (E 122) as a food additive, 2009. . *EFSA J.* 7, 1332. <https://doi.org/10.2903/j.efsa.2009.1332>
- Scientific Opinion on the re-evaluation of Ponceau 4R (E 124) as a food additive, 2009. . *EFSA J.* 7, 1328. <https://doi.org/10.2903/j.efsa.2009.1328>
- Scientific Opinion on the re-evaluation of Quinoline Yellow (E 104) as a food additive, 2009. . *EFSA J.* 7, 1329. <https://doi.org/10.2903/j.efsa.2009.1329>
- Scientific Opinion on the re-evaluation of Sunset Yellow FCF (E 110) as a food additive, 2009. . *EFSA J.* 7, 1330. <https://doi.org/10.2903/j.efsa.2009.1330>
- Singh, V., Aballay, A., 2006. Heat-shock transcription factor (HSF)-1 pathway required for *Caenorhabditis elegans* immunity. *Proc. Natl. Acad. Sci. U. S. A.* 103, 13092–13097. <https://doi.org/10.1073/pnas.0604050103>
- Stahl, W., Sies, H., 2003. Antioxidant activity of carotenoids. *Mol. Aspects Med.* 24(6), 345–351. [https://doi.org/10.1016/S0098-2997\(03\)00030-X](https://doi.org/10.1016/S0098-2997(03)00030-X)
- Stevens, L.J., Burgess, J.R., Stochelski, M.A., Kuczek, T., 2015. Amounts of artificial food dyes and added sugars in foods and sweets commonly consumed by children. *Clin. Pediatr. (Phila).* 54, 309–321. <https://doi.org/10.1177/0009922814530803>
- Stevens, L.J., Kuczek, T., Burgess, J.R., Hurt, E., Arnold, L.E., 2011. Dietary sensitivities and ADHD symptoms: thirty-five years of research. *Clin. Pediatr. (Phila).* 50, 279–293. <https://doi.org/10.1177/0009922810384728>
- Stringham, E.G., Candido, E.P.M., 1994. Transgenic *hsp 16-Lacz* strains of the soil

- nematode *Caenorhabditis elegans* as biological monitors of environmental stress. Environ. Toxicol. Chem. 13, 1211–1220. <https://doi.org/10.1002/etc.5620130802>
- Torroja, L., Ortuño-Sahagún, D., Ferrús, A., Hämmerle, B., Barbas, J.A., 1998. Scully, an essential gene of *Drosophila*, is homologous to mammalian mitochondrial type II L-3-hydroxyacyl-CoA dehydrogenase/amyloid- $\beta$  peptide- binding protein. J. Cell Biol. 141, 1009–1017. <https://doi.org/10.1083/jcb.141.4.1009>
- Vashlishan, A.B., Madison, J.M., Dybbs, M., Bai, J., Sieburth, D., Ch'ng, Q., Tavazoie, M., Kaplan, J.M., 2008. An RNAi screen identifies genes that regulate GABA synapses. Neuron 58, 346–361. <https://doi.org/10.1016/j.neuron.2008.02.019>
- Wrolstad, R.E., Culver, C.A., 2012. Alternatives to Those Artificial FD&C Food Colorants. Annu. Rev. Food Sci. Technol. 3, 59–77. <https://doi.org/10.1146/annurev-food-022811-101118>
- Yang, S.Y., He, X.Y., Miller, D., 2007. HSD17B10: A gene involved in cognitive function through metabolism of isoleucine and neuroactive steroids. Mol. Genet. 92(1-2), 36-42. Metab. <https://doi.org/10.1016/j.ymgme.2007.06.001>
- Zschocke, J., 2012. HSD10 disease: Clinical consequences of mutations in the HSD17B10 gene. J. Inherit. Metab. Dis. 35, 81–89. <https://doi.org/10.1007/s10545-011-9415-4>

## **Chapter XV. Conclusions**



The results obtained in this Thesis allow the following conclusions to be drawn:

1. The synthesis of betalains is not restricted to plants. Close-related pigments are present in fungi *Amanita* and *Hygrocybe* due to the condensation of betalamic acid with amine compounds but for the first time, dopaxanthin, the only pigment of *Glottiphyllum* plants has been detected in microbial hosts due to the activity of a 4,5-DOPA-extradiol-dioxygenase (DODA) enzyme.
2. Microbial dioxygenases described in this Thesis present higher activity and affinity than those characterized up to now from plants. Thanks to the DODA enzyme from *Gluconacetobacter diazotrophicus*, the evolution of the intermediate compounds 2,3- and 4,5-seco-DOPA has been shown for the first time. A mechanism for the cyclization of 4,5-seco-DOPA to yield betalamic acid has been proposed.
3. A biotechnological procedure to obtain individual betalains has been developed based on the novel dioxygenases from bacterial hosts. This process is scalable and its optimization in terms of concentration of substrates, culture conditions and oxygenation's effect led to production in 2 L bioreactors. These yielded up to 70 mg/L of individual pure betalains, higher than the methods previously employed.
4. Betalains interact with metals giving rise to complexes that substantially change their spectroscopic properties. This complexation is reversible and betalains can recover their absorbance and fluorescence properties in presence of agents that compete for the metal thus releasing the pigment. Taking this into account, complexation of betalains with  $\text{Eu}^{3+}$  has been proposed as an effective signal in the detection of *Bacillus* spores due to the strong affinity of dipicolinic acid, a major spores' component, for this metal.
5. Betalamic acid is able to interact with amine groups of polymeric compounds. The Schiff condensation between betalamic acid and available amines in polymers yield new materials. These can combine betalains' properties and those of the starting material. In the case of the polymeric chitosan-betaxanthin, the novel polymer combines the properties of the pigments, such as color, fluorescence and complexation with metals, with the properties of chitosan, a polymer derived from chitin widely used for medical applications.

6. The novel methodology described for obtaining betalains has allowed studies on the *in vivo* health-promoting effects of individual pure compounds. The animal model *Caenorhabditis elegans* was chosen for this purpose and the work with the automatic platform “lifespan machine” originally developed by the University of Harvard was optimized. Modifications on the original design have allowed a higher homogeneity of the results and a reduction in the loss of specimens due to desiccated and/or contaminated plates.
7. The combination of the biotechnological obtention of betalains and the measure of the lifespan of *C. elegans* has led to demonstrate that individual pure betalains present health-promoting effects in an *in vivo* system. These results expand the previous information obtained from plants’ extracts. The analysis of seventeen pure pigments show the relationships between chemical structures and their bioavailability and the increase of worms’ lifespan, identifying the most active betalains.
8. The first microarrays performed with betalain-treated worms show that the health-promoting effects of betalains are due to the modulation of different pathways that converge in the expression of *hsp* genes. Thus, betalains promote an increase of lifespan and protect against oxidative stress not only as a result of their antioxidant properties, but also due to the over-expression of heat shock proteins’ genes.
9. Baicalein and related flavonoids also present a health-promoting effect in *C. elegans* due to the modulation of genes involved in longevity pathways. Despite these pathways are the same that those modulated by betalains, target genes of flavonoids are different, such as genes involved in fat accumulation, showing a high potential in the treatment against obesity.
10. The administration of artificial food dyes to *C. elegans* also modulates the expression of genes related to aging. They produce damage such as increased oxidative stress, lipofuscin accumulation, shortening of lifespan, alterations in movement patterns, and alterations in the production of dopamine receptors.

## **Annexes**





## Annex I. Culture media recipes

All recipes are described for a final volume of 1L

### Luria-Bertani (LB)

Tryptone	10 g
Yeast extract	5 g
NaCl	10 g

For solid culture, add 15 g of Agar

### NZCYM

Tryptone	10 g
Yeast extract	5 g
NaCl	5 g
Casamino acids	1 g
MgSO <sub>4</sub>	1 g

### Nutrient-broth (NB)

Beef extract	10 g
Peptone	10 g
NaCl	5 g

### Gluconacetobacter's culture

D-manitol	25 g
Yeast extract	5 g
Peptone	3 g

For solid culture, add 15 g of Agar

### BG-11

NaNO <sub>3</sub>	1.5 g
CaCl <sub>2</sub> ·2H <sub>2</sub> O	0.036 g
Na <sub>2</sub> -EDTA	0.001 g
MgSO <sub>4</sub> ·7H <sub>2</sub> O	0.075 g
K <sub>2</sub> HPO <sub>4</sub>	0.04 g
FeNH <sub>4</sub> -Citrate	0.012 g
Na <sub>2</sub> CO <sub>3</sub>	0.02 g
Trace metals solution <sup>a</sup>	1 mL

<sup>a</sup> Trace metals solution:

H <sub>3</sub> Bo <sub>3</sub>	2.86 g
FeSO <sub>4</sub> ·7H <sub>2</sub> O	0.69 g
MnCl <sub>2</sub> ·4H <sub>2</sub> O	1.81 g
ZnSO <sub>4</sub> ·7H <sub>2</sub> O	0.222 g
CuSO <sub>4</sub> ·5H <sub>2</sub> O	0.079 g
Na <sub>2</sub> MoO <sub>4</sub> ·2H <sub>2</sub> O	0.391 g
Co(NO <sub>3</sub> ) <sub>2</sub>	0.05 g

### M9 buffer

KH <sub>2</sub> PO <sub>4</sub>	3 g
Na <sub>2</sub> HPO <sub>4</sub>	6 g
NaCl	5 g
MgSO <sub>4</sub> 1M*	1 mL

\*add after autoclave

### Nematode grown media (NGM)

Peptone	2.5 g
NaCl	3 g
Agar	17 g

Autoclave and then add:

CaCl <sub>2</sub> 1M	1 mL
Cholesterol in ethanol (5mg/mL)	1 mL
MgSO <sub>4</sub> 1M	1 mL
KPO <sub>4</sub> 1 M	25 mL

### S medium

S Basal <sup>b</sup>	974 mL
Potassium citrate 1M pH 6.0	10 mL
Trace metals solution <sup>c</sup>	10 mL
CaCl <sub>2</sub> 1M	3 mL
MgSO <sub>4</sub> 1M	3 mL

<sup>b</sup> S Basal:

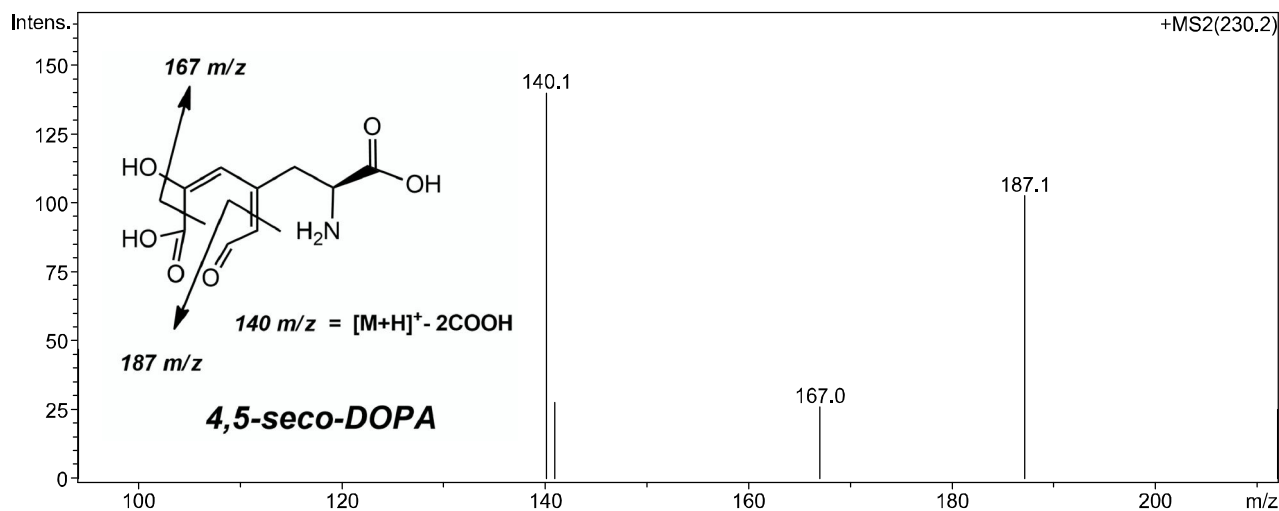
NaCl	5.8 g
K <sub>2</sub> HPO <sub>4</sub>	1 g
KH <sub>2</sub> PO <sub>4</sub>	6 g
Cholesterol in ethanol (5mg/mL)	1 mL

<sup>c</sup> Trace metals solution:

Na <sub>2</sub> -EDTA	1.86 g
FeSO <sub>4</sub> ·7H <sub>2</sub> O	0.69 g
MnCl <sub>2</sub> ·4H <sub>2</sub> O	0.20 g
ZnSO <sub>4</sub> ·7H <sub>2</sub> O	0.29 g
CuSO <sub>4</sub> ·5H <sub>2</sub> O	0.025 g

## Annex II. Supporting information of Chapter IV

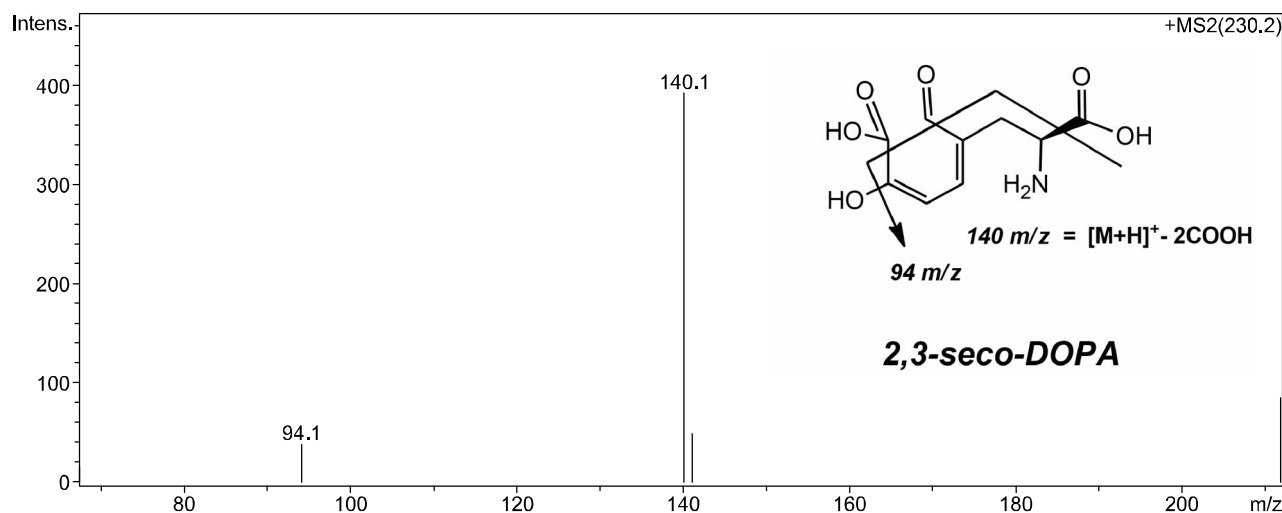
### Compound Mass Spectrum List Report - MS



#### MS Peak List:

#	m/z	Res.	FWHM	I	I %	S/N
1	94.1			47	34	
2	140.1			140	100	
3	140.9			28	20	
4	167.0			26	19	
5	187.1			102	73	
6	211.9			25	18	

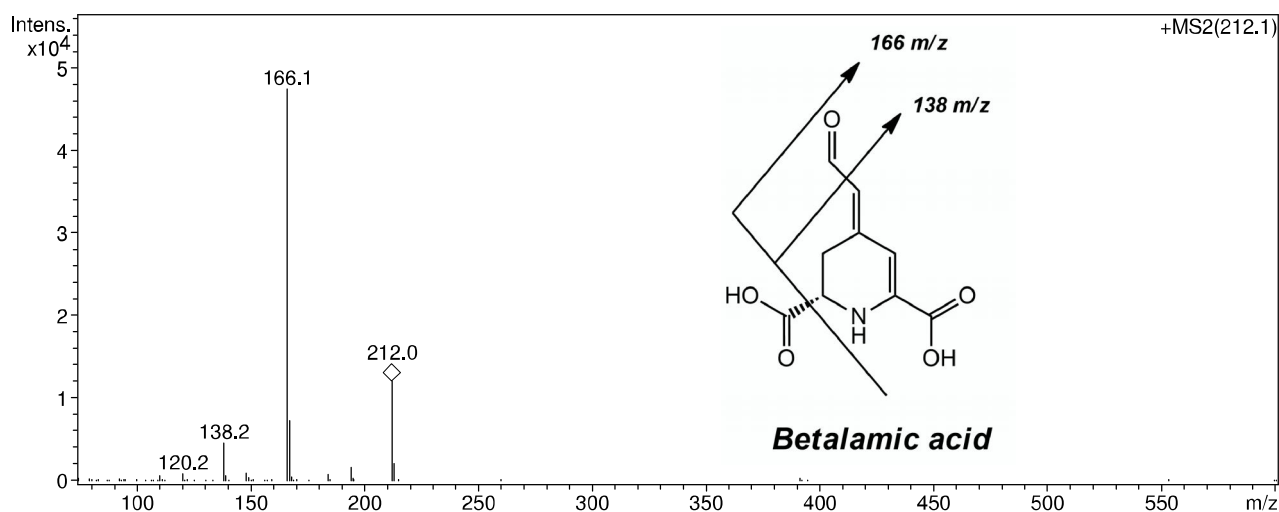
# Compound Mass Spectrum List Report - MS



## MS Peak List:

#	m/z	Res.	FWHM	I	I %	S/N
1	67.5			15	4	
2	94.1			37	10	
3	140.1			391	100	
4	141.2			48	12	
5	211.8			84	22	

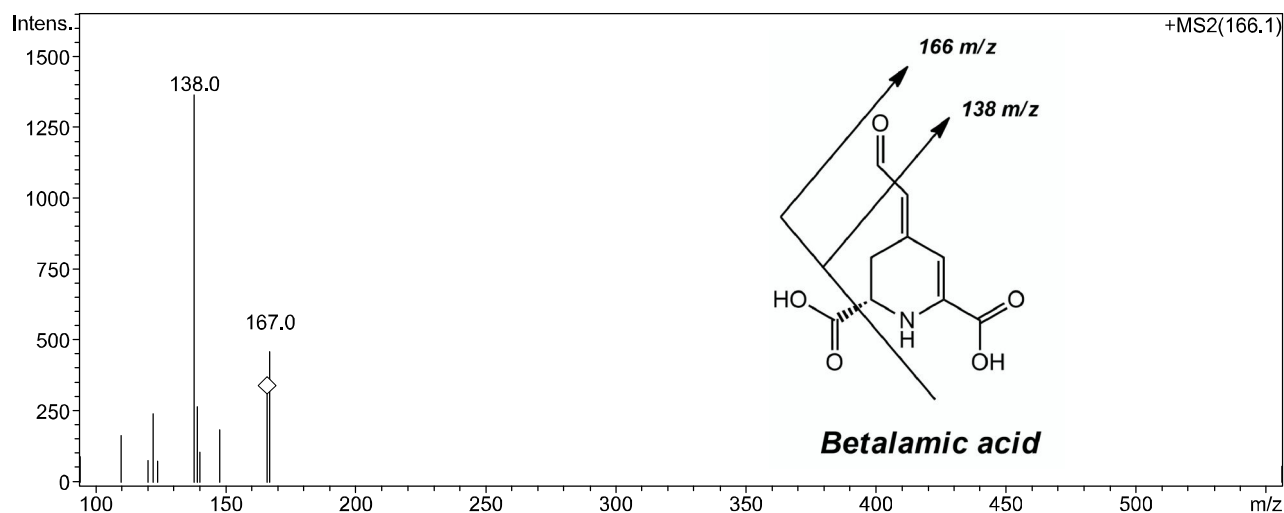
# Compound Mass Spectrum List Report - MS



## MS Peak List:

#	m/z	Res.	FWHM	I	I %	S/N
1	138.2			4518	10	
2	166.1			47362	100	
3	167.0			7204	15	
4	212.0			11977	25	

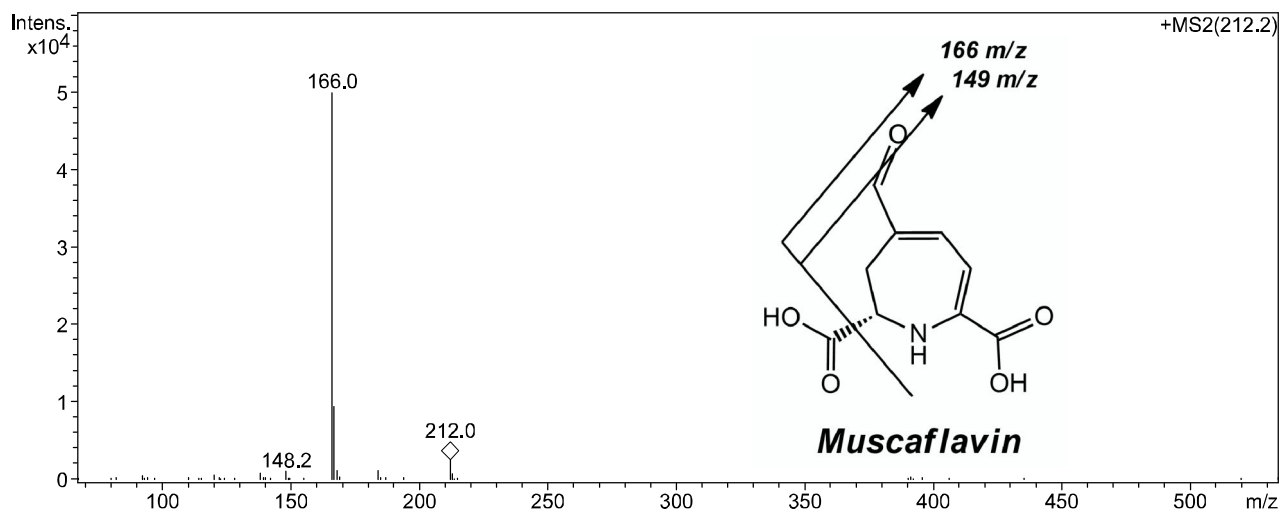
# Compound Mass Spectrum List Report - MS



## MS Peak List:

#	m/z	Res.	FWHM	I	I %	S/N
1	94.2			86	6	
2	110.0			163	12	
3	120.1			75	5	
4	122.1			237	17	
5	124.0			72	5	
6	138.0			1362	100	
7	139.0			263	19	
8	140.1			103	8	
9	148.0			184	14	
10	166.1			308	23	
11	167.0			458	34	
12	555.8			53	4	

# Compound Mass Spectrum List Report - MS

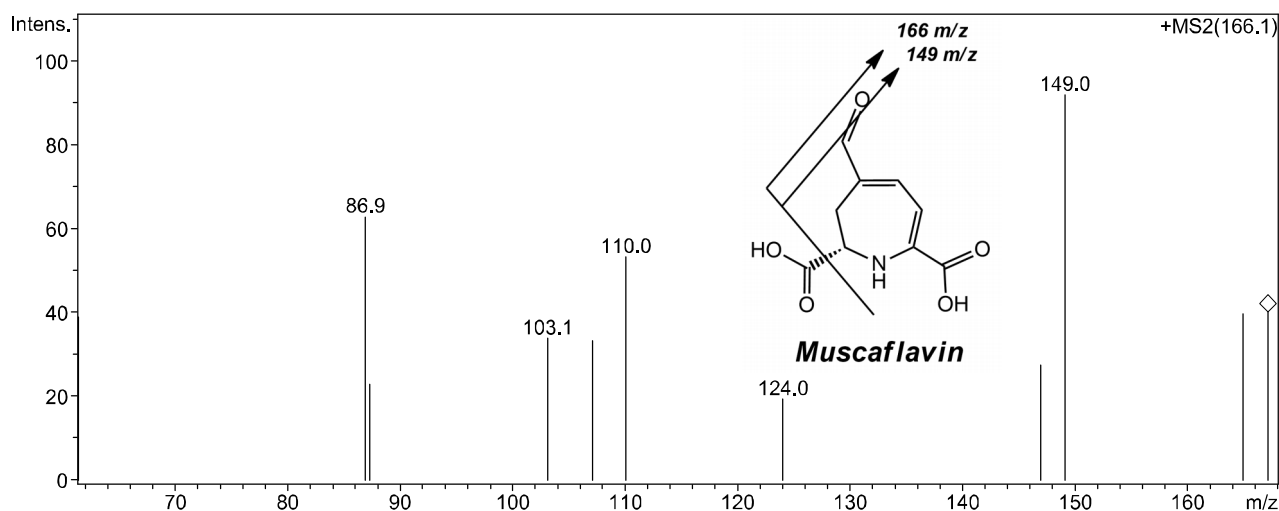


## MS Peak List:

#	m/z	Res.	FWHM	I	I %	S/N
1	67.4			83	0	
2	80.3			61	0	
3	82.2			154	0	
4	92.2			419	1	
5	93.2			50	0	
6	94.3			128	0	
7	97.1			32	0	
8	110.3			176	0	
9	114.2			64	0	
10	115.4			22	0	
11	120.1			501	1	
12	122.2			154	0	
13	122.8			15	0	
14	124.1			38	0	
15	128.2			60	0	
16	138.2			687	1	
17	139.3			115	0	
18	140.2			111	0	
19	142.1			91	0	
20	148.2			933	2	
21	149.2			91	0	
22	149.7			53	0	
23	155.2			24	0	
24	166.0			49883	100	
25	167.0			9323	19	
26	168.0			1038	2	
27	169.0			221	0	
28	184.0			1011	2	
29	185.0			112	0	
30	187.0			165	0	
31	194.0			175	0	
32	212.0			2507	5	
33	213.0			617	1	
34	213.8			18	0	



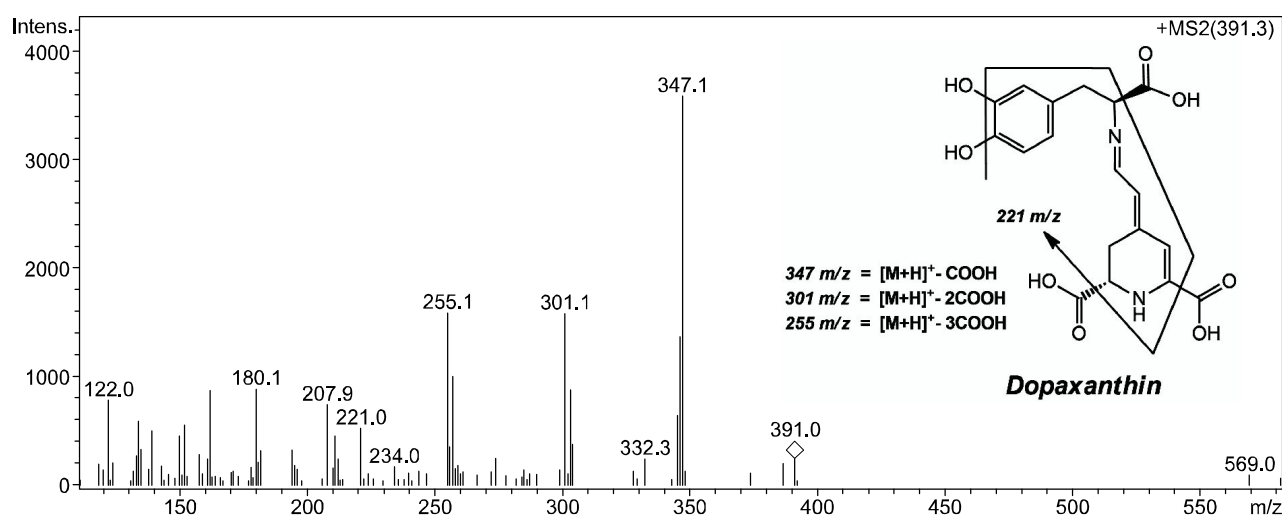
# Compound Mass Spectrum List Report - MS



## MS Peak List:

#	m/z	Res.	FWHM	I	I %	S/N
1	61.4			39	42	
2	86.9			63	68	
3	87.3			23	25	
4	103.1			34	37	
5	107.1			33	36	
6	110.0			53	58	
7	124.0			19	21	
8	146.9			27	30	
9	149.0			92	100	
10	164.9			40	43	
11	167.1			40	44	

## Compound Mass Spectrum List Report - MS

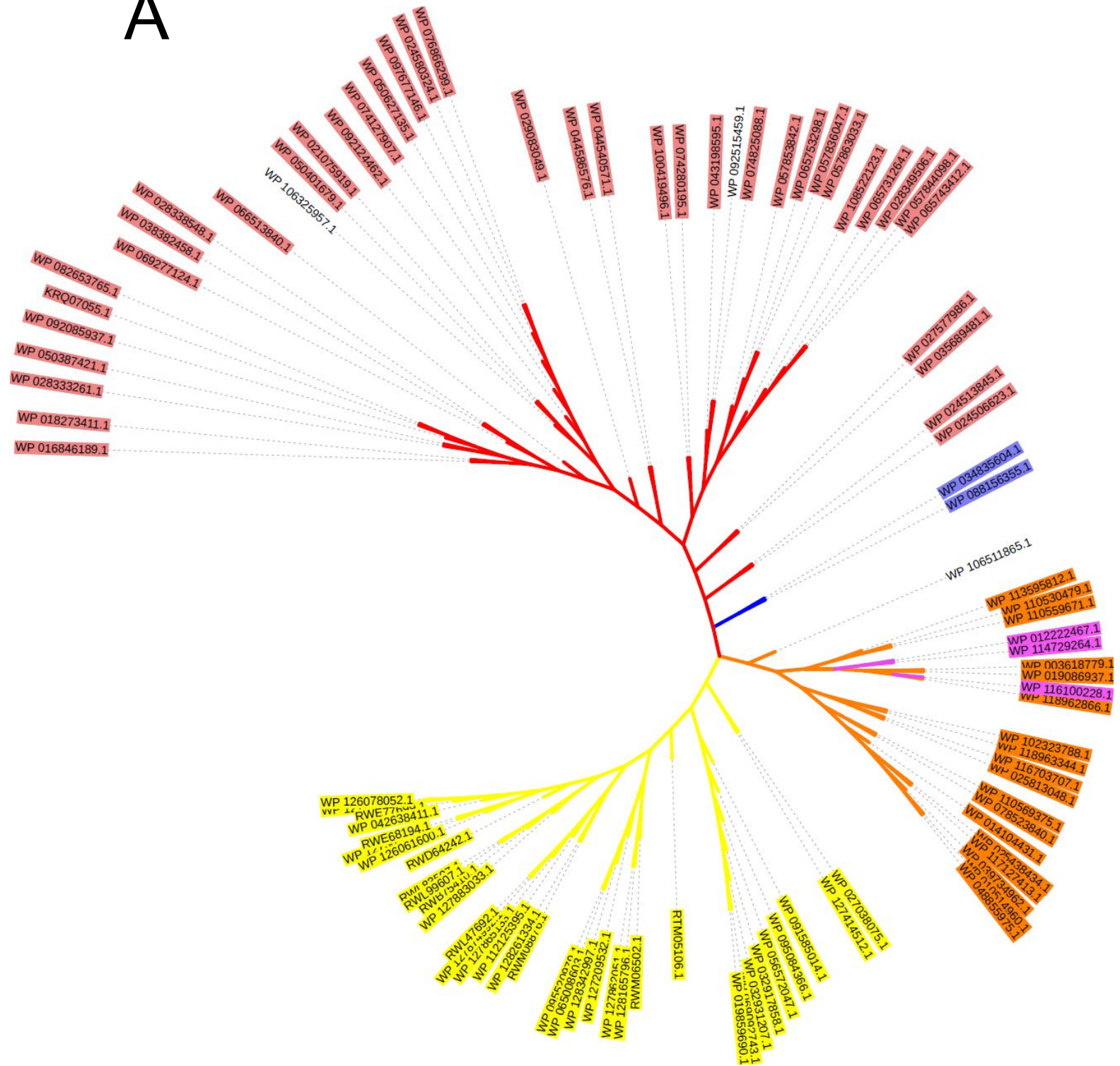


### MS Peak List:

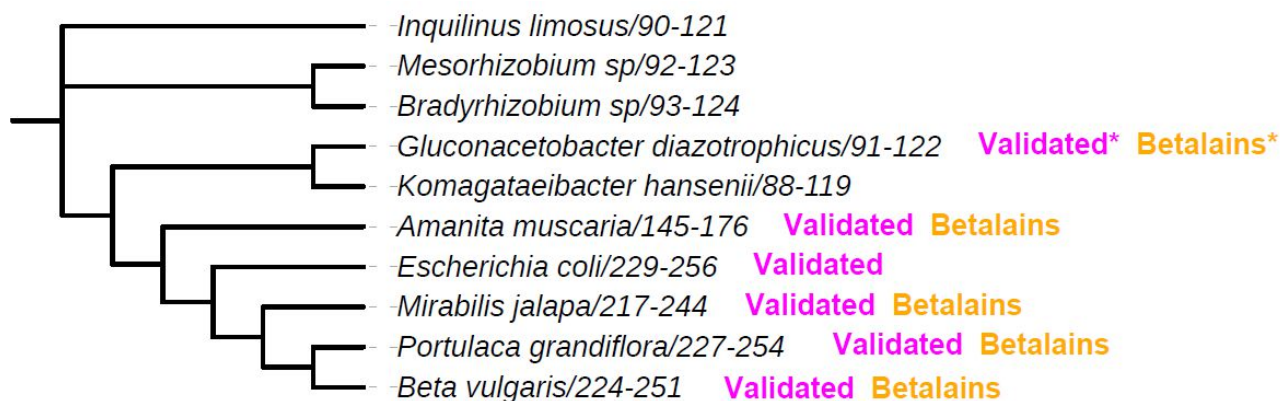
#	m/z	Res.	FWHM	I	I %	S/N
1	122.0			777	22	
2	134.0			582	16	
3	135.0			327	9	
4	139.1			495	14	
5	150.0			449	13	
6	152.1			553	15	
7	162.0			866	24	
8	180.1			880	25	
9	207.9			736	21	
10	210.8			445	12	
11	221.0			517	14	
12	255.1			1582	44	
13	256.0			346	10	
14	257.1			996	28	
15	301.1			1576	44	
16	303.2			876	24	
17	304.0			370	10	
18	345.1			633	18	
19	346.0			1364	38	
20	347.1			3582	100	

**Figure Annex II.1. ESI-MS fragment spectra of betalains and intermediate compounds identified in this work.** MS2 spectra of all compounds are provided with structures and annotations.

A



# B



**Validated:** Enzyme functionally characterized on L-DOPA

**Betalains:** Betalamic acid derivatives found naturally

**\* \*:** Described in this work

**Figure Annex II.2. Extended phylogenetic analysis of the novel betalain-forming dioxygenase from *G. diazotrophicus*.** **A:** The novel enzyme was searched against similar enzymes and the 100 most similar sequences were used to construct a Neighbour-Joining phylogenetic tree. The tree shows the presence of three main clades comprising species of *Bradyrhizobium* (red), *Komagataeibacter* (orange), and *Mesorhizobium* (yellow). Sequences corresponding to *Inquilingus* are shown in blue and those corresponding to *Acetobacter*, in pink. **B:** The block among residues His91 and Asp122 in GdDODA (see main text in chapter IV for details) was used to construct a larger tree with all the betalain-forming characterized enzymes and including bacterial members of the different classes identified in A. In this tree, experimentally validated enzymes are labelled. The presence of betalamic acid derivatives (betalains) is also indicated. Additional sequences corresponding to bacterial members are WP\_027577986 (*Bradyrhizobium*), WP\_003618779 (*Komagataeibacter*), RWL99607 (*Mesorhizobium*), and WP\_034835604 (*Inquilingus*).



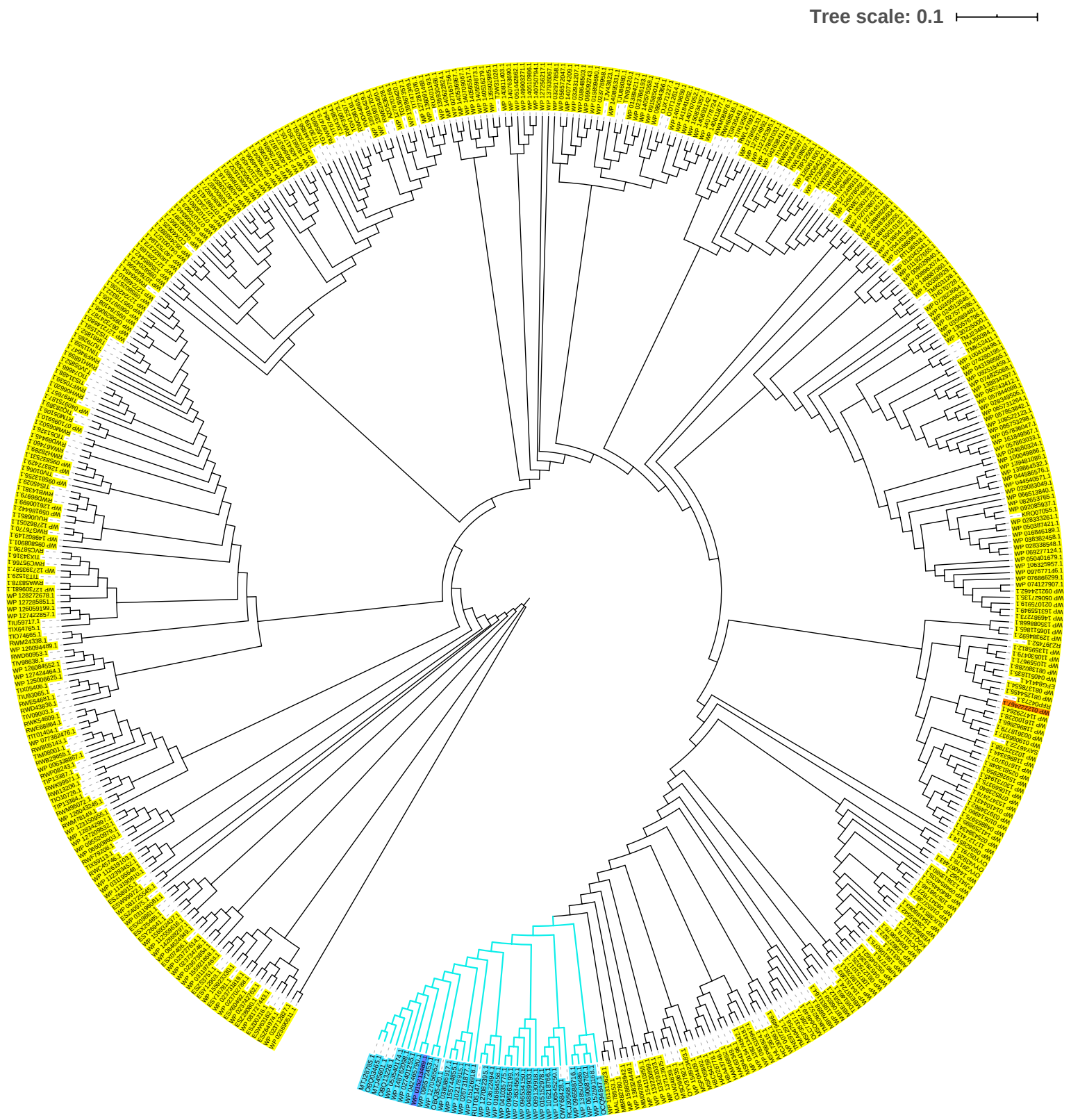


**Figure Annex III. Phylogenetic analysis of dioxygenase enzymes related to *Gluconacetobacter diazotrophicus* (orange).** These enzymes correspond to the phylum proteobacteria (yellow) and cyanobacteria (blue), including *Anabaena cylindrica* (navy blue).



## Annex IV. Statistical analysis of Chapter XII

### 1. One-way ANOVA Statistical analysis for the fluorescence measurements of LD01 worms treated with 25 $\mu\text{M}$ of indoline carboxylic acid-betacyanin vs control worms.

Summary of Data			
	Treatments		
	1	2	Total
N	13	19	32
$\Sigma X$	7602055.68	28468278.2	36070333.8
Mean	584773.514	1498330.43	1127197.93
$\Sigma X^2$	4.7252E+12	4.4777E+13	4.9502E+13
Std.Dev.	152688.499	343361.513	534122.016

Result Details				
Source	SS	df	MS	
Between-treatments	6.442E+12	1	6.442E+12	F = 80.46038
Within-treatments	2.4019E+12	30	8.0064E+10	
Total	8.8439E+12	31		

The f-ratio value is 80.46038. The  $p$ -value is  $< 0.00001$ . The result is significant at  $p < 0.05$ .

### 2. One-way ANOVA Statistical analysis for the fluorescence measurements of LD01 worms treated with 25 $\mu\text{M}$ of Indicaxanthin vs control worms.

Summary of Data			
	Treatments		
	1	2	Total
N	15	20	35
$\Sigma X$	1.67	1.214	2.884
Mean	0.2088	0.2023	0.206
$\Sigma X^2$	0.3634	0.2486	0.612
Std.Dev.	0.046	0.0245	0.0372



Result Details				
Source	SS	df	MS	
Between-treatments	0.0001	1	0.0001	F = 0.09515
Within-treatments	0.0178	12	0.0015	
Total	0.0179	13		

The f-ratio value is 0.09515. The  $p$ -value is 0.763014. The result is not significant at  $p < 0.05$ .

### 3. Chi-square Statistical analysis for the fluorescence measurements of TJ356 worms treated with 100 $\mu$ M of Indicaxanthin vs control worms.

Results				
	Nuclear	Intermediate	Cytosolic	Row Totals
Control	2 (29.04) [25.18]	45 (47.25) [0.11]	54 (24.71) [34.73]	101
Indicaxanthin	65 (37.96) [19.27]	64 (61.75) [0.08]	3 (32.29) [26.57]	132
Column Totals	67	109	57	233 (Grand Total)

The chi-square statistic is 105.933. The  $p$ -value is  $< 0.00001$ . The result is significant at  $p < 0.05$ .

### 4. Chi-square Statistical analysis for the fluorescence measurements of TJ356 worms treated with 100 $\mu$ M of Indoline carboxylic acid-betacyanin vs control worms.

Results				
	Nuclear	Intermediate	Cytosolic	Row Totals
Control	6 (20.32) [10.09]	44 (46.85) [0.17]	42 (24.83) [11.86]	92
Indoline carboxylic acid-betacyanin	30 (15.68) [13.08]	39 (36.15) [0.22]	2 (19.17) [15.37]	71
Column Totals	36	83	44	163 (Grand Total)

The chi-square statistic is 50.8026. The  $p$ -value is  $< 0.00001$ . The result is significant at  $p < 0.05$ .

**5. Chi-square Statistical analysis for the fluorescence measurements of TJ356 worms treated with 100  $\mu$ M of Dopaxanthin vs control worms.**

<b>Results</b>				
	Nuclear	Intermediate	Cytosolic	Row Totals
<b>Control</b>	42 (51.79) [1.85]	44 (35.44) [2.07]	6 (4.77) [0.32]	92
<b>Dopaxanthin</b>	34 (24.21) [3.96]	8 (16.56) [4.43]	1 (2.23) [0.68]	43
<b>Column Totals</b>	76	52	7	135 (Grand Total)

The chi-square statistic is 13.3041. The  $p$ -value is 0.001291. The result is significant at  $p < 0.05$ .

**6. Chi-square Statistical analysis for the fluorescence measurements of TJ356 worms treated with 100  $\mu$ M of Phenylalanine-betaxanthin vs control worms.**

<b>Results</b>				
	Nuclear	Intermediate	Cytosolic	Row Totals
<b>Control</b>	6 (16.73) [6.88]	44 (54.12) [1.89]	42 (21.16) [20.54]	92
<b>Phenylalanine-betaxanthin</b>	28 (17.27) [6.66]	66 (55.88) [1.83]	1 (21.84) [19.89]	95
<b>Column Totals</b>	34	110	43	187 (Grand Total)

The chi-square statistic is 57.695. The  $p$ -value is  $< 0.00001$ . The result is significant at  $p < 0.05$ .

**7. One-way ANOVA Statistical analysis for the fluorescence measurements of Wild-type N2 worms treated with 10  $\mu$ M of Dopaxanthin vs control worms.**

Summary of Data			
	Treatments		
	1	2	Total
<b>N</b>	8	11	19
<b><math>\Sigma X</math></b>	562648.602	1616085.708	2178734.31
<b>Mean</b>	70331.0753	146916.8825	114670.227
<b><math>\Sigma X^2</math></b>	4.1106E+10	2.51663E+11	2.9277E+11
<b>Std.Dev.</b>	14804.5383	37725.9744	48838.003

Result Details				
Source	SS	df	MS	
<b>Between-treatments</b>	2.7166E+10	1	2.7166E+10	F = 29.29095
<b>Within-treatments</b>	1.5767E+10	17	927453640	
<b>Total</b>	4.2933E+10	18		

The f-ratio value is 29.29095. The  $p$ -value is 0.000047. The result is significant at  $p < 0.05$ .

**8. One-way ANOVA Statistical analysis for the fluorescence measurements of Wild-type N2 worms treated with 100  $\mu$ M of Dopaxanthin vs control worms.**

Summary of Data			
	Treatments		
	1	2	Total
<b>N</b>	8	6	14
<b><math>\Sigma X</math></b>	562648.602	2942871.371	3505519.97
<b>Mean</b>	70331.0753	490478.5618	250394.284
<b><math>\Sigma X^2</math></b>	4.1106E+10	1.4581E+12	1.4992E+12
<b>Std.Dev.</b>	14804.5383	54188.7974	218639.356

Result Details				
Source	SS	df	MS	
Between-treatments	6.0522E+11	1	6.0522E+11	F = 447.8627
Within-treatments	1.6216E+10	12	1351362439	
Total	6.2144E+11	13		

The f-ratio value is 447.8627. The  $p$ -value is  $< .00001$ . The result is significant at  $p < 0.05$ .

**9. One-way ANOVA Statistical analysis for the fluorescence measurements of TJ375 worms treated with 25  $\mu$ M of Aniline-betaxanthin vs control worms.**

Summary of Data			
	Treatments		
	1	2	Total
N	7	8	15
$\Sigma X$	75.72	52.81	128.53
Mean	10.8171	6.6013	8.569
$\Sigma X^2$	821.8852	351.2321	1173.1173
Std.Dev.	0.6845	0.6118	2.2644

Result Details				
Source	SS	df	MS	
Between-treatments	66.3553	1	66.3553	F = 158.82579
Within-treatments	5.4312	13	0.4178	
Total	71.7866	14		

The f-ratio value is 158.82579. The  $p$ -value is  $< 0.00001$ . The result is significant at  $p < 0.05$ .

**10. One-way ANOVA Statistical analysis for the fluorescence measurements of TJ375 worms treated with 25  $\mu$ M of Betanidin vs control worms.**

Summary of Data			
	Treatments		
	1	2	Total
<b>N</b>	7	9	16
<b><math>\Sigma X</math></b>	75.72	33.73	109.45
<b>Mean</b>	10.8171	3.7478	6.841
<b><math>\Sigma X^2</math></b>	821.8852	131.0741	952.9593
<b>Std.Dev.</b>	0.6845	0.7633	3.6901

Result Details				
Source	SS	df	MS	
<b>Between-treatments</b>	196.7802	1	196.7802	F = 368.66505
<b>Within-treatments</b>	7.4727	14	0.5338	
<b>Total</b>	204.2529	15		

The f-ratio value is 368.66505. The  $p$ -value is  $< 0.00001$ . The result is significant at  $p < 0.05$ .

**11. One-way ANOVA Statistical analysis for the fluorescence measurements of TJ375 worms treated with 25  $\mu$ M of Dopaxanthin vs control worms.**

Summary of Data			
	Treatments		
	1	2	Total
<b>N</b>	7	9	16
<b><math>\Sigma X</math></b>	75.72	15.6	91.32
<b>Mean</b>	10.8171	1.7333	5.708
<b><math>\Sigma X^2</math></b>	821.8852	29.6684	851.5536
<b>Std.Dev.</b>	0.6845	0.5732	4.6929

<b>Result Details</b>				
<b>Source</b>	<b>SS</b>	<b>df</b>	<b>MS</b>	
<b>Between-treatments</b>	324.9052	1	324.9052	F = 836.22325
<b>Within-treatments</b>	5.4395	14	0.3885	
<b>Total</b>	330.3447	15		

The f-ratio value is 836.22325. The  $p$ -value is  $< 0.00001$ . The result is significant at  $p < 0.05$ .

## 12. One-way ANOVA Statistical analysis for the fluorescence measurements of TJ375 worms treated with 25 $\mu$ M of Indoline carboxylic acid-betacyanin vs control worms.

<b>Summary of Data</b>			
	<b>Treatments</b>		
	1	2	Total
<b>N</b>	7	8	15
<b><math>\Sigma X</math></b>	75.72	19.84	95.56
<b>Mean</b>	10.8171	2.48	6.371
<b><math>\Sigma X^2</math></b>	821.8852	49.2436	871.1288
<b>Std.Dev.</b>	0.6845	0.076	4.3289

<b>Result Details</b>				
<b>Source</b>	<b>SS</b>	<b>df</b>	<b>MS</b>	
<b>Between-treatments</b>	259.4964	1	259.4964	F = 1183.02713
<b>Within-treatments</b>	2.8515	13	0.2193	
<b>Total</b>	262.3479	14		

The f-ratio value is 1183.02713. The  $p$ -value is  $< 0.00001$ . The result is significant at  $p < 0.05$ .

**13. One-way ANOVA Statistical analysis for the fluorescence measurements of TJ375 worms treated with 25  $\mu$ M of Miraxanthin I vs control worms.**

Summary of Data			
	Treatments		
	1	2	Total
<b>N</b>	7	10	17
<b><math>\Sigma X</math></b>	75.72	99.38	175.1
<b>Mean</b>	10.8171	9.938	10.3
<b><math>\Sigma X^2</math></b>	821.8852	993.5832	1815.4684
<b>Std.Dev.</b>	0.6845	0.8127	0.8638

Result Details				
Source	SS	df	MS	
<b>Between-treatments</b>	3.1825	1	3.1825	F = 5.45203
<b>Within-treatments</b>	8.7559	15	0.5837	
<b>Total</b>	11.9384	16		

The f-ratio value is 5.45203. The  $p$ -value is 0.033853. The result is significant at  $p < 0.05$ .

**14. One-way ANOVA Statistical analysis for the fluorescence measurements of TJ375 worms treated with 25  $\mu$ M of Phenylalanine-betaxanthin vs control worms.**

Summary of Data			
	Treatments		
	1	2	Total
<b>N</b>	7	11	18
<b><math>\Sigma X</math></b>	75.72	37.04	112.76
<b>Mean</b>	10.8171	3.3673	6.264
<b><math>\Sigma X^2</math></b>	821.8852	132.5144	954.3996
<b>Std.Dev.</b>	0.6845	0.8826	3.8196

<b>Result Details</b>				
<b>Source</b>	<b>SS</b>	<b>df</b>	<b>MS</b>	
<b>Between-treatments</b>	237.4191	1	237.4191	F = 358.3089
<b>Within-treatments</b>	10.6018	16	0.6626	
<b>Total</b>	248.0208	17		

The f-ratio value is 358.3089. The  $p$ -value is  $< 0.00001$ . The result is significant at  $p < 0.05$ .

**15. One-way ANOVA Statistical analysis for the fluorescence measurements of TJ375 worms treated with 25  $\mu$ M of Pyrrolidine-betaxanthin vs control worms.**

<b>Summary of Data</b>			
	<b>Treatments</b>		
	<b>1</b>	<b>2</b>	<b>Total</b>
<b>N</b>	7	7	14
<b><math>\Sigma X</math></b>	75.72	62.68	138.4
<b>Mean</b>	10.8171	8.9543	9.886
<b><math>\Sigma X^2</math></b>	821.8852	563.7444	1385.6296
<b>Std.Dev.</b>	0.6845	0.6442	1.1585

<b>Result Details</b>				
<b>Source</b>	<b>SS</b>	<b>df</b>	<b>MS</b>	
<b>Between-treatments</b>	12.1458	1	12.1458	F = 27.49525
<b>Within-treatments</b>	5.3009	12	0.4417	
<b>Total</b>	17.4467	13		

The f-ratio value is 27.49525. The  $p$ -value is 0.000207. The result is significant at  $p < 0.05$ .



**16. One-way ANOVA Statistical analysis for the fluorescence measurements of TJ375 worms treated with 25  $\mu$ M of Tryptophan-betaxanthin vs control worms.**

Summary of Data			
	Treatments		
	1	2	Total
<b>N</b>	7	9	16
<b><math>\Sigma X</math></b>	75.72	74.84	150.56
<b>Mean</b>	10.8171	8.3156	9.41
<b><math>\Sigma X^2</math></b>	821.8852	623.3462	1445.2314
<b>Std.Dev.</b>	0.6845	0.3553	1.3775

Result Details				
Source	SS	df	MS	
<b>Between-treatments</b>	24.6406	1	24.6406	F = 90.27846
<b>Within-treatments</b>	3.8212	14	0.2729	
<b>Total</b>	28.4618	15		

The f-ratio value is 90.27846. The  $p$ -value is  $< 0.00001$ . The result is significant at  $p < 0.05$ .

**17. One-way ANOVA Statistical analysis for the fluorescence measurements of TJ375 worms treated with 25  $\mu$ M of Valine-betaxanthin vs control worms.**

Summary of Data			
	Treatments		
	1	2	Total
<b>N</b>	7	5	12
<b><math>\Sigma X</math></b>	75.72	52.84	128.56
<b>Mean</b>	10.8171	10.568	10.713
<b><math>\Sigma X^2</math></b>	821.8852	562.229	1384.1142
<b>Std.Dev.</b>	0.6845	0.9767	0.7867

Result Details				
Source	SS	df	MS	
Between-treatments	0.181	1	0.181	F = 0.27319
Within-treatments	6.627	10	0.6627	
Total	6.8081	11		

The f-ratio value is 0.27319. The  $p$ -value is 0.612582. The result is not significant at  $p < 0.05$ .

#### 18. One-way ANOVA Statistical analysis for the fluorescence measurements of TJ375 worms treated with 25 $\mu$ M of Vulgaxanthin I vs control worms.

Summary of Data			
	Treatments		
	1	2	Total
N	7	11	18
$\Sigma X$	75.72	49.09	124.81
Mean	10.8171	4.4627	6.934
$\Sigma X^2$	821.8852	221.9065	1043.7917
Std.Dev.	0.6845	0.5321	3.2392

Result Details				
Source	SS	df	MS	
Between-treatments	172.7307	1	172.7307	F = 489.81103
Within-treatments	5.6424	16	0.3526	
Total	178.373	17		

The f-ratio value is 489.81103. The  $p$ -value is  $< 0.00001$ . The result is significant at  $p < 0.05$ .

**19. One-way ANOVA Statistical analysis for the fluorescence measurements of TJ375 worms treated with 25  $\mu$ M of Vulgaxanthin II vs control worms.**

Summary of Data			
	Treatments		
	1	2	Total
<b>N</b>	7	7	14
<b><math>\Sigma X</math></b>	75.72	69.86	145.58
<b>Mean</b>	10.8171	9.98	10.399
<b><math>\Sigma X^2</math></b>	821.8852	700.7024	1522.5876
<b>Std.Dev.</b>	0.6845	0.7637	0.821

Result Details				
Source	SS	df	MS	
<b>Between-treatments</b>	2.4528	1	2.4528	F = 4.6641
<b>Within-treatments</b>	6.3107	12	0.5259	
<b>Total</b>	8.7636	13		

The f-ratio value is 4.6641. The  $p$ -value is 0.051743. The result is not significant at  $p < 0.05$ .

**20. One-way ANOVA Statistical analysis for the fluorescence measurements of TJ375 worms treated with 25  $\mu$ M of Vulgaxanthin III vs control worms.**

Summary of Data			
	Treatments		
	1	2	Total
<b>N</b>	7	9	16
<b><math>\Sigma X</math></b>	75.72	68.21	143.93
<b>Mean</b>	10.8171	7.5789	8.996
<b><math>\Sigma X^2</math></b>	821.8852	522.2065	1344.0917
<b>Std.Dev.</b>	0.6845	0.8101	1.8139

<b>Result Details</b>				
<b>Source</b>	<b>SS</b>	<b>df</b>	<b>MS</b>	
<b>Between-treatments</b>	41.2898	1	41.2898	F = 71.70467
<b>Within-treatments</b>	8.0616	14	0.5758	
<b>Total</b>	49.3514	15		

The f-ratio value is 71.70467. The  $p$ -value is  $< 0.00001$ . The result is significant at  $p < 0.05$ .

## 21. One-way ANOVA Statistical analysis for the fluorescence measurements of TJ375 worms treated with 25 $\mu$ M of Vulgaxanthin VI vs control worms.

<b>Summary of Data</b>			
	<b>Treatments</b>		
	<b>1</b>	<b>2</b>	<b>Total</b>
<b>N</b>	7	9	16
<b><math>\Sigma X</math></b>	75.72	56.15	131.87
<b>Mean</b>	10.8171	6.2389	8.242
<b><math>\Sigma X^2</math></b>	821.8852	352.5967	1174.4819
<b>Std.Dev.</b>	0.6845	0.5342	2.417

<b>Result Details</b>				
<b>Source</b>	<b>SS</b>	<b>df</b>	<b>MS</b>	
<b>Between-treatments</b>	82.5316	1	82.5316	F = 226.8139
<b>Within-treatments</b>	5.0942	14	0.3639	
<b>Total</b>	87.6258	15		

The f-ratio value is 226.8139. The  $p$ -value is  $< 0.00001$ . The result is significant at  $p < 0.05$ .